THE UNIVERSITY OF CHICAGO

APPLICATION AND DEVELOPMENT OF THE REACTIONS OF OXYALLYL CATIONS AND SYNTHETIC STUDIES TOWARDS AMBIGUINE Q

A DISSERTATION SUBMITTED TO

THE FACULTY OF THE DIVISION OF THE PHYSICAL SCIENCES

IN CANDIDACY FOR THE DEGREE OF

DOCTOR OF PHILOSOPHY

DEPARTMENT OF CHEMISTRY

BY

FERDINAND J. TAENZLER

CHICAGO, ILLINOIS

AUGUST 2021

For my family

TABLE OF CONTENTS

LIST OF SCHEMES vii

LIST OF TABLES x

LIST OF FIGURES xi

LIST OF ABBREVIATIONS xxiii

Acknowledgements xxviii

Abstract xxxi

Chapter 1: Oxyallyl Cations: Development, Application, and Asymmetric Transformations 1

1.2 Generation/transition states 1

1.3 Alpha halo ketones 4

1.4 Total Synthesis of Lasidiol by Föhlisch 7

1.5 Alkoxy-stabilized Oxyallyl Cations 8

1.6 Total Synthesis of Urechitol by Watanabe 12

1.7 Benzylic Cations as Oxyallyl Equivalents 13

1.8 Total Synthesis of Frondosin B 16

1.9 Metal Carbene and Metal Allyl Cation [4+3] 17

1.10 Total Synthesis of Englerin A by Theodorakis 19

Conclusion 20

Chapter 2: [4+3] Cycloaddition of 3-Alkenyl Indoles and Oxyallyl Cations 21

2.1: Introduction 21

2.2 Initial Discovery of the [4+3] Cycloaddition of 3-alkenyl Indoles 23

2.3 Substrate Scope of the [4+3] Cycloaddition 25

2.4 Mechanistic Discussion and Limitations 28

2.5 Intramolecular [4+3] Cycloaddition Using a Tethered Oxyallyl Cation 31

2.6 Investigations into Alternative Oxyallyl Cations 33

2.7 Isomerization of Cycloadducts 35

2.8 Catalysis of the [4+3] Cycloaddition 37

2.8 Conclusion 42

Chapter 3 Synthetic Studies Toward Ambiguine Q 44

3.1 Introduction to the Ambiguines 44

3.2.1 Sarpong's Synthesis of Ambiguine P 46

3.2.2 Rawal Synthesis of Ambiguine P 49

3.3 Retrosynthetic Analysis of Ambiguine Q 51

3.3 Model Studies for Route B 54

3.4 Model Studies Route B – Gem Dimethylated Analogue 55

3.5 Setting the C15 Stereocenter 57

3.6 Synthesis of the key 3-alkenyl indole 59

3.7 Investigation of the Key [4+3] Cycloaddition 61

3.8 Use of dimethyl oxyallyl cation precursors 64

3.9 Elaborating the [4+3] cycloadduct towards Ambiguine Q 64

3.10 Alternative Approaches to Introduce the gem-dimethyl Quaternary Center: 68

3.11 Conclusion 73

Chapter 4: Chiral Brønsted Acid Catalysis for Asymmetric [4+3] Cycloadditions 75

4.1 Introduction: Asymmetric Induction in acetal substitutions 75

4.2 Initial Discovery of the Transformation 77

4.3 Proposed catalytic cycle: 81

4.4 Substrate Table for the Assymetric [4+3] Cycloaddition 83

4.5 Additional Cycloadditions Attempted with Oxyallyl Cations 85

4.6 Attempts at Asymmetric Acetal Substitution with IDPi Catalysis 87

4.7 Conclusion 89

Chapter 5: Experimental Details 90

5.1.1 Experimental Details for Chapter 2 – Formation of 3-Acetyl Indoles 91

5.1.2 Experimental Details for Chapter 2 – Formation of 3-Alkenyl Indoles 100

5.1.3 Experimental Details for Chapter 2 – [4+3] cycloaddition of 3-alkenyl indoles 118

5.1.4 Experimental Details for Chapter 2 – Intramolecular Cyclization substrate 136

5.1.5 Experimental Details for Chapter 2 – Isomerization/Reduction of Cycloadducts 140

5.1.6 Experimental Details for Chapter 2 – Asymmetric [4+3] cycloaddition of 3-alkenyl indoles 144

5.2.1 Experimental Details for Chapter 3 – Model Studies for Route B..... 147

5.2.2 Experimental Details for Chapter 3 – Construction of the Methyl/Vinyl Skeleton..... 158

5.2.3 Experimental Details for Chapter 3 – Completion of the ambiguine skeleton 171

5.3 Experimental Details for Chapter 4..... 180

Chapter 6: Selected Spectra 198

LIST OF SCHEMES

Scheme 1: Formation and reaction of azaoxyallyl cations 6

Scheme 2: Enantioselective [4+3] with prolinol catalysis 7

Scheme 3: Föhlisch synthesis of lasidiol 8

Scheme 4: [4+3] cycloaddition of stabilized oxyallyl cations 9

Scheme 5: Chiral Stabilized Oxyallyl Cations 10

Scheme 6: Harmata's enantioselective [4+3] 11

Scheme 7: Jacobson enantioselective [4+3] 11

Scheme 8: Urechitol A retrosynthetic analysis for key intermediate 12

Scheme 9: Watanabe's Synthesis of (±)-Urechitol A 13

Scheme 10: 3-benzylic alcohols as oxyallyl cations 14

Scheme 11: Acid catalyzed [4+3] of C-2 benzylic alcohols 15

Scheme 12: Acid catalyzed [4+3] of C-2 benzylic alcohols 16

Scheme 13: Li's Synthesis of Frondosin B and epi-Liphagal 17

Scheme 14: Metal Carbenoid as oxyallyl equivalents 18

Scheme 15: Theodorakis Synthesis of (-)englerin A 20

Scheme 16: Synthesis of the Model Diene **91** 23

Scheme 17: Construction of Various Indole Dienes 26

Scheme 18: Proposed Mechanism for the Cycloaddition 28

Scheme 19: Stereo / Electronic Limitations of the [4+3] Cycloaddition 30

Scheme 20: [4+3] of 3-alkenyl pyrrole 31

Scheme 21: Approach Towards an Intramolecular Cycloaddition 32

Scheme 22: Attempts Towards an Intramolecular Cycloaddition..... 33

Scheme 23: Unsuccessful Oxyallyl Cations..... 34

Scheme 24: Use of Stabilized Zwitterionic Cation **116** 35

Scheme 25: Isomerization/Deoxygenation of Cycloadducts..... 36

Scheme 26: Proposed Deoxygenation/Isomerization Mechanism 37

Scheme 27: Sarpong's Construction of the Pentacyclic Core..... 47

Scheme 28: Sarpong's completion of the skeleton..... 48

Scheme 29: Completion of ambiguine P 49

Scheme 30: Rawal construction of pentacyclic core..... 50

Scheme 31: Rawal's synthesis of Ambiguine P..... 51

Scheme 32: Model studies towards Route B..... 55

Scheme 33: [4+3] Cycloaddition of Model Compound **182** 55

Scheme 34: synthesis of the gem-dimethyl Model Compound 186..... 56

Scheme 35: [4+3] Cycloaddition of gem-dimethylated Model Compound **186** 57

Scheme 36: Summary of C15 Diastereoselectivity..... 58

Scheme 37: Setting the stereocenter at C15 59

Scheme 38: Construction of 3-alkenyl indole **171** 60

Scheme 39: Proposed Mechanism of the [4+3] cycloaddition 63

Scheme 40: attempted cycloaddition with alkylated oxyallyl cations 64

Scheme 41: Rearomatization of the Indole and Deoxygenation 66

Scheme 42: Formation of Enone **208** 69

Scheme 43: Investigation into the use of enolates 70

Scheme 44: Attempted alkylation of silyl enol ether **211** 71

Scheme 45: Completion of the Ambiguine Skeleton 72

Scheme 46: Proposed Endgame Strategy Towards Ambiguine Q 73

Scheme 47: Mechanisms for Acetal Substitution 76

Scheme 48: Initial Discovery of the IDPi Catalyzed [4+3] with Furan 78

Scheme 49: Proposed Catalytic Cycle for the Enantioselective [4+3] 82

Scheme 50: Attempts at an IDPi Catalyzed [3+2] Cycloaddition Reaction 86

Scheme 51: Attempts at an IDPi Catalyzed Dearomative [3+2] Cycloaddition Reaction 87

Scheme 52: Results of Initial Investigations into Asymmetric Acetal Substitutions 89

LIST OF TABLES

Table 1: Cycloaddition of α-halo ketones with furan..... 5

Table 2: Optimization of the [4+3] cycloaddition..... 24

Table 3: Substrate Scope for the [4+3] Cycloaddition..... 27

Table 4: Initial catalyst Screen..... 39

Table 5: Screen of IDPi catlaysts..... 41

Table 6: Continued Screen of Reaction Conditions..... 42

Table 7: Optimization of Conditions for the [4+3] cycloaddition..... 61

Table 8: Attempts at C24 gem-di-methylation..... 67

Table 9: Initial Solvent/Temperature Optimizations..... 79

Table 10: Additional Optimizations of Catalysts..... 81

Table 11: [4+3] Cycloaddition of Substituted Furans..... 83

LIST OF FIGURES

Figure 1: Transition states of oxyallyl cations 2

Figure 2: Reaction mechanisms of oxyallyl cations 3

Figure 3: Cyclohepta[b]indole Motif in Bioactive Compounds 21

Figure 4: [4+3] Disconnections of the Ambiguine Skeleton 22

Figure 5: The Ambiguine Alkaloids 45

Figure 6: Retrosynthetic analysis of ambiguine Q 52

Figure 7: Retrosynthesis of diene **171** 53

Figure 8: ^{1}H NMR Spectrum of **90** (500MHz, $CDCl_3$) 199

Figure 9: ^{13}C NMR Spectrum of **90** (100MHz, $CDCl_3$) 200

Figure 10: ^{1}H NMR Spectrum of **94a** (400MHz, $CDCl_3$) 201

Figure 11: ^{13}C NMR Spectrum of **94a** (100MHz, $CDCl_3$) 202

Figure 12: ^{1}H NMR Spectrum of **94b** (400MHz, $CDCl_3$) 203

Figure 13: ^{13}C NMR Spectrum of **94b** (100MHz, $CDCl_3$) 204

Figure 14: ^{1}H NMR Spectrum of **94b** (400MHz, $CDCl_3$) 205

Figure 15: ^{13}C NMR Spectrum of **94c** (100MHz, $CDCl_3$) 206

Figure 16: ^{1}H NMR Spectrum of **94d** (400MHz, $CDCl_3$) 207

Figure 17: ^{13}C NMR Spectrum of **94d** (100MHz, $CDCl_3$) 208

Figure 18: ^{1}H NMR Spectrum of **94e** (400MHz, $CDCl_3$)..... 209

Figure 19: ^{13}C NMR Spectrum of **94e** (100MHz, $CDCl_3$)..... 210

Figure 20: ^{1}H NMR Spectrum of **94f** (400MHz, $CDCl_3$) 211

Figure 21: ^{13}C NMR Spectrum of **94f** (100MHz, $CDCl_3$) 212

Figure 22: ^{1}H NMR Spectrum of **94g** (400MHz, $CDCl_3$)..... 213

Figure 23: ^{13}C NMR Spectrum of **94g** (100MHz, $CDCl_3$) 214

Figure 24: ^{1}H NMR Spectrum of **94h** (400MHz, $CDCl_3$) 215

Figure 25: ^{13}C NMR Spectrum of **94h** (100MHz, $CDCl_3$) 216

Figure 26: ^{1}H NMR Spectrum of **91** (500MHz, $CDCl_3$)..... 217

Figure 27: ^{13}C NMR Spectrum of **91** (100MHz, $CDCl_3$) 218

Figure 28: ^{1}H NMR Spectrum of **91b** (500MHz, $CDCl_3$) 219

Figure 29: ^{13}C NMR Spectrum of **91b** (100MHz, $CDCl_3$) 220

Figure 30: ^{1}H NMR Spectrum of **92** (500MHz, $CDCl_3$)..... 221

Figure 31: ^{13}C NMR Spectrum of **92** (100MHz, $CDCl_3$) 222

Figure 32: ^{1}H NMR Spectrum of **92b** (500MHz, $CDCl_3$) 223

Figure 33: ^{13}C NMR Spectrum of **92b** (100MHz, $CDCl_3$) 224

Figure 34: ^{1}H NMR Spectrum of **95a** (500MHz, $CDCl_3$)..... 225

Figure 35: ^{13}C NMR Spectrum of **95a** (100MHz, $CDCl_3$) 226

Figure 36: ^{1}H NMR Spectrum of **95b** (500MHz, $CDCl_3$) 227

Figure 37: ^{13}C NMR Spectrum of **95b** (100MHz, $CDCl_3$) 228

Figure 38: ^{1}H NMR Spectrum of **95c** (400MHz, $CDCl_3$)..... 229

Figure 39: ^{13}C NMR Spectrum of **95c** (100MHz, $CDCl_3$)..... 230

Figure 40: ^{1}H NMR Spectrum of **95d** (400MHz, $CDCl_3$) 231

Figure 41: ^{13}C NMR Spectrum of **95d** (100MHz, $CDCl_3$) 232

Figure 42: ^{1}H NMR Spectrum of **95e** (400MHz, $CDCl_3$)..... 233

Figure 43: ^{13}C NMR Spectrum of **95e** (100MHz, $CDCl_3$)..... 234

Figure 44: ^{1}H NMR Spectrum of **95f** (400MHz, $CDCl_3$) 235

Figure 45: ^{13}C NMR Spectrum of **95f** (100MHz, $CDCl_3$) 236

Figure 46: ^{1}H NMR Spectrum of **95g** (400MHz, $CDCl_3$)..... 237

Figure 47: ^{13}C NMR Spectrum of **95g** (100MHz, $CDCl_3$) 238

Figure 48: ^{1}H NMR Spectrum of **95h** (400MHz, $CDCl_3$) 239

Figure 49: ^{13}C NMR Spectrum of **95h** (100MHz, $CDCl_3$) 240

Figure 50: ^{1}H NMR Spectrum of **95i** (400MHz, $CDCl_3$) 241

Figure 51: ^{13}C NMR Spectrum of **95i** (100MHz, $CDCl_3$) 242

Figure 52: ^{1}H NMR Spectrum of **95j** (400MHz, $CDCl_3$) 243

Figure 53: ^{13}C NMR Spectrum of **95j** (100MHz, $CDCl_3$) 244

Figure 54: ^{1}H NMR Spectrum of **95k** (400MHz, $CDCl_3$) 245

Figure 55: ^{13}C NMR Spectrum of **95k** (100MHz, $CDCl_3$) 246

Figure 56: ^{1}H NMR Spectrum of **95l** (400MHz, $CDCl_3$) 247

Figure 57: ^{13}C NMR Spectrum of **95l** (100MHz, $CDCl_3$) 248

Figure 58: ^{1}H NMR Spectrum of **95m** (400MHz, $CDCl_3$) 249

Figure 59: ^{13}C NMR Spectrum of **95m** (100MHz, $CDCl_3$) 250

Figure 60: ^{1}H NMR Spectrum of **95n** (400MHz, $CDCl_3$) 251

Figure 61: ^{13}C NMR Spectrum of **95n** (100MHz, $CDCl_3$) 252

Figure 62: ^{1}H NMR Spectrum of **95o** (400MHz, $CDCl_3$) 253

Figure 63: ^{13}C NMR Spectrum of **95o** (100MHz, $CDCl_3$) 254

Figure 64: ^{1}H NMR Spectrum of **95p** (400MHz, $CDCl_3$) 255

Figure 65: ^{13}C NMR Spectrum of **95p** (100MHz, $CDCl_3$) 256

Figure 66: ^{1}H NMR Spectrum of **93** (500MHz, $CDCl_3$) 257

Figure 67: ^{13}C NMR Spectrum of **93** (100MHz, $CDCl_3$) 258

Figure 68: ^{1}H NMR Spectrum of **93b** (500MHz, $CDCl_3$) 259

Figure 69: ^{13}C NMR Spectrum of **93b** (100MHz, $CDCl_3$) 260

Figure 70: ^{1}H NMR Spectrum of **93c** (500MHz, $CDCl_3$) 261

Figure 71: ^{13}C NMR Spectrum of **93c** (100MHz, $CDCl_3$) 262

Figure 72: ^{1}H NMR Spectrum of **97a** (500MHz, $CDCl_3$) 263

Figure 73: ^{13}C NMR Spectrum of **97a** (100MHz, $CDCl_3$) 264

Figure 74: ^{1}H NMR Spectrum of **97b** (500MHz, $CDCl_3$) 265

Figure 75: ^{13}C NMR Spectrum of **97b** (100MHz, $CDCl_3$) 266

Figure 76: ^{1}H NMR Spectrum of **97c** (500MHz, $CDCl_3$) 267

Figure 77: ^{13}C NMR Spectrum of **97c** (100MHz, $CDCl_3$) 268

Figure 78: ^{1}H NMR Spectrum of **97d** (500MHz, $CDCl_3$) 269

Figure 79: ^{13}C NMR Spectrum of **97d** (100MHz, $CDCl_3$) 270

Figure 80: ^{1}H NMR Spectrum of **97e** (500MHz, $CDCl_3$)..... 271

Figure 81: ^{13}C NMR Spectrum of **97e** (100MHz, $CDCl_3$)..... 272

Figure 82: ^{1}H NMR Spectrum of **97f** (500MHz, $CDCl_3$) 273

Figure 83: ^{13}C NMR Spectrum of **97f** (100MHz, $CDCl_3$) 274

Figure 84: ^{1}H NMR Spectrum of **97g** (500MHz, $CDCl_3$)..... 275

Figure 85: ^{13}C NMR Spectrum of **97g** (100MHz, $CDCl_3$) 276

Figure 86: ^{1}H NMR Spectrum of **97h** (500MHz, $CDCl_3$) 277

Figure 87: ^{13}C NMR Spectrum of **97h** (100MHz, $CDCl_3$) 278

Figure 88: ^{1}H NMR Spectrum of **97i** (400MHz, $CDCl_3$) 279

Figure 89: ^{13}C NMR Spectrum of **97i** (100MHz, $CDCl_3$) 280

Figure 90: ^{1}H NMR Spectrum of **97j** (500MHz, $CDCl_3$) 281

Figure 91: ^{13}C NMR Spectrum of **97j** (100MHz, $CDCl_3$) 282

Figure 92: ^{1}H NMR Spectrum of **97k** (400MHz, $CDCl_3$) 283

Figure 93: ^{13}C NMR Spectrum of **97k** (100MHz, $CDCl_3$) 284

Figure 94: ^{1}H NMR Spectrum of **97l** (400MHz, $CDCl_3$) 285

Figure 95: ^{13}C NMR Spectrum of **97l** (100MHz, $CDCl_3$) 286

Figure 96: ^{1}H NMR Spectrum of **97m** (400MHz, $CDCl_3$) 287

Figure 97: ^{13}C NMR Spectrum of **97m** (100MHz, $CDCl_3$) 288

Figure 98: ^{1}H NMR Spectrum of **97n** (400MHz, $CDCl_3$) 289

Figure 99: ^{13}C NMR Spectrum of **97n** (100MHz, $CDCl_3$) 290

Figure 100: ^{1}H NMR Spectrum of **97o** (400MHz, $CDCl_3$)..... 291

Figure 101: ^{13}C NMR Spectrum of **97o** (100MHz, $CDCl_3$) 292

Figure 102: ^{1}H NMR Spectrum of **97p** (400MHz, $CDCl_3$) 293

Figure 103: ^{13}C NMR Spectrum of **97p** (100MHz, $CDCl_3$) 294

Figure 104: ^{1}H NMR Spectrum of **103** (500MHz, $CDCl_3$)..... 295

Figure 105: ^{13}C NMR Spectrum of **103** (100MHz, $CDCl_3$) 296

Figure 106: ^{1}H NMR Spectrum of **104** (400MHz, $CDCl_3$)..... 297

Figure 107: ^{13}C NMR Spectrum of **104** (100MHz, $CDCl_3$) 298

Figure 108: ^{1}H NMR Spectrum of **101a** (500MHz, $CDCl_3$)..... 299

Figure 109: ^{1}H NMR Spectrum of **101b** (500MHz, $CDCl_3$) 300

Figure 110: ^{1}H NMR Spectrum of **101c** (500MHz, $CDCl_3$)..... 301

Figure 111: ^{1}H NMR Spectrum of **101d** (400MHz, $CDCl_3$) 302

Figure 112: ^{13}C NMR Spectrum of **101d** (100MHz, $CDCl_3$) 303

Figure 113: ^{1}H NMR Spectrum of **101e** (400MHz, $CDCl_3$)..... 304

Figure 114: ^{13}C NMR Spectrum of **101e** (100MHz, $CDCl_3$)..... 305

Figure 115: ^{1}H NMR Spectrum of **101f** (400MHz, $CDCl_3$) 306

Figure 116: ^{13}C NMR Spectrum of **101f** (100MHz, $CDCl_3$) 307

Figure 117: ^{1}H NMR Spectrum of **101g** (400MHz, $CDCl_3$)..... 308

Figure 118: ^{13}C NMR Spectrum of **101g** (100MHz, $CDCl_3$) 309

Figure 119: ^{1}H NMR Spectrum of **101h** (400MHz, $CDCl_3$) 310

Figure 120: ^{13}C NMR Spectrum of **101h** (100MHz, $CDCl_3$) 311

Figure 121: ^{1}H NMR Spectrum of **101j** (400MHz, $CDCl_3$) 312

Figure 122: ^{13}C NMR Spectrum of **101j** (100MHz, $CDCl_3$) 313

Figure 123: ^{1}H NMR Spectrum of **110** (500MHz, $CDCl_3$)..... 314

Figure 124: ^{1}H NMR Spectrum of **111** (500MHz, $CDCl_3$)..... 315

Figure 125: ^{1}H NMR Spectrum of **112** (500MHz, $CDCl_3$)..... 316

Figure 126: ^{1}H NMR Spectrum of **108** (400MHz, $CDCl_3$)..... 317

Figure 127: ^{13}C NMR Spectrum of **108** (100MHz, $CDCl_3$) 318

Figure 128: ^{1}H NMR Spectrum of **106** (500MHz, $CDCl_3$)..... 319

Figure 129: ^{1}H NMR Spectrum of **117** (500MHz, $CDCl_3$)..... 320

Figure 130: ^{13}C NMR Spectrum of **117** (100MHz, $CDCl_3$) 321

Figure 131: ^{1}H NMR Spectrum of **118a** (400MHz, $CDCl_3$)..... 322

Figure 132: ^{13}C NMR Spectrum of **118a** (100MHz, $CDCl_3$) 323

Figure 133: 1H NMR Spectrum of **118b** (400MHz, CDCl3) 324

Figure 134: ^{13}C NMR Spectrum of **118b** (100MHz, $CDCl_3$) 325

Figure 135: ^{1}H NMR Spectrum of **122** (400MHz, $CDCl_3$)..... 326

Figure 136: ^{13}C NMR Spectrum of **122** (100MHz, CDCl3)..... 327

Figure 137: ^{1}H NMR Spectrum of **115b** (500MHz, $CDCl_3$) 328

Figure 138: ^{1}H NMR Spectrum of **115c** (400MHz, $CDCl_3$)..... 329

Figure 139: ^{1}H NMR Spectrum of **115d** (500MHz, $CDCl_3$) 330

Figure 140: ^{1}H NMR Spectrum of **115e** (500MHz, $CDCl_3$)..... 331

Figure 141: ^{1}H NMR Spectrum of **115f** (500MHz, $CDCl_3$) 332

Figure 142: ^{1}H NMR Spectrum of **176** (400MHz, $CDCl_3$)..... 333

Figure 143: ^{13}C NMR Spectrum of **176** (100MHz, $CDCl_3$) 334

Figure 144: ^{1}H NMR Spectrum of **180** (400MHz, $CDCl_3$)..... 335

Figure 145: ^{13}C NMR Spectrum of **180** (100MHz, $CDCl_3$) 336

Figure 146: ^{1}H NMR Spectrum of **181** (400MHz, $CDCl_3$)..... 337

Figure 147: ^{13}C NMR Spectrum of **181** (100MHz, $CDCl_3$) 338

Figure 148: ^{1}H NMR Spectrum of **182** (400MHz, $CDCl_3$)..... 339

Figure 149: ^{13}C NMR Spectrum of **182** (100MHz, $CDCl_3$) 340

Figure 150: ^{1}H NMR Spectrum of **183** (400MHz, $CDCl_3$)..... 341

Figure 151: ^{13}C NMR Spectrum of **183** (100MHz, $CDCl_3$) 342

Figure 152: ^{1}H NMR Spectrum of **185** (400MHz, $CDCl_3$)..... 343

Figure 153: ^{13}C NMR Spectrum of **185** (100MHz, $CDCl_3$) 344

Figure 154: ^{1}H NMR Spectrum of **185b** (400MHz, $CDCl_3$) 345

Figure 155: ^{1}H NMR Spectrum of **186** (500MHz, $CDCl_3$)..... 346

Figure 156: ^{13}C NMR Spectrum of **186** (100MHz, $CDCl_3$) 347

Figure 157: ^{1}H NMR Spectrum of **187** (500MHz, $CDCl_3$)..... 348

Figure 158: ^{13}C NMR Spectrum of **187** (100MHz, $CDCl_3$) 349

Figure 159: 1H NMR Spectrum of **188** (500MHz, $CDCl_3$)..... 350

Figure 160: ^{13}C NMR Spectrum of **188** (100MHz, $CDCl_3$) 351

Figure 161: ^{1}H NMR Spectrum of **190** (500MHz, $CDCl_3$)..... 352

Figure 162: ^{1}H NMR Spectrum of **191** (500MHz, $CDCl_3$)..... 353

Figure 163: ^{1}H NMR Spectrum of **199** (500MHz, $CDCl_3$)..... 354

Figure 164: ^{1}H NMR Spectrum of **193** (400MHz, $CDCl_3$)..... 355

Figure 165: ^{13}C NMR Spectrum of **193** (100MHz, $CDCl_3$) 356

Figure 166: ^{1}H NMR Spectrum of **189a** (500MHz, $CDCl_3$)..... 357

Figure 167: ^{1}H NMR Spectrum of **189b** (500MHz, $CDCl_3$) 358

Figure 168: ^{1}H NMR Spectrum of **189c** (500MHz, $CDCl_3$)..... 359

Figure 169: ^{1}H NMR Spectrum of **189d** (400MHz, $CDCl_3$) 360

Figure 170: ^{13}C NMR Spectrum of **189d** (100MHz, $CDCl_3$) 361

Figure 171: ^{1}H NMR Spectrum of **194** (400MHz, $CDCl_3$)..... 362

Figure 172: ^{13}C NMR Spectrum of **194** (100MHz, $CDCl_3$) 363

Figure 173: ^{1}H NMR Spectrum of **195** (400MHz, $CDCl_3$)..... 364

Figure 174: ^{13}C NMR Spectrum of **195** (100MHz, $CDCl_3$) 365

Figure 175: ^{1}H NMR Spectrum of **175b** (400MHz, $CDCl_3$) 366

Figure 176: ^{13}C NMR Spectrum of **175b** (100MHz, $CDCl_3$) 367

Figure 177: ^{1}H NMR Spectrum of **175** (400MHz, $CDCl_3$)..... 368

Figure 178: ^{13}C NMR Spectrum of **175** (100MHz, $CDCl_3$) 369

Figure 179: ^{1}H NMR Spectrum of **171** (400MHz, $CDCl_3$)..... 370

Figure 180: ^{13}C NMR Spectrum of **171** (100MHz, $CDCl_3$) 371

Figure 181: ^{1}H NMR Spectrum of **170** (400MHz, $CDCl_3$)..... 372

Figure 182: ^{13}C NMR Spectrum of **171** (100MHz, $CDCl_3$) 373

Figure 183: ^{1}H NMR Spectrum of **197** (400MHz, $CDCl_3$)..... 374

Figure 184: ^{13}C NMR Spectrum of **197** (100MHz, $CDCl_3$) 375

Figure 185: ^{1}H NMR Spectrum of **92c** (400MHz, $CDCl_3$)..... 376

Figure 186: ^{13}C NMR Spectrum of **92c** (100MHz, $CDCl_3$)..... 377

Figure 187: ^{1}H NMR Spectrum of **204** (400MHz, $CDCl_3$)..... 378

Figure 188: ^{13}C NMR Spectrum of **204** (100MHz, $CDCl_3$) 379

Figure 189: ^{1}H NMR Spectrum of **208** (400MHz, $CDCl_3$)..... 380

Figure 190: ^{13}C NMR Spectrum of **208** (100MHz, $CDCl_3$) 381

Figure 191: ^{1}H NMR Spectrum of **205** (400MHz, $CDCl_3$)..... 382

Figure 192: ^{13}C NMR Spectrum of **205** (100MHz, $CDCl_3$) 383

Figure 193: ^{1}H NMR Spectrum of **211** (400MHz, $CDCl_3$)..... 384

Figure 194: ^{13}C NMR Spectrum of **211** (100MHz, $CDCl_3$) 385

Figure 195: ^{1}H NMR Spectrum of **207** (400MHz, $CDCl_3$)..... 386

Figure 196: ^{13}C NMR Spectrum of **207** (100MHz, $CDCl_3$) 387

Figure 197: ^{1}H NMR Spectrum of **206** (400MHz, $CDCl_3$)..... 388

Figure 198: ^{13}C NMR Spectrum of **206** (100MHz, $CDCl_3$) 389

Figure 199: ^{1}H NMR Spectrum of **92d** (400MHz, $CDCl_3$) 390

Figure 200: ^{13}C NMR Spectrum of **92d** (100MHz, $CDCl_3$) 391

Figure 201: ^{1}H NMR Spectrum of **228** (400MHz, $CDCl_3$)..... 392

Figure 202: ^{13}C NMR Spectrum of **228** (100MHz, $CDCl_3$) 393

Figure 203: ^{1}H NMR Spectrum of **234a** (400MHz, $CDCl_3$)..... 394

Figure 204: ^{13}C NMR Spectrum of **234a** (100MHz, $CDCl_3$) 395

Figure 205: ^{1}H NMR Spectrum of **234b** (400MHz, $CDCl_3$) 396

Figure 206: ^{13}C NMR Spectrum of **234b** (100MHz, $CDCl_3$) 397

Figure 207: ^{1}H NMR Spectrum of **234c** (400MHz, $CDCl_3$)..... 398

Figure 208: ^{13}C NMR Spectrum of **234c** (100MHz, $CDCl_3$)..... 399

Figure 209: ^{1}H NMR Spectrum of **234d** (400MHz, $CDCl_3$) 400

Figure 210: ^{13}C NMR Spectrum of **234d** (100MHz, $CDCl_3$) 401

Figure 211: ^{1}H NMR Spectrum of **234e** (400MHz, $CDCl_3$)..... 402

Figure 212: ^{13}C NMR Spectrum of **234e** (100MHz, $CDCl_3$)..... 403

Figure 213: ^{1}H NMR Spectrum of **234f** (400MHz, $CDCl_3$) 404

Figure 214: ^{13}C NMR Spectrum of **234f** (100MHz, $CDCl_3$) 405

Figure 215: ^{1}H NMR Spectrum of **234g**(400MHz, $CDCl_3$)..... 406

Figure 216: ^{13}C NMR Spectrum of **234g** (100MHz, $CDCl_3$) 407

Figure 217: ^{1}H NMR Spectrum of **234h**(400MHz, $CDCl_3$) 408

Figure 218: ^{13}C NMR Spectrum of **234h** (100MHz, $CDCl_3$) 409

Figure 219: ^{1}H NMR Spectrum of **241**(400MHz, $CDCl_3$)..... 410

Figure 220: ^{13}C NMR Spectrum of **241** (100MHz, $CDCl_3$) 411

Figure 221: ^{1}H NMR Spectrum of **243 (**400MHz, $CDCl_3$)..... 412

Figure 222: ^{13}C NMR Spectrum of **243** (100MHz, $CDCl_3$) 413

Figure 223: ^{1}H NMR Spectrum of **244 (**400MHz, $CDCl_3$)..... 414

Figure 224: ^{13}C NMR Spectrum of **244** (100MHz, $CDCl_3$) 415

Figure 225: ^{1}H NMR Spectrum of **IDPi-a** (500MHz, $CDCl_3$) 416

Figure 226: ^{1}H NMR Spectrum of **IDPi-b** (500MHz, CD_2Cl_2)..... 417

Figure 227: ^{1}H NMR Spectrum of **DPi-b** (202 MHz, CD_2Cl_2) 418

Figure 228: ^{1}H NMR Spectrum of **IDPi-c** (500MHz, $CDCl_3$) 419

Figure 229: ^{1}H NMR Spectrum of **IDPi-d** (400MHz, $CDCl_3$)..... 420

Figure 230: ^{31}P NMR Spectrum of **IDPi-d** (202MHz, $CDCl_3$) 421

LIST OF ABBREVIATIONS

Ac	acetyl
AIBN	2,2’-azobis(2-methylpropionitrile)
BNDHP	1,1′-Binaphthyl-2,2′-diyl hydrogenphosphate
Bn	benzyl
Boc	*tert*-butoxylcarbonyl
brsm	based on recovered starting material
Bu	butyl
CSA	camphorsulfonic acid
COSY	correlation spectroscopy
DBH	1,3-dibromo-5,5-dimethylhydantoin
DBU	1,8-diazabicyclo[5.4.0]undec-7-ene
DCE	dichloroethane
DCC	dicyclohexylcarbodiimide
DCM	dichloromethane
DCE	dichloroethane
DDQ	2,3-dichloro-5,6-dicyano-1,4-benzoquinone

decalin	decahydronaphthalene
DIBAL-H	diisobutylaluminum hydride
DIPEA	*N*,*N*-diisopropylethylamine
DMAP	4-(dimethylamino)pyridine
DMDO	dimethyldioxirane
DME	1,2-dimethoxyethane
DMF	*N*,*N*-dimethylformamide
DMP	Dess–Martin periodinane
DMSO	dimethylsulfoxide
dr	diastereomeric ratio
DTBP	2,6-di-*tert*-butylpyridine
ee	enantiomeric excess
Et	ethyl
GC	gas chromatography
h	hours
HRMS	high resolution mass spectrometry
HPLC	high performance liquid chromatography
Hz	Hertz

IDPi	imidodiphosphorimidate
IBX	2-iodoxybenzoic acid
IR	infrared
KHMDS	potassium bis(trimethylsilyl)amide
LDA	lithium diisopropylamide
LiHMDS	lithium bis(trimethylsilyl)amide
L-Selectride	lithium tri-*sec*-butylborohydride
m-CPBA	3-chloroperbenzoic acid
Me	methyl
Ms	methanesulfonyl
MTBE	methyl tertbutyl ether
NBS	*N*-bromosuccinimide
NCS	*N*-chlorosuccinimide
NMR	nuclear magnetic resonance
NOESY	nuclear Overhauser effect spectroscopy
OTf	trifluoromethanesulfonate
PDC	pyridinium dichromate
Ph	phenyl

PhH	benzene
phen	phenanthroline
PhMe	toluene
PPTS	pyridinium *p*-toluenesulfonate
Pr	propyl
PTSA	*p*-toluenesulfonic acid
Pyr	pyridine
R_f	retention factor
r.t.	room temperature
TBCO	2,4,4,6-tetrabromo-2,5-cyclohexadienone
TBHP	*tert*-butyl hydroperoxide
TBS	*tert*-butyldimethylsilyl
TBSOTf	*tert*-butyldimethylsilyltrifluoromethanesulfonate
TCA	trichloroacetic acid
TCDI	1,1'-thiocarbonyldiimidazole
TES	triethylsilyl
Tf	trifluoromethanesulfonyl
TFA	trifluoroacetic acid

TFE	2,2,2-trifluoroethanol
TFEF	2,2,2-trifluoroethyl formate
THF	tetrahydrofuran
TIPS	triisopropylsilyl
TLC	thin layer chromatography
TMS	tetramethylsilane
TMSOTf	trimethylsilyl trifluoromethanesulfonate
TBAF	tetrabutylammonium fluoride
Ts	*p*-toluenesulfonyl

Acknowledgements

First and foremost, I must thank Professor Viresh Rawal for all of his patience and support over the past five years. His baffling memory of the chemical literature has been a source of envy, bewilderment, and respect, not only is his knowledge about organic chemistry arresting but also inspiring. I appreciate his patience for my shenanigans and disorganized manner. I can say his understanding and open nature were instrumental in his mentorship and I deeply thank him for it. His soft and encouraging nature shine through in his discussion which have been dubbed as "soul-saving" talks by past group members, and I understand how they came to be known as such. During the most difficult parts of my projects he remained confident in my abilities. It's been a privilege to have learned from him.

I am very grateful to Professor Guangbin Dong and Professor Scott Snyder for their willingness to serve on my dissertation committee, for all their insightful comments, suggestions about my synthesis, and most importantly their time.

During my graduate years at Chicago, I crossed paths with many great chemists. I would like to thank Dr. Chintan Sumaria, Dr. Thomas Montgomery, Johnathan Keim, and Dr. Lan Luo for existing, providing excellent conversations and gossip and being generally pleasant people to be around. I owe special thanks to Dr. Jiasu Xu, Dr. Michael Rombola, Dr. Pavel Elkin (DrDJPDPPPEPE), and Dr. Julius Reyes for teaching me everything about working on a total synthesis, for their help, and mentoring me during my graduate years. If that weren't enough, they've made the long days brighter through good banter and much needed coffee runs. Your friendship is precious to me. Dr. Jiasu Xu was my mentor in lab, his ideas and approaches were an inspiration and I owe him for laying the groundwork for my first successful project. Dr. Michael

Rombola and I have had very good conversations outside of chemistry and I can count on him in the event of total economic collapse. Dr. Pavel Elkin is a good friend, who got me into martial arts and has helped learn the ropes of lab management, ordering, pump repair, etc. Every technical aspect of keeping lab work going, I learned from him. Julius I only knew for a brief time, but even so I appreciate his help and guidance.

Kyle Cassaidy has been a good friend over the last three years, he's had great input on my thesis, both in editing and in aid to my various projects. Thank you! I couldn't have asked for a better friend in lab than you. I will remember our coffee runs, our various conversions, and the projects we've worked on. Additionally, thank you for correcting my typo ~~leadened~~ ladled; thesis. I doubt I could have ever finished it otherwise.

The Rawal lab has been a less populated place than it was when I joined, but even so the comradery is excellent. The reason for that is simple good people, and so I would like to also thank Lingbowei Hu and Nathanial Durfee who have both been good friends over the last 4 and 3 years respectively and I'm happy to have known them during my graduate years. Lastly, Sudhakar has only been with us for a short while, but I'm happy to know him for his good spirit and personal encouragement. His work on the ambiguine synthesis has already helped, and I'm sure he can continue my work and carry it further than I ever could.

In the Department of Chemistry, I would like to thank Melinda Moore, Dr. Vera Dragisich, Mike Reedy, and Laura Luburich. Dr. Valerie Keller has known me for too long, and her patience for my grading practices along with her kindness and help is very much appreciated. Special thanks to Dr. Antoni Jurkiewicz and Dr. Josh Kurtz for their tireless efforts in maintaining our NMR facilities, Dr. Alexander Filatov for his help in solving X-ray crystallographic structures, and Dr. Jin Qin for his assistance in mass spectroscopy.

Most importantly, I would like to thank my family and close friends. I keep few close relationships, but at least so many I need two hands to count them all. The support I have had from those I hold dear is instrumental in my life and the respect, love, and appreciation I have for them cannot be overstated. My parents have kept me honest for my entire life and always supported and encouraged me in times of trouble. I've always looked to them for advice in life and work, and I love them dearly. My brother, Phil, I know we're an odd set of siblings with an odder history, but I'm proud of you and love you all the same.

I must thank my closest friend Miles, who I've known and relied on for the best part of twenty years. I treasure your friendship and I can say confidently that I wouldn't have made it to this point without you. Trevor, David, Matt, and you are terrific friends, and I think we'll continue to support one another for many years to come. Lastly, I must thank Jo, whose unwavering love and support has been key to my happiness these past two years; thank you.

– April 29, 2021 –

Abstract

Cycloadditions have long been held as the premier for economical constructions in organic synthesis, the use of which has led to the completion of innumerable total syntheses and methodologies. Towards this end, the Rawal group has a long-standing interest in cycloaddition methodologies and applications in total synthesis. This thesis details the exploration of a novel approach to cyclohepta[b] indoles via a [4+3] cycloaddition reaction of 3-alkenyl indoles and stabilized oxyallyl cations. The transformation was explored fully, and a catalytic, enantioselective approach via highly acidic imidodiphosphorimidates (IDPi) was discovered and used to showcase a general enantioselective [4+3] cycloaddition reaction of stabilized oxyallyl cations. Finally, a novel approach towards the ambiguine alkaloids has been explored, and significant progress towards amibiguine Q has been made. Additionally, through the use of our novel [4+3] cycloaddition methodology, a generalizable route towards pentacyclic ambiguines has been achieved.

Chapter 1: Oxyallyl Cations: Development, Application, and Asymmetric Transformations

First observed by Fort as an intermolecular trapping of a Favorskii intermediate by furan, the [4+3] cycloaddition between an oxyallyl species and a diene has found widespread adoption analogous to the Diels-Alder reaction.[1,2] The ease of access and diversity of oxyallyl precursors has allowed for extensive exploration of the chemical space and has facilitated the total synthesis of many complex molecules featuring the cycloheptane motif. Owing to the breadth of methodology and application of the [4+3], this chapter will focus mostly on the "3" component: the oxyallyl cation. While a simple three atom component, the use and development of this relatively simple species is extensive and has served as the key linchpin in many total syntheses.

1.2 Generation/transition states

The general structure of the oxyallyl cation is that of a zwitterionic-1,3 dipole; unlike the Diels-Alder reaction, however, the transition state and precise mechanism are more complex. Similar to the Diels-Alder, the "3" component of a [4+3] cycloaddition is equivalent to the dienophile with similar LUMO energy level considerations. While the Diels-Alder reaction is generally a concerted, orbital symmetry-controlled cycloaddition with two possible transition states, endo and exo, the [4+3] has three possible conformations of the oxyallyl cation (Figure **1**): "W", "Sickle", and "U", as well as endo/exo equivalents: compact and extended, respectively. Typically, the "W" conformation is most commonly observed for acyclic dienes owing to it being

[1] Fort, A. W. *J. Am. Chem. Soc*. **1962**, *84*, 4979–4981.
[2] For general reviews: (a) P. Knochel; Molander G. A.; Mascarenas, J. Comprehensive organic synthesis II, **2014,** *5*, 595-655. (b) Hoffmann, H. M. R. *Angew. Chem., Int. Ed*. Engl. **1984**, *23*, 1−19. (c) Rigby, J. H.; Pigge, F. C. [4 + 3] Cycloaddition Reactions. In Organic Reactions; Paquette, L. A., Eds.; John Wiley and Sons: New York, **1997**, *51*, 351−478. (d) Harmata, M. Adv. Synth. Catal. **2006**, *348*, 2297−2306. (e) Harmata, M. *Chem. Commun*. **2010**, *46*, 886 −8903. (f) Harmata, M. *Chem. Commun*. **2010**, 46, 8904−8922. (f) Lohse, A. G.; Hsung, R. P. *Chem. - Eur. J*. **2011**, *17*, 3812−3822.

lowest in energy relative to the other conformations. The compact transition state leads to a di-equatorial arrangement of "R" groups on the resulting cycloadduct, whereas the extended transition state results in a di-axial substituted product. "U" transitions states tend to only be involved with cyclic oxyallyl cations. The "Sickle" conformation was previously used to justify the formation of axial/equatorial substituted products, but the alternative stepwise mechanism is more often used to explain these results.[3] DFT studies are concordant with empirical results and expectations, i.e. "W" conformer and compact transition states are preferred.[4]

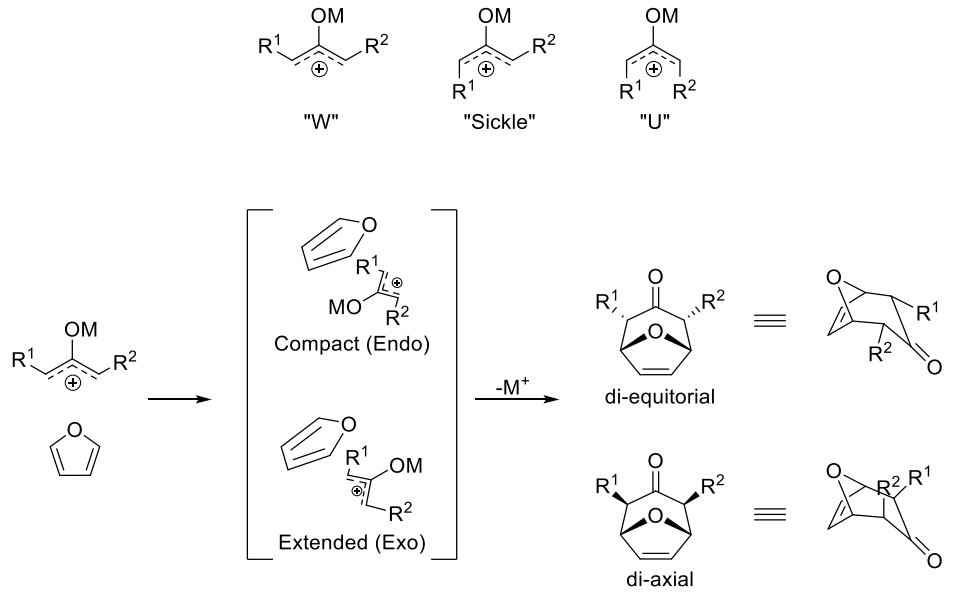

Figure 1: Transition states of oxyallyl cations

Owing to the multiple transition states, conformations, and mechanisms, more complex reaction mixtures and products are generally obtained with [4+3] cycloadditions. Unlike the Diels-Alder reaction, the [4+3] can occur asynchronously, as a nucleophilic attack by the diene onto the oxyallyl cation followed by the enolate closing onto the resulting allylic cation. Evidence for this

[3] (a) Harmata, M. *Accounts of Chemical Research* **2001**, *34*, 595-605. (b) Krenske, E. H.; Houk, K. N.; Harmata, M. *Org. Lett*. **2010**, *12*, 444–447.
[4] Amoah, A.; Tia, R.; Adei, E. *Tetrahedron.* **2020**, *76,* 131422.

stepwise mechanism is seen through to the presence of unexpected "sickle" products isolated during initial experiments by Hoffman; the R^1 and R^2 groups being axial/equatorial to one another. Alternatively, the oxyallyl cation can undergo a [3+2] cycloaddition with electron rich dienes, and subsequently rearrange to furnish the [4+3] adduct (Figure **2**).

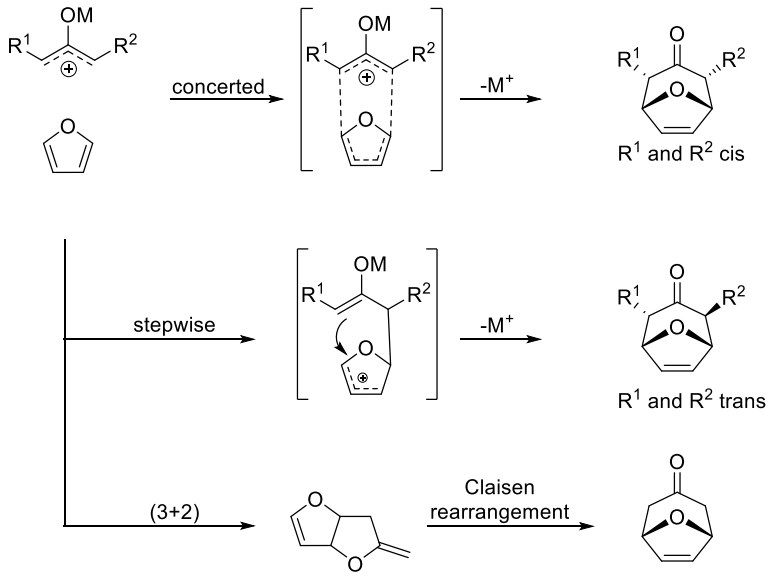

Figure 2: Reaction mechanisms of oxyallyl cations

The intermediates and stereochemical outcomes of the reaction are heavily influenced by the electronic character of the oxyallyl cation and diene; more electrophilic oxyallyl cations and more electron rich dienes typically proceed via stepwise cyclization.[5] While the reaction itself possesses many potential intermediates and reaction pathways, the overall generation of the oxyallyl species can be just as varied, with unique reactivity and selectivity. Since its discovery, the [4+3] cycloaddition has seen use in the synthesis of a variety of natural products featuring a cycloheptane core, notably the ambiguines, sesquiterpenoids, and several alkaloids.[6]

[5] Cramer, C. J.; Barrows, S. E. *J. Phys. Org. Chem*. **2000**, *13*, 176–186.
[6] Yin, Z.; He, Y.; Chiu, P. *Chem. Soc. Rev*., **2018**, *47*, 8881 —8924.

1.3 Alpha halo ketones

The most common and easily accessible precursor for generating an oxyallyl cation is the α-halo ketone, **1**. The reaction mechanism neatly parallels the Favorskii rearrangement, wherein an alpha halo ketone is deprotonated, and the resulting enolate eliminates the halide leading to the formation of an oxyallyl cation. This intermediate is not limited to the [4+3] and has found use in other dipolar cycloaddition reactions such as the [3+3] and [3+2].[7,8] Initially, the reaction suffered from low reactivity and lengthy reaction times. Improvements of the original procedure were based on increasing ionization using non-nucleophilic and cheap reagents. Lithium perchlorate, silver tetrafluoroborate, and polyfluorinated alcohol solvents like trifluoroethanol or HFIP with their corresponding alkali bases have been employed successfully.[9] Initial experiments found that the cycloaddition required, >40 equivalents of furan in order to effectively trap the transient oxyallyl cation, however with improvements to the reaction conditions, such as the use of sodium TFE in trifluoroethanol, the reaction proceeds quickly, giving predominantly the endo product **2** in high yield.

[7] (a) Cordier, M.; Archambeau, A. *Org. Lett.* **2018**, *20*, 2265−2268. (b) Hu, L.; Rombola, M.; Rawal, V. H. *Org. Lett.* **2018**, *20*, 5384-5388.
[8] Li, H.; Hughes, R. P.; Wu J.; *J. Am. Chem. Soc.* **2014**, *136*, 6288-6296.
[9] (a) Herter, R.; Föhlisch, B. *Synthesis* **1982**, *11*, 976–979. (b) Föhlisch, B.; Gehrlach, E.; Geywitz, B. *Chem. Ber*. **1987**, *120*, 1815–1824.

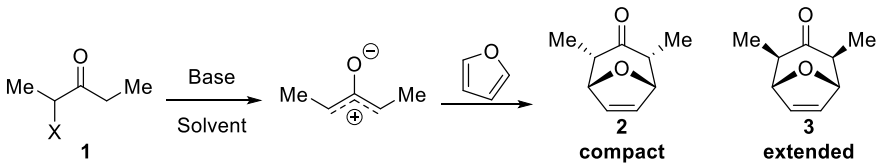

Entry	X	Base	Solvent, Time	Yield (**2**:**3**)
1	Br	Et_3N (1eq)	MeOH, 7d	40% (--)
2	Br	Et_3N (2eq)	MeOH, 3d	52% (--)
3	Cl	Et_3N (2eq)	MeOH, 77d	65% (--)
4	Br	K_2CO_3 (1eq)	MeOH, 7d	26% (--)
5	Br	NaTFE (1eq)	TFE, 1d	93% (95:5)
6	Cl	$LiClO_4/Et_3N$ (2eq)	Et_2O, 6h	78% (81:19)
7	Br	$LiClO_4/Et_3N$ (2eq)	Et_2O, 2.5h	75% (82:18)

Table 1: Cycloaddition of α-halo ketones with furan

In addition to simple mono-halo ketones, polyhalo-ketonesperform well in the generation of oxyallyl cations.[10] Di-, tri-, and tetra- halo ketones, while less accessible, offer improved reactivity for the [4+3] cycloaddition. Typically, regioselectivity and reactivity both improve under standard basic conditions over the mono-halogenated ketones. Alternatively, treatment of polyhalo-ketones with reducing metals such as zinc-copper couple, copper/sodium iodide, or iron allows for alternative metal enolates and de-halogenated products.[11,12] While the α-halo-ketones constitute simple and readily accessible precursors, α-tosyloxy-ketones, perform equally well under most conditions.

Not limited to 3 carbon units, α-bromo hydroxamates, **4**, can be used to form azaoxyallyl or azaallyl (**5**) cations[13]; which have been used in both [3+3][14] and [4+3][15] cycloaddition reactions.

[10] H. M. R. Hoffmann and J. G. Vinter, *J. Org. Chem.*, **1974**, *39*, 3921.
[11] Ashcroft, M. R.; Hoffmann, H. M. R. *Org. Synth*. **1978**, *58*, 17.
[12] Takaya, H.; Makino, S.; Hayakawa, Y.; Noyori, R. *J. Am. Chem. Soc*. **1978**, *100*, 1765–1777.
[13] (a) I. Lengyel, J.C. Sheehan *Angew. Chem. Int. Ed*. **1968**, *7*, 25 (b) Kende, A. S.; Huang, H. *Tetrahedron Lett*. **1997**, *38*, 3353–3356.
[14] R. Chen , S. Sun , G. Wang and H. Guo , *Tetrahedron Lett*., **2018**, *59* , 1916.
[15] C.S. Jeffrey, K.L. Barnes, J.A. Eickhoff, C.R. Carson *J. Am. Chem. Soc.*, **2011,** *133*, 7688.

Particularly exciting and novel is the use of the azaoxyallyl to generate the benzodiazepine skeleton **6**, a highly useful pharmaceutical framework.[16] Much like the all-carbon oxyallyl cation, the azaoxyallyl cation is most readily generated in the presence of base in a fluorinated alcoholic solvent to enhance the stability of the zwitterionic intermediate. Both heterogeneous, inorganic bases, such as carbonate salts, or homogenous amine bases work well to initiate the reaction.

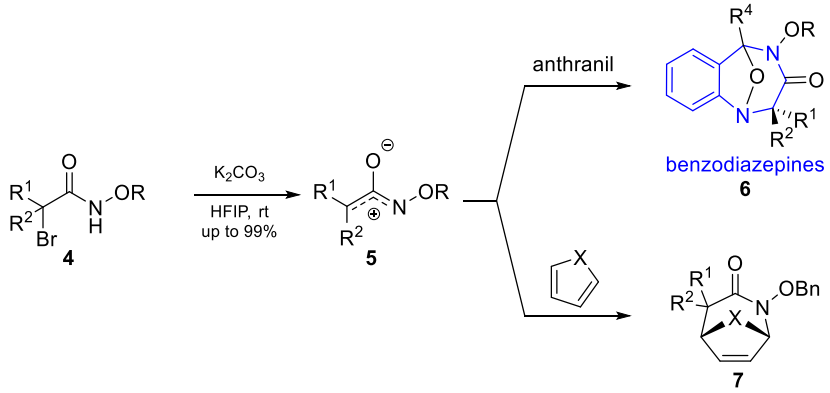

Scheme 1: Formation and reaction of azaoxyallyl cations

Typically, highly reactive dienes such as furan or cyclopentadiene are used to ensure adequate trapping of the transient oxyallyl cation. The first example of the formation of asymmetric 8-oxabicyclo[3.2.1]octene derivatives comes from Davies[17] who employed a cyclopropanation/Cope strategy using chiral auxiliaries, a formal [4+3] cycloaddition. Additionally, Lautens[18] demonstrated a true [4+3] strategy for accessing the same skeletons using enantiomerically enriched furanyl alcohols proceeding via chelation control. These initial strategies proved highly successful in delivering the cycloadducts with high selectivity. Harmata[19],

[16] Feng, J.; Zhou, M.; Lin, X.; Lu, A.; Zhang, X.; Zhao, M.; *Org. Lett*. **2019**, *21*, 6245-6248.
[17] Davies, H. M. L.; Ahmed, G.; Churchill, M. R. *J. Am. Chem. Soc.* **1996**, *118*, 10774.
[18] Lautens, M.; Aspiotis, R.; Colucci, J. *J. Am. Chem. Soc* **1996**, *118*, 10930-10931.
[19] Topinka, M.; Zawatzky, K.; Barnes, C. L.; Welch C. J.; Harmata M. *Org. Lett*. **2017**, *19*, 4106-4109.

one of the most prominent researchers in the area of [4+3] cycloadditions, reported a prolinol-catalyzed [4+3] cycloaddition delivering very high enantioselectivities and yields. Harmata employed α-tosyloxy ketone **8**, which upon treatment with prolinol **9**, in the presence of potassium phosphate allows for the formation of tetracycle **10** in up to 93% ee, however the reaction suffers from long reaction times.

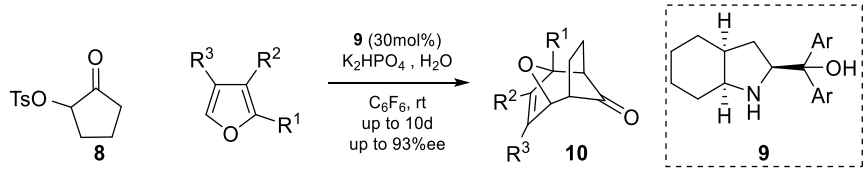

Scheme 2: Enantioselective [4+3] with prolinol catalysis

1.4 Total Synthesis of Lasidiol by Föhlisch

The sesquiterpenoid, lasidiol (**15**), was isolated from the leaves of *Lasianthae fruitocosa* (daisy) and features the carotene skeleton found in carotol and siol acetate.[20] This cis-fused 5,7-skeleton provides an excellent target for a [4+3] cycloaddition approach (Scheme **3**). Föhlish and Kreiselmeier envisioned an intramolecular cycloaddition through the use of an α-dibromo ketone **13**. The synthesis is remarkably concise, with the installation of the key alpha halo ketone in only seven steps. Conversion of alcohol **12** to the corresponding bromide should have enabled an enolate displacement with ethyl propionate which would have curtailed the synthesis by two steps; unfortunately, this transformation was unsuccessful.

[20] Kreiselmeier, G.; Föhlisch, B. *Tetrahedron Lett*. **2000**, *41*, 1375-1379.

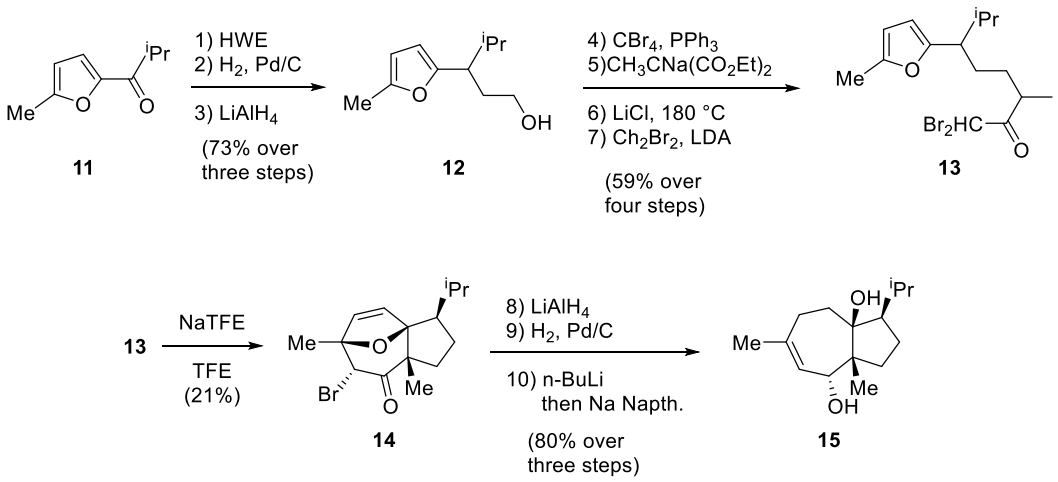

Scheme 3: Föhlisch synthesis of lasidiol

The NaTFE-promoted intramolecular [4+3] cycloaddition of **13** gave a complex mixture of products; the main complications included Favorskii rearrangement products, incorporation of TFE, and stereocontrol issues. The desired cycloadduct was isolated in only 21%, and as a result, the overall yield of the synthesis sits at only 7%. Overall, the synthesis is highly efficient and offers key insights into the complications associated with the [4+3] cycloaddition.

1.5 Alkoxy-stabilized Oxyallyl Cations

The first use of so-called stabilized oxyallyl cations, came from Föhlish[21]: α-chloro-α-alkoxy ketones, in the presence of base, generate 1-alkoxy stabilized oxyallyl cations. Subsequent developments by Albizati and Hoffman, [22,23] reported the use of silylenol acetals; **16** treated with a suitable Lewis acid generates the vinyl-oxocarbenium **17**. This modus of activation allows for highly stabilized oxy- and aza-allyl cations to participate in cycloadditions. In contrast to the alpha halo ketones, these stabilized oxyallyl cations can offer improved reactivity and increased endo

[21] Föhlisch, B.; Krimmer, D.; Gehrlach, E.; Kashammer, D. *Chem. Ber*. **1988**, *121*, 1585–1593.
[22] Murray, D. H.; Albizati, K. F. *Tet. Lett*. **1990**, *31*, 4109–4112.
[23] Pierau, S.; Hoffmann, H. M. R. *Synlett* **1999**, *2*, 213–215.

selectivity. Although there are no kinetic or DFT studies, typically the increased electrophilicity of these oxyallyl cations results in a stepwise cyclization mechanism.

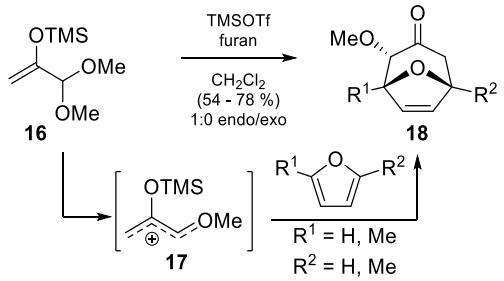

Scheme 4: [4+3] cycloaddition of stabilized oxyallyl cations

When mixed acetals, such as **19** (scheme **5**) are used, the vinyloxocarbenium can be generated by selectively eliminating the less hindered alcohol. Typically, complete abstraction of the methyl ether predominates allowing for the generation of a chiral vinyl oxocarbenium **20**. When subsequently trapping with furan, the resulting oxabicycle can be obtained with high diastereoselectivity; the first "asymmetric" [4+3] using stabilized oxyallyl cations.[24] The original benzyl ether, only delivered the cycloadduct **21** in 76% diastereoselectivity, however use of the naphthyl substituent proved to be a marked improvement, delivering the cycloadduct as a single diastereomer.

[24] Stark, C. B. W.; Pierau, S.; Wartchow, R.; Hoffmann, H. M. R. *Chem. Eur. J.* **2000**, *6*, 684–691.

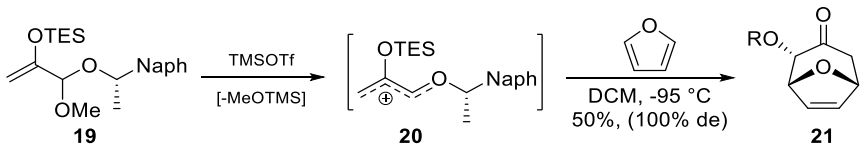

Scheme 5: Chiral Stabilized Oxyallyl Cations

The inherent stability of the intermediate oxyallyl cation can be exploited to increase the regio- and diastereoselectivity of the cycloaddition reaction. Typically, stabilized oxyallyl cations allow for lower reaction temperatures, and higher yields. Truly asymmetric, catalytic [4+3] cycloadditions, using stabilized oxyallyl cations were reported by Harmata (Scheme **6**).[25] Pentadienal **22**, was previously used in cycloadditions promoted by $SnCl_4$ in good yield and high diastereoselectivity.[26] While previous examples relied on chiral auxiliaries; the use of organocatalyst **24**, allows for the formation of chiral iminium **23** through acid catalyzed condensation. Subsequent cycloaddition and hydrolysis allows for the formation of oxabicycle **25**, in high yield and enantioselectivity.

[25] Harmata, M.; Ghosh, S. K.; Hong, X. C.; Wacharasindhu, S.; Kirchhoefer, P. *J. Am. Chem. Soc.* **2003**, *125*, 2058–2059.
[26] Ohno, M.; Mori, K.; Hattori, T.; Eguchi, S. *J. Org. Chem.* **1990**, *55*, 6086–6091.

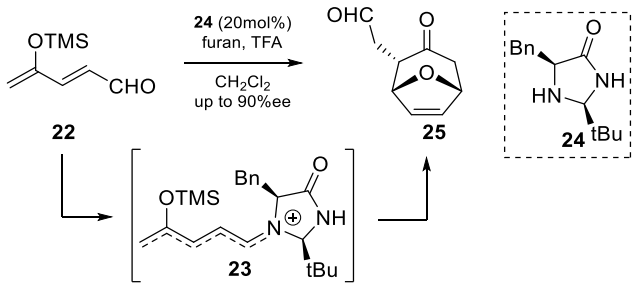

Scheme 6: Harmata's enantioselective [4+3]

These initial disclosures where pivotal in introducing asymmetry in organocatalyzed [4+3] cycloadditions with stabilized oxyallyl cations. The most recent advance in catalytic asymmetric [4+3] reactions was made by the Jacobson group using squaramide catalysis (scheme **7**).[27]

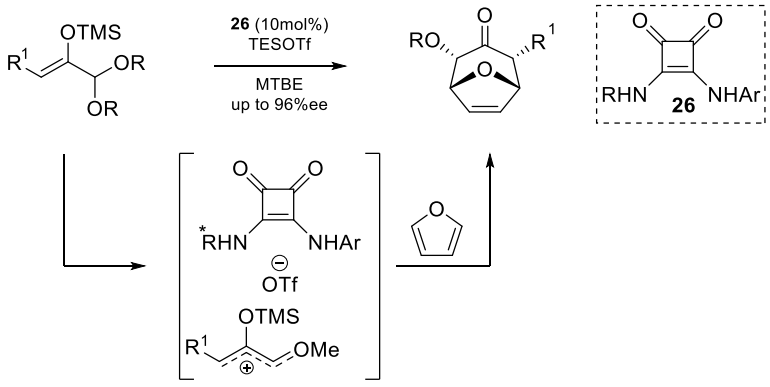

Scheme 7: Jacobson enantioselective [4+3]

A novel catalytic system composed of TESOTf and squaramides (**26)** allows for the enhancement of the Lewis acidity of the squaramide while creating an ion pair capable of inducing enantioselectivity in both acetal substitutions and cycloadditions. The reported yields and enantioselectivities are remarkable and have set the standard for future methodologies.

[27] Banik, S. M.; Levina, A.; Hyde, A. M.; Jacobsen, E. N., *Science* **2017**, *358,* 761-764.

1.6 Total Synthesis of Urechitol by Watanabe

Found in the root extract of *Pentalinon andrieuxii* and a traditional Yucatecan medicine, urechitol A has a remarkable tricyclic skeleton bearing a 6,7-fused bicycle making it the perfect framework to showcase the [4+3].[28] As originally conceived, the late stage allylation and oxygenation were unnecessary as appropriately substituted oxyallyl cation and furan fragment **29** contained the necessary handles (scheme **8** route a) to assemble a direct precursor to key intermediate **27**.

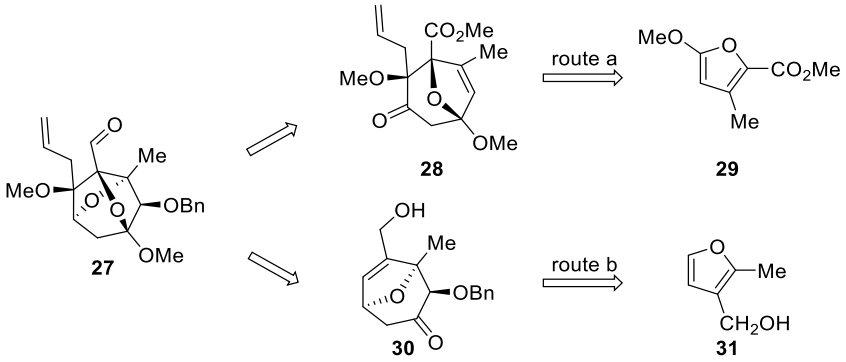

Scheme 8: Urechitol A retrosynthetic analysis for key intermediate

Unfortunately, the resulting cycloaddition gave exclusively the incorrect regio- and stereoisomers mandating a slightly more elaborate construction, route b. In the revised synthesis, the cycloaddition produced the desired cycloadduct which upon directed epoxidation gave **33** in modest yield. Subsequent treatment with acidic methanol afforded the hemiacetal, which upon protection and oxidation gave product **34** in good overall yield. The construction of the last hemiacetal proceeds in a very classic strategy; ultimately delivering urechitol A (**35**) in 2.3% overall yield over 12 steps (scheme **9**). While impressively concise, the complications arising from this approach highlight the importance of regio- and stereocontrol in these cycloaddition reactions.

[28] T. Sumiya, K. Ishigami, H. Watanabe, *Angew. Chem. Int. Ed.* **2010**, 49, 5527-5528.

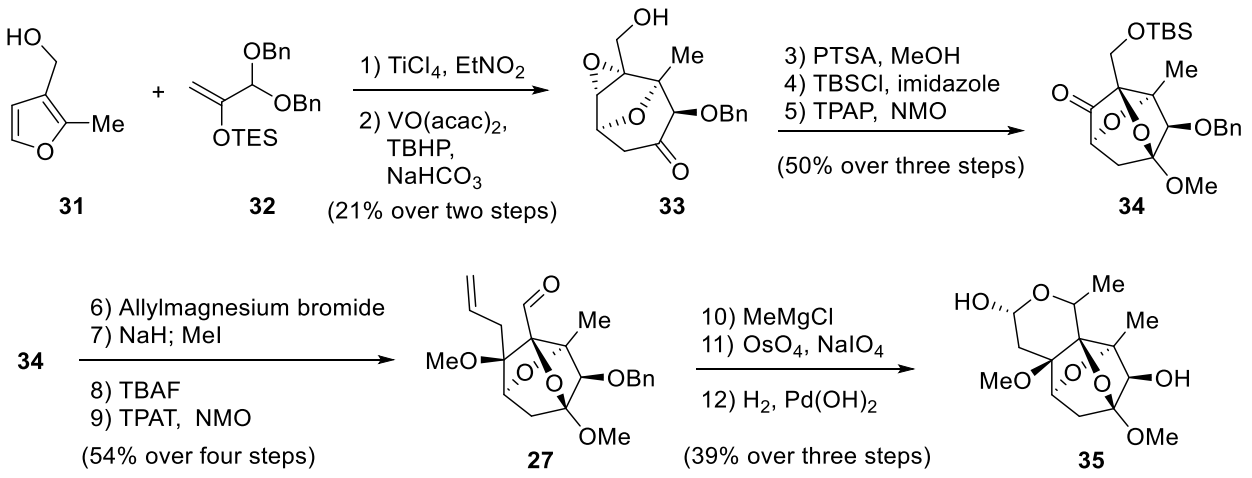

Scheme 9: Watanabe's Synthesis of (±)-Urechitol A

The use of these stabilized oxy-allyl cations is less extensive than the alpha halo ketone method, mostly due to the lack of synthetic utility of the alpha alkoxy ketone product. Even so several syntheses have featured their use and ongoing research may deliver further applications.

1.7 Benzylic Cations as Oxyallyl Equivalents

Benzo-fused cycloheptanes are a key structure in many natural products and their construction through [4+3] cycloaddition is empowering. Owing to the stability of benzylic cations the generation of the oxyallyl is facile, thus the dehydration of benzylic alcohols is often employed. While many heterocyclic alcohols have been used in this cycloaddition, in practice furans[29], benzofurans, and indoles are most successful owing to the facile access to the requisite alcohols. Work by Li[30], showed the construction of fused tricyclic skeletons through the dehydration of 3-benzylic alcohols of benzofuran and indole. The electronic consideration for the 3-benzylic cation is more similar to those of stabilized oxyallyl cations than traditional zwitterionic cations. The

[29] Winne, J. M.; Catak, S.; Waroquier, M.; Speybroeck, V. V. *Angew. Chem., Int. Ed*. **2011**, *50*, 11990.
[30] Gong, W.; Liu, Y.; Zhang, J.; Jiao, Y.; Xue, J.; Li, Y. *Chem. Asian J*. **2013**, *8*, 546-551.

cycloaddition of indole benzylic alcohols performs well, however complications owing to polymerization of the isoprene resulted in lower yields with benzofuran. Indole stabilized benzylic alcohols reacted cleanly under mildly Lewis acidic conditions, giving the cycloadduct with cyclopentadiene with high diastereoselectivity.

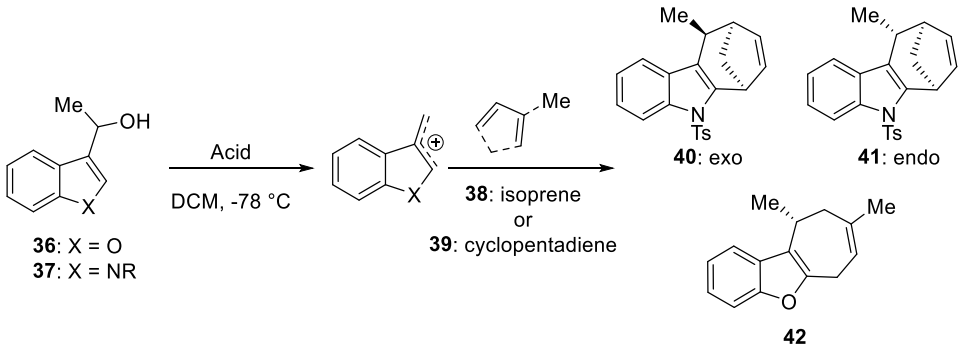

Entry	Alcohol	Diene	Acid	Yield (d.r.)
1	**37**	**39**	$ZnCl_2$[a]	92% (2:1)
2	**36**	**38**	TfOH[b]	25%
3	**36**	**38**	Tf_2O	48%
4	**37**	**39**	Tf_2O	72% (2:1)
5	**37**	**39**	TMSOTf	62% (2:1)

[a] reaction run at r.t.; [b] reaction was warmed from -78 °C to r.t.

Scheme 10: 3-benzylic alcohols as oxyallyl cations

In addition to C-3 stabilized cations, the use of indole and benzofuran C-2 benzylic alcohols has been widely investigated. Unlike the C-3 allylic cations, the C-2 benzylic cations bear more similarity to the electronics of true zwitterionic-oxyallyl cations discussed earlier. Development into the reactivity of C-2 benzylic alcohols is less extensive, however reports by Speyboreck and Zheng,[31] have detailed the use of various acids in the promotion of the generation of the oxyallyl cation and its interception with various dienes to give the cyclohepta[b]- indoles or benzofurans (Scheme **11**). The reaction is well tolerant of various heterocycles including benzofurans, indoles,

[31] Cao, K.; Bian, H.; Zheng, W. *Org. Biomol. Chem.*, **2015**, *13*, 6449.

and benzothiophenes (**43-45**) giving the desired cycloadducts **49** in excellent yields and selectivity (d.r. >20:1).

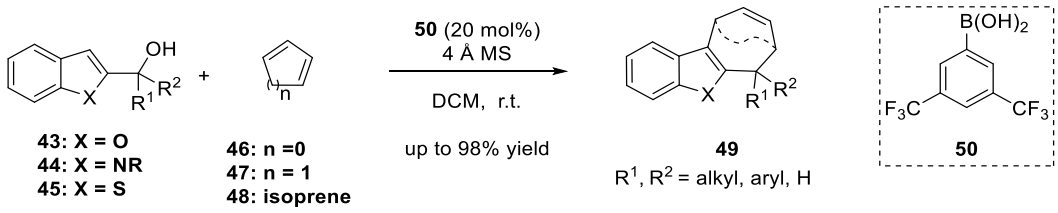

Scheme 11: Acid catalyzed [4+3] of C-2 benzylic alcohols

As the reaction can be promoted by the acid-catalyzed dehydration of benzylic alcohols, attempts were made to induce enantioselectivity by use of chiral phosphoric acids. The Masson group[32] used TRIP-phosphoric acid (**54)** in the presence of 4 Å molecular sieves to form cyclohepta[*b*] indoles in excellent yields and enantioselectivities from indole 3-benzylic alcohols **51** and various carbamate dienes **52** (scheme **12**). Overall, the reaction is extremely tolerant of electronic derivations of indole, excepting electron withdrawing substituents on the indole. While the reaction proceeds well, the yields are variable and depend heavily on the substitution of the diene. Terminal substitutions are well tolerated, but substituents at R^4 and R^5 led to a decrease in diastereoselectivity. Coordination between the carbamate diene and the phosphoryl oxygen, allows for a highly ordered transition state and explains the enantioselectivity.

[32] Gelis, C.; Levitre, G.; Merad, J.; Retailleau, P.; Neuville, L.; Masson, G. *Angew. Chem. Int. Ed.* **2018**, *57*, 12121.

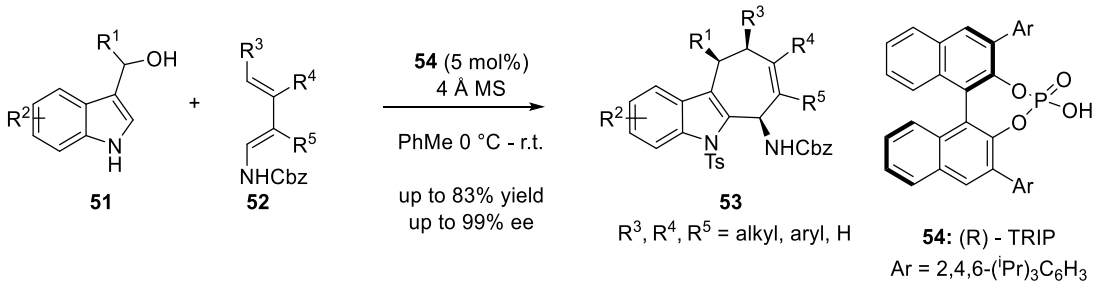

Scheme 12: Acid catalyzed [4+3] of C-2 benzylic alcohols

1.8 Total Synthesis of Frondosin B

Frondosin B (**61**), a meroterpenoid isolated from marine sponge and possessing excellent activity as an IL-8 receptor agonist, has been the target of numerous syntheses. While the target is relatively simple, the approach by Li et al.[33] utilizes the [4+3] cycloaddition to rapidly establish the tetracyclic framework. The C-2 benzylic alcohols **55** and **56** upon treatment with CSA in the presence of the requisite dienes **57** and **58** gives the desired cyclohepta[*b*] benzofurans in good yield. The generation of the oxyallyl cation uses protic conditions, as Lewis acids such as $SnCl_4$, $TiCl_4$, etc. generated homopolymers of the dienes. Protoisomerization of cycloadduct **59** and unmasking of the C5 alcohol completes the synthesis of racemic Frondosin B in four steps from commercially available material in 33% yield. Structurally similar Liphagal can be constructed in an analogous fashion; the [4+3] cycloaddition proceeds well, even with the more substituted diene **58**. Unfortunately, the hydrogenation of the cycloadduct, gives the wrong epimer, ultimately delivering *epi*-Liphagal in two additional steps. [34] The use of this [4+3] strategy gives both Frondosin B and epi-Liphagal in a concise fashion synthesis of epi-Liphagal in an additional two steps.

[33] Zhang, J.; Li, L.; Wang, Y.; Wang, W.; Xue, J.; Li, Y. *Org. Lett.* **2012**, *14*, 4528.
[34] George, J. H.; Baldwin, J. E.; Adlington, R. M. *Org. Lett.* **2010**, *12*, 2394.

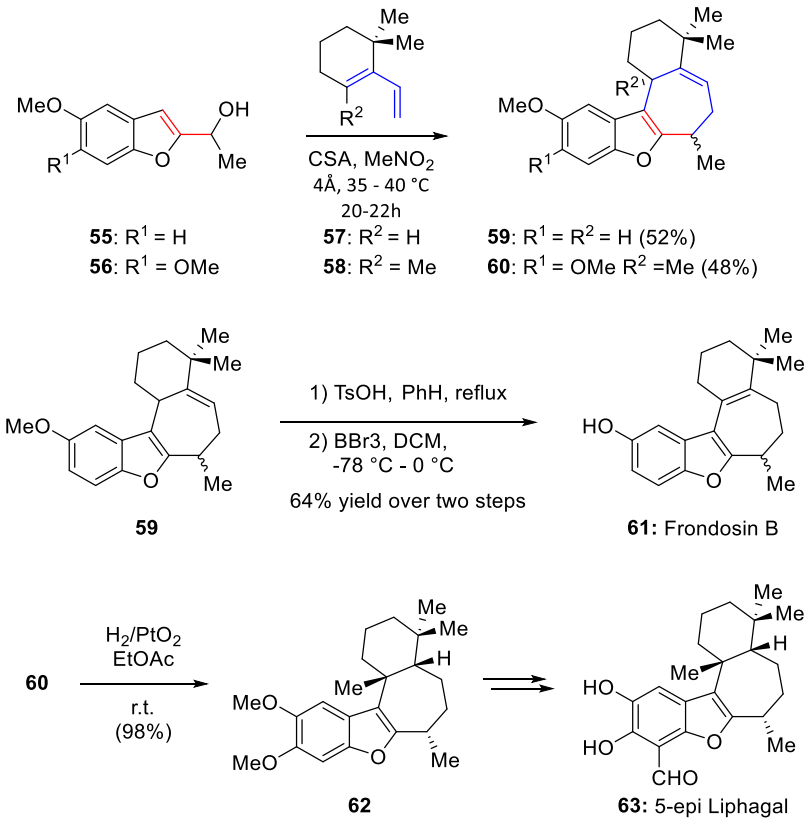

Scheme 13: Li's Synthesis of Frondosin B and epi-Liphagal

1.9 Metal Carbene and Metal Allyl Cation [4+3]

Unlike the oxyallyl cation-based [4+3] cycloadditions above which furnished cycloheptyl carbocycles through either an orbital symmetry-controlled cycloaddition or stepwise annulation; the metal carbenoid [4+3] gives rise to the same motifs through more varied mechanisms. Discussed below will be the role of vinyl carbene reactions, focusing primarily on the generation through propargylic esters. The vinyl carbenoid serves as a key intermediate for all proposed [4+3] cycloaddition reaction mechanisms, though the precise mechanism in any one particular case is often unknown. A representative example through the formation of a cyclohepta[*b*]indole by way

of propargylic ether **64** (Scheme **14**). [35] Similar mechanistic considerations exist for rhodium[36], palladium[37], and platinum[38] vinyl carbenes.

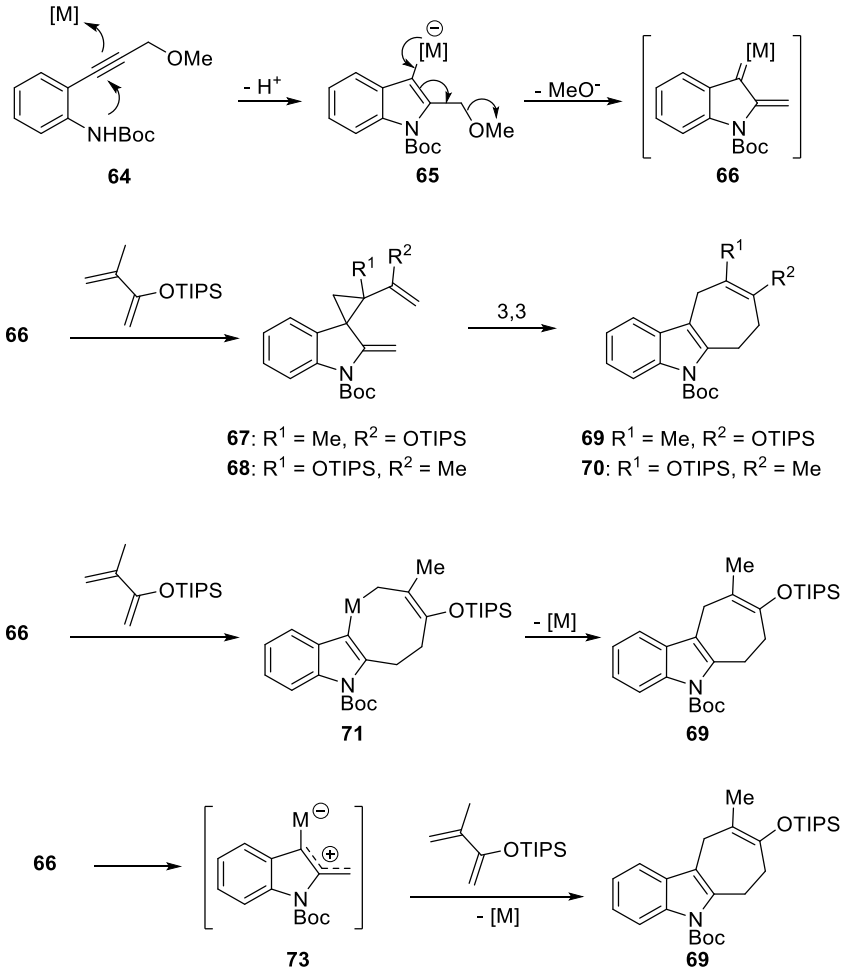

Scheme 14: Metal Carbenoid as oxyallyl equivalents

[35] Shu, D.; Song, W.; Li, X.;Tang, W. *Angew. Chem. Int. Ed*., **2013**, *52*, 3237-3240.
[36] Davies, H. M. L. *Tetrahedron* **1993**, *49*, 5203–5223.
[37] Liu, Y.; Wang Z.; Huang Z.; Zheng X.; Yang W.; Deng W. *Angewandte Chemie* **2020,** *132*, 1254-1258. (b). Huang, Z. Murhade G. M.; Trost, B. M. *Science* 2018, *362*, 564-568.
[38] Shu, D.; Song, W.; Li, X.; Tang, W. *Angew. Chem. Int. Ed*., **2013**, *52*, 3237-3240.

Following the formation of metal vinyl carbenoid **66**, three possible mechanisms can explain the formation of cycloadduct **69**. Cyclopropanation and subsequent [3,3]-rearrangement could give the cycloadduct as shown, however the isolated regioisomer **69** is inconsistent with the expected cyclopropanation trends of the diene. Based on the selectivity of cyclopropanation towards electron rich alkenes, cyclopropane **68** should predominate which upon rearrangement should give cycloadduct **70**; which was not observed. A subsequent report by Gaich et al. utilized the cyclopropanation/Cope sequence to furnish the same skeleton.[39] Alternatively, a [4+4] cycloaddition between the vinyl carbene and diene gives an intermediate metallocycle (**71**) which could also eliminate the metal and thereby giving the cyclohelpta[*b*]indole. Finally, a [4+3] cycloaddition between **73** and the siloxy diene with concomitant metal elimination would furnish the same skeleton.

1.10 Total Synthesis of Englerin A by Theodorakis

The total synthesis of englerin A perfectly encapsulates the potency of the metal mediated [4+3]. A sesquiterpene isolated from a Tanzanian shrub boasting activity against Renal Cell Carcinoma was synthesized contemporaneously by both the Ma and Nicolaou groups; Ma publishing one week prior to Nicolaou.[40,41] While Ma's synthesis used a gold-catalyzed enyne cyclization to give the oxabicyclic core, the Nicolaou group utilized a [5+2] cycloaddition as one of their key steps. A later report by Theodorakis, meanwhile, took advantage of a rhodium-catalyzed [4+3] cycloaddition instead.[42] This convergent synthesis allows for the formation of the key intermediate **75** in high yield and diastereoselectivity. The subsequent reduction and Rubottom

[39] Gritsch, P. J.; Stempel, E.; Gaich, T. *Org. Lett.* **2013**, *15*, 5472−5475.
[40] Zhou, Q.; Chen, X.; Ma, D. *Angew. Chem. Int. Ed*, **2010**, *49*, 3513-3516.
[41] Nicolaou, K. C.; Kang, Q.; Ng, S. Y.; Chen, D. Y-K. *J. Am. Chem. Soc.* **2010**, *132*, 8219-8222.
[42] Xu, J.; Caro-Diaz, E. J.; Batova, A.; Sullivan, S. D.; Theodorakis E. A. *Chem Asian J.* **2012**, *7*, 1052-1060.

oxidation give **76** with further elaboration giving intermediate **78**; the same intermediate was used by Ma, thereby completing the formal synthesis of (-)-englerin A.

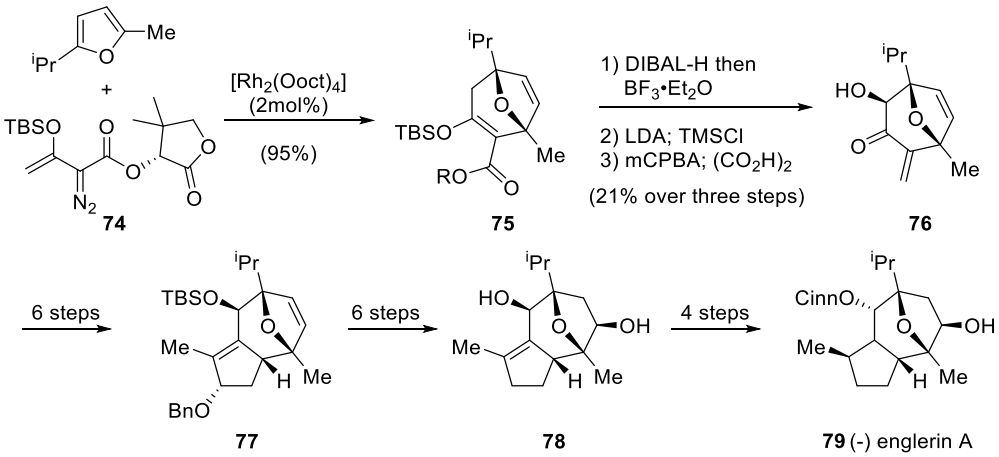

Scheme 15: Theodorakis Synthesis of (-)englerin A

Conclusion

The use and development of the [4+3] cycloaddition has produced a multitude of useful methodologies and total syntheses. The "3" component can have multiple precursors and various electronic considerations, as was seen in the case of Urechitol A, which can complicate strategy and approaches towards natural products. Given the complexity and ubiquity of the formed cycloheptanone skeletons, development and expansion in the study of oxyallyl cations remains an unanswered challenge. Further developments in reactivity and access to new scaffolds can allow more efficient synthesis of natural products and pharmaceutical agents.

Chapter 2: [4+3] Cycloaddition of 3-Alkenyl Indoles and Oxyallyl Cations

2.1: Introduction

Indole containing natural products are some of the most studied classes of compounds, drawing intense interest owing to their structural complexity and biological activity. Polycyclic frameworks such as carbazoles, found in the Strychnos class of natural products, are readily accessible through a variety of methods. Congruently, the cyclohepta[*b*]indole, i.e., a cycloheptene wherein the alkene carbons comprise the C2–C3 atoms of an indole, highlighted in blue (Figure **3**), has been dubbed a privileged motif and can be found in many natural products and pharmaceutical agents.[1]

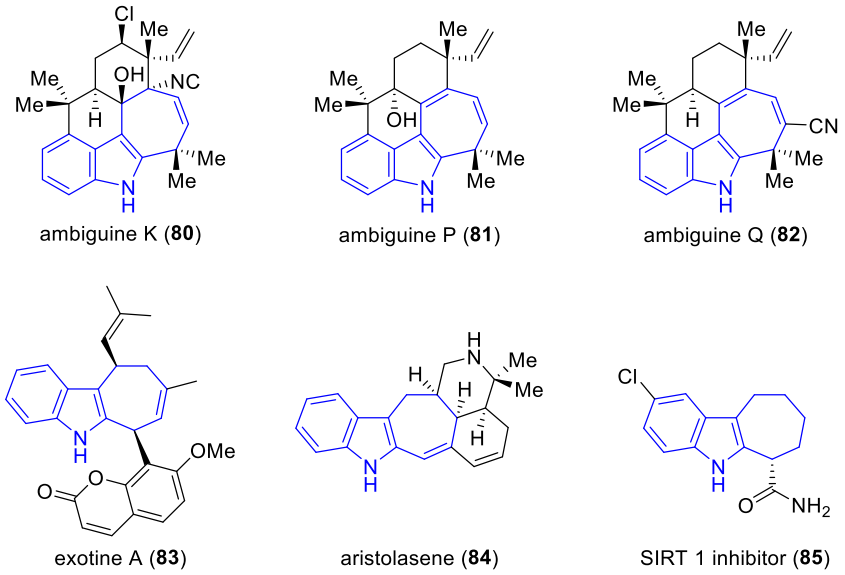

Figure 3: Cyclohepta[b]indole Motif in Bioactive Compounds

Our group has had a long-standing interest in the total synthesis of indole containing natural products, and recently our attention has been focused on the synthesis of pentacyclic ambiguines.

[1] Stempel, E. and Gaich, T. *Acc. Chem. Res.* **2016**, *49*, 2390–2402.

Initially, we were inspired by a potential [4+3] cycloaddition as the key step in synthesizing this motif (Figure **4**) and saw two possible approaches. Route A, which is comprised of an indole benzylic cation intercepting a suitable diene, and found literature support through the works of Li, Wu, and Zheng.[2,3,4] Using this route Dr. Jiasu Xu completed the synthesis of ambiguine P.[5] Alternatively, we also considered a different disconnection comprising a 3-alkenyl indole acting as a diene and an oxyallyl cation undergoing a dearomative [4+3] cycloaddition reaction, route B.

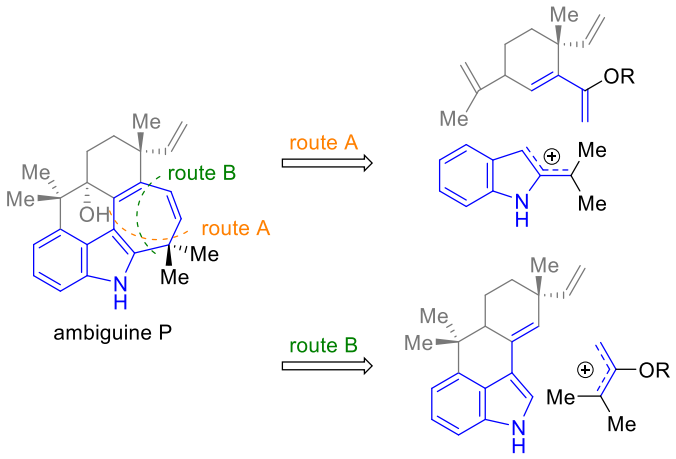

Figure 4: [4+3] Disconnections of the Ambiguine Skeleton

While cycloadditions of 3-alkenyl indoles have been shown to behave well in the Diels-Alder reaction,[6] an extensive search of the literature revealed no reports of [4+3] cycloadditions between 3-alkenyl indoles and oxyallyl cations. As a result, before pursuing the synthesis of

[2] (a) Zhang, J.; Li, L.; Wang, Y.; Wang, W.; Xue, J.; Li Y. *Org. Lett.* **2012**, *14*, 17, 4528-4530 .(b) Gong, W.; Liu, Y.; Zhang, J.; Jiao, Y.; Xue, J.; Li, Y. *Chem. Asian J.*, **2013**, *8*, 546-551. (c) Zhang, J.; Shao, J. D.; Xue, J.-J.; Wang, Y.-X.; Li, Y. *RSC Adv.*, **2014**, *4*, 63850.
[3] Han, X.; Li, H.; Hughes, R. P.; Wu, J. *Angew. Chem. Int. Ed.* **2012**, *51*, 10390−10393.
[4] Cao, K.-S.; Bian, H.-X.; Zheng, W.-H. *Org. Biomol. Chem.*, **2015**, ***13***, 6449.
[5] Xu, J.; Rawal, V. H. *J. Am. Chem. Soc.* **2019**, *141*, 4820–4823.
[6] (a) Gioia, C., Hauville, A., Bernardi, L., Fini, F. and Ricci, A. *Angew. Chem. Int. Ed*, **2008**, *47*, 9236-9239. (b) Enders, D.; Joie, C; Deckers, K. *Chem. Eur. J.*, **2013**, *19*, 10818-10821. (c) Gharagozloo, P.; Miyauchi, M.; Birdsall, B.; Birdsall, N. J. M. *J. Org. Chem.* **1998**, *63*, 6, 1974-1980.

pentacyclic ambiguines using route B, we devoted time to explore this potential methodology: the scope, limitations, and potential catalysis of the transformation are presented below. While writing up our manuscript for this transformation the Rossi group disclosed a related [4+3] cycloaddition between 2-alkenyl indoles and un-stabilized oxyallyl cations.[7]

2.2 Initial Discovery of the [4+3] Cycloaddition of 3-alkenyl Indoles

Our work started with model substrate **91**, initially prepared by Dr. Jiasu Xu during his pursuit of ambiguine P. The tricyclic core of diene **91** was chosen as it comprises the A, B, and C rings of the pentacyclic ambiguines, and contains a rotationally locked, sterically unencumbered diene (Scheme **16**).

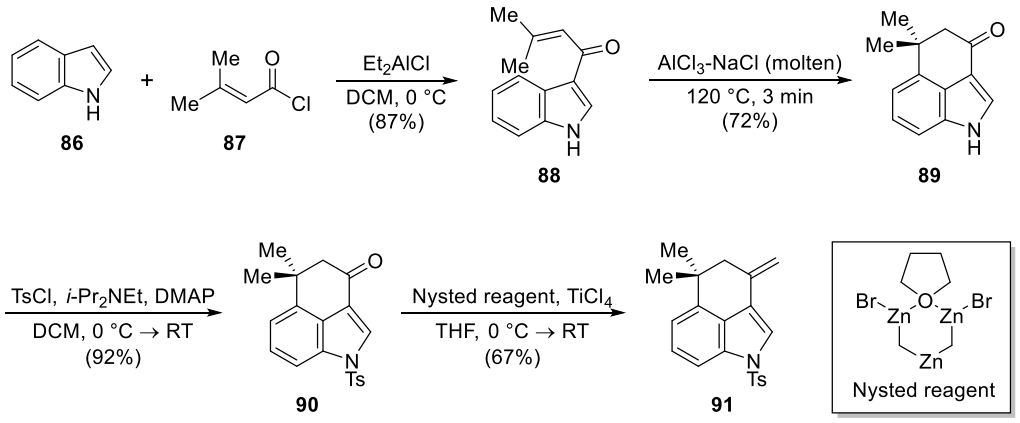

86 **87** **88** **89** **90** **91**

Scheme 16: Synthesis of the Model Diene **91**

After the formation of diene **91**, an initial screen was conducted to determine which conditions, if any, could promote the desired transformation (Table **2**). The use of common Lewis acids, such as tin(IV) chloride, led to deleterious protoisomerization of diene **91**. Based on this observation, we considered that Lewis acids which readily generate HCl to be less useful at

[7] Pirovano, V.; Brambilla, E.; Moretti , A.; Rizzato, S.; Abbiati, G.; Nava, D.; Rossi, E. *J. Org. Chem.*, **2020**, *85* , 3265–3276.

promoting the cycloaddition. Instead, potentially less protic conditions were tried and subsequently TMSOTf was found to be an optimal Lewis acid. Based on our understanding of the reaction mechanism, we postulated that highly stabilizing solvents such as diethyl ether, THF, or nitroethane would be required to produce the desired product in high yields. We found this to be the case, and THF or nitroethane were ultimately found to produce the best results. Ultimately, after optimization, the desired cycloadduct **93** was formed, in excellent yield and complete diastereoselectivity. The ease of this reaction led us to pursue this transformation as a simple, convergent approach to the cyclohepta[*b*] indole motif, and after our initial discovery, Dr. Xu, focused on route A successfully utilizing the strategy to deliver ambiguine P in an elegant synthesis. Left with this encouraging result and no direct precedent in the literature, we felt that a thorough examination into the substrate scope was warranted, as the polycyclic frameworks we developed could be of great synthetic utility.

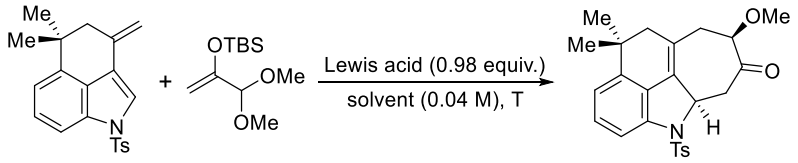

91 **92** **93**

Entry[a]	Lewis acid	Solvent	T	NMR Yield
1	$SnCl_4$[b]	DCM	–78 °C	-[c]
2	$ZnCl_2$[d]	DCM	0 °C	50%
3	TMSOTf	DCM	–78 °C	67%
4	TMSOTf	PhMe	–78 °C	62%
5	TMSOTf	*t*-BuOMe	–78 °C	54%
6	TMSOTf	Et_2O	–78 °C	85%
7	TMSOTf	THF	–78 °C	97%
8	TMSOTf	$EtNO_2$	–78 °C	95%

[a] yield was determined with ^{1}HNMR with internal standard. [b]1 equiv. of $SnCl_4$ was used. [c]Decomposition of starting materials. [d]1.1 equiv. of $ZnCl_2$ was used.

Table 2: Optimization of the [4+3] cycloaddition

2.3 Substrate Scope of the [4+3] Cycloaddition

In order to better understand the limits of this transformation, we considered selection of 3-alkenyl indoles bearing substitutions of various steric and electronic character. Access to such 3-alkenyl indoles was well precedented, and we explored several routes to access this class of compounds (Scheme **17**). Dienes could be synthesized through a sequence of (a) acylation, protection, and olefination (Scheme **17a**), (b) Suzuki cross coupling of indole 3-boronic acid (Scheme **17b**), or (c) through oxidative Heck coupling with suitable styrenes to give 3-styrenyl indoles (Scheme **17c**).[8] This three-pronged approach allowed for rapid preparation of 3-alkenyl indoles (**95a-q**) and allowed us to explore a variety of substrates quickly and efficiently. Olefination of N-benzenesulfonyl-3-acetyl indole proved challenging using typical Wittig olefination conditions, possibly due to the increased acidity of the methyl group.[9] To overcome this, Nysted's reagent or alternatively, bis(cyclopentadienyl)-dimethyltitanium (Petasis reagent),[10] were found to be highly effective allowing for the olefination of **95a** on large scale in high yield (Scheme **17**).

[8] Grimster, N.P.; Gauntlett, C.; Godfrey, C.R.A.; Gaunt, M.J. *Angew. Chem. Int. Ed.*, **2005**, *44*, 3125-3129.
[9] Noland, W. E.; Etienne, C. L.; Lanzatella, N. P. *J. Heterocycl. Chem*. **2011**, *48*, 381.
[10]Petasis, N. A.; Bzowej, E. I. *J. Am. Chem. Soc.* **1990**, *112*, 6392-6394.

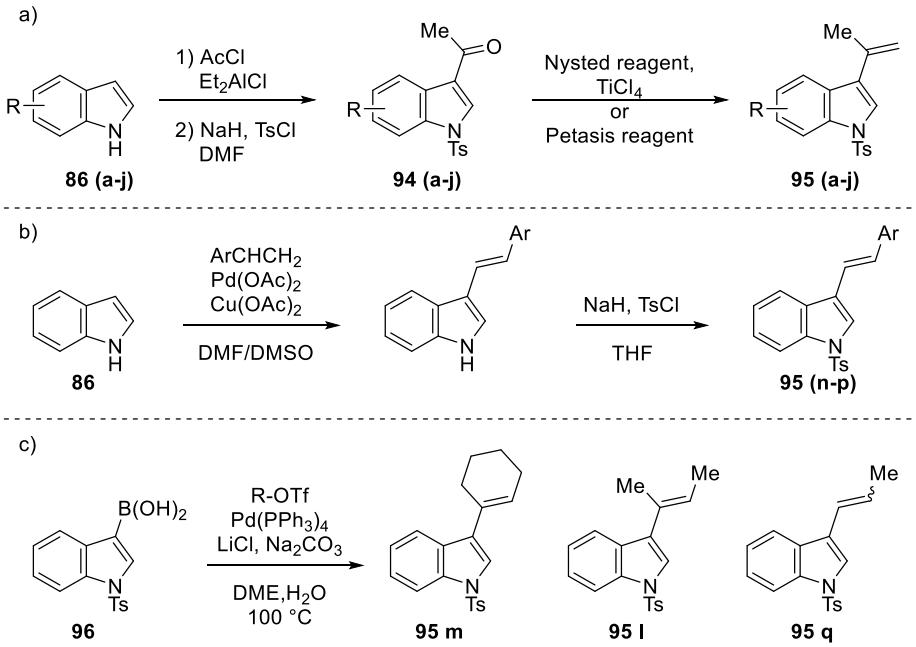

Scheme 17: Construction of Various Indole Dienes

After preparing a library of 3-alkenyl dienes, we attempted the cycloaddition reaction based on our optimized conditions. To our delight, the reaction proceeds well with most substrates, giving the desired cyclohepta[*b*] indole motif in high yields and high diastereoselectivity. The use of THF proved necessary for most substrates, as the use of nitroethane as the solvent for the 3-isopropenyl indole substrates saw a reduction in diastereoselectivity from >20:1 to ~4:1. This result is consistent with the reports by Hoffman, who saw a decrease in diastereoselectivity when using nitroalkane solvents relative to less stabilizing solvents such as DCM.[11] More puzzling is that with styryl indole **95n**, the opposite effect is observed; the use of ethereal solvents like THF, saw a decrease in yield and diastereoselectivity whereas nitroethane gave the cycloadduct in high yield as a single diastereomer.

[11] Pierau, S.; Hoffmann, H. M. R. Synlett **1999**, *2*, 213–215.

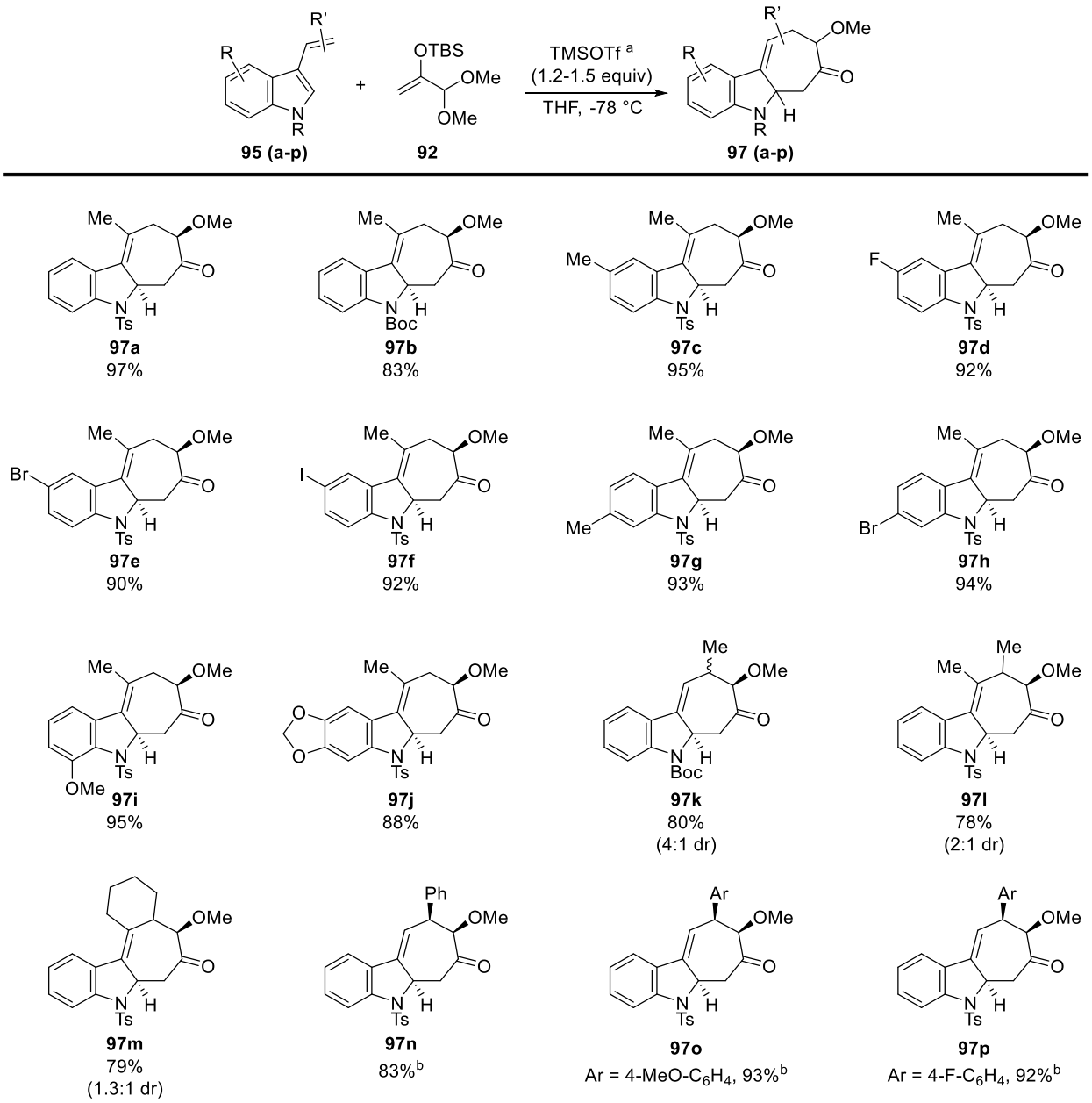

[a] TMSOTf equivalents were varried between 1.2 to 1.5 equivalents based on TLC. [b] Nitroethane was used as the solvent

Table 3: Substrate Scope for the [4+3] Cycloaddition

In all cases reactions proceed quickly at – 78 °C, with most cycloadditions reaching complete conversion within an hour, cleanly affording the products with only 1.5 equivalents of acetal **92**. Substrates **95l** and **95m** saw a plateau in reaction progress (TLC), with additional equivalents of acetal **92** or TMSOTf not further improving their conversion. After the reaction is

complete, clean *Z*-3-propenyl indole can be recovered which upon re-subjection to the reaction conditions gave none of the desired cycloadduct. We attribute the lack of reactivity of the Z olefin to steric interactions with the indole C2 hydrogen. We propose that the increased allylic strain causes a disruption of the planarity of the diene which could inhibit the reactivity of the 3-alkenyl indole.

2.4 Mechanistic Discussion and Limitations

Based on our observed diastereoselectivity and the known reactivities of stabilized oxyallyl cations, we propose the following mechanism (Scheme **18**). As was discussed in Chapter One, the relative stereochemistry between the substituents of an oxyallyl cation can help elucidate if a mechanism is concerted or stepwise. The syn relationship between the highlighted hydrogen and methyl groups, as well as the anti-conformation between the methyl and methoxy groups suggests a stepwise mechanism. Initially, oxyallyl cation precursor **92b** reacts with one equivalent of TMSOTf, resulting in the loss of methyl TMS ether. The resultant oxacarbenium ion **98** is intercepted by the 3-alkenyl indole **91**.

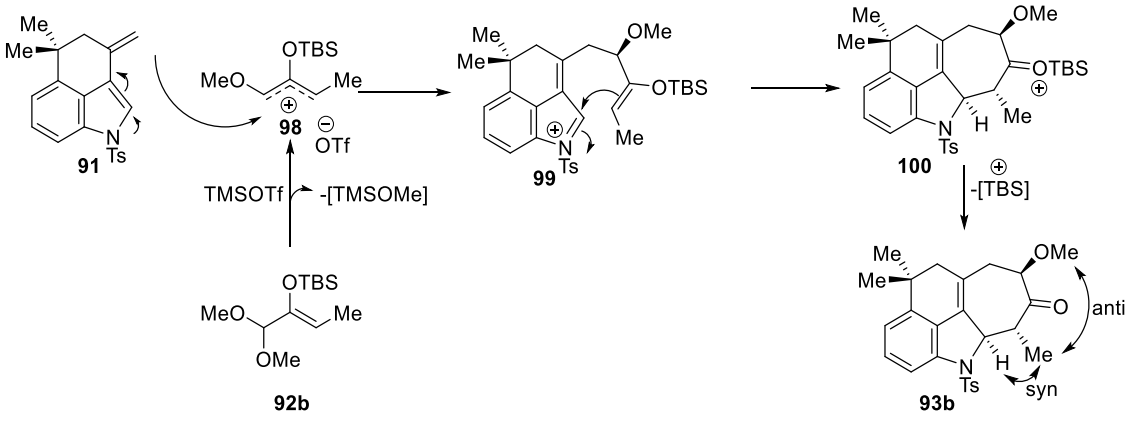

Scheme 18: Proposed Mechanism for the Cycloaddition

The resulting iminium **99** is then intercepted in a Mannich-type process by the silyl enol ether leading to the cyclohepta[*b*] indole framework containing the siloxycarbenium intermediate **100**; which upon loss of TBSOTf generates the final cycloadduct **93b**. This mechanism explains the ability of the reaction to proceed with sub-stoichiometric amounts of TMSOTf, as the generation of silyl triflate over the course of the mechanism could promote the reaction and has inspired us to pursue a catalytic method for this transformation.

While the reaction tolerates various substitutions on the benzene ring as well as the dienes, several attempted dienes were unreactive (Scheme **19**). The effects of decreasing the nucleophilicity of the 3-alkenyl indoles, as well as steric disruption to the planarity of the diene were identified as a major factor for their lack of reactivity. In these cases, varying reaction conditions such as solvent or temperature did not improve the reactivity of the diene. These complications were expected given the similarity to the Diels-Alder reaction and the stereoelectronic requirements of the "4" component. In our case the electronic limitations could be explained by the diminished ability of the diene to add into oxocarbenium **98**, which is manifested in the unreactive nature of substrates lacking sufficient electronic density around the terminal carbon of the diene. Several compounds containing electron withdrawing substituents on the diene were examined (**101a-j**), but no reactivity in the [4+3] cycloaddition was observed for these substrates.

We postulated that changes to the indole protecting group could alleviate this electronic limitation; for instance, changing from N-tosyl to a less deactivating group, such as N-Boc or N-Me, might improve the reactivity of the dienes. In support of this conclusion, the use of N-tosyl 3-propenyl indole **101a** does not undergo the cycloaddition, however the N-Boc 3-propenyl indole **95k** delivers the cycloadduct in good yield. Unfortunately, changes to the indole protecting group

did not change the outcome of the reaction in the case of **101c**. Attempts to change the outcomes of the reaction by changes in solvent or temperature also did not alter the outcome of the reaction.

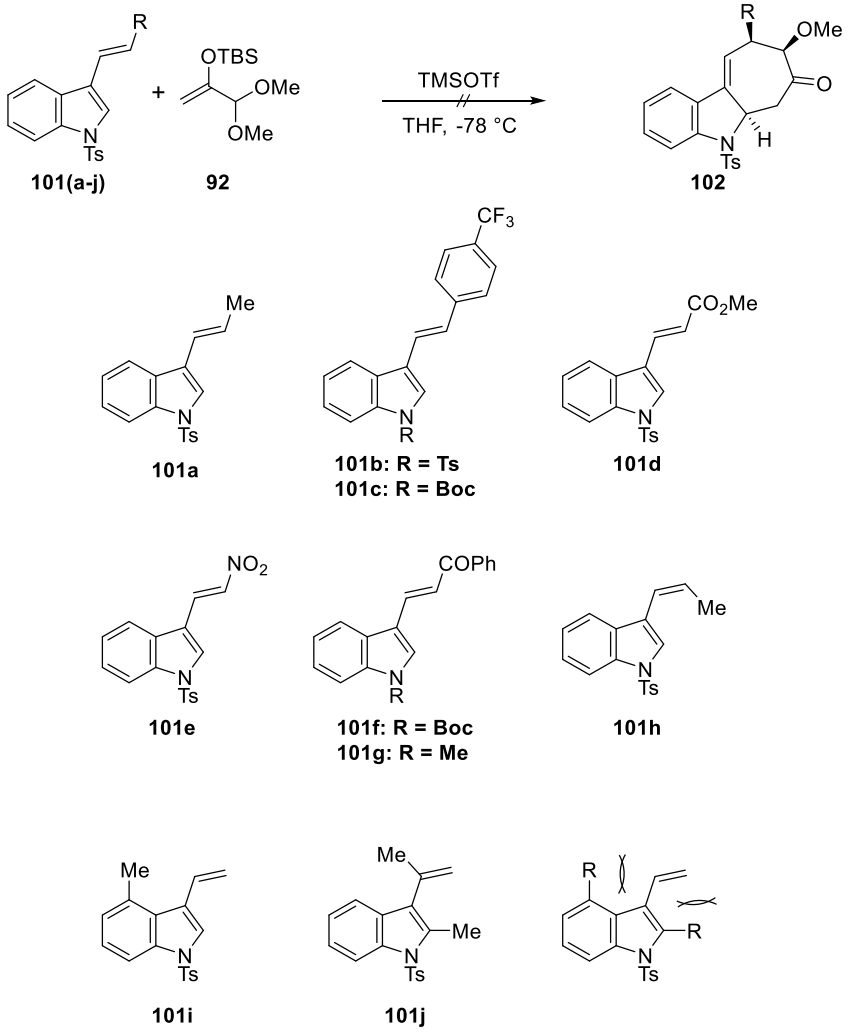

Scheme 19: Stereo / Electronic Limitations of the [4+3] Cycloaddition

Logically, N-alkyl indoles would also work, but those substrates primarily gave uncyclized products. The decreased electrophilicity of the intermediate aza-allyl cation **99** may make cyclization onto C-2 less favorable, allowing side reactions to compete. For this reason, such substrates were not pursued or studied farther.

In our investigations we examined related 3-alkenyl heterocycles such as 3-isopropenyl-benzofuran or 3-isopropenyl-benzothiophene. However, these substrates did not participate in the [4+3] under the standard reaction conditions, possibly due to either insufficient nucleophilicity of the participating 3-alkenyl group, or a higher energy barrier of dearomatization in these heterocycles. However, N-tosyl-3-isopropenyl pyrrole **103**, undergoes the cycloaddition cleanly giving the cycloadduct **104** as a single diastereomer in moderate yield (scheme **20**). This result is interesting as it breaks from previous reports which detail the use of pyrrole as the "4" component in [4+3] cycloadditions, leading to products of the type **104b**; strangely, the freely rotating diene was more prone to react than the s-cis locked diene.[12]

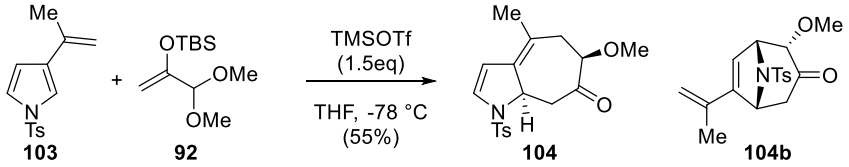

Scheme 20: [4+3] of 3-alkenyl pyrrole

2.5 Intramolecular [4+3] Cycloaddition Using a Tethered Oxyallyl Cation

During our investigation into the intermolecular [4+3] cycloaddition, an attempt was made to engineer an intramolecular cycloaddition using a tethered α-keto-acetal at either the C3 or N1 position of indole (Scheme **21**). We only actively pursued the N-acylation strategy, as functionalization onto the C3 through Wittig olefination posed too many challenges. Our plan was to N-acylate an unprotected, 3-alkenyl indole **107** with a carboxylic acid bearing a distal α-keto-

[12] (a) Intramolecular [4+3] cycloaddition of pyrrole: Cameron A., Fisher B., Fisk N., Hummel J., White J. M., Krenske E. H., Rizzacasa M. A. *Org. Lett.* **2015**, *17*, 24, 5998-6001. (b) Shibata, M.; Fuchigami, R.; Kotaka, R.; Namba, K.; Tanino, K. *Tetrahedron* **2015**, *71*, 26-27, 4495 – 4499.

acetal **108**. This approach allowed us to make use of previously synthesized material and would allow access for unique tetracyclic substrates.

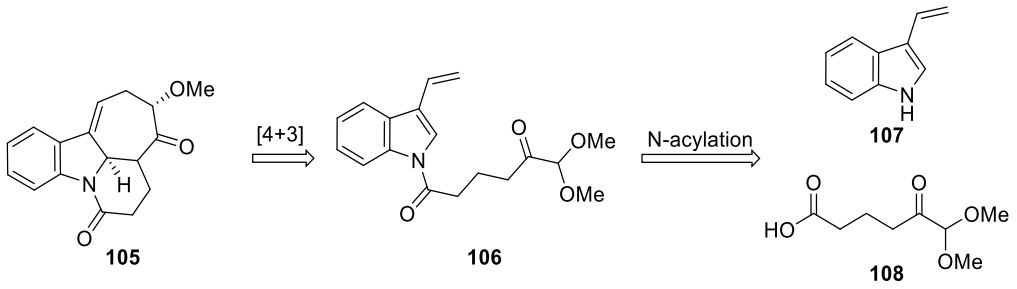

Scheme 21: Approach Towards an Intramolecular Cycloaddition

Synthesis of acid **106** (Scheme **22**) begins with the alkenylation of commercially available 5-oxohexanoic acid **109** with benzaldehyde in a Knoevenagel reaction. Subsequent methyl ester formation proceeds in near quantitative yield; the methyl ester was necessary as the glyoxal of **108** is insoluble in most organic solvents owing to its polarity. After subjecting methyl ester **111** to ozonolysis and acetal formation, the resulting products were a mixture of the acetal, and ketal-acetal. To combat this problem, a careful hydrolysis of the ketal was attempted. Through careful control of temperature and reaction time, the exclusive hydrolysis of the mixed ketal/acetal in acidic, aqueous methanol can be resolved to furnish exclusively the acetal. Subsequent saponification gives acid **108** in moderate overall yield. Acylation of 3-vinyl indole **107** with activated acid **108** led to indole **106** in modest yield, however the sequence was scalable, and large quantities of acid **108** could be prepared.

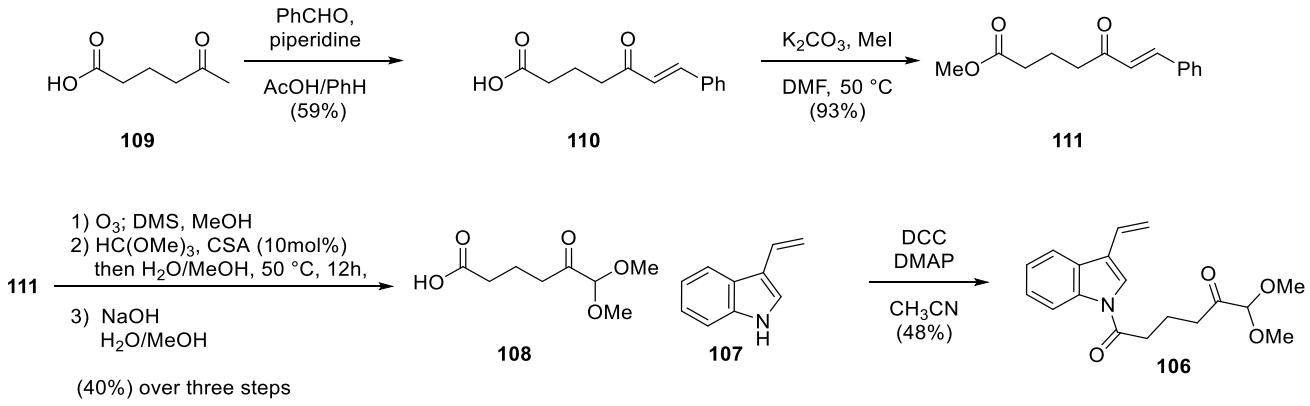

Scheme 22: Attempts Towards an Intramolecular Cycloaddition

Unfortunately, the formation of the necessary silyl enol ether of **106** was never realized, and so this pursuit was discontinued. While the tetracyclic structure of **105** is not found in natural products, the complexity of the framework made the pursuit a worthwhile investment.

2.6 Investigations into Alternative Oxyallyl Cations

During our investigations we naturally examined several alternative and well developed oxyallyl cation precursors discussed in Chapter One (Scheme **23**). These attempts included vinyl α,α'-dihalo ketones **115a**,[13] epoxide **115d**,[14] azaoxyallyl cations **115c**,[15] and 1-methoxy-3-tosyloxy propanone **115f**.[16] Disappointingly, the standard conditions unique to each oxyallyl precursor, gave none of the expected cycloadduct. Strangely, oxyallyl cations derived from **101b**, or **101d**, which have similar electronic character to oxocarbenium **98** did not give the desired cycloadduct, producing instead a complex mixture of products. To rule out experimental error,

[13] (a) Hoffmann, H. M. R.; Clemens, K. E.; Smithers, R. H. *J. Am. Chem. Soc.* **1972**, *94*, 3940–3946. (b) Takaya, H.; Makino, S.; Hayakawa, Y.; Noyori, R. *J. Am. Chem. Soc*. **1978**, *100*, 1765–1777. (c) Rawson, D. I.; Carpenter, B. K.; Hoffmann, H. M. R. *J. Am. Chem. Soc.* **1979**, *101*, 1786–1793. (d) Handy, S. T.; Okello, M. *Synlett*, **2002**, 3, p. 489 – 491.
[14] Lo, B.; Chiu, P. *Org. Lett.* **2011**, *13*, 864 – 867.
[15] Jeffrey, C. S.; Barnes, K. L.; Eickhoff, J. A.; Carson, C. R. *J. Am. Chem. Soc*. **2011**, *133*, 7688–7691.
[16] Föhlisch, B.; Krimmer, D.; Gehrlach, E.; Kaeshammer, D. *Chem. Ber*. **1988**, *121*,1585-1594.

standard dienes such as furan were used as a control and in these cases, the [4+3] cycloadditions gave yields consistent with literature results.

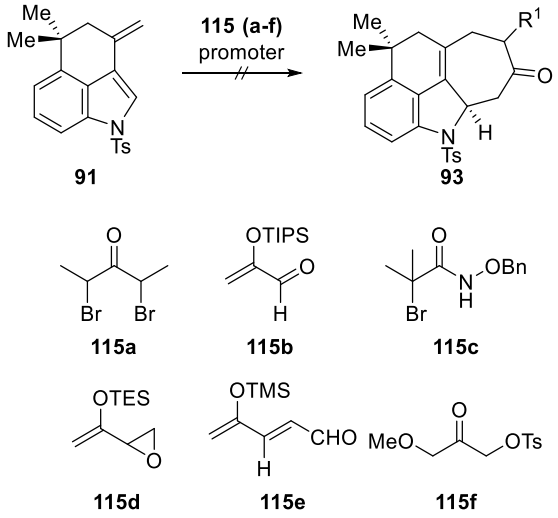

Scheme 23: Unsuccessful Oxyallyl Cations

While disappointing, the lack of reactivity with zwitterionic oxyallyl cations lends credence to our proposed mechanism. The most revelatory result was the lack of reactivity of the tosyloxy methoxy ketone **115f**, which upon treatment with base would generate the 1-methoxy stabilized zwitterionic oxyallyl cation **116** (Scheme **24**). The zwitterionic oxyallyl **116** serves as an analogue to the cationic oxyallyl cation **98** that we suspect to be the active species in our reaction. Using standard conditions, sodium carbonate in HFIP, the cycloaddition with furan gave complete conversion to oxobicycle **18**, however diene **91** did not react. The reason for this discrepancy in reactivity could be due to the lower electrophilicity of the zwitterionic versus cationic intermediates.

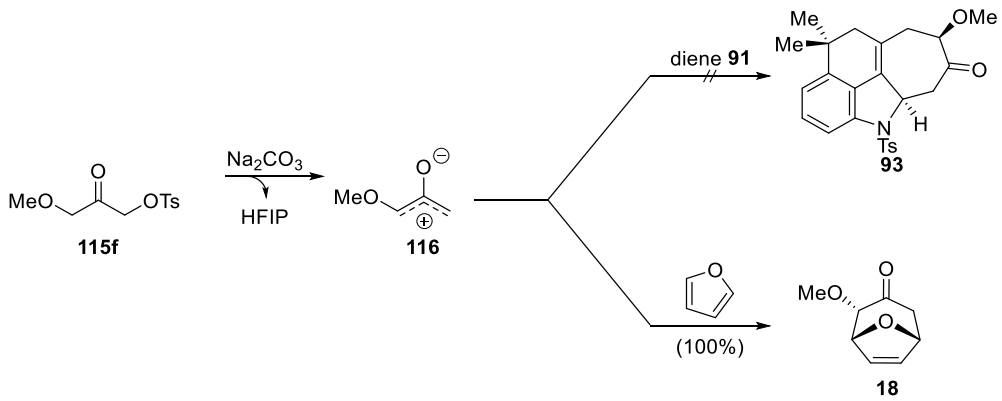

Scheme 24: Use of Stabilized Zwitterionic Cation **116**

Strangely, α,α'-dihalo ketones react with 2-vinyl indoles as was recently disclosed by the Rossi group.[17] In contrast, our examination of 2-vinyl indoles led us to conclude that the desired cycloaddition reaction does not takes place under our conditions using stabilized oxyallyl cations. The reason for this discrepancy is unknown.

2.7 Isomerization of Cycloadducts

During the investigation of the cycloaddition, many attempts were made to rearomatize the pyrrolo-ring of the cycloadducts to regenerate the indole. Standard acidic, basic, and metal Lewis acids were tried, but initially no reliable approach was found.[18] Literature conditions such as iron (III) trifluoromethanesulfonate seemed promising, as this procedure had been used previously to isomerize tetrasubstituted alkenes in similar indoline systems. Attempts at isomerizing cycloadduct **93** with iron(III) triflate, or trifluoroacetic acid, led to the formation of the desired indole **117**, albeit in low yield. As the reactivity of the cycloadducts was unknown, our attempts

[17] Pirovano, V.; Brambilla, E.; Moretti , A.; Rizzato, S.; Abbiati, G.; Nava, D.; Rossi, E. *J. Org. Chem.*, **2020**, *85*, 3265–3276.
[18] (a) Simoji, Y.; Saito, F.; Tomita, K.; Morisawa, Y. *Heterocycles* **1991**, *32*, 2389–2397. (b) Tan, B.; Hernández-Torres, G.; Barbas III, C. F. *J. Am. Chen. Soc.* **2011**, *133*, 12354–12357. (c) Nakano, S.; Inoue, N.; Hamada, Y.; Nemoto, T. *Org. Lett.* **2015**, *17*, 2622–2625. (d) Kundal, S.; Jalal, S.; Paul, K.; Jana, U. *Eur. J. Org. Chem.* **2015**, 5513–5517.

at utilizing the methoxy-ketone handle led to attempts at TMSI mediated ether cleavage (Scheme **25**). To our surprise, treatment of **93** with an excess of in situ generated TMSI, led to the formation of the deoxygenated ketone **118a**. The concomitant deoxygenation/isomerization led us to try the reaction with only 20 mol% of TMSI; with these conditions, only the isomerization reaction was observed. In both cases, the protoisomerization is diastereoselective, as the C2 hydrogen directs the isomerization to the indole in a selective manner, although the precise mechanism is unknown. When the N-Boc tetracycle **93c** was subjected to the reaction condition, using five equivalents of TMSI, the isomerization, deprotection, and deoxygenation proceeded in concert giving the deprotected indole product **118b** in excellent yield.

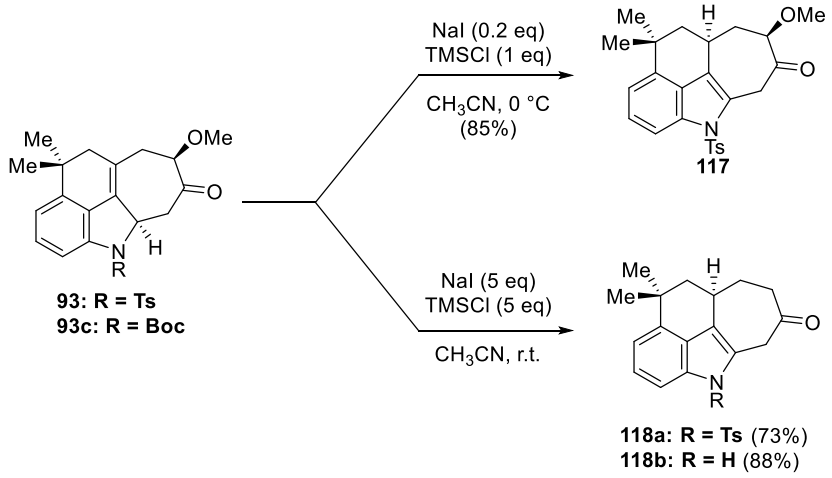

Scheme 25: Isomerization/Deoxygenation of Cycloadducts

A proposed mechanism of the transformation is shown in Scheme **26**.[19] The TMSI promoted iodide displacement of the α-methoxy ketone **97a** leads to α-iodo ketone **119**. An additional equivalent of TMSI is needed to reduce the α-iodo ketone to the silyl enol ether **121**. Subsequent hydrolysis and isomerization with TMSI, leads to the cycloheptanone **122** in 71% yield. Unfortunately, the

[19] (a) Olah, G. A.; Arvanaghi, M.; Vankar, Y. D., *J. Org. Chem*. **1980**, *45*, 3531. (b) Ho, T.-L., *Synth. Commun*. **1979**, *9*, 665.

intermediates could not isolated, however the proposed mechanism is consistent with reports in the literature.

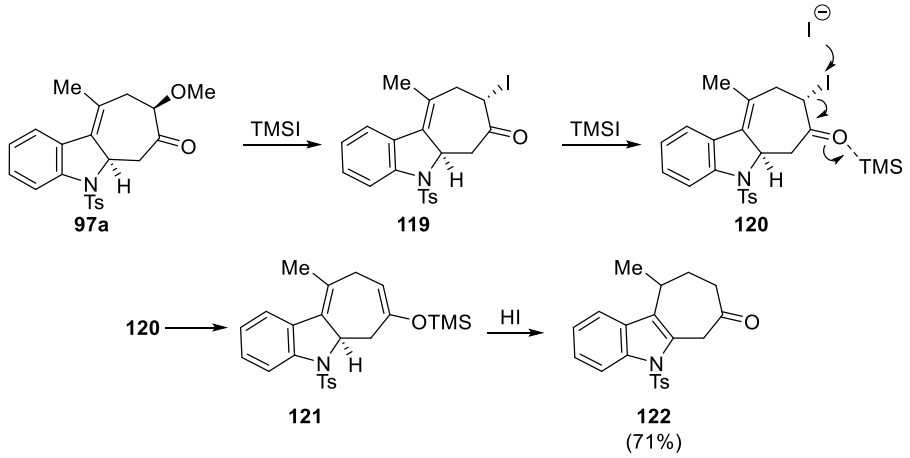

Scheme 26: Proposed Deoxygenation/Isomerization Mechanism

In every case the isomerization/deoxygenation proceeded smoothly giving the corresponding indoles in high yields and as single diastereomers. As the reaction requires at least two equivalents of TMSI, an additional set of experiments was conducted to probe the role of hydroiodic acid. Subjecting cycloadduct **93** to 20 mol% of hydroiodic acid, no reaction is observed; the reason behind this is unknown. This same reaction is explored in the synthetic studies towards ambiguine Q, but again, no other readily available transformation has been found to rearomatize the indole.

2.8 Catalysis of the [4+3] Cycloaddition

While this methodology provides ready access to a challenging structural motif, a catalytic or enantioselective method would be far more impactful. To this end, an extensive search for asymmetric acetal substitution conditions was conducted. In keeping with our understanding of the reaction mechanism, the key step requires the formation of an oxocarbenium ion; as a result, Lewis and Brønsted acids of sufficient strength are required to facilitate the transformation. An

initial screen of suitable Lewis and Brønsted acids was conducted using 3-isopropenyl indole **95a** and acetal **92**, including conditions that have an asymmetric variant (Table **4**). The use of 3-isopropenyl indole **95a** was necessary, as we were concerned about potential protoisomerization of diene **91**. Upon screening the most common Lewis acids, scandium(III) trifluoromethanesulfonate,[20] presented itself as viable at catalyzing the racemic transformation, so efforts were directed at using reported chelated complexes to test the feasibility of the asymmetric transformation.[21] Unfortunately, none of the ligated complexes possessed sufficient reactivity to give the desired product. We propose that the lower Lewis acidity of the complexes may have hindered the formation of the key oxocarbenium ion. So far, no Lewis acid complexes we have examined gave the desired cycloadduct and so efforts were shifted to other potential solutions.

[20] Scandium: (a) Kobayashi, S., *Chem. Lett*. **1991**, 2187. (b) Kobayashi, S.; Araki, M.; Hachiya, I., *J. Org. Chem*. **1994**, *59*, 3758. Ytterbium: Kobayashi, S.; Hachiya, I.; Takahori, T., *Synthesis* **1993**, 371.
[21] Copper: (a) Krebs, A.; Bolm, C. *Synlett*, **2011**, *5*, 671 – 673. (b) Evans, D. A.; Kozlowski, M. C.; Murry, J. A.; Burgey, C. S.; Campos, K. R.; Connell, B. T.; Staples R. J. *J. Am. Chem. Soc.* **1999**, 121, 4, 669-685. Tin: Iwasawa, N.; Yura, T.; Mukaiyama, T., *Tetrahedron* **1989**, *45*, 1197.

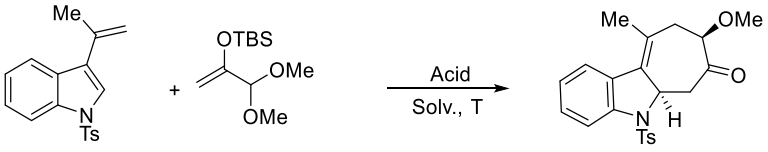

95a **92** **97a**

Lewis Acid	Solvent	Temp. (°C)	Yield
$Cu(OTf)_2$/BINAP	DCM	r.t.	NR
$Sc(OTf)_3$	DCM	r.t.	>90%[b]
$Sc(OTf)_3$/BINOL	DCM	r.t.	NR
$Sc(OTf)_3$/PyBox	DCM	r.t.	NR
$Yb(OTf)_3$/BINOL	DCM	r.t.	NR
$Ti(OiPr)_4$/BINOL	DCM	r.t.	NR
$Sn(OTf)_2$	DCM	r.t.	NR
BNDHP (0.2 eq)	DCM	r.t.	NR
Phosphoramide (0.2 eq)	DCM	r.t.	NR
TMSOTf (1 eq)	$EtNO_2$	-78	95%[a]
TMSOTf (0.5 eq)	$EtNO_2$	-78	70%[a]
TMSOTf (0.1 eq)	$EtNO_2$	-78	51%[a]
HOTf (0.1 eq)	$EtNO_2$	-78	39%[a]

[a]Yield in isolation [b]Yield Determined 1HNMR.

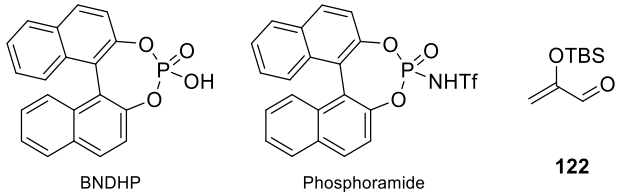

Table 4: Initial catalyst Screen

The most promising results were found in the case sub-stoichiometric amounts of TMSOTf and triflic acid, which could give the desired cycloadduct in good yield. Unfortunately, no reactivity was observed with chiral Brønsted acids such as BINOL phosphoric acid or the more acidic N-trifluoromethanesulfonyl triflamide.[22,23] As the key to the reaction lies in the formation of the oxocarbenium intermediate, and we had demonstrated that triflic acid was capable of generating this key intermediate, our focus shifted to Brønsted acids that were sufficiently acidic. With the knowledge that strong enough Brønsted acids can promote the reaction, another attempt

[22] Luan, Y.; Qi, Y.; Gao, H.; Ma, Q.; Schaus, S.E. *Eur. J. Org. Chem.* **2014**, 6868-6872.
[23] Nakashima D.; Yamamoto H. *J. Am. Chem. Soc.* **2006**, *128*, 9626-9627.

was made using the highly acidic imidodiphosphorimidate (IDPi) catalysts developed by List et al.[24] The time investment to produce even one catalyst initially dampened our pursuit, but we had confidence that these catalysts could lead to an unprecedented asymmetric [4+3] cycloaddition.

After synthesizing IDPi-**a**, a screen of relevant reaction conditions was conducted using diene **91**, 5 mol% IDPi-**a**, and acetal **92** (table **5**). To our great delight the desired cycloadduct was obtained cleanly as a single diastereomer, albeit in moderate yield and enantioselectivity. The chief complication was attributed to the hydrolysis of acetal **91** to the α-siloxy acrolein **122**. We hypothesized that changes to the catalyst, such as increasing either the acidity or the steric bulk may improve the reactivity of acetal **92**, so the more acidic IDPi-**b**, and the more hindred IDPi-**c** were prepared and examined. Based on our findings, the reaction works better with the more acidic catalysts, however the increased steric congestion of the bulkier catalysts can drastically reduce the enantioselectivity. Additionally, we decided to run the reaction at lower catalyst loadings and found that even 1 mol% was sufficient to catalyze the reaction.

[24] For a review: Schreyer , L.; Properzi, R.; List, B. IDPi Catalysis, *Angew. Chem., Int. Ed.* **2019**, *58*, 12761-12777.

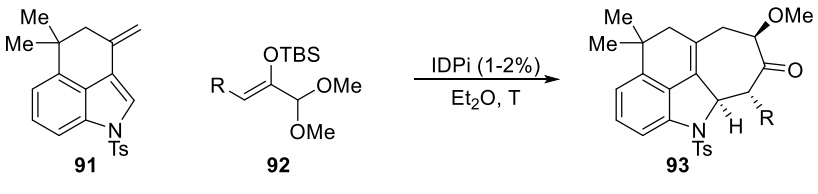

entry	IDPi - R'	R	temp. (°C)	yield[a](ee)
1	R' = Ph	Me	r.t.	46% (14)
2	R' = 4-tBuC$_6$H$_4$	Me	r.t.	38% (3)
3	R' = 3,5-(CF$_3$)$_2$C$_6$H$_3$	Me	r.t.	68% (31)
4	R' = Ph	H	r.t.	65%(13)
5	R' = 4-tBuC$_6$H$_4$	H	r.t.	41%(11)
6	R' = 3,5-(CF$_3$)$_2$C$_6$H$_3$	H	r.t.	79%(11)
7	R' = 3,5-(CF$_3$)$_2$C$_6$H$_3$	Me	-20	64% (31%)[b]
8	R' = 3,5-(CF$_3$)$_2$C$_6$H$_3$	Me	-40	21% (32%)[b]

[a]Yield determined by ^{1}H NMR relative to internal standard [b]protoisomerization not seen in NMR

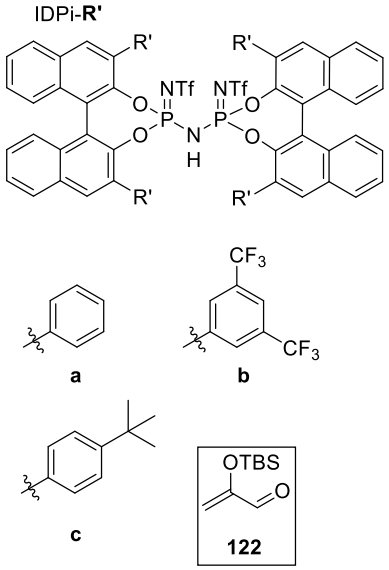

Table 5: Screen of IDPi catlaysts

With a suitable catalyst in hand, we next sought to explore reaction conditions such as temperature, solvent, and additives such as molecular sieves, to improve the yield and enantioselectivities of the reaction (Table **6**). We had hoped that by increasing the coordination between the oxocarbenium ion and the IDPi catalyst, through the use of less polar solvents such as MTBE and decreasing the temperature, that the reaction would give the cycloadduct in better enantioselectivity. To our surprise this was not the case, decreasing the temperature only decreased the yield with a comparative increase of the hydrolysis of acetal **92**. Additionally, no improvement in the enantioselectivity was found at lower temperatures, or with the use silylated IDPi catalysts. This puzzling development is confounded further with our findings on the effects of molecular sieves.

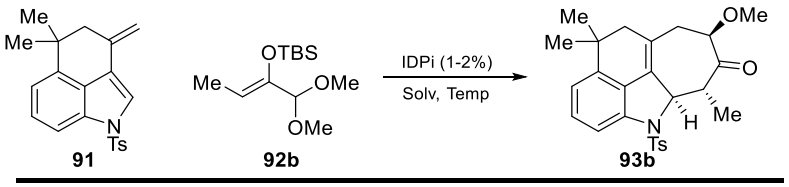

entry	IDPi (CF_3)$_2$	M.S.	temp.	solv.	yielda(ee)
1	X = TBS	--	r.t.	Et_2O	83% (30)
2	X = TBS	--	-20 °C	Et_2O	56% (31)
3	X = TBS	5Å	r.t.	Et_2O	quant (31)
4	X = TBS	5Å	-20 °C	Et_2O	quant (40)
5	X = H	4Å	r.t.	MTBE	NR
6	X = H	4Å	-20 °C	MTBE	NR
7	X = TMS	4Å	r.t.	Et_2O	NR
8	X = TBS	4Å	-20 °C	Et_2O	NR

Yield determined by ^{1}H NMR relative to internal standard

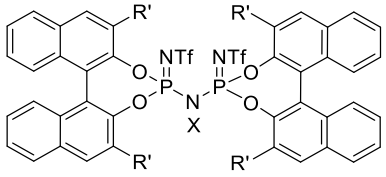

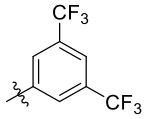

3,5-$(CF_3)_2C_6H_3$

Table 6: Continued Screen of Reaction Conditions

Our hypothesis was that by adding molecular sieves, trace water would be sequestered, decreasing the rate of the hydrolysis of acetal **92**, thereby increasing the formation of the desired cycloadduct **93b**. Surprisingly, 4Å molecular sieves completely inhibited the reaction, whereas the use of 5Å molecular sieves improved the reaction by decreasing the hydrolysis of **92** and improved the enantioselectivity at lower temperatures. The reason behind this anomalous result is unknown, however this result suggests that water could be a key part in the transformation and is needed to generate the oxocarbenium. So far, only dienes **91** and **95a** have been examined and the promising initial results gave us cause to pursue these catalysts as a general avenue towards asymmetric [4+3] cycloaddition reactions and acetal substitutions, henceforth the results will be presented in Chapter Four. Currently efforts are underway to improve the enantioselectivity and expand our limited scope by trying different oxyallyl cation precursors.

2.8 Conclusion

We have developed a useful methodology for the access to cyclohepta[*b*]indoles using a [4+3] cycloaddition reaction between 3-alkenyl indoles and oxyallyl cations. The reaction scope

has been fully explored with the stereoelectronic limits of the reaction having been well established. During our investigation, we have come across a novel application of imidodiphosphorimidate (IDPi) catalysts to achieve the [4+3] cycloaddition reaction enantioselectively with high yields and moderate selectivity.

Chapter 3 Synthetic Studies Toward Ambiguine Q

3.1 Introduction to the Ambiguines

Indole alkaloids have long been prized as synthetic targets for their structural complexity and biological activity. Of particular interest to our group are those isolated from the *Stigonemataceae* family of cyanobacteria.[1] Efforts by the Moore group saw a new class of hapalindoles arise from extracts of terrestrial cyanophytes *Fischerella ambigua, Hapalosiphon hibernicus*, and *Westiellopsis prolifica* 1.[2] Ambiguines A–F (Figure 3.1). Further study of related bacteria, such as *Hapalosiphon delicatulus*, [3] found the first nitrile group containing product, ambiguine G. The ambiguines are a family of indole alkaloid natural products, which possess the core structure of hapalindoles, but most members have an additional seven-membered ring that connects the C-2 position of indole with the distal cyclohexane ring. Tetracyclic ambiguines contain a reverse prenyl group at the C2, which helped elucidate the biosynthetic pathway of the pentacyclic ambiguines. Beyond the synthetic challenge, the bioactivity of these compounds has served as justification for their synthesis. Notably ambiguine I, has been shown to be a potent inhibitor (IC_{50} = 30nM), of NF-κB, expression of which inhibits apoptosis in cancer cell lines; other ambiguines exhibit considerable antifungal activity. With such a challenging framework to work towards, a unified route towards all of the pentacyclic ambiguines would be empowering to chemists and biologists alike, and therefore warrant significant effort be spent on its realization.

---

[1] Review of hapalindole family alkaloids: Bhat, V.; Dave, A.; Mackay, J. A.; Rawal, V. H. Chapter Two – The Chemistry of Hapalindoles, Fischerindoles, Ambiguines and Welwitindolinones. *The Alkaloids: Chemistry and Biology*; Elsevier, Inc.: 2014; Vol. 73, pp 65−160.
[2] Smitka, T.A.; Bonjouklian, R.; Doolin, L.; Jones, N. D.; Deeter, J. B.; Yoshida, W. Y.; Prinsep, M. R.; Moore, R. E.; Patterson, G. M. L. *J. Org. Chem.* **1992**, *57*, 857.
[3] Huber, U.; Moore, R. E.; Patterson, G. M. L. *J. Nat. Prod.* **1998**, *61*, 1304.

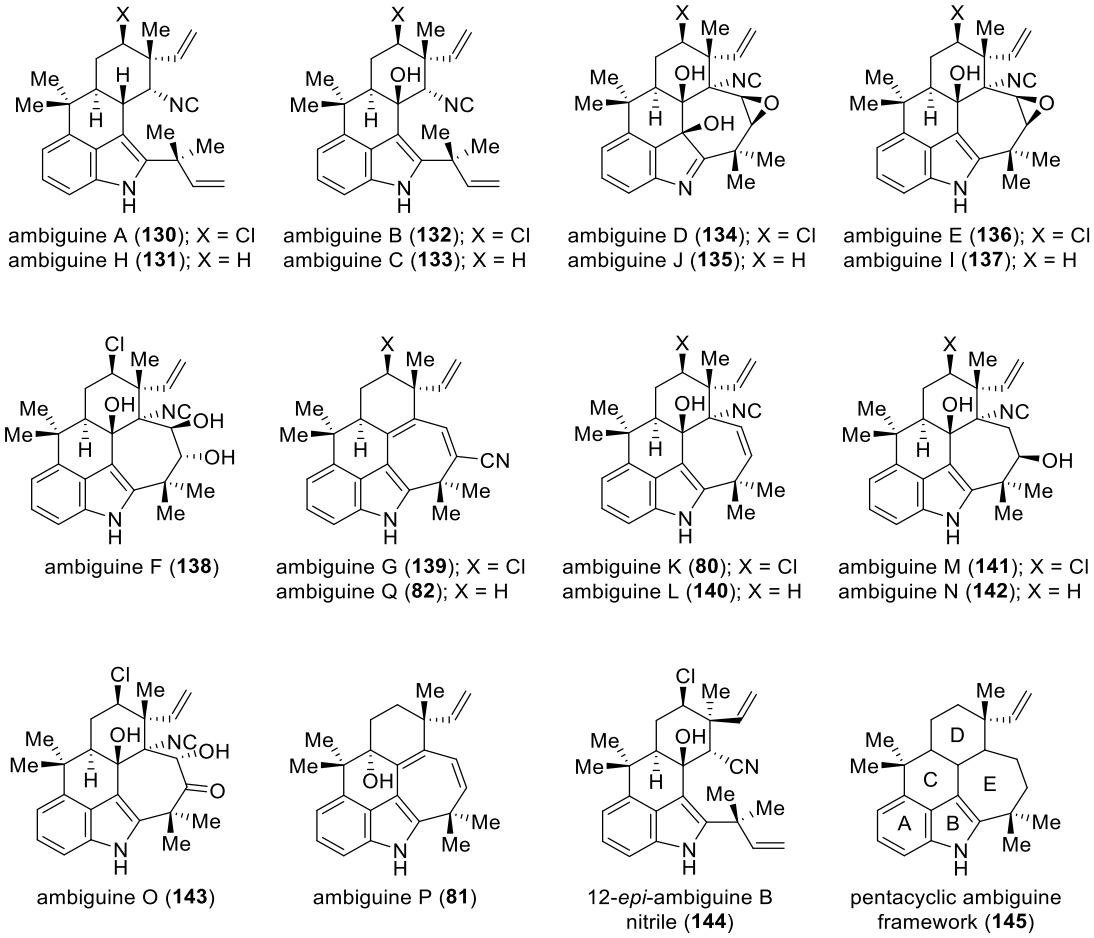

Figure 5: The Ambiguine Alkaloids

Synthesis of the pentacyclic ambiguines has been a long-standing challenge that has eluded the efforts of many research groups for several decades. To date, most members of the hapalindoles, including many tetracyclic ambiguines, have been synthesized. However, to date only one pentacyclic ambiguine, ambiguine P, has been successfully synthesized by both the Sarpong and Rawal groups.

3.2.1 Sarpong's Synthesis of Ambiguine P

In the first publication of the total synthesis of a pentacyclic ambiguine, the Sarpong group's work proved foundational and expansive in the area of total synthesis.[4] The construction of the pentacyclic core takes full advantage of well-established disconnections, but through the use of a seldom seen Nicholas reaction the construction of the petacycle is remarkably elegant.

The synthesis (Scheme **27**) starts with Baran's copper mediated coupling of (S)-carvone to the C3 of indole to give **147**,[5] setting the C15 stereocenter. Initial 1,2-addition of propargyl alcohol **148**, and subsequent oxidative transposition sets the stage for the key cyclization onto C2 through a Nicholas reaction, affording the seven-membered E ring over cyclization to either C3 or C4. Cyclization of the isopropenyl group onto C4 gave the complete skeleton in excellent yield and regioselectivity. This construction also sets a convenient handle for conjugate nitrile addition at C11, serving as both a functional handle to install an isonitrile, and as a directing group for setting the C12 quaternary center.

[4] Johnson, R. E.; Ree, H.; Hartmann, M.; Lang, L.; Sawano, S.; Sarpong, R. *J. Am. Chem. Soc*. **2019**, *141*, 2233.
[5] Richter J. M.; Ishihara, Y.; Masuda, T.; Whitefield, B. W.; Llamas, T.; Pohjakallio, A.; Baran P. S. *J. Am. Chem. Soc.* **2008**, *130*, 17938-17954.

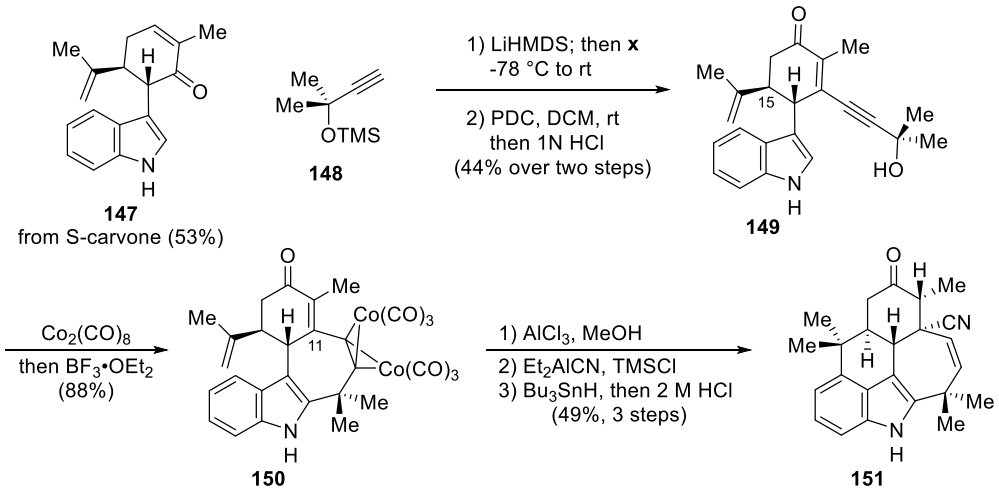

Scheme 27: Sarpong's Construction of the Pentacyclic Core

With such a reliable route in hand, efforts turned towards the construction of the C12-methyl, vinyl center. Direct attempts at vinylation failed to give the correct stereochemistry. Instead, hydration of the nitrile, formylation, and subsequent reduction gave a handle with the correct relative stereochemistry **152** (scheme **28**). Treatment with triflic anhydride, revealed cyano-aldehyde **153**, and subsequent Barton-McCombie deoxygenation gave aldehyde **154** in modest yield. Using a Peterson-like olefination generates the necessary C12 quaternary center along with a primary amide at C11, which serves as the handle for installing the required isonitrile group **155**.

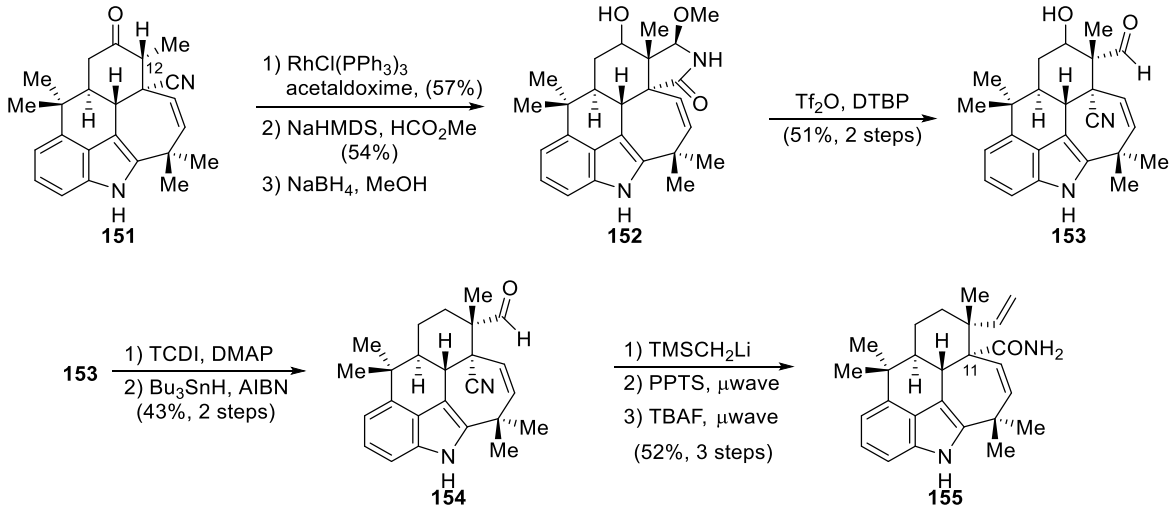

Scheme 28: Sarpong's completion of the skeleton

Hypervalent iodine-mediated Hoffman rearrangement of **155** afforded amine **156** in modest yield (Scheme **29**), with complications arising from the presence of indolenine formation through C2-C3 aziridation and subsequent ring opening. Formylation/dehydration of primary amine **156** gave the desired isonitrile **157** in excellent yield. Elimination of the isonitrile with potassium tert-butoxide and allylic oxidation gave ambiguine P in 21 steps and 0.016% from tricycle **147**.

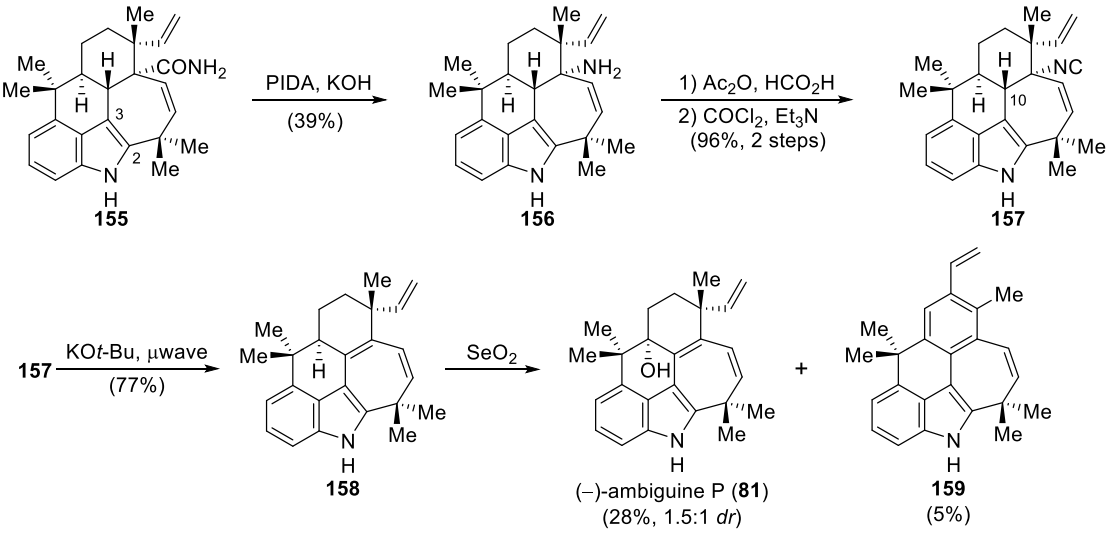

Scheme 29: Completion of ambiguine P

While the C11-isonitrile group is a feature in more complex pentacyclic ambiguines, the published route ablated the handle in favor of delivering ambiguine P. Sarpong et al. have made great strides towards the synthesis of the pentacyclic ambiguines, and additional members of the family may yield to synthetic efforts soon.

3.2.2 Rawal Synthesis of Ambiguine P

The Rawal synthesis of ambiguine P, begins with the synthesis of the Mehta-Baran ketone, **160**, which is converted to enone **161** by sequential triflation and Stille coupling.[6,7] Formation of the silyl enol ether **162** proceeds through standard conditions (Scheme **30**). Treating a 2:1 mixture of silyl alcohol **163**, and diene **162**, with an equivalent of TMSOTf, gives enone **164**, an incomplete cyclized product which arises presumably due to the poor stability of the intermediate

[6] Xu, J.; Rawl, V. H. J. Am. Chem. Soc. **2019**, *141*, 4820.
[7] (a) Baran, P. S.; Maimone, T. J.; Richter, J. M. *Nature* **2007**, *446*, 404. (b) Mehta, G.; Acharyulu, P.V.R.; *J. Chem. Soc., Chem. Commun*. **1994**, 2759-2760.

siloxycarbenium ion. Intramolecular Michael cyclization and subsequent Brønsted-Acid catalyzed cyclization onto C-4 gives the pentacyclic indole framework **165** in good overall yield.

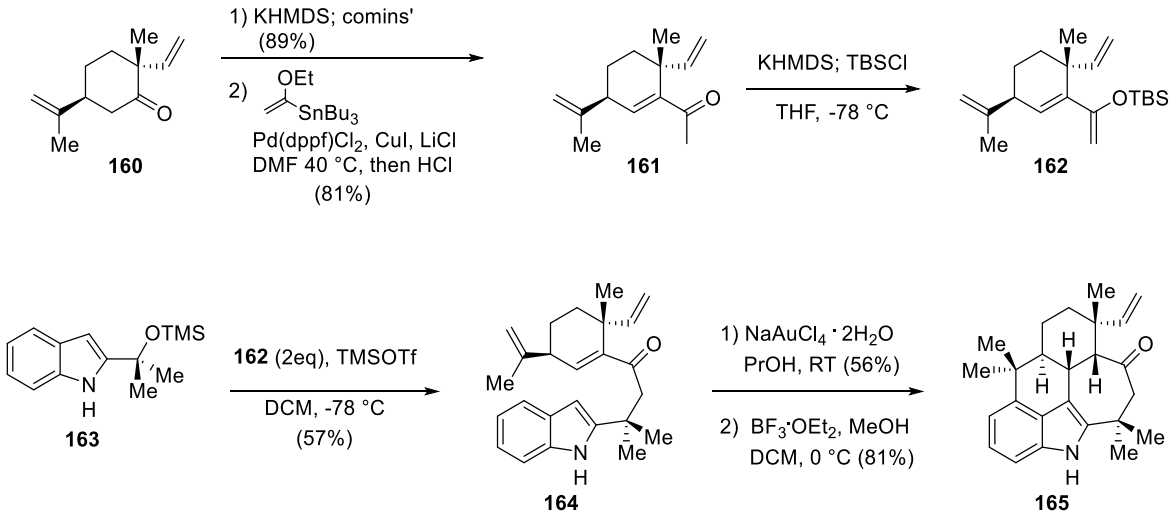

Scheme 30: Rawal construction of pentacyclic core

After construction of the complete skeleton **165**, a sequence of oxidations and protection leads to enone **166**. Reduction of enone **166**, and elimination of the allylic alcohol led to triene **167**. Boc-deprotection of indole **167**, and subsequent treatment with NBS leads to the formation of ambiguine P (**82**). Initially, our route envisioned direct functionalization at C23, however serendipitous oxidation occurred at C15 leading to formation of ambiguine P in 10 steps and 4.8% overall yield from ketone **160** (scheme **31**).

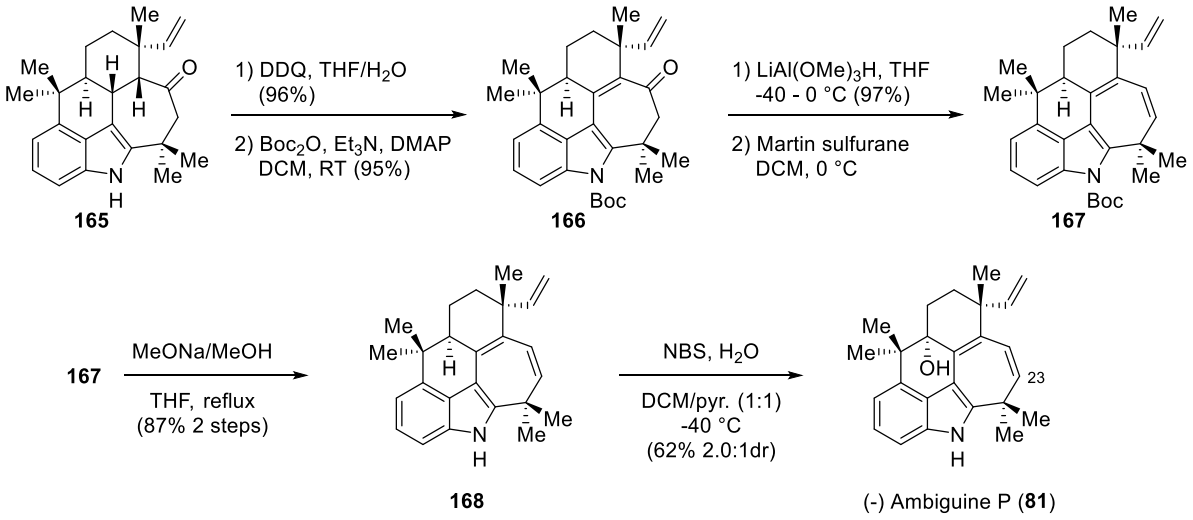

Scheme 31: Rawal's synthesis of Ambiguine P

One difficulty both routes faces is the ablation of the stereocenter at C15; thus an unavoidable complication results as the oxidation of C15 is favored over C23 functionalization. As such any synthesis which uses this intermediate en route to a different ambiguine will face similar challenges. One of the goals of the present work was to develop a strategy wherein the stereocenter at C15 would not be ablated in the later stages of the synthesis. To this end, we sought to employ our [4+3] cycloaddition methodology to access the ambiguine skeleton diastereoselectively. Ultimately, our goal is to establish a unified route to the ambiguines through a common intermediate. As a proof of concept, our first target is the relatively simple ambiguine Q.

3.3 Retrosynthetic Analysis of Ambiguine Q

Our retrosynthetic analysis of ambiguine Q sees the C23 nitrile arising as from a carbonyl handle in enone **169** through either a cyanohydrin elimination or a palladative cyanation of the corresponding vinyl halide. Enone **169** would arise from the isomerization and subsequent di-methylation of cycloadduct **170**, taking advantage of the increased acidity of the α-phenyl ketone

to complete the skeleton. Lastly, elimination of methanol would result in the formation of the desired enone **169**. Cycloadduct **170** is the expected product of our [4+3] cycloaddition methodology from Chapter Two, and the requisite diene **171**, can be either a tri- or tetracyclic compound, depending on whether or not the bond to C4 is established.

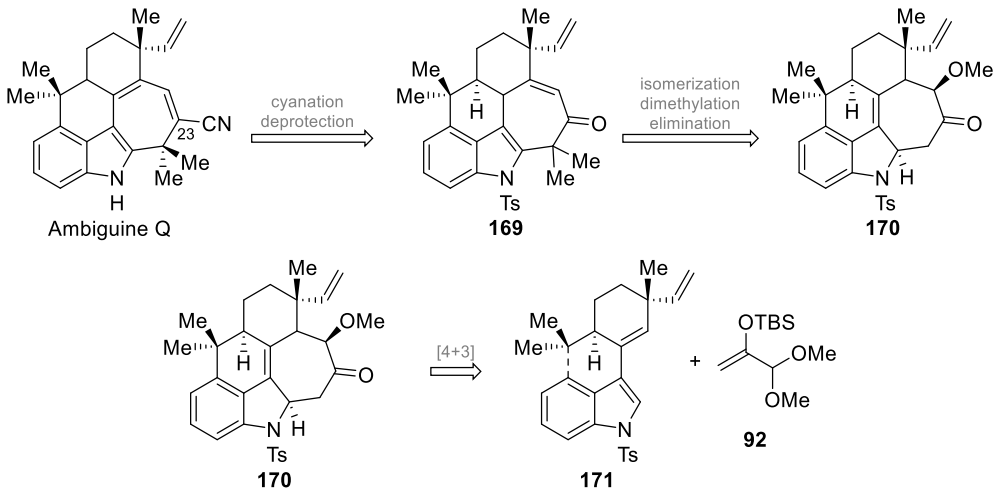

Figure 6: Retrosynthetic analysis of ambiguine Q

The key [4+3] cycloaddition should be possible with either the tricyclic diene **173**, made through route A or the tetracyclic diene **171** made through route B (Figure **7**). In route A: Suzuki cross-coupling reaction between the N-tosyl indole-3-boronic acid **96** and the corresponding decorated cyclohexenyl-triflate **174** would parallel the 3-cyclohexenyl indole developed during our study of the methodology. Alternatively, route B would more closely resemble the use of the original tricyclic diene **91**, as the diene is rotationally locked and the indole C4 bond is already in place. We recognized that route A, might suffer additional complications arising from the presence of the isopropenyl group. Friedel-Crafts cyclization of the isopropenyl onto the C-4 of indole is complicated by attack at C-3 and subsequent migration to C-2 to give the cyclopenta[*b*]indole framework found in fischerindoles. This was used in the synthesis of various fischerindoles by

Baran where this transformation was used to converted hapalindoles into fischerindoles.[8] Due to this reactivity, the [4+3] would need to be performed first to avoid this potential deleterious skeletal rearrangement.

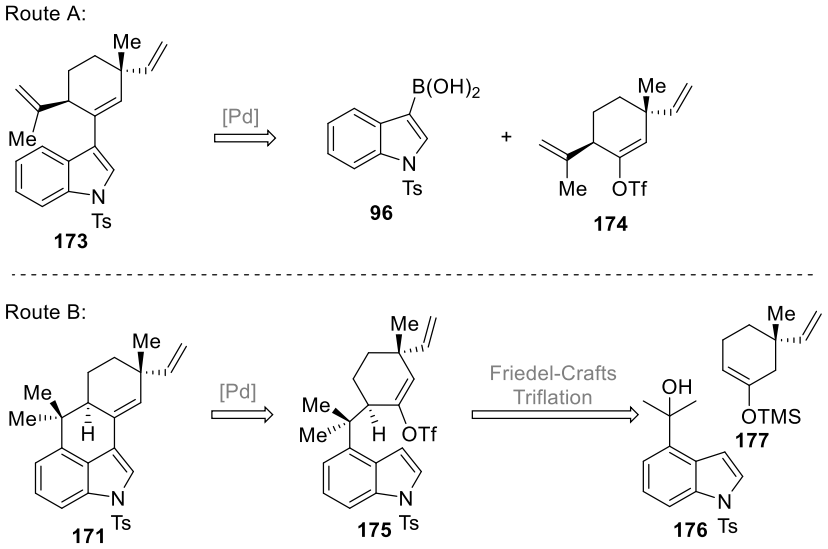

Figure 7: Retrosynthesis of diene **171**

Despite our best efforts, attempts at studying route A were unsuccessful. Problems arose during substrate preparation as well as the key [4+3] cycloaddition, which failed to provide any of the desired cycloadduct. These difficulties prompted us to abandon this approach and instead focus on route B. Based on the extensive alkaloid work by Natsume,[9] route B would take advantage of the Friedel-Crafts reaction between tertiary benzylic alcohol **176** and silyl enol ether **177**. The resulting ketone can then be used to generate enol triflate **175** and subsequent palladium mediated C-3 alkenylation would lead to the desired diene.[10] While this approach is less direct, we predicted

[8] (a) Baran, P. S.; Richter, J. M. *J. Am. Chem. Soc*. **2004**, *126*, 7450. (b) Richter, J. M.; Ishihara, Y.; Masuda, T.; Whitefield, B. W.; Llamas, T.; Pohjakallio, A.; Baran, P. S. *J. Am. Chem. Soc.* **2008**, *130*, 17938-17954.
[9] Muratake, H.; Natsume, M. *Tetrahedron* **1990**, *46*, 6331.
[10] Lane, B. S.; Brown M. A.; Sames D. *J. Am. Chem. Soc.* **2005**, *127*, 8050-8057.

that the *s*-cis-locked diene would be more adept at undergoing the [4+3] cycloaddition. Additionally, chirality can potentially be introduced through enantioencriched silyl enol ether **177** by utilizing chemistry developed by Alexakis.[11]

3.3 Model Studies for Route B

The synthesis of the model system for route B (Scheme **32**) starts with commercially available methyl indole-4-carboxylate **178**. Protection of the indole nitrogen and subsequent methyl Grignard addition delivered key tertiary alcohol **176** as a crystalline solid. Friedel-Crafts addition with the commercially available silyl enol ether of cyclohexanone **179** gave ketone **180** in excellent yield. Triflation of the ketone gives the desired enol triflate **181** in excellent yield and palladium-mediated intramolecular arylation gives the 3-alkenyl indole **182** in near quantitative yield. Cyclization onto C3 must proceed through a two-step triflation and palladium-mediated alkenylation to avoid the formation of the more thermodynamically stable endocyclic alkene isomer, which is observed via Lewis acid mediated cyclization as the sole product as described by Natsume.[74]

[11] Alexakis, A. and Benhaim, C. *Eur. J. Org. Chem*., **2002**, 3221-3236. (b) Tissot, M., Poggiali, D., Hénon, H.; Müller, D.; Guénée, L.; Mauduit, M.; Alexakis, A. *Chem. Eur. J*., **2002**, *18*, 8731-8747.

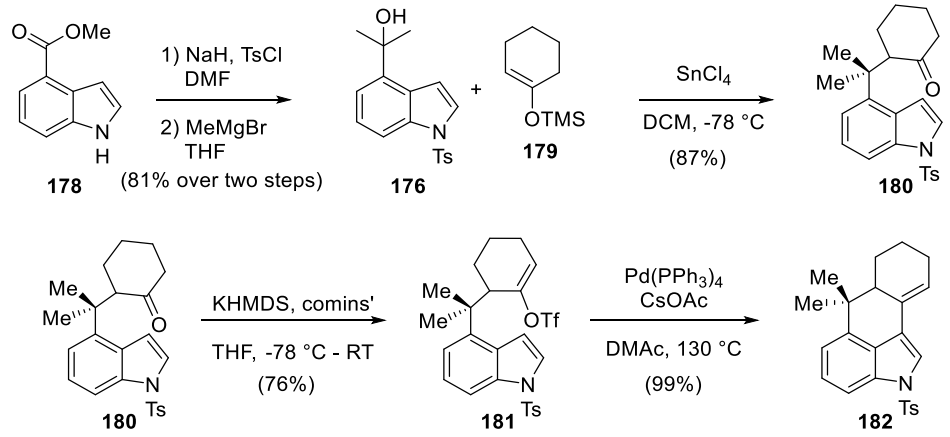

Scheme 32: Model studies towards Route B

With rotationally locked alkenyl indole **182** in hand, hopes were high that this model substrate would deliver the pentacyclic framework in higher yield than was observed with diene **95m**. Upon subjecting diene **182** to our optimized reaction conditions from the methodology, the dearomative [4+3] cycloaddition reaction proceeds smoothly to give the desired cycloadduct in 95% yield as a single diastereomer (Scheme **33**). With such a promising result in hand, efforts turned to exploring a more sterically encumbered substrate before advancing to the real system.

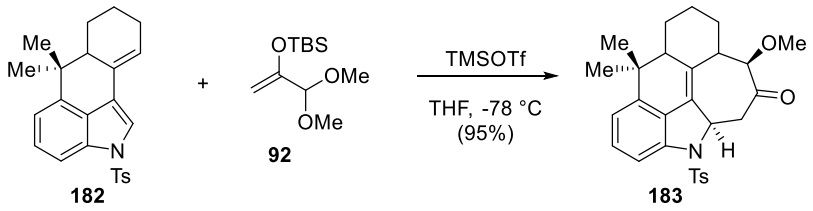

Scheme 33: [4+3] Cycloaddition of Model Compound **182**

3.4 Model Studies Route B – Gem Dimethylated Analogue

With positive results from the simple model substrate, efforts turned towards to a more directly comparable model with similar steric concerns. The synthesis of the 3-alkenyl indole **186** begins, as before with tertiary benzylic alcohol **176**. Friedel-Crafts alkylation with 3,3-dimethyl silyl enol ether **184** gives ketone **185** on gram-scale albeit in modest yield. The cyclization to give

the 3-alkenyl indole **186** is carried out analogously to the previous model; the overall yield of this sequence is significantly lower, especially the triflation which only proceeds in 26% yield. Presumably this result is due to the increased steric congestion around the 5 position of the cyclohexanone. However, the palladium cyclization proceeds in only slightly lower yield giving the 3-alkenyl indole in 82% yield (Scheme **34**).

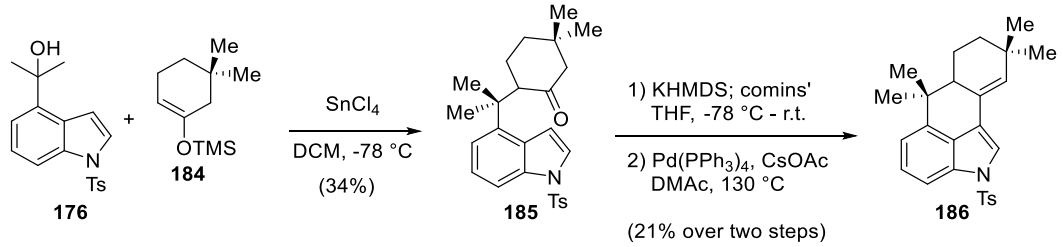

Scheme 34: synthesis of the gem-dimethyl Model Compound 186

Upon synthesis of 3-alkenyl indole **186**, the [4+3] cycloaddition reaction was examined to test the feasibility of pursuing the ambiguine skeleton bearing the methyl/vinyl quaternary center. Initial attempts at the cycloaddition with previously optimized reaction conditions gave none of the desired cyclohepta[*b*] indole (Scheme **35**). In contrast to the high yield of model compound **183**, the cycloaddition reaction of the di-methylated model compound **186**, did not proceed under the same conditions. Presumably the increased steric congestion of the quaternary center of the alkene slows the initial stages of the reaction. We suspect that if the reaction were to undergo a stepwise cyclization, then the use of stabilizing, polar additives such as nitroalkanes would stabilize the charged intermediates, thereby enabling the desired cycloaddition. Initially, running the reaction in nitroethane furnished the desired cycloadduct **187** in good yield, however we rationalized that further improvements could be realized by increasing the temperature of the reaction. Continued experiments under this assumption saw a drastic improvement in the reaction and an isolated yield of 50%, increasing further to 56% upon warming to -63 °C (Scheme **35**). We

suspect that at higher temperatures the trapping of the transient oxocarbenium ion generated by the reaction of **92** and TMSOTf is more facile. In this vein, an even higher temperature was tried, and to our surprise, the isolated product was cyclopentenone **188** which was obtained in 81% yield as a colorless crystal. Overall, a 56% yield for a sterically congruent system was sufficient for pursuing the methyl-vinyl quaternary center found in the ambiguines.

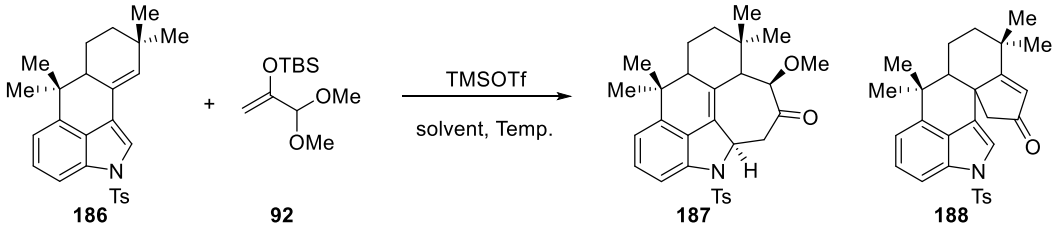

Entry	Solvent	Temp. (°C)	Result
1	THF	-78	NR
2	$EtNO_2$	-78	44%[a]
3	$EtNO_2$	-78	50%[b]
4	$EtNO_2$	-45 - r.t.	81% **188**[b]
5	$EtNO_2$	-63	56%[c]

[a] determined by ^{1}H-NMR relative to **186**; [b] yield in isolation;
[c] yield on 1mmol scale

Scheme 35: [4+3] Cycloaddition of gem-dimethylated Model Compound **186**

3.5 Setting the C15 Stereocenter

Upon completion of the model substrates and preliminary examination of the key [4+3] cycloaddition, efforts turned towards the construction of the 3-alkenyl indole bearing the methyl-vinyl quaternary center. Our synthesis begins with the Lewis acid-catalyzed Friedel-Crafts alkylation just as in the model system, however due to the presence of the chiral quaternary center the diastereoselectivity of the reaction becomes an issue. The reaction of kinetic silyl-enol ether of 3-methyl-3-vinyl cyclohexanone **177** and alcohol **176** gave the alkylation product in 51% yield, the product was formed as a 1: 1.2 ratio of diastereomers at C15. This poor selectivity was rationalized as a result of the small difference between the A values of a methyl and vinyl group,

1.7 and 1.68 kcal/mol respectively. [12] From this result, we speculated that by controlling the relative size of the vinyl group, we might be able to tune the diastereoselectivity of the Friedel-Crafts reaction between silyl enol ethers **177 a-d** and alcohol **176** (Scheme **36**).

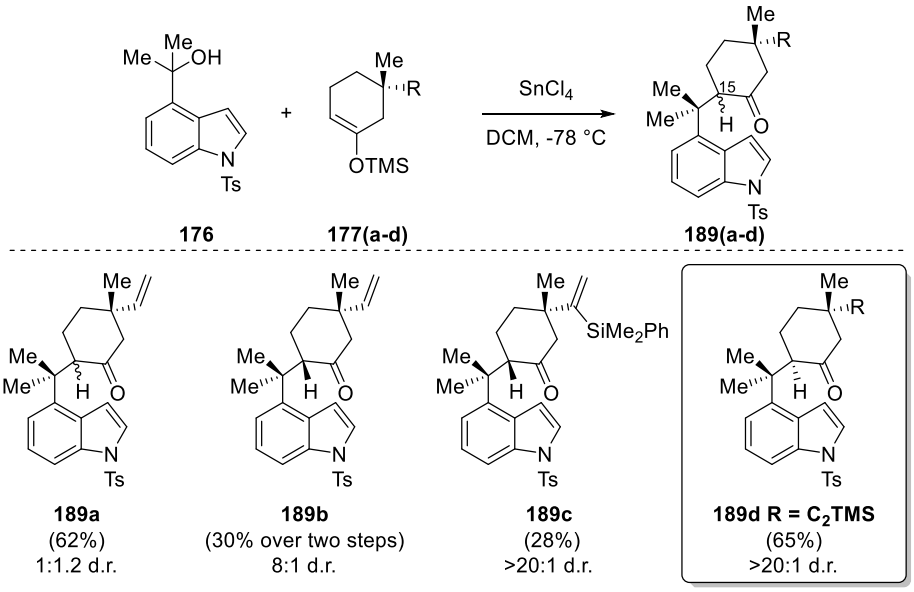

Scheme 36: Summary of C15 Diastereoselectivity

Increasing the size of the vinyl group can be achieved through the addition of bromine across the alkene to give **191**, increasing its size relative to vinyl; potentially as much as an isopropyl group (A-value ≈ 2.15 kcal/mol). Formation of the kinetic silyl enol ether **177b** and Friedel-Crafts alkylation gives the desired adduct, which is then dehalogenated with zinc dust and sonication, giving adduct **189b** in 30% overall yield with an 8:1 ratio of diastereomers (Scheme **37 a**). Additionally, the vinyl silane **177c** was used to form ketone **189c** as a single diastereomer in 28% yield, however as expected, in both cases the undesired diastereomer was obtained as the major product. Instead we theorized that the relative size of the vinyl group could be reduced by instead using the methyl-alkynyl ketone **193**. (A-value of TMS alkyne ≈ 0.5 kcal/mol). Conjugate

[12] Eliel, E. L. *J. Org. Chem.* **1981**, *46*, 1959.

addition of lithium trimethylsilylacetylide to 3-methyl cyclohexen-2-one gives the methyl-alkynyl ketone **193** in excellent yield. Formation of the kinetic silyl enol ether proceeds smoothly under soft enolization conditions and the Friedel-Crafts alkylation with tertiary alcohol **176** gives the desired adduct **189d** in high yield and diastereoselectivity (Scheme **37 b**).

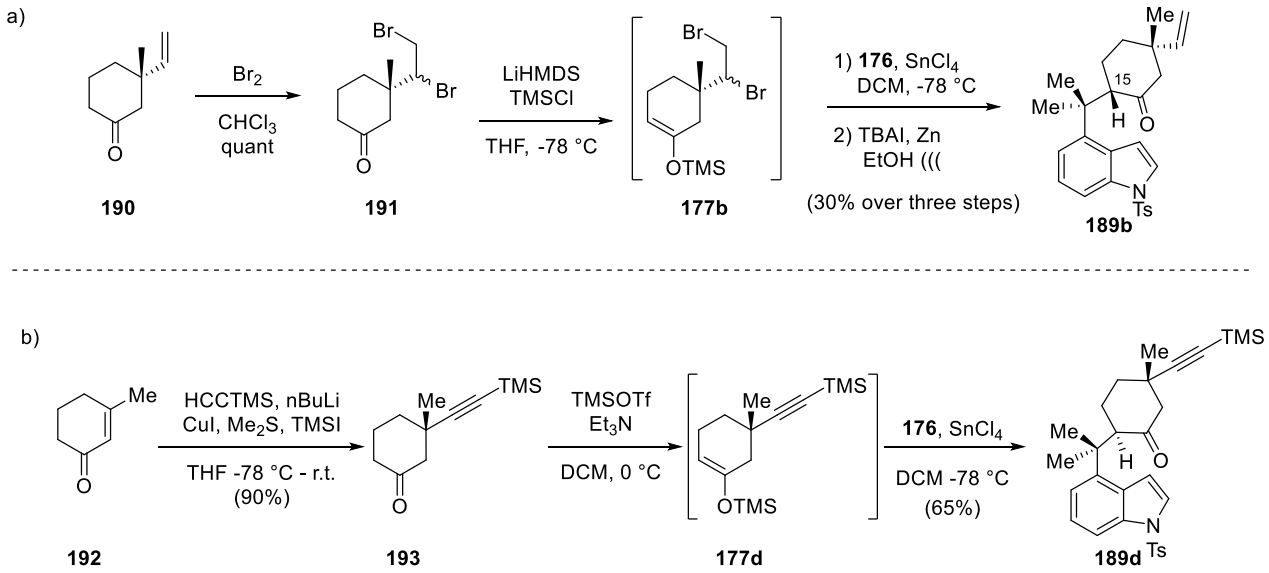

Scheme 37: Setting the stereocenter at C15

3.6 Synthesis of the key 3-alkenyl indole

With the desired stereocenter at C15 set, elaboration towards 3-alkenyl indole **171** proceeds well (Scheme **38**). The conversion of methyl-alkynyl ketone **189d** to the desired methyl-vinyl ketone **195** proceeds in quantitative yield through fluoride promoted protodesilylation in the presence of pivalic acid to form alkyne **194** and subsequent partial hydrogenation with Lindlar's conditions. The protodesilylation proceeds well under a variety of conditions, however prolonged treatment with base epimerizes the C15 center. With ketone **194** in hand, formation of the enol triflate **175**, was optimized by using KHMDS to give the desired product in 84% yield; LDA

affords the desired product in < 50% yield. The palladium cyclization proceeds well giving the key 3-alkenyl indole **171** in 71% yield, but the results are inconsistent and no clear reason for this inconsistency has been identified. The reaction performs equally well with various phosphine ligands (e.g. $P(o\text{-}tol)_3$ or $P(tBu)_3$), however yield decreases significantly if run at lower temperatures. This stands in contrast to the simple model triflate **181**, which could be cyclized in near quantitative yield even at lower temperatures.

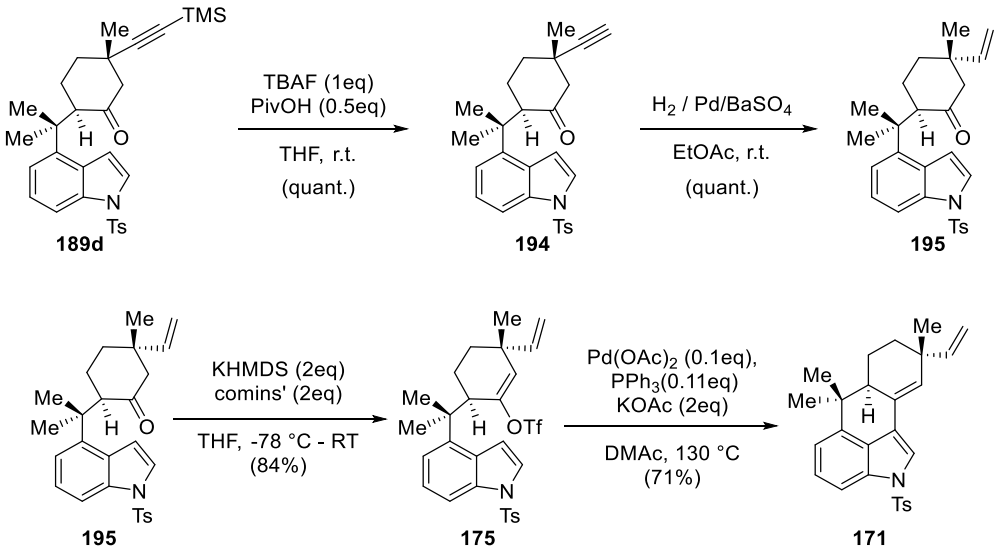

Scheme 38: Construction of 3-alkenyl indole **171**

Based on our investigations with model compound **186**, we hypothesized that steric effects caused by the quaternary center decreases the reactivity in the [4+3] cycloaddition. As a result, we considered performing the partial hydrogenation after the [4+3] cycloaddition. To this end, triflation of **189d** was carried out to give enol triflate **175b** in high yield, however the subsequent palladium cyclization did not give any of the 3-alkenyl indole. The reason behind the lack of reactivity of the enol triflate of **189d** with palladium is unknown, however a chelation effect between the alkyne and palladium is suspected. With the key 3-alkenyl indole **171** prepared, investigations into the cycloaddition could be carried out analogously to model system **186**.

3.7 Investigation of the Key [4+3] Cycloaddition

While significant efforts were devoted to the general cycloaddition reaction of 3-alkenyl indoles, the total synthesis demanded a more specific look into its optimum conditions. Initially, the reaction suffered from several issues chiefly: low yields, low diastereoselectivity, and deleterious side reactions (e.g. incomplete cyclization or [3+2] cycloaddition). To address each of these issues, a systematic screen was conducted to ferret out more optimum conditions, an abridged overview of which can be seen in Table **7**. Firstly, the solvent of the reaction was determined to be crucial as a nitroalkane solvent is needed to stabilize the oxocarbenium intermediate formed by the reaction of the acetal **92** and TMSOTf.

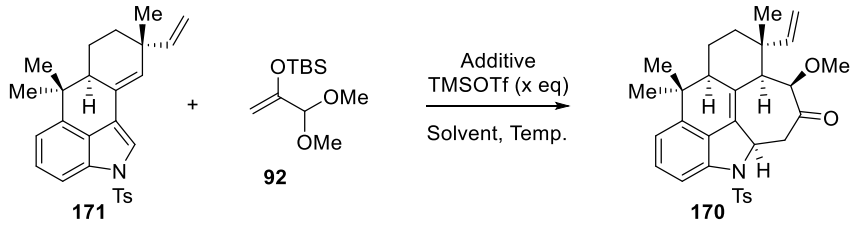

Additive	Solvent (0.1M)	Temperature (°C)	TMSOTf (eq)	Result
None	DCM	-78	excess	NR
None	THF	-78	excess	NR
None	$EtNO_2$	-78	excess	NR
None	$EtNO_2$	-40	excess	20%[a]
None	$^{i}PrNO_2$	-78	excess	NR
None	DCM, $iPrNO_2$ (1:1)	-78	excess	NR
None	DCM, $EtNO_2$ (1:1)	-45	excess	31%[b]
2,6($tBu)_2$ - 4MePyr (10 mol%)	DCM, $EtNO_2$ (5:1)	-78	2	24%[b,c]
2,6($tBu)_2$ - 4MePyr (10 mol%)	DCM, $EtNO_2$ (20:1)	-78 - -60	0.7	34%[b,c]

[a] conversion by 1H NMR; [b] yield in isolation; [c] no deleterious side reactions observed

Table 7: Optimization of Conditions for the [4+3] cycloaddition

When the reaction was carried out in less polar solvents such as THF or DCM none of the desired cycloadduct was observed. When attempting to run the reaction in nitroethane at -78 °C, the insolubility of the 3-alkenyl indole **171** complicated the reaction and no desired product was obtained. However, when nitroethane or 1-nitropropane were used at slightly elevated

temperatures, the cycloadduct **170** was obtained as the major product, albeit as a mixture of diastereomers in 20% yield. Reactions run at higher temperatures saw the presence of **197**, an adduct similar to that obtained during our model studies with diene **186**. Other nitroalkanes, such as 2-nitropoane or nitromethane were unable to afford the desired product. We rationalized this observation as being the result of the stabilizing influence of the nitroethane on the oxocarbenium intermediate. We hypothesized that in order to improve the selectivity of the reaction a decrease in the temperature would be needed. Unfortunately, the poor solubility of **171** in nitroethane would inhibit the reaction, so instead using a cosolvent such as DCM would allow us to run the reaction at lower temperatures. Initial experiments using a 1:1 mixture of solvents gave none of the desired cycloadduct at -78 °C, but increasing the temperature worked to deliver the desired product in 31% yield, but unfortunately solubility remained an issue. The most important discovery was that the inclusion of a small amount (5%) of nitroethane to the solvent mixture was effective in promoting the reaction, reliably increasing both the yield and diastereoselectivity of the reaction (relative stereochemistry assigned by 1D NOESY spectroscopy). Based on the presumptive reaction mechanism (Scheme **39**), the addition of additional equivalents of **92** should improve the yield of the reaction as the active oxacarbenium **98** would, over time, be quenched. Unfortunately, no improvement of yield was observed upon the addition of more equivalents of **92**. Further changes in order of addition or rate of addition did not improve the yield of the reaction, so far, the reason behind this observation is unknown.

On recovering unreacted starting material, large quantities of the endocyclic alkene isomer of **171** were found, which can be rationalized by way of triflic acid induced isomerization. To avoid decomposition to an unreactive, inseparable material, 2,6-ditertbutyl-4-methyl-pyridine was added to the cycloaddition reaction. Initial trials revealed that the deleterious protoisomerization

was easily prevented, however at higher loadings of the pyridine base, the reaction was inhibited. Ultimately, the inclusion of substoichiometric amounts (10-20 mol%) of 2,6-ditertbutyl-4-methyl-pyridine allowed for the reaction to proceed in >90% brsm.

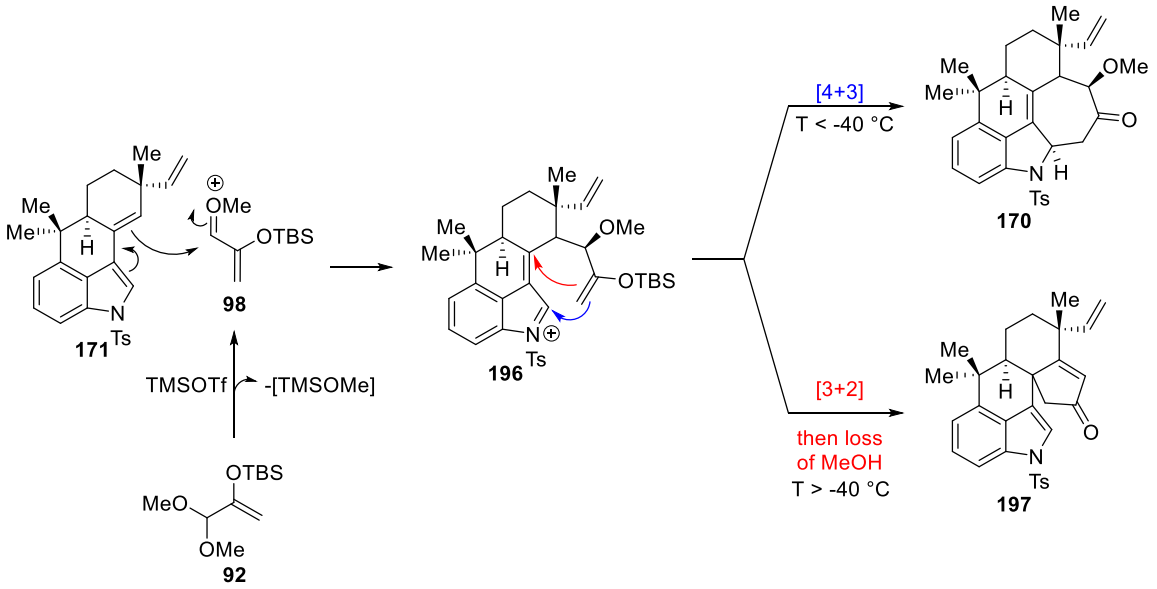

Scheme 39: Proposed Mechanism of the [4+3] cycloaddition

The effect of temperature is twofold. First, the effect on reactivity is obvious, as the interception of the oxocarbenium ion **98** is slow at low temperatures. This step also sets the relative stereochemistry for all atoms on the E ring, which means that in order to achieve high diastereoselectivity lower temperatures are required. While ultimately inconsequential, interpretation of spectra of late stage intermediates was difficult when working on mixtures of diastereomers and ultimately this work only accelerated after single diastereomers were isolated for the first time. Another deleterious effect of increasing the temperature is the increase in the formation of the undesired [3+2] adduct **197**, which can be obtained in significant yields (>80%) above 0 °C but starts forming around -40 °C. The formation of this compound is best rationalized as the addition of the silyl enol ether into the benzylic cation as opposed to the C-2 of the indole,

resulting in a cyclopentanone which rapidly loses methanol in the presence of excess TMSOTf (Scheme **39**). As it stands the key step has been optimized to give the desired product in a moderate yield: 39% (97% brsm) as a single diastereomer.

3.8 Use of dimethyl oxyallyl cation precursors

While the formation of cycloadduct **170** marks a key milestone in the synthesis of ambiguine Q, the reaction with either mono or dimethyl oxyallyl precursors, (**92b** or **92c**), would be advantageous as either would deliver the ambiguine skeleton in a more efficient manner. Particularly acetal **92c** would complete the skeleton in a single step and drastically improve the efficiency of the route. Unfortunately, neither of the oxyallyl precursors **92b** or **92c**, gave the cycloadducts **201** or **202**. We rationalize this as the result of the increased steric demands of the reaction, decreasing the reactivity of the [4+3] cycloaddition. (Scheme **40**). Attempts at increasing the temperature, or solvent composition did not alter the outcome. As it stands, efforts are still being devoted to this route as the benefits of a one-step construction of the pentacycle would warrant significant efforts.

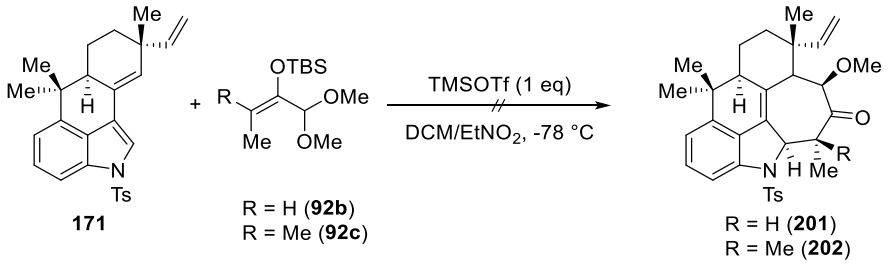

Scheme 40: attempted cycloaddition with alkylated oxyallyl cations

3.9 Elaborating the [4+3] cycloadduct towards Ambiguine Q

The construction of the pentacyclic framework marks an important milestone towards the final product and as a useful handle to access more functionalized pentacyclic ambiguines.

Completion of the ambiguine skeleton requires gem-dimethylation at C24, a transformation we initially thought of as simple owing to the neighboring carbonyl group. Additionally, protoisomerization of the cycloadduct **170** to indole **203** is needed; based on our work presented in Chapter Two, the transformation is non-trivial and attempts were made using all previously examined conditions. Just like the simple model substrates discussed during our methodology work, the rearomatization of the cycloadduct **170** to indole **203** via protoisomerization of the alkene proved quite difficult. Several common protocols for protoisomerization of alkenes were examined, including refluxing TFA, DBU, or catalytic $Fe(OTf)_3$.[13] Disappointingly, in all cases only minor conversion to desired indole was observed. Fortunately, the use of catalytic TMSI, generated in situ, afforded the desired indole **203** cleanly and in good yield. However, attempts at methylation of **203** failed to produce any of the desired gem-di-methylated product. The use of a large excess of TMSI, generated in situ, accomplished both the deoxygenation and isomerization to afford ketone **204** in 96% yield. (Scheme **41**). As the yield of the concomitant deoxygenation/isomerization is higher than just isomerization, larger quantities of **204** could be produced, as such efforts were directed towards studying the reactivity of ketone **204**.

[13] (a) Simoji, Y.; Saito, F.; Tomita, K.; Morisawa, Y. *Heterocycles* **1991**, *32*, 2389–2397. (b) Tan, B.; Hernández-Torres, G.; Barbas III, C. F. *J. Am. Chen. Soc.* **2011**, *133*, 12354–12357. (c) Nakano, S.; Inoue, N.; Hamada, Y.; Nemoto, T. *Org. Lett.* **2015**, *17*, 2622–2625. (d) Kundal, S.; Jalal, S.; Paul, K.; Jana, U. *Eur. J. Org. Chem.* **2015**, 5513–5517.

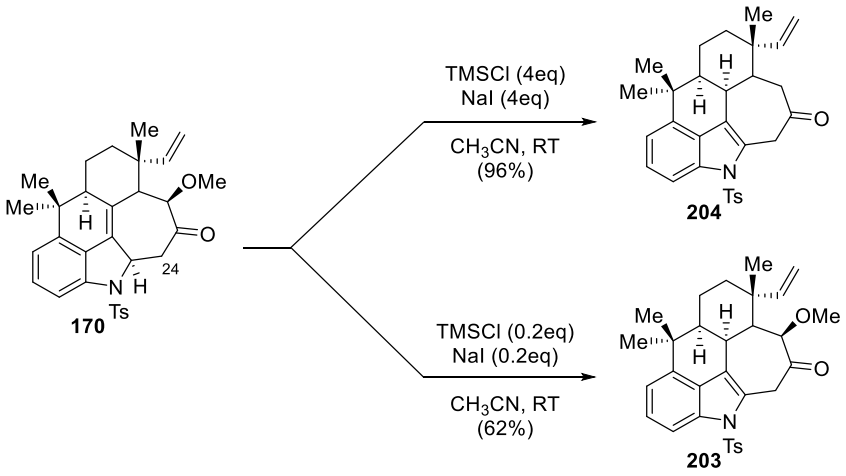

Scheme 41: Rearomatization of the Indole and Deoxygenation

Completion of the skeleton requires di-methylation at C24, which is well precedented in the literature owing to the acidic nature of α-phenyl ketones. Typical phase transfer conditions are in most cases sufficient to dimethylate tetralones in excellent yields. In our system, the only product was the monomethylated ketone **205** in 93% yield; which can be obtained in excellent yield as single diastereomer. Changes in the reaction setup such as alternative methylating reagents or phase transfer catalysts failed to improve the reaction, and under no phase-transfer conditions was the gem-dimethylated ketone observed. Alternatively, sodium hydride in DMF, which has been used successfully in related systems gave only a 1:2 mixture of the monomethylated ketone **205** and the methyl enol ether **207**. [14] An extensive search of conditions was attempted, however the gem-dimethylated ketone **206**, was only ever observed in trace quantities.

[14] Dattatraya, D. *Org. Chem. Front.* **2015**, *2*, 548-551.

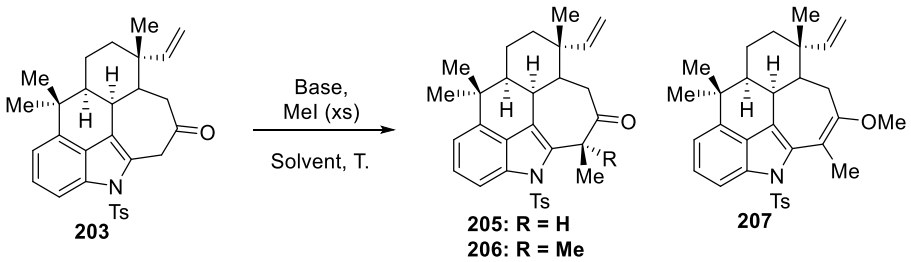

Base	Solvent	Temp. (°C)	Result
KOH (50% aq. sol.)	PhMe	r. t. - 40	93% **205**, 1:0 dr[a]
NaOH (50% aq. sol.)	PhMe	90	91% **205**, 1:0.6 dr[a]
MeONa (15%)	MeOH	r.t. - 40	78% **205**[a]
NaH	DMF	-10 - r.t.	1:2 **205**:**207**[b]
KOtBu	THF	0 - r.t.	NR
KH	THF	0 - r.t.	67% **205**[b]
KH	THF	0 - 65.	decomposition
LDA	Et_2O	-78 - r.t.	NR
LDA	THF	-78 - r.t.	47% **205**[b]
LHMDS	THF	-45 - r.t.	12% **205**[b]

[a] yield in isolation, [b] determined by ^{1}H-NMR relative to **203**

Table 8: Attempts at C24 gem-di-methylation

While the monomethylated product **205**, could be obtained cleanly and as a single diastereomer, the difficulties in obtaining the demethylated compound **206** limited the potential of this construction. The reason behind this difficulty is unknown, but a possible complication is allylic strain involving the tosyl protecting group. Several commonly employed conditions to remove the indole tosyl group were examined (e.g. Mg/MeOH, NaOH/MeOH, Li/Napth., TBAF/THF, etc.) however, the deprotected indole was not observed. The resistance of tosyl indole **203** towards deprotection was unexpected. An extensive search for feasible detosylation reactions was undertaken, but no viable method was found. This stands in stark contrast to earlier materials where, attempts at deprotections resulted in near quantitative removal of the tosyl group under mild conditions. Further investigation into both deprotection and direct di-methylation are underway, but to date, no reliable conditions have been found to affect either transformation.

Attempts to convert the mono-methylated product to the di-methylated skeleton were partially successful, but the yields were irreproducible, and failure of the reaction resulted in decomposition to baseline materials. Attempts at reacting mono-methylated ketone **205** to produce the corresponding silyl enol ether also produced no viable leads. "Soft" enolization with TMSI or TMSOTf produced none of the silyl enol ether, a possible alternative handle to complete the skeleton. Due to this lackluster set of results, alternative methods for completing the skeleton were attempted and thoroughly investigated.

3.10 Alternative Approaches to Introduce the gem-dimethyl Quaternary Center:

The ease and reliability of the mono-methylation led us to consider the use of the alpha methylenated enone, **208**, as a key intermediate for further study (Scheme **42**). Several standard conditions were examined, including the use of paraformaldehyde as the one carbon unit, but the most promising was results came with the use of in situ generated Eschenmoser salt, which produced enone **208** as the sole product in 88% yield. Initially, our plan was to form the α-cyclopropyl ketone **209** through Johnson–Corey–Chaykovsky cyclopropanation[15] and subsequent hydrogenolysis with Adam's catalyst.[16] Unfortunately, the cyclopropanation of **208** failed to provide any ketone **209**.

[15] (a) Corey, E. J.; Chaykovsky, M. *J. Am. Chem. Soc*. **1965**, *87*, 1353–1364. (b) Johnson, A.W.; LaCount, R.B. *J. Am. Chem. Soc.* **1961**, *83*, 417–423.
[16] Schultz A. L. *J. Org. Chem*. **1971**, *36*, 383.

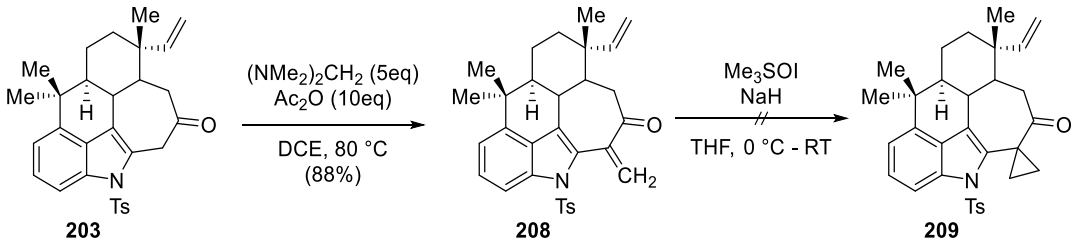

Scheme 42: Formation of Enone **208**

Treatment of enone **208** with L-selectride would form the metal enolate **210**, allowing for trapping with either TMSCl or MeI (Scheme **43**).[17] Treatment of the intermediate enolate **210**, with methyl iodide results in the formation of methyl enol ether **207** in 61% yield; much to our disappointment, the desired gem-di-methylated product **206** only formed in trace amounts under these conditions. However, trapping the intermediate enolate **210** with TMSCl, leads to the formation of the desired silyl enol ether in excellent yield. The silyl enol ether is very prone to hydrolysis, so an additional amine base is added to avoid complications arising from trace water or acid. With reliable access to a handle at C24, efforts turned towards the derivatization of silylenol ether **211**.

[17] Wilson, M. S.; Woo, J. C. S.; Dake, G. R., *J. Org. Chem.* **2006**, *71*, 4237.

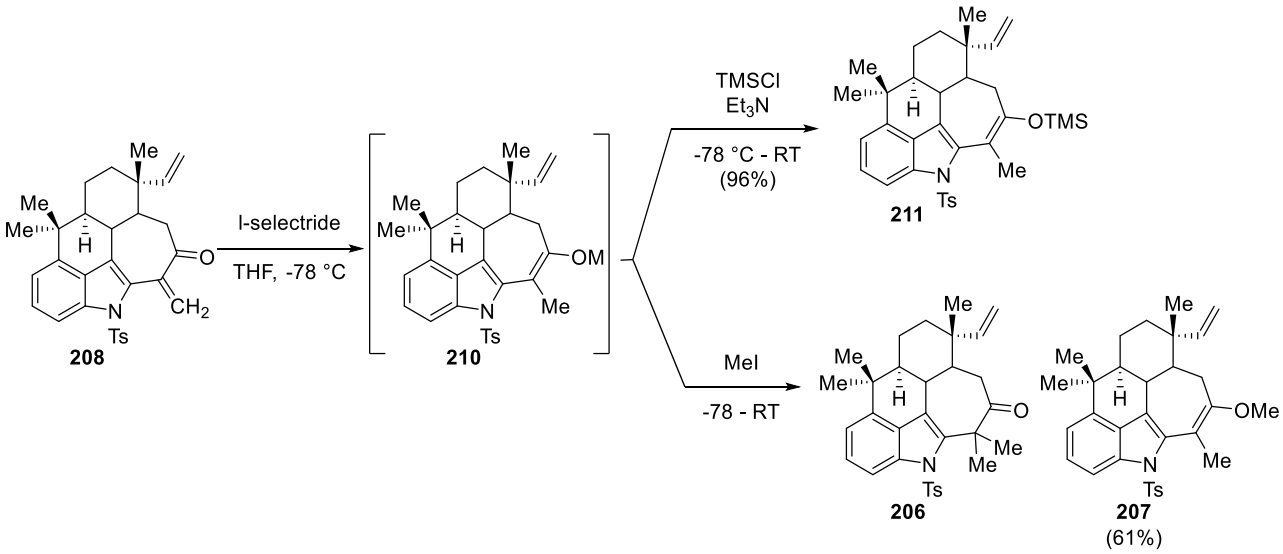

Scheme 43: Investigation into the use of enolates

The difficulty in direct enolate alkylation made us consider alternative approaches for alkylating silyl enol ethers such as: the Patterson thioalkyation procedure, cyclopropanation/hydrolysis, methylaluminum bis(4-bromo-2,6-di-tert-butylphenoxide) (MABR) mediated methylation, or anhydrous fluoride-mediated enolate alkylation.[18,19,20] Complications were prevalent for each of these ventures as the silyl enol ether is unusually unstable to trace acids with hydrolysis to the monomethyl ketone occurring rapidly even at low temperatures. Patterson thioalkylation was unsuccessful at delivering the desired thioether **212**, even when using more active species such as the iodomethylphenylsulfide. In all cases, acid rapidly hydrolyzed the silyl enol ether to give ketone **205**. The same complications were observed under dry benzyltrimethylammonium fluoride and MABR methylation conditions (Scheme **44**). The use of the less acid labile TBS enol ether failed to provide any of the desired products. Additionally,

[18] (a) Paterson, I. *Tetrahedron* **1988**, *44*, 4207. (b) Paterson, I.; Fleming, I. *Tetrahedron Lett*. **1979**, 995. (c) Paterson, I.; Fleming, I. *Tetrahedron Lett*. **1979**, 2179.
[19] Kuwajima, I.; Nakamura, E.; Shimizu M.; *J. Am. Chem. Soc.* **1982**, *104*, 1025-1030.
[20] Maruoka, K.; Sato, J.; Yamamoto, H. *J. Am. Chem. Soc.* **1992**, *114*, 4422-4423.

attempts at regenerating the lithium enolate from silyl enol ether **211** and subsequent trapping with methyl iodide only gave methyl enol ether **207** in 81% yield. Owing to its higher hydrolytic stability methyl enol ether **207**, may yield better results under these conditions, however, neither Paterson's thioalkylation nor Yamamoto's MABR methylation have been attempted on alkoxy ethers.

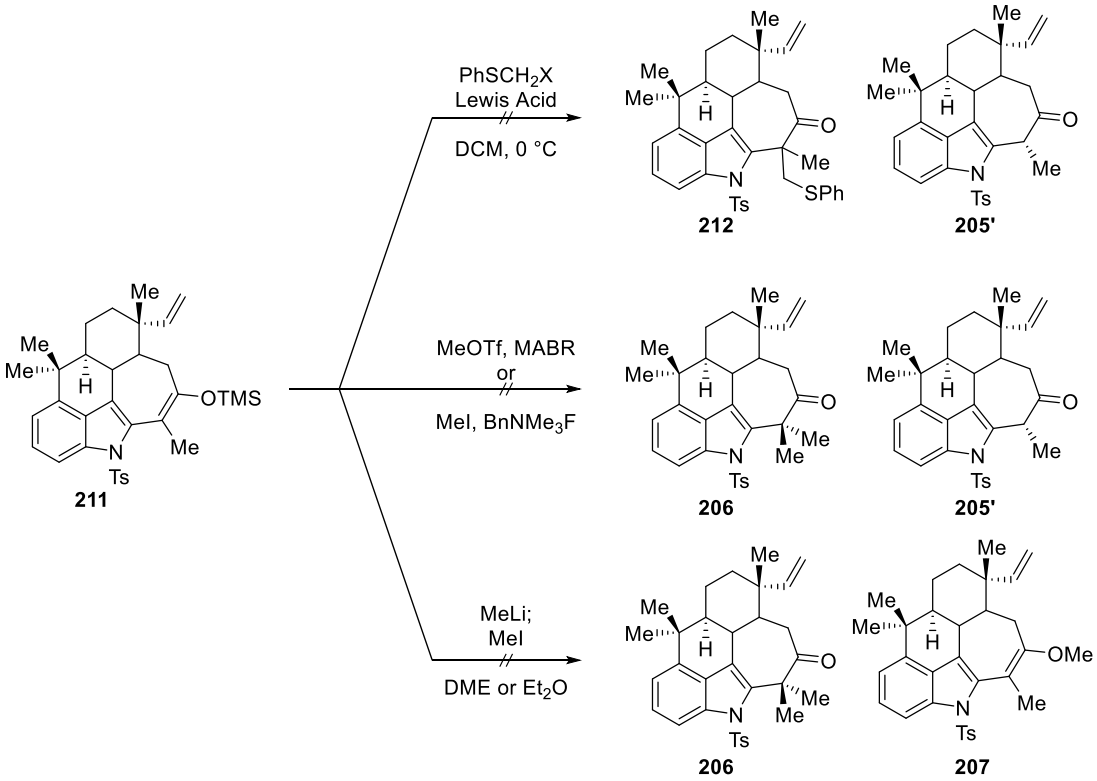

Scheme 44: Attempted alkylation of silyl enol ether **211**

After exhausting other pathways, the less direct cyclopropanation/hydrolysis pathway was examined (Scheme **45**). [21] Treatment of silyl enol ether **211**, with diethylzinc and diiodomethane resulted in the formation of the desired cyclopropanol **213**, however this procedure was found to

[21] Charette, A.B.; Beauchemin, A. (**2004**). Simmons-Smith Cyclopropanation Reaction. In Organic Reactions, (Ed.) (b) Ernest Wenkert, Arrhenius, T. S.; Bookser, B.; Guo, M.; Mancini, P. *J. Org. Chem.* **1990**, *55*, 1185-1193. (c) A. Abad, C. Agulló, A.C. Cuñat, I. de Alfonso Marzal, A. Gris, I. Navarro, C. Ramírez de Arellano *Tetrahedron*, **2007**, *63*, 1664-1679.

be wildly inconsistent, leading us to examine factors such as: reagent purity, temperature, and addition rates. Still unable to improve the reliability of the reaction, alternatives such as zinc/copper and zinc/silver couple were examined. Zinc/copper proved unsuccessful, degrading starting materials, while zinc/silver couple allowed for the clean formation of the product with up to 70% conversion by ^{1}H-NMR. Overall, the reaction was still highly variable, and alternative metal systems such as samarium or aluminum may prove more reliable and as such are under investigation.

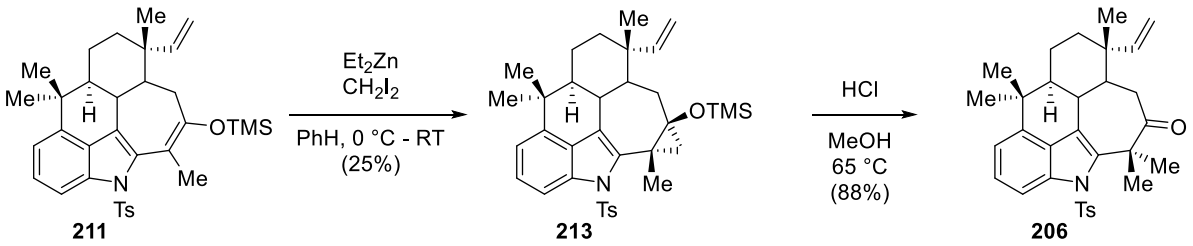

Scheme 45: Completion of the Ambiguine Skeleton

Hydrolysis of the cyclopropanol had its own difficulties, as anionic and radical intermediates were liable to expand the C ring, giving the cycloocto[*b*] indole.[22] Unwilling to risk such a deleterious skeletal rearrangement, we treated crude **213** with methanolic hydrochloric acid to furnish the complete skeleton **206** in 22% yield from **211**. While the synthesis rests here, additional reactions were performed to reconnoiter likely avenues of progress; such as deprotection of the indole, which proceeds smoothly on the dimethylated compound **206**.

[22] (a) Tsuchida, H.; Tamura, M.; Hasegawa, E. *J. Org. Chem.* **2009**, *74*, 2467-2475. (b) Hasegawa, E.; Nemoto, K.; Nagumo, R.; Tayama, E.; Iwamoto, H. *J. Org. Chem* **2016**, *8*, 2692-2703.

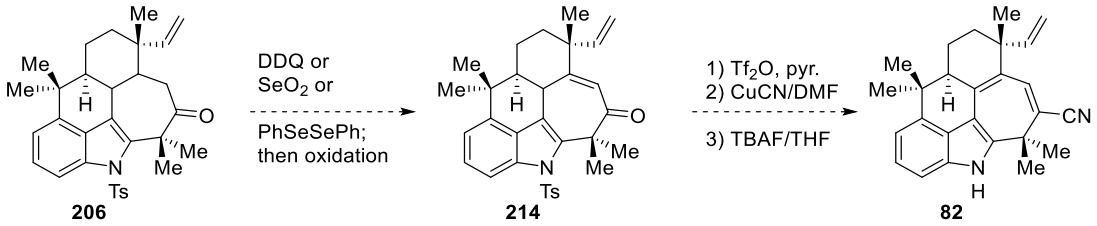

Scheme 46: Proposed Endgame Strategy Towards Ambiguine Q

The current plan for the synthetic endgame is outlined in Scheme **46**; the remaining transformations: nitrile formation, deprotection, and oxidation could be carried out in any order, however preliminary experiments revealed difficulties with the nitrile formation through a cyanohydrin/elimination sequence. As such, the proposed route would be oxidation of ketone **206** to enone **214** through Saegusa-Ito oxidation, [23] DDQ, [24] or selenoxide elimination[25]. After which the formation of the dienol triflate of ketone **214**, would be facilitated owing to the higher acidity of the γ hydrogen. Cyanation and deprotection would then give the final product, ambiguine Q.[26] Efforts by Dr. Sudhakar Athe are underway to build on this synthesis.

3.11 Conclusion

While this synthesis remains incomplete, the current progress towards the target has revealed interesting chemistry, challenges, and avenues that can be used to fully develop a unified approach to other ambiguines bearing more complex functional groups. The current construction of the skeleton could use improvements, the direct gem- demethylation may yet be possible, however

[23] Ito, Y.; Hirao, T. and Saegusa, T., *J. Org. Chem.*, **1978**, *43*, 1011.
[24] (a) Harada, N.; Sugioka, T.; Yusuke, A.; Uda, H.; Kuriki T. *J. Am. Chem. Soc.* **1988**, *110*, 8483-8487. (b) Chai K. B.; Sampson P. *J. Org. Chem.* **1993**, *58*, 6807-6813. (c) Harada, N.; Sugioka, T.; Uda, H.; Kuriki T., *J. Org. Chem.* **1990**, *55*, 3158-3163.
[25] (a) Sugihara, Y.; Sugimura, T.; Murata, I. *J. Am. Chem. Soc.* **1981**, *103*, 6738-6739. (b) Sato, S.; Fukuda, Y.; Ogura, Y.; Kwon, E.; Kuwahara, S.; *Angew. Chem. Int. Ed*. **2017**, *56*, 10911.
[26] Snider B. B.; Vo N. H.; O'Nei S. V.; Foxman B. M. *J. Am. Chem. Soc.* **1996**, *118*, 7644-7645. (b) Kou K. G. M.; Kulyk S.; Marth, C. J.; Lee, J. C.; Doering N. A.; Li B. X.; Gallego G. M.; Lebold T. P.; Sarpong R. *J. Am. Chem. Soc.* **2017**, *139*, 13882-13896.

work on the endgame takes priority. Overall, the high diastereoselectivity and facile construction of the pentacyclic core makes for an exciting project.

Chapter 4: Chiral Brønsted Acid Catalysis for Asymmetric [4+3] Cycloadditions

4.1 Introduction: Asymmetric Induction in acetal substitutions

Acetals are a ubiquitous, accessible, and useful protecting group in organic synthesis finding their way into key steps of several total syntheses.[1] While typically used as a protecting group in organic synthesis, the acetal handle has seen widespread investigation in carbohydrate chemistry, as sugars naturally adopt a cyclic hemi-acetal form.[2] Even with limited research, investigations into acetal substitutions have led to mechanistic elucidations and several enantioselective transformations. As carbohydrate chemistry was at the heart of acetal substitutions, early mechanistic studies by Denmark, Sammakia, and Heathcock focused on the substitution of cyclic acetals, with only limited exploration of acyclic acetal substitution.[3]

Based on this early mechanistic work, we can understand acetal substitution promoted by either Lewis or Brønsted acids, as undergoing either an S_N1 or S_N2 type mechanism (Scheme **47**). Acetals prove to be a unique scaffold for substitution, with various reaction mechanisms that can be classified according to the extent of dissociation of the acetal. The pathway can be truly ionic, wherein a free ion pair (FIP) is generated, leaving a naked oxocarbenium ion for substitution by a suitable nucleophile. The extent to which the ion pair is truly dissociated is mostly a result of the solvent, as more polar, stabilizing solvents improve the stability of the oxocarbenium. Alternatively, a contact ion pair (CIP) could form, wherein the dissociated alkoxide weakly coordinates to the oxocarbenium. Finally, the reaction could undergo an S_N2-like mechanism

[1] Overman, L. E.; Thompson, A. S. *J. Am. Chem. Soc.* **1988**, 1110, 7, 2248-2256.
[2] Clode, D. M. *Chem. Rev.* **1979** 79, 6, 491-513.
[3] (a) Denmark, S. E.; Wilson, T. M. *J. Am. Chem. Soc.* **1989** 111, 9, 3475-3476. (b) Smith, R. S.; Sammakia, T. *J. Org. Chem.* **1992**, 57, 11, 2997-3000. (c) Ishihara, K.; Yamamoto, H.; Heathcock, C. H. *Tet. Lett.* **1989** 30, 14, 1825-1828.

wherein the Lewis or Brønsted acid facilitates the displacement of one of the alkoxy groups by a suitable nucleophile, but no oxocarbenium ion is formed during the course of the reaction.

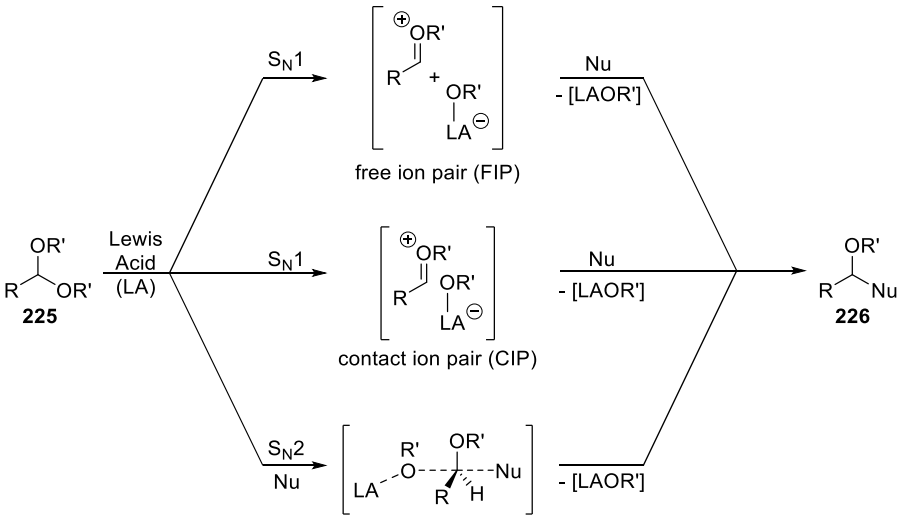

Scheme 47: Mechanisms for Acetal Substitution

While asymmetric transformations of acetal substrates are rare, they have been the subject of much study, as the reactions can proceed under mild conditions and the scaffold is easy to access. Many nucleophilic substitutions have been developed including the formation of protected cyanohydrins, aldol reactions, and the addition of allyl and alkynyl groups. To date, Lewis acid complexes employing copper, nickel, and niobium have been used to afford asymmetric acetal substitutions. However, an additional Lewis acid promoter, such as BF_3-OEt_2, is typically added to generate the oxocarbenium intermediate.[4] Brønsted acid catalysis is less well studied, however an imidodiphosphorimidate (IDPi) catalyzed substitution of cyclic oxocarbenium ions has been

[4] (a) Dasgupta, S.; Rivas, T.; Watson, M. P. *Angew. Chem. Int. Ed.* **2015**, 54, 47, 14154-14158. (b) Srinivas, H. D.; Maity, P.; Yap, G. P. A.; Watson, M. P. *J. Org. Chem.* **2015**, 80, 8, 4003-4016. (c) Maity, P.; Srinivas, H. D.; Watson, M. P. *J. Am. Chem. Soc* **2011**, 133, 43, 17142-17145. (d) Kobayashi, S.; Arai, K.; Yamakawa, T.; Chem, Y-J.; Salter, M. M.; Yamashita, T.; *Adv. Synth. Catal.* **2011**, 353, 1927-1932. (e) Ye. P; Liu, X.; Wang, G.; Liu, L. *Chin. Chem. Lett.* **2020**

reported, along with numerous racemic transformations.[5] The development of an operationally simple, general access to asymmetric acetal reactions would be a useful development in the field; to this end we have attempted to explore the use of highly acidic imidodiphosphorimidate catalysts to promote asymmetric reactions of acyclic acetals, exploring the asymmetric [4+3], [3+2], and acetal substitutions.

4.2 Initial Discovery of the Transformation

Over the course of our studies into the cycloaddition of 3-alkenyl indoles and stabilized oxyallyl cations, we sought to develop catalytic conditions to affect the enantioselectivity of the transformation. As discussed in Chapter Two, List's IDPi catalysts were found to be suitably acidic to promote the [4+3] cycloaddition, giving good enantioselectivities for several substrates. Since the requisite catalysts and oxyallyl precursors were already prepared, we sought to explore the chemical space by exploring the [4+3] cycloadditions of using furan. Originally, limits in our instrumentation necessitated installing a UV active handle, as such we attempted the [4+3] with di-benzyl acetal **92d** assuming that the larger handle would not be deleterious to the enantioselectivity of the transformation. Our initial hit came with catalyst IDPi-**a** and dibenzyl acetal **92d** (Scheme **48**), where reactions using either furan or 2,5-dimethylfuran were run in diethyl ether, our optimum conditions for the 3-alkenyl indoles from Chapter Two. It was anticipated that the reaction with 2,5-dimethylfuran would be less selective owing to the increased steric congestion. Unfortunately, 2,5-dimethylfuran participated in the cycloaddition in high yield, but the reaction gave only a racemic cycloadduct. To our surprise, the dibenzyl acetal proved itself very resistant to hydrolysis to the α-siloxyacrolein **122**; which could reflect a slower rate of formation of the oxocarbenium ion compared to the dimethyl acetal **92**. The reactivity of the 2,5-

[5] Lee, S.; Kaib, P. S. J.; List, B. *J. Am. Chem. Soc* **2017**, 139, 6, 2156-2159.

dimethyl furan suggests that substitutions at either the 2 or 5 positions of furan may have deleterious effects on the enantioselectivity of the transformation. The high yield of the reaction could suggest that the background reaction is readily catalyzed at room temperature. We attribute this background reactivity to trace water, which could, in the presence of the acidic IDPi catalyst, promote the racemic reaction through a hydronium species.

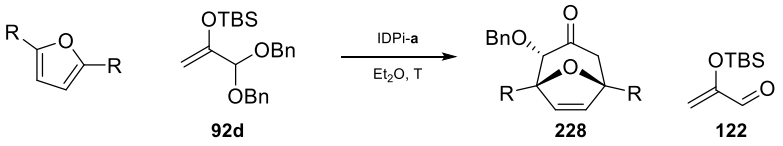

entry	R	T (°C)	Yield[a] (ee)
1	Me	r.t.	72% (0)
2	Me	-35	NR
3	H	r.t.	51% (50)
4	H	-35	NR

[a] Yield Determined by ^{1}HNMR relative to internal standard

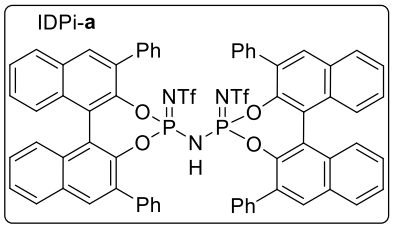

Scheme 48: Initial Discovery of the IDPi Catalyzed [4+3] with Furan

After our initial hit, we sought to investigate the effects of less polar solvents, as well as the effect that temperature might have on the yield and enantioselectivity of the reaction (Table **9**). Based on our understanding of the reaction, we proposed that using non-polar solvents such as methyl tert-butyl ether or methyl-cyclohexane would engender tighter coordination between the intermediate oxocarbenium ion and the IDPi catalyst, thereby leading to higher enantioselectivities. After our initial screen, we were delighted to find that our assumption was correct, but incomplete. Based on our initial results methylcyclohexane proved to be an excellent solvent, giving the desired product in moderate yield and selectivity. However, the yield and enantioselectivity in DCM was better than in MTBE, a less polar solvent. The reason behind this is unknown. Strangely, the reaction did not proceed below 0 °C using dibenzyl acetal **92d**, while dimethyl acetal **92**, on the other hand the desired cycloadduct with furan even at -10 °C. A possible

reason for this is the increased lability of the methyl acetal compared to the dibenzyl acetal, leading to an increased rate of oxocarbenium ion formation at lower temperatures.

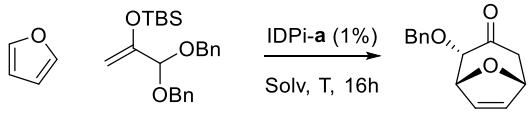

entry	Solv	T (°C)	Yield (ee)
1	MeCy	r.t.	59% (56)
2	DCM	r.t.	43% (51)
3	MTBE	r.t.	40% (21)
4	MeCy	-10	NR
5	MeCy	-5	NR
6	MeCy	0	NR

Yield Determined by ^{1}HNMR relative to internal standard

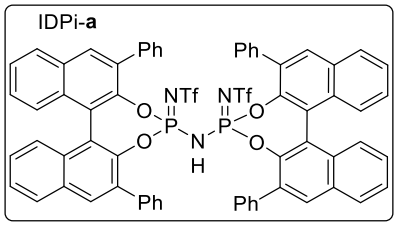

Table 9: Initial Solvent/Temperature Optimizations

With suitable conditions identified, we sought to explore the breadth of catalysts at our disposal to promote the [4+3] cycloaddition. We expected that the decreased size of the diene, would enable the use sterically more congested catalysts such as IDPi-**c** and IDPi-**d**. To our surprise the use of these catalysts resulted in no conversion to the desired cycloadduct, instead giving only the hydrolyzed acetal **122**. This result would suggest that a primary factor in the outcome in the reaction is the size of the silyl group, rather than the size of the diene. Additionally, we examined both chromium and cobalt salen catalysts (**229a,b**) which have previously been used to promote enantioselective Diels-Alder reactions between acroleins and various dienes (Table **10**).[6] Unfortunately, these catalysts failed to deliver any of the desired cycloadduct.

Through our examination of the transformation, we came to the conclusion that the reaction requires either IDPi-**a** or IDPi-**b** to reach high yields and enantioselectivities. The temperature of

[6] (a) Huang, Y.; iwama, T.; Rawal, V. H. *J. Am. Chem. Soc.* **2002**, 124, 21, 5950-5951. (b) Schaus, S. E.; Brånalt, J.; Jacobsen, E. N. *J. Org. Chem* **1998**, 63, 2, 403-405.

the reaction determines whether the key intermediate oxocarbenium could be generated; an approximate lower bound for the temperature is 0 °C. The use of molecular sieves is important, but poorly understood. Reactions run with 4Å molecular sieves for any of the dienes resulted in a complete inhibition of the reaction. However, the use of 5Å molecular sieves promotes the reaction primarily by inhibiting the hydrolysis of acetal **92**, to α-tert-butyldimethylsilyloxyacrolein **122**. As a result, the turnover of the reaction improves over longer reaction times, the same effect is seen with dimethyl acetal **92**. Additionally, it could be that the molecular sieves inhibit the racemic background reaction which we propose is caused by trace moisture, or alcohol liberated from the acetal.

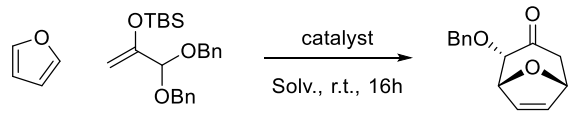

92d **228**

entry	catalyst	M.S.	Solv.	Yield
1	IDPi-**a**	-	MeCy	59% (56)[a]
2	IDPi-**b**	-	MeCy	43% (51)[a]
3	IDPi-**c**	-	MeCy	NR
4	IDPi-**d**	-	MeCy	NR
5	Co Salen (**229a**)	-	MTBE	NR
6	Cr Salen (**229b**)	-	MTBE	NR
7	IDPi-**b**	4 Å	MeCy	NR
8	IDPi-**b**	5 Å	MeCy	87%(53)[b]

[a] Yield Determined by ^{1}HNMR relative to internal standard;
[b] Yield Determined in Isolation

IDPi-**x**

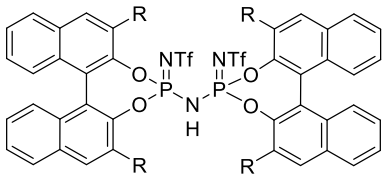

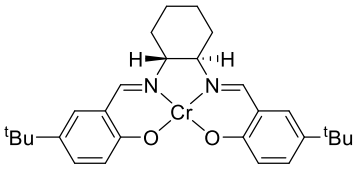

229a

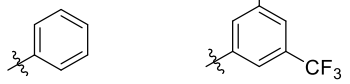

a **b**

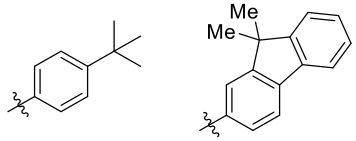

c **d**

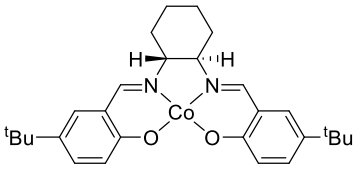

229b

Table 10: Additional Optimizations of Catalysts

4.3 Proposed catalytic cycle:

Based on our understanding of the [4+3] cycloaddition and the catalytic cycle of TMSOTf promoted [4+3] cycloaddition we have proposed in Chapter Two, we propose a similar cycle for the enantioselective [4+3] cycloaddition reaction with IDPi catalysts. The catalytic cycle (Scheme **49**) starts with IDPi **230** (X=H) reacting with an equivalent of the dibenzyl acetal **92d**, which leads to the elimination of benzyl alcohol and forming an ion pair, **231**, between the deprotonated IDPi

and the oxocarbenium. The coordination between the deprotonated IDPi and the oxocarbenium ion can be rationalized as engendering the enantioselectivity of the reaction. This consideration led us to using non-polar solvents and lower temperatures in an attempt to tighten this coordination. Upon oxocarbenium ion **231** reacting with an equivalent of furan, the siloxycarbenium ion **232** forms, which upon transferring a silyl group to the IDPi anion loses cycloadduct **228**. As a result, the silylated IDPi (X=TBS) is generated and can then react with another equivalent of **92d**. At this point, the mechanism is the same, except that silylilium is used to generate the oxocarbenium **231** instead of a proton. Sililium IDPi catalysts are known and can be generated by reacting the IDPi catalyst with and equivalent of a silyl ketene acetal.

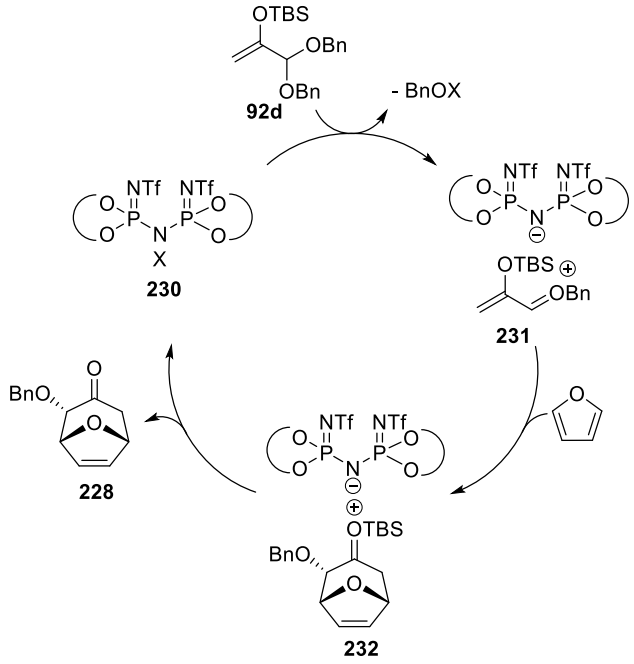

Scheme 49: Proposed Catalytic Cycle for the Enantioselective [4+3]

Based on this catalytic cycle, inferences can be made about our experimental observations, such as difficulties with more sterically hindered catalysts. Intermediate **231** bearing a bulky TBS group may not be able to bind well with bulky IDPi catalysts, such as IDPi-**c** and IDPi-**d**. A

possible solution to this issue may be to decrease the size of the oxyallyl precursor by using the methyl enol ether instead of the silyl enol ether. However, the IDPi catalysts will not be able to transfer a methyl as easily as a proton or silyl cation.

4.4 Substrate Table for the Assymetric [4+3] Cycloaddition

With a preliminary optimization being complete, several furan substrates were prepared to probe the efficacy of the transformation. To test the effects of substitution, both C3 substituted furans and monomethylated oxyallyl cations were used to gauge the scope of the transformation. We expected that by increasing the substitution at either C3 of furan or using the monomethylated oxyallyl cation **92b**, we would see an improvement in the enantioselectivity.

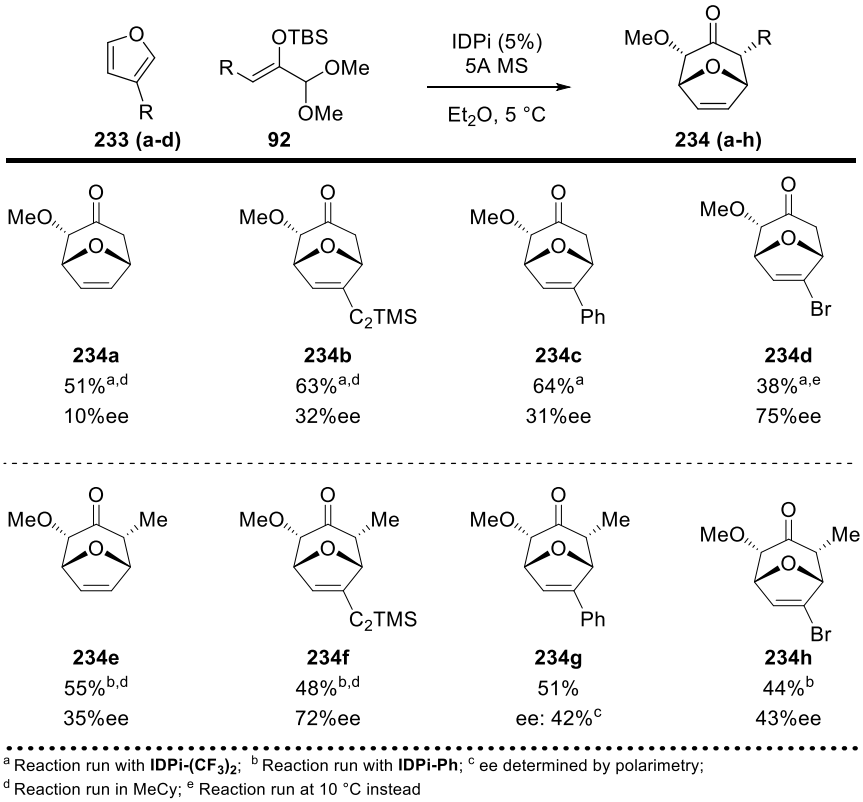

Table 11: [4+3] Cycloaddition of Substituted Furans

Originally, we had planned to run these reactions with the dibenzyl acetal **92d**; however, when the products were evaluated for their enantioenrichment we were unable to separate the enantiomers in either chiral HPLC or GC. This set back was addressed by using the dimethyl acetal **92** instead and using chiral GC to assess the enantioselectivity when possible.

Overall, the yields of the reaction were moderate, with the best enantioselectivity being 75%. In each case the IDPi catalyzed reaction delivered the cycloadduct as a single regio and diastereomer, while the racemic transformation delivered **234c** and **234d** as a mixture of products. While these results are promising, the overall trend of the reaction in terms of yield and enantioselectivity is hard to gauge. Generally, an increase in the enantioselectivity was observed when using monomethyl acetal **92b**. However, trends in enantioselectivity are hard to gauge between substrates, with the best enantioselectivities not correlating with either yield or substituent size, (e.g. **234b**, **234d** vs **234f**, **234h**). While the reactivity was comparable between acetal **92** and **92d** in terms of yield, it is possible that the enantioselectivity with the dibenzyl acetals was better, given the results with substrate **234a**. The dimethyl acetal gave the cycloadduct in only 10% ee, while the dibenzyl acetal gave cycloadduct **228** in up to 56% ee. Based on the relative stereochemistry of substrates **234e-h**, the [4+3] may be concerted, unlike the results obtained for the [4+3] cycloaddition of 3-alkenyl indoles. As discussed in Chapters One and Two, the relative stereochemistry between the alkoxide and alkyl substituents may provide insight into the reaction mechanism. The syn relationship between the two substituents as well as the anti-relationship between the substituents and the bridging oxygen supports a concerted reaction proceeding through an endo transition state. While we were correct in our assumptions that the 3-substitution of furan and the monomethylated acetal **92b** improved the enantioselectivity, additional optimization is needed to improve these results. The overall poor enantioselectivities observed for

furan indicates that either a racemic background reaction catalyzed by trace water is reducing the enantioselectivity or that the chiral pocket is poorly setup to induce enantioselectivity. Perhaps longer, naphthenyl or anthracenyl substituents on the IDPi catalyst may improve the transformation without being so bulky as to inhibit the reaction.

This operationally simple method helps demonstrate the viability of IDPi catalyzed [4+3] cycloadditions, with substituted furans giving the desired cycloadducts as single diastereomers in moderate yields and up to 75% ee. While this work is not yet complete, additional examples may be able to improve the enantioselectivity and make for a useful method for accessing oxabicyclic systems through [4+3] cycloadditions.

4.5 Additional Cycloadditions Attempted with Oxyallyl Cations

While our primary focus was the [4+3] cycloaddition of furan and stabilized oxyallyl cations, we also briefly explored similar transformations including the [3+2] cycloaddition reaction.[7] The literature is sparse on the [3+2] cycloaddition of stabilized oxyallyl cations, but examples of 1-sulfide stabilized oxyallyl cations has been reported.[8] Based on this report, we hypothesized that suitably electron rich olefins should react with a stabilized oxyallyl cation and deliver the desired cycloadduct (Scheme **50**). Of particular interest was **235b** which could be used for an asymmetric access to diquinanes.

[7] For a general review: Li, H.; Wu, J. *Synthesis*, **2015**, 47, 22-33.
[8] (a) Masuya, K.; Domon, K.; Tanino, K.; Kuwajima, I. *Synlett* **1996**, 157. (b) Masuya, K.; Domon, K.; Tanino, K.; Kuwajima, I. *J. Am. Chem. Soc.* **1998**, *120*, 1724.

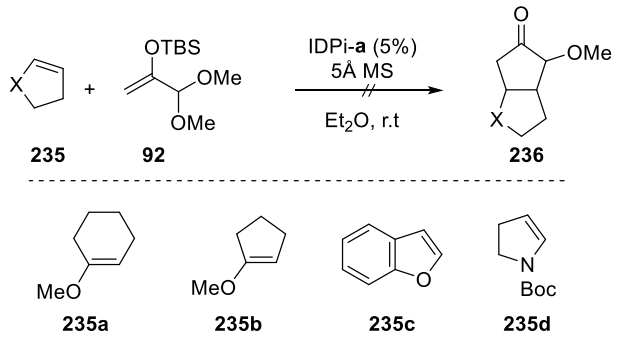

Scheme 50: Attempts at an IDPi Catalyzed [3+2] Cycloaddition Reaction

Based on this premise, we attempted several [3+2] cycloaddition reactions with a diverse array of olefins including: enols, styrene, and dihydropyrrole acting as the "2" component, but no cycloadducts were formed.[9] In all cases, only degradation of the starting material was observed, principally hydrolysis in the case of enol ethers, and polymerization in cases using styrene. This result is unfortunate, but not unexpected owing to the dearth of research on the [3+2] cycloaddition of oxyallyl cations.

In addition to our attempts at asymmetric [3+2] cycloadditions, attempts were made to expand upon the dearomative [4+3] cycloaddition of 3-alkenyl indoles. As disclosed by the Wu group, indole can act as the "2" component in [3+2] cycloadditions with oxyallyl cations wherein N-alkyl substituted indoles were reacted with α-halo ketones to furnish the cyclopenta[*b*]indoline.[10] While this report was limited to unstabilized oxyallyl cations, we had hoped that the reactivity of 1-stabilized oxyallyl cations would be comparable. Enantioinduction of α-tosyloxy ketones with prolinol catalysis has been disclosed by the MacMillan group, however outside of an example in the supporting information the reactions only furnished the 3-substituted indoles rather than the

[9] Hayakawa, Y.; Yokoyama, K.; Noyori, R. *J. Am. Chem. Soc*. **1978**, 100, 1799−1806.
[10] Li H.; Hughes R. P.; and Wu J. *J. Am. Chem. Soc.* **2014** 136, 17, 6288-6296.

fully cyclized products.[11] In addition to the works of Wu and MacMillan, the work of Kerr et al. gave us some hope that the stepwise annulation would be possible.[12] With limited literature precedent, we performed several probative experiments on simple indoles to gauge the viability of this project (Scheme **51**). Unfortunately, the rate of the reaction with the IDPi system was unperceptively slow at room temperatures, and no improvement in conversion was observed even after extended reaction at higher temperatures. As a result, we discontinued our investigations into the cyclopentannulation, and instead focused on the catalytic, enantioselective [4+3] and acetal substitution reaction.

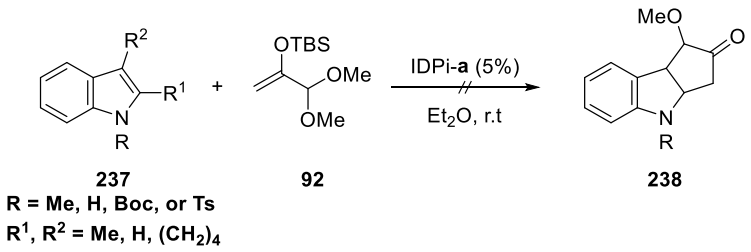

Scheme 51: Attempts at an IDPi Catalyzed Dearomative [3+2] Cycloaddition Reaction

4.6 Attempts at Asymmetric Acetal Substitution with IDPi Catalysis

While our attempts at catalyzing the [3+2] cycloaddition failed, we considered other avenues which, based on our understanding of the [4+3] cycloaddition, would be more fruitful. Mechanistically, the initial step in the [4+3] is the formation of the oxocarbenium of an acetal, therefore we hypothesized that various acyclic acetals could be substituted with suitable nucleophiles using IDPi catalysis. As multiple nucleophilic transformations of acetals are known, including the Mukaiyama aldol, Hosomi-Sakurai, and cyanohydrin formation, we chose to

[11] Liu C.; Oblak E. Z.; Vander Wal M. N.; Dilger A. K.; Almstead D. K.; and MacMillan D. W. C. *J. Am. Chem. Soc* **2016** 138, 7, 2134-2137.
[12] England, D. B.; Kuss, T. D. O.; Keddy, R. G.; Kerr, M. A. *J. Org. Chem*. **2001**, 66, 4704−4709.

examine these simple transformations on a simple model substrate; benzaldehyde dimethyl acetal **240** (Scheme **52**). Using commericially available cyclohexenyl TMS ether **179**, the aldol reaction proceeded in excellent yield. In contrast, commercial 2-trimethylsiloxypropene, gave none of the desired aldol product. Unfortunately, all attempts at gauging the enantioselectivity of the aldol reaction failed; neither chiral HPLC nor GC separated the enantiomers of **241**, and the optical rotation is unknown. Further attempts to determine the enantioselectivity are underway by separating derivatives of **241**. Additionally, the cyanohydrin formation with TMSCN, typically catalyzed with mild Lewis and Brønsted acids was attempted using IDPi-**a** (Scheme **52b**). The reaction proceeded smoothly giving the desired cyanohydrin **243** in 95% yield; unfortunately, cyanohydrin **243** was obtained as a racemate. We propose this is most likely due to the relatively small size of cyanide, or the high reactivity between cyanide and an oxocarbenium, which based on the literature is a diffusion controlled reaction.[13] Lastly, using allyl-TMS, the Hosomi-Sakurai reaction proceeds smoothly giving the desired homo-allylic ether **244** in good yield. Unfortunately, the enantiomers could not be resolved using HPLC or GC, as such, the enantioselectivity was determined to be a modest 23% by polarimetry. While currently, the scope of transformations is limited, we hope that this methodology develops into a useful, general tool towards asymmetric acetal substitutions.

[13] (a) Lucius, R.; Loos, R.; Mayr, H. *Angew. Chem. Int. Ed.* **2002**, 41, 1, 91-95. (b) Ofial, A. R.; Mayr, H. *J. Phys. Org. Chem.* **2008**, 21, 584-595.

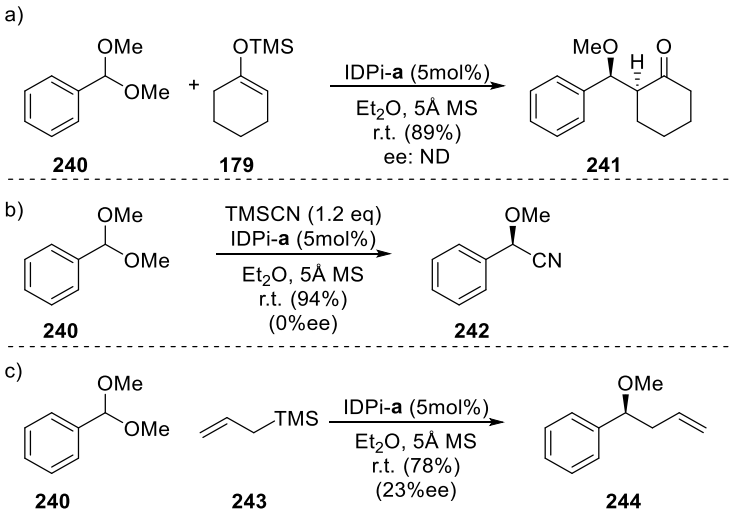

Scheme 52: Results of Initial Investigations into Asymmetric Acetal Substitutions

This avenue of research is promising, acetals are readily accessible, and the absence of the bulkier silyl group as compared to acetal **92**, should allow for the use of more hindered catalysts.

4.7 Conclusion

Through the use of chiral imidodiphosphorimidate catalysis, we have been able to successfully demonstrate enantioselective [4+3] cycloadditions between stabilized oxyallyl cations and furan as well as various acetal substitutions. Although currently the yields of the simple acetal substitutions are excellent the enantioselectivity for some reactions has yet to be determined. Also, much work remains on testing additional transformations of acetals. While this avenue of research needs further development, particular in the exploration of additional catalysts for the [4+3], the methods we have examined should be enabling to synthetic chemists.

Chapter 5: Experimental Details

1. Materials and Methods

Unless stated otherwise, reactions were performed under a nitrogen atmosphere using oven- or flame-dried glassware and stir bars. Ambient temperature refers to 22–26 °C. Higher than ambient temperatures were maintained using pre-heated oil baths. Lower temperatures were maintained using acetone/CO_2(s) (−78 °C), MeCN/CO_2(s) (−40 °C) and water/ice (0 °C) baths. Dichloromethane (CH_2Cl_2 or DCM), tetrahydrofuran (THF), and dimethylformamide (DMF) were dried by passage through an activated alumina column purification system (Innovative Technology Inc. Pure Solv^{TM}). Commercially obtained reagents were used as received, unless stated otherwise.

Thin-layer chromatography (TLC) was performed using EMD Millipore silica gel 60 Å plates with UV fluorescence quenching (254 nm), KMnO4, or Seebach's stain. Flash column chromatography was performed on SiliCycle SiliaFlash P60 (40-63 μm particle size) using ACS or HPLC grade solvents purchased from Fisher Scientific. ^{1}H NMR spectra were recorded on Bruker 500 spectrometers (at 500 MHz) at 294-297 K. ^{13}C NMR spectra were recorded on Bruker 500 and Bruker 400 spectrometers (at 125 MHz and 100 MHz, respectively) at 294-297 K. ^{1}H spectra were calibrated from internal standard TMS (δ 0.0). ^{13}C spectra were calibrated from solvent resonance ($CDCl_3$: δ 77.16). NMR data are reported as: chemical shift (δ ppm) (multiplicity, coupling constant (Hz), and integration). High-resolution mass spectral analysis was measured on Agilent Technologies 6224 TOF LC/MS (electrospray ionization). IR spectra were recorded on a Thermo Scientific Nicolet iS50 FT-IR spectrometer and are reported as frequency of absorption (cm^{-1}).

Experimental Procedures and Characterization Data

5.1.1 Experimental Details for Chapter 2 – Formation of 3-Acetyl Indoles

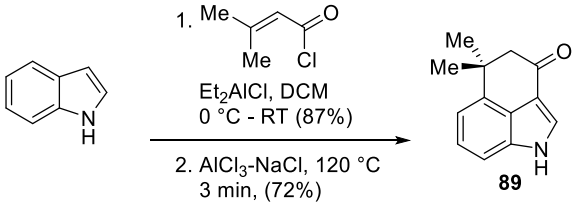

5,5-dimethyl-4,5-dihydrobenzo[cd]indol-3(1*H*)-one (89).

Prepared according to the literature.[1, 2, 3]

^{1}H NMR (500 MHz, $CDCl_3$): δ 8.75 (s, 1H), 7.74 (d, *J* = 2.8 Hz, 1H), 7.31 – 7.28 (m, 2H), 7.19 (t, *J* = 3.9 Hz, 1H), 2.76 (s, 2H), 1.44 (s, 6H).

^{13}C NMR (100 MHz, $CDCl_3$): δ 194.7, 139.0, 133.9, 127.8, 124.7, 123.7, 116.1, 114.5, 109.6, 55.9, 39.3, 29.5.

HRMS (ESI): calcd for $C_{13}H_{14}NO^+$ $[M+H]^+$: 200.1070, found: 200.1072.

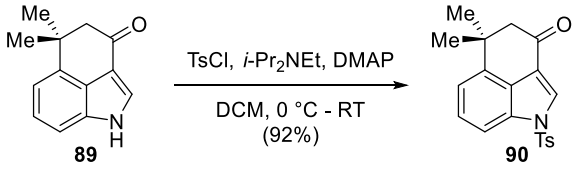

[1] Okauchi, T.; Itonaga, M.; Minami, T.; Owa, T.; Kitoh, K.; Yoshino, H. *Org. Lett.* **2000**, *2*, 1485.
[2] Kumar, V.; Bulumulla, H. N. K.; Wimalasiri, W. R.; Reisch, J. *Phytochemistry* **1994**, *36*, 879.
[3] (a) Bergmann, J.; Venemalm, L.; Gogoll, A. *Tetrahedron*, **1990**, *46*, 6067. (b) Chandra, A.; Johnston, J. N. *Angew. Chem. Int. Ed.* **2011**, *50*, 7641.

5,5-dimethyl-1-tosyl-4,5-dihydrobenzo[*cd*]indol-3(1*H*)-one (90).

A 50 mL flask with a magnetic stir bar was charged with tricyclic ketone **1b** (407 mg, 2.04 mmol, 1 equiv.) and 10 mL DCM to afford a yellow solution. *i*-Pr_2NEt (0.569 mL, 3.26 mmol, 1.6 equiv.) was added, and the mixture was cooled to 0 °C. DMAP (12.5 mg, 0.102 mmol, 0.05 equiv.) and TsCl (467 mg, 2.45 mmol, 1.2 equiv.) were added sequentially. After 15 min, the cold bath was removed, and the reaction mixture was stirred at ambient temperature for 1.5 h. The mixture was quenched with 6 mL saturated aqueous $NaHCO_3$, and partitioned between 20 mL 1:1 brine:H_2O and 20 mL DCM. The aqueous layer was extracted with DCM (15 mL × 2), and the combined organic layers were dried over Na_2SO_4, and concentrated under reduced pressure. Purification by flash chromatography (20:80 EtOAc:hexanes) provided **1** (661 mg, 1.87 mmol, 92% yield) as a white solid.

^{1}H NMR (500 MHz, $CDCl_3$): δ 8.04 (s, 1H), 7.87 (d, *J* = 8.4 Hz, 2H), 7.78 (d, *J* = 8.3 Hz, 1H), 7.39 (t, *J* = 7.4 Hz,1H), 7.30 (d, *J* = 8.1 Hz, 2H), 7.27 – 7.23 (m, 1H), 2.70 (s, 2H), 2.38 (s, 3H), 1.37 (s, 6H).

^{13}C NMR (100 MHz, $CDCl_3$): δ 194.2, 146.0, 139.8, 134.9, 133.3, 130.4, 128.9, 127.4, 126.7, 124.1, 118.7, 118.0, 111.6, 55.9, 39.3, 29.5, 21.8.

HRMS (ESI): calcd for $C_{20}H_{20}NO_3S^+$ $[M+H]^+$: 354.1158, found: 354.1165.

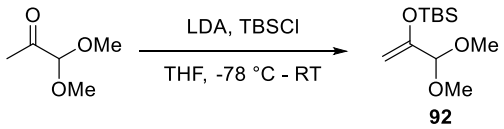

92

Tert-butyl((3,3-dimethoxyprop-1-en-2-yl)oxy)dimethylsilane (92).

Prepared according to the literature,[4] and analytical data matched the reported values.

^{1}H NMR (500 MHz, $CDCl_3$): δ 4.56 (s, 1H), 4.56 (d, *J* = 1.1 Hz, 1H), 4.33 (d, *J* = 1.3 Hz, 1H), 3.33 (s, 6H), 0.93 (s, 9H), 0.18 (s, 6H).

^{13}C NMR (100 MHz, $CDCl_3$): δ 153.6, 102.1, 92.6, 53.2, 25.7, 18.2, −4.6.

HRMS (ESI): calcd for $C_{11}H_{25}O_3Si^+$ $[M+H]^+$: 233.1567, found: 233.1555.

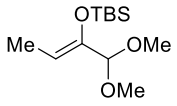

92b

(*Z*)-*tert*-butyl((1,1-dimethoxybut-2-en-2-yl)oxy)dimethylsilane (92b).

Prepared according to the literature.[5]

^{1}H NMR (500 MHz, $CDCl_3$): δ 5.01 (qd, *J* = 6.8, 0.8 Hz, 1H), 4.50 (s, 1H), 3.31 (s, 6H), 1.60 (dd, *J* = 6.8, 0.9 Hz, 3H), 0.96 (s, 9H), 0.14 (s, 6H).

^{13}C NMR (100 MHz, $CDCl_3$): δ 146.0, 105.3, 103.0, 53.3, 26.0, 18.6, 10.4, −3.9.

HRMS (ESI): calcd for $C_{12}H_{27}O_3Si^+$ $[M+H]^+$: 247.1724, found: 247.1707.

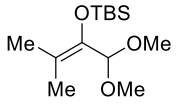

200

(*Z*)-*tert*-butyl((1,1-dimethoxybut-2-en-2-yl)oxy)dimethylsilane (92c)

[4] T*ürkmen, Y. Ph.D. Thesis, The University of Chicago, 2012.*
[5] (a) Pierau, S.; Hoffmann, H, M. R. *Synlett* **1999**, 213. (b) Pichon, N.; Harrison-Marchand, A.; Toupet, L.; Maddaluno, J. *J. Org. Chem.* **2006**, *71*, 1892.

Prepared according to the literature.[6]

^{1}H NMR (400 MHz, $CDCl_3$) δ 4.87 (s, 1H), 3.32 (s, 6H), 1.72 (s, 3H), 1.67 (s, 3H), 0.95 (s, 9H), 0.11 (s, 6H).

^{13}C NMR (101 MHz, $CDCl_3$) δ 140.21, 114.91, 106.46, 101.60, 54.12, 26.20, 26.11, 18.75, 18.53, 17.95, -3.93.

HRMS (ESI): calcd for $C_{13}H_{28}O_3Si^+$ $[M+Na]^+$: 183.1705, found: 283.1697

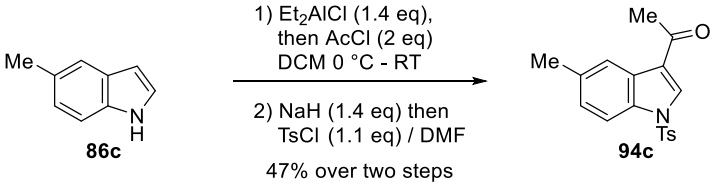

1-(5-methyl-1-tosyl-1H-indol-3-yl)ethan-1-one (94c)

Representative Procedure for synthesis of Acetyl Indoles: **Procedure A**

A 50 mL round-bottomed flask with a magnetic stir bar was charged with 5-methylindole (327mg, 2.5 mmol, 1 equiv.) and 10 mL DCM to afford a colorless solution, which was cooled to 0 °C. Et_2AlCl solution (1.0 M in hexanes; 3.5 mL, 3.5 mmol, 1.4 equiv.) was added over 5 min, and the mixture was stirred at 0 °C for 35 min. Then acetyl chloride (0.36 mL, 5 mmol, 2 equiv.) was added over 10 min using a total of 1 mL DCM, and the mixture turned orange. After 2 h stirring at 0 °C, the reaction mixture was quenched with 50 mL saturated aqueous $NaHCO_3$ and allowed to warm to ambient temperature. The mixture was partitioned with 30 mL DCM, and the aqueous layer was extracted with DCM (20 mL × 2). The combined organic layers were dried over

[6] Prepared according to the doctoral thesis of: Pierau, S. "Neue Methoden zur diastereo- und enantioselektiven Synthese von 8-oxabicyclo(3.2.1)oct-6-en-3-onen" **1997**

Na_2SO_4, filtered, and concentrated under reduced pressure to furnish the 3-acetyl indole as a tan solid which was clean enough to proceed to the next step. Crude acetyl indole was dissolved in 25 mL DMF and treated with NaH (60% dispersion in oil; 140 mg, 3.5 mmol,1.4 eq). The reaction was allowed to stir for one hour under nitrogen during which elution of hydrogen was observed. Tosyl chloride (524 mg, 2.75 mmol, 1.1 eq) was added in one portion and left to stir for two hours. The reaction mixture was then poured into 100 mL water, and extracted with ethyl acetate (25mL x 4). The combined organic layers were diluted with hexanes (100 mL), and then washed with water (25 mL x 4) and brine (25 mL x 1). The combined organic layers were dried over Na_2SO_4, and concentrated under reduced pressure. Purification by flash chromatography (33:67 EtOAc:hexanes) provided indole **94c** (384 mg, 1.17 mmol, 47% yield) as an off white solid.

^{1}H NMR (400 MHz, $CDCl_3$) δ 8.16 (s, 1H), 8.12 (s, 1H), 7.80 (t, *J* = 8.8 Hz, 3H), 7.27 (d, *J* = 8.1 Hz, 2H), 7.18 (dd, *J* = 8.5, 1.8 Hz, 1H), 2.56 (s, 3H), 2.43 (s, 3H), 2.36 (s, 3H).

^{13}C NMR (101 MHz, $CDCl_3$) δ 193.63, 145.84, 134.76, 134.60, 133.17, 132.33, 130.21, 127.72, 127.14, 127.11, 122.89, 121.45, 112.68, 27.81, 21.65, 21.40.

HRMS (ESI): calcd for $C_{18}H_{17}NO_3S$+ [M+H]+: 328.1002, found: 328.0993.

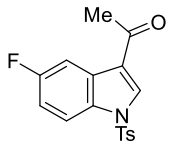

1-(5-fluoro-1-tosyl-1H-indol-3-yl)ethan-1-one (94d)

Following **Procedure A**

5-fluoro indole (405 mg, 3 mmol, 1eq) was subjected to **general procedure A** to furnish **94d** (416 mg, 1.25 mmol, 42%) as a white solid.

^{1}H NMR (400 MHz, $CDCl_3$) δ 8.22 (s, 1H), 8.01 (dd, *J* = 9.1, 2.6 Hz, 1H), 7.86 (dd, *J* = 8.6, 4.3 Hz, 1H), 7.82 (d, *J* = 8.6 Hz, 2H), 7.30 (d, *J* = 8.3 Hz, 0H), 7.10 (td, *J* = 9.0, 2.7 Hz, 1H), 2.56 (s, 3H), 2.38 (s, 3H).

^{13}C NMR (101 MHz, $CDCl_3$) δ 193.12, 161.75, 159.35, 146.20, 134.34, 133.35, 131.22, 130.36, 128.74, 128.64, 127.12, 121.40, 121.36, 114.20, 114.13, 114.10, 113.87, 109.10, 108.85, 27.68, 21.69, 0.01.

HRMS (ESI): calcd for $C_{17}H_{14}FNO_3S$+ [M+H]+: 332.0751, found: 332.0748

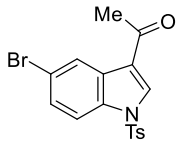

1-(5-bromo-1-tosyl-1H-indol-3-yl)ethan-1-one (94e)

Following **Procedure A**

5-bromo indole (588 mg, 3 mmol, 1eq) was subjected to **general procedure A** to furnish **94e** (903 mg, 1.25 mmol, 76%) as a white solid.

^{1}H NMR (400 MHz, $CDCl_3$) δ 8.50 (d, *J* = 1.8 Hz, 1H), 8.18 (s, 1H), 7.80 (t, *J* = 8.2 Hz, 3H), 7.51 – 7.43 (m, 1H), 7.30 (d, *J* = 8.0 Hz, 2H), 2.56 (s, 2H), 2.38 (s, 3H). **^{13}C NMR** (101 MHz, $CDCl_3$) δ 193.02, 146.30, 134.25, 133.60, 132.87, 130.39, 129.13, 128.82, 127.13, 125.91, 120.87, 118.71, 114.45, 27.74, 21.70.

HRMS (ESI): calcd for $C_{17}H_{14}BrNO_3S$+ [M+H]+: 391.99511, found: 391.9942

.

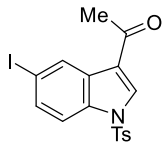

1-(5-iodo-1-tosyl-1H-indol-3-yl)ethan-1-one (94f)

Following **Procedure A**

5-iodo indole (729 mg, 3 mmol, 1eq) was subjected to **general procedure A** to **94f** (762 mg, 1.74 mmol, 57%) as a tan solid.

^{1}H NMR (400 MHz, $CDCl_3$) δ 8.70 (dd, *J* = 1.7, 0.7 Hz, 1H), 8.14 (s, 1H), 7.81 (d, *J* = 8.4 Hz, 2H), 7.71 – 7.60 (m, 2H), 7.34 – 7.28 (m, 2H), 7.29 (d, *J* = 8.5 Hz, 0H), 2.38 (s, 3H). **^{13}C NMR** (101 MHz, $CDCl_3$) δ 193.04, 146.30, 134.42, 134.24, 134.16, 132.54, 132.00, 130.39, 129.55, 127.14, 120.64, 114.81, 89.56, 30.96, 27.75, 21.70. HRMS (ESI): calcd for $C_{17}H_{14}INO_3S$+ [M+H]+: 439.9812, found: 439.9801.

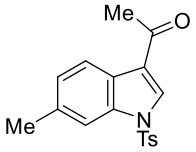

1-(6-methyl-1-tosyl-1H-indol-3-yl)ethan-1-one (94g)

Following **Procedure A**

6-methyl indole (393.5 mg, 3 mmol, 1eq) was subjected to **general procedure A** to **94g** (569 mg, 1.25 mmol, 58%) as a tan solid.

^{1}H NMR (400 MHz, $CDCl_3$) δ 8.18 (d, *J* = 8.1 Hz, 1H), 8.14 (s, 1H), 7.82 (d, *J* = 8.4 Hz, 1H), 7.72 (s, 1H), 7.28 (d, *J* = 8.1 Hz, 2H), 7.16 (d, *J* = 8.2 Hz, 0H), 7.20 – 7.12 (m, 0H), 2.55 (s, 2H), 2.47 (s, 2H), 2.37 (s, 2H).

^{13}C NMR (101 MHz, $CDCl_3$) δ 193.54, 145.84, 136.05, 135.35, 134.69, 131.71, 130.25, 127.09, 126.41, 125.22, 122.64, 121.67, 113.06, 27.75, 21.99, 21.66.

HRMS (ESI): calcd for $C_{18}H_{17}NO_3S$+ [M+H]+: 328.1002, found: 328.0983.

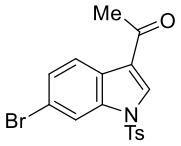

1-(6-bromo-1-tosyl-1H-indol-3-yl)ethan-1-one (94h)

Following **Procedure A**

6-bromo indole (1.176 g, 6 mmol, 1eq) was subjected to **general procedure A** to furnish **94h** (1.282 g, 3.28 mmol, 54.6%) as a tan solid.

^{1}H NMR (400 MHz, $CDCl_3$) δ 8.19 (d, *J* = 8.5 Hz, 1H), 8.15 (s, 1H), 8.10 (d, *J* = 1.7 Hz, 1H), 7.45 (dd, *J* = 8.5, 1.7 Hz, 1H), 7.32 (d, *J* = 8.1 Hz, 2H), 2.55 (s, 3H), 2.40 (s, 3H).

^{13}C NMR (101 MHz, $CDCl_3$) δ 193.16, 146.33, 135.54, 134.28, 132.33, 130.46, 128.28, 127.15, 126.41, 124.38, 121.35, 119.62, 116.16, 27.74, 21.72.

HRMS (ESI): calcd for $C_{17}H_{14}BrNO_3S$+ [M+H]+: 391.9951, found: 391.9940.

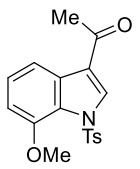

1-(7-methoxy-1-tosyl-1H-indol-3-yl)ethan-1-one (94i)

Following **Procedure A**

7-methoxy indole (441.2 mg, 3 mmol, 1eq) was subjected to **general procedure A** to furnish **1i** (349.9 mg, 1.02 mmol, 34%) as a pale yellow solid.

^{1}H NMR (400 MHz, $CDCl_3$) δ 8.49 (s, 1H), 7.99 (d, *J* = 7.9 Hz, 1H), 7.76 (d, *J* = 8.3 Hz, 2H), 7.30 (d, *J* = 8.2 Hz, 2H), 7.23 (t, *J* = 8.0 Hz, 1H), 6.74 (d, *J* = 7.9 Hz, 1H), 3.68 (s, 3H), 2.60 (s, 3H), 2.42 (s, 3H).

^{13}C NMR (101 MHz, $CDCl_3$) δ 193.54, 146.86, 145.01, 136.32, 134.84, 130.37, 129.56, 127.59, 125.77, 125.13, 119.99, 115.46, 107.89, 55.42, 27.82, 21.67.

HRMS (ESI): calcd for $C_{18}H_{17}NO_4S$+ [M+H]+: 344.0951, found: 344.0950.

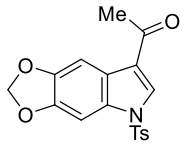

1-(5-tosyl-5H-[1,3]dioxolo[4,5-f]indol-7-yl)ethan-1-one (94h)

Following **Procedure A**

5H-[1,3]dioxolo[4,5-f]indole[7] (161 mg, 1 mmol, 1eq) was subjected to **general procedure A** to furnish **94j** (131 mg, 0.367 mmol, 36.7%) as a white solid.

^{1}H NMR (400 MHz, $CDCl_3$) δ 8.06 (s, 1H), 7.79 (d, *J* = 8.4 Hz, 2H), 7.72 (s, 1H), 7.39 (s, 1H), 7.29 (d, *J* = 8.2 Hz, 2H), 5.99 (s, 2H), 2.52 (s, 3H), 2.39 (s, 3H).

[7] Sinhababu A. K. and Borchardt R. T. *J. Org Chem* **1983** 48 (19), 3347-3349

^{13}C NMR (101 MHz, $CDCl_3$) δ 193.51, 147.23, 146.38, 145.95, 134.50, 130.71, 130.29, 129.89, 127.09, 121.95, 121.76, 101.84, 101.61, 94.39, 27.57, 21.68.

HRMS (ESI): calcd for $C_{18}H_{15}NO_5S$+ [M+H]+: 358.0744, found: 358.0734.

5.1.2 Experimental Details for Chapter 2 – Formation of 3-Alkenyl Indoles

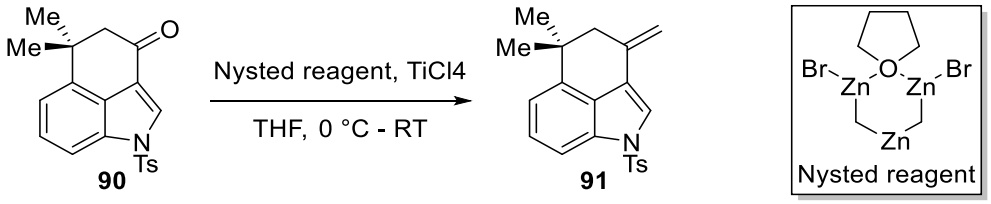

Representative Procedure for synthesis of Dienes using Nysted's reagent: **Procedure B**

5,5-dimethyl-3-methylene-1-tosyl-1,3,4,5-tetrahydrobenzo[*cd*]indole (91)

A 100 mL flask with a magnetic stir bar was charged with 12 mL THF, and cooled to 0 °C. Nysted reagent solution (20 wt% in THF; 4.71 mL, 2.45 mmol, 1.1 equiv.) was added to form a white suspension. $TiCl_4$ (0.269 mL, 2.45 mmol, 1.1 equiv.) was added dropwise, and the suspension turned purple. After 10 min, *N*-tosyl indole **1** (788 mg, 2.23 mmol, 1 equiv.) was added using a total of 10 mL THF. Then the cold bath was removed, and the grey slurry was stirred at ambient temperature for 2 h. The mixture was carefully quenched with 50 mL 1 M HCl, and partitioned between 20 mL H_2O and 30 mL 1:1 Et_2O:hexanes. The aqueous layer was extracted with 30 mL 1:1 Et_2O:hexanes, and the combined organic layers were washed with brine, dried over Na_2SO_4, and concentrated under reduced pressure. Purification by flash chromatography

(10:90 EtOAc:hexanes) provided tricyclic diene **91** (521 mg, 1.48 mmol, 66% yield) as a white solid.

^{1}H NMR (500 MHz, $CDCl_3$): δ 7.81 (d, *J* = 8.4 Hz, 2H), 7.72 (d, *J* = 8.2 Hz, 1H), 7.54 (s, 1H), 7.28 (t, *J* = 7.8 Hz, 1H), 7.24 (d, *J* = 7.9 Hz, 2H), 7.13 (d, *J* = 7.4 Hz, 1H), 5.44 (d, *J* = 1.4 Hz, 1H), 5.09 (d, *J* = 1.4 Hz, 1H), 2.45 (s, 2H), 2.35 (s, 3H), 1.27 (s, 6H).

^{13}C NMR (100 MHz, $CDCl_3$): δ 145.0, 141.4, 136.0, 135.7, 133.5, 130.1, 127.9, 127.0, 125.7, 120.5, 117.5, 117.5, 111.1, 110.4, 48.5, 36.3, 28.8, 21.7.

HRMS (ESI): calcd for $C_{21}H_{22}NO_2S^+$ $[M+H]^+$: 352.1366, found: 352.1359.

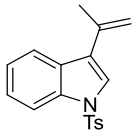

3-(prop-1-en-2-yl)-1-tosyl-1H-indole (95a)

Following **Procedure B**

1-(1-tosyl-1H-indol-3-yl)ethan-1-one (321 mg, 1.03 mmol, 1 equiv.) was subjected to **general procedure B** with modifications: Nysted reagent solution (25 wt% in THF; 2.56 mL, 1.33 mmol, 1.3 equiv.) and $TiCl_4$ solution (1.0 M in DCM; 1.33 mL, 1.33 mmol, 1.3 equiv.). To furnish *N*-tosyl-3-isopropenyl indole **95a** (244 mg, 0.784 mmol, 77% yield) as a white solid.

^{1}H NMR (500 MHz, $CDCl_3$): δ 8.00 (dt, *J* = 8.4, 0.9 Hz, 1H), 7.81 (dt, *J* = 8.0, 1.1 Hz, 1H), 7.80 – 7.74 (m, 2H), 7.56 (s, 1H), 7.32 (ddd, *J* = 8.4, 7.2, 1.3 Hz, 1H), 7.30 – 7.24 (m, 1H), 7.25 – 7.19 (m, 2H), 5.51 (s, 1H), 5.25 – 5.20 (m, 1H), 2.34 (s, 3H), 2.17 (dd, *J* = 1.5, 0.8 Hz, 3H).

^{13}C NMR (100 MHz, $CDCl_3$): δ 145.1, 136.3, 135.7, 135.3, 130.0, 129.0, 127.0, 124.8, 124.1, 123.7, 123.6, 121.5, 113.9, 113.8, 23.2, 21.7.

HRMS (ESI): calcd for $C_{18}H_{18}NO_2S^+$ $[M+H]^+$: 312.1053, found: 312.1060.

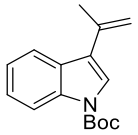

tert-butyl 3-(prop-1-en-2-yl)-1H-indole-1-carboxylate (5b)

Following **Procedure B**

tert-butyl 3-acetyl-1H-indole-1-carboxylate (321 mg, 2 mmol, 1 equiv.) was subjected to general procedure B with modifications: Nysted reagent solution (25 wt% in THF; 5 mL, 2.6 mmol, 1.3 equiv.) and $TiCl_4$ solution (1.0 M in DCM; 2.6 mL, 2.6 mmol, 1.3 equiv.). To furnish **95b** (298 mg, 1.16 mmol, 58% yield) as a yellow oil.

^{1}H NMR (500 MHz, CDCl3) δ 8.20 – 8.15 (m, 1H), 7.85 (d, J = 7.8 Hz, 1H), 7.58 (s, 1H), 7.36 – 7.29 (m, 1H), 7.29 – 7.21 (m, 1H), 5.54 (s, 1H), 5.21 (s, 1H), 2.18 (s, 3H), 1.67 (s, 9H).

^{13}C NMR (126 MHz, CDCl3) δ 149.78, 136.75, 136.03, 128.67, 124.41, 123.42, 122.90, 122.30, 120.94, 115.36, 113.02, 83.82, 30.36, 28.24, 23.11.

HRMS (ESI): calcd for $C_{16}H_{19}NO_2^+$ $[M+H]^+$: 258.1489, found: 258.1493.

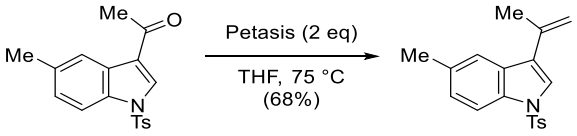

5-methyl-3-(prop-1-en-2-yl)-1-tosyl-1H-indole (95c) Representative Procedure for synthesis of 3-alkenyl indoles with Petasis reagent : **General procedure C**

To a 50mL dry recovery flask and stir bar was added **94c** (164 mg, 0.5 mmol, 1 eq) and 5 mL dry THF under nitrogen. After dissolution, Petasis reagent (0.5M solution in THF, 4mL, 2eq), was added in one portion, and the septum was replaced by a water jacketed reflux

condenser. The reaction as then lowered into an oil bath preheated to 75 °C, and the reaction was left to stir overnight. The following day, the reaction mixture was taken up in 10mL ether and filtered through a short plug of silica gel. The resulting yellow solution was concentrated and purified by column chromatography (10:90 EtOAc:hexanes) providing **95c** (110.6 mg, 0.34 mmol, 68% yield) as a white solid.

^{1}H NMR (400 MHz, $CDCl_3$) δ 7.87 (d, *J* = 8.5 Hz, 1H), 7.74 (d, *J* = 8.4 Hz, 2H), 7.58 (d, *J* = 0.8 Hz, 1H), 7.51 (s, 1H), 7.19 (d, *J* = 8.2 Hz, 2H), 7.13 (dd, *J* = 8.5, 1.7 Hz, 1H), 5.50 (s, 1H), 5.21 (t, *J* = 1.5 Hz, 1H), 2.41 (s, 3H), 2.31 (s, 3H), 2.15 (s, 2H).

^{13}C NMR (101 MHz, $CDCl_3$) δ 144.89, 136.33, 135.18, 133.84, 133.14, 129.88, 129.15, 126.81, 126.06, 123.82, 123.77, 121.33, 113.63, 113.40, 23.12, 21.56, 21.54.

HRMS (ESI): calcd for $C_{19}H_{19}NO_2S$+ [M+H]+: 398.1421, found: 398.1417.

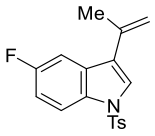

5-fluoro-3-(prop-1-en-2-yl)-1-tosyl-1H-indole (95d)

Following **Procedure C**

94d (161 mg, 1 mmol, 1eq) was subjected to **general procedure C** to furnish **95d** (78.9 mg, 0.24 mmol, 48%) as a white solid.

^{1}H NMR (400 MHz, $CDCl_3$) δ 7.94 (dd, *J* = 9.1, 4.6 Hz, 1H), 7.75 (d, *J* = 8.5 Hz, 2H), 7.58 (s, 1H), 7.45 (dd, *J* = 9.6, 2.5 Hz, 1H), 7.23 (d, *J* = 7.9 Hz, 1H), 7.05 (td, *J* = 8.9, 2.5 Hz, 1H), 5.42 (d, *J* = 1.2 Hz, 1H), 5.22 (p, *J* = 1.5 Hz, 1H), 2.35 (s, 3H), 2.15 (s, 3H).

^{13}C NMR (101 MHz, $CDCl_3$) δ 161.02, 158.63, 145.22, 135.86, 134.94, 131.89, 130.00, 129.92, 129.83, 128.24, 126.82, 125.14, 123.86, 123.82, 114.75, 114.65, 113.78, 112.80, 112.54, 107.34, 107.10, 23.00, 21.60.

HRMS (ESI): calcd for $C_{18}H_{16}FNO_2S$+ [M+H]+: 330.0959, found: 330.0950.

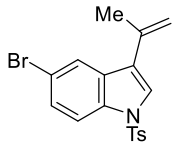

5-bromo-3-(prop-1-en-2-yl)-1-tosyl-1*H*-indole (95e)

Following **Procedure B**

94e (390 mg, 1.0 mmol, 1eq) was subjected to **general procedure B** with modifications: Nysted reagent solution (25 wt% in THF; 2.9 mL, 1.5 mmol, 1.5 equiv.) and $TiCl_4$ solution (1.0 M in DCM; 1.5 mL, 1.5 mmol, 1.5 equiv.). To furnish **95e** (171 mg, 0.44 mmol, 44% yield) as a white solid.

^{1}H NMR (400 MHz, $CDCl_3$) δ 7.92 (d, *J* = 1.9 Hz, 1H), 7.87 (d, *J* = 8.8 Hz, 1H), 7.74 (d, *J* = 8.4 Hz, 2H), 7.54 (s, 1H), 7.41 (dd, *J* = 8.8, 1.9 Hz, 1H), 7.29 – 7.11 (m, 2H), 5.43 (d, *J* = 1.1 Hz, 1H), 5.23 (d, *J* = 1.5 Hz, 1H), 2.34 (s, 3H), 2.14 (s, 2H).

^{13}C NMR (101 MHz, $CDCl_3$) δ 145.36, 135.66, 134.85, 134.25, 130.61, 130.05, 127.61, 126.84, 124.60, 124.16, 123.40, 117.19, 115.11, 114.20, 77.38, 77.06, 76.74, 23.06, 21.61.

HRMS (ESI): calcd for $C_{18}H_{16}BrNO_2S$+ [M+H]+: 390.0158, found 390.0145.

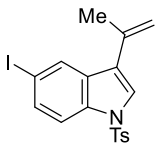

5-iodo-3-(prop-1-en-2-yl)-1-tosyl-1*H*-indole (95f)

Following **Procedure B**

94f (438 mg, 1.0 mmol, 1eq) was subjected to **general procedure B** with modifications: Nysted reagent solution (25 wt% in THF; 2.9 mL, 1.5 mmol, 1.5 equiv.) and $TiCl_4$ solution (1.0 M in DCM; 1.5 mL, 1.5 mmol, 1.5 equiv.). To furnish **95f** (197 mg, 0.45 mmol, 45% yield) as a white solid.

^{1}H NMR (400 MHz, $CDCl_3$) δ 8.12 (d, *J* = 1.6 Hz, 1H), 7.75 (dd, *J* = 8.5, 6.4 Hz, 2H), 7.59 (dd, *J* = 8.8, 1.6 Hz, 1H), 7.50 (s, 1H), 7.24 (d, *J* = 8.0 Hz, 2H), 5.43 (s, 1H), 5.29 – 5.20 (m, 1H), 2.35 (s, 2H), 2.14 (s, 3H).

^{13}C NMR (101 MHz, $CDCl_3$) δ 145.35, 135.65, 134.86, 134.79, 133.22, 131.16, 130.30, 130.05, 126.84, 124.20, 123.17, 115.50, 114.27, 87.90, 23.07, 21.62.

HRMS (ESI): calcd for $C_{18}H_{16}INO_2S$+ [M+H]+: 438.0019, found: 438.0010.

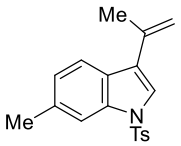

6-methyl-3-(prop-1-en-2-yl)-1-tosyl-1*H*-indole (95g)

Following **Procedure C**

94g (163.5 mg, 0.5 mmol, 1eq) was subjected to **general procedure C** to furnish **95g** (101 mg, 0.355mmol, 71%) as a white solid.

^{1}H NMR (400 MHz, $CDCl_3$) δ 7.83 – 7.78 (m, 1H), 7.76 (d, *J* = 8.4 Hz, 2H), 7.67 (d, *J* = 8.2 Hz, 1H), 7.48 (s, 1H), 7.22 (d, *J* = 7.8 Hz, 2H), 7.08 (dd, *J* = 8.2, 1.5 Hz, 1H), 5.50 (s, 1H), 5.20 (t, *J* = 1.5 Hz, 1H), 2.47 (s, 4H), 2.34 (s, 4H), 2.15 (t, *J* = 1.1 Hz, 4H).

^{13}C NMR (101 MHz, $CDCl_3$) δ 144.89, 136.32, 136.00, 135.32, 134.84, 129.91, 126.80, 126.61, 125.02, 123.84, 123.07, 120.95, 113.80, 113.50, 23.00, 21.84, 21.58.

HRMS (ESI): calcd for $C_{19}H_{19}NO_2S$+ [M+H]+: 326.1209, found: 326.1204.

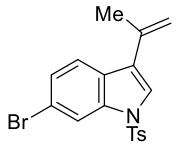

6-bromo-3-(prop-1-en-2-yl)-1-tosyl-1H-indole (95h)

Following **Procedure C**

94h (195.5 mg, 0.5 mmol, 1eq) was subjected to **general procedure C** to furnish **95h** (91.4 mg, 0.235 mmol, 47%) as a white solid.

^{1}H NMR (400 MHz, $CDCl_3$) δ 8.18 (d, *J* = 1.8 Hz, 1H), 7.77 (d, *J* = 8.4 Hz, 2H), 7.65 (d, *J* = 8.5 Hz, 1H), 7.51 (s, 1H), 7.37 (dd, *J* = 8.5, 1.8 Hz, 1H), 7.25 (d, *J* = 8.5 Hz, 0H), 5.44 (s, 1H), 5.22 (t, *J* = 1.4 Hz, 1H), 2.36 (s, 3H), 2.20 – 2.12 (m, 3H).

^{13}C NMR (101 MHz, $CDCl_3$) δ 145.38, 136.21, 135.80, 134.92, 130.12, 127.75, 126.86, 126.83, 123.90, 123.78, 122.51, 118.43, 116.74, 114.08, 23.02, 21.63.

HRMS (ESI): calcd for $C_{18}H_{16}BrNO_2S$+ [M+H]+: 390.0158, found: 390.0147.

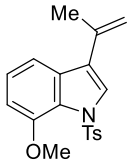

7-methoxy-3-(prop-1-en-2-yl)-1-tosyl-1*H*-indole (95i)

Following **Procedure B**

94i (343mg, 1 mmol, 1eq) was subjected to **general procedure B** with modifications: Nysted reagent solution (25 wt% in THF; 2.9 mL, 1.5 mmol, 1.5 equiv.) and $TiCl_4$ solution (1.0 M in DCM; 1.5 mL, 1.5 mmol, 1.5 equiv.). To furnish **95i** (134 mg, 0.39 mmol, 39% yield) as a white solid.

^{1}H NMR (400 MHz, $CDCl_3$) δ 7.84 (s, 2H), 7.73 (d, *J* = 8.4 Hz, 2H), 7.45 (d, *J* = 8.1 Hz, 1H), 7.16 (t, *J* = 8.0 Hz, 2H), 6.70 (d, *J* = 7.0 Hz, 1H), 5.51 (s, 2H), 5.24 (p, *J* = 1.6 Hz, 2H), 3.66 (s, 5H), 2.40 (s, 6H), 2.21 (s, 2H).

^{13}C NMR (101 MHz, $CDCl_3$) δ 147.40, 144.10, 137.49, 136.41, 131.72, 129.35, 127.21, 126.21, 125.42, 124.18, 121.87, 113.87, 113.43, 107.06, 55.47, 23.27, 21.62.

HRMS (ESI): calcd for $C_{19}H_{19}NO_3S$+ [M+H]+: 342.1158, found: 342.1152.

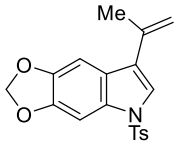

7-(prop-1-en-2-yl)-5-tosyl-5H-[1,3]dioxolo[4,5-f]indole (95j)

Following **Procedure B**

94j (122mg, 0.342 mmol, 1eq) was subjected to **general procedure B** with modifications: Nysted reagent solution (25 wt% in THF; 1 mL, 0.513 mmol, 1.5 equiv.) and $TiCl_4$ solution (1.0 M in DCM; 0.513 mL, 0.513 mmol, 1.5 equiv.). To furnish **95j** (43 mg, 0.12 mmol, 35% yield) as a white solid.

^{1}H NMR (500 MHz, $CDCl_3$) δ 7.74 (d, *J* = 8.4 Hz, 2H), 7.50 (s, 1H), 7.43 (s, 1H), 7.24 (d, *J* = 8.2 Hz, 2H), 7.17 (s, 1H), 5.98 (s, 2H), 5.37 (s, 1H), 5.18 (s, 1H), 2.36 (s, 2H), 2.12 (s, 3H).

^{13}C NMR (126 MHz, $CDCl_3$) δ 146.31, 145.37, 145.00, 136.31, 135.06, 130.45, 129.95, 126.83, 124.19, 123.02, 122.56, 113.28, 101.42, 100.24, 95.24, 23.10, 21.61.

HRMS (ESI): calcd for $C_{19}H_{17}NO_4S$+ [M+H]+: 356.0951, found: 356.0950.

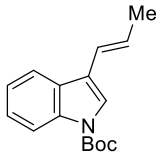

tert-butyl (E)-3-(prop-1-en-1-yl)-1H-indole-1-carboxylate (95k)

Based on a procedure by Terada[8]

To a suspension of ethyltriphenylphosphonium bromide (744 mg, 2 mmol, 1eq) in 10 mL dry THF was added phenyllithium in (1.6 M n-Bu_2O solution, 1.24 mL, 2 mmol, 1eq) at room temperature and the mixture was stirred for 10 min. The solution was cooled to -78 °C and tert-butyl 3-formylindole-1-carboxylate (490 mg, 2 mmol, 1eq) in 5mL dry Et_2O was added dropwise. The reaction was stirred for 5 min at -78 °C and then for 30 min at -30 °C, whereupon an additional equivalent of phenyllithium was added and the reaction mixture was kept at -30 °C for 5 min. This reaction was treated with hydrogen chloride (2.0 M Et_2O solution, 1.1 mL, 2.2 mmol, 1.1 eq), t-

[8] Terada, M.; Moriya, K.; Kanomata, K,; Sorimachi, K. *Angew. Chem. Int. Ed*. **2011**, 50: 12586-12590.

butanol (0.29 mL, 3 mmol, 1.5 eq), and potassium t-butoxide (337 mg, 3 mmol, 1.5 eq). The mixture was stirred for 2 h at room temperature. After cooling to 0 °C, the reaction mixture was quenched by saturated aqueous NH_4Cl solution and extracted with Et_2O (×3). The combined organic layers were washed with brine, dried over anhydrous sodium sulfate, and evaporated under reduced pressure. Purification by flash chromatography (10:90 EtOAc/Hexanes) to give **95k** as a colorless oil (262 mg, 1.02 mmol, 51% yield) (E/Z = 1:0.6)

^{1}H NMR (400 MHz, $CDCl_3$) δ 8.12 (d, *J* = 7.7 Hz, 1H), 7.74 (d, *J* = 7.5 Hz, 0H), 7.59 (d, *J* = 6.0 Hz, 1H), 7.57 (s, 0H), 7.37 – 7.29 (m, 1H), 7.28 (d, *J* = 0.8 Hz, 0H), 6.56 – 6.48 (m, 1H), 5.92 (dq, *J* = 11.3, 7.0 Hz, 1H), 1.93 (td, *J* = 6.4, 5.7, 1.7 Hz, 3H), 1.68 (d, *J* = 8.3 Hz, 6H).

^{13}C NMR (101 MHz, $CDCl_3$) δ 206.97, 130.57, 127.56, 126.37, 124.50, 123.45, 122.70, 122.59, 121.97, 119.88, 119.27, 119.14, 117.35, 115.29, 115.13, 83.75, 30.94, 28.23, 19.00, 15.62.

HRMS (ESI): calcd for $C_{16}H_{19}NO_2$+ [M+H]+: 258.1489, found: 258.1482.

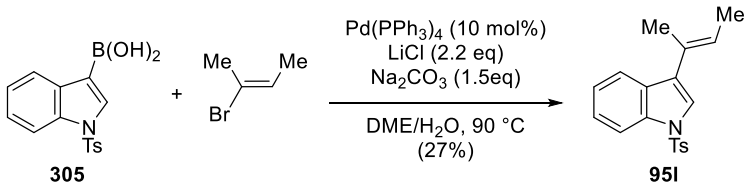

305 **95l**

(E)-3-(but-2-en-2-yl)-1-tosyl-1H-indole (95l)

(1-tosyl-1H-indol-3-yl)boronic acid **305** (315.2 mg, 1 mmol, 1eq), $Pd(PPh_3)_4$ (115mg, 0.1 mmol, 1eq), LiCl (93.3 mg, 2.2 mmol, 2.2 eq), were combined in a 5 mL round-bottom flask fitted with a water jacketed condenser. The system was evacuated and backfilled with argon, twice. Na_2CO_3 (2M solution in H_2O, 1.5 mmol, 0.75 mL, 1.5 eq), , E-2-bromo-2-butene (0.1 mL, 1 mmol, 1 eq), and 2 mL of degassed DME were added, and the flask was placed in an oil bath

preheated to 90 °C and left to stir for two hours. The reaction was cooled to room temperature, transferred with DCM (2 x 5mL) to a 25 mL separatory funnel containing 10 mL DI water. The aqueous layer was extracted with DCM 2 x 10 mL. The combined organic extracts were dried over sodium sulfate, filtered, and concentrated under reduced pressure. Purification with silica gel chromatography (gradient elution 6:94 to 12:88 EtOAc:Hexanes) gives **95l** as a colorless oil that slowly solidifies (88 mg, 0.27 mmol, 27%)

^{1}H NMR (400 MHz, $CDCl_3$) δ 7.99 (dt, *J* = 8.2, 1.0 Hz, 1H), 7.78 – 7.64 (m, 3H), 7.46 (s, 1H), 7.30 (ddd, *J* = 8.4, 7.2, 1.3 Hz, 1H), 7.25 – 7.17 (m, 3H), 6.03 (qq, *J* = 6.9, 1.4 Hz, 1H), 2.33 (s, 3H), 2.04 (p, *J* = 1.1 Hz, 3H), 1.83 (dq, *J* = 6.9, 1.1 Hz, 3H).

^{13}C NMR (101 MHz, $CDCl_3$) δ 144.81, 135.55, 135.26, 129.85, 129.28, 128.13, 126.82, 126.41, 124.52, 123.72, 123.23, 122.27, 121.25, 113.76, 21.57, 16.41, 14.02.

HRMS (ESI): calcd for $C_{19}H_{19}NO_2S$+ [M+H]+: 326.1209, found: 326.1206.

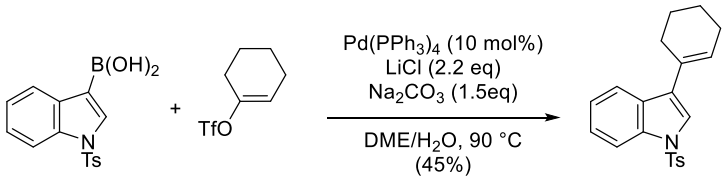

3-(cyclohex-1-en-1-yl)-1-tosyl-1H-indole (95m)

Prepared analogously to **(E)-3-(but-2-en-2-yl)-1-tosyl-1H-indole (95m)** from (1-tosyl-1H-indol-3-yl)boronic acid (200 mg, 0.635 mmol, 1eq) and to give **95m** as a white solid (101 mg, 0.288 mmol, 45%)

^{1}H NMR (400 MHz, $CDCl_3$) δ 7.99 (d, *J* = 8.1 Hz, 1H), 7.76 (t, *J* = 8.6 Hz, 2H), 7.46 (s, 1H), 7.34 – 7.17 (m, 6H), 6.27 (dt, *J* = 4.0, 2.2 Hz, 1H), 2.40 (ddt, *J* = 6.3, 4.1, 1.9 Hz, 2H), 2.33 (s, 2H), 2.29 – 2.19 (m, 2H), 1.80 (dtt, *J* = 11.5, 7.7, 4.4 Hz, 2H).

^{13}C NMR (101 MHz, $CDCl_3$) δ 144.81, 135.60, 135.26, 129.85, 129.78, 129.20, 126.81, 126.17, 125.08, 124.53, 123.25, 121.97, 121.34, 113.75, 28.35, 25.71, 22.85, 22.16, 21.57.

HRMS (ESI): calcd for $C_{21}H_{21}NO_2S$+ [M+H]+: 352.1366, found: 352.1358.

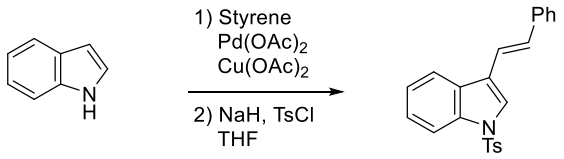

(E)-3-styryl-1-tosyl-1H-indole (95n)

To a 50 mL oven-dried round-bottom flask and stir bar was added 3-styrenyl indole[9] (219 mg, 1mmol, 1 eq) and dry THF 15 mL. NaH (60% dispersion in mineral oil, 60 mg, 1.5mmol, 1.5 eq) was added in one portion. The mixture was allowed to stir for one hour after which Tosyl chloride (229 mg, 1.2 mmol, 1.2 eq) was added in one portion and the reaction was left to stir for two hours. The reaction was quenched with DI water 50 mL, and transferred to a separatory funnel containing 50 mL of 1:1 EtOAc/Hexanes. The layers were separated and the aqueous fraction was extracted 3 x 25 mL 1:1 EtOAc/Hexanes. The combined organic layers were dried over sodium sulfate, filtered, and concentrated under reduced pressure. Purification by flash chromatography (15:85 EtOAc:hexanes) provided **95n** (360 mg, 0.96 mmol, 97% yield) as a light yellow foam that darkens over time.

[9] Grimster, N.P., Gauntlett, C., Godfrey, C.R.A. and Gaunt, M.J. *Angew. Chem. Int. Ed.*, **2005**, 44: 3125-3129

^{1}H NMR (500 MHz, $CDCl_3$) δ 8.02 (d, *J* = 8.1 Hz, 1H), 7.83 (d, *J* = 7.6 Hz, 1H), 7.77 (d, *J* = 8.2 Hz, 2H), 7.72 (s, 1H), 7.50 (d, *J* = 7.5 Hz, 2H), 7.35 (q, *J* = 7.0 Hz, 5H), 7.27 (dq, *J* = 20.6, 6.8, 6.0 Hz, 4H), 7.18 (d, *J* = 8.2 Hz, 3H), 7.16 (s, 2H), 2.29 (s, 3H).

^{13}C NMR (126 MHz, $CDCl_3$) δ 145.12, 137.39, 135.65, 135.09, 129.98, 129.85, 129.13, 128.79, 127.71, 126.89, 126.28, 125.09, 123.96, 123.63, 120.86, 120.48, 119.20, 113.89, 21.60.

HRMS (ESI): calcd for $C_{23}H_{19}NO_2S$+ [M+H]+: 374.1209, found: 374.1181.

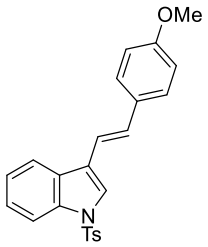

(E)-3-(4-methoxystyryl)-1-tosyl-1H-indole (95o)

Prepared analogously to **(E)-3-styryl-1-tosyl-1H-indole (95n)**

(E)-3-(4-methoxystyryl)-1H-indole (124.7 mg, 0.5 mmol, 1eq) yielded **95o** (110mg, 0.27 mmol, 55%)

^{1}H NMR (500 MHz, $CDCl_3$) δ 8.01 (d, *J* = 8.1 Hz, 1H), 7.82 (d, *J* = 7.6 Hz, 1H), 7.78 (d, *J* = 8.4 Hz, 2H), 7.68 (s, 1H), 7.44 (d, *J* = 8.7 Hz, 2H), 7.32 (dt, *J* = 25.9, 7.2 Hz, 2H), 7.20 (d, *J* = 8.1 Hz, 2H), 7.13 (d, *J* = 16.5 Hz, 1H), 7.02 (d, *J* = 16.5 Hz, 1H), 6.91 (d, *J* = 8.7 Hz, 2H), 3.83 (s, 3H), 2.32 (s, 3H).

^{13}C NMR (126 MHz, $CDCl_3$) δ 159.39, 144.99, 135.66, 130.19, 129.91, 129.46, 129.25, 127.47, 126.85, 124.97, 123.50, 123.30, 121.16, 120.40, 116.98, 114.23, 113.87, 55.35, 21.56.HRMS (ESI): calcd for $C_{24}H_{21}NO_3S$+ [M+H]+: 404.1315, found: 398.1417.

HRMS (ESI): calcd for $C_{24}H_{21}NO_3S$+ [M+H]+: 404.1315, found: 304.1308.

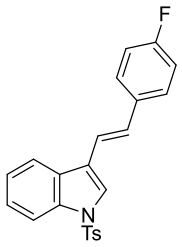

(E)-3-(4-fluorostyryl)-1-tosyl-1H-indole (95p)

Prepared analogously to **(E)-3-styryl-1-tosyl-1H-indole (95n)**

3-[(E)-2-(4-fluorophenyl)ethenyl]-1H-indole (237 mg, 1 mmol, 1eq) yielded **95p** (253mg, 0.647 mmol, 65%)

^{1}H NMR (400 MHz, $CDCl_3$) δ 8.02 (d, *J* = 7.4 Hz, 1H), 7.82 (d, *J* = 7.9 Hz, 2H), 7.71 (s, 2H), 7.50 – 7.42 (m, 3H), 7.33 (dtd, *J* = 21.4, 7.3, 1.3 Hz, 3H), 7.21 (d, *J* = 8.1 Hz, 3H), 7.18 – 7.00 (m, 7H), 2.32 (s, 3H).

^{13}C NMR (101 MHz, $CDCl_3$) δ 163.60, 161.14, 145.11, 135.62, 135.10, 133.60, 133.56, 129.96, 129.03, 128.61, 127.77, 127.70, 126.88, 125.09, 123.88, 123.60, 120.67, 120.36, 118.99, 118.97, 115.82, 115.61, 113.89, 21.59.HRMS (ESI): calcd for $C_{23}H_{18}FNO_2S$+ [M+H]+: 392.1115, found: 398.1417.

HRMS (ESI): calcd for $C_{23}H_{18}FNO_2S$+ [M+H]+: 392.1115, found: 392.1106.

Failed Substrates

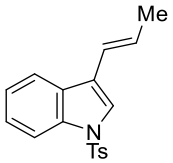

101a

(E)-3-(prop-1-en-1-yl)-1-tosyl-1H-indole (101a)

Prepared Analogously to **95m**

N-Tosyl indole-3-boronic acid (0.5 mmol, 158 mg, 1 eq) and E-Bromopropene gave **101a**, as a white solid (74 mg, 0.24 mmol, 48%). Spectral data is consistent with literature values.[10]

^{1}H NMR (500 MHz, CDCl3) δ 8.17 (d, J = 8.4 Hz, 1H), 7.84 – 7.27 (m, 6H), 7.21 – 7.12 (m, 4H), 7.04 (dd, J = 15.0, 2.4 Hz, 1H), 6.59 (s, 1H), 6.21 – 6.10 (m, 1H), 2.31 (s, 3H), 1.95 (dd, J = 6.8, 1.9 Hz, 3H).

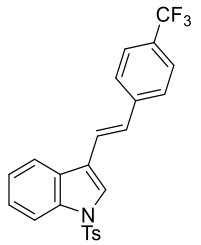

101b

(E)-1-tosyl-3-(4-(trifluoromethyl)styryl)-1H-indole (101b)

Prepared analogously to **95n**

^{1}H NMR (500 MHz, $CDCl_3$) δ 8.03 (d, *J* = 8.2 Hz, 1H), 7.85 (d, *J* = 7.7 Hz, 1H), 7.83 – 7.75 (m, 3H), 7.67 – 7.52 (m, 4H), 7.41 – 7.30 (m, 2H), 7.26 – 7.16 (m, 4H), 2.35 (s, 3H).

[10] del Hoyo, A. M.; Herraiz, A. G.; Suero, M. G. *Angew. Chemie Int. Ed.* **2017**, 56 (6), 1610–1613

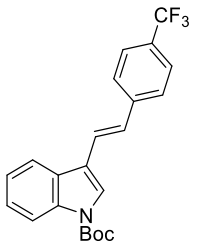

101c

tert-butyl (E)-3-(4-(trifluoromethyl)styryl)-1H-indole-1-carboxylate (101c)

Prepared analogously to **95n**

^{1}H NMR (500 MHz, CDCl3) δ 8.21 (s, 1H), 7.91 (d, J = 7.8 Hz, 1H), 7.79 (s, 1H), 7.62 (s, 4H), 7.42 – 7.32 (m, 3H), 7.22 (d, J = 16.4 Hz, 1H), 1.70 (s, 9H).

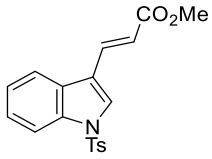

101d

methyl (E)-3-(1-tosyl-1H-indol-3-yl)acrylate (101d)

Prepared according to the literaturefrom indole-3 carboxylate.[11]

^{1}H NMR: (400 MHz, $CDCl_3$) δ 8.00 (d, *J* = 8.0 Hz, 1H), 7.84 (s, 1H), 7.83 – 7.75 (m, 3H), 7.42 – 7.32 (m, 2H), 7.28 – 7.21 (m, 3H), 6.52 (d, *J* = 16.1 Hz, 1H), 3.82 (s, 3H), 2.35 (s, 3H).

^{13}C NMR: (101 MHz, CDCl3) δ 167.54, 145.56, 135.87, 135.61, 134.78, 130.12, 128.43, 128.12, 127.01, 125.52, 124.11, 120.66, 118.13, 117.90, 113.85, 51.73, 21.62.

[11] Nocquet, P.-A.; Corbu, A.; Meerpoel, L.; Stansfield, I.; Berthelot, D.; Angibaud, P.; Cossy, J. *Eur. J. Org. Chem*. **2017**: 3343-3354.

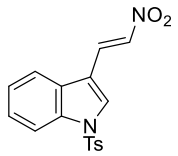

101e

(E)-3-(2-nitrovinyl)-1-tosyl-1H-indole (101e)

Prepared according to the literaturefrom N-tosyl indole 3- carboxylate.[12]

^{1}H NMR (400 MHz, $CDCl_3$) δ 8.15 (d, *J* = 13.8 Hz, 1H), 8.03 (d, *J* = 10.4 Hz, 2H), 7.83 (d, *J* = 8.5 Hz, 2H), 7.74 (d, *J* = 13.5 Hz, 1H), 7.70 (d, *J* = 6.7 Hz, 1H), 7.48 – 7.34 (m, 2H), 7.29 (d, *J* = 8.6 Hz, 2H), 7.33 – 7.27 (m, 2H), 2.37 (s, 3H).

^{13}C NMR (101 MHz, $CDCl_3$) δ 146.09, 136.35, 134.41, 131.62, 130.82, 130.31, 127.16, 126.18, 124.71, 120.63, 114.10, 21.68.

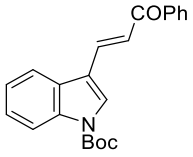

101f

tert-butyl (E)-3-(3-oxo-3-phenylprop-1-en-1-yl)-1H-indole-1-carboxylate (101f)

Prepared from **(E)-3-(1H-indol-3-yl)-1-phenylprop-2-en-1-one**

^{1}H NMR (400 MHz, $CDCl_3$) δ 8.23 (d, *J* = 7.9 Hz, 1H), 8.09 – 7.91 (m, 5H), 7.66 (d, *J* = 15.9 Hz, 1H), 7.64 – 7.48 (m, 3H), 7.40 (pd, *J* = 7.3, 1.5 Hz, 2H), 1.70 (s, 9H).

^{13}C NMR (101 MHz, $CDCl_3$) δ 190.54, 136.77, 132.65, 129.60, 128.65, 128.46, 127.99, 125.39, 123.72, 121.35, 120.37, 117.44, 115.70, 28.16.

[12] Kinsman, A. C.; Kerr M. A. *Org. Lett.* **2001** 3 (20), 3189-3191

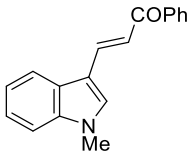

101g

(E)-3-(1-methyl-1H-indol-3-yl)-1-phenylprop-2-en-1-one (101g)

Prepared according to the literature from N-methyl indole 3-carboxylate.[13]

^{1}H NMR (400 MHz, $CDCl_3$) δ 8.13 – 7.97 (m, 4H), 7.60 – 7.46 (m, 5H), 7.42 – 7.28 (m, 3H), 3.85 (s, 3H).

^{13}C NMR (101 MHz, $CDCl_3$) δ 190.78, 139.19, 138.69, 134.61, 132.13, 128.50, 128.30, 123.20, 121.60, 120.86, 117.10, 110.15, 33.32, 30.94.

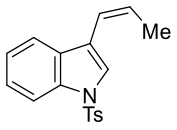

101h

(Z)-3-(prop-1-en-1-yl)-1-tosyl-1H-indole (101h)

Prepared analogously to **101a** from N-tosyl indole 3-boronic acid.[14]

^{1}H NMR (400 MHz, CDCl3) δ 7.99 (dd, J = 8.3, 0.9 Hz, 1H), 7.83 – 7.72 (m, 2H), 7.57 – 7.50 (m, 1H), 7.23 – 7.19 (m, 2H), 7.13 (d, J = 7.9 Hz, 1H), 6.52 – 6.40 (m, 1H), 5.94 (dd, J = 11.3, 7.1 Hz, 1H), 2.32 (s, 3H), 1.93 (dd, J = 7.1, 1.8 Hz, 3H).

^{13}C NMR (101 MHz, CDCl3) δ 129.87, 129.51, 128.50, 126.80, 126.63, 124.86, 123.58, 123.23, 119.58, 118.76, 113.59, 25.62, 21.56, 15.67.

[13] Chen, K. *Eur. J. Med. Chem.* ***2018*** 156: p.722-737
[14] del Hoyo, A. M.; Herraiz, A. G.; Suero, M. G. *Angew. Chemie Int. Ed*. **2017**, 56 (6), 1610–1613

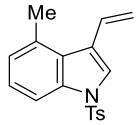

101i

4-methyl-1-tosyl-3-vinyl-1H-indole (101i)

Prepared according to literature procedure.[15]

^{1}H NMR (500 MHz, $CDCl_3$) δ 7.73 (d, *J* = 8.1 Hz, 2H), 7.39 – 7.32 (m, 5H), 7.29 (d, *J* = 8.2 Hz, 2H), 7.14 (dt, *J* = 3.3, 1.4 Hz, 1H), 7.01 (t, *J* = 1.9 Hz, 1H), 6.44 (dd, *J* = 3.3, 1.7 Hz, 1H), 5.42 (d, *J* = 1.2 Hz, 1H), 5.19 (d, *J* = 1.2 Hz, 1H), 2.41 (s, 3H).

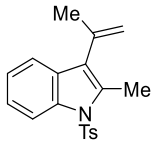

101j

2-methyl-3-(prop-1-en-2-yl)-1-tosyl-1H-indole (101j)

^{1}H NMR (400 MHz, CDCl3) δ 8.19 (d, J = 8.3 Hz, 3H), 7.66 (d, J = 8.4 Hz, 5H), 7.40 (d, J = 7.5 Hz, 3H), 7.26 (td, J = 8.3, 7.8, 1.6 Hz, 2H), 7.21 (t, J = 7.5 Hz, 9H), 5.39 – 5.32 (m, 5H), 4.92 (s, 1H), 2.55 (s, 8H), 2.35 (s, 8H), 2.04 (s, 10H).

^{13}C NMR (101 MHz, CDCl3) δ 144.61, 137.32, 136.44, 136.21, 132.23, 129.85, 129.56, 126.39, 124.28, 123.92, 123.29, 119.32, 117.76, 114.51, 23.60, 21.57, 13.44.

5.1.3 Experimental Details for Chapter 2 – [4+3] cycloaddition of 3-alkenyl indoles

[15]Marcin, L. R.; Denhart, D. J.; Mattson R. J. *Org. Lett.* **2005** 7 (13), 2651-2654

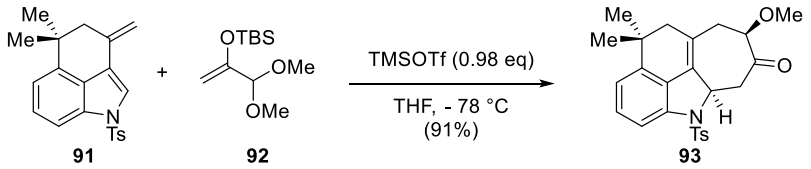

7-methoxy-10,10-dimethyl-4-tosyl-4a,5,7,8,9,10-hexahydrobenzo[*cd*]cyclohepta[*hi*]isoindol-6(4*H*)-one (93)

Representative Procedure for the [4+3] Cycloaddition: **Procedure D**

A 10 mL recovery flask with a magnetic stir bar was charged with TBS enol ether **92** (52.3 mg, 0.225 mmol, 1 equiv.) and tricyclic diene **91** (79.1 mg, 0.225 mmol, 1 equiv.). 4.5 mL THF was added to give a colorless solution, which was cooled to −78 °C. TMSOTf (0.040 mL, 0.221 mmol, 0.98 equiv.) was added dropwise, and the mixture became light yellow immediately. After 1.5 h stirring at −78 °C, the reaction mixture was quenched with 3 mL saturated aqueous $NaHCO_3$, and allowed to warm to ambient temperature. The mixture was partitioned between 30 mL 1:1 brine:H_2O and 20 mL 1:1 EtOAc:hexanes, and the aqueous layer was extracted with 20 mL 1:1 EtOAc:hexanes. The combined organic layers were washed with brine, dried over Na_2SO_4, and concentrated under reduce pressure. The crude material was purified by flash chromatography (gradient elution 25:75 → 30:70 EtOAc:hexanes) to afford tetracycle **93** (89.2 mg, 0.204 mmol, 91% yield) as a white solid.

^{1}H NMR (500 MHz, $CDCl_3$): δ 7.66 (d, *J* = 8.4 Hz, 2H), 7.43 (d, *J* = 8.1 Hz, 1H), 7.23 (d, *J* = 8.0 Hz, 2H), 7.18 (t, *J* = 7.9 Hz, 1H), 6.92 (d, *J* = 7.5 Hz, 1H), 4.89 (d, *J* = 11.4 Hz, 1H), 4.27 (dd, *J* = 9.7, 4.4 Hz, 1H), 3.49 (dd, *J* = 15.3, 4.6 Hz, 1H), 3.36 (s, 3H), 2.99 (dd, *J* = 15.3, 11.5 Hz, 1H), 2.60 (d, *J* = 17.4 Hz, 1H), 2.45 – 2.28 (m, 2H), 2.37 (s, 3H), 2.05 (d, *J* = 17.4 Hz, 1H), 1.28 (s, 3H), 1.00 (s, 3H)

^{13}C NMR (125 MHz, $CDCl_3$): δ 208.4, 144.4, 140.6, 140.1, 134.4, 129.9, 129.9, 129.8, 127.5, 126.5, 123.7, 119.0, 113.4, 84.4, 61.4, 57.9, 48.4, 47.1, 38.4, 34.5, 29.9, 27.5, 21.7.

HRMS (ESI): calcd for $C_{25}H_{28}NO_4S^+$ $[M+H]^+$: 438.1734, found: 438.1728. m.p. = 160–162 °C.

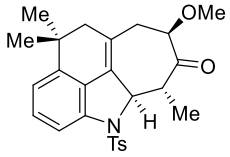

93b

(4a*R*,5*R*,7*R*)-7-methoxy-5,10,10-trimethyl-4-tosyl-4a,5,7,8,9,10-hexahydrobenzo[*cd*]cyclohepta[*hi*]isoindol-6(4*H*)-one (93b)

Prepared according to the representative procedure for the [4+3] cycloaddition (**Procedure D**) from diene **91** (55.4 mg, 0.158 mmol, 1 equiv.), TBS enol ether **92b** (58.3 mg, 0.237 mmol, 1.5 equiv.), and TMSOTf (0.042 mL, 0.233 mmol, 1.48 equiv.).Tetracycle **93b** (62.9 mg, 0.139 mmol, 88% yield) was obtained as a white solid.

^{1}H NMR (500 MHz, $CDCl_3$): δ 7.44 (d, *J* = 7.9 Hz, 1H), 7.34 (d, *J* = 8.3 Hz, 2H), 7.19 (t, *J* = 7.8 Hz, 1H), 7.07 (d, *J* = 8.0 Hz, 2H), 6.94 (d, *J* = 7.5 Hz, 1H), 4.72 (d, *J* = 10.7 Hz, 1H), 4.39 (dd, *J* = 9.7, 5.1 Hz, 1H), 3.30 (s, 3H), 2.80 (dq, *J* = 10.6, 7.2 Hz, 1H), 2.71 – 2.64 (m, 1H), 2.29 (s, 3H), 2.28 – 2.19 (m, 2H), 1.97 (d, *J* = 17.4 Hz, 1H), 1.53 (d, *J* = 7.5 Hz, 3H), 1.23 (s, 3H), 0.72 (s, 3H).

^{13}C NMR (100 MHz, $CDCl_3$): δ 212.4, 144.1, 140.5, 139.9, 133.2, 130.7, 129.4, 129.3, 129.1, 127.7, 124.2, 120.2, 117.1, 82.7, 66.6, 57.8, 53.3, 47.1, 38.7, 34.2, 29.7, 26.9, 21.5, 15.0.

HRMS (ESI): calcd for $C_{26}H_{30}NO_4S^+$ $[M+H]^+$: 452.1890, found: 452.1886.

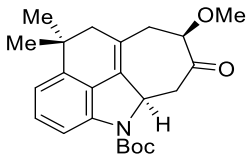

93c

***tert*-butyl (4a*R*,7*R*)-7-methoxy-10,10-dimethyl-6-oxo-5,6,7,8,9,10-hexahydrobenzo[*cd*]cyclohepta[*hi*]isoindole-4(4*aH*)-carboxylate (93c)**

Prepared according to the representative procedure for the [4+3] cycloaddition (**Procedure D**) from diene **91b** (121 mg, 0.408 mmol, 1 equiv.), TBS enol ether 92 (142 mg, 0.612 mmol, 1.5 equiv.), and TMSOTf (0.109 mL, 0.604 mmol, 1.48 equiv.). Tetracycle **91b** (131 mg, 0.342 mmol, 84% yield) was obtained as a light yellow solid. The product exists as two rotamers in $CDCl_3$ at room temperature in a ratio of 1.6:1.

^{1}H NMR (500 MHz, $CDCl_3$, * denotes minor rotamer): δ 7.58 (br s, 1H*), 7.20 (br s, 1H), 7.15 (br s, 1H and 1H*), 6.90 (d, *J* = 7.5 Hz, 1H and 1H*), 5.40 (br s, 1H), 5.08 (br s, 1H*), 4.50 (br s, 1H), 4.32 (br s, 1H*), 3.66 (d, *J* = 16.7 Hz, 1H), 3.44 – 3.24 (m, 1H*), 3.36 (s, 3H and 3H*), 2.76 (br d, *J* = 19.7 Hz, 1H and 1H*), 2.65 (br s, 1H and 1H*), 2.41 (br s, 2H and 2H*), 2.09 (br d, *J* = 16.9 Hz, 1H and 1H*), 1.60 (s, 9H and 9H*), 1.34 (s, 3H and 3H*), 1.13 (s, 3H and 3H*).

^{13}C NMR (100 MHz, $CDCl_3$): δ 209.3, 208.6, 152.6, 140.3, 139.8, 130.8, 130.0, 129.6, 125.8, 122.6, 117.6, 113.1, 84.9, 83.3, 82.4, 81.8, 59.3, 58.4, 58.0, 47.4, 46.8, 46.3, 38.8, 38.1, 34.4, 30.0, 28.5, 27.4.

HRMS (ESI): calcd for $C_{23}H_{29}NO_4Na^+$ $[M+Na]^+$: 406.1989, found: 406.1984.

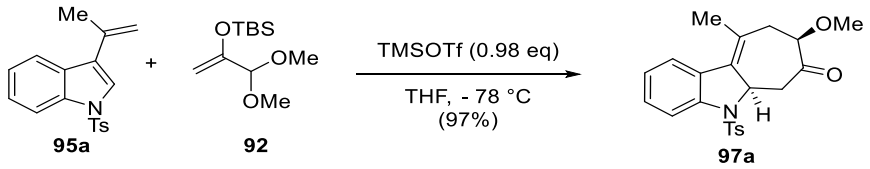

8-methoxy-10-methyl-5-tosyl-5a,6,8,9-tetrahydrocyclohepta[*b*]indol-7(5*H*)-one (97a)

Prepared according to the representative procedure for the [4+3] cycloaddition (**Procedure D)** from diene **95a** (76.9 mg, 0.247 mmol, 1 equiv.), TBS enol ether **92** (86.1 mg, 0.371 mmol, 1.5 equiv.), and TMSOTf (0.066 mL, 0.366 mmol, 1.48 equiv.). Tricycle **97a** (94.9 mg, 0.239 mmol, 97% yield) was obtained as a white solid.

^{1}H NMR (500 MHz, $CDCl_3$): δ 7.76 (ddd, *J* = 8.2, 1.2, 0.6 Hz, 1H), 7.63 – 7.57 (m, 2H), 7.49 (d, *J* = 7.9 Hz, 1H), 7.24 (ddd, *J* = 8.4, 7.4, 1.3 Hz, 1H), 7.19 (dt, *J* = 8.0, 0.7 Hz, 2H), 7.07 (td, *J* = 7.6, 1.1 Hz, 1H), 4.79 (ddq, *J* = 11.2, 3.4, 1.7 Hz, 1H), 4.16 (ddd, *J* = 7.3, 5.1, 0.9 Hz, 1H), 3.33 (s, 3H), 3.31 (ddd, *J* = 14.3, 3.5, 0.9 Hz, 1H), 2.92 (dd, *J* = 14.3, 11.3 Hz, 1H), 2.61 – 2.53 (m, 2H), 2.35 (s, 3H), 2.07 (d, *J* = 1.8 Hz, 3H).

^{13}C NMR (100 MHz, $CDCl_3$): δ 207.1, 144.5, 143.4, 134.3, 132.3, 129.9, 129.4, 128.7, 127.3, 127.3, 125.0, 124.5, 116.1, 84.9, 61.5, 57.9, 49.4, 41.1, 23.4, 21.7.

HRMS (ESI): calcd for $C_{22}H_{24}NO_4S^+$ $[M+H]^+$: 398.1421, found: 398.1417.

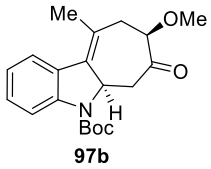

tert-butyl 8-methoxy-10-methyl-7-oxo-6,7,8,9-tetrahydrocyclohepta[b]indole-5(5aH)-carboxylate (97b)

Prepared according to the representative procedure for the [4+3] cycloaddition (**Procedure D)** from diene **95b** (52 mg, 0.2 mmol, 1 equiv.), TBS enol ether **92** (57 mg, 0.3mmol, 1.5 equiv.),

and TMSOTf (0.05 mL, 0.3 mmol, 1.5 equiv.), tricycle **97b** (57.6 mg, 0.167 mmol, 83% yield) was obtained as a yellow oil.

^{1}H NMR (500 MHz, CDCl3) δ 7.99 (br. s, 1H), 7.58 (d, J = 7.8 Hz, 1H), 7.21 (t, J = 7.7 Hz, 1H), 7.03 (t, J = 7.5 Hz, 1H), 4.96 (br. d, J = 184.0 Hz, 1H), 4.04 (br. s, 1H), 3.31 (s, 3H), 2.69 (br. s, 2H), 2.20 (s, 2H), 1.59 (s, 9H), 1.26 (s, 3H), 0.90 (s, 2H).

^{13}C NMR (101 MHz, CDCl3) δ 207.76, 182.02, 128.38, 125.96, 124.49, 122.76, 122.58, 115.58, 115.40, 90.77, 60.42, 57.69, 46.80, 34.77, 32.89, 31.61, 30.33, 28.42, 28.35, 28.23, 25.29, 22.67, 21.21, 21.08, 14.22, 14.14.

HRMS (ESI): calcd for $C_{20}H_{25}NO_4^+$ $[M+Na]^+$: 366.1681, found: 366.1668.

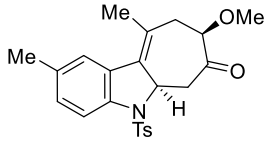

8-methoxy-2,10-dimethyl-5-tosyl-5a,6,8,9-tetrahydrocyclohepta[*b*]indol-7(5*H*)-one (97c)

Prepared according to the representative procedure for the [4+3] cycloaddition (**Procedure D)** from diene **95c** (50 mg, 0.154 mmol, 1 equiv.), TBS enol ether **92** (53.6 mg, 0.231mmol, 1.5 equiv.), and TMSOTf (0.03 mL, 0.154 mmol, 1.5 equiv.), tricycle **97c** (60.2 mg, 0.146 mmol, 95% yield) was obtained as a white solid.

^{1}H NMR (500 MHz, $CDCl_3$) δ 7.65 (d, *J* = 8.4 Hz, 1H), 7.59 (d, *J* = 8.2 Hz, 2H), 7.28 (s, 1H), 7.19 (d, *J* = 8.1 Hz, 2H), 7.05 (d, *J* = 8.2 Hz, 1H), 4.75 (d, *J* = 10.1 Hz, 1H), 4.15 (dd, *J* = 6.9, 5.3 Hz, 1H), 3.33 (s, 3H), 3.28 (dd, *J* = 14.2, 3.4 Hz, 1H), 2.90 (dd, *J* = 14.3, 11.4 Hz, 1H), 2.58 – 2.53 (m, 2H), 2.35 (s, 3H), 2.32 (s, 3H), 2.07 (s, 3H).

^{13}C NMR (126 MHz, $CDCl_3$) δ 206.96, 144.17, 141.12, 134.21, 133.97, 132.40, 129.73, 129.37, 129.28, 127.20, 126.84, 125.38, 115.89, 84.90, 61.57, 57.76, 49.28, 40.99, 23.29, 21.53, 21.30.

HRMS (ESI): calcd for $C_{23}H_{25}NO_4S^+$ $[M+H]^+$: 412.1577, found: 412.1582.

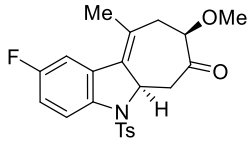

2-fluoro-8-methoxy-10-methyl-5-tosyl-5a,6,8,9-tetrahydrocyclohepta[*b*]indol-7(5*H*)-one (97d)

Prepared according to the representative procedure for the [4+3] cycloaddition (**Procedure D)** from diene **95d** (50 mg, 0.152 mmol, 1 equiv.), TBS enol ether **92** (86.1 mg, 0.371 mmol, 1.5 equiv.), and TMSOTf (0.03 mL, 0.154 mmol,, 1.01 equiv.), tricycle **97d** (58.2 mg, 0.239 mmol, 92% yield) was obtained as a white solid.

^{1}H NMR (500 MHz, $CDCl_3$) δ 7.72 (dd, *J* = 8.9, 4.8 Hz, 1H), 7.57 (d, *J* = 8.2 Hz, 1H), 7.21 (d, *J* = 8.1 Hz, 2H), 7.17 (dd, *J* = 9.5, 2.5 Hz, 1H), 6.95 (td, *J* = 8.7, 2.6 Hz, 1H), 4.75 (d, *J* = 10.2 Hz, 1H), 4.16 – 4.08 (m, 2H), 3.32 (s, 3H), 3.27 (dd, *J* = 14.0, 3.1 Hz, 1H), 2.93 (dd, *J* = 14.1, 11.4 Hz, 1H), 2.63 – 2.48 (m, 3H), 2.37 (s, 2H), 2.05 (s, 3H).

^{13}C NMR (101 MHz, $CDCl_3$) δ 206.75, 161.21, 158.81, 144.55, 139.33, 139.31, 133.71, 131.73, 131.70, 130.94, 130.85, 129.87, 129.13, 127.21, 117.07, 116.99, 115.17, 114.93, 111.89, 111.63, 84.90, 61.96, 57.81, 49.10, 40.95, 23.27, 21.59.

HRMS (ESI): calcd for $C_{22}H_{22}FNO_4S^+$ $[M+H]^+$: 416.1326, found: 416.1325.

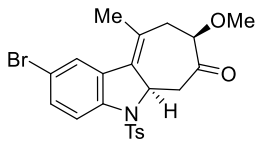

2-bromo-8-methoxy-10-methyl-5-tosyl-5a,6,8,9-tetrahydrocyclohepta[*b*]indol-7(5*H*)-one (97e)

Prepared according to the representative procedure for the [4+3] cycloaddition (**Procedure D)** from diene **95e**(50 mg, 0.247 mmol, 1 equiv.), TBS enol ether **92** (86.1 mg, 0.371 mmol, 1.5 equiv.), and TMSOTf (0.066 mL, 0.366 mmol, 1.48 equiv.), tricycle **97e** (94.9 mg, 0.239 mmol, 90% yield) was obtained as a white solid.

^{1}H NMR (400 MHz, $CDCl_3$) δ 7.64 (d, *J* = 8.6 Hz, 1H), 7.61 – 7.55 (m, 3H), 7.34 (dd, *J* = 8.6, 2.0 Hz, 1H), 7.22 (d, *J* = 7.9 Hz, 2H), 4.72 (d, *J* = 11.0 Hz, 1H), 4.11 (dd, *J* = 8.1, 3.5 Hz, 1H), 3.32 (s, 3H), 3.27 (dd, *J* = 14.0, 2.6 Hz, 1H), 2.92 (dd, *J* = 13.9, 11.3 Hz, 1H), 2.66 – 2.48 (m, 2H), 2.37 (s, 3H), 2.07 (s, 3H).

^{13}C NMR (101 MHz, $CDCl_3$) δ 206.72, 144.68, 142.36, 133.82, 131.25, 131.20, 129.95, 129.37, 127.67, 127.15, 117.46, 117.29, 84.98, 61.82, 57.81, 49.01, 40.95, 23.52, 21.61.

HRMS (ESI): calcd for $C_{22}H_{22}BrNO_4S^+$ $[M+H]^+$: 476.0526, found: 476.0511.

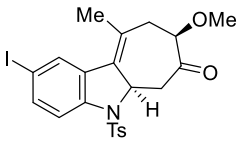

2-iodo-8-methoxy-10-methyl-5-tosyl-5a,6,8,9-tetrahydrocyclohepta[*b*]indol-7(5*H*)-one (97f)

Prepared according to the representative procedure for the [4+3] cycloaddition (**Procedure D)** from diene **95f** (50 mg, 0.1144 mmol, 1 equiv.), TBS enol ether **92** (40 mg, 0.1716 mmol, 1.5 equiv.), and TMSOTf (0.02 mL, 0.1144mmol, 1 equiv.), tricycle **97f** (94.9 mg, 0.239 mmol, 92% yield) was obtained as a white/tan solid.

^{1}H NMR (400 MHz, $CDCl_3$) δ 7.77 (s, 1H), 7.59 (d, *J* = 8.3 Hz, 2H), 7.52 (d, *J* = 0.9 Hz, 2H), 7.22 (d, *J* = 8.0 Hz, 2H), 4.70 (d, *J* = 10.5 Hz, 1H), 4.10 (dd, *J* = 7.9, 3.7 Hz, 1H), 3.31 (s, 3H), 3.26 (dd, *J* = 13.6, 2.9 Hz, 1H), 2.91 (dd, *J* = 13.9, 11.2 Hz, 1H), 2.37 (s, 3H), 2.06 (s, 3H).

^{13}C NMR (101 MHz, CH_3CN+D_2O) δ 204.16, 142.13, 140.54, 134.63, 131.36, 131.02, 129.00, 128.57, 127.42, 126.71, 124.60, 115.20, 85.44, 82.48, 59.13, 55.27, 46.46, 38.40, 21.00, 19.07.

HRMS (ESI): calcd for $C_{22}H_{22}INO_4S^+$ $[M+H]^+$: 524.0387, found: 524.0392.

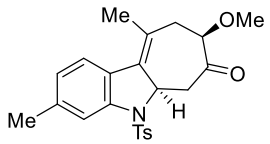

8-methoxy-3,10-dimethyl-5-tosyl-5a,6,8,9-tetrahydrocyclohepta[*b*]indol-7(5*H*)-one (97g)

Prepared according to the representative procedure for the [4+3] cycloaddition (**Procedure D)** from diene **95g** (50 mg, 0.154 mmol, 1 equiv.), TBS enol ether **92** (53.6 mg, 0.231mmol, 1.5 equiv.), and TMSOTf (0.03 mL, 0.154 mmol, 1 equiv.), tricycle **97g** (94.9 mg, 0.239 mmol, 93% yield) was obtained as a white solid.

^{1}H NMR (500 MHz, $CDCl_3$) δ 7.60 (d, *J* = 8.4 Hz, 3H), 7.36 (d, *J* = 7.9 Hz, 1H), 7.20 (d, *J* = 8.1 Hz, 2H), 6.88 (d, *J* = 7.9 Hz, 1H), 4.78 (d, *J* = 10.4 Hz, 1H), 4.16 (dd, *J* = 7.9, 4.5 Hz, 1H), 3.33 (s, 2H), 3.29 (dd, *J* = 14.3, 3.2 Hz, 1H), 2.90 (dd, *J* = 14.4, 11.4 Hz, 1H), 2.55 (qd, *J* = 16.6, 6.0 Hz, 3H), 2.38 (s, 3H), 2.36 (s, 3H), 2.04 (s, 3H).

^{13}C NMR (126 MHz, $CDCl_3$) δ 206.98, 144.25, 143.51, 139.01, 134.39, 132.15, 129.77, 127.14, 126.70, 125.64, 125.33, 124.51, 116.57, 84.83, 61.63, 57.76, 49.35, 40.93, 23.12, 21.70, 21.54.

HRMS (ESI): calcd for $C_{23}H_{25}NO_4S^+$ $[M+H]^+$: 412.1577, found: 412.1582.

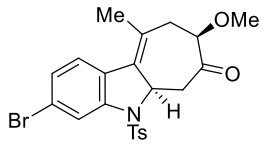

3-bromo-8-methoxy-10-methyl-5-tosyl-5a,6,8,9-tetrahydrocyclohepta[*b*]indol-7(5*H*)-one (97h)

Prepared according to the representative procedure for the [4+3] cycloaddition (**Procedure D)** from diene **95h** (50 mg, 0.129 mmol, 1 equiv.), TBS enol ether **92** (44.7 mg, 0.193mmol, 1.5 equiv.), and TMSOTf (0.03 mL, 0.154 mmol, 1.2 equiv.), tricycle **97h** (94.9 mg, 0.239 mmol, 93% yield) was obtained as a white solid.

^{1}H NMR (500 MHz, $CDCl_3$) δ 7.93 (d, *J* = 1.7 Hz, 1H), 7.63 (d, *J* = 8.2 Hz, 2H), 7.32 (d, *J* = 8.4 Hz, 1H), 7.24 (d, *J* = 8.2 Hz, 2H), 7.19 (dd, *J* = 8.4, 1.7 Hz, 1H), 4.76 (d, *J* = 10.7 Hz, 1H), 4.13 (dd, *J* = 7.7, 4.2 Hz, 1H), 3.33 (s, 3H), 3.28 (dd, *J* = 14.0, 3.2 Hz, 1H), 2.91 (dd, *J* = 14.0, 11.3 Hz, 1H), 2.55 (qd, *J* = 16.3, 5.6 Hz, 2H), 2.38 (s, 3H), 2.04 (s, 3H).

^{13}C NMR (126 MHz, $CDCl_3$) δ 206.61, 144.71, 144.46, 134.03, 131.46, 129.98, 128.23, 128.18, 127.40, 127.16, 125.71, 122.25, 118.93, 84.93, 61.85, 57.81, 49.09, 40.98, 23.41, 21.59.

HRMS (ESI): calcd for $C_{22}H_{22}BrNO_4S^+$ $[M+H]^+$: 476.0526, found: 476.0511.

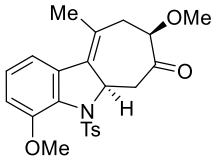

4,8-dimethoxy-10-methyl-5-tosyl-5a,6,8,9-tetrahydrocyclohepta[b]indol-7(5*H*)-one (97i)

Prepared according to the representative procedure for the [4+3] cycloaddition (**Procedure D)** from diene **95i** (50 mg, 0.247 mmol, 1 equiv.), TBS enol ether **92** (86.1 mg, 0.371 mmol, 1.5 equiv.), and TMSOTf (0.066 mL, 0.366 mmol, 1.48 equiv.), tricycle **97i** (94.9 mg, 0.239 mmol, 93% yield) was obtained as a white solid.

^{1}H NMR (400 MHz, $CDCl_3$) δ 7.68 (d, *J* = 8.3 Hz, 1H), 7.26 (d, *J* = 8.0 Hz, 2H), 7.17 (d, *J* = 7.8 Hz, 1H), 7.06 (t, *J* = 8.0 Hz, 1H), 6.76 (d, *J* = 8.0 Hz, 1H), 5.60 (d, *J* = 11.2 Hz, 1H), 4.28 (dd, *J* = 8.1, 4.8 Hz, 1H), 3.55 (s, 3H), 3.34 (s, 3H), 3.13 (dd, *J* = 14.3, 3.5 Hz, 1H), 2.92 – 2.79 (m, 2H), 2.54 (dd, *J* = 16.8, 8.1 Hz, 1H), 2.42 (s, 3H), 2.09 (s, 3H).

^{13}C NMR (101 MHz, $CDCl_3$) δ 206.73, 149.96, 143.19, 138.03, 132.84, 132.79, 132.67, 129.05, 127.25, 126.89, 126.10, 117.27, 112.30, 84.29, 61.30, 57.84, 55.35, 49.12, 41.04, 22.80, 21.54.

HRMS (ESI): calcd for $C_{23}H_{25}NO_5S^+$ $[M+H]^+$: 428.1526, found: 428.1517.

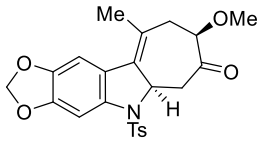

8-methoxy-10-methyl-5-tosyl-5a,6,8,9-tetrahydrocyclohepta[*b*][1,3]dioxolo[4,5-*f*]indol-7(5*H*)-one (97i)

Prepared according to the representative procedure for the [4+3] cycloaddition (**Procedure D)** from diene **95i** (50 mg, 0.247 mmol, 1 equiv.), TBS enol ether **92** (86.1 mg, 0.371 mmol, 1.5 equiv.), and TMSOTf (0.066 mL, 0.366 mmol, 1.48 equiv.), tricycle **97i** (94.9 mg, 0.239 mmol, 93% yield) was obtained as a white solid.

^{1}H NMR (400 MHz, $CDCl_3$) δ 7.58 (d, *J* = 8.3 Hz, 2H), 7.35 (s, 1H), 7.22 (d, *J* = 8.0 Hz, 2H), 6.95 (s, 1H), 6.01 (d, *J* = 1.2 Hz, 1H), 5.97 (d, *J* = 1.3 Hz, 1H), 4.75 – 4.68 (m, 2H), 4.12 (dd, *J* = 7.4, 4.7 Hz, 1H), 3.32 (s, 3H), 3.23 (dd, *J* = 14.3, 3.0 Hz, 1H), 2.89 (dd, *J* = 14.3, 11.3 Hz, 1H), 2.52 (d, *J* = 6.7 Hz, 2H), 2.37 (s, 3H), 1.98 (s, 3H)

^{13}C NMR (101 MHz, $CDCl_3$) δ 207.03, 148.02, 145.24, 144.37, 138.34, 133.72, 132.12, 129.85, 127.27, 123.75, 122.75, 104.47, 101.86, 98.79, 84.98, 62.09, 57.80, 49.26, 40.89, 22.94, 21.61.

HRMS (ESI): calcd for $C_{23}H_{23}NO_6S^+$ $[M+H]^+$: 442.1319, found: 442.1296.

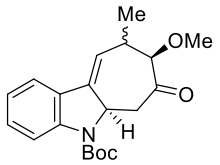

tert-butyl-8-methoxy-9-methyl-7-oxo-6,7,8,9-tetrahydrocyclohepta[*b*]indole-5(5a*H*)-carboxylate (97k)

Prepared according to the representative procedure for the [4+3] cycloaddition (**Procedure D)** with modifications from diene **95k** (200 mg, 0.777 mmol, 1 equiv.), TBS enol ether **92** (221.8 mg, 1.166 mmol, 1.5 equiv.), and TMSOTf (0.14 mL, 0.777 mmol, 1 equiv.) in nitroethane 15 mL. NMR analysis showed no **E-95k** diene remaining. Purification with silica gel chromatography (gradient elution 5:95 → 15:85 Acetone:Hexanes) gives **Z**-9**5k** (54mg, 0.212 mmol) and tricycle **97k** (133.3 mg, 0.389 mmol, 3:1 dr, 80% yield) was obtained as a colorless oil. Yield based on ratio of E/Z in parent diene

^{1}H NMR (400 MHz, $CDCl_3$) δ 7.75 (d, *J* = 8.1 Hz, 1H), 7.35 – 7.29 (m, 2H), 7.21 (t, *J* = 7.8 Hz, 2H), 6.96 (t, *J* = 7.5 Hz, 1H), 6.06 (dd, *J* = 6.4, 3.1 Hz, 2H), 5.05 (s, 1H), 3.71 (d, *J* = 4.5 Hz, 1H),

3.42 (s, 4H), 3.01 – 2.86 (m, 3H), 2.22 (dd, *J* = 13.1, 11.0 Hz, 2H), 1.59 (s, 9H), 1.27 (d, *J* = 6.7 Hz, 3H).

^{13}C NMR (101 MHz, $CDCl_3$) δ 208.36, 206.43, 152.15, 129.54, 126.86, 124.60, 122.98, 122.76, 121.74, 119.77, 116.72, 115.86, 115.70, 90.22, 88.34, 81.86, 65.58, 61.80, 59.04, 58.09, 51.18, 45.17, 35.00, 29.88, 28.40, 28.33, 28.21, 21.07.

HRMS (ESI): calcd for $C_{20}H_{25}NO_4^+$ $[M+H]^+$: 344.1856, found: 344.1818.

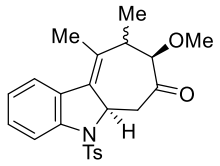

8-methoxy-9,10-dimethyl-5-tosyl-5a,6,8,9-tetrahydrocyclohepta[*b*]indol-7(5*H*)-one (97l)

Prepared according to the representative procedure for the [4+3] cycloaddition (**Procedure D)** with modifications from diene **95l** (50 mg, 0.154 mmol, 1 equiv.), TBS enol ether **92** (44 mg, 0.231 mmol, 1.5 equiv.), and TMSOTf (0.03 mL, 0.165 mmol, 1.07 equiv.) in nitroethane 3mL. tricycle **97l** (49.3 mg, 0.12 mmol, 2:1 dr, 78% yield) was obtained as a colorless oil

^{1}H NMR (400 MHz, $CDCl_3$) δ 7.80 (d, *J* = 8.1 Hz, 2H), 7.74 – 7.61 (m, 2H), 7.56 (dd, *J* = 11.0, 8.5 Hz, 2H), 7.40 (d, *J* = 7.7 Hz, 1H), 7.19 (ddd, *J* = 14.6, 9.3, 5.6 Hz, 7H), 7.10 – 6.97 (m, 2H), 4.93 – 4.87 (m, 1H), 4.70 (s, 0H), 4.26 (s, 0H), 3.88 (d, *J* = 2.5 Hz, 1H), 3.47 (s, 2H), 3.25 (s, 1H), 3.08 (dt, *J* = 12.7, 6.7 Hz, 1H), 2.98 – 2.88 (m, 1H), 2.81 – 2.60 (m, 1H), 2.36 (s, 3H), 2.34 (s, 2H), 2.24 – 2.03 (m, 4H), 1.94 (d, *J* = 2.3 Hz, 3H), 1.23 (d, *J* = 7.0 Hz, 2H), 1.18 (d, *J* = 6.7 Hz, 3H).

^{13}C NMR (101 MHz, $CDCl_3$) δ 208.14, 144.20, 135.81, 129.74, 129.67, 128.44, 128.02, 127.47, 127.12, 124.39, 124.33, 124.21, 124.12, 116.01, 115.62, 91.56, 90.04, 69.05, 59.06, 48.71, 35.79, 34.17, 29.69, 21.58, 17.37, 15.38, 14.33.

HRMS (ESI): calcd for $C_{23}H_{25}NO_4S^+$ $[M+H]^+$: 412.1577, found: 412.1540.

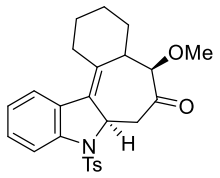

5-methoxy-8-tosyl-1,3,4,4a,5,7,7a,8-octahydrobenzo[3,4]cyclohepta[1,2-*b*]indol-6(2*H*)-one (97m)

Prepared according to the representative procedure for the [4+3] cycloaddition (**Procedure D)** with modifications from diene **95m** (50 mg, 0.142 mmol, 1 equiv.), TBS enol ether **92** (50 mg, 0.214 mmol, 1.5 equiv.), and TMSOTf (0.025 mL, 0.142 mmol, 1 equiv.) in nitroethane 3 mL. Tetracycle **97m** (49.1 mg, 0.111 mmol, 1.3:1 dr, 79% yield) was obtained as a colorless oil.

^{1}H NMR (400 MHz, $CDCl_3$) δ 7.77 (d, *J* = 8.2 Hz, 2H), 7.66 (d, *J* = 8.3 Hz, 1H), 7.59 (d, *J* = 8.2 Hz, 1H), 7.54 (d, *J* = 7.9 Hz, 1H), 7.02 (dt, *J* = 14.6, 7.6 Hz, 2H), 4.98 (t, *J* = 3.2 Hz, 1H), 4.77 (s, 1H), 4.26 (s, 1H), 3.74 (d, *J* = 3.5 Hz, 1H), 3.44 (s, 1H), 3.27 (s, 2H), 3.09 (s, 0H), 2.90 – 2.61 (m, 4H), 2.51 – 2.39 (m, 2H), 2.37 (s, 2H), 2.35 (s, 2H), 1.74 (dq, *J* = 12.6, 5.9, 5.2 Hz, 3H), 1.65 – 1.55 (m, 6H).

^{13}C NMR (101 MHz, $CDCl_3$) δ 207.86, 207.69, 144.59, 144.18, 144.10, 137.40, 137.08, 134.68, 134.49, 130.59, 129.72, 129.63, 128.83, 128.46, 128.05, 127.39, 127.22, 127.17, 127.14, 124.77, 124.47, 124.33, 124.10, 116.52, 115.80, 91.10, 90.15, 68.55, 65.64, 59.40, 59.10, 47.88, 46.19, 38.27, 34.58, 31.25, 29.05, 26.51, 26.02, 23.63, 22.16, 21.58, 21.56, 20.55, 20.22.

HRMS (ESI): calcd for $C_{25}H_{27}NO_4S^+$ $[M+H]^+$: 438.1734, found: 438.1720.

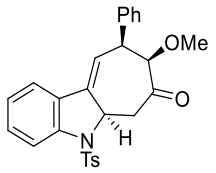

8-methoxy-9-phenyl-5-tosyl-5a,6,8,9-tetrahydrocyclohepta[*b*]indol-7(5*H*)-one (97n)

Prepared according to the representative procedure for the [4+3] cycloaddition (**Procedure D)** with modifications from diene **95n** (55 mg, 0.147 mmol, 1 equiv.), TBS enol ether **92** (52 mg, 0.221mmol, 1.5 equiv.), and TMSOTf (0.03 mL, 0.165 mmol, 1.12 equiv.) in nitroethane 3 mL. **97n** (49.1 mg, 0.111 mmol, 83% yield) was obtained as a yellow/white foam.

^{1}H NMR (400 MHz, $CDCl_3$) δ 7.82 (d, *J* = 8.2 Hz, 1H), 7.66 (d, *J* = 8.3 Hz, 1H), 7.35 – 7.20 (m, 7H), 7.16 – 7.08 (m, 2H), 7.05 (q, *J* = 7.8, 7.4 Hz, 1H), 5.96 (t, *J* = 3.1 Hz, 1H), 5.56 (ddt, *J* = 11.2, 5.3, 2.9 Hz, 1H), 3.96 (q, *J* = 3.8 Hz, 1H), 3.87 (d, *J* = 4.2 Hz, 1H), 3.73 (dd, *J* = 17.6, 5.1 Hz, 1H), 3.53 (s, 2H), 2.93 (dd, *J* = 17.5, 11.3 Hz, 1H), 2.37 (s, 2H).

^{13}C NMR (101 MHz, $CDCl_3$) δ 206.15, 144.60, 143.08, 139.99, 138.64, 133.32, 129.98, 129.80, 129.11, 128.82, 128.46, 127.54, 127.48, 124.57, 120.33, 117.24, 116.37, 92.16, 59.02, 58.36, 50.81, 49.35, 21.60.

HRMS (ESI): calcd for $C_{27}H_{25}NO_4S^+$ $[M+H]^+$: 460.1577, found: 460.1545.

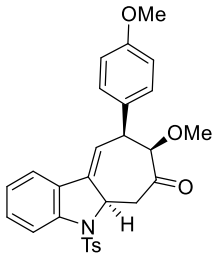

8-methoxy-9-(4-methoxyphenyl)-5-tosyl-5a,6,8,9-tetrahydrocyclohepta[*b*]indol-7(5*H*)-one (97o)

Prepared according to the representative procedure for the [4+3] cycloaddition (**Procedure D)** with modifications from diene **95o** (50 mg, 0.124mmol, 1 equiv.), TBS enol ether **92** (44 mg, 0.186mmol, 1.5 equiv.), and TMSOTf (0.03 mL, 0.165 mmol, 1.3 equiv.) in nitroethane 3 mL. **97o** (56.4 mg, 0.115 mmol, 93% yield) was obtained as a pale neon-yellow foam.

^{1}H NMR (400 MHz, CDCl3) δ 7.82 (d, J = 8.2 Hz, 1H), 7.65 (d, J = 8.3 Hz, 1H), 7.33 – 7.23 (m, 1H), 7.22 (d, J = 8.3 Hz, 1H), 7.03 (d, J = 8.7 Hz, 2H), 6.83 (d, J = 8.7 Hz, 1H), 5.94 (t, J = 3.4 Hz, 1H), 5.57 (dq, J = 8.1, 2.3 Hz, 1H), 3.93 (q, J = 3.9 Hz, 1H), 3.84 (d, J = 4.4 Hz, 1H), 3.77 (s, 2H), 3.73 (dd, J = 17.7, 5.2 Hz, 1H), 3.53 (s, 3H), 2.92 (dd, J = 17.7, 11.3 Hz, 1H), 2.37 (s, 3H). **^{13}C NMR** (101 MHz, CDCl3) δ 206.37, 158.92, 144.60, 143.04, 138.26, 133.28, 131.84, 129.92, 129.80, 129.49, 129.21, 127.49, 124.57, 120.30, 117.52, 116.36, 114.20, 92.39, 58.98, 58.34, 55.28, 50.86, 48.52, 21.60.

HRMS (ESI): calcd for $C_{28}H_{27}NO_5S^+$ $[M+H]^+$: 490.1683, found: 490.1678.

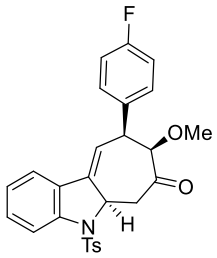

9-(4-fluorophenyl)-8-methoxy-5-tosyl-5a,6,8,9-tetrahydrocyclohepta[*b*]indol-7(5*H*)-one (97p)

Prepared according to the representative procedure for the [4+3] cycloaddition (**Procedure D)** with modifications from diene **95p** (50 mg, 0.128mmol, 1 equiv.), TBS enol ether **92** (45 mg, 0.192mmol, 1.5 equiv.), and TMSOTf (0.03 mL, 0.165 mmol, 1.3 equiv.) in nitroethane 3 mL. **97p** (55.4 mg, 0.115 mmol, 91% yield) was obtained as a pale colorless foam.

^{1}H NMR (500 MHz, CDCl3) δ 7.82 (d, J = 8.2 Hz, 1H), 7.65 (d, J = 8.2 Hz, 2H), 7.31 (t, J = 7.8 Hz, 1H), 7.28 – 7.25 (m, 2H), 7.23 (d, J = 8.2 Hz, 2H), 7.12 – 7.07 (m, 3H), 7.05 (t, J = 7.6 Hz, 1H), 7.02 – 6.97 (m, 2H), 5.91 (t, J = 3.2 Hz, 1H), 5.55 (ddt, J = 11.1, 5.3, 3.0 Hz, 1H), 3.95 (q, J = 4.0 Hz, 1H), 3.83 (d, J = 4.3 Hz, 1H), 3.74 (dd, J = 17.6, 5.1 Hz, 1H), 3.53 (s, 3H), 2.91 (dd, J = 17.5, 11.3 Hz, 1H), 2.37 (s, 3H).

^{13}C NMR (126 MHz, CDCl3) δ 206.08, 163.06, 161.09, 144.60, 143.15, 138.87, 135.82, 133.37, 130.10, 130.03, 129.96, 129.79, 128.95, 127.47, 124.57, 120.32, 116.90, 116.38, 115.78, 115.61, 92.12, 59.00, 58.37, 50.84, 48.59, 21.58.

HRMS (ESI): calcd for $C_{27}H_{24}NO_4S^+$ $[M+H]^+$: 478.1483, found: 478.1457.

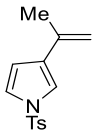

3-(prop-1-en-2-yl)-1-tosyl-1*H*-pyrrole (7)

Following **general procedure B**

1-(1-tosyl-1H-pyrrol-3-yl)ethan-1-one (263mg, 1 mmol, 1eq) was subjected to **general procedure B** with modifications: Nysted reagent solution (25 wt% in THF; 2.9 mL, 1.5 mmol, 1.5 equiv.) and

$TiCl_4$ solution (1.0 M in DCM; 1.5 mL, 1.5 mmol, 1.5 equiv.). To furnish **7** (115mg, 0.44 mmol, 49% yield) as a tan solid.

^{1}H NMR (500 MHz, CDCl3) δ 7.74 (d, J = 7.9 Hz, 2H), 7.31 – 7.24 (m, 3H), 7.10 (s, 2H), 6.45 (s, 1H), 5.21 (s, 1H), 4.90 (s, 1H), 2.40 (s, 3H), 1.98 (s, 3H).

^{13}C NMR (126 MHz, CDCl3) δ 145.04, 136.01, 135.00, 130.63, 130.04, 126.87, 121.43, 116.92, 111.32, 110.83, 21.63, 21.02

HRMS (ESI): calcd for $C_{14}H_{15}NO_2S^+$ $[M+H]^+$: 262.0896, found: 262.0889.

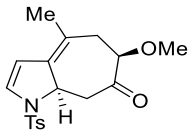

6-methoxy-4-methyl-1-tosyl-5,6,8,8a-tetrahydrocyclohepta[*b*]pyrrol-7(1*H*)-one (8)

8 was prepared according to the representative procedure for the [4+3] cycloaddition (**Procedure D)** from diene **7** (50 mg, 0.268 mmol, 1 equiv.), TBS enol ether **3a** (51.1 mg, 0.268 mmol, 1.5 equiv.), and TMSOTf (0.07 mL, 0.402 mmol, 1.5 equiv.), tricycle **8** (94.9 mg, 0..147 mmol, 55% yield) was obtained as a tan solid.

^{1}H NMR (400 MHz, CDCl3) δ 7.68 (d, J = 8.2 Hz, 2H), 7.33 (d, J = 8.0 Hz, 2H), 6.67 (d, J = 4.8 Hz, 1H), 5.76 (d, J = 4.1 Hz, 1H), 4.29 (d, J = 10.6 Hz, 1H), 4.08 (dd, J = 9.1, 4.0 Hz, 1H), 3.34 (s, 3H), 3.21 (dd, J = 14.6, 3.5 Hz, 1H), 2.89 (dd, J = 14.6, 11.5 Hz, 1H), 2.44 (s, 3H), 2.41 – 2.23 (m, 2H).

^{13}C NMR (101 MHz, CDCl3) δ 207.81, 144.34, 137.30, 133.17, 132.94, 129.98, 127.55, 120.74, 112.11, 85.15, 58.92, 57.75, 47.48, 38.74, 22.17, 21.64.

HRMS (ESI): calcd for $C_{18}H_{21}NO_4S^+$ $[M+H]^+$: 348.1264, found: 348.1247.

5.1.4 Experimental Details for Chapter 2 – Intramolecular Cyclization substrate

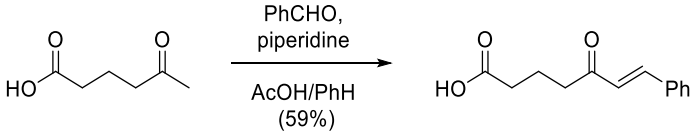

109 **110**

(E)-5-oxo-7-phenylhept-6-enoic acid (110)

To a stirred solution of 5-oxohexanoic acid (8mL, .067 mol, 1equiv.) in toluene (50mL, 1.25M) was added benzaldehyde (6.84mL, 0.067 mol, 1 equiv.), piperidine (2.65mL, 0.0268 mol, 0.4 equiv), and acetic acid (8 mL) in a 200 mL round bottom flask. A dean-stark and condenser were attached and the reaction was set to reflux for three days whereupon it was cooled to r.t., diluted with water and extracted with Et_2O 3 x 100mL. The combined organic fraction was dried over sodium sulfate, concentrated in vacuo and taken up into 1:4 Et_2O/Hexanes, and subsequently diluted to 1:9 Et_2O/Hexanes whereupon yellow crystals formed. The solids were collected by vacuum filtration to give **110** (8g, .036 mol, 54% yield).

^{1}H NMR (500 MHz, CDCl3) δ 7.62 – 7.52 (m, 3H), 7.40 (q, J = 3.5 Hz, 4H), 6.74 (d, J = 16.2 Hz, 1H), 2.79 (t, J = 7.2 Hz, 3H), 2.48 (t, J = 7.1 Hz, 3H), 2.03 (t, J = 7.2 Hz, 2H), 1.45 (d, J = 185.7 Hz, 3H).

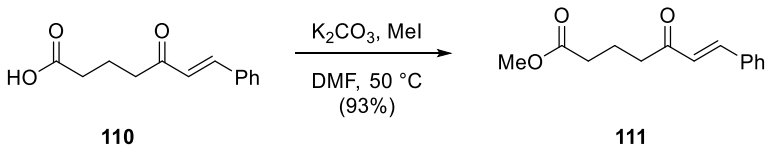

methyl (E)-5-oxo-7-phenylhept-6-enoate (111)

To an ovendried 100 mL recovery falsk and stirbar was added **111** (2.18g, 10 mmol, 1 equiv.), K_2CO_3 (2.21 g, 16 mmol, 1.6 equiv) and DMF (40 mL, anhydrous). The reaction was brought to 50 °C under nitrogen whereupon MeI (0.93 mL, 15 mmol, 1.5 equiv.) was added dropwise. The reaction was left to stir for 4 hours and subsequently cooled to ambient temperature. The reaction was transferred to a 250 mL separatory funnel containing 100mL deionized water and 50 mL 4:1 Et_2O/Hexanes. The layers were separated, and the aqueous layer was extracted three times with the same ratio of ether/hexanes. The combined organic layers were washed with water 2 x 50 mL, and 1 x 50 mL brine. The combined organic layers were then dried over sodium sulfate, filtered and concentrated in vacuo to give **111** (2.16g, 9.3 mmol, 93% yield)

^{1}H NMR (500 MHz, CDCl3) δ 7.60 – 7.52 (m, 3H), 7.42 – 7.38 (m, 3H), 6.73 (d, J = 16.2 Hz, 1H), 3.69 (s, 3H), 2.76 (t, J = 7.2 Hz, 2H), 2.42 (t, J = 7.2 Hz, 2H), 2.06 – 1.97 (m, 2H).

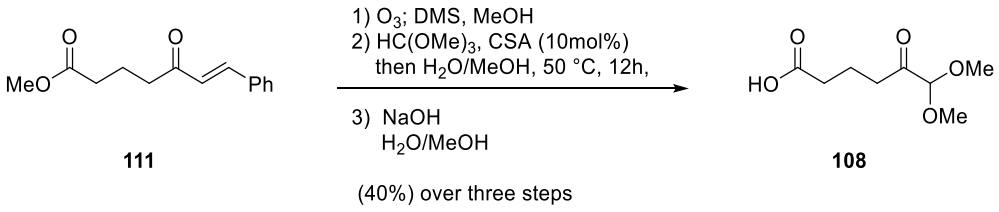

6,6-dimethoxy-5-oxohexanoic acid (108)

To a 200 mL recovery flask was added **111** (2.16 g, 9.3 mmol, 1 equiv) and a stir bar. After the addition of 40 mL the reaction was placed in a – 78 °C cold bath and ozone was passed through the mixture while stirring with a scintered glass tube. Over two hours the reaction turned green

and finally blue whereupon DMS (10mL) was added and the reaction was warmed to r.t. and concentrated slightly in vacuo. The crude ozonized product was combined with trimethyl orthoformate (8 mL) and CSA (200mg) and left to stir at r.t. overnight with slight heating ~30 °C. The next day, the reaction was concentrated and partitioned between brine and ether in a 250 mL separatory funnel. The organic phase was dried over sodium sulfate, filtered, and concentrated in vacuo. The product was a mixture of the desired acetal and bis ketal/acetal. Partial hydrolysis of this undesired ketal is carried out as follows:

To a solution of the crude product in methanol/water (25mL/0.25mL) was added AcOH (25mL) and the mixture was left to stir for 16 hours at 50 °C under nitrogen. Increasing temperature leads to conversion to the methyl vinyl ether within an hour.

The reaction mixture is quenched with sodium bicarbonate and extracted with Et_2O, 3 x 100 mL. The combined organic layers are dried over sodium sulfate, filtered, and concentrated to give the acetal in 41% yield as a colorless liquid (553 mg)

^{1}H NMR (500 MHz, CDCl3) δ 4.47 (s, 1H), 3.69 (s, 3H), 3.43 (s, 8H), 2.65 (t, J = 7.1 Hz, 4H), 2.37 (t, J = 7.3 Hz, 5H), 1.94 (q, J = 7.2 Hz, 4H).

To a 50 mL roundbottom flask and stir bar was added the acetal (500 mg, 2.5 mmol, 1 equiv.), NaOH (150 mg, 3.75 mmol, 1.5 equiv) and aqueous methanol (10 mL) The reaction was left to stir at ambient temperature overnight and subsequently transferred to a 250 mL separatory funnel. The mixture was acidified by addition of 12 N HCl, pH ~3, appearance of an oily residue on the side of the funnel was noted. Et_2O 100 mL was added to the funnel, the layers were separated, and the organic phase was drained. The aqueous phase was extracted with ether 2 x 50

mL, and the combined organic layers were dried over sodium sulfate, filtered and concentrated in vacuo to give **108** (473 mg, 2.49 mmol, 99.6% yield) as a colorless liquid.

^{1}H NMR (500 MHz, CDCl3) δ 4.46 (s, 1H), 3.42 (s, 7H), 2.40 (t, J = 7.3 Hz, 3H), 1.92 (t, J = 7.2 Hz, 2H).

^{13}C NMR (101 MHz, CDCl3) δ 204.96, 179.21, 104.05, 54.84, 36.09, 32.94, 32.85, 30.92, 19.49, 17.87.

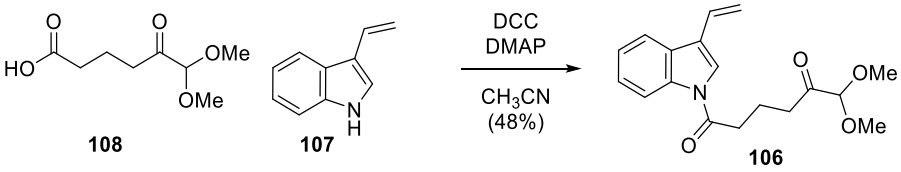

6,6-dimethoxy-1-(3-vinyl-1H-indol-1-yl)hexane-1,5-dione (106)

To a 50 mL ovendried round-bottom flask and stir bar, was added **107** (143 mg, 1 mmol, 1 equiv), **108** (209 mg, 1.1 mmol, 1.1 equiv), DCC (227 mg, 1.1 mmol, 1.1 equiv), DMAP (122 mg, 1 mmol, 1 equiv.), and acetonitrile (10 mL). The reaction was left to stir for 48 hours, and subsequently quenched with the addition of 0.5 M HCl 10mL. The reaction mixture was transferred to a 100 mL separatory funnel containing DCM (25mL), the layers were separated. The aqueous phase was extracted 3 x 50 mL DCM. The combined organic phase was dried over sodium sulfate, filtered, and concentrated in vacuo. Crude **206** was purified with column chromatography (20:80 EtOAc/Hexanes -> 40:60 EtOAc/Hexanes) to give **206** (154 mg, 0.49 mmol, 48.9% yield) as a white solid.

^{1}H NMR (500 MHz, CDCl3) δ 8.49 (d, J = 8.1 Hz, 1H), 7.80 (d, J = 7.6 Hz, 1H), 7.54 (s, 1H), 7.42 – 7.31 (m, 1H), 5.38 (d, J = 11.4 Hz, 1H), 4.49 (s, 0H), 3.42 (s, 2H), 2.97 (q, J = 7.1, 4.9 Hz, 2H), 2.79 (q, J = 6.5, 4.9 Hz, 2H), 2.19 – 2.09 (m, 2H).

5.1.5 Experimental Details for Chapter 2 – Isomerization/Reduction of Cycloadducts

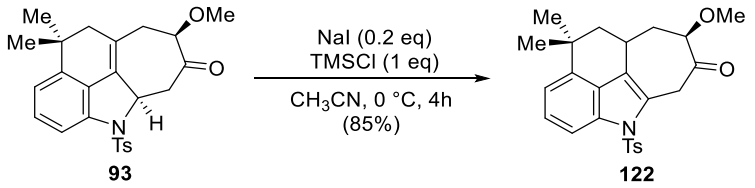

(4a*R*,7*R*)-7-methoxy-10,10-dimethyl-4-tosyl-4a,5,7,8,9,10-hexahydrobenzo[*cd*]cyclohepta-[*hi*]isoindol-6(4*H*)-one (122).

A 10 mL recovery flask with a magnetic bar was charged with cycloadduct **93** (25.0 mg, 0.057 mmol, 1 equiv.) and 3 mL acetonitrile to give a colorless solution. To this mixture was added sodium iodide (2 mg, 0.0128 mmol, 0.2 equiv.) was added, followed by TMSCl (7 mg, 0.057 mmol, 1 equiv.) as a solution in acetonitrile. The resulting solution was left to stir at 0 °C. The reaction mixture was quenched with 4 mL saturated aqueous $NaHCO_3$ and sodium thiosulfate saturated solution (2 mL), then partitioned between 20 mL 1:1 brine:H_2O and 20 mL DCM. The aqueous layer was extracted with DCM 2 x 15 mL, and the combined organic layers were dried over Na_2SO_4, and concentrated under reduced pressure. Purification by flash chromatography (20:80 EtOAc:hexanes) provided rearomatized tetracycle **122** (21.2 mg, 0.0544 mmol, 85% yield) as a white solid.

^{1}H NMR (500 MHz, $CDCl_3$): δ 7.88 (d, *J* = 8.2 Hz, 1H), 7.72 (d, *J* = 8.4 Hz, 2H), 7.29 – 7.21 (m, 3H), 7.12 (d, *J* = 7.3 Hz, 1H), 4.46 (dd, *J* = 15.9, 2.2 Hz, 1H), 4.07 (d, *J* = 16.1 Hz, 1H), 4.01 (dd, *J* = 10.2, 5.4 Hz, 1H), 3.40 (s, 3H), 2.96 (tdd, *J* = 12.0, 5.0, 2.6 Hz, 1H), 2.36 (s, 3H), 2.26 (ddd, *J* = 13.4, 5.4, 3.0 Hz, 1H), 1.78 – 1.65 (m, 2H), 1.59 – 1.51 (m, 1H), 1.40 (s, 3H), 1.17 (s, 3H).

^{13}C NMR (125 MHz, $CDCl_3$): δ 205.1, 144.9, 140.2, 136.2, 135.2, 130.1, 126.7, 126.7, 125.5, 125.4, 122.2, 117.9, 112.5, 86.6, 57.9, 46.9, 40.1, 37.6, 34.7, 30.2, 28.1, 27.8, 21.7.

HRMS (ESI): calcd for $C_{25}H_{28}NO_4S^+$ $[M+H]^+$: 438.1734, found: 438.1736.

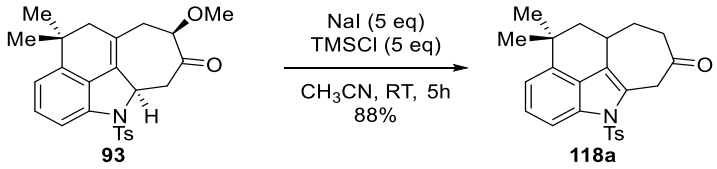

10,10-dimethyl-4-tosyl-5,7,8,8a,9,10-hexahydrobenzo[cd]cyclohepta[hi]isoindol-6(4H)-one (118a)

To a stirred solution of **93b** (20 mg, 0.052 mmol, 1eq) in 10 mL acetonitrile was added sodium iodide (39 mg, 0.26 mmol, 5 eq). The system was then evacuated and backfilled with nitrogen twice. TMSCl (28 mg, 0.26 mmo, 5eq) was added in one portion and the reaction was allowed to proceed for five hours. The reaction was quenched with the addition of saturated sodium thiosulfate solution 5 mL, and saturated sodium bicarbonate solution 5 mL. The mixture was transferred to a 50mL separatory funnel and the aqueous layer extracted 5 x 10 mL DCM. The combined organic fractions were dried over anhydrous sodium sulfate, filtered, and concentrated under reduced pressure. Purification by silica gel chromatography (30:70 EtOAc:Hexanes) produced **118a** (11.6 mg, 0.045 mmol, 88% yield) as a white solid.

^{1}H NMR (400 MHz, CDCl3) δ 7.90 (dd, J = 8.3, 0.7 Hz, 1H), 7.75 – 7.66 (m, 2H), 7.29 – 7.19 (m, 4H), 7.12 (dd, J = 7.4, 0.7 Hz, 1H), 4.26 (t, J = 2.4 Hz, 2H), 2.96 (tdd, J = 12.8, 4.7, 2.6 Hz, 1H), 2.89 – 2.72 (m, 2H), 2.35 (s, 3H), 2.03 (dtd, J = 14.0, 4.6, 3.1 Hz, 1H), 1.85 (dddd, J = 14.0, 12.0, 11.1, 4.4 Hz, 1H), 1.72 (dd, J = 12.9, 4.4 Hz, 1H), 1.62 – 1.51 (m, 2H), 1.40 (s, 3H), 1.19 (s, 3H).

^{13}C NMR (101 MHz, CDCl3) δ 206.35, 144.74, 140.19, 136.12, 135.13, 129.98, 126.85, 126.53, 125.16, 124.76, 122.40, 117.80, 112.35, 46.78, 44.47, 43.18, 34.66, 31.88, 30.01, 29.64, 28.14, 21.60.

HRMS (ESI): calcd for $C_{24}H_{25}NO_3S^+$ $[M+Na]^+$: 430.1453, found: 430.1454.

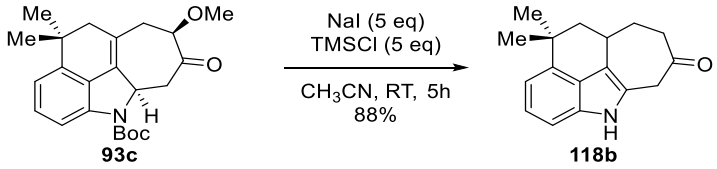

10,10-dimethyl-5,7,8,8a,9,10-hexahydrobenzo[*cd*]cyclohepta[*hi*]isoindol-6(4*H*)-one (118b)

To a stirred solution of **93c** (20 mg, 0.052 mmol, 1eq) in 10 mL acetonitrile was added sodium iodide (39 mg, 0.26 mmol, 5 eq). The system was then evacuated and backfilled with nitrogen twice. TMSCl (28 mg, 0.26 mmo, 5eq) was added in one portion and the reaction was allowed to proceed for five hours. The reaction was quenched with the addition of saturated sodium thiosulfate solution 5 mL, and saturated sodium bicarbonate solution 5 mL. The mixture was transferred to a 50mL separatory funnel and the aqueous layer extracted 5 x 10 mL DCM. The combined organic fractions were dried over anhydrous sodium sulfate, filtered, and concentrated under reduced pressure. Purification by silica gel chromatography (30:70 EtOAc:Hexanes) produced **118b** (11.6 mg, 0.045 mmol, 88% yield) as a white solid.

^{1}H NMR (400 MHz, CDCl3) δ 7.63 (s, 1H), 7.16 – 7.06 (m, 2H), 6.98 (dd, J = 6.7, 1.3 Hz, 1H), 4.06 (dd, J = 15.7, 2.2 Hz, 1H), 3.75 (d, J = 15.7 Hz, 1H), 3.20 (t, J = 11.7 Hz, 1H), 3.00 – 2.81 (m, 2H), 2.21 – 2.09 (m, 1H), 1.83 – 1.68 (m, 2H), 1.62 (d, J = 12.4 Hz, 1H), 1.45 (s, 3H), 1.27 (s, 3H).

^{13}C NMR (101 MHz, CDCl3) δ 206.82, 139.86, 133.80, 126.59, 122.62, 122.54, 114.32, 113.34, 107.59, 47.49, 44.78, 44.70, 35.10, 32.69, 31.89, 30.22, 28.05. HRMS (ESI): calcd for $C_{17}H_{19}NO^+$ $[M+H]^+$: 254.1539, found: 254.1530

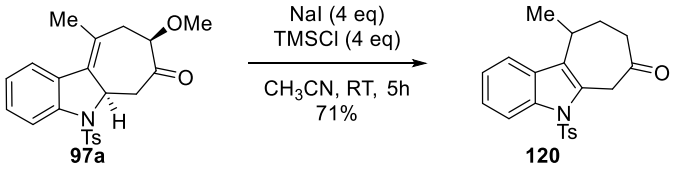

10-methyl-6,8,9,10-tetrahydrocyclohepta[*b*]indol-7(5*H*)-one (120)

Prepared in an analogous fashion to **118a**. To a stirred solution of **97a** (20 mg, 0.0504 mmol, 1 equiv.) and sodium iodide (30 mg, 0.2 mmol, 4 equiv.) in wet acetonitrile (5 mL) was added TMSCl (0.03 mL, 0.2 mmol, 4 equiv.) Left to stir for five hours and worked up and purified as with **118a**, to give **120** (13mg, 0.0355 mmol, 71% yield) as a white solid.

^{1}H NMR (400 MHz, CDCl3) δ 8.20 (d, J = 8.2 Hz, 1H), 7.65 (d, J = 8.4 Hz, 2H), 7.45 – 7.38 (m, 1H), 7.34 – 7.28 (m, 1H), 7.24 (dd, J = 7.3, 1.0 Hz, 1H), 7.19 (d, J = 8.0 Hz, 2H), 4.37 (d, J = 2.4 Hz, 2H), 3.36 – 3.24 (m, 1H), 2.72 (ddd, J = 17.1, 9.8, 3.7 Hz, 1H), 2.58 (ddd, J = 17.1, 7.7, 3.8 Hz, 1H), 2.34 (s, 3H), 2.32 – 2.18 (m, 1H), 2.05 (dtd, J = 14.9, 7.9, 3.8 Hz, 1H), 1.26 (d, J = 7.0 Hz, 3H).

^{13}C NMR (101 MHz, CDCl3) δ 206.61, 144.79, 137.02, 135.58, 130.05, 129.80, 126.74, 126.53, 125.94, 124.65, 123.57, 118.62, 115.62, 40.41, 40.33, 30.11, 28.60, 21.58, 19.88. HRMS (ESI): calcd for $C_{21}H_{21}NO_3S^+$ $[M+H]^+$: 368.1315 found: 368.1297

5.1.6 Experimental Details for Chapter 2 – Asymmetric [4+3] cycloaddition of 3-alkenyl indoles

General Procedure **E**

To an oven dried 2-dram vial and stirbar was added 3-alkenyl indole **95a** (10 mg, 0.022 mmol, 1 equiv.), **92** (10 mg, 0.044 mmol, 2 equiv.), and solvent (0.6 mL). The vial was purged with argon and left to stir at room temperature. To this mixture was added the appropriate promotor, and the reaction was left to stir for 24 hours whereupon the reaction was treated with saturated sodium bicarbonate solution, 3 mL, and extracted with DCM 5 x 3 mL. The combined organic layers were then dried over sodium sulfate, filtered and concentrated in vacuo to give the crude product which was examined with ^{1}H-NMR. If an internal standard was used to determine yield, it was added along with the sodium bicarbonate solution. The products were purified on preparatory TLC (35:65 EtOAc/Hexanes) if any desired product was observed in NMR.

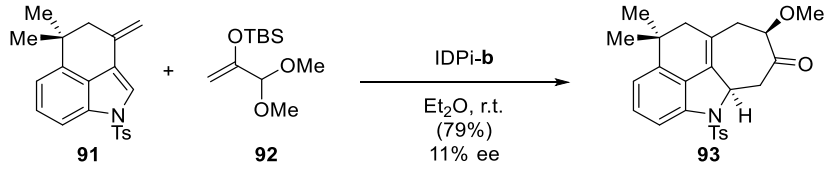

Following general procedure **E**, reacting **91**, **92**, and IDPi-**b**. (5 mol%) in diethyl ether to give **93** (79% yield, 11% ee). Yield determined by internal standard in ^{1}H-NMR. Analysis of enantioenrichment was possible with chiral HPLC: 20% IPA/Hexanes 1 mL/min OD-H column: t-major: 8.4 min, t-minor: 13.8 min.

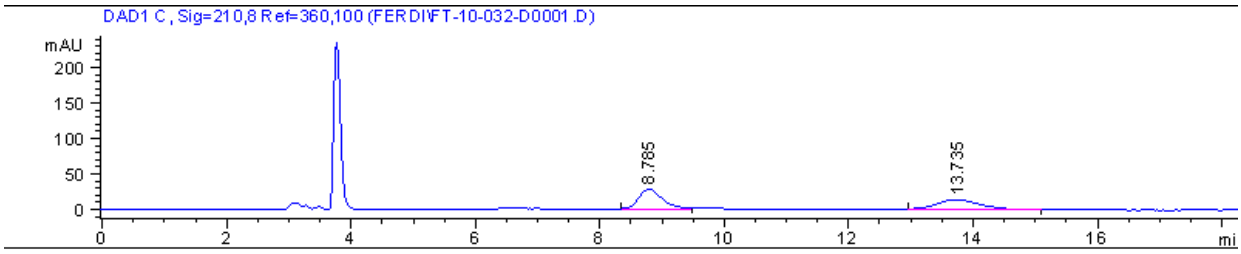

Signal 2: DAD1 C, Sig=210,8 Ref=360,100

Peak #	RetTime [min]	Type	Width [min]	Area [mAU*s]	Height [mAU]	Area %
1	8.785	BB	0.3764	731.50806	27.67297	51.0970
2	13.735	VB	0.5881	700.09814	14.22739	48.9030
Totals :				1431.60620	41.90036	

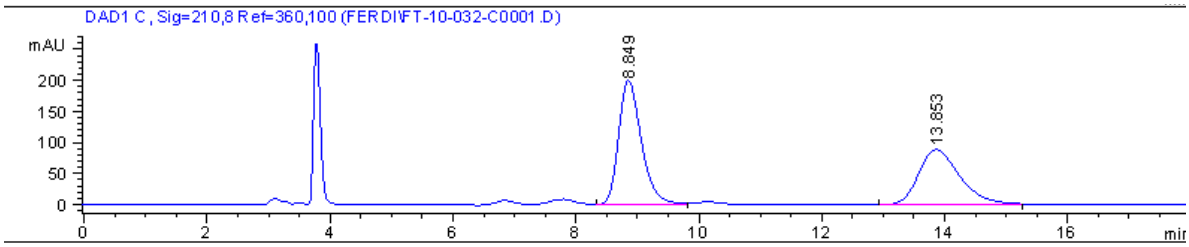

Signal 2: DAD1 C, Sig=210,8 Ref=360,100

Peak #	RetTime [min]	Type	Width [min]	Area [mAU*s]	Height [mAU]	Area %
1	8.849	VB	0.3935	5173.28320	200.19624	55.7934
2	13.853	BB	0.6437	4098.92383	88.27328	44.2066
Totals :				9272.20703	288.46952	

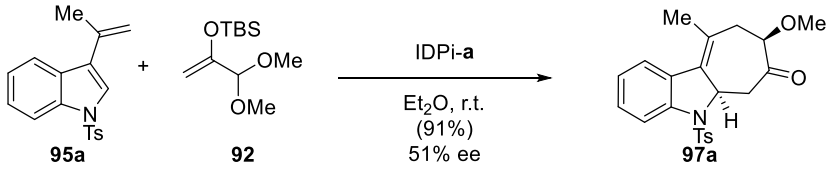

Tricycle (97a)

Following general procedure **E**, reacting **95a** (10 mg, 0.032 mmol, 1 equiv.), **92** (15 mg, 0.064 mmol, 2 equiv.), and IDPi-**a**. (5 mol%) to give **97a** (91% yield, 51% ee). Yield determined by internal standard in ^{1}H-NMR. Analysis of enantioenrichment was possible with chiral HPLC: 20% IPA/Hexanes 1 mL/min OD-H column, t-major: 8.5 min, t-minor: 12.2 min.

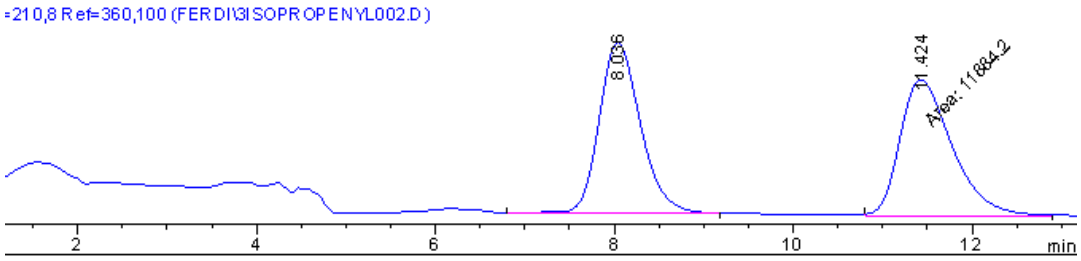

Signal 2: DAD1 C, Sig=210,8 Ref=360,100

Peak #	RetTime [min]	Type	Width [min]	Area [mAU*s]	Height [mAU]	Area %
1	8.036	VB	0.4909	1.17425e4	365.45111	49.7002
2	11.424	MM	0.6796	1.18842e4	291.43304	50.2998
Totals :				2.36267e4	656.88416	

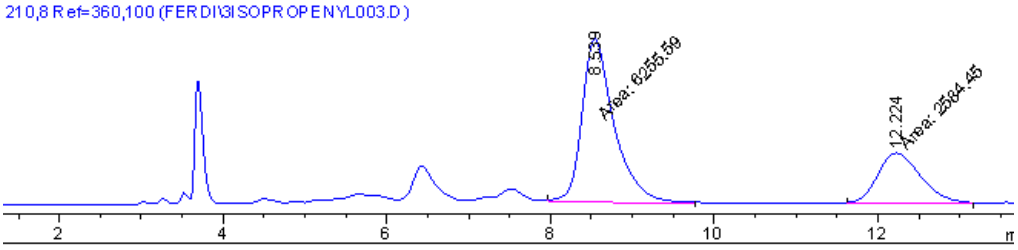

Signal 2: DAD1 C, Sig=210,8 Ref=360,100

Peak #	RetTime [min]	Type	Width [min]	Area [mAU*s]	Height [mAU]	Area %
1	8.539	MM	0.4602	6255.59424	226.54701	70.7643
2	12.224	MM	0.6144	2584.44873	70.11169	29.2357
Totals :				8840.04297	296.65871	

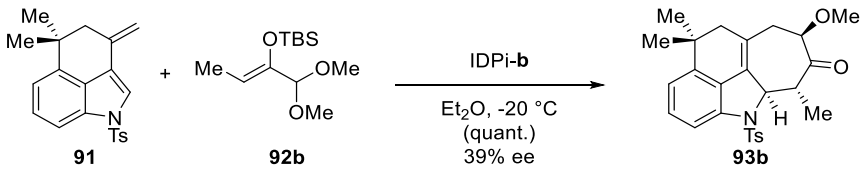

Following general procedure **E**, reacting **91**(10 mg, 0.022 mmol, 1 equiv.), **92b** (11 mg, 0.044 mmol, 2 equiv.), and IDPi-**b**. (5 mol%) to give **93b** (100% yield, 39.7%ee). Analysis of enantioenrichment was possible with chiral HPLC: 20% IPA/Hexanes 1 mL/min OD-H column, t-major: 6.9 min, t-minor: 9.4 min.

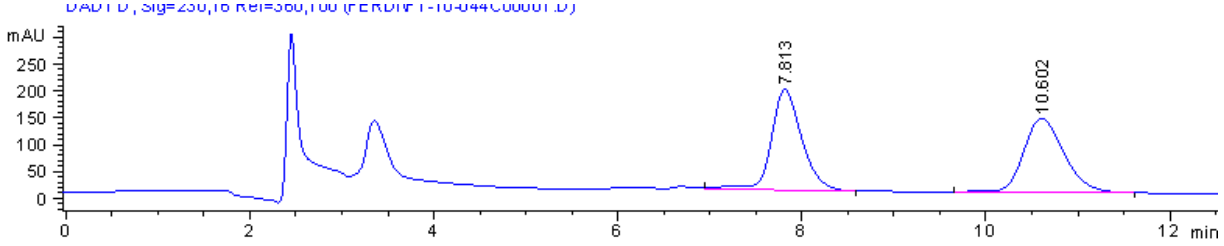

Signal 3: DAD1 D, Sig=230,16 Ref=360,100

Peak #	RetTime [min]	Type	Width [min]	Area [mAU*s]	Height [mAU]	Area %
1	7.813	VB	0.3503	4327.48877	186.78487	50.5304
2	10.602	BB	0.4743	4236.64258	137.93851	49.4696
Totals :				8564.13135	324.72337	

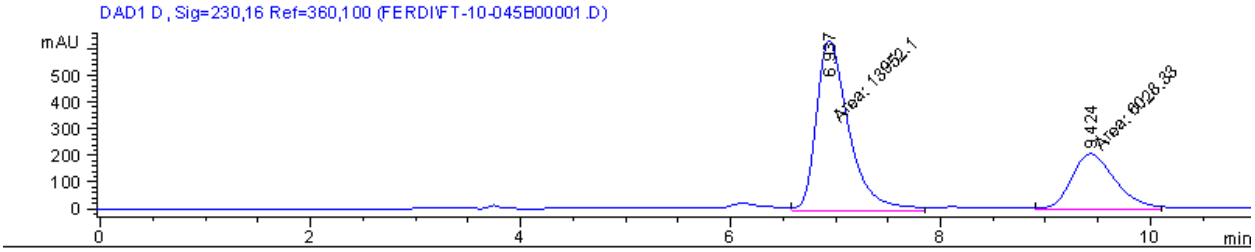

Signal 3: DAD1 D, Sig=230,16 Ref=360,100

Peak #	RetTime [min]	Type	Width [min]	Area [mAU*s]	Height [mAU]	Area %
1	6.937	MM	0.3629	1.39521e4	640.72003	69.8288
2	9.424	MM	0.4837	6028.32568	207.69487	30.1712
Totals :				1.99804e4	848.41490	

5.2.1 Experimental Details for Chapter 3 – Model Studies for Route B

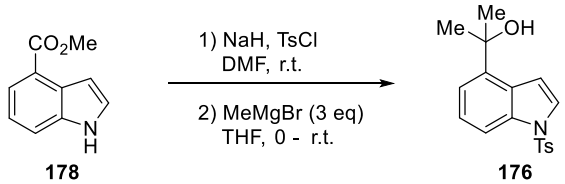

2-(1-tosyl-1H-indol-4-yl)propan-2-ol (176)

Methyl Indole-4-carboxylate (5.25g, 30 mmol, 1 equiv.) and sodium hydride 60% suspension (1.8g, 45 mmol, 1.5equiv.) were added to a 250mL oven dried flask and stirbar.

Anhydrous DMF 75mL was added under nitrogen, and the reaction was allowed to proceed at ambient temperature for 1 hour before the addition of tosyl chloride (6.1g, 32 mmol, 1.06 equiv.) in one portion. Additional DMF was poured down the side to dissolve caked on material. The reaction was allowed to proceed overnight. The reaction was quenched by the addition of water (100mL) and acidified slightly by the addition of a few mL of 1M HCl. The resulting solids were filtered off and the filtrate extracted 3x100ml EtOAc. The filtered solids were dissolved in the organic extracts and 200mL of hexanes were added. The combined organic extracts were then washed 4 x 100mL H_2O and 1x 50mL brine. The organic phase was then dried with anhydrous sodium sulfate and treated with ~20-40 mL of silica gel before filtering through a glass frit. The solvent was removed in vacuo to give the product as a white solid which was pure enough to proceed without additional purification.

N-Tosyl methyl indole-4-carboxylate (8.26g, 25mmol, 1equiv.) was transferred to a 250mL oven dried flask and stirbar. The material was then dissolved in 100mL of anhydrous THF, put under nitrogen, and cooled to 0 °C in an ice bath. MeMgBr (3M in Et_2O, 75mmol, 25mL) was added over ten minutes and the reaction was allowed to warm up over the course of 4 hours. The reaction was quenched by the addition of EtOAc 10mL and water 10mL both added slowly. The reaction was transferred to a 500mL separatory funnel containing 200mL diethyl ether and 75mL 1M HCl. The layers were separated, and the aqueous phase was extracted once with 100mL of diethyl ether. The combined organic extracts were washed once with water (75mL) and once with 1:1 brine: sat. Sodium bicarbonate solution (75mL). The organic phase was then collected, dried over sodium sulfate and concentrated to give the desired product as a lightly yellow oil which foams under high vacuum. Crystalizing from chloroform gives the desired alcohol **176** (7.99 g, 24.3 mmol, 81% yield) as a clear colorless crystal.

Spectra are consistent with literature values.[16]

^{1}H NMR (400 MHz, CDCl3) δ 7.91 (ddd, J = 7.2, 2.0, 0.8 Hz, 1H), 7.77 (d, J = 8.4 Hz, 2H), 7.57 (d, J = 3.8 Hz, 1H), 7.28 – 7.17 (m, 4H), 7.10 (dd, J = 3.7, 0.9 Hz, 1H), 2.33 (s, 3H), 1.66 (s, 6H).

^{13}C NMR (101 MHz, CDCl3) δ 144.91, 141.59, 135.59, 135.37, 129.90, 127.89, 126.93, 125.40, 124.13, 118.84, 112.58, 109.87, 73.36, 31.05, 21.58.

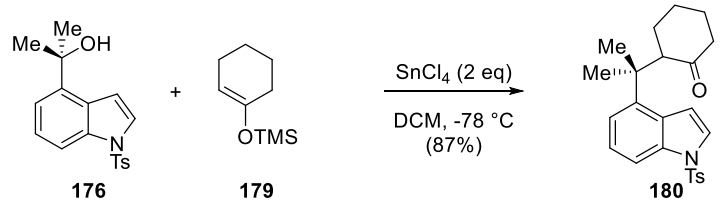

2-(2-(1-tosyl-1H-indol-4-yl)propan-2-yl)cyclohexan-1-one (180)

To a 500 mL ovendried roundbottom flask was added: **176** (3.29 g, 10 mmol, 1 equiv.) and **179** (3.4 g, 20 mmol, 2 equiv.) and subsequently dissolved in 150 mL dry DCM. The system was cooled to -78 °C under nitrogen, and after fifteen minutes neat tin (IV) chloride (2.37 mL, 20 mmol, 2 equiv.) was added over five minutes. The reaction was left to stir for another two hours at -78 °C before being quenched by the addition of saturated $NaHCO_3$ solution (5-10 mL). The reaction was then allowed to warm to r.t. Addition of anhydrous sodium sulfate, silica, and filtration; allows for the workup of the reaction without tin emulsions forming. The crude mixture was concentrated and purified by flash column chromatography (10:90 EtOAc/Hexanes) to afford ketone **180** (3.56g, 8.7 mmol, 87 % yield) as a pale-yellow oil.

[16] Muratake, H.; Natsume, M. *Tetrahedron* **1990**,.*46*, 6331 - 6342

^{1}H NMR (400 MHz, CDCl3) δ 7.84 (d, J = 8.0 Hz, 1H), 7.77 (d, J = 8.4 Hz, 2H), 7.58 (d, J = 3.8 Hz, 1H), 7.28 – 7.14 (m, 4H), 6.85 (dd, J = 3.9, 0.9 Hz, 1H), 3.13 (dd, J = 11.7, 5.0 Hz, 1H), 2.35 (s, 3H), 2.33 – 2.22 (m, 2H), 1.80 – 1.62 (m, 1H), 1.60 (s, 3H), 1.50 (s, 3H), 1.48 – 1.27 (m, 2H).

^{13}C NMR (101 MHz, CDCl3) δ 211.89, 144.93, 142.89, 135.65, 135.34, 129.90, 127.55, 126.98, 124.95, 124.11, 121.09, 111.52, 109.16, 57.97, 44.08, 40.66, 30.29, 28.26, 26.42, 25.95, 23.78, 21.60.

HRMS (ESI): calcd for $C_{24}H_{27}NO_3S^+$ $[M+H]^+$: 410.1784 found: 410.1781

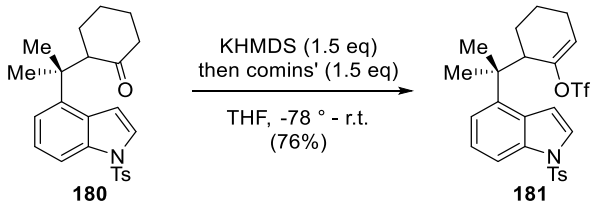

6-(2-(1-tosyl-1H-indol-4-yl)propan-2-yl)cyclohex-1-en-1-yl trifluoromethanesulfonate (181)

A magnetically stirred solution of **180** (1.636g, 4 mmol, 1 equiv.), in anhydrous THF (100mL), was cooled to -78 °C, and allowed to stir at that temperature for fifteen minutes. KHMDS, (6 mL, 6 mmol, 1M in THF, 1.5eq), was added dropwise over twenty minutes. The reaction turned amber and was left to stir at -78 °C for an additional two hours. The septum was removed, and comins' reagent (2.36 g, 6 mmol, 1.5 equiv) was added in one portion. The septum was replaced, the system re-purged with nitrogen, and left to warm to RT overnight. The next day, the reaction was quenched by the addition of 1M HCl (25 ml) and transferred to a 250 mL separatory funnel containing 100 mL of DCM. The layers were separated, and the aqueous layer was extracted 2x50mL DCM. The combined organic layers were dried over anhydrous sodium sulfated, concentrated in vacuo, and purified with column chromatography (10:90 EtOAc/Hexanes) to afford **181** (2.4671g, 4.56, 76%) as a pale-yellow oil.

^{1}H NMR (400 MHz, CDCl3) δ 7.90 (d, J = 8.3 Hz, 1H), 7.75 (d, J = 8.3 Hz, 2H), 7.60 (d, J = 3.8 Hz, 2H), 7.27 – 7.16 (m, 3H), 7.11 (dd, J = 7.7, 0.9 Hz, 2H), 6.86 (dd, J = 3.9, 0.8 Hz, 1H), 5.92 – 5.85 (m, 1H), 3.44 – 3.35 (m, 1H), 2.32 (s, 3H), 2.14 – 1.98 (m, 2H), 1.56 (s, 3H), 1.56– 1.52 (m, 2H), 1.40 (s, 3H), 1.41 – 1.17 (m, 3H).

^{13}C NMR (101 MHz, CDCl3) δ 151.74, 144.87, 142.04, 135.71, 135.25, 129.81, 128.02, 126.90, 125.36, 124.34, 122.26, 120.23, 112.02, 109.20, 45.14, 41.84, 27.97, 27.23, 25.10, 24.42, 21.51, 20.75.

HRMS (ESI): calcd for $C_{25}H_{26}F_3NO_5S_2^+$ $[M+H]^+$: 544.1277 found: 542.1281

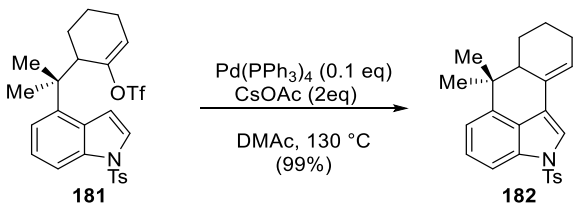

6,6-dimethyl-2-tosyl-2,6,6a,7,8,9-hexahydronaphtho[1,2,3-cd]indole (182)

To a 50 mL concentration flask was added **181** (1.08g, 2 mmol, 1 equiv.), CsOAc (768mg, 4mmol, 2 equiv.), $Pd(PPh_3)_4$ (231 mg, 0.2 mmol, 0.1 equiv.) , and DMAc (20mL, anhydrous), the system was put under vacuum and then backfilled with argon 3x. The reaction was left to stir at 130 °C overnight under argon. The next day, the reaction was diluted with Et_2O/Hexanes 1:1 100mL and filtered through a 2cm pad of silicagel to remove the palladium black. The filtrate was then washed 5x40mL H_2O to remove the residual DMAc. The combined organic layers were then dried over sodium sulfate, concentrated in vacuo, and purified with column chromatography (5:95

-> 10:90 EtOAc/Hexanes) to give tetracyclic diene **182** (774 mg, 1.98 mmol, 99% yield) as a pale-yellow oil.

^{1}H NMR (400 MHz, CDCl3) δ 7.79 (d, J = 8.4 Hz, 2H), 7.70 (dd, J = 8.2, 0.7 Hz, 1H), 7.42 (s, 1H), 7.27 – 7.19 (m, 3H), 7.13 (dd, J = 7.5, 0.7 Hz, 1H), 6.40 – 6.33 (m, 1H), 2.51 – 2.34 (m, 1H), 2.33 (s, 3H), 2.17 (s, 1H), 2.02 (dd, J = 4.3, 1.5 Hz, 1H), 1.92 (s, 3H), 1.66 – 1.50 (m, 2H), 1.44 (s, 3H), 0.94 (s, 3H).

^{13}C NMR (101 MHz, CDCl3) δ 144.65, 142.61, 135.66, 133.45, 129.85, 129.02, 127.28, 126.86, 125.47, 124.65, 120.74, 116.98, 116.04, 110.91, 45.89, 38.53, 25.72, 25.66, 23.92, 23.52, 22.75, 21.57.

HRMS (ESI): calcd for $C_{24}H_{25}NO_2S^+$ $[M+H]^+$: 392.1679 found: 392.1669

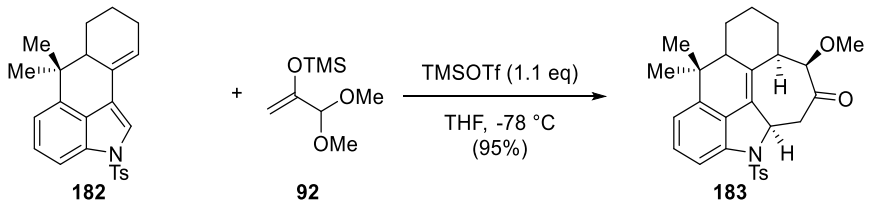

9-methoxy-5,5-dimethyl-1-tosyl-5a,6,7,8,8a,9,11,11a-octahydro-1H-1-azacyclohepta[mno]aceanthrylen-10(5H)-one (183)

To a 25 mL oven dried round bottom flask and stir-bar was added **182**(100 mg, 0.256 mmol, 1 equiv.), **92** (100mg, 0.52 mmol, 2 equiv.), and anhydrous THF (10 mL). The flask was cooled to – 78 °C under nitrogen and left to stir for 10 minutes. TMSOTf (0.05mL, 0.282 mmol, 1.1 equiv.), was added in one portion, and the reaction was left to stir for an additional 2 hours at – 78 °C. The reaction was then quenched with saturated sodium bicarbonate solution (10 mL), and the flask was warmed to ambient temperature slowly. The reaction mixture was transferred to a

125 mL separatory funnel containing 50 mL DCM and 10 mL DI H_2O. The layers were separated, and the aqueous fraction was extracted with DCM (2 x 20 mL). The combined organic layers were dried over anhydrous sodium sulfate, filtered, and concentrated in vacuo. The residue was purified with column chromatography (10:90 -> 20:80 EtOAc/Hexanes) to give **183** (115.7 mg, 0.243mmol, 95% yield) as a tan solid.

^{1}H NMR (500 MHz, CDCl3) δ 7.65 (d, J = 8.2 Hz, 2H), 7.39 (d, J = 8.1 Hz, 1H), 7.22 (d, J = 7.9 Hz, 2H), 7.11 (t, J = 7.8 Hz, 1H), 6.88 (d, J = 7.6 Hz, 1H), 4.84 (d, J = 4.6 Hz, 1H), 4.22 (s, 1H), 3.58 (s, 3H), 3.39 (dd, J = 10.2, 4.4 Hz, 1H), 2.77 (dd, J = 14.0, 5.6 Hz, 1H), 2.53 – 2.44 (m, 1H), 2.36 (s, 2H), 2.29 (dd, J = 15.3, 8.2 Hz, 2H), 1.83 (dd, J = 39.1, 12.1 Hz, 3H), 1.73 – 1.60 (m, 2H), 1.55 (s, 3H), 1.31 (s, 3H), 1.31 – 1.21 (m, 2H), 0.76 (s, 3H).

^{13}C NMR (101 MHz, CDCl3) δ 208.82, 144.16, 141.70, 140.22, 133.96, 133.33, 129.67, 129.31, 127.52, 127.16, 126.47, 118.76, 113.43, 89.71, 69.01, 59.36, 48.21, 46.10, 36.77, 32.52, 28.40, 24.28, 23.75, 23.53, 21.57, 21.15.

HRMS (ESI): calcd for $C_{28}H_{31}NO_4S^+$ $[M+]^+$: 477.1974 found: 477.1939

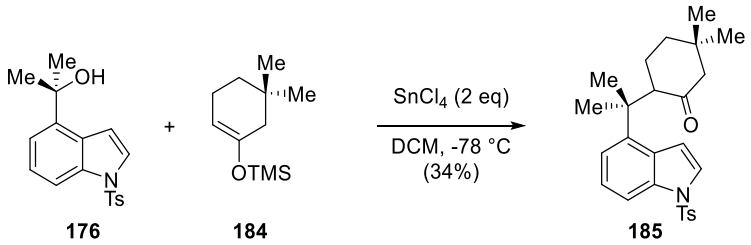

5,5-dimethyl-2-(2-(1-tosyl-1H-indol-4-yl)propan-2-yl)cyclohexan-1-one (185)

Following the procedure of **180**, alcohol **176** (6.6 g, 20mmol, 1 equiv.) and **184** (5.95 g, 30 mmol, 1.5 equiv.) was dissolved in DCM (100 mL, anhydrous), cooled to -78 °C under nitrogen, and subsequently treated with neat minutes neat tin (IV) chloride (4.74 mL, 40 mmol, 2 equiv.)

was added over five minutes. The reaction was left to stir for another two hours at -78 °C before being quenched by the addition of saturated $NaHCO_3$ solution (5-10 mL). The reaction was then allowed to warm to r.t. Addition of anhydrous sodium sulfate, silica, and filtration; allows for the workup of the reaction without tin emulsions forming. The solution is concentrated in vacuo and purified by column chromatography (5:95 -> 10:90 EtOAc/Hexanes) to furnish **185** (3 g, 6.8 mmol, 34% yield) as a tan solid.

^{1}H NMR (400 MHz, CDCl3) δ 7.85 (d, J = 8.0 Hz, 1H), 7.85 (dt, J = 8.0, 1.0 Hz, 2H), 7.81 – 7.74 (m, 2H), 7.77 (d, J = 6.6 Hz, 1H), 7.58 (d, J = 3.9 Hz, 1H), 7.30 – 7.08 (m, 4H), 6.85 (d, J = 3.8 Hz, 1H), 3.03 (dd, J = 12.3, 5.0 Hz, 1H), 2.34 (s, 3H), 2.19 (d, J = 12.4 Hz, 1H), 1.97 (d, J = 12.4 Hz, 1H), 1.60 (s, 3H), 1.60 – 1.54 (m, 1H), 1.50 (s, 3H), 1.44 – 1.39 (m, 3H), 0.97 (s, 4H), 0.83 (s, 3H).

^{13}C NMR (101 MHz, CDCl3) δ 211.33, 144.94, 142.94, 135.64, 135.32, 129.91, 127.58, 126.98, 124.97, 124.13, 121.06, 111.52, 109.17, 77.38, 77.06, 76.74, 56.84, 56.79, 40.50, 38.84, 37.01, 31.66, 26.43, 25.58, 25.25, 23.66, 21.59.

HRMS (ESI): calcd for $C_{26}H_{31}NO_3S^+$ $[M+H]^+$: 438.2097 found: 438.2093

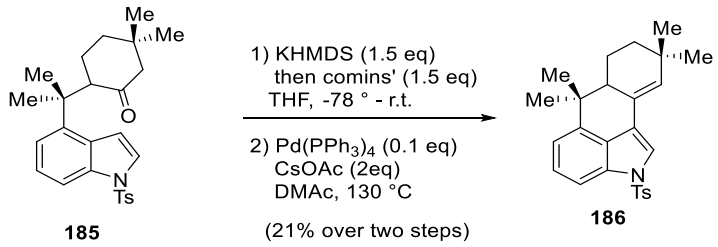

6,6,9,9-tetramethyl-2-tosyl-2,6,6a,7,8,9-hexahydronaphtho[1,2,3-cd] indole (186)

A magnetically stirred solution of **185** (2.62 g, 6 mmol, 1 equiv.), in anhydrous THF (100mL), was cooled to -78 °C under nitrogen, and allowed to stir at that temperature for fifteen

minutes. KHMDS, (9 mL, 9 mmol, 1M in THF, 1.5eq), was added dropwise over twenty minutes. The reaction turned amber and was left to stir at -78 °C for an additional two hours. The septum was removed, and comins' reagent (3.54 g, 9 mmol, 1.5 equiv.) was added in one portion. The septum was replaced, the system re-purged with nitrogen, and left to warm to RT overnight. The next day, the reaction was quenched by the addition of 1M HCl (25 ml) and transferred to a 250 mL separatory funnel containing 100 mL of DCM. The layers were separated, and the aqueous layer was extracted 2x50mL DCM. The combined organic layers were dried over anhydrous sodium sulfated, concentrated in vacuo, and purified with column chromatography (10:90 EtOAc/Hexanes) to afford **186** (887 mg, 1.56 mmol, 26% yield)

^{1}H NMR (500 MHz, CDCl3) δ 7.91 (d, J = 8.4 Hz, 1H), 7.75 (d, J = 8.4 Hz, 2H), 7.60 (d, J = 3.8 Hz, 1H), 7.29 – 7.16 (m, 5H), 7.13 (d, J = 7.6 Hz, 1H), 6.87 (d, J = 3.7 Hz, 1H), 5.60 (s, 1H), 3.35 (t, J = 7.1 Hz, 1H), 2.32 (s, 3H), 1.56 (s, 3H), 1.42 (s, 3H), 1.41 – 1.12 (m, 6H), 0.99 (d, J = 3.2 Hz, 7H).

To a 50 mL concentration flask was added **186** (887 mg, 1.56 mmol, 1 equiv.), CsOAc (600 mg, 3.12 mmol, 2 equiv.), $Pd(PPh_3)_4$ (184 mg, 0.16 mmol, 0.1 equiv.) , and DMAc (15 mL, anhydrous), the system was put under vacuum and then backfilled with argon 3x. The reaction was left to stir at 130 °C overnight under argon. The next day, the reaction was diluted with Et_2O/Hexanes 1:1 100mL and filtered through a 2cm pad of silicagel to remove the palladium black. The filtrate was then washed 5x40mL H_2O to remove the residual DMAc. The organic fraction was then dried over sodium sulfate, concentrated in vacuo, and purified with column chromatography (5:95 -> 10:90 EtOAc/Hexanes) to give tetracyclic diene **187** (536 mg, 1.28mmol, 82%) as an off-white solid.

^{1}H NMR (400 MHz, CDCl3) δ 7.80 (d, J = 8.4 Hz, 2H), 7.70 (d, J = 8.1 Hz, 1H), 7.42 (s, 1H), 7.31 – 7.19 (m, 3H), 7.13 (d, J = 7.4 Hz, 1H), 6.10 (s, 1H), 2.38 (ddd, J = 10.9, 6.2, 2.3 Hz, 1H), 2.34 (s, 3H), 1.87 (d, J = 6.4 Hz, 1H), 1.81 – 1.69 (m, 1H), 1.64 (d, J = 13.4 Hz, 2H), 1.50 (s, 3H), 1.45 (s, 3H), 1.08 (d, J = 2.3 Hz, 6H), 0.94 (s, 3H).

^{13}C NMR (101 MHz, CDCl3) δ 144.65, 142.55, 135.75, 134.60, 133.43, 129.87, 127.38, 126.89, 126.56, 125.45, 120.55, 116.91, 116.11, 110.87, 45.71, 38.40, 37.00, 31.76, 31.06, 28.46, 25.59, 23.55, 21.58, 20.42.

HRMS (ESI): calcd for $C_{26}H_{29}NO_2S^+$ $[M+H]^+$: 420.1992 found: 420.1987

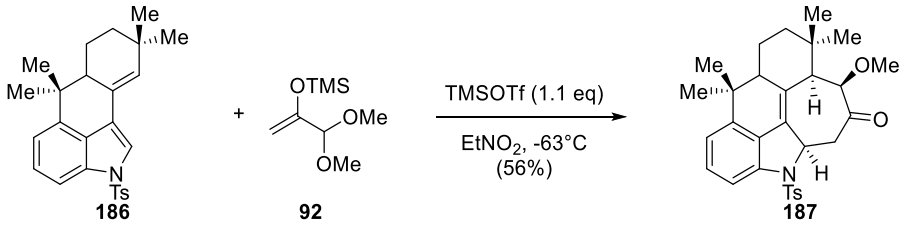

9-methoxy-5,5,8,8-tetramethyl-1-tosyl-5a,6,7,8,8a,9,11,11a-octahydro-1H-1-azacyclohepta[mno]aceanthrylen-10(5H)-one (187)

To an oven dried 50 mL recovery flask was added **186** (200 mg, 0.477 mmol, 1 equiv.), silyl enol ether **92** (285 mg, 1.5, 3 equiv.), and nitroethane (5 mL). The flask was cooled to -78 °C under nitrogen and left to stir for 10 minutes. TMSOTf (0.27 mL, 1.5 mmol, 3 equiv.) was added dropwise and the solution turned red. The reaction was allowed to warm to -63 °C, and the temperature was maintained over three hours. The reaction was quenched by the addition of a saturated solution of sodium bicarbonate (15 mL) and transferred to a 125 mL separatory funnel. The aqueous phase was extracted with DCM 4 x 25 mL. The combined organic phases were dried

over sodium sulfate, filtered and concentrated in vacuo to give the crude product which was purified by column chromatography (10:90 EtOAc/Hexanes -> 20:80 EtOAc/Hexanes) to give **187** (135 mg, 0.267 mmol, 46% yield) as an off white amorphous solid.

^{1}H NMR (400 MHz, CDCl3) δ 7.69 (d, J = 8.3 Hz, 2H), 7.38 (d, J = 8.0 Hz, 1H), 7.24 (d, J = 8.2 Hz, 2H), 7.10 (t, J = 7.9 Hz, 1H), 6.86 (d, J = 7.6 Hz, 1H), 4.87 (d, J = 5.0 Hz, 1H), 4.24 (s, 1H), 3.58 (s, 3H), 2.98 (dd, J = 12.8, 5.6 Hz, 1H), 2.84 (dd, J = 13.8, 5.6 Hz, 1H), 2.37 (s, 3H), 2.35 – 2.21 (m, 1H), 1.67 – 1.56 (m, 2H), 1.49 – 1.31 (m, 2H), 1.30 (s, 3H), 0.97 (s, 3H), 0.95 (s, 3H), 0.82 (s, 3H).

^{13}C NMR (101 MHz, CDCl3) δ 210.21, 144.20, 141.75, 140.21, 134.14, 129.75, 129.32, 127.52, 127.44, 118.45, 113.03, 90.00, 69.26, 59.43, 44.96, 44.50, 43.24, 36.93, 32.90, 31.09, 28.24, 27.97, 23.43, 22.91, 21.60, 19.75.

HRMS (ESI): calcd for $C_{30}H_{35}NO_4S^+$ $[M+Na]^+$: 528.2184 found 528.2142

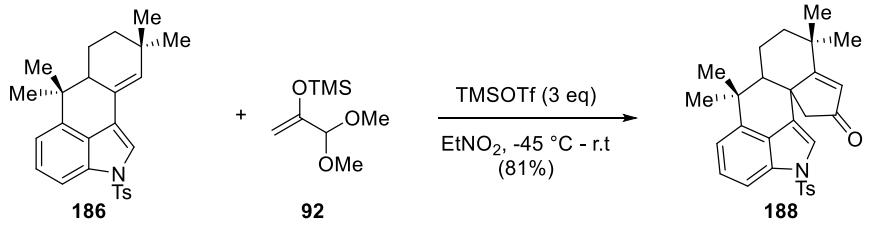

6,6,9,9-tetramethyl-2-tosyl-2,6,6a,7,8,9-hexahydrocyclopenta[8,8a]naphtho[1,2,3-cd]indol-11(12H)-one (188)

To an oven dried 50 mL recovery flask was added **186** (200 mg, 0.477 mmol, 1 equiv.), silyl enol ether **92** (285 mg, 1.5, 3 equiv.), and nitroethane (5 mL). The flask was cooled to -45 °C under nitrogen and left to stir for 10 minutes. TMSOTf (0.27 mL, 1.5 mmol, 3 equiv.) was added

dropwise and the solution turned red. The reaction was monitored by TLC, and the appearance of **186** was noted, upon warming overnight to ambient temperature, the reaction took on a brown appearance. The reaction was quenched by the addition of a saturated solution of sodium bicarbonate (15 mL) and transferred to a 125 mL separatory funnel. The aqueous phase was extracted with DCM 4 x 25 mL. The combined organic phases were dried over sodium sulfate, filtered and concentrated in vacuo to give a brown solid which was purified by column chromatography (20:80 EtOAc/Hexanes -> 50:50 EtOAc/Hexanes) to give **188** (182 mg, 0.386 mmol, 81% yield) as an off-white crystal

^{1}H NMR (500 MHz, CDCl3) δ 7.74 (dd, J = 11.3, 8.4 Hz, 5H), 7.31 (t, J = 7.9 Hz, 1H), 7.20 (d, J = 7.9 Hz, 3H), 7.12 (d, J = 7.5 Hz, 1H), 6.17 (s, 1H), 2.82 (d, J = 17.4 Hz, 1H), 2.56 (d, J = 17.4 Hz, 1H), 2.34 (s, 3H), 1.81 (ddd, J = 35.4, 13.2, 3.4 Hz, 4H), 1.51 (s, 3H), 1.47 – 1.38 (m, 3H), 1.27 (s, 3H), 1.23 (s, 3H), 1.17 – 1.08 (m, 2H), 0.66 (s, 3H).

^{13}C NMR (126 MHz, CDCl3) δ 207.62, 190.28, 144.91, 139.83, 135.49, 133.55, 129.86, 127.57, 126.82, 125.95, 125.77, 124.32, 120.27, 118.06, 111.20, 56.89, 56.21, 47.26, 39.87, 39.22, 36.23, 34.73, 30.70, 28.46, 26.50, 22.40, 21.57.

5.2.2 Experimental Details for Chapter 3 – Construction of the Methyl/Vinyl Skeleton

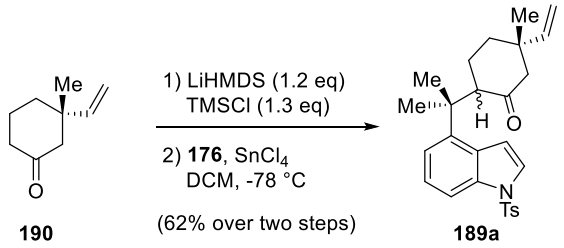

5-methyl-2-(2-(1-tosyl-1H-indol-4-yl)propan-2-yl)-5-vinylcyclohexan-1-one (189a)

To a 200 mL oven dried flask and stir bar was added **190** (1.38 g, 10 mmol, 1 equiv.), and anhydrous THF (100 mL). The reaction mixture was cooled to -78 °C under nitrogen and left to stir for 15 minutes. LiHMDS (12 mL, 12 mmol, 1M in THF, 1.2 equiv.) was added dropwise and upon complete addition, the reaction was left to stir for an additional 45 minutes. TMSCl (1.75 mL, 13 mmol, 1.3 equiv.), was added in one portion and, after one hour, the reaction was allowed to warm to ambient temperature whereupon sodium bicarbonate solution 50 mL was added. The reaction was transferred to a 500 mL separatory funnel and the aqueous phase was extracted with DCM 3 x 150 mL. The combined organic extracts were dried over sodium sulfate, filtered and concentrated before being taken on to the next step.

Crude **117a** was combined with alcohol **176** (1.64 g, 5 mmol, 0.5 equiv.), and dissolved in DCM. The resulting solution was cooled to -78 °C under nitrogen and left to stir for 15 minutes. Neat $SnCl_4$ (1.65 mL, 10 mmol, 1 equiv.) was added in one portion and the reaction was left to stir for one hour whereupon it was quenched at -78 °C by the addition of saturated sodium bicarbonate solution (10 mL) Subsequent addition of anhydrous sodium sulfate and filtration left a solution of the crude adduct which was concentrated in vacuo to give crude **189a**, which was purified by column chromatography (10:90 EtOAc/Hexanes) to give **189a** (1.391 g 3.1 mmol, 62% yield)as a tan solid.

^{1}H NMR (500 MHz, CDCl3) δ 7.91 – 7.84 (m, 3H), 7.79 (d, J = 8.2 Hz, 5H), 7.61 (dd, J = 3.7, 1.1 Hz, 3H), 7.28 – 7.17 (m, 12H), 6.90 – 6.85 (m, 3H), 5.78* (dd, J = 17.5, 10.6 Hz, 1H), 5.60 (dd, J = 17.5, 11.0 Hz, 1H), 5.08 – 4.95* (m, 2H), 4.92 (dd, J = 14.1, 2.7 Hz, 2H), 3.11* (dd, J = 12.1, 5.3 Hz, 1H), 3.01 (dd, J = 11.7, 5.0 Hz, 1H), 2.54 – 2.38 (m, 2H), 2.35 (s, 7H), 2.22 (d, J = 13.7 Hz, 1H), 2.06 (s, 3H), 1.69 – 1.58 (m, 10H), 1.55 (s, 4H), 1.47 (s, 4H), 1.04 (s, 3H), 0.96 (s, 3H).

* denotes major diastereomer

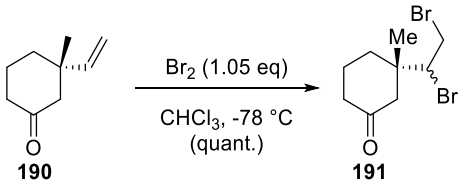

190 191

3-(1,2-dibromoethyl)-3-methylcyclohexan-1-one (191)

To a 250 mL ovendried flask was added **192** (2.76 g, 20mmol, 1 eq) and Chloroform[17] 100mL. The flask was cooled to 0 °C, and bromine (3.36 g, 21 mmol, 1.05 eq) in 20 mL of chloroform was added through a constant pressure addition funnel over thirty minutes. The funnel was then washed with an additional 5 mL of chloroform and the reaction was allowed to proceed for an additional two hours. The reaction was then treated with sodium bicarbonate, and sodium thiosulfate saturated solutions and allowed to come to room temperature. The reaction mixture was transferred to a separatory funnel, and the layers separated. The aqueous fraction was extracted twice with DCM (25 mL), and the combined organic layers were dried over sodium sulfate, filtered, and concentrated to afford **193** (5.92 g, 20mmol, 100% yield) as an orange oil.

^{1}H NMR (500 MHz, CDCl3) δ 4.17 – 4.08 (m, 1H), 4.00 (ddd, J = 16.3, 11.6, 2.8 Hz, 1H), 3.68 – 3.56 (m, 1H), 2.63 (d, J = 13.6 Hz, 1H), 2.51 (d, J = 13.7 Hz, 1H), 2.43 – 2.24 (m, 3H), 2.10 – 1.94 (m, 3H), 1.93 – 1.76 (m, 3H), 1.11 (s, 3H).

[17] The Solvent must be Chloroform as elimination products were observed with DCM.

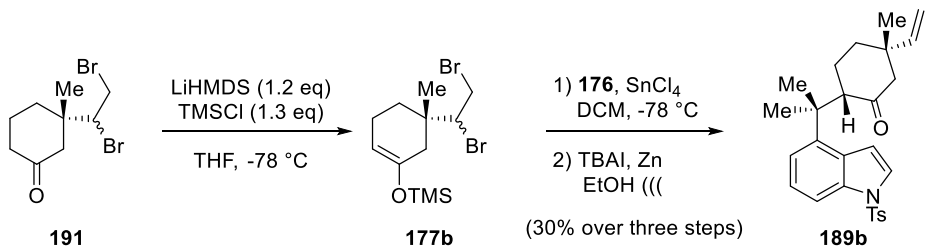

5-methyl-2-(2-(1-tosyl-1H-indol-4-yl)propan-2-yl)-5-vinylcyclohexan-1-one (189b)

To a 500 mL oven dried flask and stir bar was added **191** (5.92 g, 20 mmol, 1 equiv.), and anhydrous THF (200 mL). The reaction mixture was cooled to -78 °C under nitrogen and left to stir for 15 minutes. LiHMDS (24 mL, 24 mmol, 1M in THF, 1.2 equiv.) was added dropwise and upon complete addition, the reaction was left to stir for an additional 45 minutes. TMSCl (3.3 mL, 26 mmol, 1.3 equiv.), was added in one portion and, after one hour, the reaction was allowed to warm to ambient temperature whereupon sodium bicarbonate solution 50 mL was added. The reaction was transferred to a 500 mL separatory funnel and the aqueous phase was extracted with DCM 3 x 150 mL. The combined organic extracts were dried over sodium sulfate, filtered and concentrated before being taken on to the next step.

Crude **117b** was combined with alcohol **176** (4.38 g, 13.3 mmol, 0.67 equiv.), and dissolved in DCM. The resulting solution was cooled to -78 °C under nitrogen and left to stir for 15 minutes. Neat $SnCl_4$ (3 mL, 26 mmol, 1.3 equiv.) was added in one portion and the reaction was left to stir for one hour whereupon it was quenched at -78 °C by the addition of saturated sodium bicarbonate solution (10 mL) Subsequent addition of anhydrous sodium sulfate and filtration left a solution of the crude adduct which was concentrated in vacuo and re-dissolved in ethanol (100 mL). The solution was transferred to a 200 mL recovery flask whereupon TBAI (20 mmol, 1 equiv.) and zinc powder (5.2 g, 80 mmol, 4 equiv.) were added. The reaction was then loosely stoppered with aluminum foil and sonicated overnight. The next day, the reaction was

dissolved with ether, filtered, and concentrated to give crude **189b**, which was purified by column chromatography (10:90 EtOAc/Hexanes) to give **189b** (1.8g, 4 mmol, 30% yield) as a tan solid.

^{1}H NMR (500 MHz, CDCl3) δ 7.84 (d, J = 8.2 Hz, 1H), 7.78 (d, J = 8.2 Hz, 1H), 7.58 (d, J = 3.8 Hz, 1H), 7.24 – 7.08 (m, 2H), 7.16 (d, J = 7.6 Hz, 1H), 6.84 (d, J = 3.7 Hz, 1H), 5.57 (dd, J = 17.5, 11.0 Hz, 1H), 5.02 (d, J = 11.0 Hz, 1H), 4.96 (d, J = 17.7 Hz, 1H), 2.97 (dd, J = 11.8, 5.3 Hz, 1H), 2.40 (d, J = 14.3 Hz, 1H), 2.36 (s, 3H), 2.18 (d, J = 12.7 Hz, 1H), 1.92 – 1.79 (m, 1H), 1.59 (s, 2H), 1.44 (s, 2H), 1.27 (d, J = 7.0 Hz, 1H), 1.03 (s, 3H).

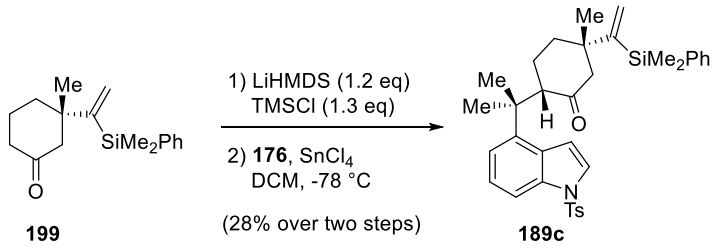

5-(1-(dimethyl(phenyl)silyl)vinyl)-5-methyl-2-(2-(1-tosyl-1H-indol-4-yl)propan-2-yl)cyclohexan-1-one (189c)

Prepared from **199** (1.36g, 5mmol) analogously to **189a**

To give **189c** (816.2 mg, 1.4 mmol, 28% yield)

^{1}H NMR (500 MHz, CDCl3) δ 7.82 (d, J = 8.2 Hz, 1H), 7.76 (d, J = 8.2 Hz, 2H), 7.55 (d, J = 3.8 Hz, 1H), 7.50 – 7.43 (m, 3H), 7.32 (d, J = 7.2 Hz, 3H), 7.30 – 7.17 (m, 5H), 7.07 (d, J = 7.6 Hz, 1H), 6.78 (d, J = 3.8 Hz, 1H), 5.75 (s, 1H), 5.57 (s, 1H), 2.85 (dd, J = 12.3, 5.4 Hz, 1H), 2.65 (dd, J = 14.1, 2.4 Hz, 1H), 2.34 (s, 3H), 2.11 – 2.03 (m, 1H), 1.84 – 1.75 (m, 2H), 1.57 (d, J = 6.6 Hz, 1H), 1.54 (s, 3H), 1.32 (s, 3H), 1.28 – 1.22 (m, 1H), 1.19 – 1.07 (m, 1H), 1.00 (s, 3H), 0.97 (d, J = 6.6 Hz, 1H), 0.89 (dd, J = 14.0, 7.4 Hz, 1H), 0.42 (s, 3H), 0.4 (s, 3H).

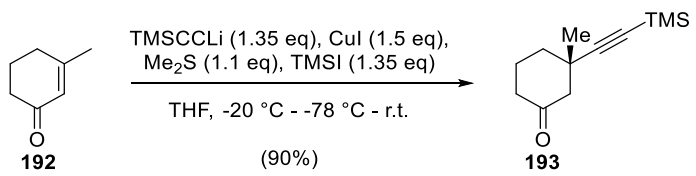

192 193

3-methyl-3-((trimethylsilyl)ethynyl)cyclohexan-1-one (193)

Following the procedure of: Rüedi and Hanson[18]

To a 500mL oven dried flask and stirbar was added anhydrous THF 250mL under nitrogen. The flask was cooled to -10 °C and TMS acetylene (5g, 50mmol, 1.35 eq) was added followed by the dropwise addition of nBuLi (1.6M in Hexanes, 31.25mL, 50mmol, 1.35 eq). The reaction was allowed to stir for an additional 30 minutes at -10 °C. Copper Iodide (10.46g, 55mmol, 1.48 eq) and Me_2S (3mL, 41.2mmol, 1.11 eq) were added at this temperature. The reaction was then cooled to -20 °C and allowed to stir for one hour before the temperature was lowered to -78 °C. Iodotrimethyl silane (6.8mL, 50mmol, 1.35 eq) was added and the reaction was stirred an addition 30 minutes before the addition of a solution of 3-Methyl-2-cyclohexenone (37mmol, 4.2mL, 1 eq) in THF (20mL)

The reaction was maintained another hour at -78 ° before being allowed to warm to RT overnight. The next day the reaction was treated with HCl (1M, 100mL) for one hour to hydrolyze the enol ether. Insoluble salts were removed by filtration, and the filtrate was transferred to a 1L separatory funnel and extracted 3x 150mL diethyl ether. The organic phase was then washed with saturated sodium thiosulfate solution (150mL) and brine 75mL. The combined organic extracts were then dried with sodium sulfate and filtered through a plug of silica before being concentrated in vacuo to give the desired ketone **193** (6.93g, 33.3 mmol, 90% yield) as a colorless oil.

[18] Rüedi, G.; Hansen, HJ., *Helv. Chem. Accta.* **2004**, *87*, 1628-1665

^{1}H NMR (400 MHz, CDCl3) δ 2.46 (d, J = 13.7 Hz, 1H), 2.34 (d, J = 13.8 Hz, 1H), 2.19 (dd, J = 12.2, 8.2 Hz, 2H), 2.14 (d, J = 5.5 Hz, 0H), 2.12 – 1.98 (m, 1H), 1.98 – 1.85 (m, 2H), 1.66 – 1.54 (m, 1H), 1.29 (s, 3H), 0.09 (d, J = 2.1 Hz, 9H).

^{13}C NMR (101 MHz, CDCl3) δ 208.95, 110.22, 87.14, 53.93, 40.40, 37.52, 36.62, 28.94, 22.60, 0.00.

HRMS (ESI): calcd for $C_{12}H_{20}OSi^{+}$ $[M+H]^{+}$: 209.1356 found 209.1356

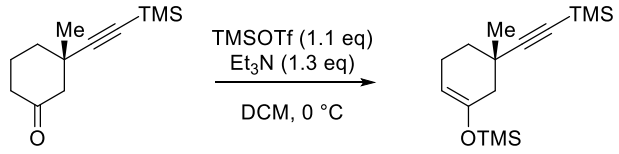

193 **177d**

To a 500mL ovendried flask was added **193** (6.24 g, 30 mmol, 1 equiv.), anhydrous DCM (200mL), and triethylamine (1.5 eq). The flask was cooled to 0 °C under nitrogen and left to stir for fifteen minutes; at which time TMSOTf (1.2 eq) was added over fifteen minutes. The reaction was left to proceed for four hours before being quenched by the addition of saturated sodium bicarbonate solution (100mL). The reaction mixture was transferred to 500mL separatory funnel and the layers separated. The aqueous phase was extracted twice with 75mL of DCM. The combined organic layers were dried over anhydrous sodium sulfate, concentrated in vacuo, and taken on to the next step without further purification.

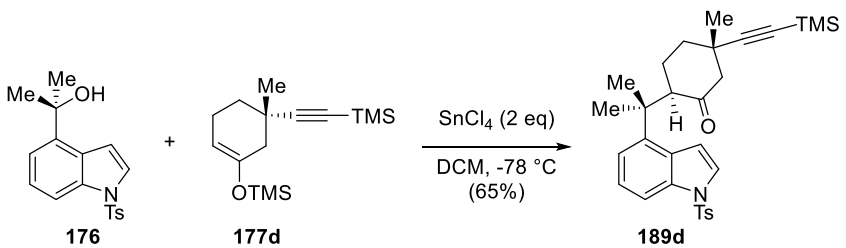

176 **177d** **189d**

5-methyl-2-(2-(1-tosyl-1H-indol-4-yl)propan-2-yl)-5-((trimethylsilyl)ethynyl)cyclohexan-1-one (187d)

To a 500mL oven dried flask and stirbar was added **176** (20 mmol, 6.58g, 1eq), **177d** (30 mmol, 8.4 g, 1.5eq), and anhydrous DCM (200mL). The flask was cooled to -78 °C under nitrogen and left for 15 minutes. Tin (IV) chloride (30 mmol, 3.51 mL, 1.5eq) was added in one portion and the reaction was left to stir at -78 °C for two hours. Saturated sodium bicarbonate solution (6mL), was added and the reaction was allowed to come to ambient temperature. The reaction was treated with anhydrous sodium sulfate and filtered through celite. The filtercake and flask being washed several times with DCM. This method avoids the formation of tin emulsions during normal aqueous workups. Solvent was removed by concentration in vacuo and the crude product was dry loaded onto silica gel. Column purification (Hexanes -> 5:95 EtOAc/Hexanes -> 15:85 EtOAc/Hexanes) gave ketone **187** (6.75 g, 13 mmol, 65% yield) as a yellow oil that solidifies over time.

^{1}H NMR (400 MHz, CDCl3) δ 7.86 (d, J = 8.1 Hz, 1H), 7.77 (d, J = 8.4 Hz, 2H), 7.59 (d, J = 3.8 Hz, 1H), 7.23 (dd, J = 7.9, 5.7 Hz, 4H), 7.16 (d, J = 7.0 Hz, 1H), 6.84 (d, J = 3.8 Hz, 1H), 3.10 (dd, J = 11.5, 5.8 Hz, 1H), 2.58 (d, J = 13.2 Hz, 1H), 2.35 (d, J = 4.8 Hz, 4H), 2.24 (dd, J = 13.2, 1.9 Hz, 1H), 1.91 – 1.76 (m, 2H), 1.73 – 1.63 (m, 2H), 1.58 (s, 3H), 1.56 – 1.50 (m, 2H), 1.49 (s, 3H), 1.47 – 1.36 (m, 2H), 1.13 (s, 3H), 0.12 (d, J = 4.0 Hz, 9H).

^{13}C NMR (101 MHz, CDCl3) δ 208.77, 144.82, 142.27, 135.53, 135.16, 129.77, 127.40, 126.84, 126.76, 124.97, 124.01, 120.88, 112.53, 111.57, 108.95, 84.19, 77.21, 77.09, 76.89, 76.57, 59.62, 56.38, 54.96, 40.52, 37.43, 35.82, 31.29, 26.44, 25.03, 24.47, 23.60, 21.46, 14.43, 0.00, -0.23.

HRMS (ESI): calcd for $C_{30}H_{37}NO_3SSi^+$ $[M+H]^+$: 520.2336 found 520.2350

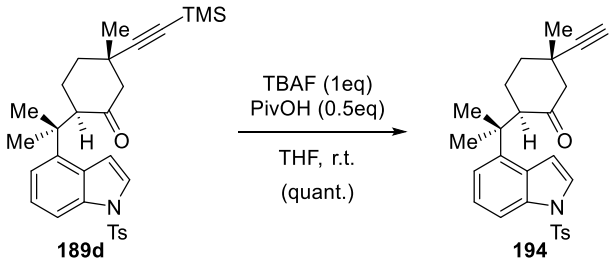

5-ethynyl-5-methyl-2-(2-(1-tosyl-1H-indol-4-yl)propan-2-yl)cyclohexan-1-one (194)

To a 100 mL roundbottom flask and stir bar was added **189d** (6.75 g, 13 mmol, 1 equiv.) and THF, 60 mL. To this mixture was added a solution of TBAF (15.4 mL, 15.4 mmol, 1M in THF) and pivalic acid (785 mg, 7.7 mmol, 0.5 equiv.) in THF 10 mL, dropwise over the course of five minutes. The reaction is left to stir until complete consumption of starting material. The reaction mixture is quenched by the addition of brine (50 mL), and transferred to a 250 mL separatory funnel. The layers are separated, and the aqueous fraction is extracted with diethyl ether 2 x 50 mL. The combined organic layers are dried over sodium sulfate, diluted with hexanes 50 mL, and passed through a plug of silica. Upon concentration **194** (5.81 g, 13 mmol, 100% yield) as a colorless oil.

^{1}H NMR (400 MHz, CDCl3) δ 7.79 (d, J = 8.2 Hz, 1H), 7.70 (d, J = 8.4 Hz, 2H), 7.52 (d, J = 3.8 Hz, 1H), 7.19 (d, J = 3.0 Hz, 1H), 7.16 (dd, J = 7.9, 6.0 Hz, 4H), 7.09 (d, J = 7.5 Hz, 1H), 6.78 (d, J = 3.8 Hz, 1H), 3.05 (dd, J = 11.2, 6.0 Hz, 1H), 2.53 (d, J = 13.3 Hz, 1H), 2.28 (d, J = 4.1 Hz, 4 H), 2.20 (dd, J = 13.3, 1.8 Hz, 1H), 2.10 (s, 1H), 1.82 – 1.70 (m, 1H), 1.68 – 1.58 (m, 1H), 1.51 (s, 3H), 1.42 (s, 3H), 1.35 (dd, J = 15.1, 8.5 Hz, 1H), 1.10 (s, 3H).

^{13}C NMR (101 MHz, CDCl3) δ 208.82, 144.98, 142.27, 135.66, 135.30, 129.92, 127.55, 126.98, 125.15, 124.15, 121.00, 111.75, 109.03, 77.34, 77.03, 76.71, 68.84, 56.42, 54.96, 40.72, 37.40, 35.06, 27.04, 26.66, 25.28, 24.50, 23.78, 21.60.

HRMS (ESI): calcd for $C_{30}H_{37}NO_3SSi^+$ $[M+H]^+$: 448.1941 found 448.1931

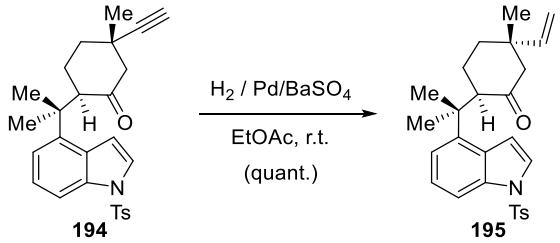

5-methyl-2-(2-(1-tosyl-1H-indol-4-yl)propan-2-yl)-5-vinylcyclohexan-1-one (195)

To a 100 mL round bottom flask and stir bar is added **194** (6.88g, 15.4 mmol, 1 equiv.) and ethyl acetate (50 mL) to afford a colorless solution. Quinoline () and $Pd/BaSO_4$ (40mol%) were added and the system was evacuated and backfilled 3x with Hydrogen. The reaction was allowed to stir for two days, replacing hydrogen and monitoring the conversion by ^{1}H NMR.

Upon complete conversion, the catalyst was removed by filtration, and the organic phase washed 2x HCl to remove quinoline. The organic phase was then separated, dried over sodium sulfate, diluted with hexanes and passed through a plug of silica. After being concentrated in vacuo **195** (5.84 g, 13 mmol, 100% yield) is obtained as a yellow oil.

^{1}H NMR (400 MHz, CDCl3) δ 7.85 (d, J = 7.9 Hz, 1H), 7.77 (d, J = 8.4 Hz, 2H), 7.58 (d, J = 3.9 Hz, 1H), 7.27 – 7.14 (m, 5H), 6.85 (d, J = 3.7 Hz, 1H), 5.76 (dd, J = 17.6, 10.6 Hz, 1H), 4.94 – 4.85 (m, 2H), 3.08 (dd, J = 11.8, 5.5 Hz, 1H), 2.33 (s, 3H), 1.61 (s, 3H), 1.58 (dd, J = 7.6, 3.0 Hz, 1H), 1.52 (s, 3H), 1.48 – 1.38 (m, 2H), 0.93 (s, 3H).

^{13}C NMR (101 MHz, CDCl3) δ 210.62, 147.54, 144.96, 142.78, 135.65, 135.32, 129.92, 127.56, 126.99, 125.03, 124.16, 121.07, 111.58, 110.42, 109.13, 77.39, 77.08, 76.76, 56.90, 54.16, 42.23, 40.55, 36.48, 26.46, 25.15, 23.65, 22.83, 21.59.

HRMS (ESI): calcd for $C_{27}H_{31}NO3S^{+}$ $[M+H]^{+}$: 450.1590 found 450.1587

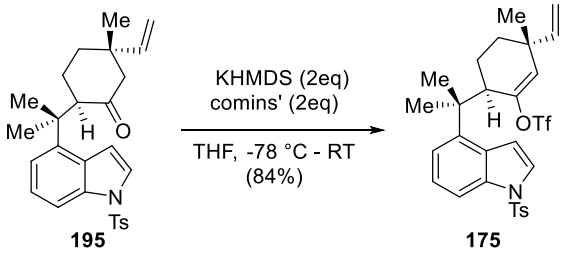

3-methyl-6-(2-(1-tosyl-1H-indol-4-yl)propan-2-yl)-3-vinylcyclohex-1-en-1-yl trifluoromethanesulfonate (175)

To a 200 mL ovendried roundbottom flask and stirbar was added **195** (2.245g, 5 mmol, 1 eq) and anhydrous THF (50 mL). The flask was cooled to -78 °C under nitrogen, and left to stir for 15 minutes. To this solution was added KHMDS (20mL, 10mmol, 2 equiv., 0.5M in PhMe) dropwise over twenty minutes. After stirring at -78 °C for 45 minutes, comins' reagent (3.927g, 10mmol, 2 equiv.) was added as a solution in anhydrous THF (10 mL). The reaction was left to warm to ambient temperature and subsequently quenched by the addition of sodium bicarbonate saturated solution (50 mL). The reaction mixture was transferred to a 250 mL separatory funnel, and the layers were separated. The aquous fraction was extracted with diethyl ether 3 x 50 mL. The combined organic layers were dried over sodium sulfate, filtered, and concentrated in vacuo to give the crude enol triflate which was purified by column chromatography (5:95 EtOAc/Hexanes) to give **175** (2.44 g, 4.2 mmol, 84% yield)

^{1}H NMR (400 MHz, CDCl3) δ 7.91 (d, J = 8.3 Hz, 1H), 7.75 (d, J = 8.4 Hz, 2H), 7.60 (d, J = 3.8 Hz, 1H), 7.23 (dd, J = 15.7, 7.9 Hz, 3H), 7.13 (dd, J = 7.7, 1.0 Hz, 1H), 6.85 (dd, J = 3.9, 0.9 Hz, 1H), 5.68 – 5.56 (m, 2H), 5.02 – 4.90 (m, 2H), 3.31 – 3.23 (m, 1H), 2.33 (s, 3H), 1.57 (s, 3H), 1.47 (s, 3H), 1.39 (dd, J = 10.1, 6.0 Hz, 2H), 1.33 – 1.22 (m, 2H), 1.05 (s, 3H).

^{13}C NMR (101 MHz, CDCl3) δ 150.94, 145.17, 144.89, 141.87, 135.72, 135.25, 129.82, 128.45, 128.09, 126.91, 125.36, 124.35, 120.31, 113.12, 112.10, 109.29, 44.85, 41.96, 39.28, 32.73, 28.84, 26.22, 26.10, 23.15, 21.52.

HRMS (ESI): calcd for $C_{28}H_{30}F_3NO_5S_2^+$ $[M+H]^+$: 582.1590 found 582.1582

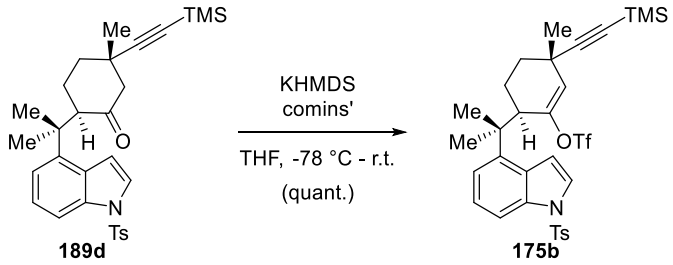

3-methyl-6-(2-(1-tosyl-1H-indol-4-yl)propan-2-yl)-3-((trimethylsilyl)ethynyl)cyclohex-1-en-1-yl trifluoromethanesulfonate (175b)

Prepared analogously to **175**,

189d (250 mg, 0.482 mmol, 1 equiv.) gave **175b** (122 mg, 0.188 mmol, 39% yield) as a white foam.

^{1}H NMR (400 MHz, CDCl3) δ 7.92 (dt, J = 8.4, 0.8 Hz, 1H), 7.75 (d, J = 8.4 Hz, 2H), 7.60 (d, J = 3.8 Hz, 1H), 7.26 – 7.17 (m, 4H), 7.11 (dd, J = 7.7, 0.9 Hz, 1H), 6.87 (dd, J = 3.9, 0.9 Hz, 1H),

5.76 (s, 1H), 3.42 – 3.34 (m, 1H), 2.33 (s, 3H), 1.64 – 1.31 (m, 5H), 1.42 (s, 4H), 1.24 (s, 3H), 0.09 (s, 9H).

^{13}C NMR (101 MHz, CDCl3) δ 151.20, 144.95, 141.67, 135.82, 135.29, 129.88, 128.12, 127.74, 126.97, 125.49, 124.44, 120.35, 112.28, 110.50, 109.34, 85.37, 44.47, 41.83, 33.99, 33.40, 27.32, 25.95, 23.56, 21.58, 0.00.

HRMS (ESI): calcd for $C_{30}H_{37}NO_3SSi^+$ $[M+H]^+$: 652.1829 found 652.1809

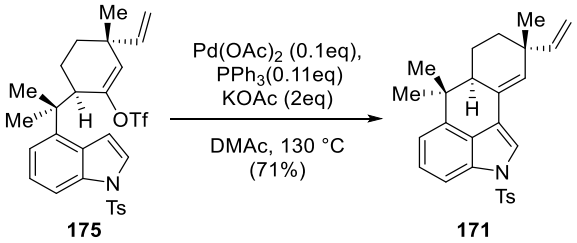

6,6,9-trimethyl-2-tosyl-9-vinyl-2,6,6a,7,8,9-hexahydronaphtho[1,2,3-cd]indole (171)

To an oven dried 50 mL recovery flask and stir bar was added **175** (1.162 g, 2 mmol, 1equiv.), Pd $(OAc)_2$ (45 mg, 0.2 mmol, 0.1 equiv.), PPh_3 (58 mg, 0.22 mmol, 0.11 equiv.) and Cesium Acetate (767 mg, 4 mmol, 2 equiv.). DMAc (10mL, anhydrous) was added and the system was evacuated and backfilled with argon three times. The reaction mixture was then suspended in a preheated oil bath, 130 °C, and left to stir overnight.

The following morning, the reaction mixture was cooled to room temperature, and then diluted with diethyl ether/Hexanes 1:1 50mL. The crude mixture was passed through a pad of silica to remove the palladium black and concentrated in vacuo to give the crude product as a yellow oil which was purified by column chromatography (Hexanes -> 5:95 EtOAc/Hexanes -> 10% EtOAc/Hexanes), to give the desired diene **171** (611 mg, 1.42 mmol, 71% yield) as a white foam.

This product is highly crystalline and only sparsely soluble in EtOAc/Hexanes mixtures transferred best with DCM.

^{1}H NMR (400 MHz, CDCl3) δ 7.84 – 7.75 (m, 2H), 7.71 (d, J = 8.1 Hz, 1H), 7.31 – 7.19 (m, 4H), 7.13 (d, J = 7.4 Hz, 1H), 6.13 (dd, J = 2.4, 1.3 Hz, 1H), 5.90 (dd, J = 17.5, 10.6 Hz, 1H), 5.12 – 4.95 (m, 2H), 2.45 – 2.36 (m, 1H), 2.34 (s, 3H), 1.99 – 1.74 (m, 1H), 1.74 – 1.56 (m, 2H), 1.46 (s, 3H), 1.19 (s, 3H), 0.97 (s, 3H).

^{13}C NMR (101 MHz, CDCl3) δ 148.04, 144.70, 142.36, 135.69, 133.42, 131.24, 129.89, 127.78, 127.28, 126.90, 125.52, 120.41, 117.01, 116.37, 110.97, 110.93, 45.49, 38.58, 37.95, 34.82, 26.12, 25.74, 23.65, 21.59, 19.94.

HRMS (ESI): calcd for $C_{27}H_{29}NO_2S^+$ $[M+H]^+$: 432.1992 found 432.1965

5.2.3 Experimental Details for Chapter 3 – Completion of the ambiguine skeleton

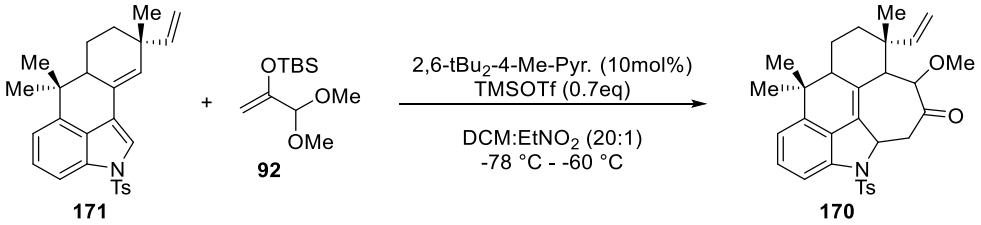

9-methoxy-5,5,8-trimethyl-1-tosyl-8-vinyl-5a,6,7,8,8a,9,11,11a-octahydro-1H-1-azacyclohepta[mno]aceanthrylen-10(5H)-one (170)

To an ovendried 50 mL recovery flask and stirbar was added **171** (500 mg, 1.16 mmol, 1 equiv.) **92** (538 mg, 2.32 mmol, 2 equiv.), and 2,6 ditertbutyl 4 methyl pyridine (18.9 mg, 0.116 mmol, 0.1 equiv.). The reagents were dissolved in a 20:1 mixture of DCM/$EtNO_2$ (10 mL). The flask was cooled to -78 °C under nitrogen and left at this temperature for five minutes. Subsequently, TMSOTf (0.15 mL, 0.812 mmol, 0.7 equiv.), was added dropwise and the reaction

was allowed to warm to -60 °C over the course of four hours. The reaction was then quenched with saturated sodium bicarbonate solution (5mL), and extracted with DCM 4 x 15 mL. The organic phase was dried over sodium sulfate and concentrated in vacuo. The crude product was purified with column chromatography (10:90 EtOAc/Hexanes -> 20:80 EtOAc/Hexanes) to afford **170** (233.9 mg, 0.45 mmol, 39% yield), as an off-white solid as a single diastereomer

^{1}H NMR (400 MHz, CDCl3) δ 7.78 (d, J = 8.4 Hz, 2H), 7.74 (dd, J = 8.3, 0.6 Hz, 1H), 7.30 (dd, J = 8.3, 7.4 Hz, 1H), 7.26 – 7.20 (m, 2H), 7.10 (dd, J = 7.5, 0.7 Hz, 1H), 6.89 (s, 1H), 6.22 (s, 1H), 5.42 (dd, J = 17.5, 10.7 Hz, 1H), 4.73 – 4.64 (m, 1H), 4.31 (d, J = 10.6 Hz, 1H), 2.85 (d, J = 17.5 Hz, 1H), 2.56 (d, J = 17.4 Hz, 1H), 2.36 (s, 3H), 1.99 – 1.71 (m, 2H), 1.50 (s, 3H), 1.44 (dd, J = 12.6, 2.8 Hz, 1H), 1.29 (d, J = 5.1 Hz, 7H).

^{13}C NMR (101 MHz, CDCl3) δ 207.45, 188.28, 144.93, 142.51, 139.63, 135.86, 133.39, 129.93, 127.99, 126.87, 125.80, 123.10, 121.20, 117.92, 111.14, 111.02, 56.56, 55.92, 47.57, 41.55, 39.26, 36.91, 34.71, 28.31, 26.55, 22.18, 21.58.

HRMS (ESI): calcd for $C_{31}H_{35}NO_4S^+$ $[M+H]^+$: 518.2360 found 518.2347

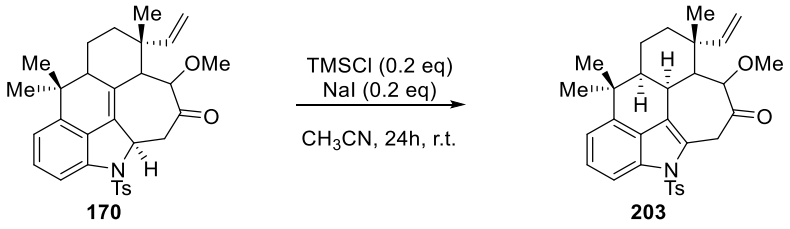

170 203

9-methoxy-5,5,8-trimethyl-1-tosyl-8-vinyl-5a,5a1,6,7,8,8a,9,11-octahydro-1H-1-azacyclohepta[mno]aceanthrylen-10(5H)-one (203)

To a 2 dram oven dried vial and stir bar was added **170** (10 mg, 0.019 mmol, 1 equiv.) was added wet acetonitrile. NaI (0.57mg, 0.0038 mmol, 0.2eq) and TMSCl (0.42 mg, 0.0038 mmol,

0.2 equiv.) were added, both as a solution in acetonitrile. The reaction was left to stir for 24 hours, quenched with saturated sodium bicarbonate and sodium thiosulfate. The reaction was extracted with DCM 3 x 5 mL, and purified with prep-TLC (30:70 EtOAc/Hexanes) to give **203** as a pale wax (6 mg, 0.0118 mmol, 62% yield).

^{1}H NMR (400 MHz, CDCl3) δ 7.86 (d, J = 8.3 Hz, 1H), 7.75 (d, J = 8.4 Hz, 2H), 7.34 – 7.27 (m, 1H), 7.17 (dd, J = 12.5, 7.8 Hz, 4H), 5.83 (dd, J = 17.7, 10.9 Hz, 1H), 5.08 (d, J = 11.8 Hz, 1H), 4.97 (d, J = 17.7 Hz, 1H), 3.78 – 3.69 (m, 1H), 3.61 (s, 2H), 3.42 – 3.32 (m, 2H), 3.27 – 3.18 (m, 1H), 2.63 (d, J = 18.2 Hz, 1H), 2.53 – 2.42 (m, 1H), 1.90 – 1.78 (m, 0H), 1.72 – 1.62 (m, 1H), 1.36 (s, 3H), 1.20 (d, J = 4.2 Hz, 5H).

^{13}C NMR (101 MHz, CDCl3) δ 204.75, 156.08, 148.29, 144.60, 135.84, 129.67, 127.16, 126.93, 126.57, 125.93, 118.42, 112.93, 111.83, 81.39, 57.91, 43.24, 40.02, 38.75, 34.61, 33.18, 29.71, 28.52, 25.37, 24.61, 21.60, 21.06, 20.36.

HRMS (ESI): calcd for $C_{31}H_{35}NO_4S^+$ $[M+H]^+$: 518.2360 found 518.2315

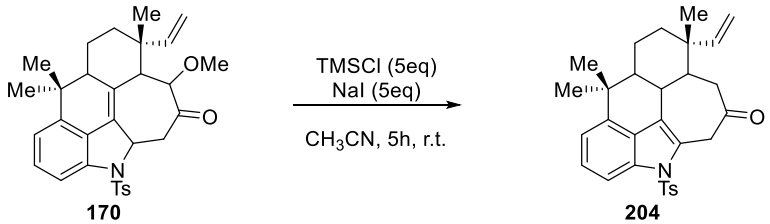

5,5,8-trimethyl-1-tosyl-8-vinyl-5a,5a1,6,7,8,8a,9,11-octahydro-1H-1-azacyclohepta[mno]aceanthrylen-10(5H)-one (204)

To a solution of **170** (230 mg, 0.445 mmol, 1equiv.) in acetonitrile 10 mL was added sodium iodide (331 mg, 2.22 mmol, 5equiv.). The flask was evacuated and backfilled three times with nitrogen. TMSCl (0.29 mL, 2.22 mmol, 5equiv.), was added in one portion and the reaction

quickly turned rust brown. The reaction was allowed to continue for five hours and subsequently quenched with the addition of 10mL of a solution of sodium bicarbonate and sodium thiosulfate. The mixture was transferred to a 125mL separatory funnel, and extracted 5 x 25mL DCM. The combined organic fraction was dried over sodium sulfate, and concentrated in vacuo. The crude product was purified by column chromatography (20:80 EtOAc/Hexanes) to give **204** (208.1 mg, 0.427 mmol, 96% yield) as a white crystalline solid.

^{1}H NMR (400 MHz, CDCl3) δ 7.90 (d, J = 8.2 Hz, 1H), 7.68 (d, J = 8.3 Hz, 2H), 7.27 (t, J = 7.9 Hz, 1H), 7.20 (d, J = 8.0 Hz, 2H), 7.17 (d, J = 7.4 Hz, 1H), 5.78 (dd, J = 17.6, 10.9 Hz, 1H), 5.08 (dd, J = 10.9, 0.9 Hz, 1H), 4.96 (dd, J = 17.6, 0.9 Hz, 1H), 4.55 (d, J = 18.1 Hz, 1H), 4.09 (dd, J = 18.1, 2.7 Hz, 1H), 3.36 (dd, J = 12.0, 2.7 Hz, 1H), 2.49 (d, J = 15.4 Hz, 1H), 2.44 (d, J = 10.1 Hz, 1H), 2.35 (s, 3H), 1.87 – 1.77 (m, 1H), 1.62 (dd, J = 13.5, 3.5 Hz, 2H), 1.38 (s, 3H), 1.22 (s, 3H), 1.20 (s, 3H) .

^{13}C NMR (101 MHz, CDCl3) δ 207.97, 147.80, 144.68, 141.46, 136.02, 135.52, 129.89, 127.22, 126.60, 125.26, 124.41, 122.09, 118.11, 112.64, 112.06, 43.56, 40.81, 40.20, 39.27, 37.44, 33.01, 29.05, 25.45, 25.40, 24.72, 21.61, 20.24.

HRMS (ESI): calcd for $C_{30}H_{33}NO_3S^+$ $[M+H]^+$: 488.2254 found 488.2248

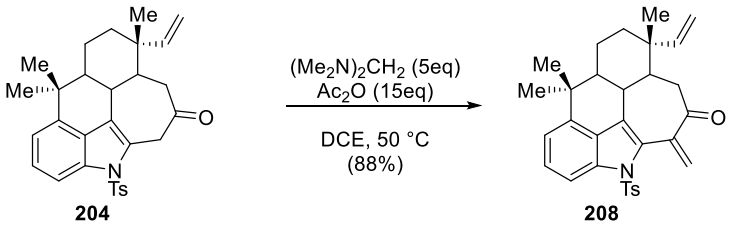

5,5,8-trimethyl-11-methylene-1-tosyl-8-vinyl-5a,5a1,6,7,8,8a,9,11-octahydro-1H-1-azacyclohepta[mno]aceanthrylen-10(5H)-one (208)

To a solution of **204** (180 mg, 0.37 mmol, 1 equiv.), in DCE (5 mL), was added N,N,N,N-Tetramethyldiaminomethane (0.28 mL, 1.85 mmol, 5 equiv.), and the system was purged with argon. Acetic anhydride (0.52 mL, 5.55 mmol, 15 equiv.) was added in one portion at ambient temperature, and subsequently the reaction was warmed to 50 °C for four hours. The reaction mixture was then cooled, quenched by the addition of saturated sodium bicarbonate, and extracted with DCM 4 x 20 mL. The combined organic phases were dried over sodium sulfate and concentrated in vacuo. The crude product was then purified with column chromatography (20:80 EtOAc/Hexanes) to afford enone **208** (162 mg, 0.326 mmol, 88% yield)

^{1}H NMR (400 MHz, CDCl3) δ 8.04 (d, J = 7.9 Hz, 1H), 7.39 – 7.31 (m, 1H), 7.22 (dd, J = 7.7, 5.8 Hz, 3H), 7.02 (d, J = 8.0 Hz, 2H), 6.68 (d, J = 1.2 Hz, 1H), 6.14 (s, 1H), 5.75 (dd, J = 17.6, 10.9 Hz, 1H), 5.07 (dd, J = 10.9, 1.0 Hz, 1H), 4.93 (dd, J = 17.6, 0.9 Hz, 1H), 3.27 (dd, J = 12.1, 5.9 Hz, 1H), 2.28 (s, 4H), 2.08 (dd, J = 10.0, 5.7 Hz, 1H), 1.92 (dd, J = 14.3, 10.1 Hz, 1H), 1.77 (dt, J = 9.9, 5.0 Hz, 2H), 1.67 – 1.52 (m, 5H), 1.37 (s, 3H), 1.31 (dd, J = 12.7, 4.4 Hz, 2H), 1.24 (s, 3H), 1.13 (s, 3H).

^{13}C NMR (101 MHz, CDCl3) δ 200.86, 147.74, 144.58, 141.85, 137.25, 135.58, 135.08, 132.69, 129.39, 128.87, 127.97, 126.60, 126.16, 124.60, 118.98, 114.54, 111.83, 44.10, 39.81, 39.34, 38.99, 37.61, 32.94, 29.29, 25.75, 25.39, 24.54, 21.55, 19.95.

HRMS (ESI): calcd for $C_{31}H_{33}NO_3S^+$ $[M+H]^+$: 500.2254 found 500.2250

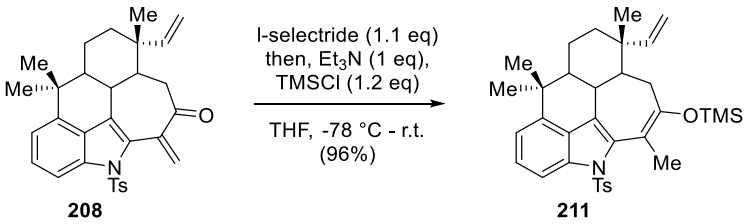

5,8,11-tetramethyl-1-tosyl-10-((trimethylsilyl)oxy)-8-vinyl-5,5a,5a1,6,7,8,8a,9-octahydro-1H-1-azacyclohepta[mno]aceanthrylene (211)

Enone **211** (150 mg, 0.3 mmol, 1 equiv.), was transferred to a 25mL oven dried recovery flask, and subsequently dissolved in dry THF (10 mL). the flask was cooled to -78 °C under nitrogen and left to stir for 15 minutes. L-selectride (0.33mL, 0.33mmol, 1 M in THF, 1.1 equiv.), was added dropwise, whereupon the reaction turned neon yellow. After 90 minutes, the reaction was treated with triethylamine (0.05mL, 0.3 mmol, ~1 equiv.), and then TMSCl (0.05mL, 0.36 mmol, 1.2 equiv.). The reaction was then allowed to warm slowly to room temperature over the course of 3 hours. The reaction was then quenched with DI water (10 mL). The mixture was transferred to a 125 mL separatory funnel and quantified with Et_2O (2 x 25mL). The layers were separated, and the organic phase was washed with 1M HCl (20mL 2x), and brine (10 mL). The organic layer was then dried over anhydrous sodium sulfate, diluted with hexanes 50 mL, decolorized with silica gel, filtered, and concentrated in vacuo to give silyl enol ether **211** (165 mg, 0.288 mmol, 96% yield), as a yellow/orange wax.

^{1}H NMR (400 MHz, CDCl3) δ 7.84 – 7.77 (m, 1H), 7.16 (d, J = 8.1 Hz, 3H), 7.06 (dd, J = 7.6, 0.7 Hz, 1H), 6.94 – 6.87 (m, 1H), 5.92 (dd, J = 17.7, 10.9 Hz, 1H), 5.06 (dd, J = 10.9, 1.3 Hz, 1H), 4.96 (dd, J = 17.7, 1.4 Hz, 1H), 3.03 (dd, J = 12.2, 7.4 Hz, 1H), 2.24 (s, 3H), 2.12 – 2.08 (m, 4H), 2.03 – 1.94 (m, 1H), 1.93 – 1.81 (m, 2H), 1.17 (s, 3H), 1.15 (s, 3H), 1.13 – 1.10 (m, 2H), 1.09 (s, 3H).

^{13}C NMR (101 MHz, CDCl3) δ 154.64, 148.31, 142.69, 140.07, 136.30, 135.34, 132.01, 130.19, 127.40, 127.34, 126.30, 126.05, 123.93, 118.68, 114.42, 109.68, 108.29, 49.41, 44.18, 38.11, 36.62, 33.08, 32.35, 30.41, 30.27, 28.17, 25.92, 25.68, 25.51, 24.77, 24.50, 23.14, 20.54, 18.94, 16.38, 13.65, 12.75, 12.46, 9.15, 0.70, 0.53, 0.00, -0.03.

HRMS (ESI): calcd for $C_{34}H_{43}NO_3SSi^+$ $[M+]^+$: 573.2733 found 573.2768

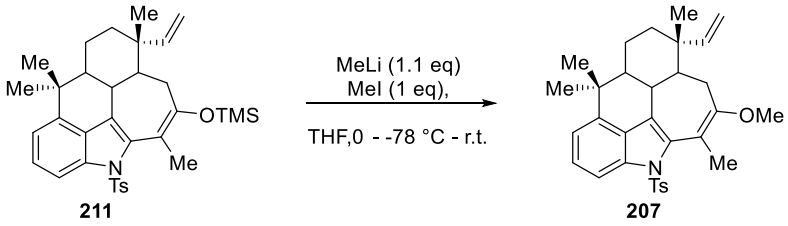

10-methoxy-5,5,8,11-tetramethyl-1-tosyl-8-vinyl-5,5a,5a1,6,7,8,8a,9-octahydro-1H-1-azacyclohepta[mno]aceanthrylene (207)

To a 25 mL flame dried flask and stir bar was added silyl enol ether **211** (25 mg, 0.044 mmol, 1 equiv.) and anhydrous THF (5 mL). The reaction was cooled to 0 °C, and methyl lithium (0.03 mL, 0.0484 mmol, 1.6M in Et_2O, 1.1 equiv.) was added dropwise. The solution was left to stir at 0 °C for two hours before being cooled to -78 °C. Iodomethane (6.4 mg, 0.045 mmol, 1 equiv.), was added as a solution in THF (0.5mL) in one portion, and the reaction was left to slowly warmed to room temperature. The reaction was quenched by the addition of brine, and extracted with DCM 2 x 10 mL. The combined organic layers were dried over sodium sulfate, filtered, and concentrated to give **207** (18.4 mg, 0.356 mmol, 81% yield)

^{1}H NMR (400 MHz, CDCl3) δ 7.81 (d, J = 8.0 Hz, 1H), 7.19 (t, J = 7.8 Hz, 1H), 7.13 (d, J = 8.3 Hz, 1H), 7.08 (d, J = 7.5 Hz, 1H), 6.91 (d, J = 8.1 Hz, 1H), 5.91 (dd, J = 17.8, 10.8 Hz, 1H), 5.09

(dd, J = 10.9, 1.1 Hz, 1H), 4.99 (d, J = 17.7 Hz, 0H), 3.68 (s, 2H), 3.04 (dd, J = 12.5, 7.4 Hz, 1H), 2.36 (d, J = 13.7 Hz, 1H), 2.25 (s, 2H), 2.14 (s, 2H), 1.45 – 1.31 (m, 2H), 1.31 – 1.20 (m, 4H), 1.16 (s, 2H), 1.09 (s, 2H).

^{13}C NMR (101 MHz, CDCl3) δ 159.24, 148.79, 143.64, 140.95, 136.97, 135.82, 132.80, 128.27, 127.57, 126.86, 124.91, 119.53, 115.43, 110.98, 109.20, 56.14, 50.76, 48.38, 44.92, 39.31, 37.49, 33.25, 29.12, 26.74, 26.53, 26.28, 23.95, 21.44, 19.80, 16.43.

HRMS (ESI): calcd for $C_{32}H_{37}NO_3S^+$ $[M+]^+$: 515.2494 found 515.2481

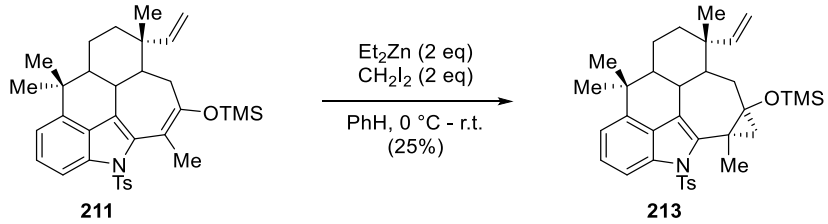

3,6,6,10b-tetramethyl-10-tosyl-1a-((trimethylsilyl)oxy)-3-vinyl-1,1a,2,2a,2a1,3,4,5,5a,6,10,10b-dodecahydro-10-azacyclopropa[5,6]cyclohepta[1,2,3,4-mno]aceanthrylene (213)

To a 25 mL flamedried round bottom flask and stirbar was added **211** (25 mg, 0.044 mmol, 1 equiv.) and benzene (5 mL). The flask was cooled to 0 °C under argon, and left to stir for 15 minutes. To this solution was added diethyl zinc (0.09 mL, 0.09 mmol, 1M in Hex, 2 equiv.), the reaction was left to stir until the smoke had dissipated, whereupon diiodomethane (23 mg, 0.088 mmol, 2 equiv.) in benzene (0.5 mL) was added dropwise. Upon complete addition, a yellow solid formed. The reaction was allowed to come to ambient temperature and left to stir overnight. The next day, the reaction was quenched by the addition of sodium bicarbonate saturated solution (5

mL). The layers were separated, and the aqueous fraction was extracted with diethyl ether 3 x 10 mL. The combined organic layers were dried over sodium sulfate, filtered, and concentrated in vacuo to give crude **213**. Yield based on composition in ^{1}HNMR, relative to SM, partially hydrolyzed **211** and mass. Due to fears of oxidation and poor separation on TLC, crude **213** was taken on as is.

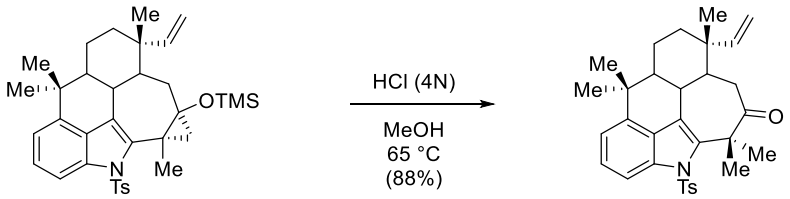

213 **206**

5,5,8,11,11-pentamethyl-1-tosyl-8-vinyl-5a,5a1,6,7,8,8a,9,11-octahydro-1H-1-azacyclohepta[mno]aceanthrylen-10(5H)-one (206)

To a 25 mL round bottom flask was added **213**, and acidic methanol (5 mL, 4 N HCl) The flask was fitted with a reflux condenser, and left to stir at 65 °C for 8 hours. The reaction was cooled to ambient temperature, and poured into saturated sodium bicarbonate solution 25 mL. The reaction mixture was transferred to a 125 mL separatory funnel, and extracted with DCM 5 x 20 mL. The combined organic layers were washed with sodium bicarbonate saturated solution 2 x 25 mL, dried over sodium sulfate, filtered, and concentrated. Preparatory TLC (20:80 EtOAc/Hexanes) gave **206** (5.1 mg, 0.0145 mmol, 22.5% yield overall) as a pale-yellow solid.

^{1}H NMR (400 MHz, CDCl3) δ 8.13 (d, J = 8.4 Hz, 2H), 7.89 (d, J = 8.3 Hz, 1H), 7.47 – 7.39 (m, 1H), 7.33 (d, J = 8.2 Hz, 2H), 7.22 (d, J = 7.4 Hz, 1H), 5.96 (dd, J = 17.6, 10.9 Hz, 1H), 5.09 (d, J = 10.9 Hz, 1H), 4.96 (d, J = 17.8 Hz, 1H), 3.70 (d, J = 1.9 Hz, 1H), 3.22 (dd, J = 11.4, 4.9 Hz, 1H),

2.41 (s, 3H), 1.97 – 1.88 (m, 1H), 1.83 (d, J = 10.4 Hz, 1H), 1.75 – 1.58 (m, 1H), 1.43 (s, 3H), 1.36 (s, 3H), 1.25 (s, 4H), 1.22 (s, 3H), 1.07 (s, 3H).

^{13}C NMR (101 MHz, CDCl3) δ 216.54, 146.63, 142.21, 134.92, 128.63, 128.60, 126.80, 126.75, 123.90, 122.38, 118.81, 113.58, 110.91, 105.71, 95.41, 55.55, 48.79, 43.72, 39.55, 38.64, 38.09, 32.48, 31.93, 30.57, 28.68, 27.21, 24.89, 24.34, 24.06, 21.64, 20.50, 17.22, 13.10.

HRMS (ESI): calcd for $C_{32}H_{37}NO_3S^+$ $[M+]^+$: 515.2494 found 515.2501

5.3 Experimental Details for Chapter 4

General Procedure for Racemic Sample preparation: **General Procedure A**

To an oven dried 2-dram vial and stirbar was added furan **233a-d** (1 eq), oxyallyl cation **92**, **92b**, or **92d** (2 eq), and anhydrous DCM. The vial is then cooled to -78 °C under nitrogen and left to stir for 10 minutes. TMSOTf (1.1 eq) is added, and the reaction mixture is left to stir at -78 °C for one hour, where upon sodium bicarbonate saturated solution (3 mL) is added in one portion. The reaction mixture is allowed to warm to room temperature and subsequently transferred to a 16 x 125 mm test tube. The reaction mixture was quantitated 3 x 5 mL DCM, and the layers partitioned. The organic layer was transferred to a second 16 x 125 mm test tube. The aqueous fraction was extracted 2 x 5 mL DCM, and the combined organic layers were dried over anhydrous sodium sulfate, filtered, and concentrated in vacuo. The crude reaction mixture was purified by column chromatography (20:80 -> 30:70 EtOAc/Hexanes) to yield the cycloadduct, visualized with $KMNO_4$ stain.

General Procedure for IDPi catalyzed reactions: **General Procedure B**

To an oven dried 2-dram vial and stirbar was added furan **233a-d** (1 eq), oxyallyl cation **92**, **92b**, or **92d** (2 eq), and anhydrous solvent. After the addition of 2-4 mg of freshly dried powder 5Å

molecular sieves the vial is then cooled to -10 °C, -5 °C, 5 °C, or r.t. in a crycool under nitrogen and left to stir for 10 minutes. IDPi-**X** (5 mol%) is added as a solution, and the reaction mixture is left to stir at the initial temperature for 12-16 hours, where upon sodium bicarbonate saturated solution (3 mL) is added in one portion. The reaction mixture is allowed to warm to room temperature and subsequently transferred to a 16 x 125 mm test tube. The reaction mixture was quantitated 3 x 5 mL DCM, and the layers partitioned. The organic layer was transferred to a second 16 x 125 mm test tube. The aqueous fraction was extracted 2 x 5 mL DCM, and the combined organic layers were dried over anhydrous sodium sulfate, filtered, and concentrated in vacuo. The crude reaction mixture was purified by column chromatography (20:80 -> 30:70 EtOAc/Hexanes) to yield the cycloadduct, visualized with $KMNO_4$ stain.

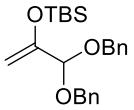

((3,3-bis(benzyloxy)prop-1-en-2-yl)oxy)(tert-butyl)dimethylsilane (92d)

To a 250 mL ovendried round-bottom flask and stir bar was added THF (100 mL) and diisorpoyl amine (5.7 mL, 36mmol, 1.2 eq). The flask was cooled to 0 °C, and left to stir for 10 minutes under nitrogen. nBuLi (1.6M in Hexanes, 22.5 mL, 36 mmol, 1.2 eq) was added dropwise; upon complete addition, the flask was cooled to -78 °C and left to stir for 10 minutes. At this point, (1,1-Bis(benzyloxy)propan-2-one (8.1g, 30 mmol, 1 eq) in THF (10 mL),[19] was added dropwise; after the addition is complete, the reaction was left to stir for 1.5 hours. TBSCl (4.97 g, 33 mmol, 1.1 eq) was added in one portion as a solution in anhydrous THF (10 mL). The reaction was left to warm up overnight and subsequently quenched by addition into 300mL of hexanes. The resulting

[19] Vidal-Pascual, M.; Marinez-Lamenca, M.; Hoffmann, H. M. R. *Org. Synth.* **2006**, 83, 61

cloudy mixture was filtered through a plug of silca and concentrated in vacuo. The crude product was purified with column chromatography (Hexanes -> 5:95 EtOAc/Hexanes) to yield **92d** (7g, 18.3mmol, 61% yield) a colorless oil.

^{1}H NMR (400 MHz, CDCl3) δ 7.28 – 7.09 (m, 10H), 4.74 (s, 1H), 4.57 (s, 1H), 4.52 – 4.36 (m, 4H), 4.22 (s, 1H), 0.75 (s, 9H), 0.06 – -0.06 (s, 6H).

^{13}C NMR (101 MHz, CDCl3) δ 153.72, 138.15, 128.33, 127.84, 127.52, 126.04, 99.16, 92.87, 67.44, 25.99, 25.65, 18.11, -4.67.

HRMS (ESI): calcd for $C_{23}H_{32}O_3Si^+$ $[M+]^+$: 385.2193 found 385.2184

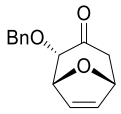

2-(benzyloxy)-8-oxabicyclo[3.2.1]oct-6-en-3-one (228)

Prepared according to general procedure **B**

From furan (68 mg, 1 mmol, 10 equiv.) and **92d** (38 mg, 0.1mmol, 1 equiv.) and IDPi-**b** (0.005mmol) in methylcyclohexane at room temperature gave **228** (19.1 mg, 0.083 mmol, 83%, 54.6% ee) as a crystalline solid.

All spectral information matches reported values.

^{1}H NMR (400 MHz, CDCl3) δ 7.43 – 7.30 (m, 5H), 6.37 – 6.27 (m, 2H), 5.03 – 4.95 (m, 2H), 4.91 (dd, J = 5.1, 1.6 Hz, 1H), 4.64 (d, J = 12.1 Hz, 1H), 4.13 (d, J = 5.1 Hz, 1H), 2.76 (dd, J = 15.5, 4.9 Hz, 1H), 2.38 (d, J = 15.5 Hz, 1H).

^{13}C NMR (101 MHz, CDCl3) δ 206.3, 137.6, 137.15, 134.84, 128.4, 128.3, 127.9, 87.5, 86.8, 84.9, 51.7, 23.1, 20.5

HPLC: chiral AD-H column 5% IPA/Hexanes 1 mL/min 254 nm absorbance: t-major: 13.4 min, t-minor: 11.7 min.

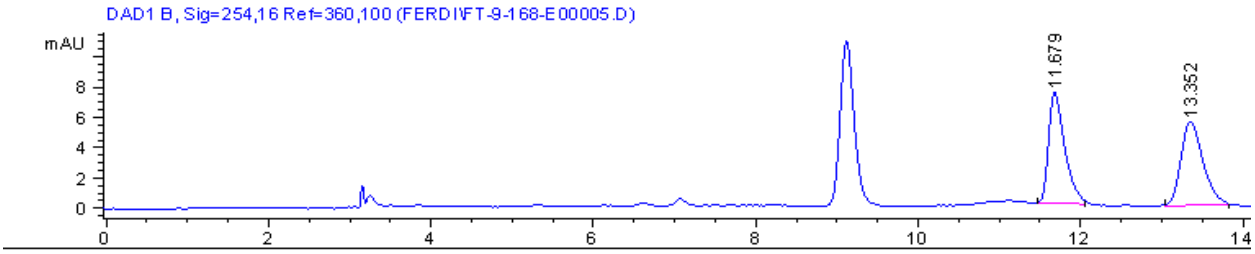

Signal 1: DAD1 B, Sig=254,16 Ref=360,100

Peak #	RetTime [min]	Type	Width [min]	Area [mAU*s]	Height [mAU]	Area %
1	11.679	BB	0.2118	101.75604	7.33741	49.2280
2	13.352	BB	0.2819	104.94760	5.51706	50.7720
Totals :				206.70364	12.85447	

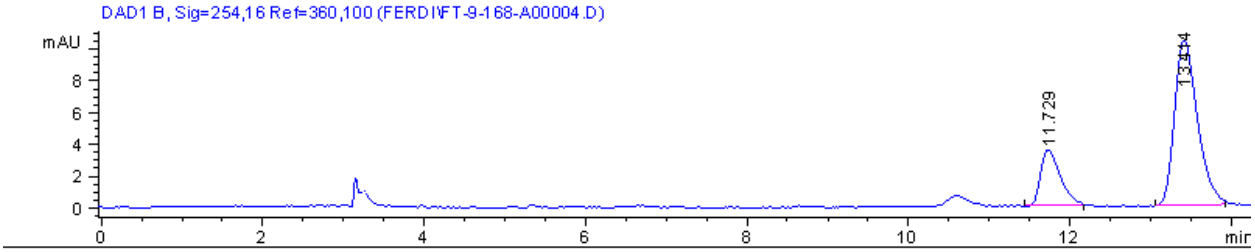

Signal 1: DAD1 B, Sig=254,16 Ref=360,100

Peak #	RetTime [min]	Type	Width [min]	Area [mAU*s]	Height [mAU]	Area %
1	11.729	BB	0.2462	59.81704	3.52190	22.6226
2	13.414	BB	0.2993	204.59560	10.40981	77.3774
Totals :				264.41263	13.93171	

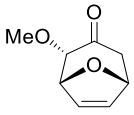

2-methoxy-8-oxabicyclo[3.2.1]oct-6-en-3-one (234a)

Prepared according to general procedure **B**

From furan (140 mg, 2 mmol, 10 equiv.) and **92** (46 mg, 0.2 mmol, 1 equiv.) and IDPi-**b** (5 mol%) in methylcyclohexane at -10 °C gave **234a** (15.7 mg, 0.102 mmol, 51% yield, 9% ee) as a colorless oil.

All spectral information matches reported values.

^{1}H NMR (400 MHz, CDCl3) δ 6.19 (s, 2H), 4.91 (dd, J = 7.5, 5.0 Hz, 2H), 3.86 (d, J = 5.0 Hz, 1H), 3.48 (s, 3H), 2.66 (dd, J = 15.4, 4.9 Hz, 1H), 2.26 (d, J = 15.4 Hz, 1H).

^{13}C NMR (101 MHz, CDCl3) δ 204.5, 134.6, 131.5, 86.9, 79.3, 78.4, 59.7, 45.9.

GC (chirocel B column): 60 °C -> 120 °C (ramp: 2 °C/min) t- major: 36.1 t -minor: 37.0

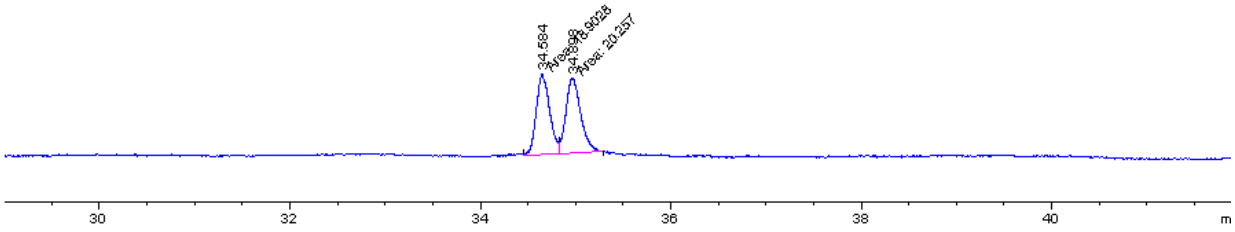

#	Time	Area	Height	Width	Area%	Symmetry
1	34.584	18.9	2	0.1583	48.271	0
2	34.898	20.3	1.9	0.181	51.729	0.709

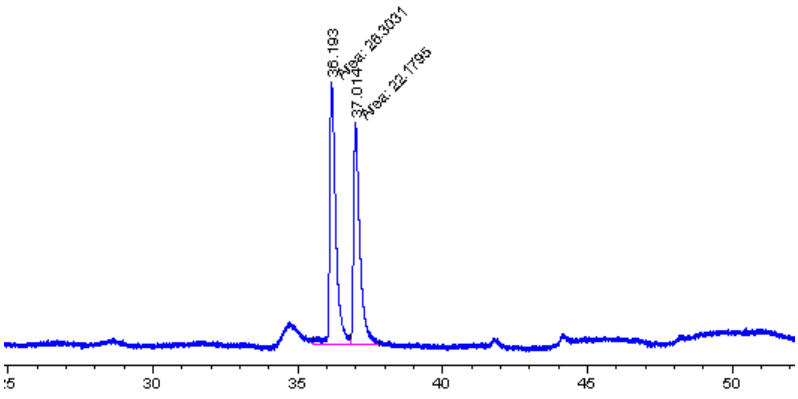

#	Time	Area	Height	Width	Area%	Symmetry
1	36.193	26.3	1.8	0.2461	54.253	0
2	37.014	22.2	1.5	0.2453	45.747	0.385

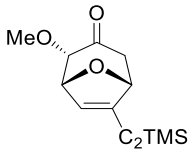

2-methoxy-6-((trimethylsilyl)ethynyl)-8-oxabicyclo[3.2.1]oct-6-en-3-one (234b)

Prepared according to general procedure **B**

From furan **233b** (16.4 mg, 0.1 mmol, 1 equiv.) and **92** (46 mg, 0.2 mmol, 2 equiv.) and IDPi-**b** (5 mol%) in methylcyclohexane at - 5 °C gave **234b** (15.7 mg, 0.063 mmol, 63% yield, 32% ee) as a colorless oil.

All spectral information matches reported values.

^{1}H NMR (400 MHz, CDCl3) δ 6.43 (d, J = 2.0 Hz, 1H), 5.06 (dd, J = 5.0, 2.0 Hz, 1H), 4.90 (d, J = 4.2 Hz, 1H), 3.95 (d, J = 5.0 Hz, 1H), 3.60 (s, 3H), 2.75 (dd, J = 15.7, 4.9 Hz, 1H), 2.58 (d, J = 15.7 Hz, 1H), 0.18 (s, 9H).

^{13}C NMR (101 MHz, CDCl3) δ 204.39, 135.71, 86.17, 81.14, 80.50, 60.26, 45.56, 0.32, -0.00.

GC (chirocel B column, 8 psi): 120 °C -> 150 °C (ramp: 1 °C/min) t- major: 43.9 t -minor: 43.5

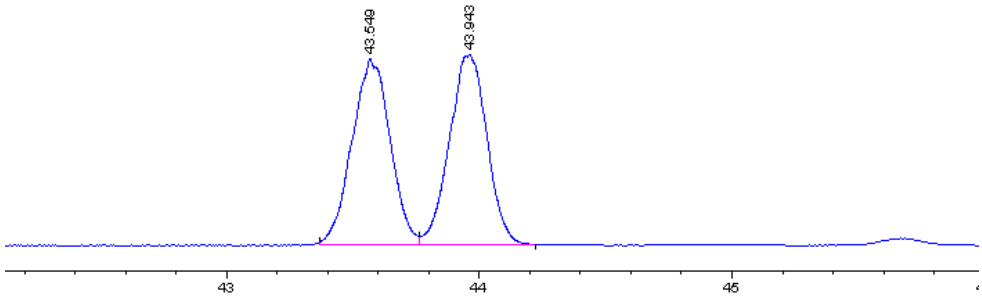

#	Time	Area	Height	Width	Area%	Symmetry
1	43.549	118.7	11.4	0.1268	49.763	0.899
2	43.943	119.8	11.6	0.1257	50.237	1.14

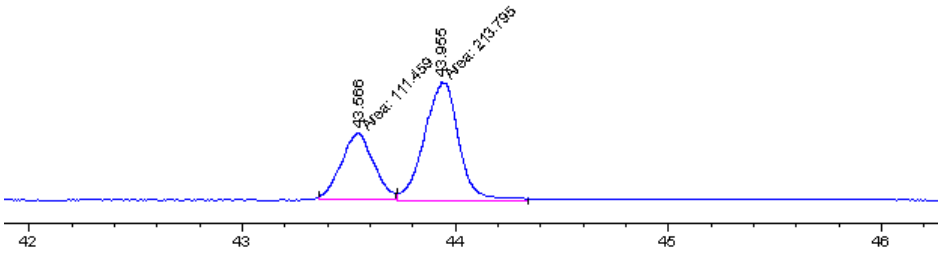

#	Time	Area	Height	Width	Area%	Symmetry
1	43.566	111.5	10.6	0.1751	34.268	1.201
2	43.955	213.8	18.8	0.1891	65.732	0.998

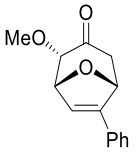

2-methoxy-6-phenyl-8-oxabicyclo[3.2.1]oct-6-en-3-one (234c)

Prepared according to general procedure **B**

From furan **233c** (14.4 mg, 0.1 mmol, 11 equiv.) and **92b** (46 mg, 0.2 mmol, 1 equiv.) and IDPi-($\mathbf{CF_3}$)$_2$ (5 mol%) in diethyl ether at - 10 °C gave **234c** (14.8 mg, 0.064 mmol, 64% yield, 32% ee) as a colorless oil.

^{1}H NMR (400 MHz, CDCl3) δ 7.40 – 7.28 (m, 5H), 6.54 (d, J = 2.1 Hz, 1H), 5.40 (d, J = 4.2 Hz, 1H), 5.17 (dd, J = 4.9, 2.1 Hz, 1H), 4.05 (d, J = 4.9 Hz, 1H), 3.63 (s, 3H), 2.90 (dd, J = 15.4, 5.0 Hz, 1H), 2.57 (d, J = 15.4 Hz, 1H).

^{13}C NMR (101 MHz, CDCl3) δ 204.31, 128.92, 128.84, 126.14, 123.34, 85.83, 80.49, 78.96, 59.88, 45.75.

GC (chirocel B column, 8 psi): 170 °C (iso 90 min.) t- major: 38.3 t -minor: 37.6

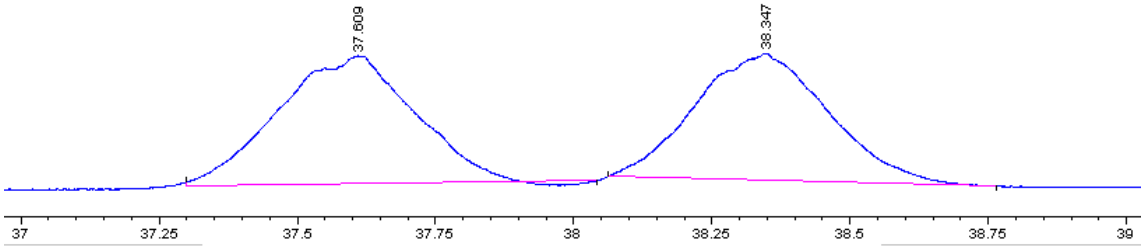

#	Time	Area	Height	Width	Area%	Symmetry
1	37.609	76.9	4.5	0.2041	50.583	1.338
2	38.347	75.1	4.5	0.2012	49.417	1.058

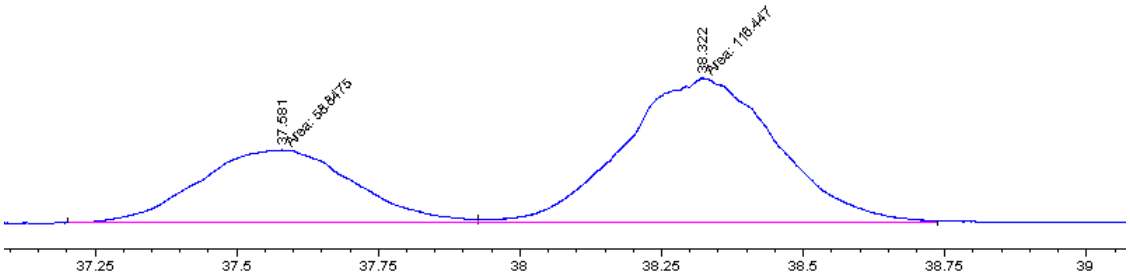

#	Time	Area	Height	Width	Area%	Symmetry
1	37.581	58.8	3.1	0.3146	33.571	0
2	38.322	116.4	6.2	0.3133	66.429	1.033

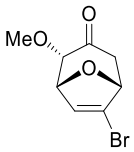

6-bromo-2-methoxy-8-oxabicyclo[3.2.1]oct-6-en-3-one (234d)

From furan **233d** (14.6 mg, 0.1 mmol, 1 equiv.) and **92** (46 mg, 0.2 mmol, 2 equiv.) and IDPi-**b** (5 mol%) in diethyl ether at 10 °C gave **234d** (12.2 mg, 0.038 mmol, 38% yield, 75% ee) as a colorless oil.

Additional purification was needed for the racemic sample (10:20:70 $Et_2O/CHCl_3$/Hexanes)

^{1}H NMR (400 MHz, CDCl3) δ 6.37 (d, J = 2.0 Hz, 1H), 5.00 (dd, J = 4.8, 2.0 Hz, 1H), 4.82 (dd, J = 4.7, 1.0 Hz, 1H), 3.91 (d, J = 4.8 Hz, 1H), 3.61 (s, 3H), 2.74 (dd, J = 15.7, 4.7 Hz, 1H), 2.63 (d, J = 15.7 Hz, 1H).

^{13}C NMR (101 MHz, CDCl3) δ 203.63, 130.42, 85.15, 82.13, 80.65, 77.34, 77.02, 76.70, 60.03, 44.20.

GC (chirocel B column, 8 psi): 110 °C (iso 60 min.) t- major: 52.9 t -minor: 52.3

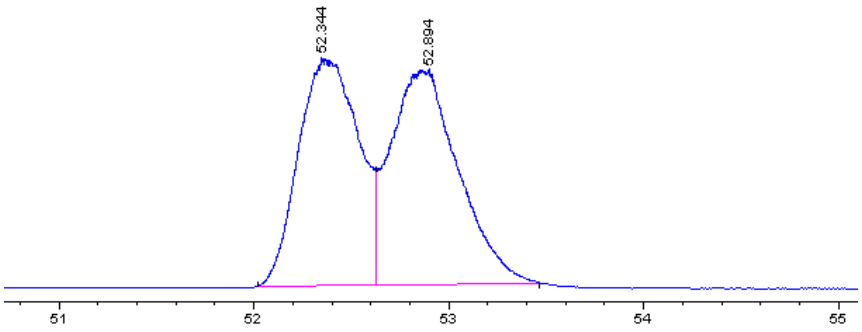

#	Time	Area	Height	Width	Area%	Symmetry
1	52.344	189.8	8.8	0.2544	48.649	0.639
2	52.894	200.4	8.3	0.2841	51.351	1.147

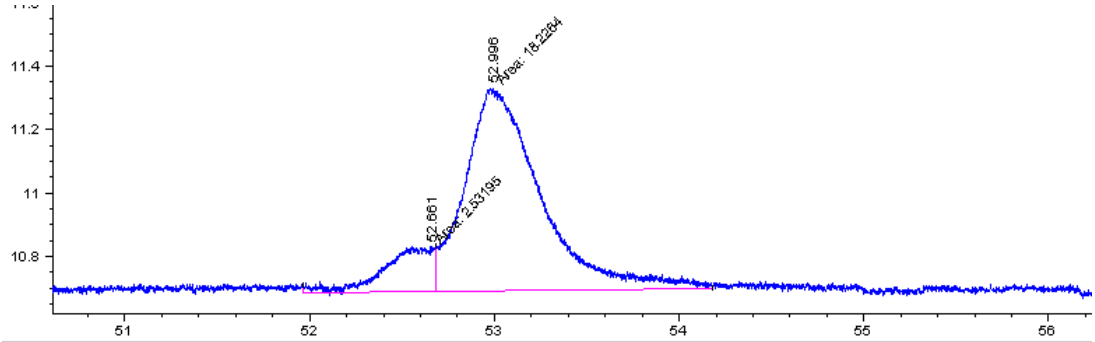

#	Time	Area	Height	Width	Area%	Symmetry
1	52.661	2.5	1.4E-1	0.2968	12.197	0
2	52.996	18.2	6.4E-1	0.4742	87.803	0.566

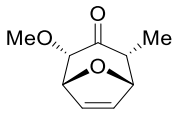

2-methoxy-4-methyl-8-oxabicyclo[3.2.1]oct-6-en-3-one (234e)

Prepared according to general procedure **B**

From furan **233a** (140 mg, 2 mmol, 10 equiv.) and **92b** (50 mg, 0.2 mmol, 1 equiv.) and IDPi-**a** (5 mol %) in methylcyclohexane at - 5 °C gave **234e** (18.5 mg, 0.11 mmol, 55% yield, 35% ee) as a colorless oil.

All spectral information matches reported values.

^{1}H NMR (400 MHz, CDCl3) δ 6.39 – 6.27 (m, 2H), 5.01 (dd, J = 4.9, 1.7 Hz, 1H), 4.83 (dd, J = 4.6, 1.5 Hz, 1H), 3.98 (dd, J = 4.9, 0.6 Hz, 1H), 3.59 (s, 3H), 2.88 – 2.77 (m, 1H), 0.98 (d, J = 6.9 Hz, 3H).

^{13}C NMR (101 MHz, CDCl3) δ 206.95, 133.43, 133.11, 86.10, 82.95, 79.99, 59.71, 50.20, 9.53**.**

GC (chirocel B column, 8 psi): 75 °C -> 110 °C (ramp: 0.25 °C/min.) t- major: 44.1 t -minor: 43.9

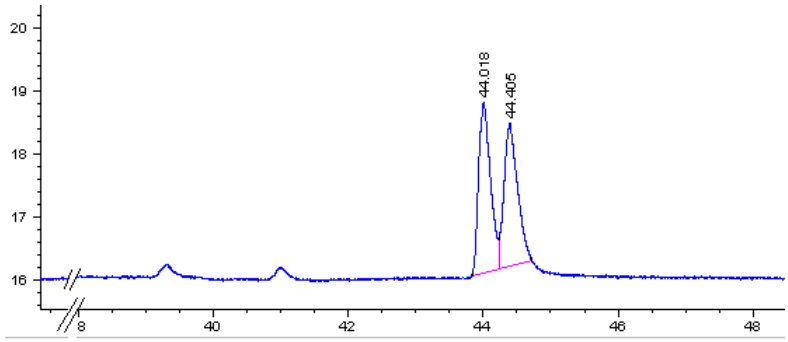

#	Time	Area	Height	Width	Area%	Symmetry
1	44.018	33.1	2.7	0.1493	50.758	0.724
2	44.405	32.1	2.3	0.1712	49.242	0.721

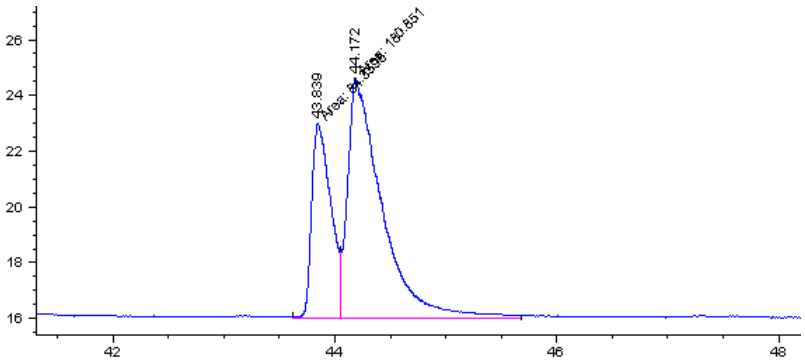

#	Time	Area	Height	Width	Area%	Symmetry
1	43.839	84.4	7	0.2015	31.809	0
2	44.172	180.9	8.6	0.3502	68.191	0.251

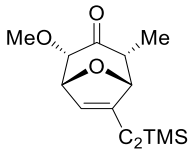

2-methoxy-4-methyl-6-((trimethylsilyl)ethynyl)-8-oxabicyclo[3.2.1]oct-6-en-3-one (234f)

Prepared according to general procedure **B**

From furan **233b** (16.4 mg, 0.1 mmol, 1 equiv.) and **92** (50 mg, 0.2 mmol, 2 equiv.) and IDPi-**a** (5 mol%) in methylcyclohexane at - 10 °C gave **234f** (12.6 mg, 0.048 mmol, 48% yield, 72% ee) as a colorless oil.

All spectral information matches reported values.

^{1}H NMR (400 MHz, CDCl3) δ 6.46 (d, J = 2.1 Hz, 1H), 5.09 – 4.99 (m, 1H), 4.76 (d, J = 4.5 Hz, 1H), 3.98 (d, J = 5.0 Hz, 1H), 3.59 (s, 3H), 2.89 (dd, J = 6.9, 4.6 Hz, 1H), 1.14 (d, J = 7.0 Hz, 3H), 0.16 (s, 9H)

GC (chirocel B column, 8 psi): 150 °C (iso 60 min.) t- major: 31.8 t -minor: 30.4

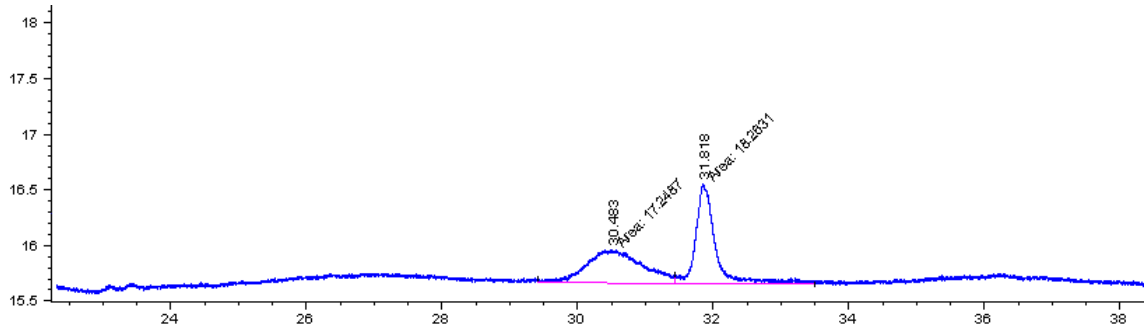

#	Time	Area	Height	Width	Area%	Symmetry
1	30.483	17.2	3E-1	0.9647	48.572	0
2	31.818	18.3	9E-1	0.3398	51.428	0.564

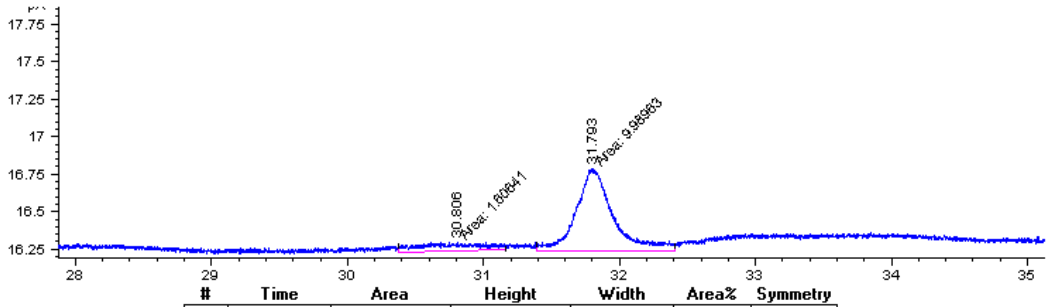

#	Time	Area	Height	Width	Area%	Symmetry
1	30.806	1.6	5.6E-2	0.4774	13.853	0
2	31.793	10	5.4E-1	0.307	86.147	0.733

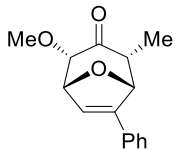

2-methoxy-4-methyl-6-phenyl-8-oxabicyclo[3.2.1]oct-6-en-3-one (234g)

Prepared according to general procedure **B**

From furan **233c** (14.4 mg, 0.1 mmol, 11 equiv.) and **92b** (50 mg, 0.2 mmol, 1 equiv.) and IDPi-**a** (5 mol %) in methylcyclohexane at - 5 °C gave **234g** (12.4 mg, 0.051 mmol, 51% yield, 42% ee) as a colorless oil.

All spectral information matches reported values.

^{1}H NMR (400 MHz, CDCl3) δ 7.40 – 7.25 (m, 5H), 6.52 (d, J = 2.2 Hz, 1H), 5.37 (d, J = 4.6 Hz, 1H), 5.14 (dd, J = 4.9, 2.2 Hz, 1H), 4.10 (d, J = 4.9 Hz, 1H), 3.63 (s, 3H), 3.08 – 2.93 (m, 1H), 0.83 (d, J = 7.0 Hz, 3H).

^{13}C NMR (101 MHz, CDCl3) δ 200.82, 147.61, 128.68, 126.66, 124.73, 86.21, 83.11, 81.03, 59.75, 51.08, 9.93.

Polarimetry: $[\alpha]_D^{23}$ = 25.9°. compared to literature value $[\alpha]^{22.5}$ = +53.8° for 87% ee.[20]

[20] Banik, S. M.; Levina, A.; Hyde, A. M.; Jacobsen, E. N. *Science* **2017**, *358*, 761-764

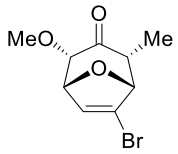

6-bromo-2-methoxy-4-methyl-8-oxabicyclo[3.2.1]oct-6-en-3-one (234h)

Prepared according to general procedure **B**

From furan **233d** (14.6 mg, 0.1 mmol, 1 equiv.) and **92** (46 mg, 0.2 mmol, 2 equiv.) and IDPi-**a** (5 mol%) in diethyl ether at 10 °C gave **234h** (10.8 mg, 0.044 mmol, 44% yield, 43% ee) as a colorless oil.

All spectral information matches reported values.

^{1}H NMR (400 MHz, CDCl3) δ 6.43 (d, J = 2.2 Hz, 1H), 4.95 (dd, J = 5.0, 2.2 Hz, 1H), 4.70 (d, J = 4.4 Hz, 1H), 3.98 (d, J = 5.0 Hz, 1H), 3.60 (s, 3H), 2.97 (tt, J = 7.2, 3.2 Hz, 1H), 1.21 (d, J = 7.1 Hz, 3H).

^{13}C NMR (101 MHz, CDCl3) δ 205.36, 131.78, 123.71, 85.83, 85.18, 81.20, 59.87, 50.68, 9.50.

GC (chirocel B column, 8 psi): 80 °C -> 120 °C (ramp: 0.3 °C/ min.) t- major: 99.5 t -minor: 99.0

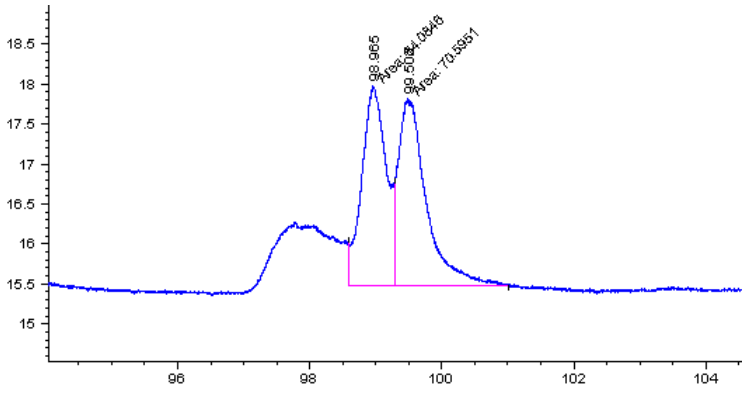

#	Time	Area	Height	Width	Area%	Symmetry
1	98.965	64.1	2.5	0.4246	47.583	0
2	99.502	70.6	2.3	0.5016	52.417	0.534

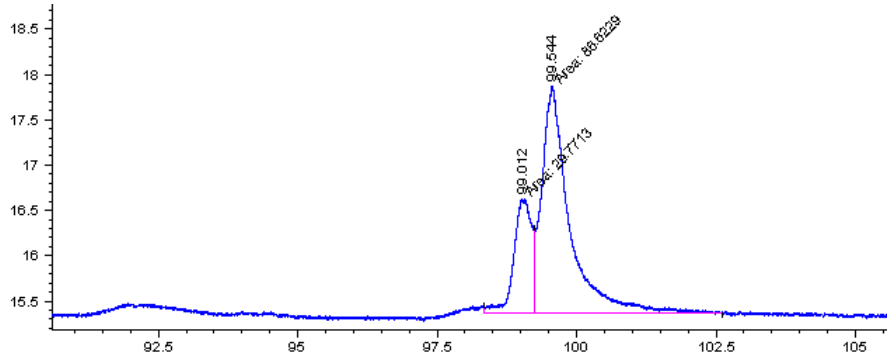

#	Time	Area	Height	Width	Area%	Symmetry
1	99.012	29.8	1.3	0.3899	25.578	0
2	99.544	86.6	2.5	0.5743	74.422	0.503

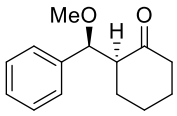

2-methoxy(phenyl)methyl)cyclohexan-1-one (241)

Prepared according to general procedure **B**

Benzaldehyde dimethyl acetal **240** (15.2 mg, 0.1 mmol, 1 equiv.), TMS enol ether **179** (34 mg, 0.2 mmol, 2 equiv.), and IDPi-**a** (5 mol%) in diethyl ether at ambient temperature. To yield **241** (19.4 mg, 0.089mmol, 89% yield)**.** The racemate was isolated as a mixture of diastereomers.

All spectral information matches reported values.

^{1}H NMR (400 MHz, CDCl3) δ 7.37 – 7.07 (m, 10H), 4.58 (d, J = 6.3 Hz, 1H), 4.39 (d, J = 9.9 Hz, 1H), 3.19 (s, 3H), 2.89 (s, 3H), 2.87 – 2.73 (m, 3H), 2.66 – 2.53 (m, 1H), 2.47 (t, J = 6.7 Hz, 1H), 1.86 (dd, J = 7.4, 4.5 Hz, 2H), 1.68 (ddt, J = 17.1, 8.5, 5.2 Hz, 6H), 1.66 – 1.49 (m, 4H), 1.42 (d, J = 3.7 Hz, 1H).

^{13}C NMR (101 MHz, CDCl3) δ 211.12, 201.83, 141.13, 139.23, 136.71, 135.61, 130.31, 128.54, 128.47, 128.35, 128.20, 128.12, 127.47, 127.38, 127.25, 83.18, 80.81, 77.36, 77.24, 77.04, 76.72, 58.17, 56.99, 56.69, 55.14, 40.36, 28.96, 28.93, 28.86, 23.91, 23.41, 21.04.

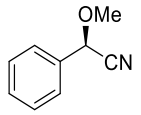

(R)-2-methoxy-2-phenylacetonitrile (242)

Prepared according to general procedure **B**

Benzaldehyde dimethyl acetal **240** (15.2 mg, 0.1 mmol, 1 equiv.) TMSCN (20 mg, 0.2 mmol, 2 equiv.) and IDPi-**a** (5 mol%) in diethyl ether at ambient temperature. To yield **242** (13.8 mg, 0.094mmol, 94% yield)**.**

All spectral information matches reported values.

^{1}H NMR (400 MHz, CDCl3) δ 7.54 – 7.38 (m, 5H), 5.20 (s, 1H), 3.54 (s, 3H).

^{13}C NMR (101 MHz, CDCl3) δ 133.28, 129.87, 129.05, 127.32, 116.96, 72.32, 57.23.

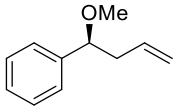

(1-methoxybut-3-en-1-yl)benzene (244)

Benzaldehyde dimethyl acetal **240** (15.2 mg, 0.1 mmol, 1 equiv.) allyl trimethyl silane, **243** (22.8 mg, 0.2 mmol, 2 equiv.) (20 mg, 0.2 mmol, 2 equiv.) and IDPi-**a** (5 mol%) in diethyl ether at ambient temperature. To yield **242** (12.6 mg, 0.078 mmol, 78% yield, 23% ee)**.**

^{1}H NMR (400 MHz, CDCl3) δ 7.40 – 7.24 (m, 5H), 5.77 (ddt, J = 17.1, 10.2, 6.9 Hz, 1H), 5.10 – 5.00 (m, 3H), 4.17 (dd, J = 7.4, 5.9 Hz, 1H), 3.22 (s, 2H), 2.58 (dd, J = 14.3, 7.2 Hz, 1H), 2.47 – 2.35 (m, 2H).

^{13}C NMR (101 MHz, CDCl3) δ 141.70, 134.83, 128.37, 127.62, 126.75, 116.89, 83.67, 77.37, 77.05, 76.73, 56.68, 42.55.

Polarimetry: $[\alpha]^{23} = -18.8°$. compared to literature value R-**244** $[\alpha]^{22.5} = +35.0°$ for 54% ee.[21]

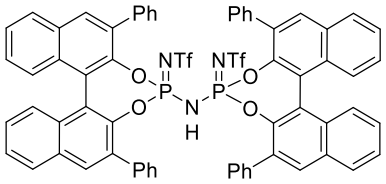

Imidodiphosphorimidate (IDPi-a)

Following to procedure of List et al. IDPi-**a** was prepared in 70% yield from the corresponding s-binol.

Spectral data matches the reported values.[22]

^{1}H NMR (500 MHz, CD2Cl2) δ 8.16 (d, J = 4.7 Hz, 1H), 8.10 (d, J = 8.1 Hz, 1H), 7.88 (d, J = 6.6 Hz, 1H), 7.74 – 7.60 (m, 2H), 7.45 (d, J = 7.6 Hz, 1H), 7.43 – 7.25 (m, 4H), 7.25 (dd, J = 13.1, 6.3 Hz, 1H), 7.05 (t, J = 7.3 Hz, 1H), 6.52 (d, J = 7.5 Hz, 1H).

[21] Hathaway, S. J.; Paquette, L. A. *J. Org. Chem.* **1983**, *48*, 3351-3353
[22] Kaib, P. S. J.; Schreyer, L.; Lee, S.; Properzi, R.; List, B. . *Angew. Chem. Int. Ed.* **2016**, *55*, 13200-13203

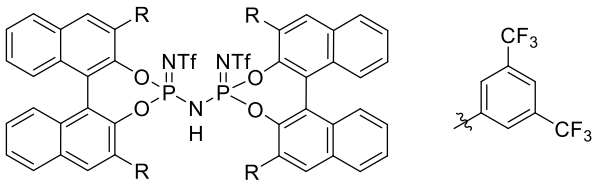

Imidodiphosphorimidate (IDPi-b)

Following to procedure of List et al. IDPi-**b** was prepared in 46% yield from the corresponding s-binol.

Spectral data matches the reported values.[23]

^{1}H NMR (500 MHz, CD2Cl2) δ 8.20 (s, 1H), 8.15 (d, J = 7.8 Hz, 2H), 8.03 – 7.89 (m, 4H), 7.84 – 7.65 (m, 1H), 7.42 (d, J = 7.5 Hz, 1H), 7.21 (d, J = 8.5 Hz, 2H), 6.73 (s, 1H).

^{31}P NMR (202 MHz, CD2Cl2) δ -16.01.

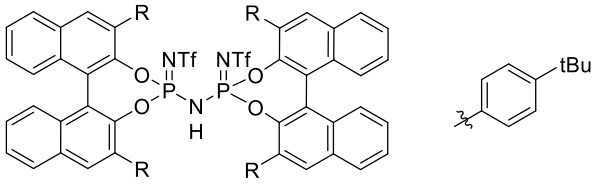

Imidodiphosphorimidate (IDPi-c)

Following to procedure of List et al. IDPi-**c** was prepared in 56% yield from the corresponding s-binol.

Spectral data matches the reported values.[24]

[23] Kaib, P. S. J.; Schreyer, L.; Lee, S.; Properzi, R.; List, B. . *Angew. Chem. Int. Ed.* **2016**, *55*, 13200-13203
[24] Lee, S.; Kaib, P. S. J.; List, B. *J. Am. Chem. Soc.* **2017**, *139*, 2156-2159

^{1}H NMR (400 MHz, CDCl3) δ 8.09 (s, 2H), 8.05 (d, J = 8.2 Hz, 2H), 8.00 (d, J = 8.4 Hz, 2H), 7.77 (s, 2H), 7.60 (d, J = 10.0 Hz, 2H), 7.53 (t, J = 7.7 Hz, 6H), 7.40 – 7.30 (m, 4H), 6.91 (s, 4H), 6.58 (d, J = 7.9 Hz, 4H), 1.80 (s, 18H).

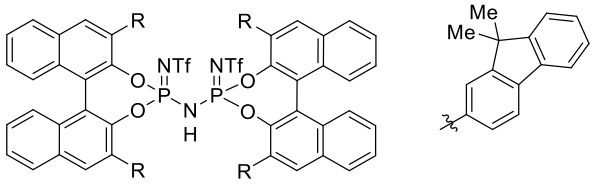

Imidodiphosphorimidate (IDPi-d)

Following to procedure of List et al. IDPi-**d** was prepared in 15% yield from the corresponding s-binol.

Spectral data matches the reported values.[25]

^{1}H NMR (400 MHz, CDCl3) δ 8.04 (d, J = 6.0 Hz, 4H), 7.89 – 7.79 (m, 2H), 7.70 (d, J = 8.1 Hz, 1H), 7.58 (d, J = 6.7 Hz, 1H), 7.48 (s, 2H), 7.45 – 7.34 (m, 6H), 7.26 – 7.12 (m, 12H), 6.70 (d, J = 8.2 Hz, 2H), 6.23 (d, J = 8.1 Hz, 1H), 1.48 (s, 3H), 1.41 (s, 3H), 1.24 (s, 3H), 1.20 (s, 3H).

^{31}P NMR (162 MHz, CDCl3) δ -8.07, -16.84.

[25] Gatzenmeier, T.; Kaib, P. S. J.; Lingnau, J. B.; Goddard, R.; List, B. *Angew. Chem. Int. Ed.* **2017**, *57*, 2464-2468

Chapter 6: Selected Spectra

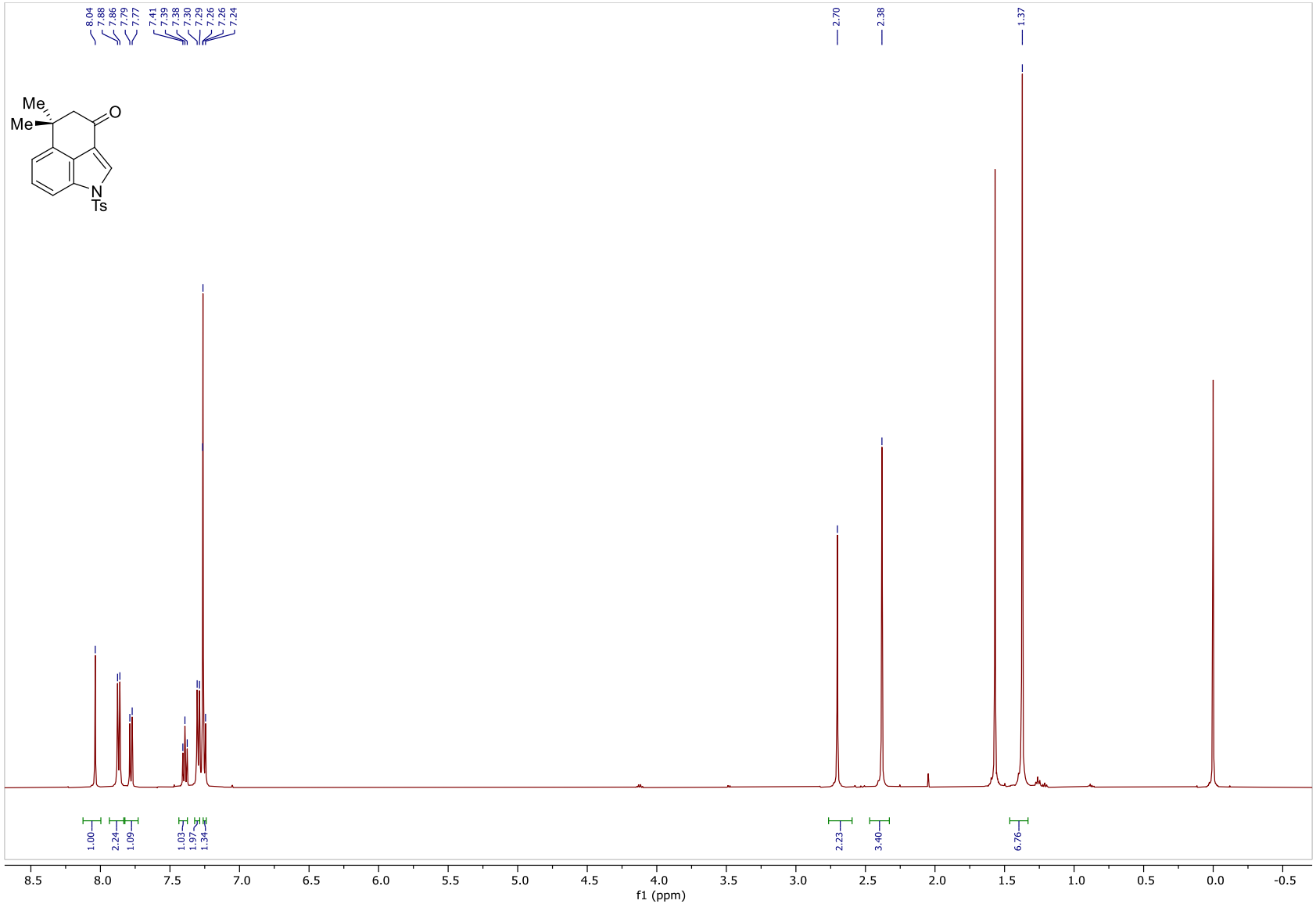

Figure 8: ^{1}H NMR Spectrum of **90** (500MHz, $CDCl_3$)

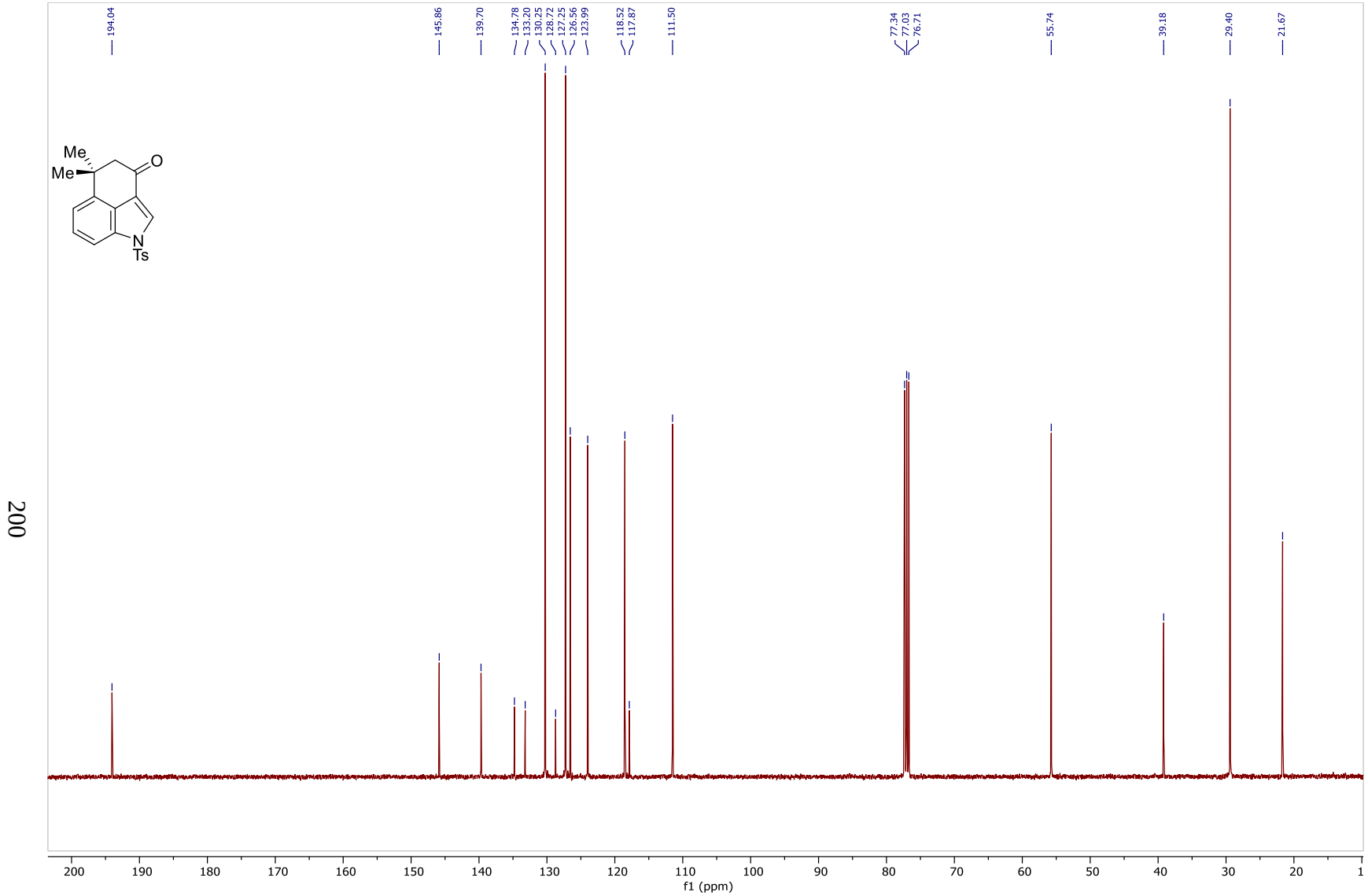

Figure 9: ^{13}C NMR Spectrum of **90** (100MHz, $CDCl_3$)

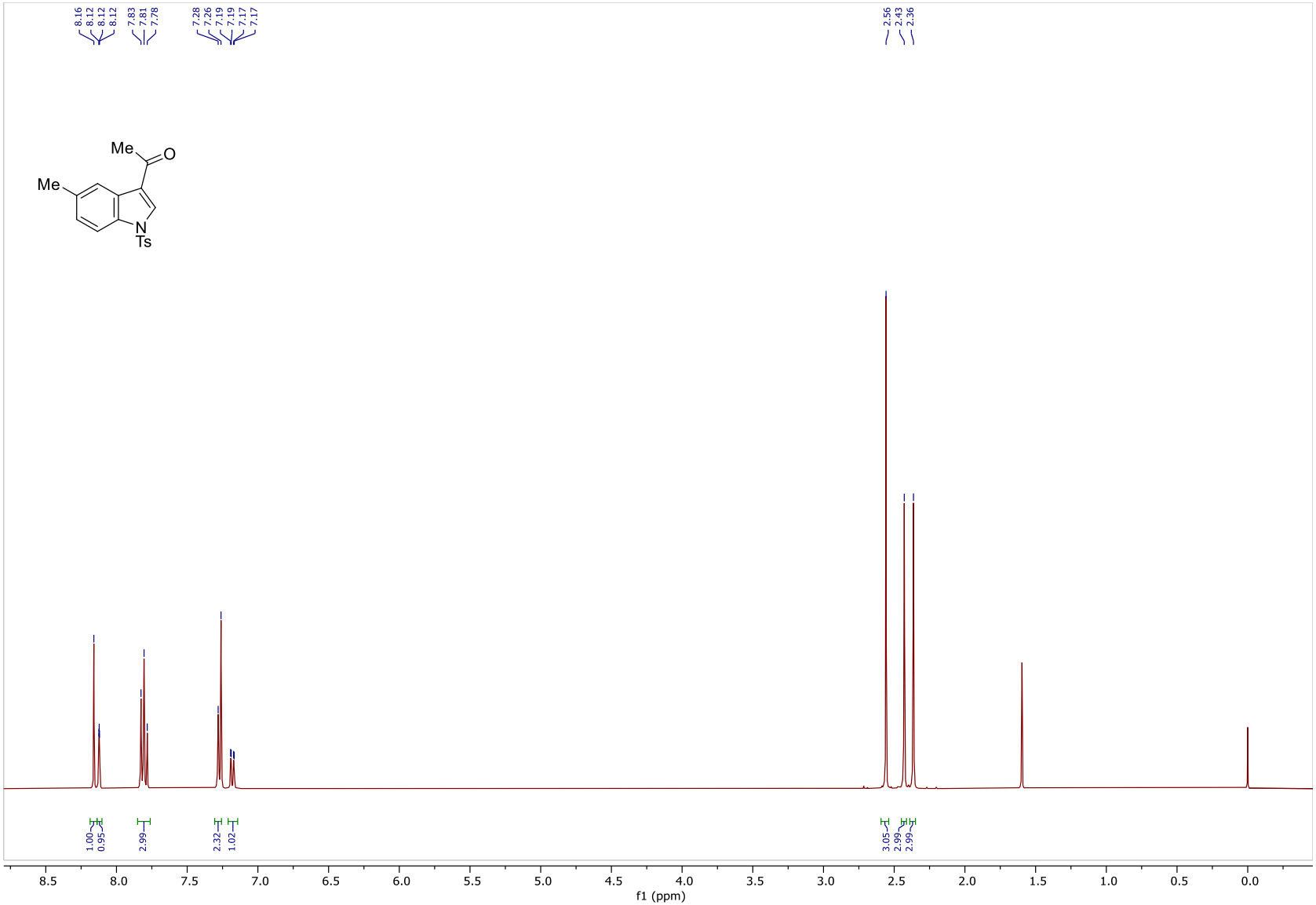

Figure 10: ^{1}H NMR Spectrum of **94a** (400MHz, $CDCl_3$)

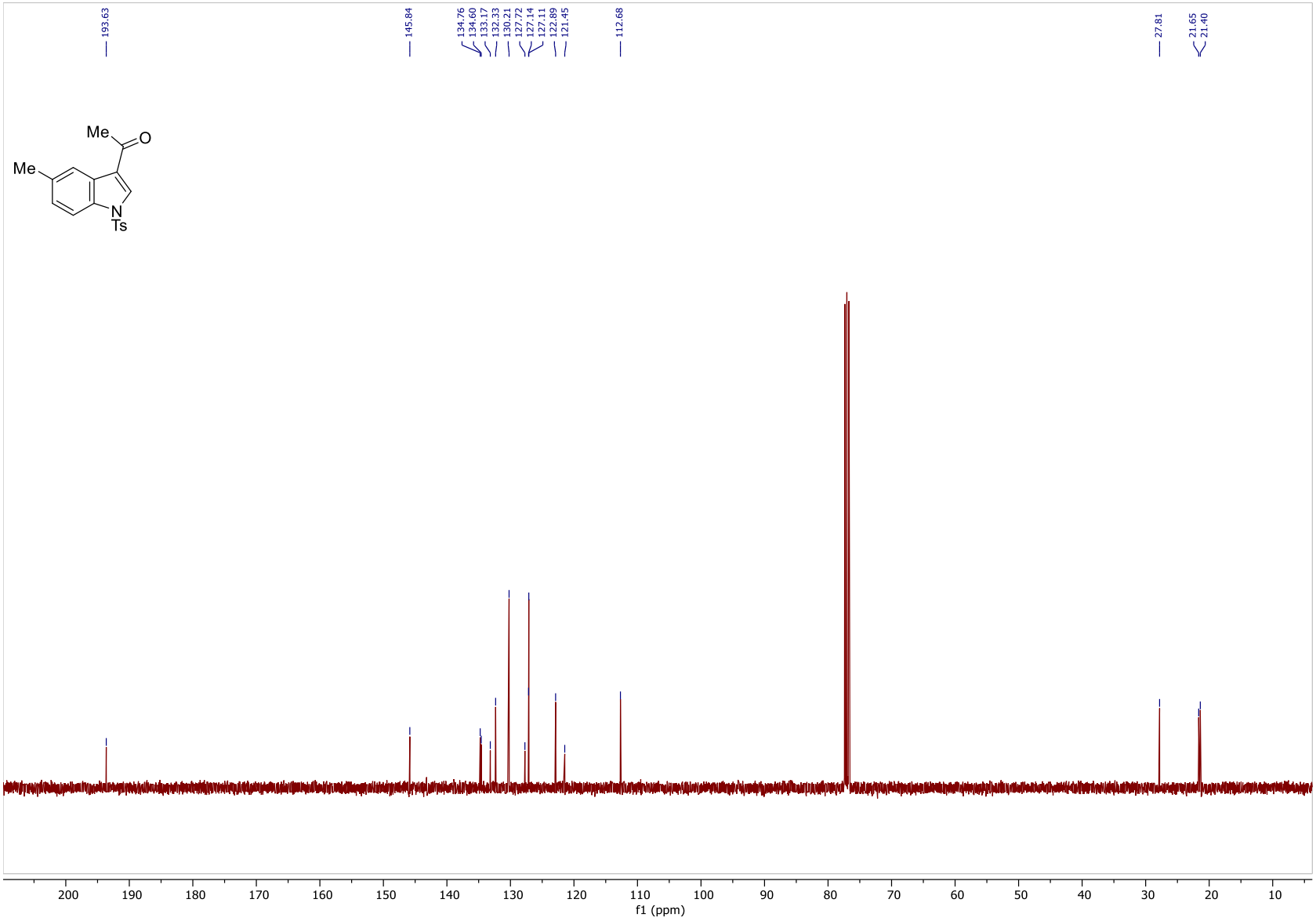

Figure 11: ^{13}C NMR Spectrum of **94a** (100MHz, $CDCl_3$)

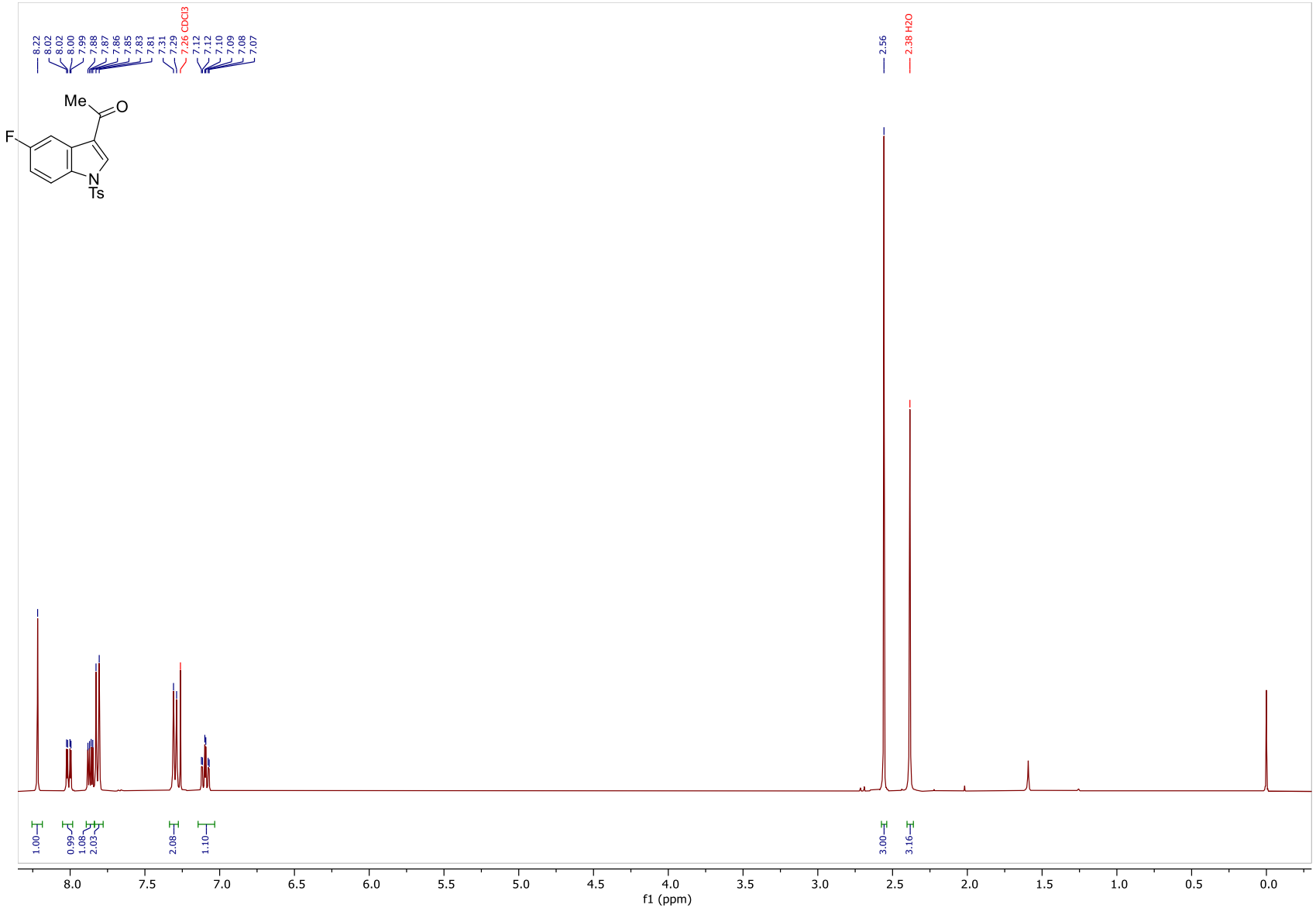

Figure 12: ^{1}H NMR Spectrum of **94b** (400MHz, $CDCl_3$)

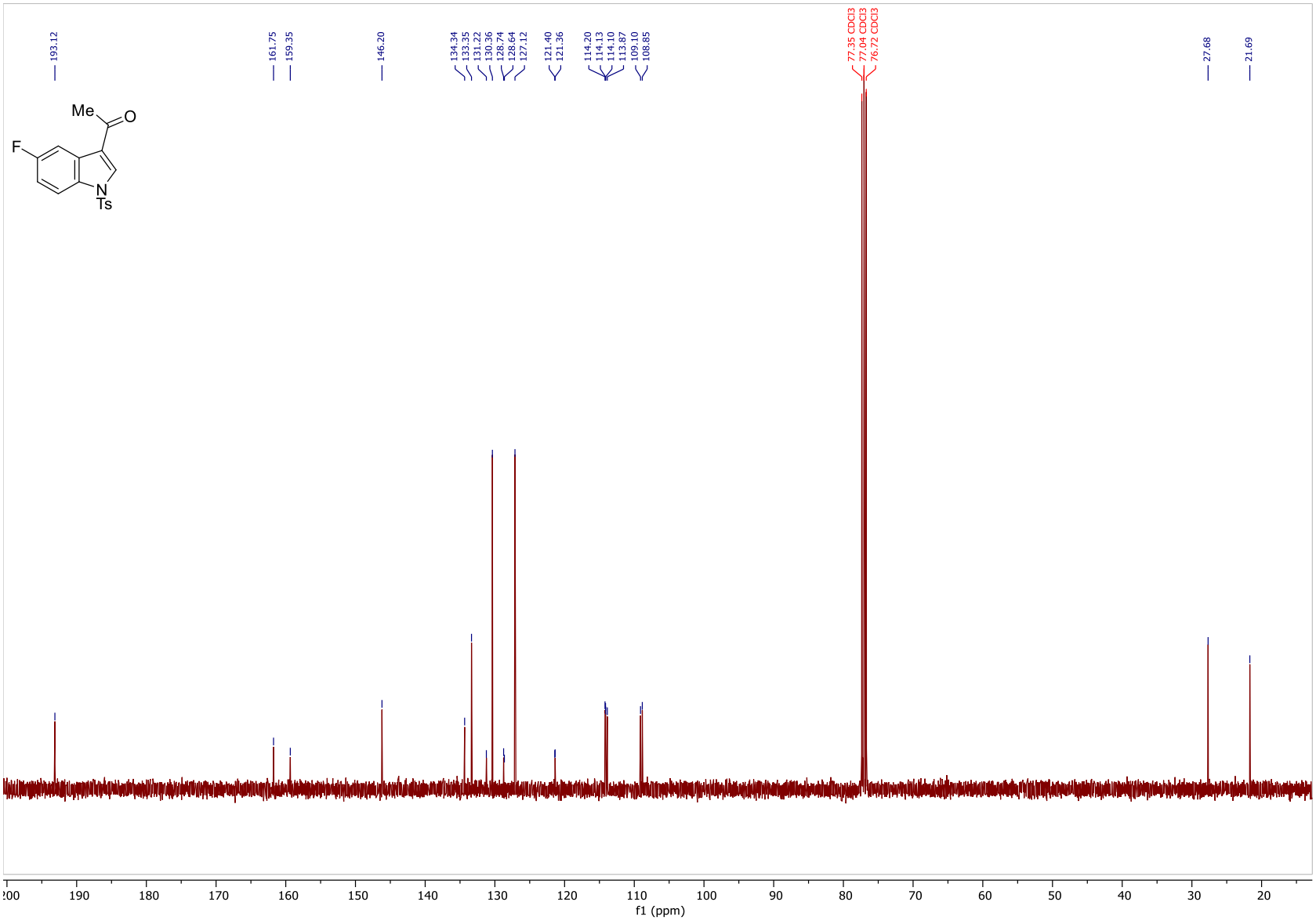

Figure 13: ^{13}C NMR Spectrum of **94b** (100MHz, $CDCl_3$)

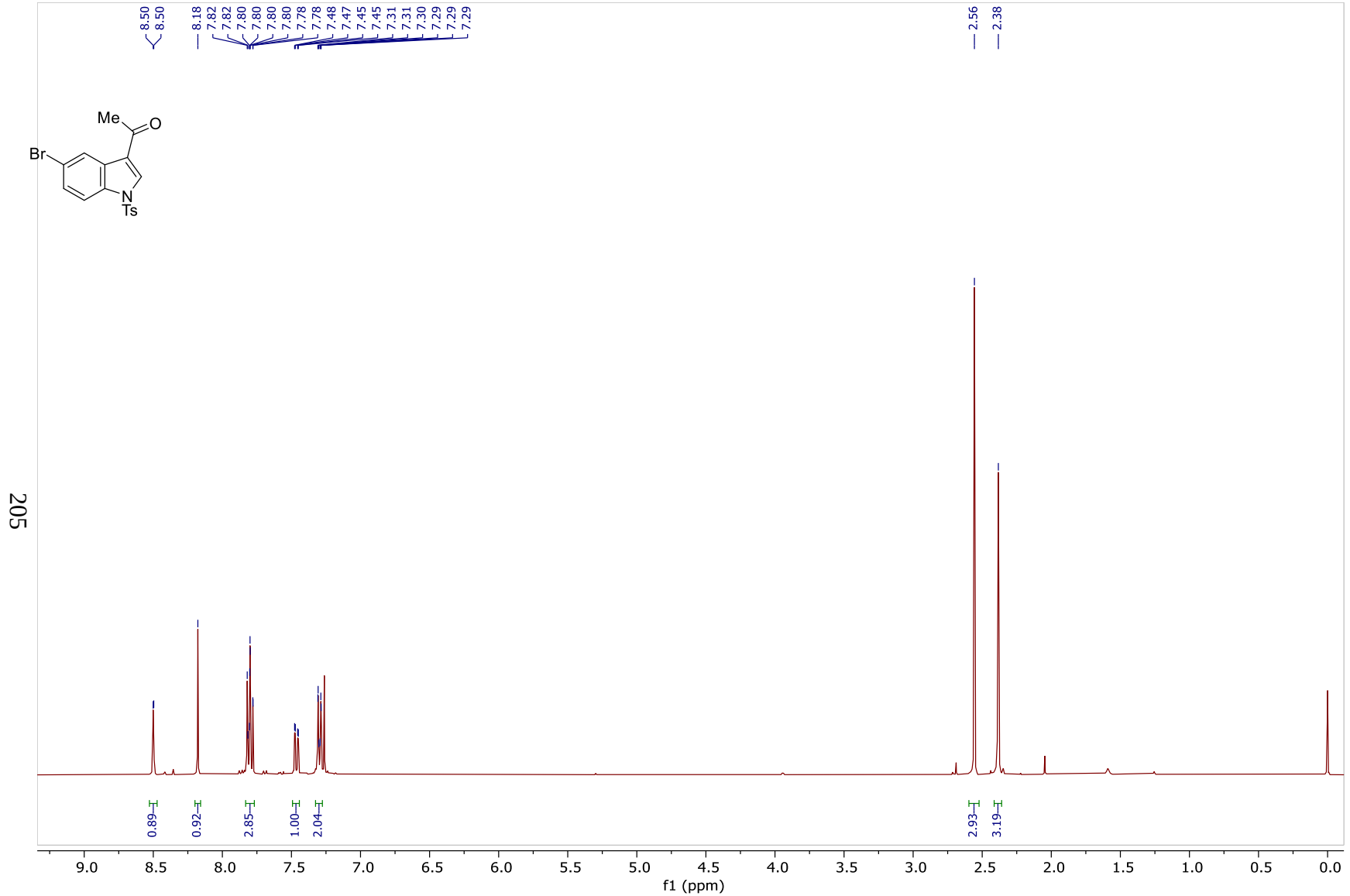

205

Figure 14: ^{1}H NMR Spectrum of **94b** (400MHz, $CDCl_3$)

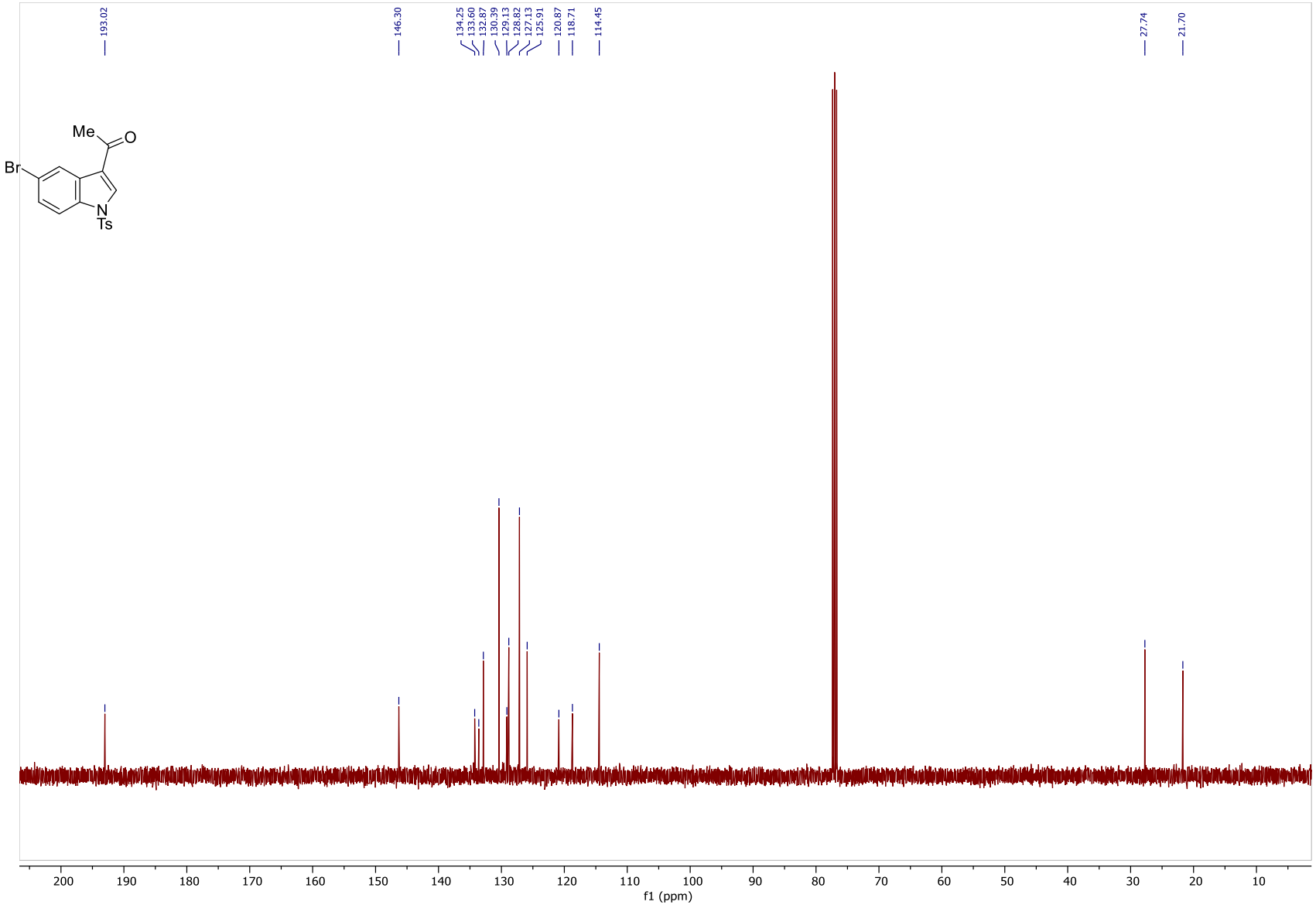

Figure 15: ^{13}C NMR Spectrum of **94c** (100MHz, $CDCl_3$)

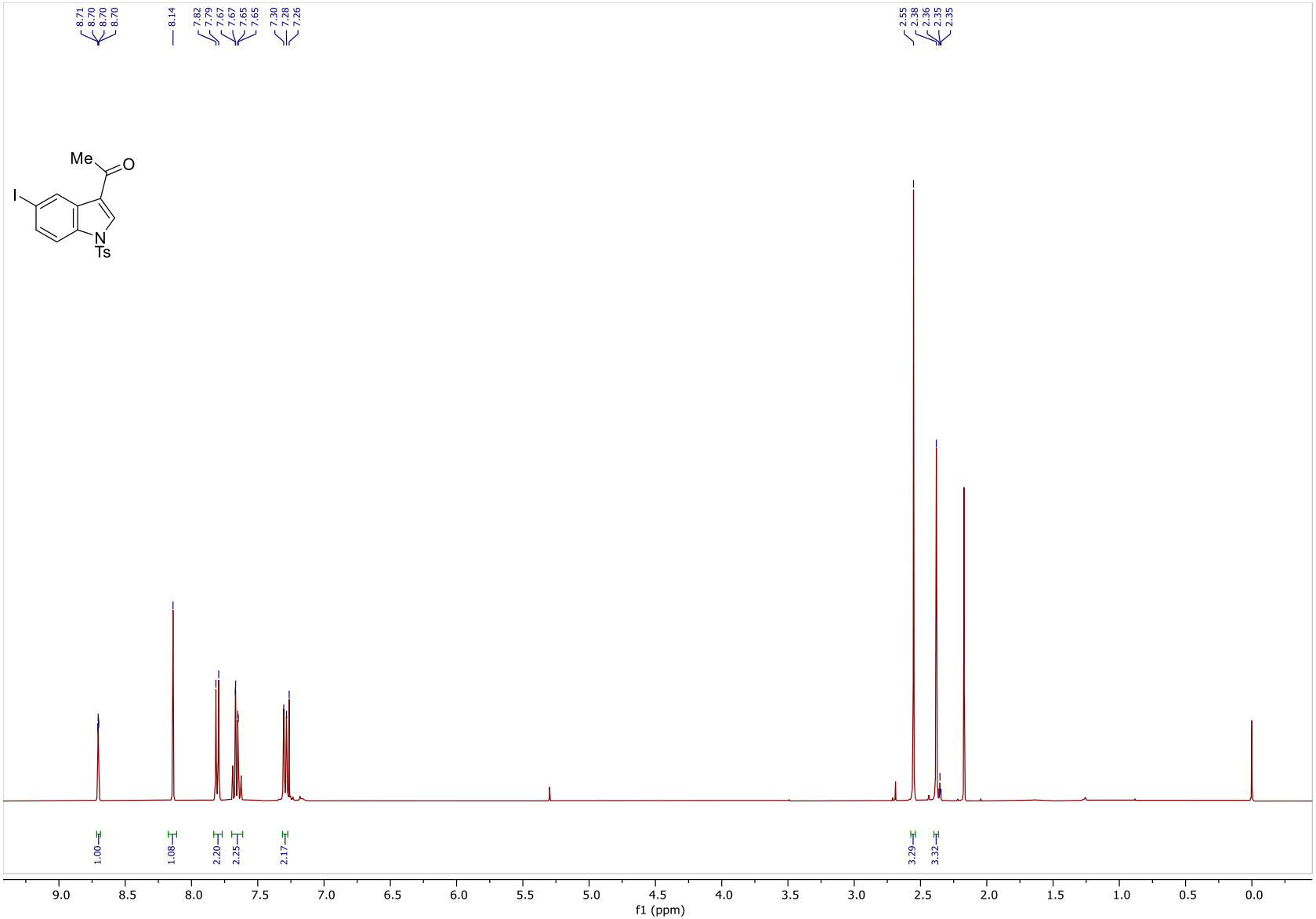

Figure 16: ^{1}H NMR Spectrum of **94d** (400MHz, $CDCl_3$)

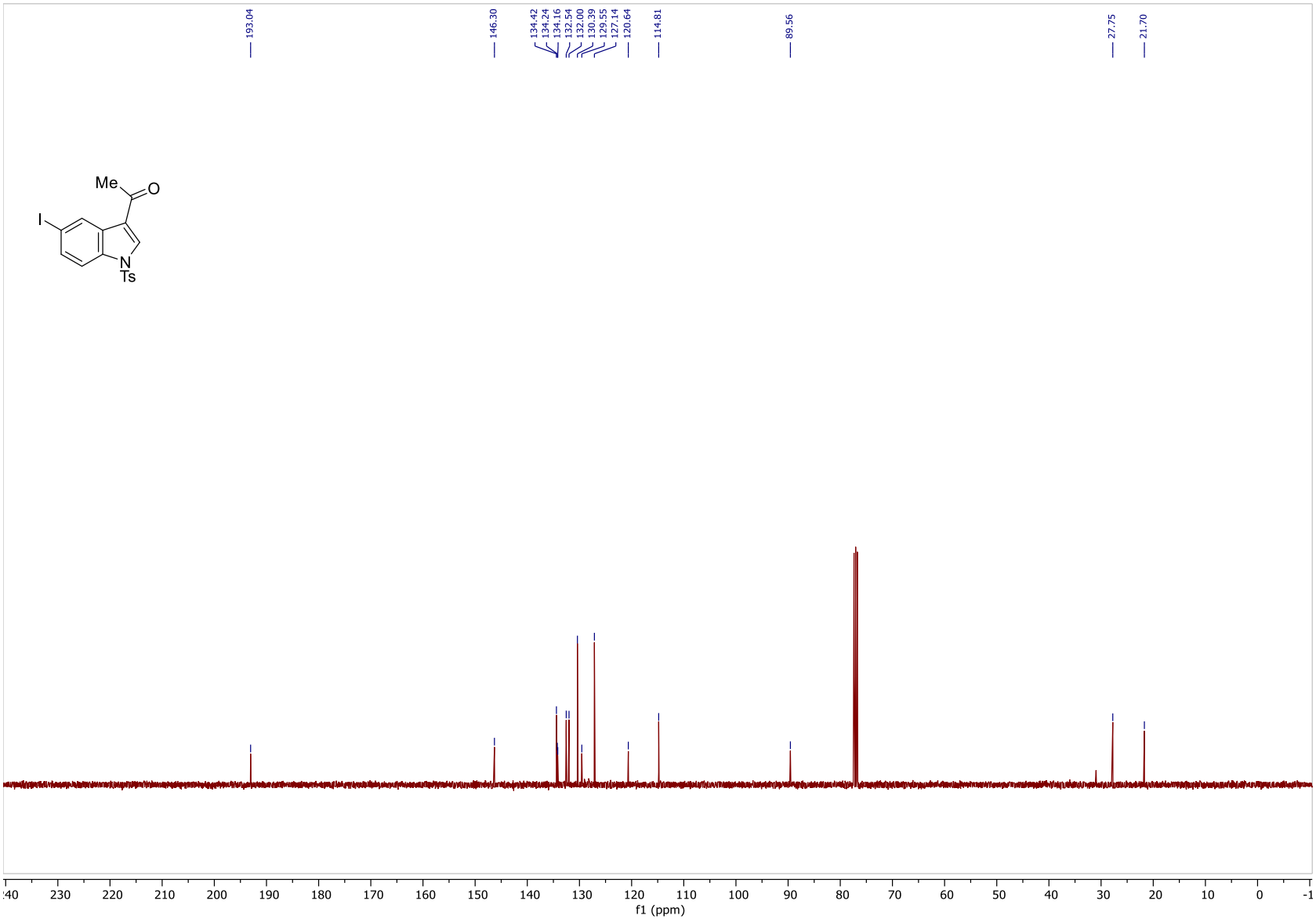

Figure 17: ^{13}C NMR Spectrum of **94d** (100MHz, $CDCl_3$)

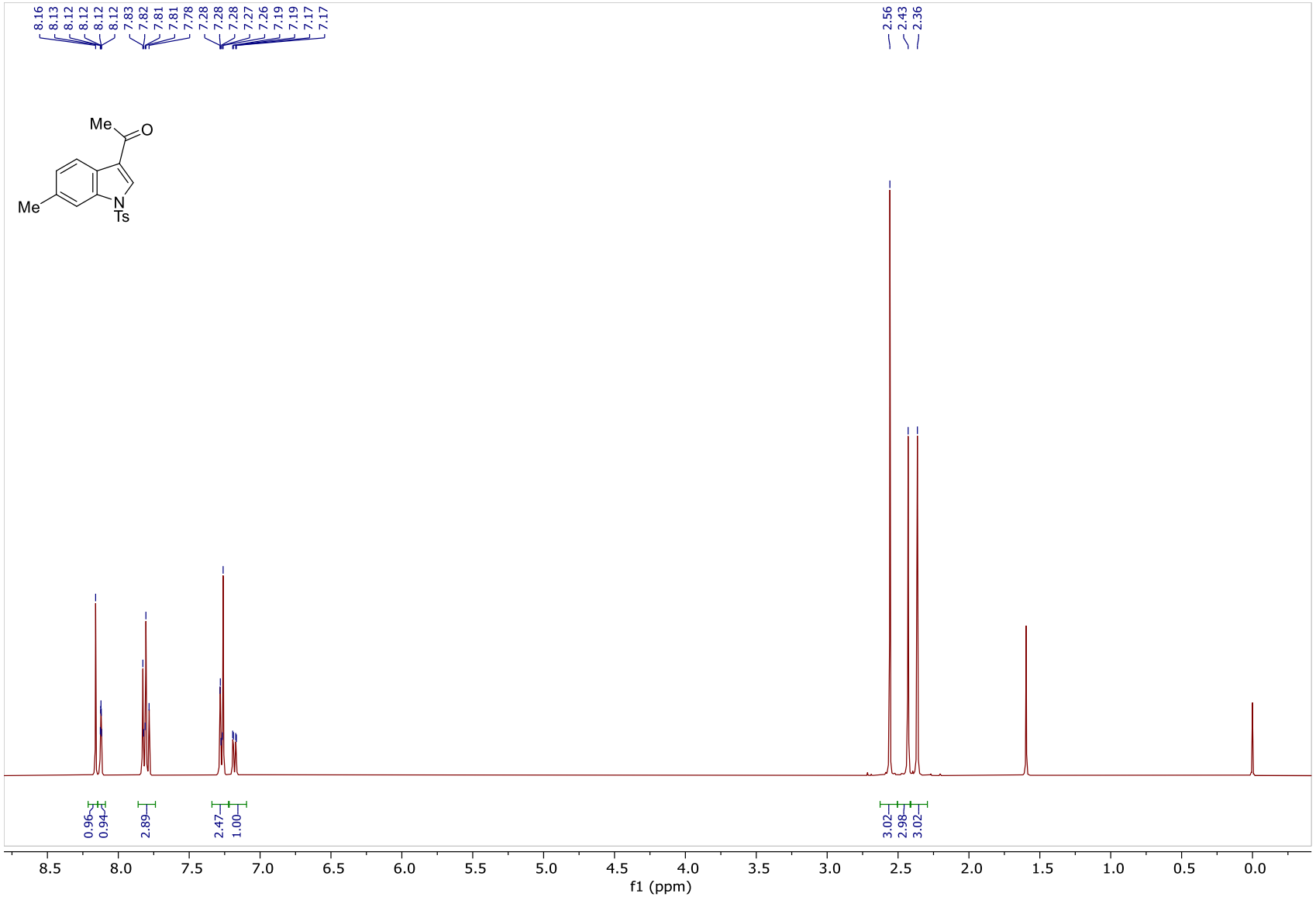

Figure 18: ^{1}H NMR Spectrum of **94e** (400MHz, $CDCl_3$)

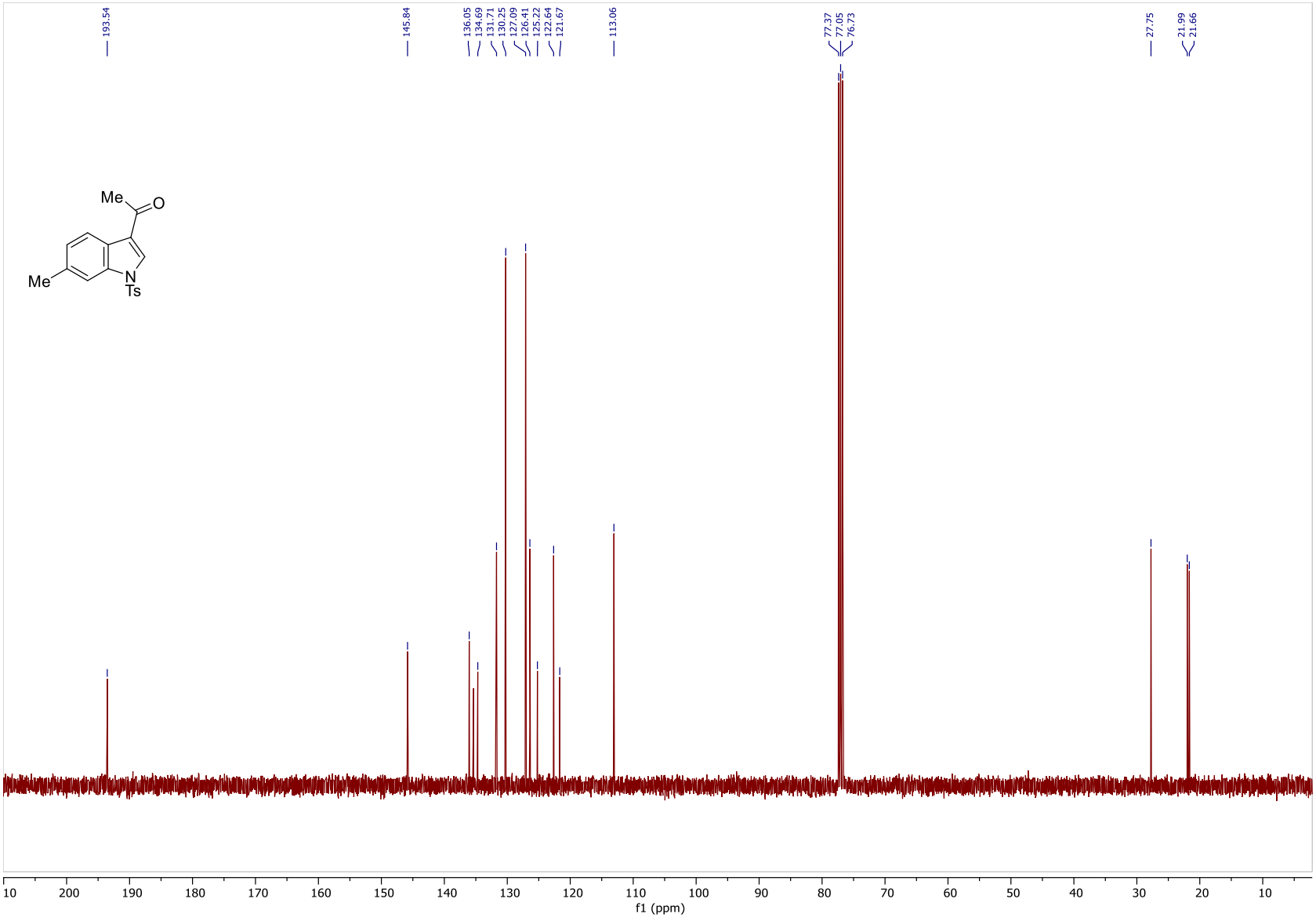

Figure 19: ^{13}C NMR Spectrum of **94e** (100MHz, $CDCl_3$)

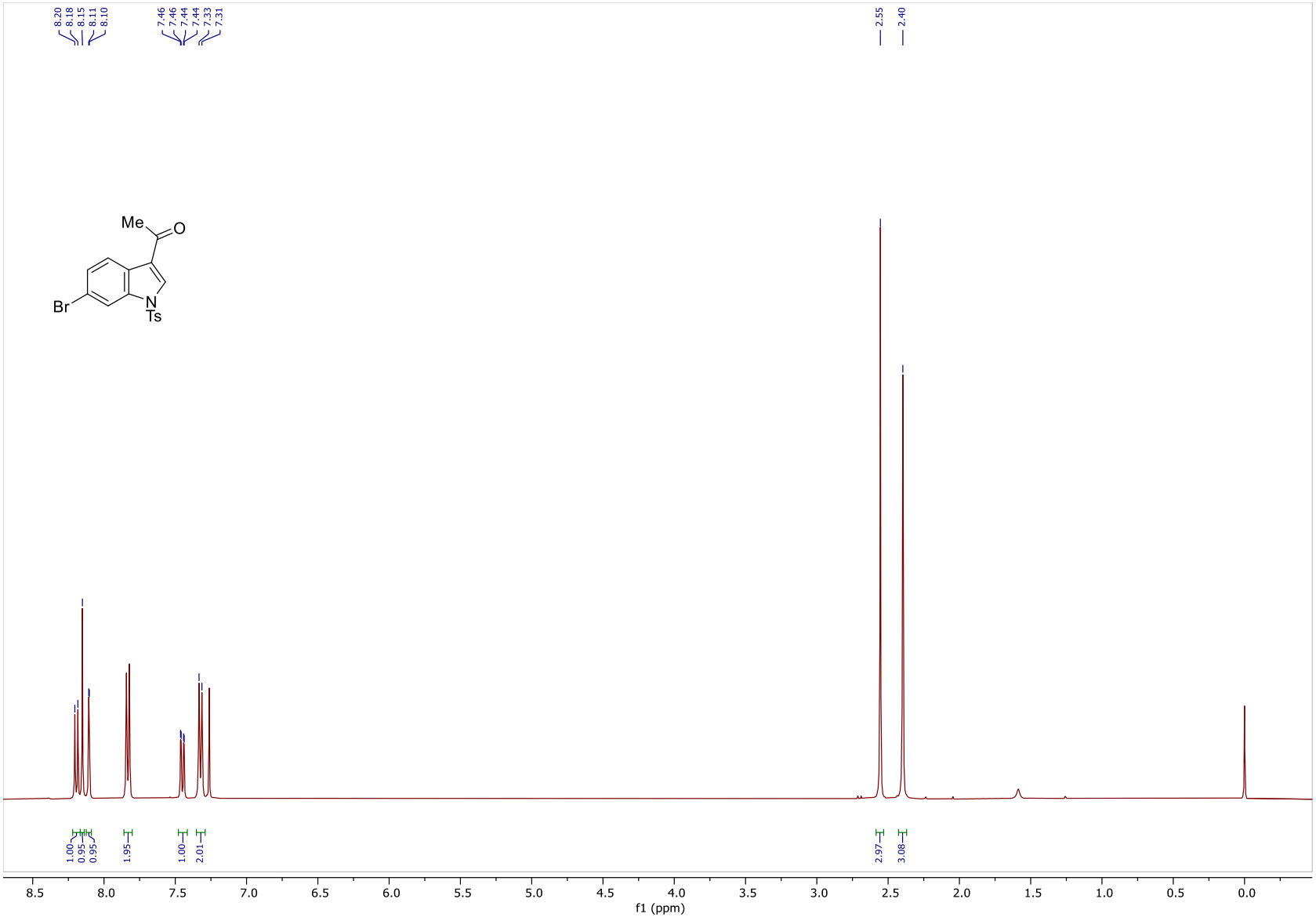

Figure 20: ^{1}H NMR Spectrum of **94f** (400MHz, $CDCl_3$)

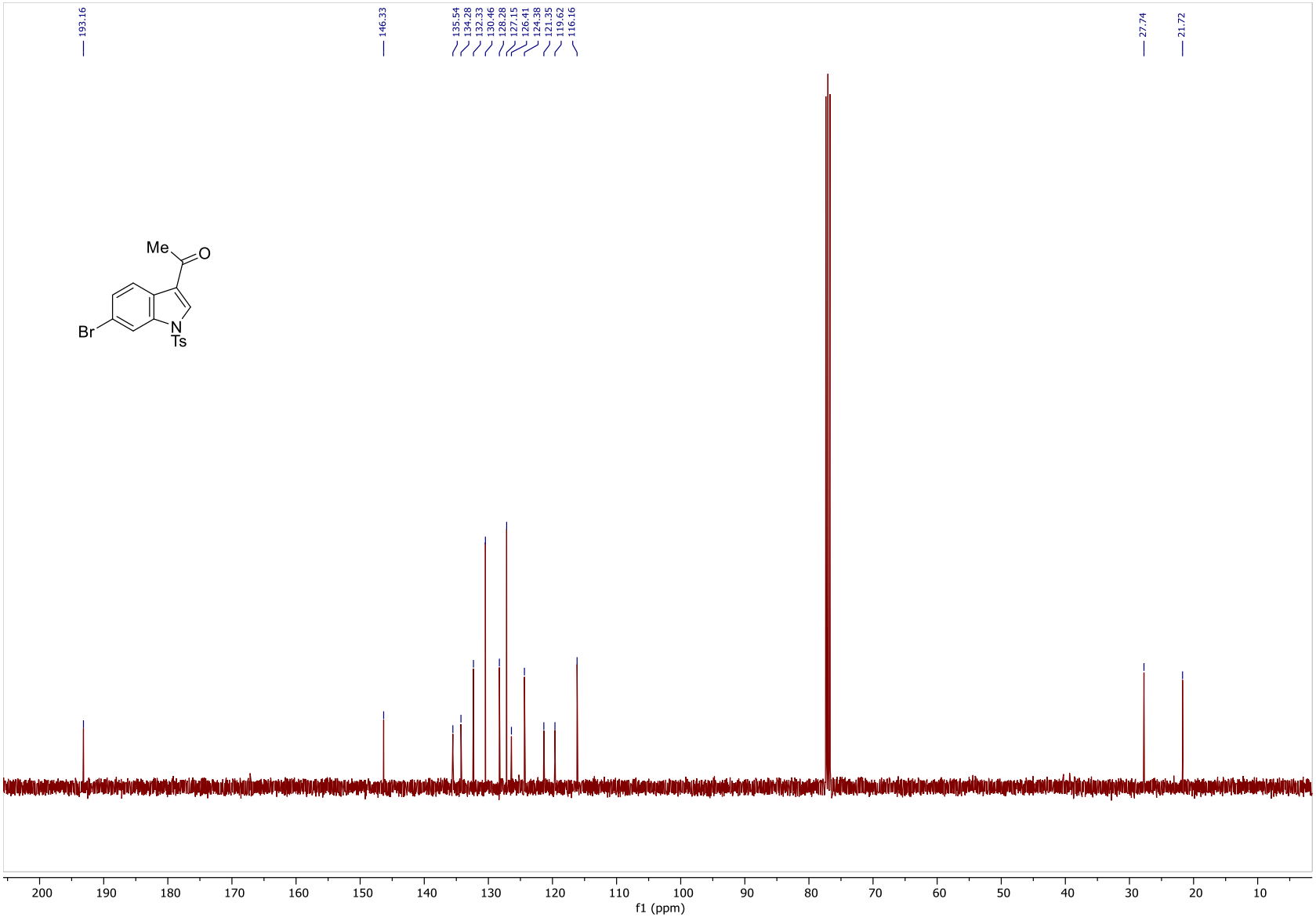

Figure 21: ^{13}C NMR Spectrum of **94f** (100MHz, $CDCl_3$)

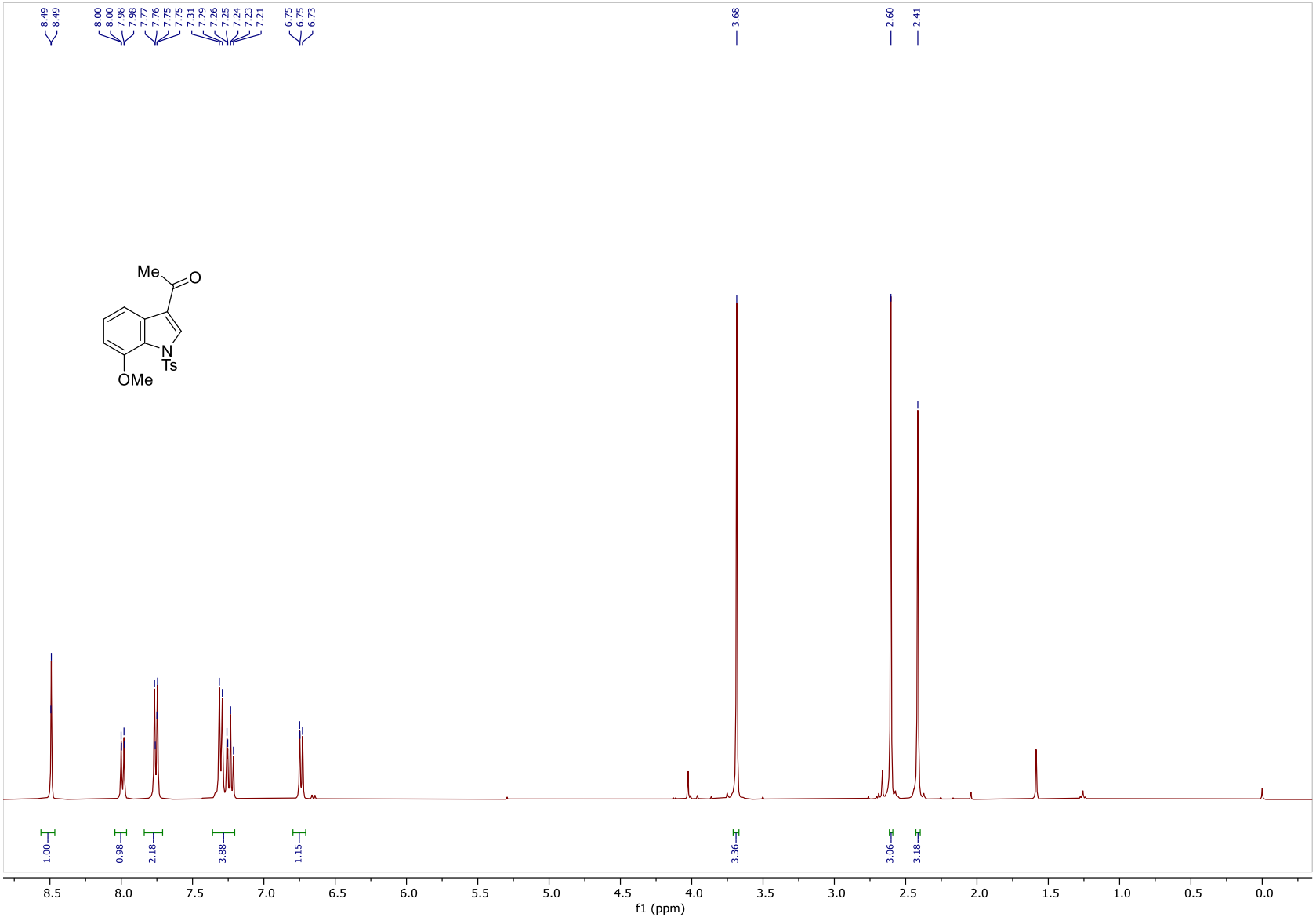

Figure 22: ^{1}H NMR Spectrum of **94g** (400MHz, $CDCl_3$)

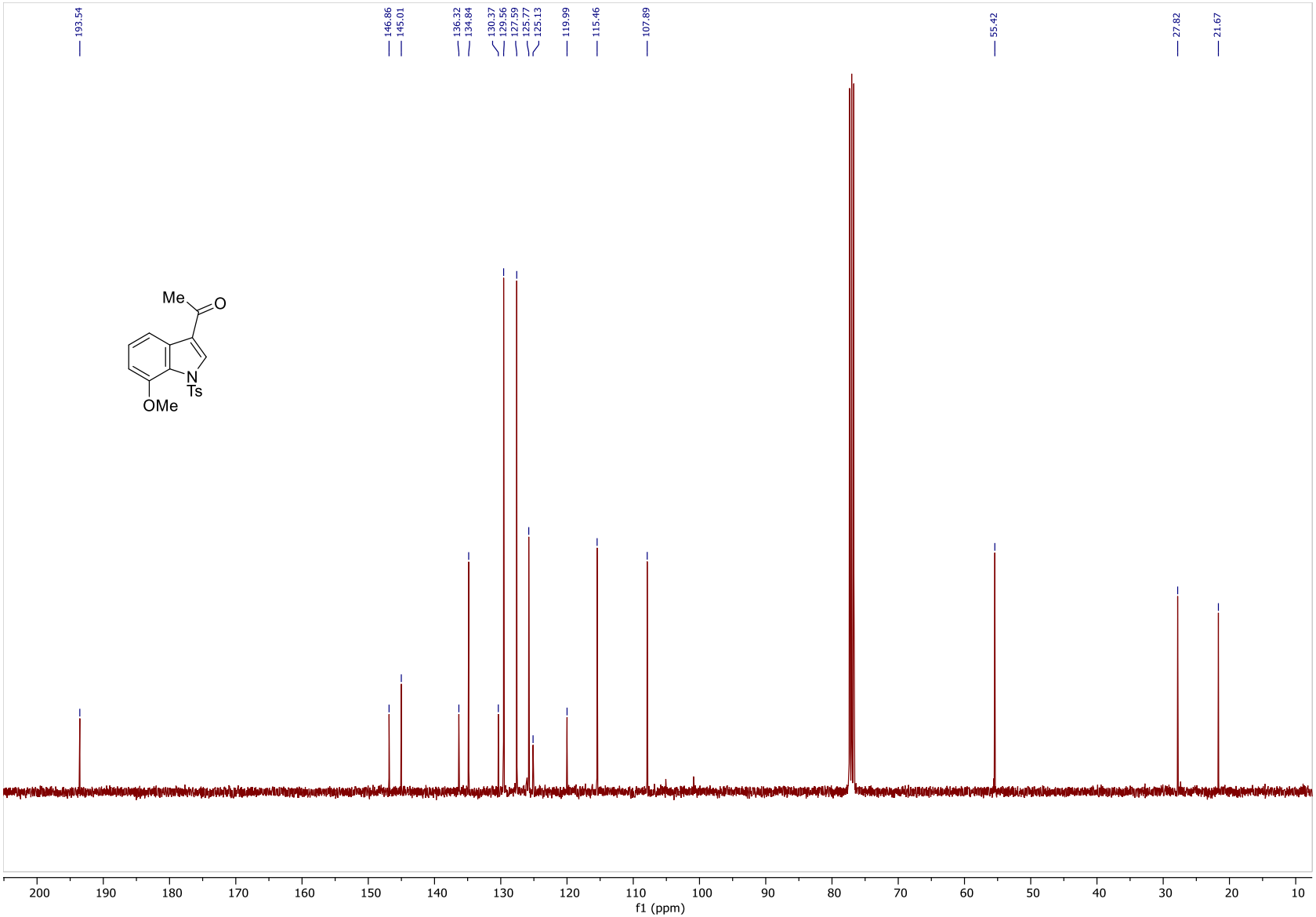

Figure 23: ^{13}C NMR Spectrum of **94g** (100MHz, $CDCl_3$)

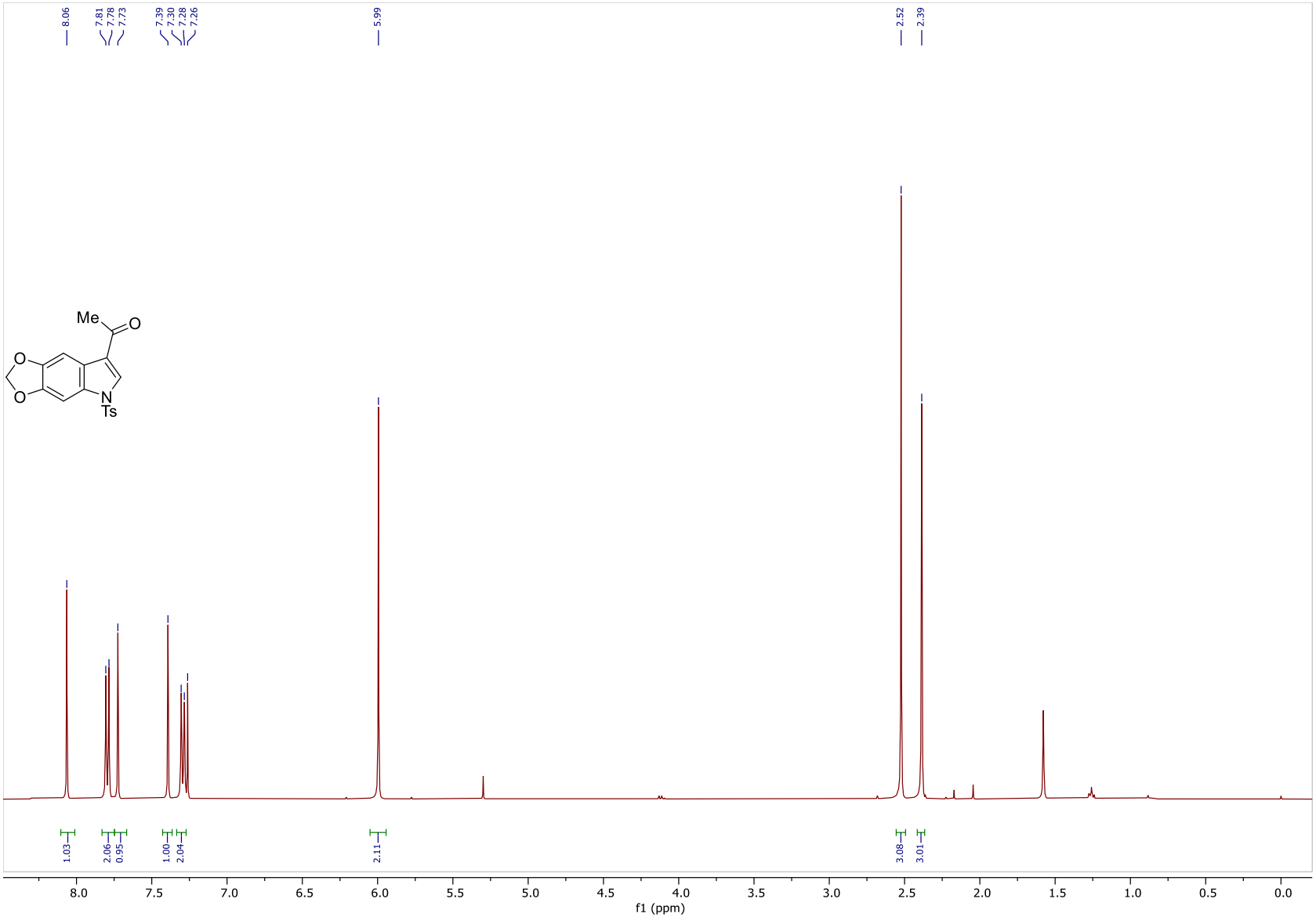

Figure 24: ^{1}H NMR Spectrum of **94h** (400MHz, $CDCl_3$)

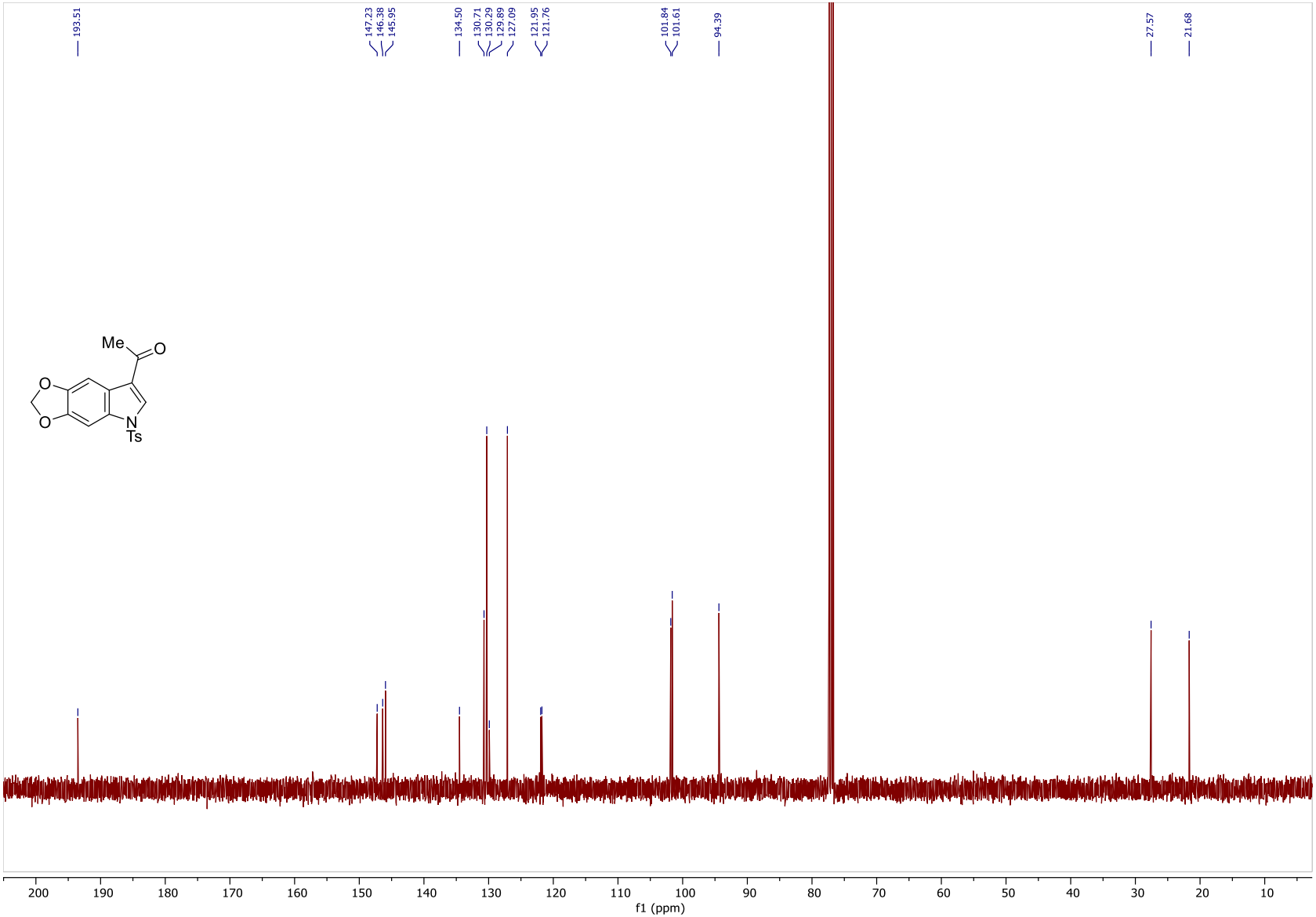

Figure 25: ^{13}C NMR Spectrum of **94h** (100MHz, $CDCl_3$)

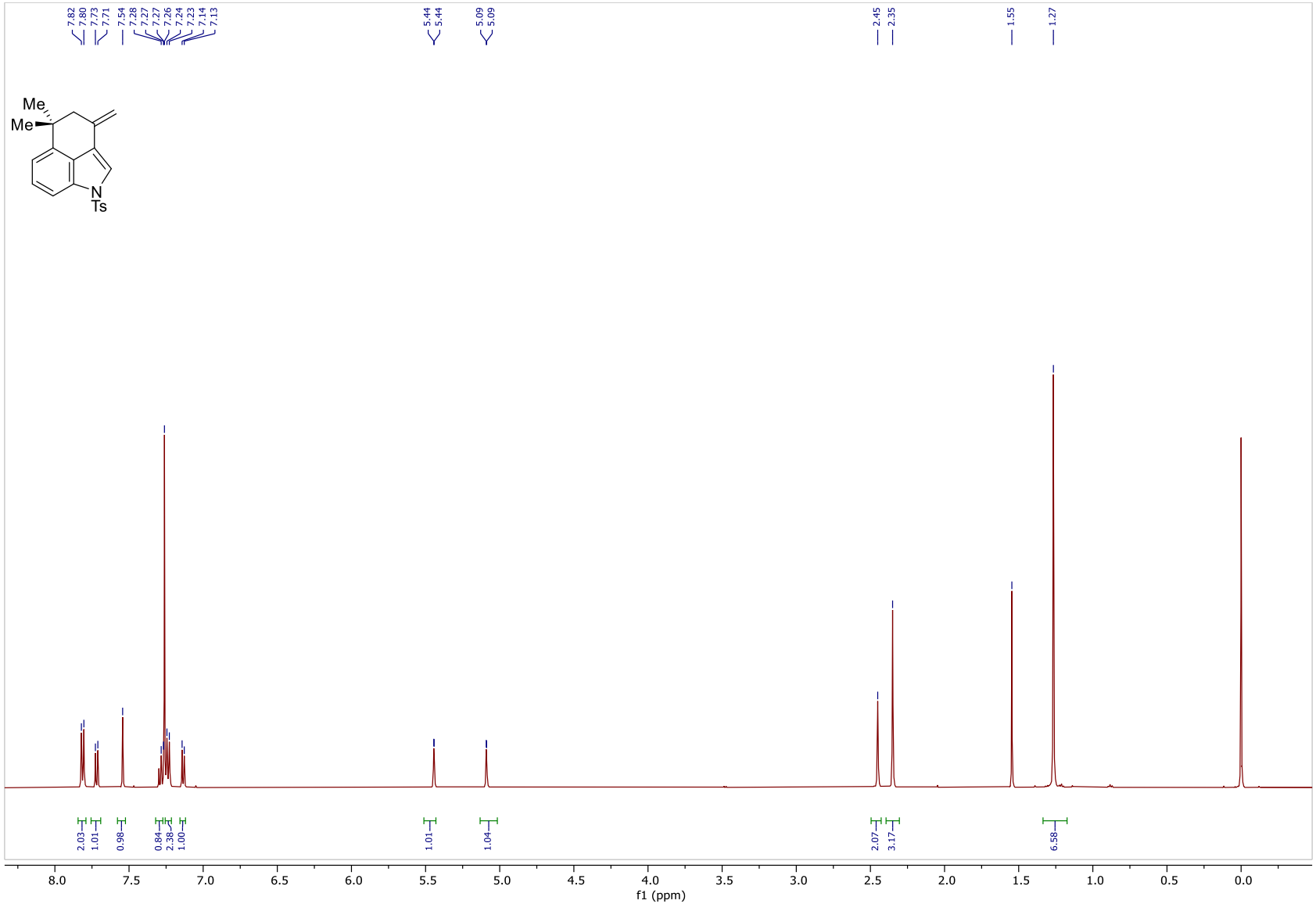

Figure 26: ^{1}H NMR Spectrum of **91** (500MHz, $CDCl_3$)

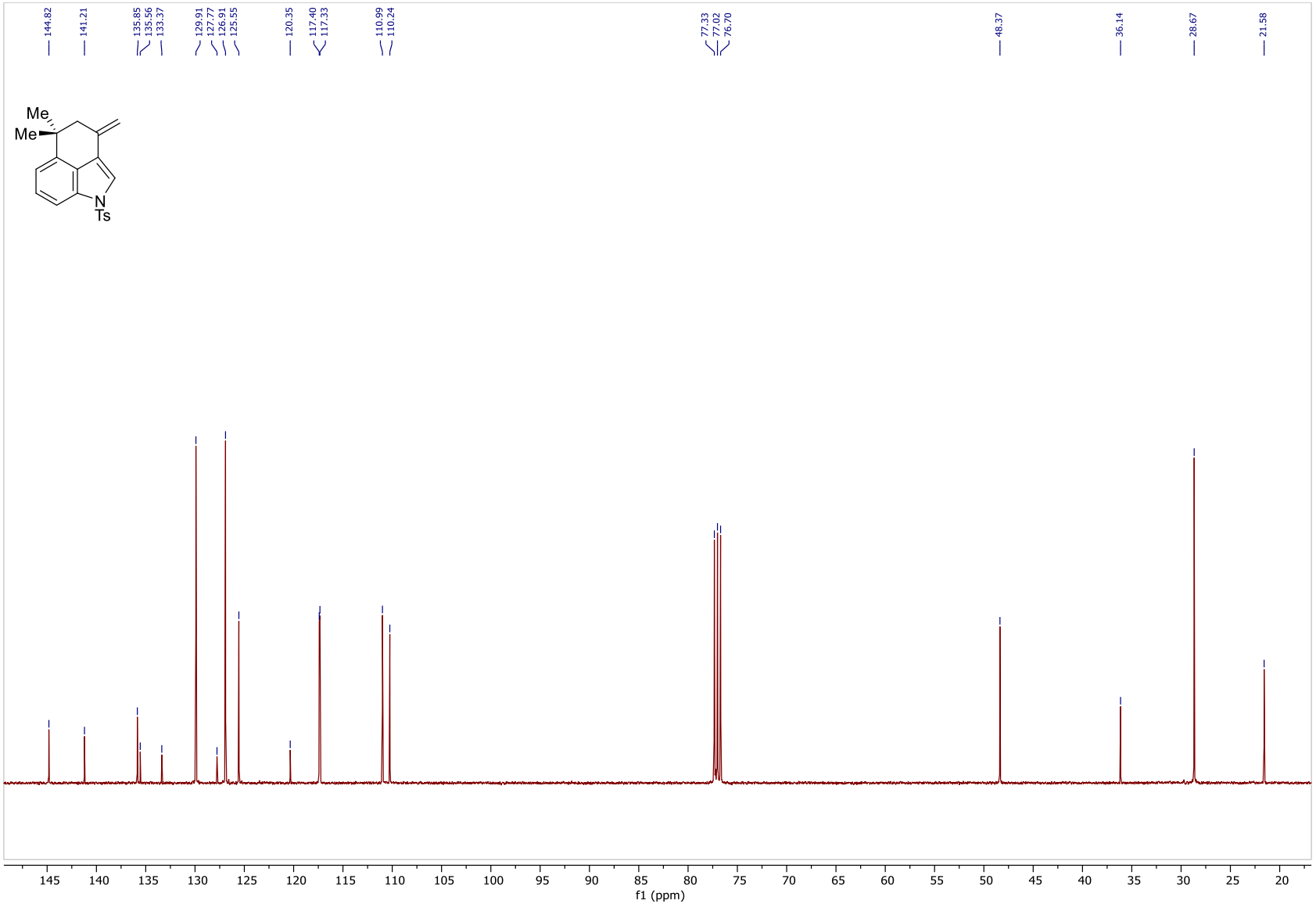

Figure 27: ^{13}C NMR Spectrum of **91** (100MHz, $CDCl_3$)

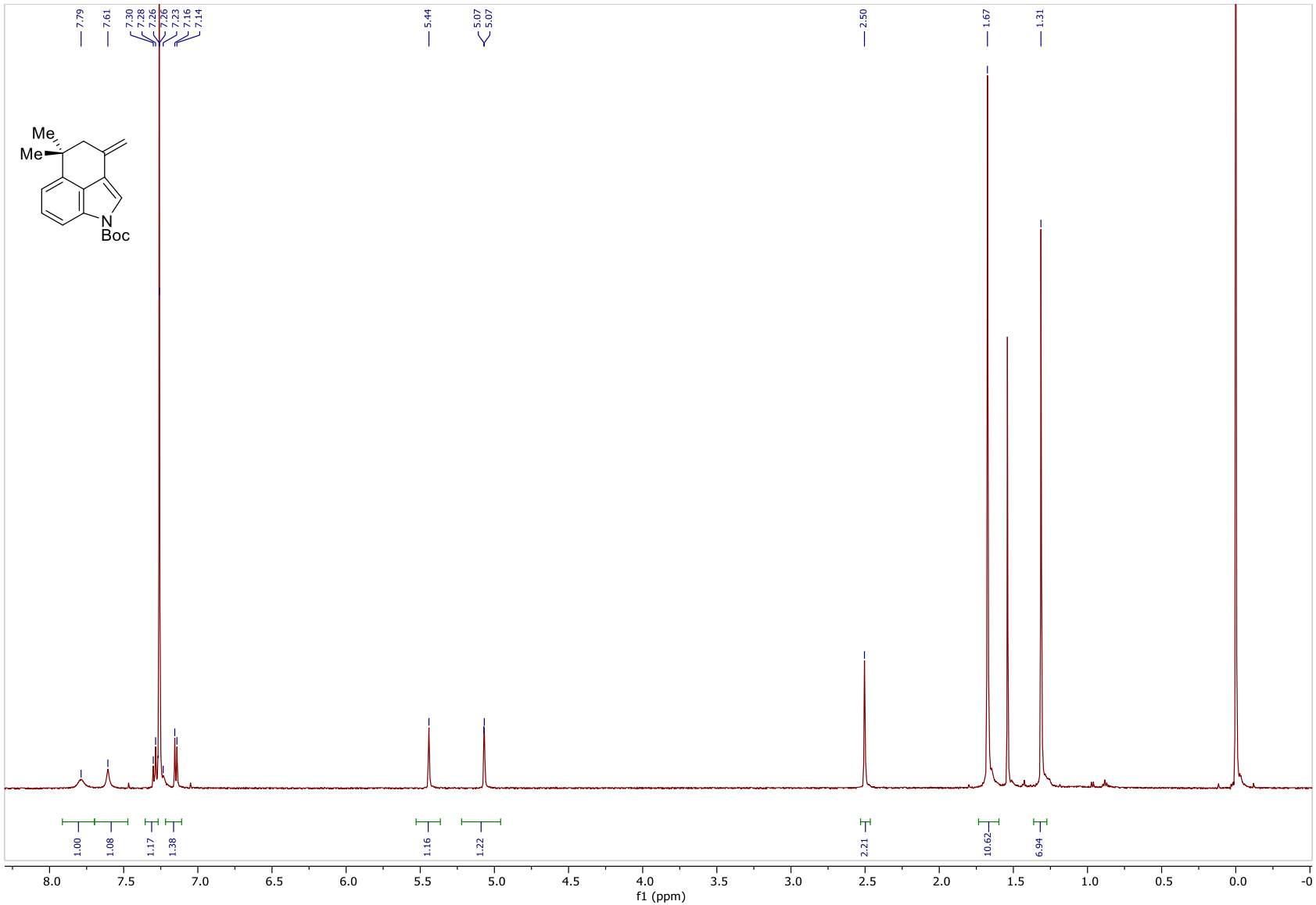

Figure 28: ^{1}H NMR Spectrum of **91b** (500MHz, $CDCl_3$)

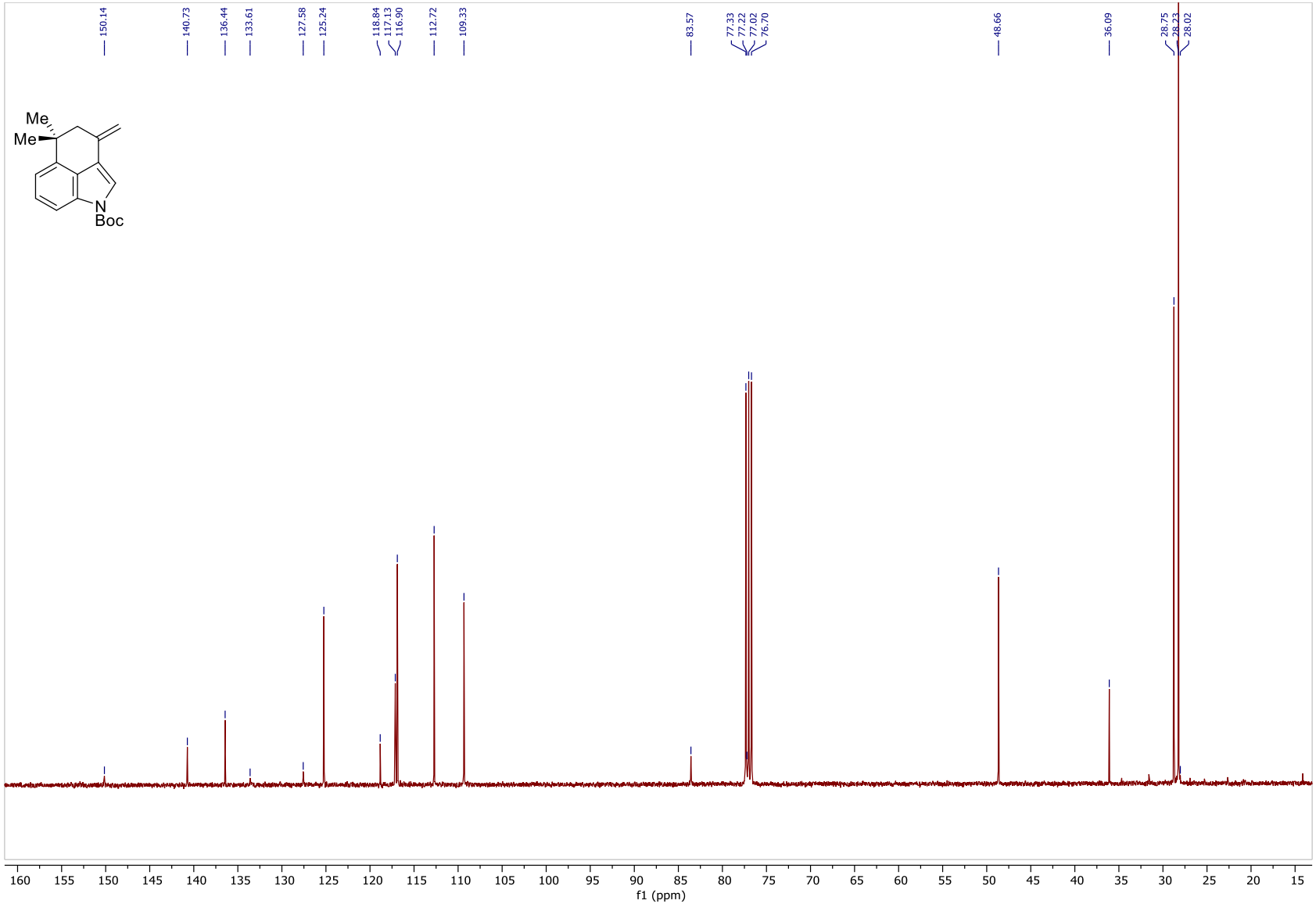

Figure 29: ^{13}C NMR Spectrum of **91b** (100MHz, $CDCl_3$)

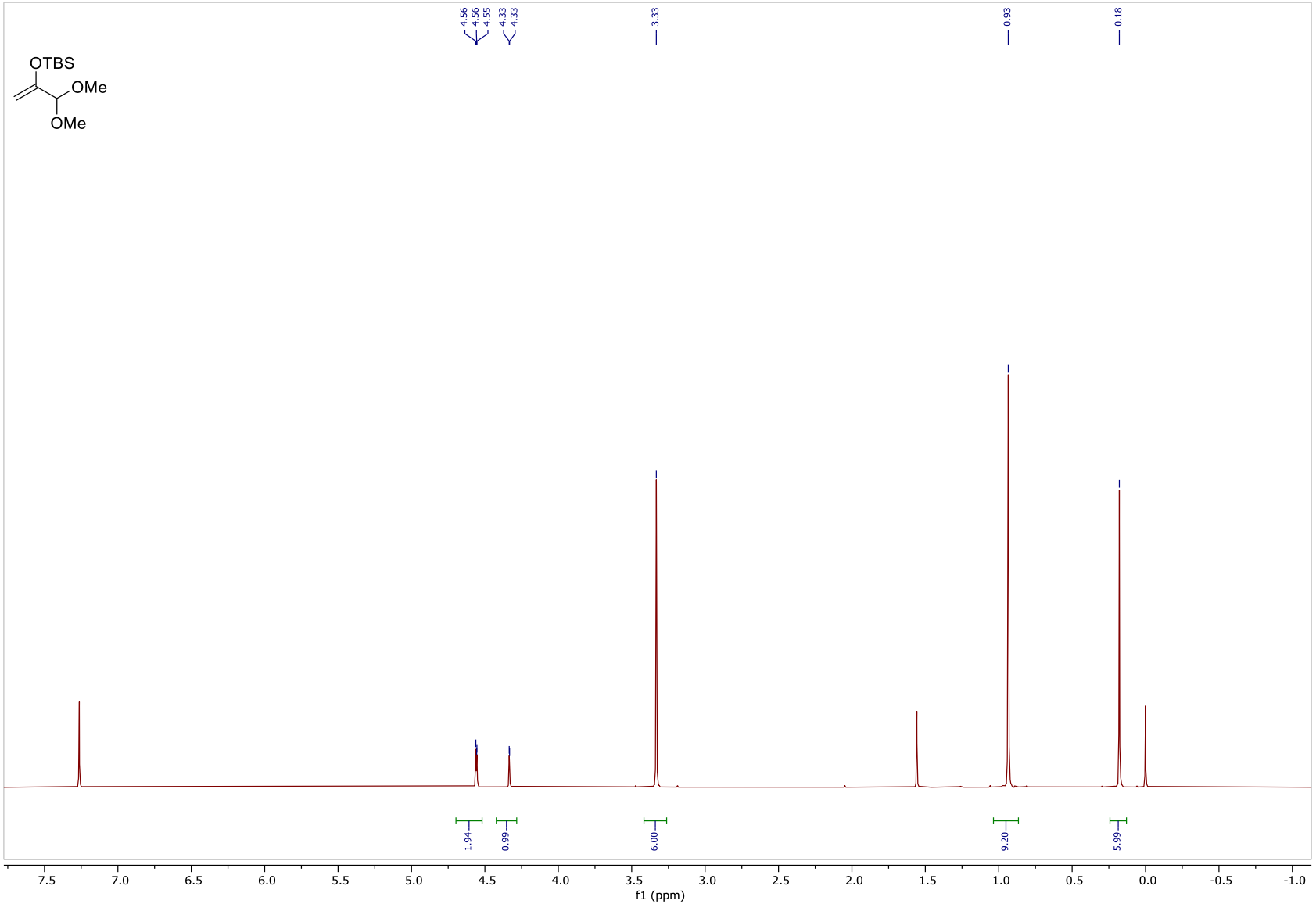

Figure 30: ^{1}H NMR Spectrum of **92** (500MHz, $CDCl_3$)

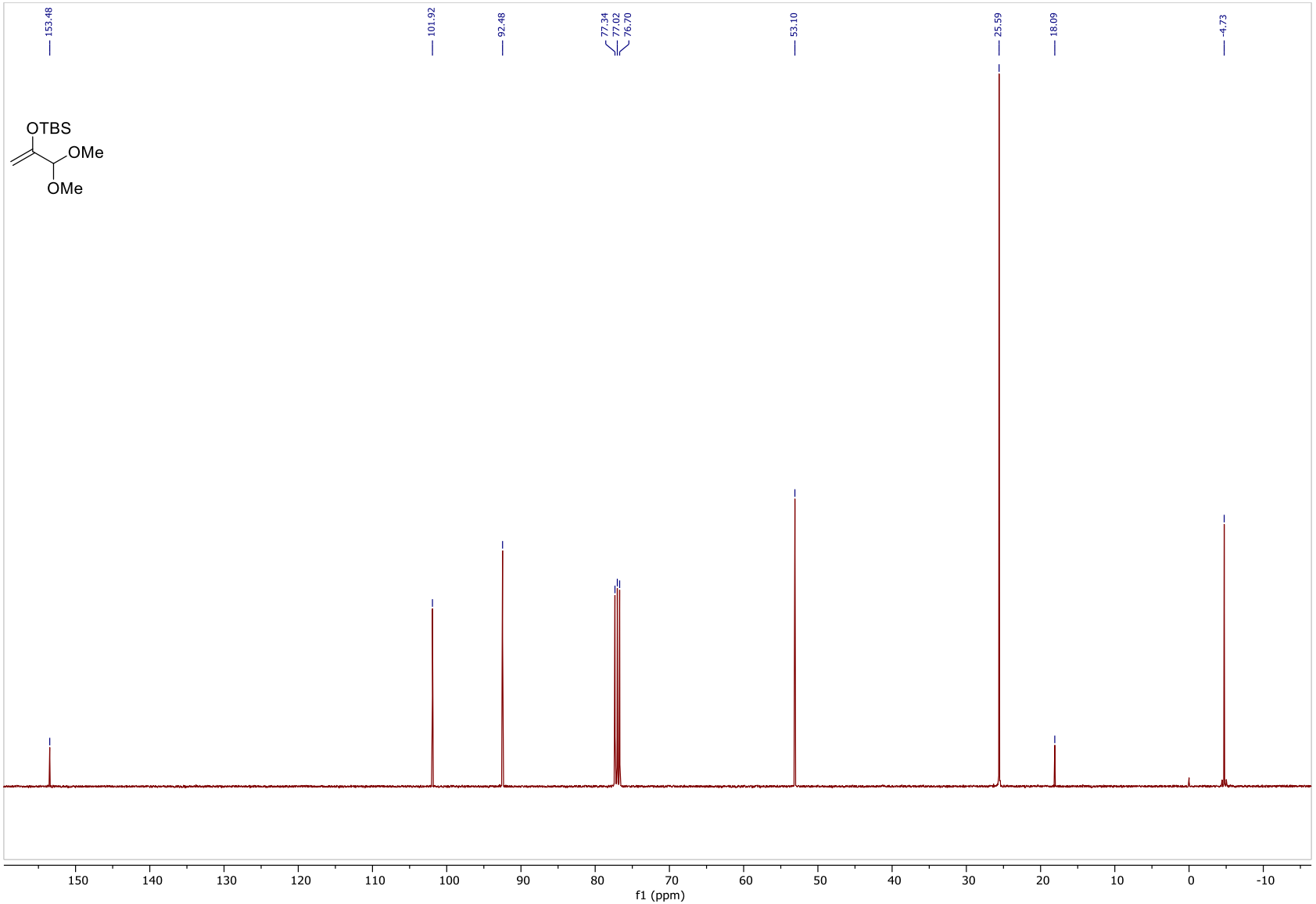

Figure 31: ^{13}C NMR Spectrum of **92** (100MHz, $CDCl_3$)

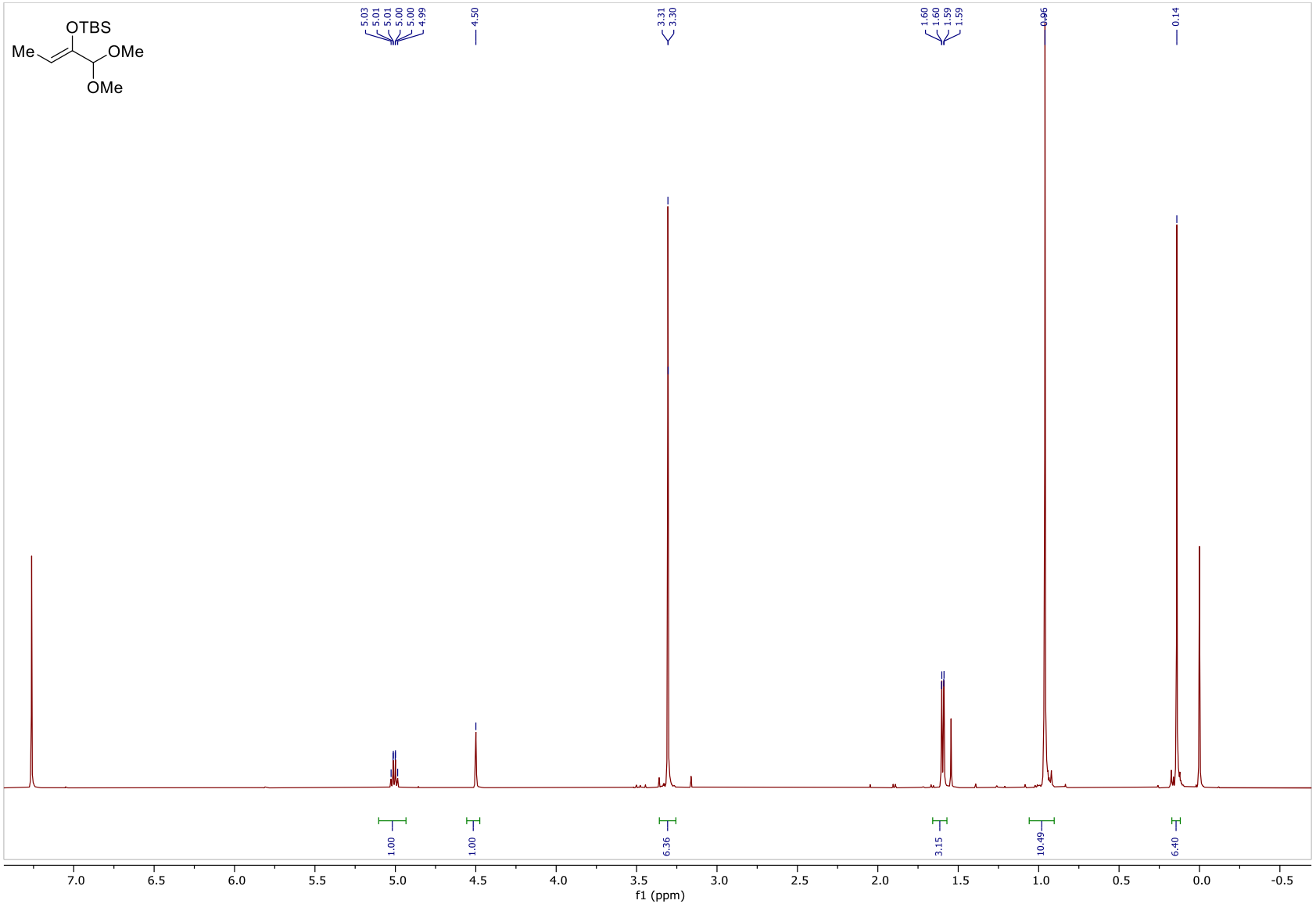

Figure 32: ^{1}H NMR Spectrum of **92b** (500MHz, $CDCl_3$)

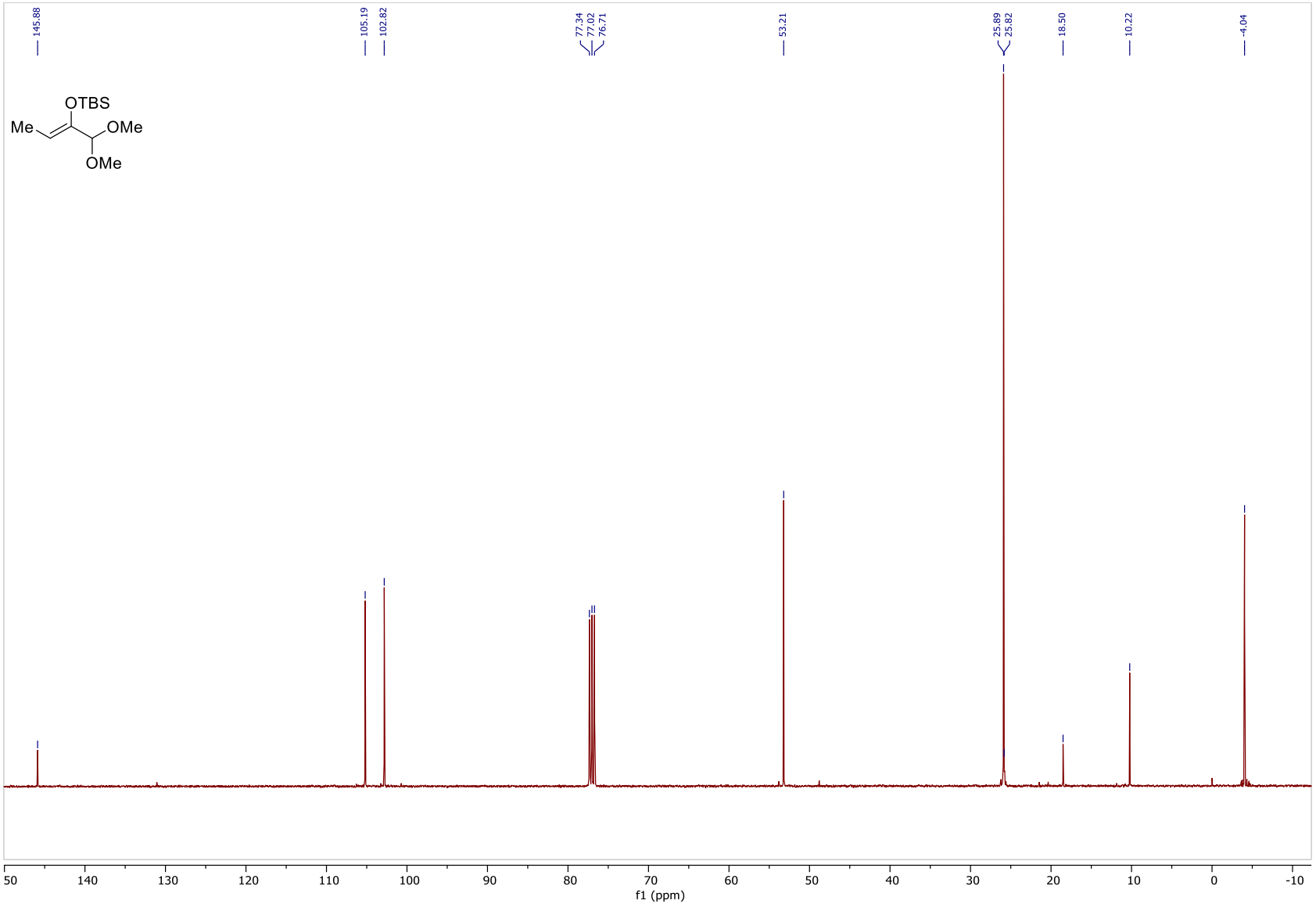

Figure 33: ^{13}C NMR Spectrum of **92b** (100MHz, $CDCl_3$)

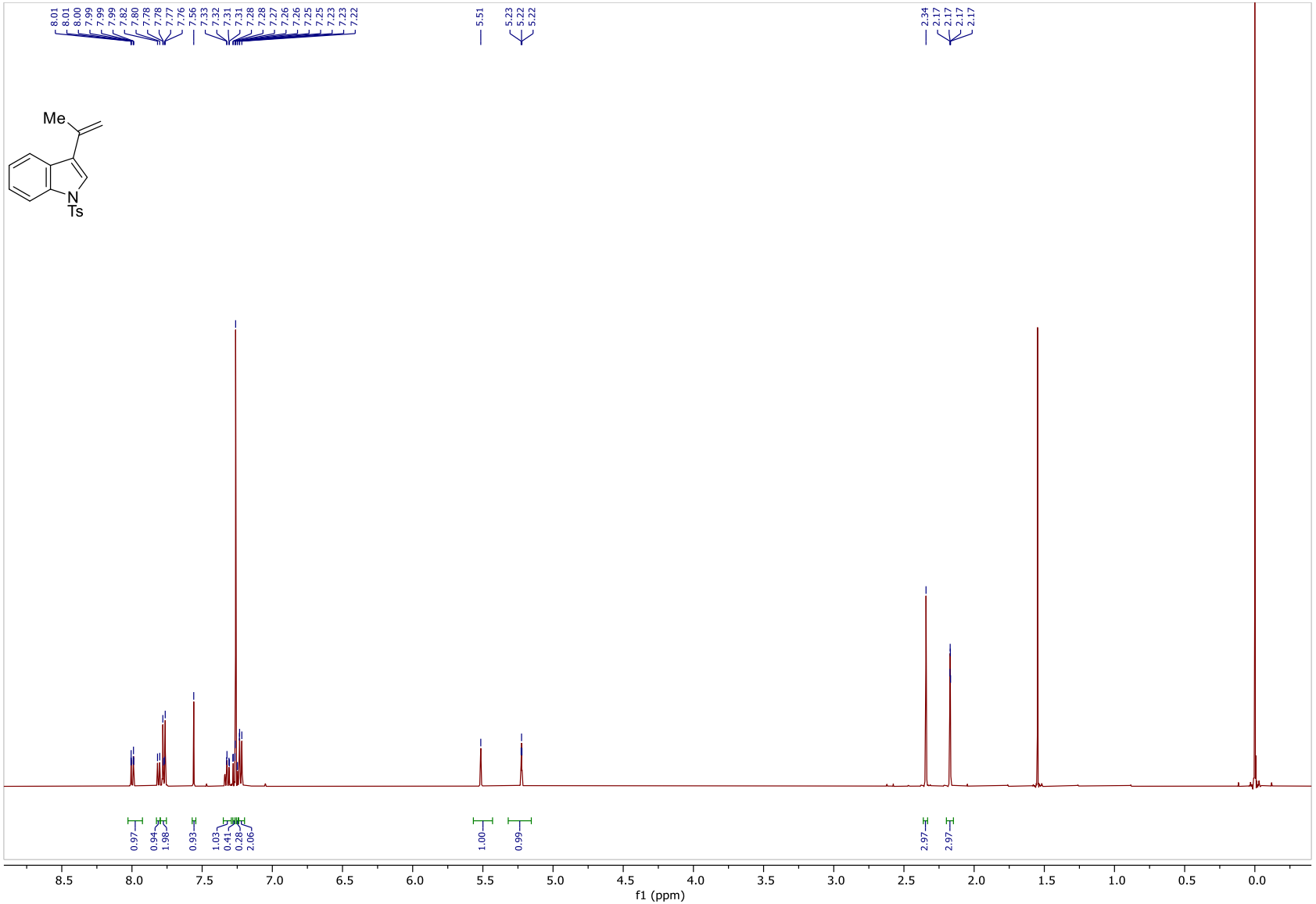

Figure 34: ^{1}H NMR Spectrum of **95a** (500MHz, $CDCl_3$)

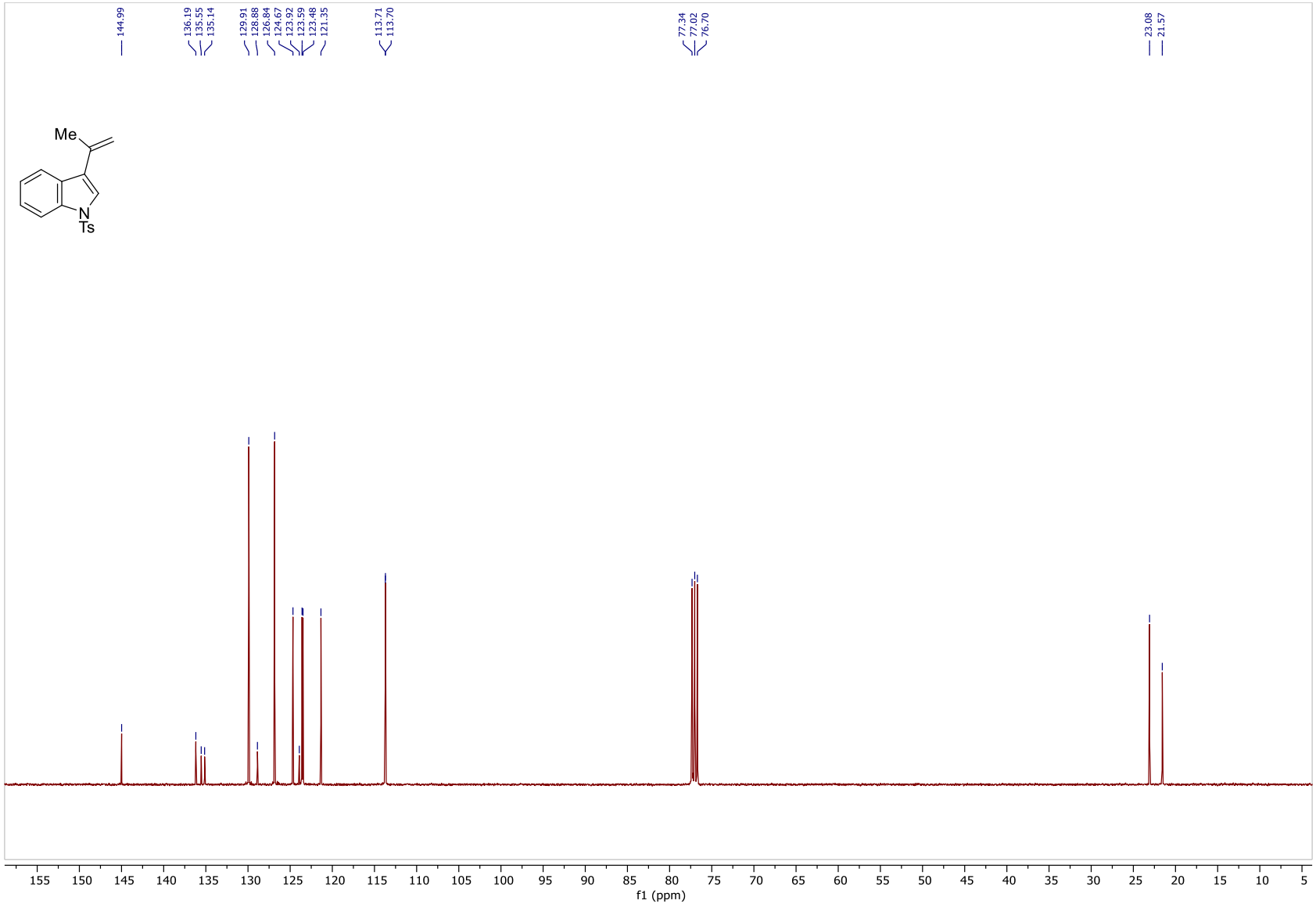

Figure 35: ^{13}C NMR Spectrum of **95a** (100MHz, $CDCl_3$)

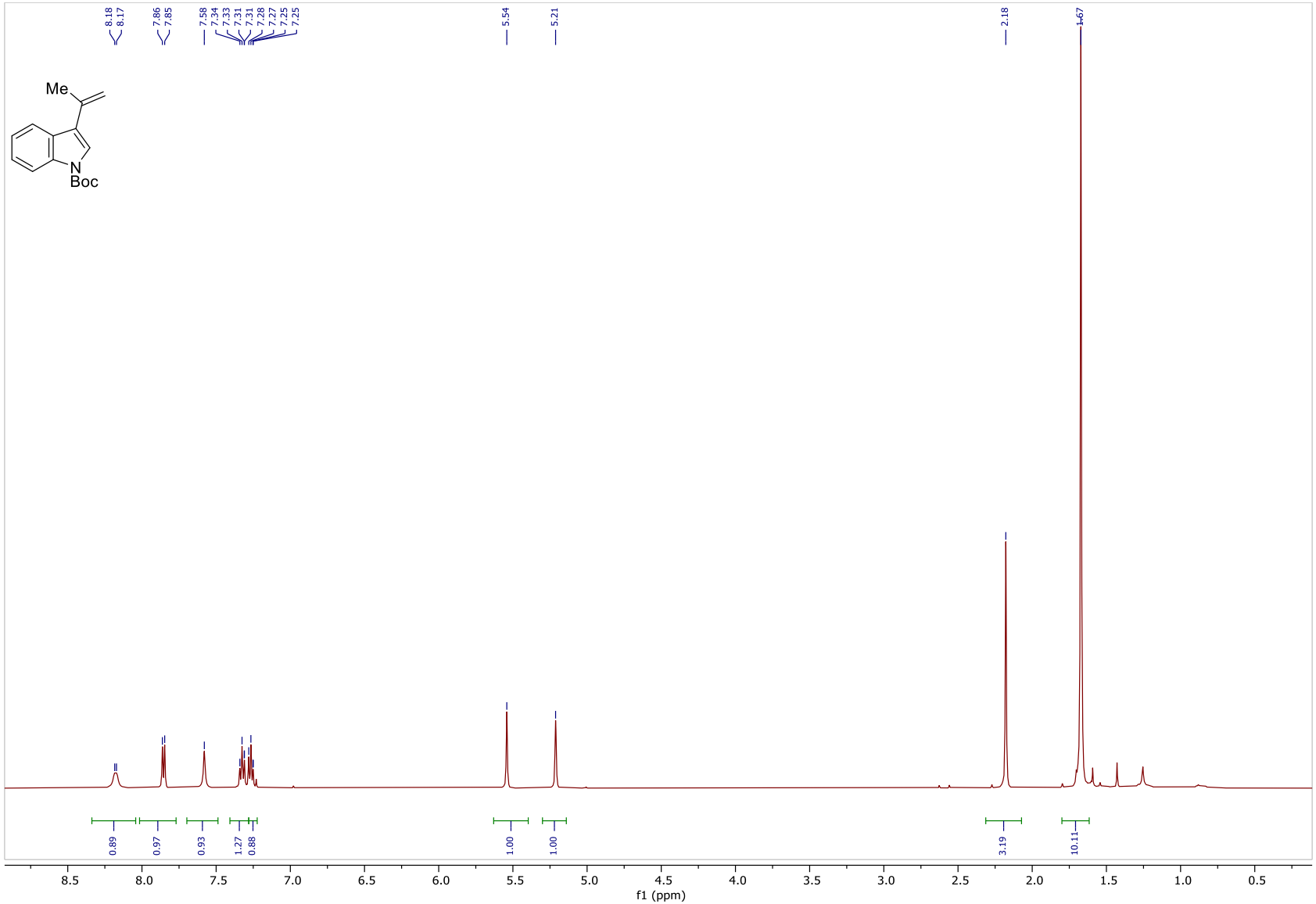

Figure 36: ^{1}H NMR Spectrum of **95b** (500MHz, $CDCl_3$)

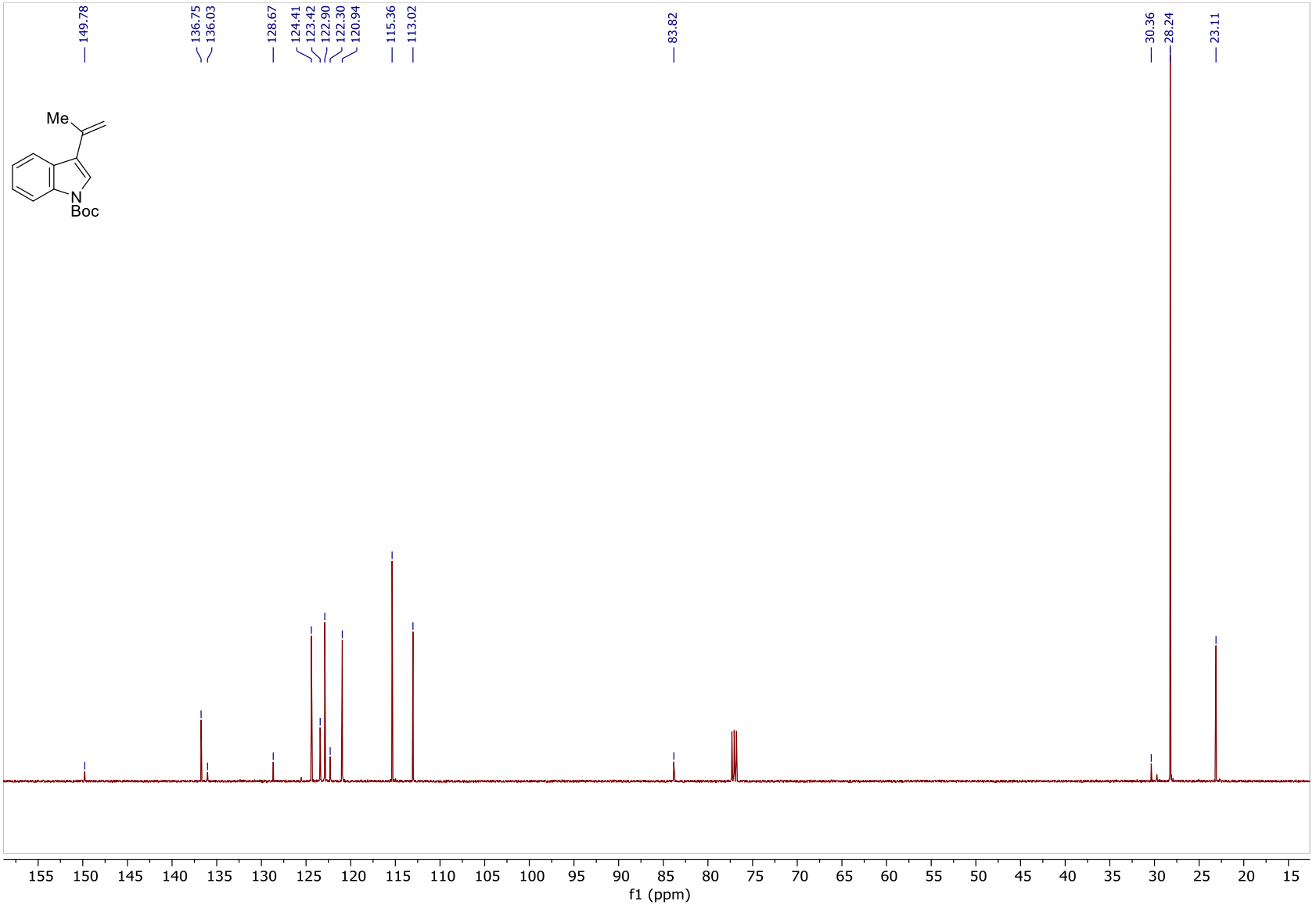

Figure 37: ^{13}C NMR Spectrum of **95b** (100MHz, $CDCl_3$)

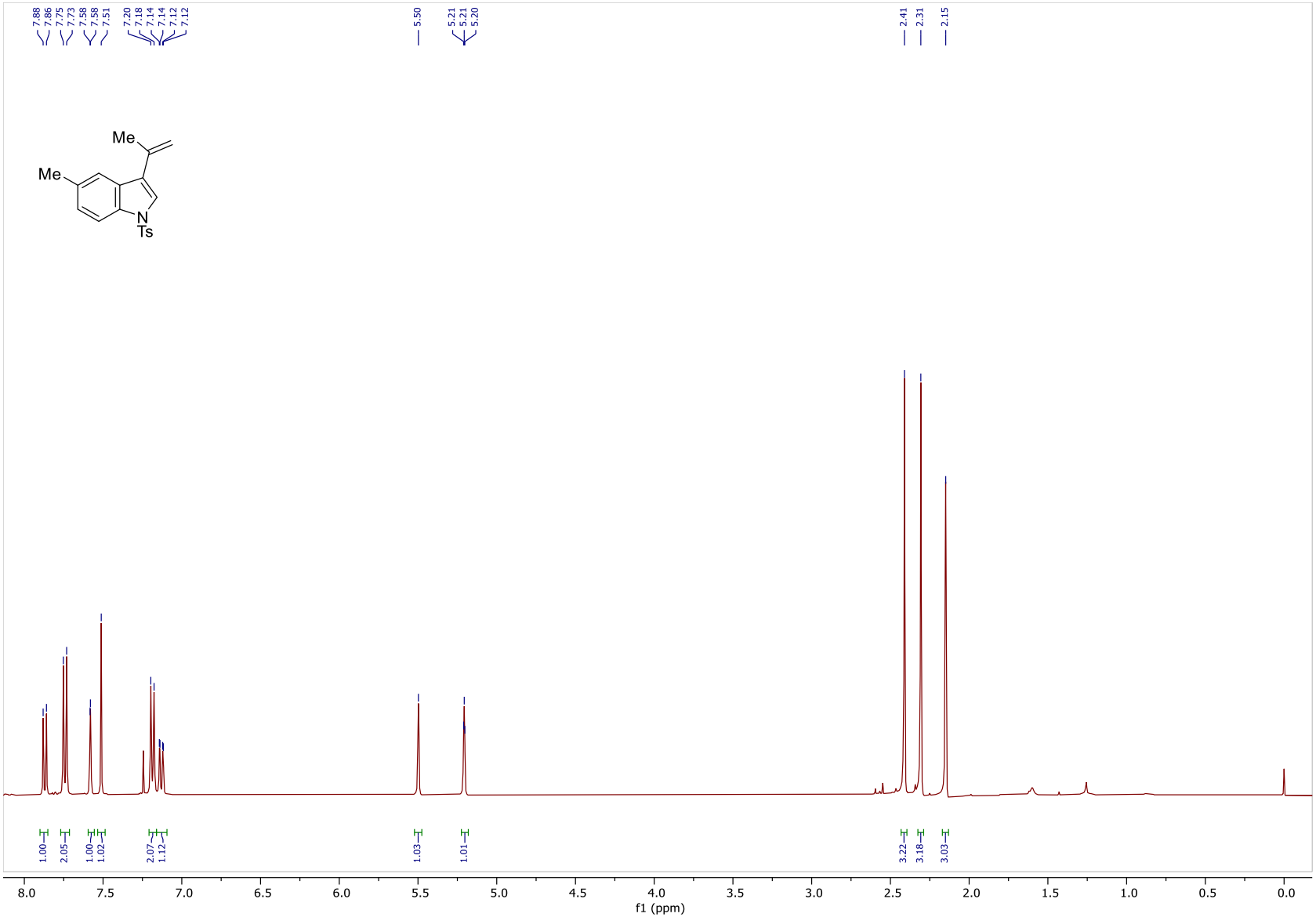

Figure 38: ^{1}H NMR Spectrum of **95c** (400MHz, $CDCl_3$)

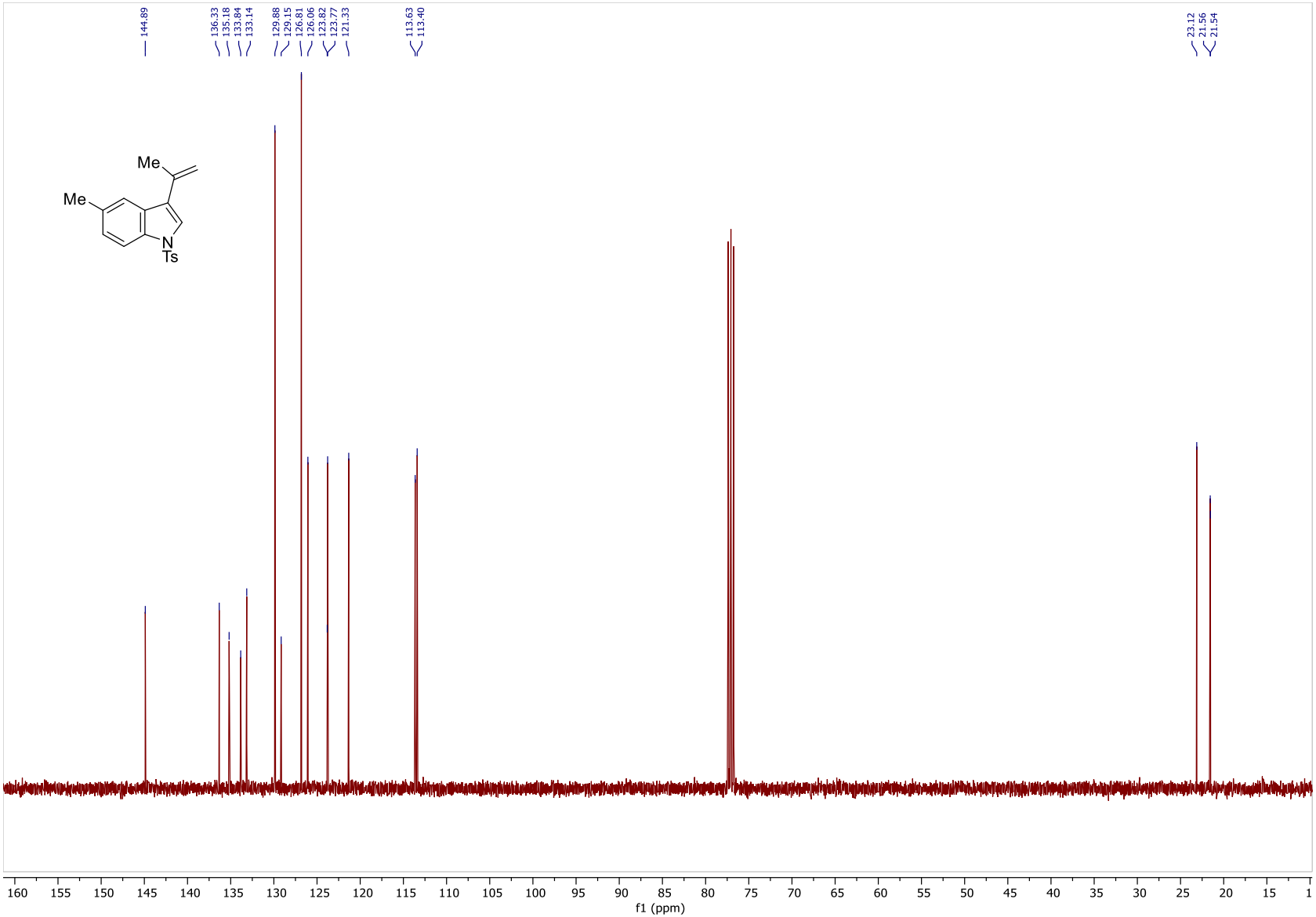

Figure 39: ^{13}C NMR Spectrum of **95c** (100MHz, $CDCl_3$)

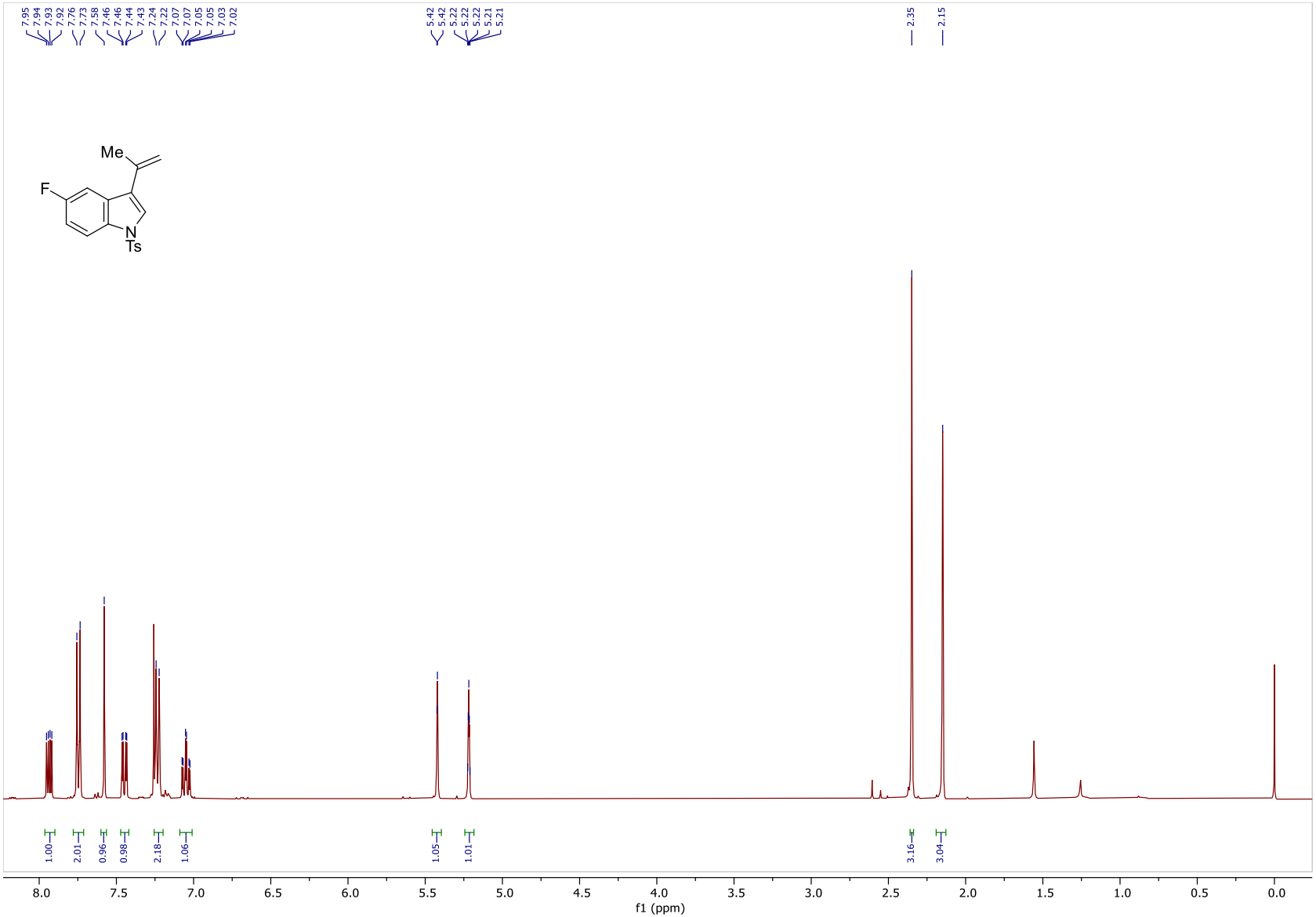

Figure 40: ^{1}H NMR Spectrum of **95d** (400MHz, $CDCl_3$)

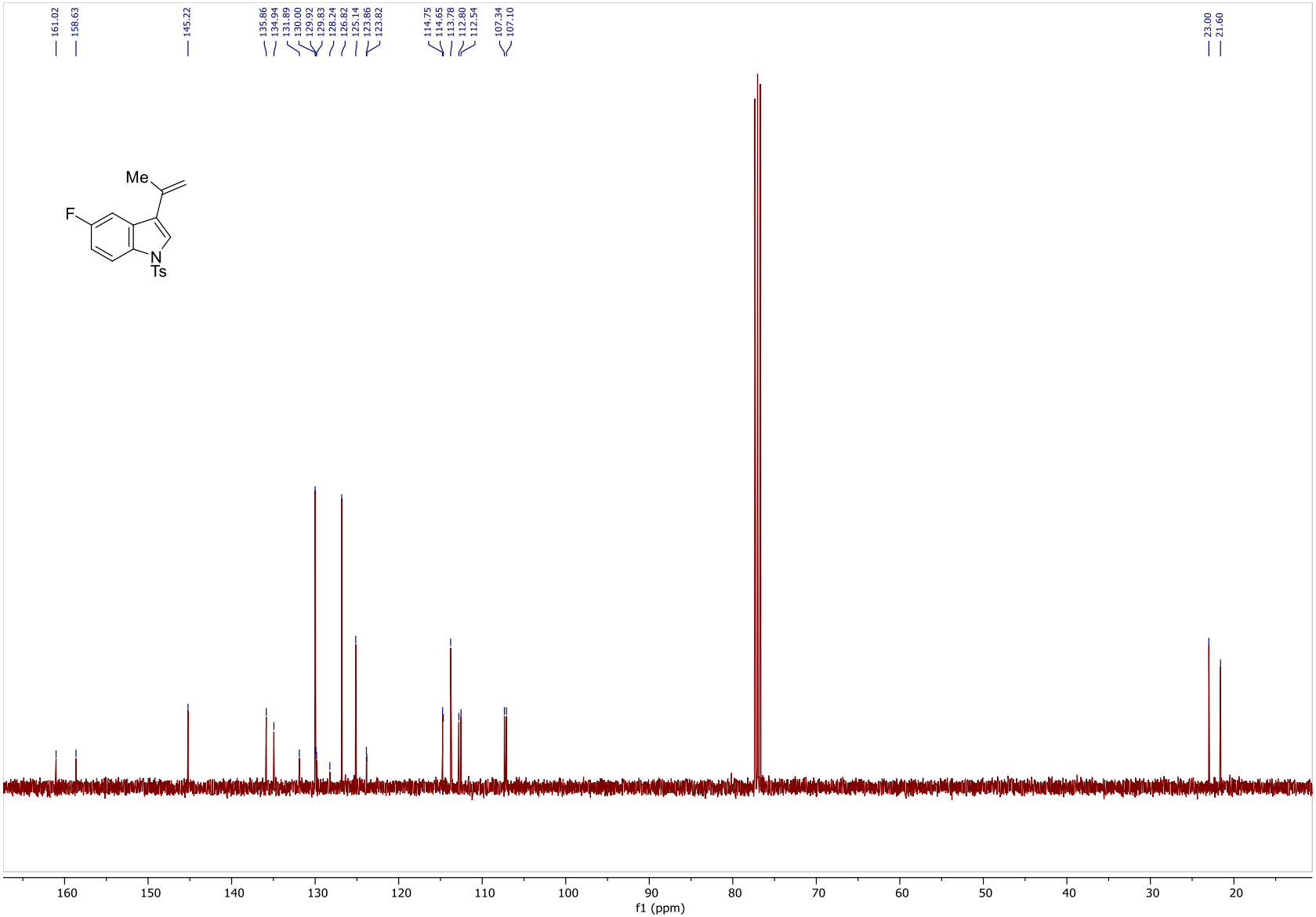

Figure 41: ^{13}C NMR Spectrum of **95d** (100MHz, $CDCl_3$)

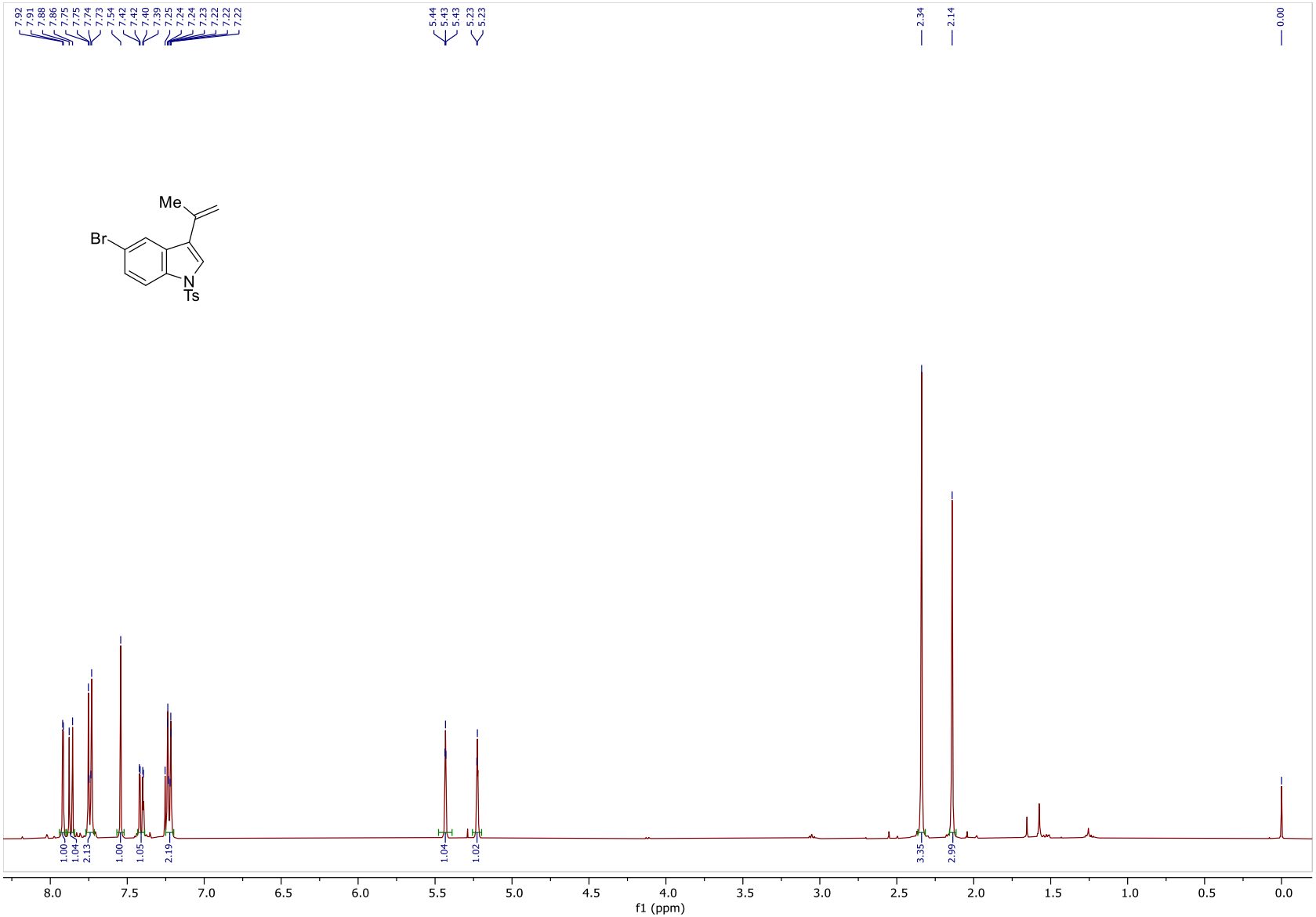

Figure 42: ^{1}H NMR Spectrum of **95e** (400MHz, $CDCl_3$)

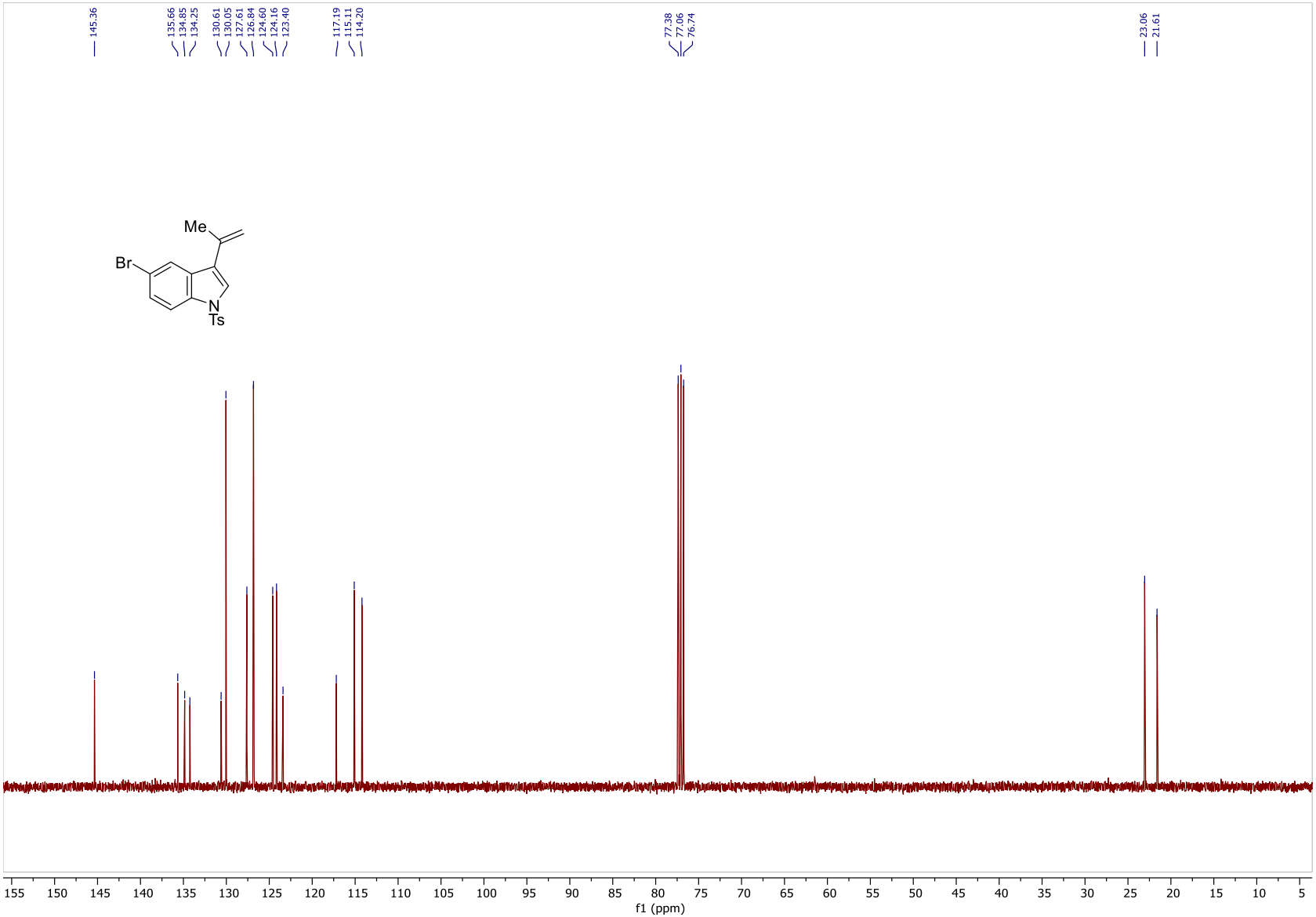

Figure 43: ^{13}C NMR Spectrum of **95e** (100MHz, $CDCl_3$)

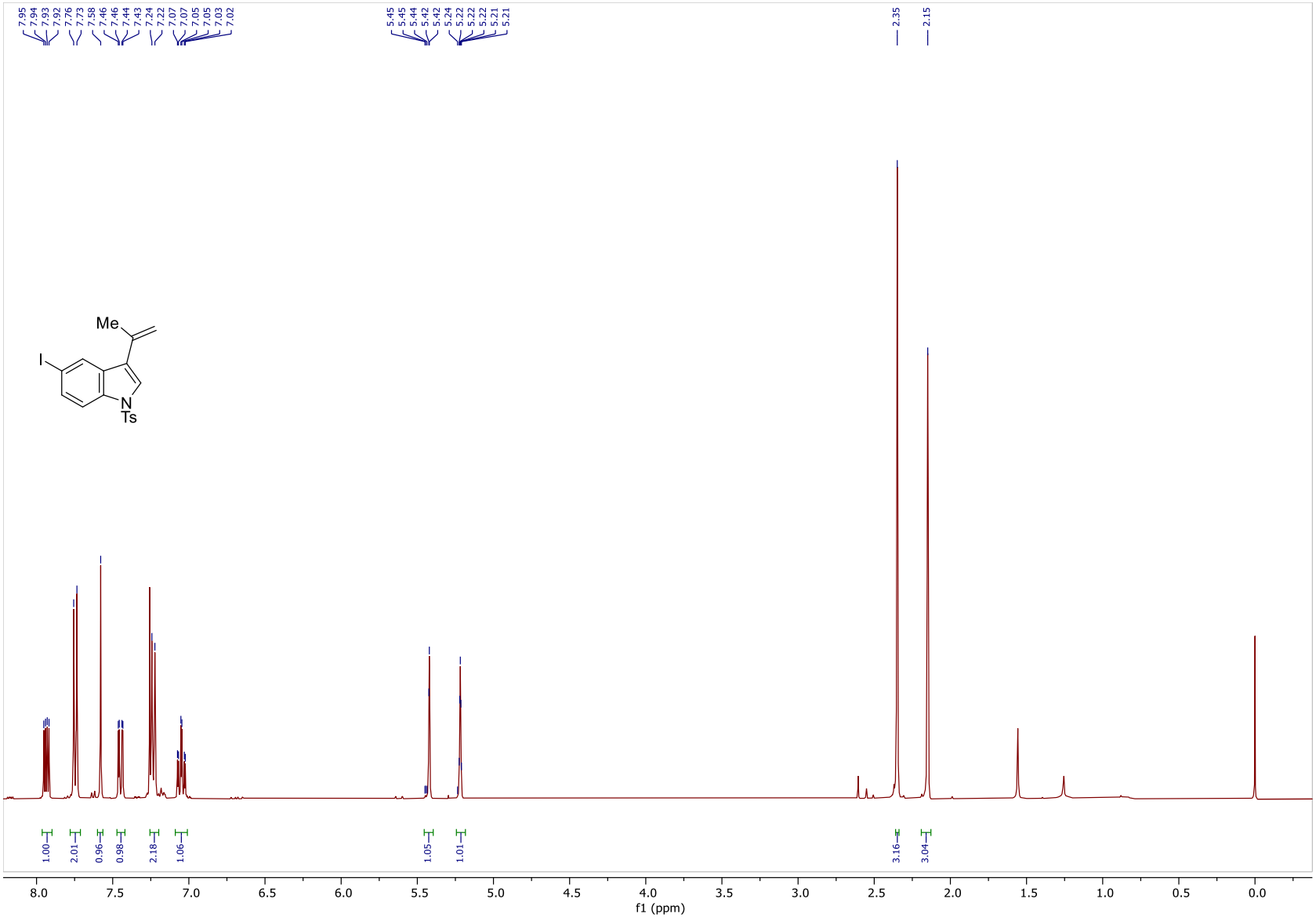

Figure 44: ^{1}H NMR Spectrum of **95f** (400MHz, $CDCl_3$)

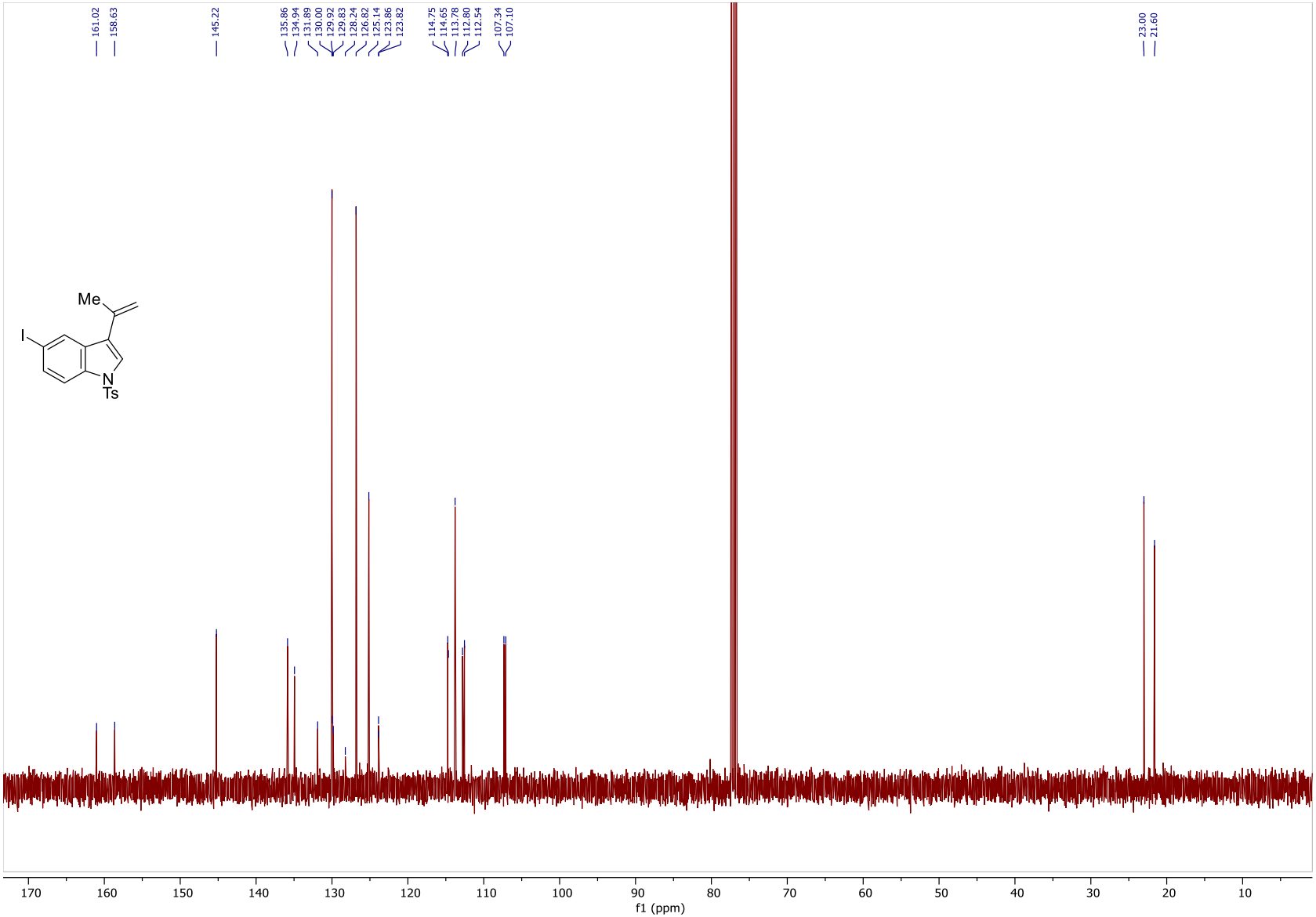

Figure 45: ^{13}C NMR Spectrum of **95f** (100MHz, $CDCl_3$)

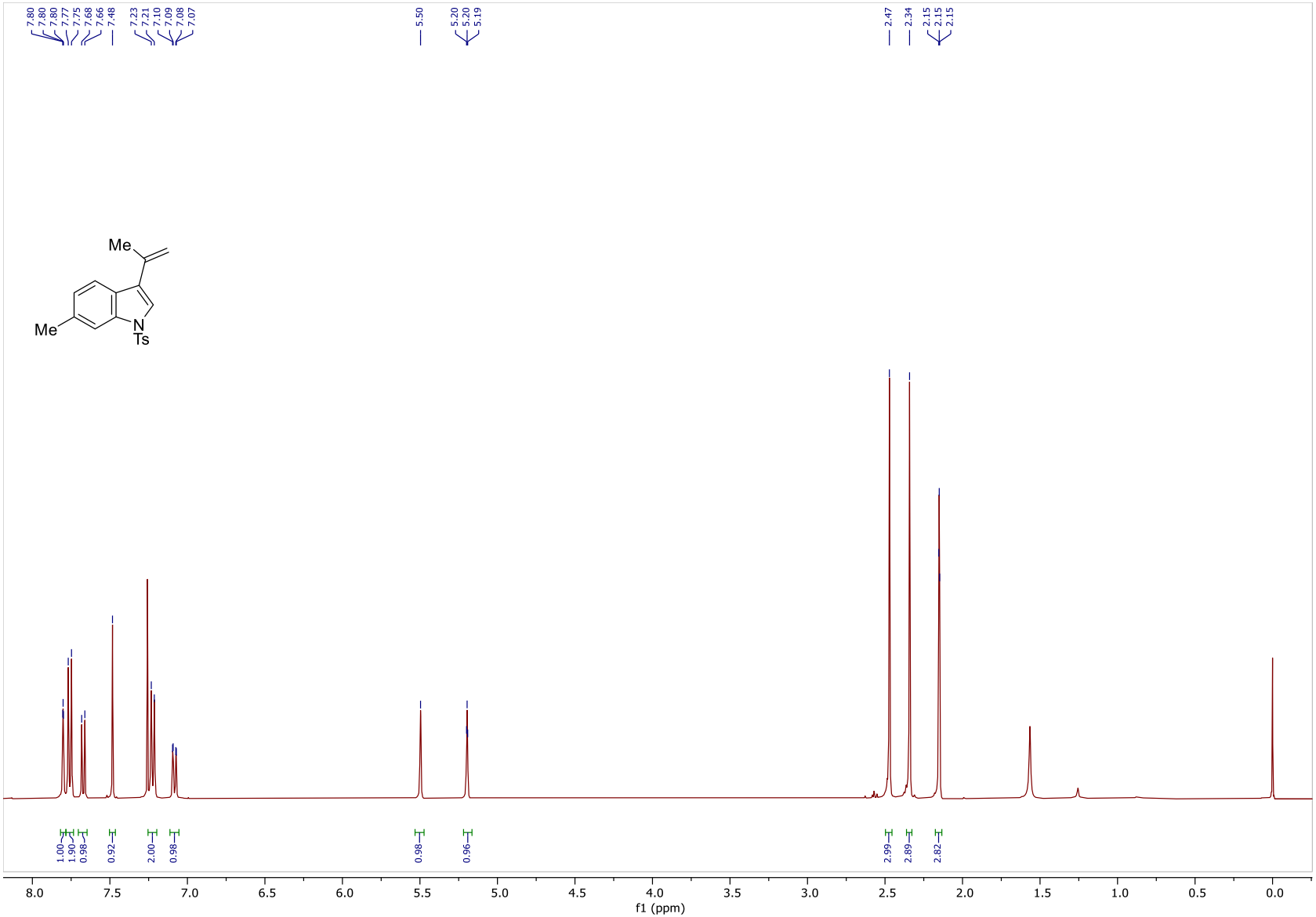

Figure 46: ^{1}H NMR Spectrum of **95g** (400MHz, $CDCl_3$)

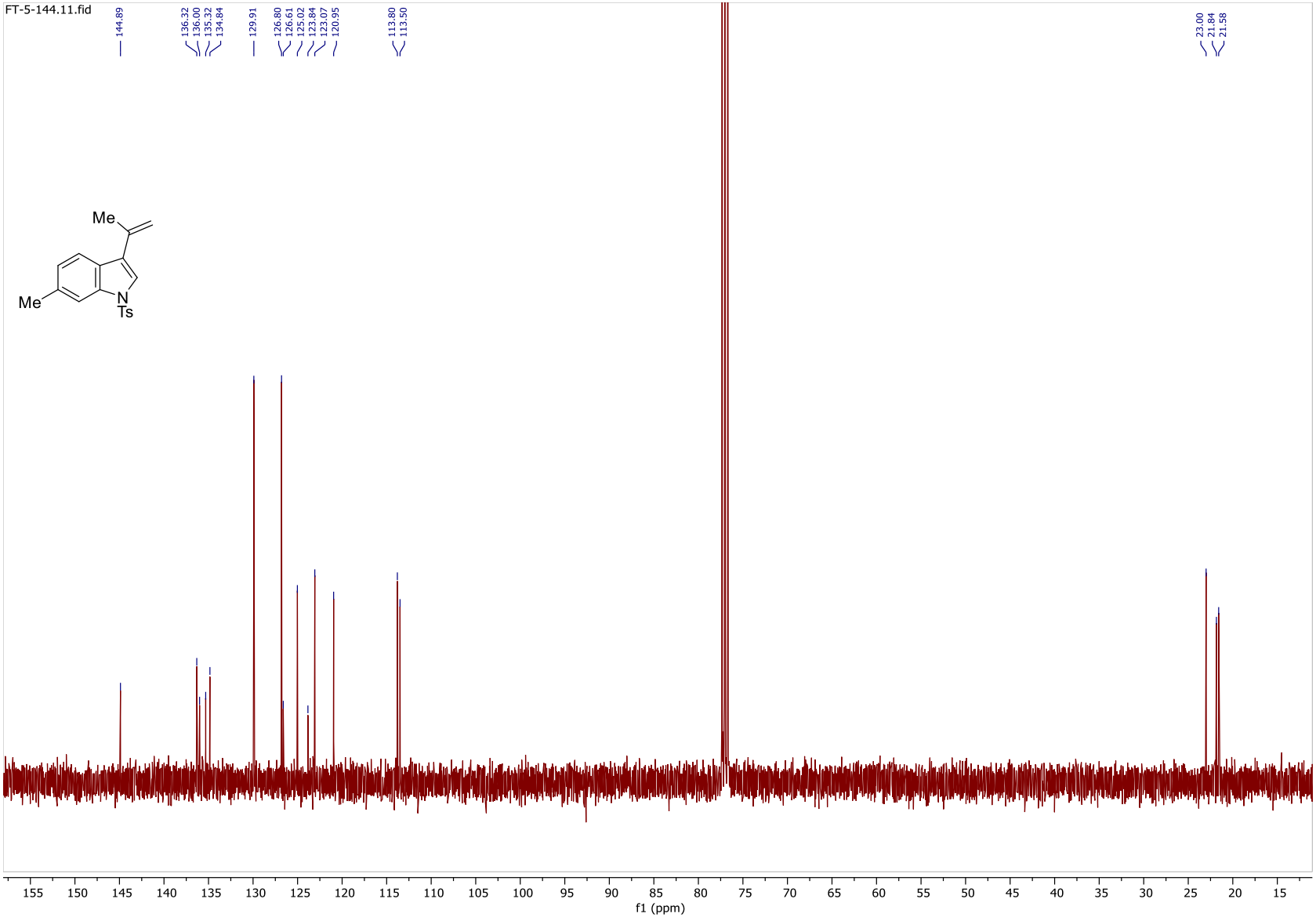

Figure 47: ^{13}C NMR Spectrum of **95g** (100MHz, $CDCl_3$)

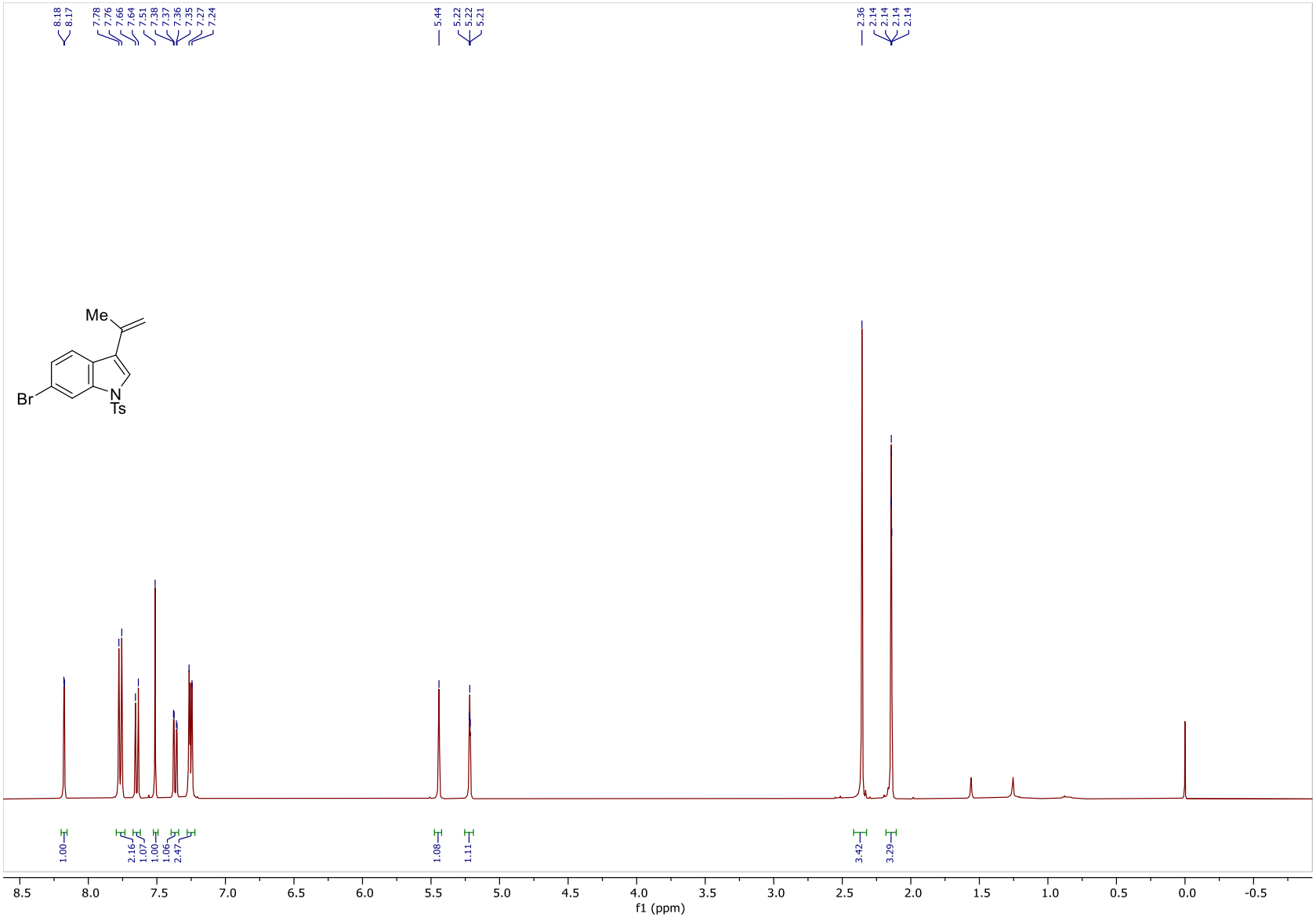

Figure 48: ^{1}H NMR Spectrum of **95h** (400MHz, $CDCl_3$)

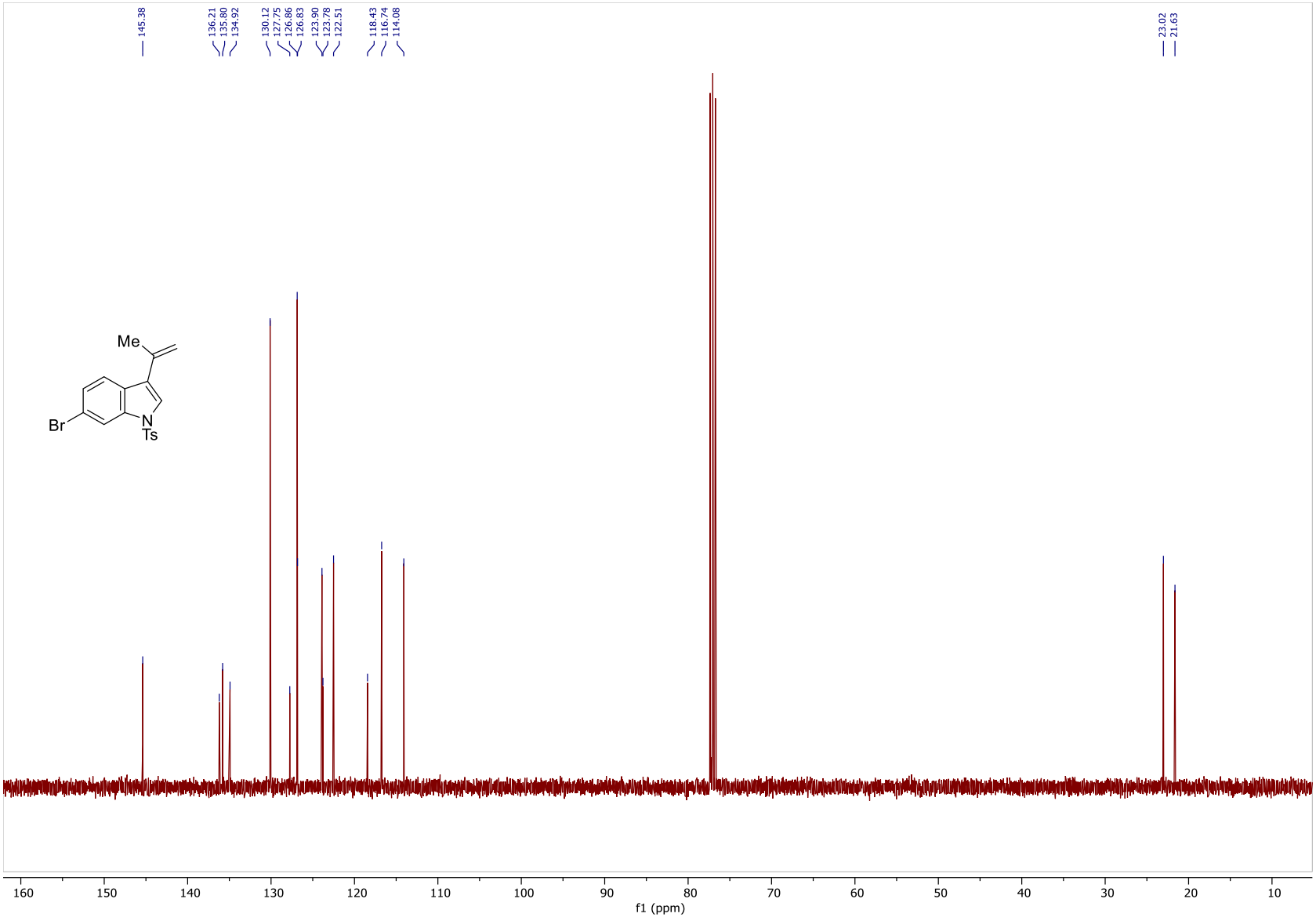

Figure 49: ^{13}C NMR Spectrum of **95h** (100MHz, $CDCl_3$)

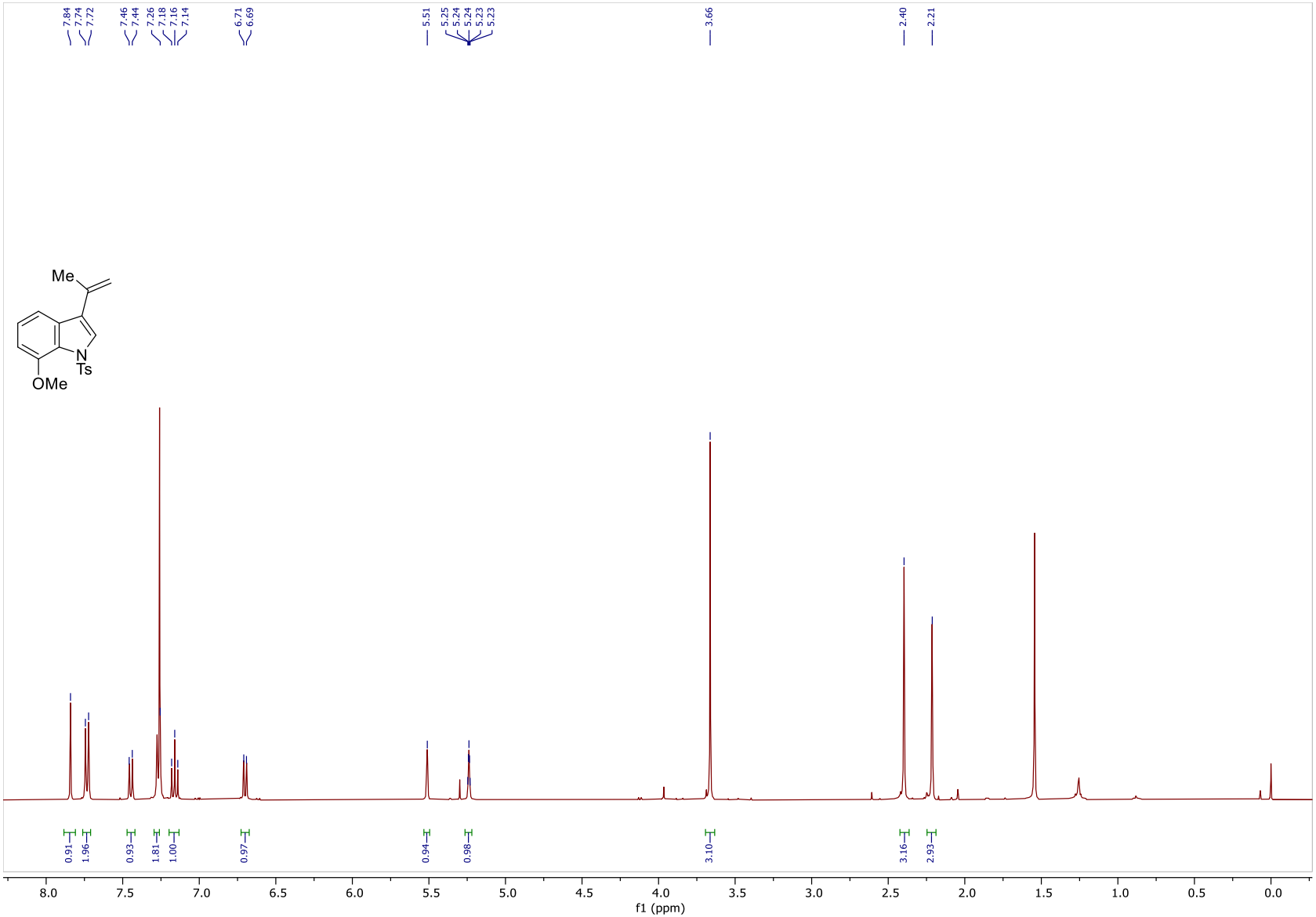

Figure 50: ^{1}H NMR Spectrum of **95i** (400MHz, $CDCl_3$)

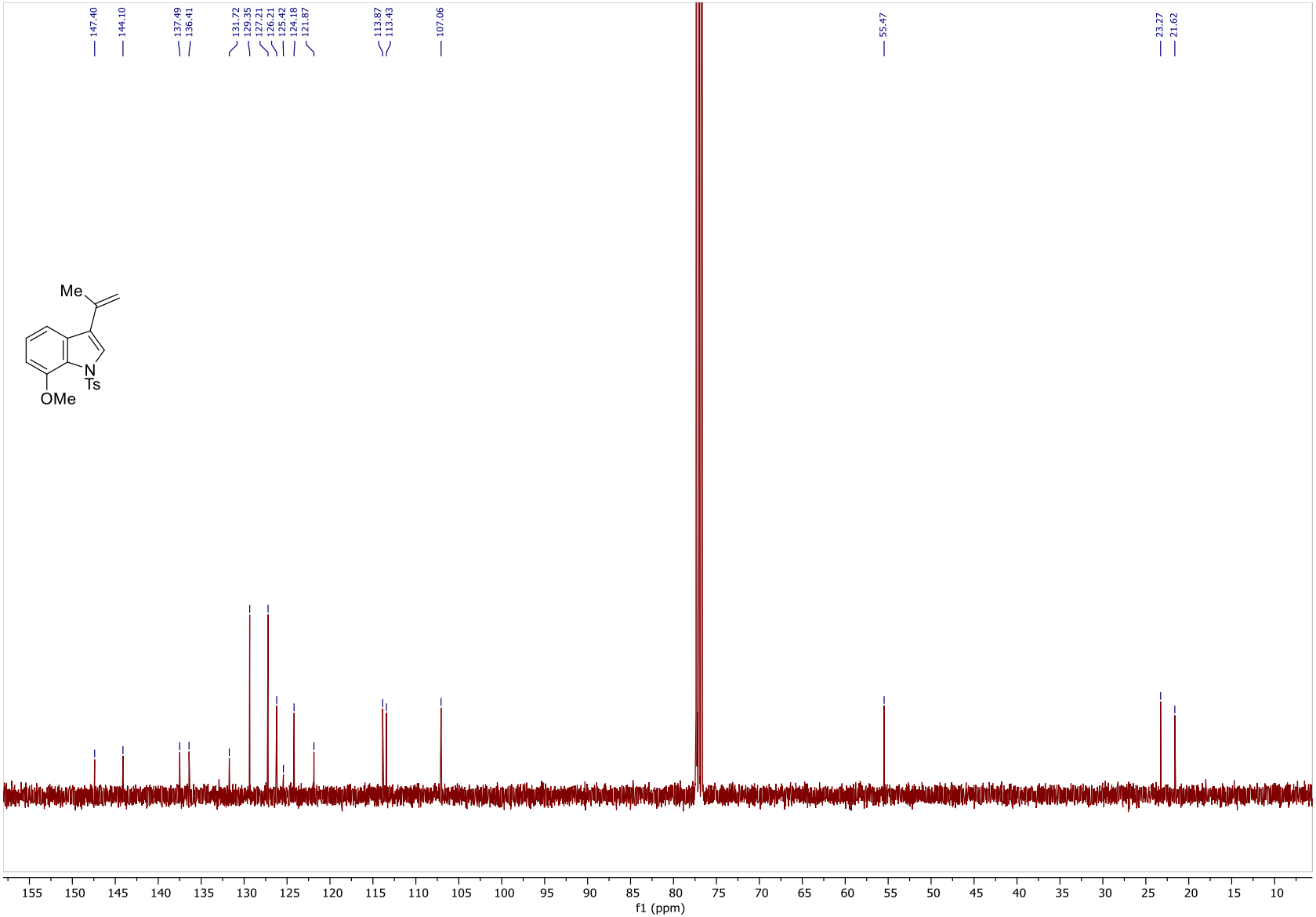

Figure 51: ^{13}C NMR Spectrum of **95i** (100MHz, $CDCl_3$)

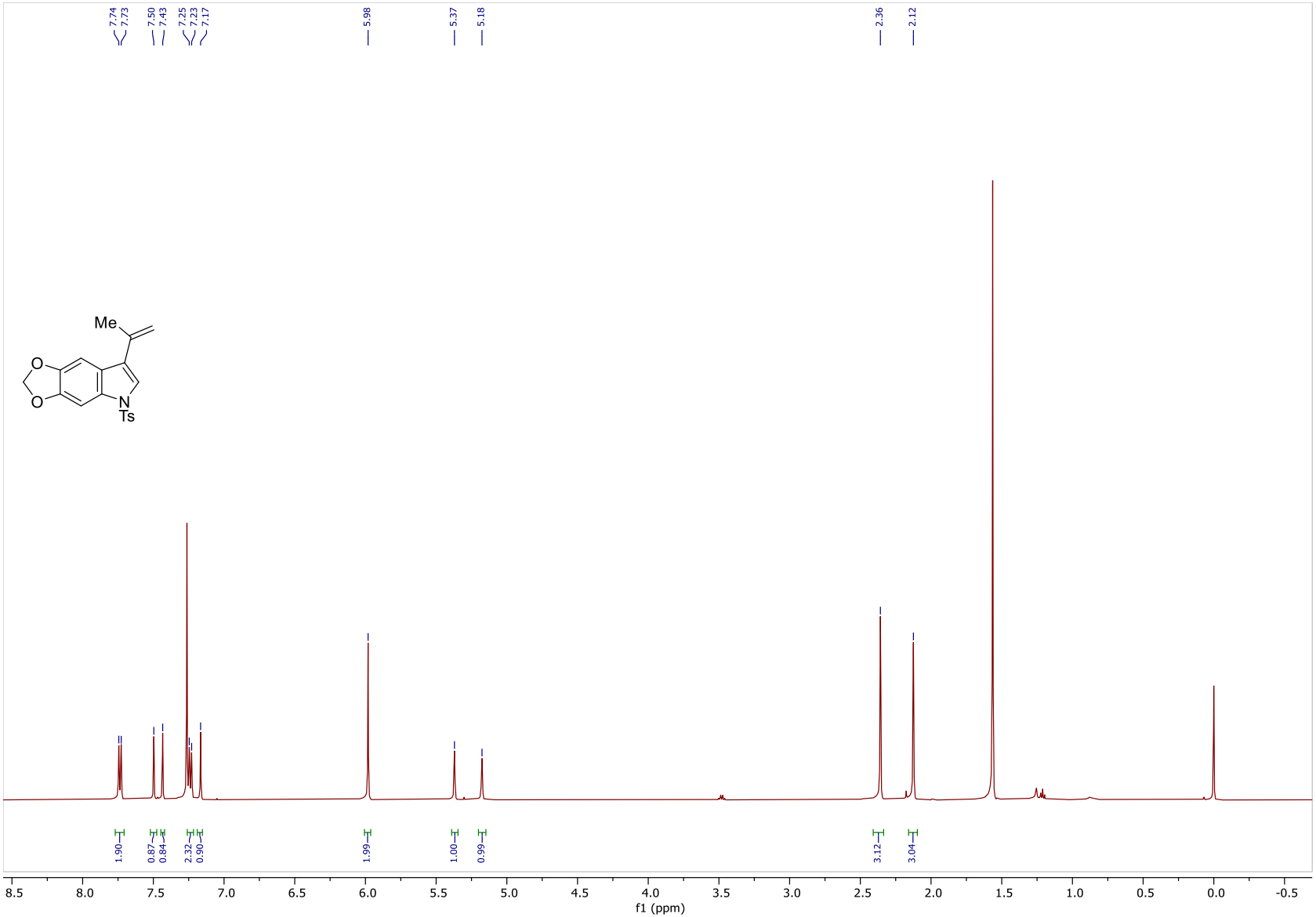

Figure 52: ^{1}H NMR Spectrum of **95j** (400MHz, $CDCl_3$)

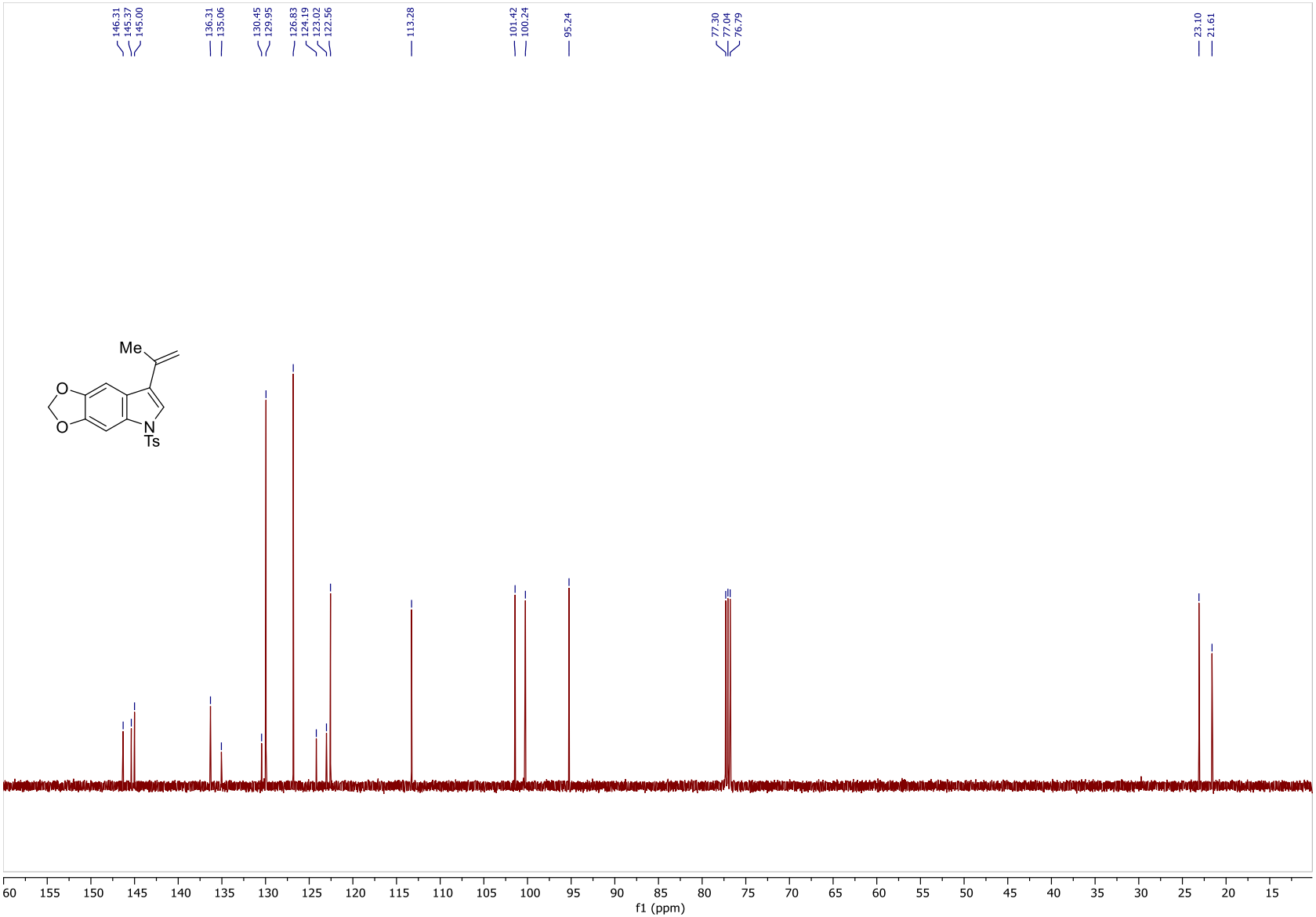

Figure 53: ^{13}C NMR Spectrum of **95j** (100MHz, $CDCl_3$)

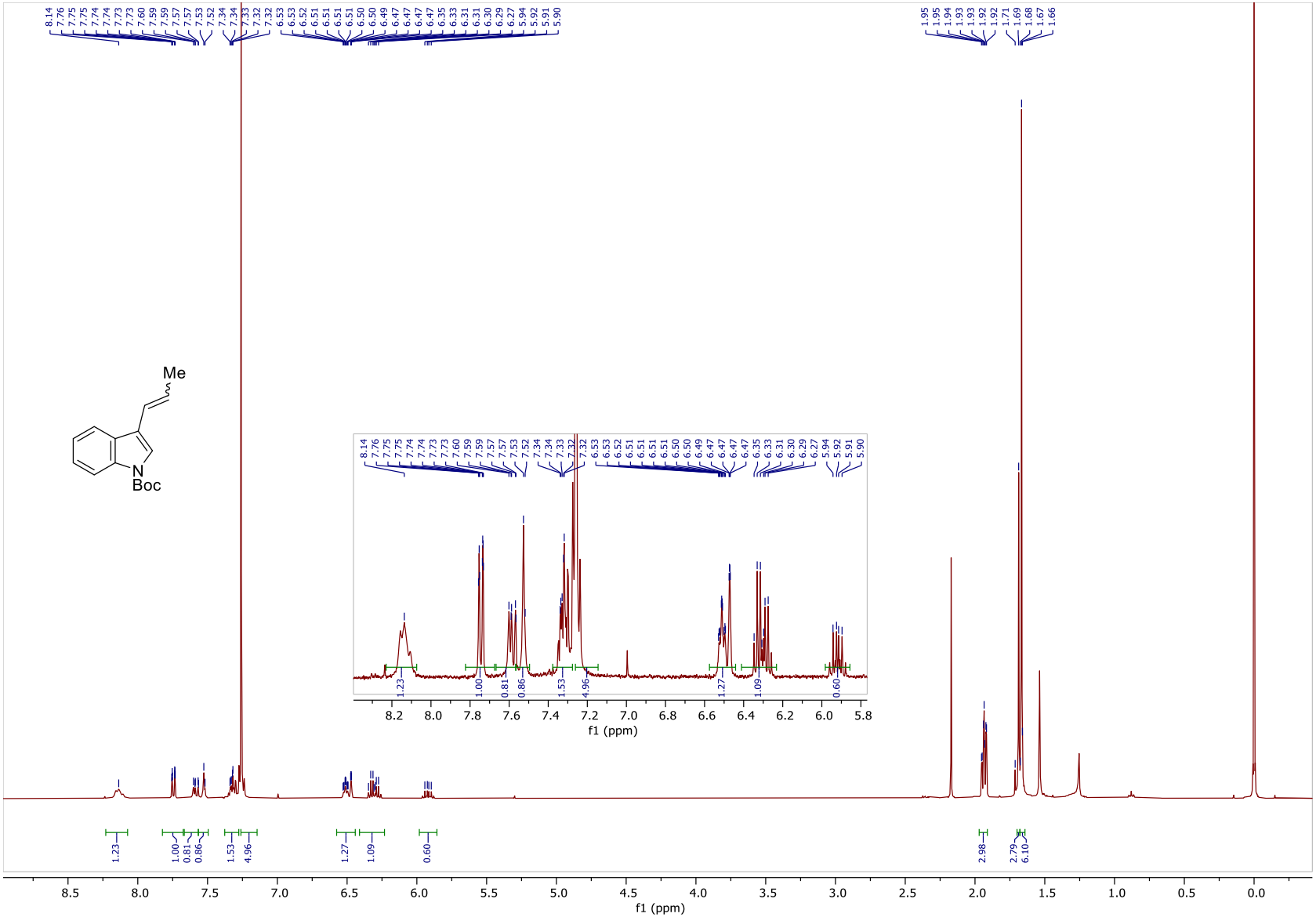

Figure 54: ^{1}H NMR Spectrum of **95k** (400MHz, $CDCl_3$)

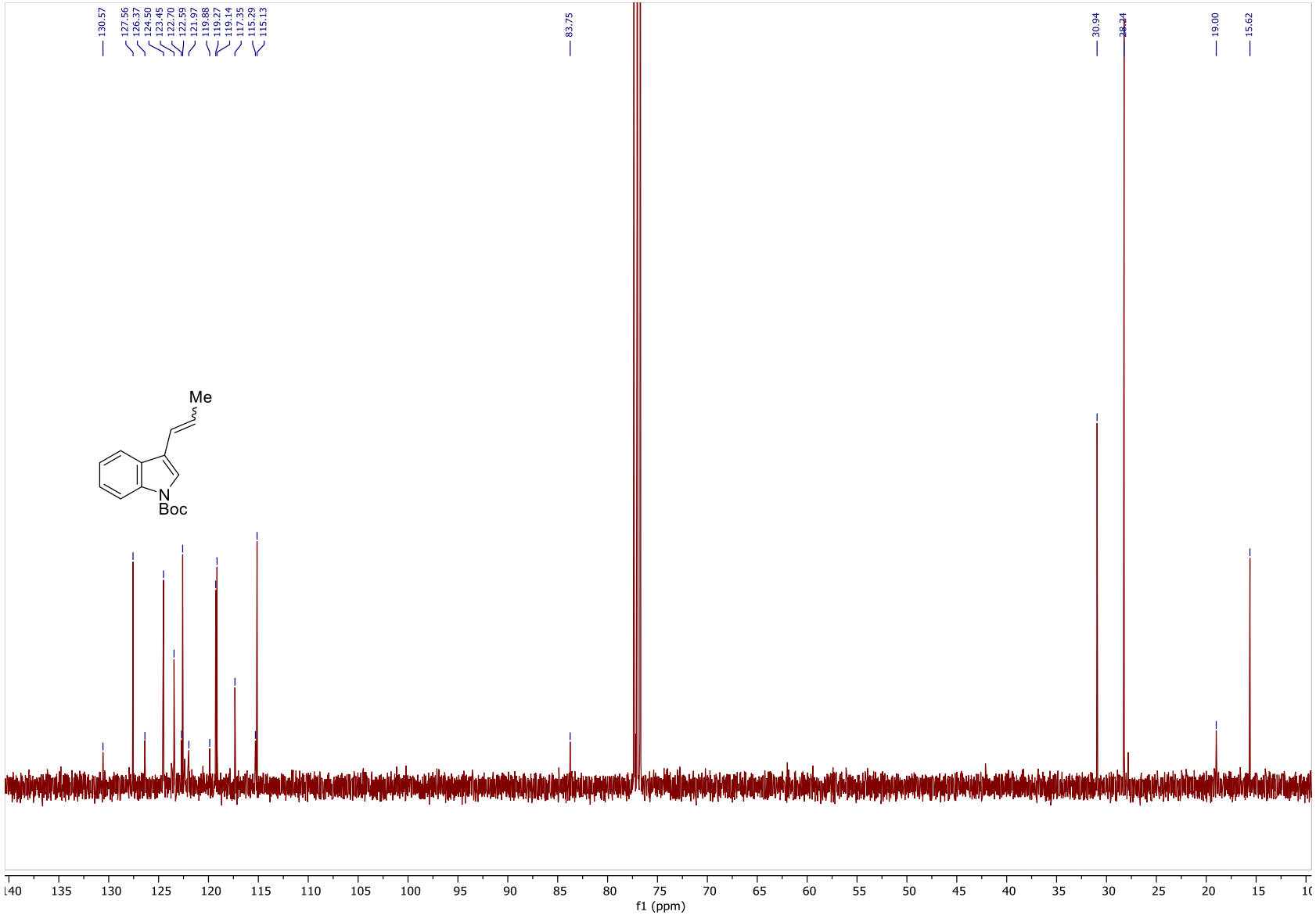

Figure 55: ^{13}C NMR Spectrum of **95k** (100MHz, $CDCl_3$)

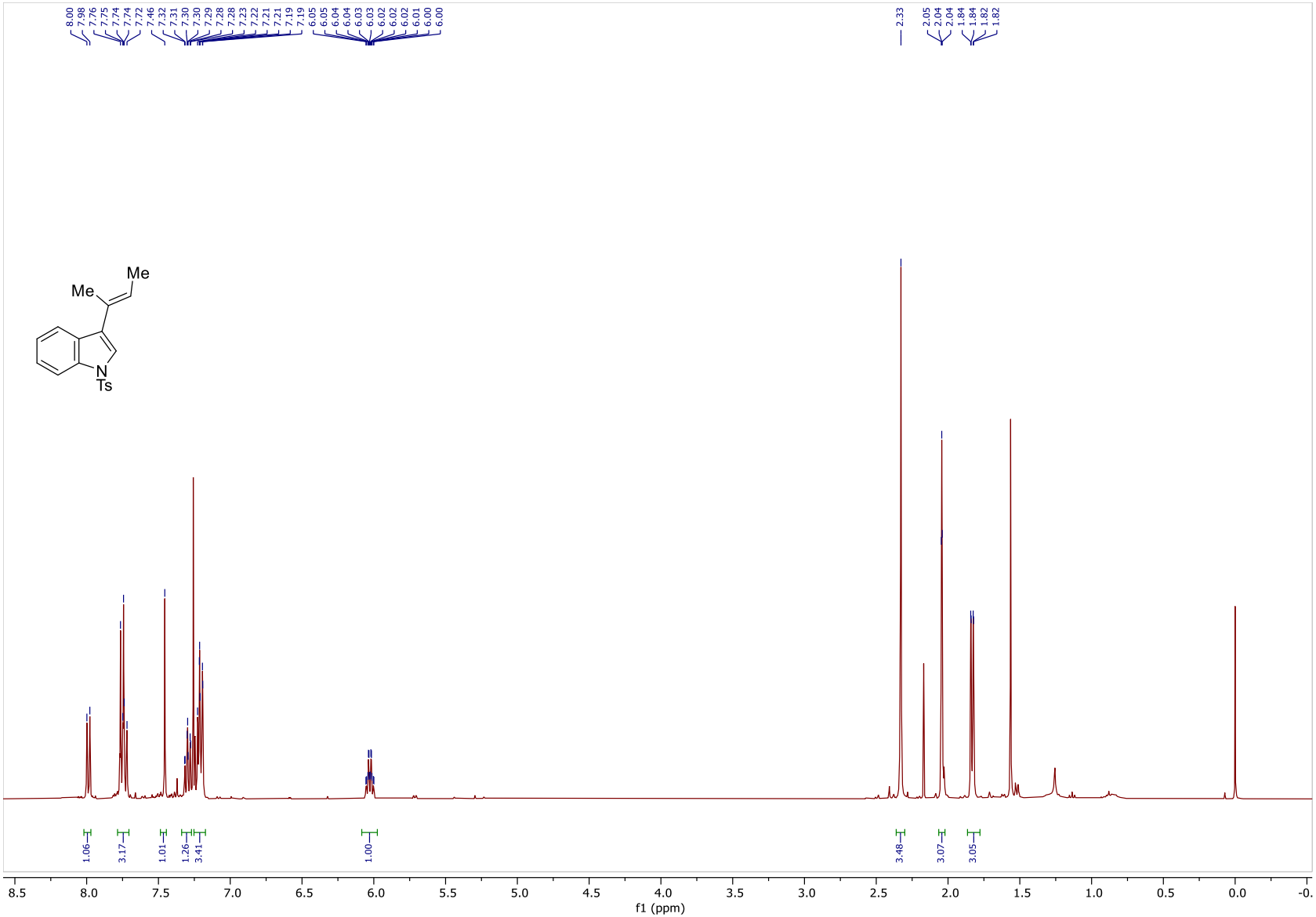

Figure 56: ^{1}H NMR Spectrum of **95l** (400MHz, $CDCl_3$)

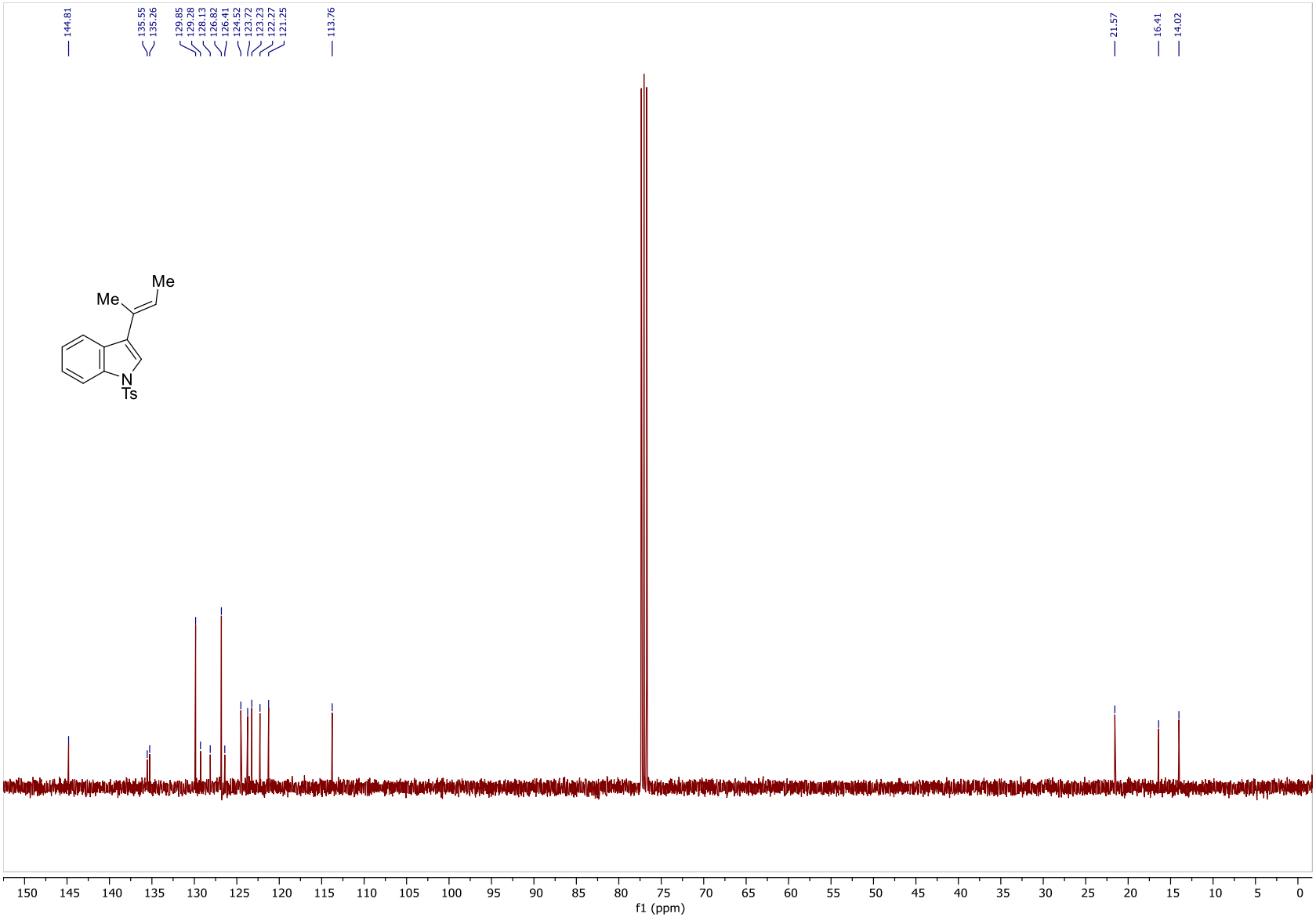

Figure 57: ^{13}C NMR Spectrum of **95l** (100MHz, $CDCl_3$)

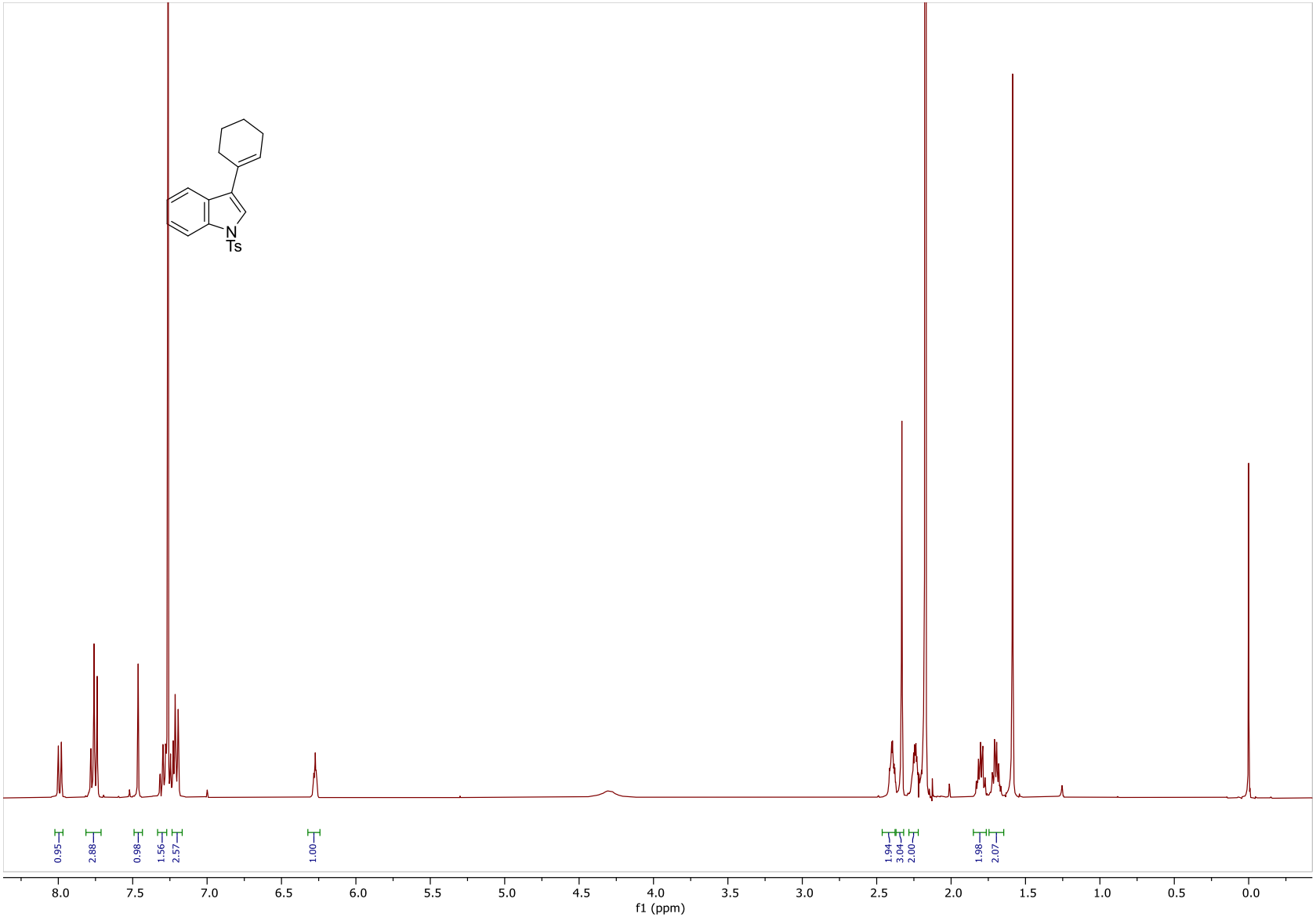

Figure 58: ^{1}H NMR Spectrum of **95m** (400MHz, $CDCl_3$)

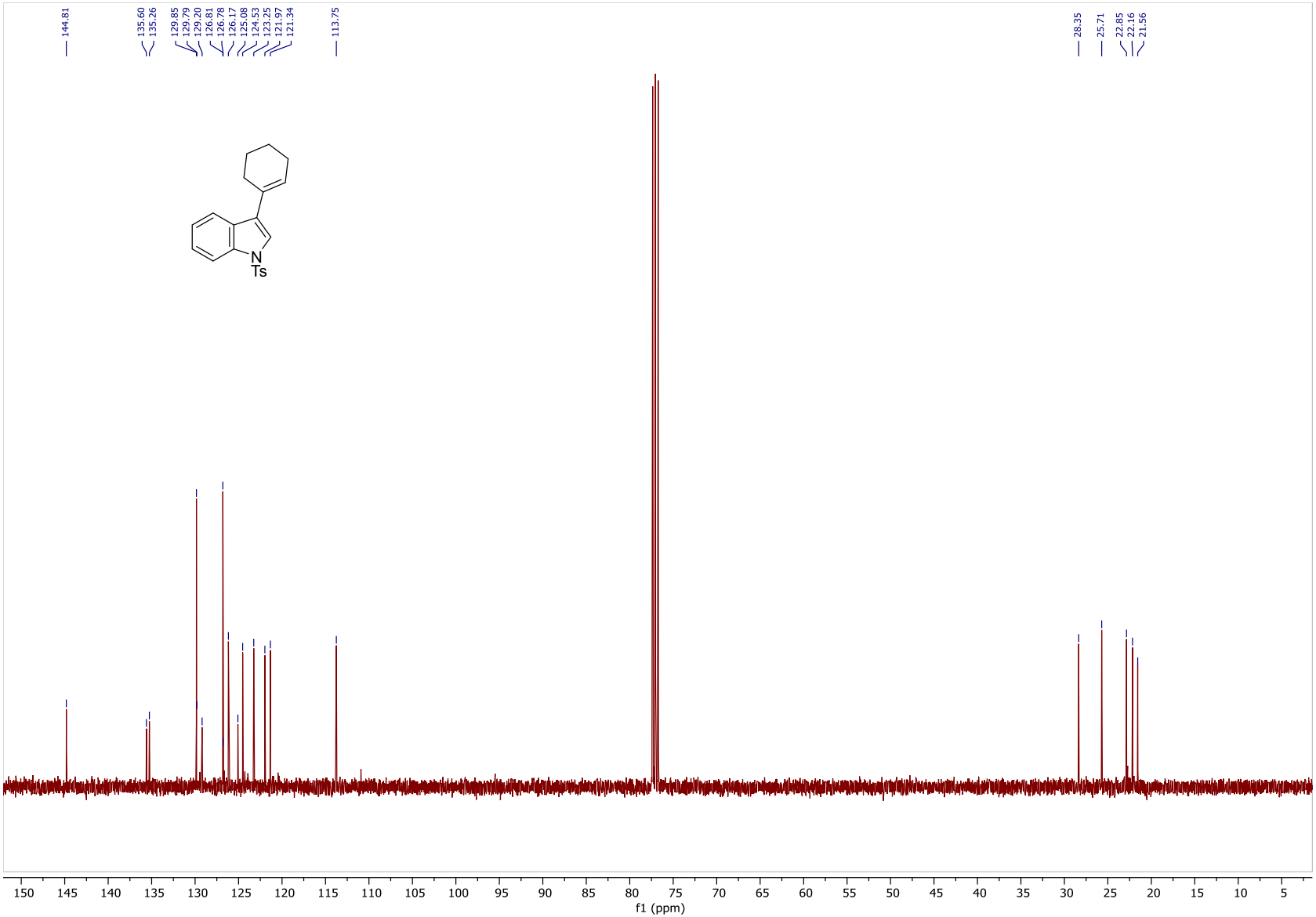

Figure 59: ^{13}C NMR Spectrum of **95m** (100MHz, $CDCl_3$)

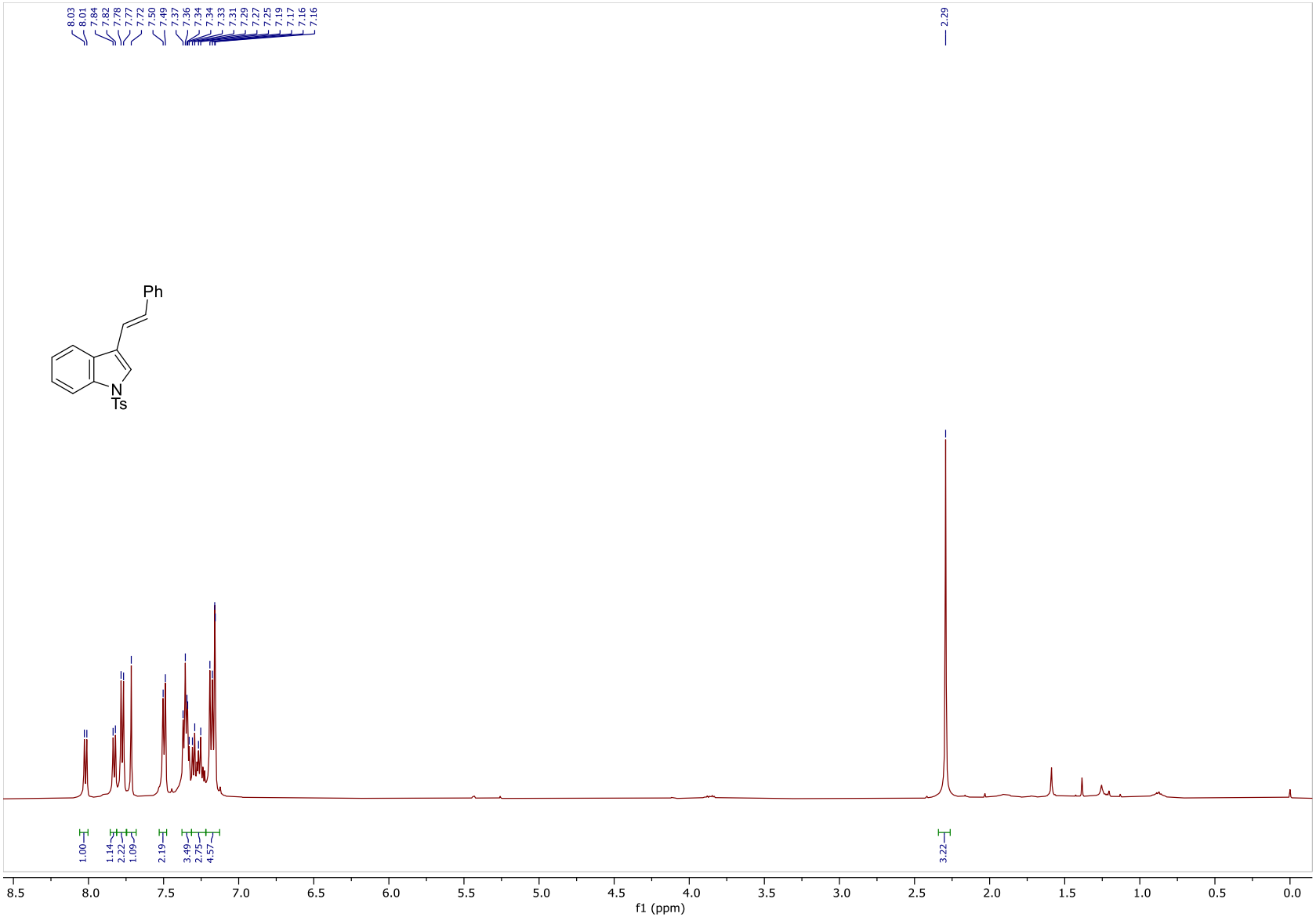

Figure 60: ^{1}H NMR Spectrum of **95n** (400MHz, $CDCl_3$)

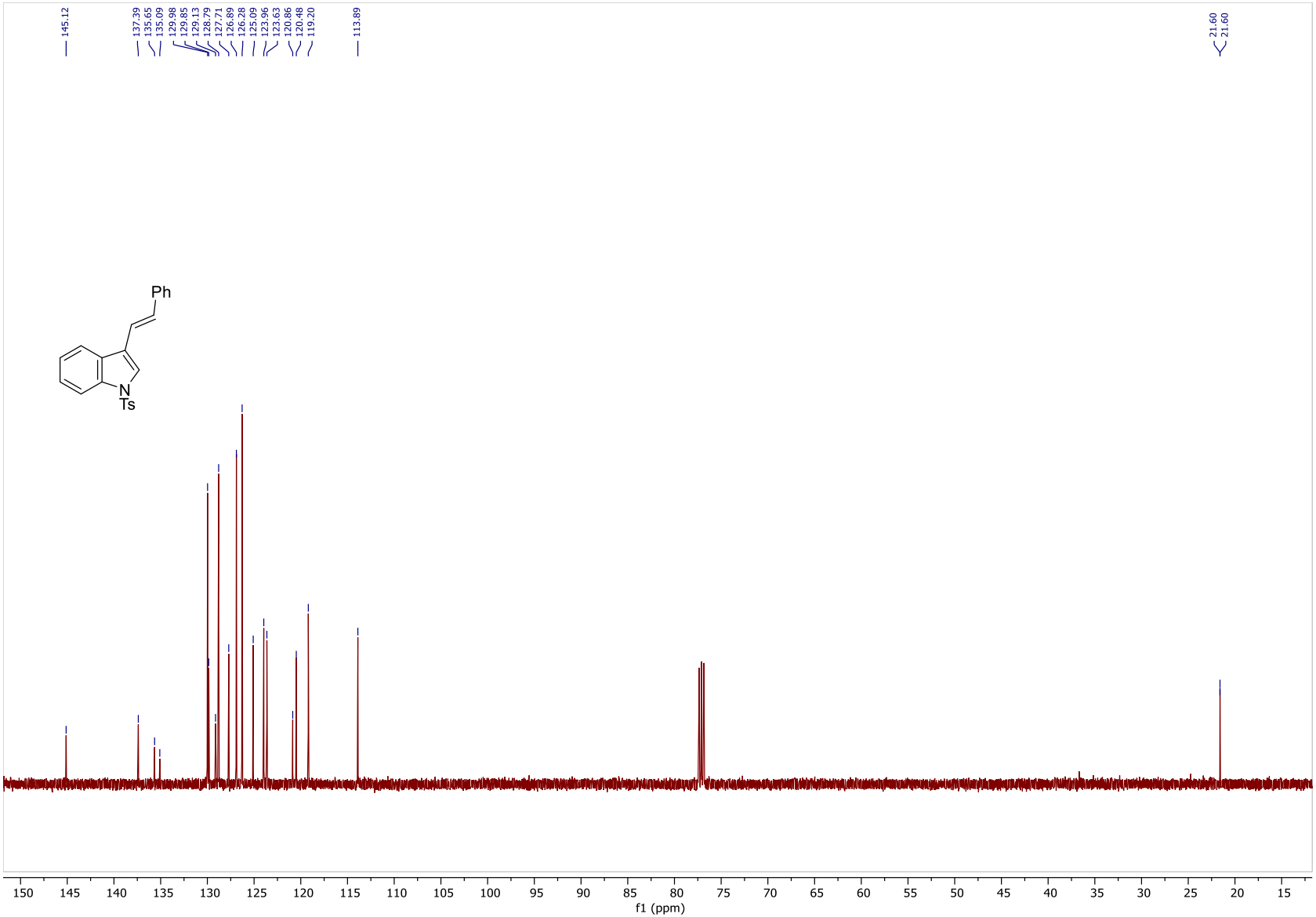

Figure 61: ^{13}C NMR Spectrum of **95n** (100MHz, $CDCl_3$)

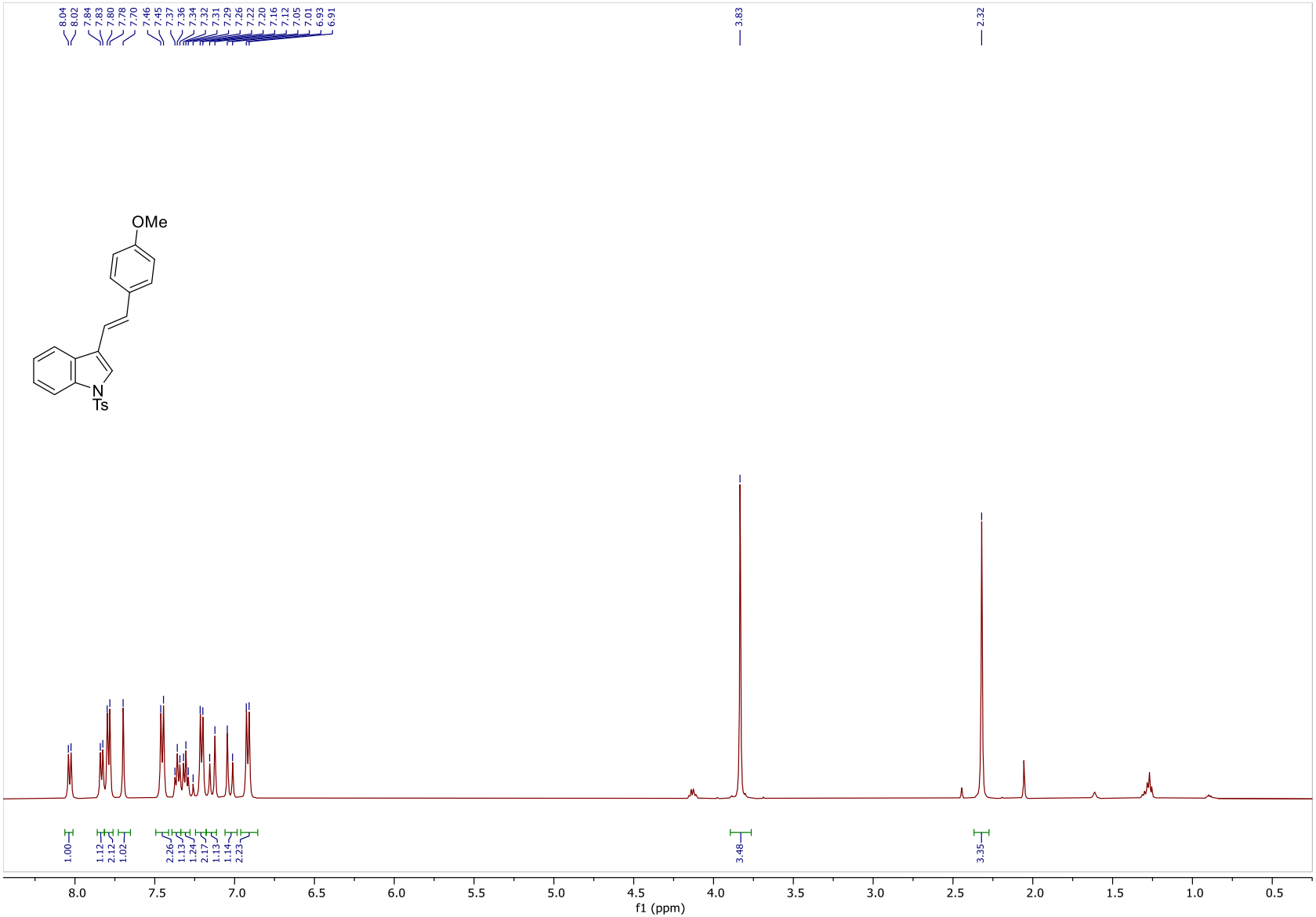

Figure 62: ^{1}H NMR Spectrum of **95o** (400MHz, $CDCl_3$)

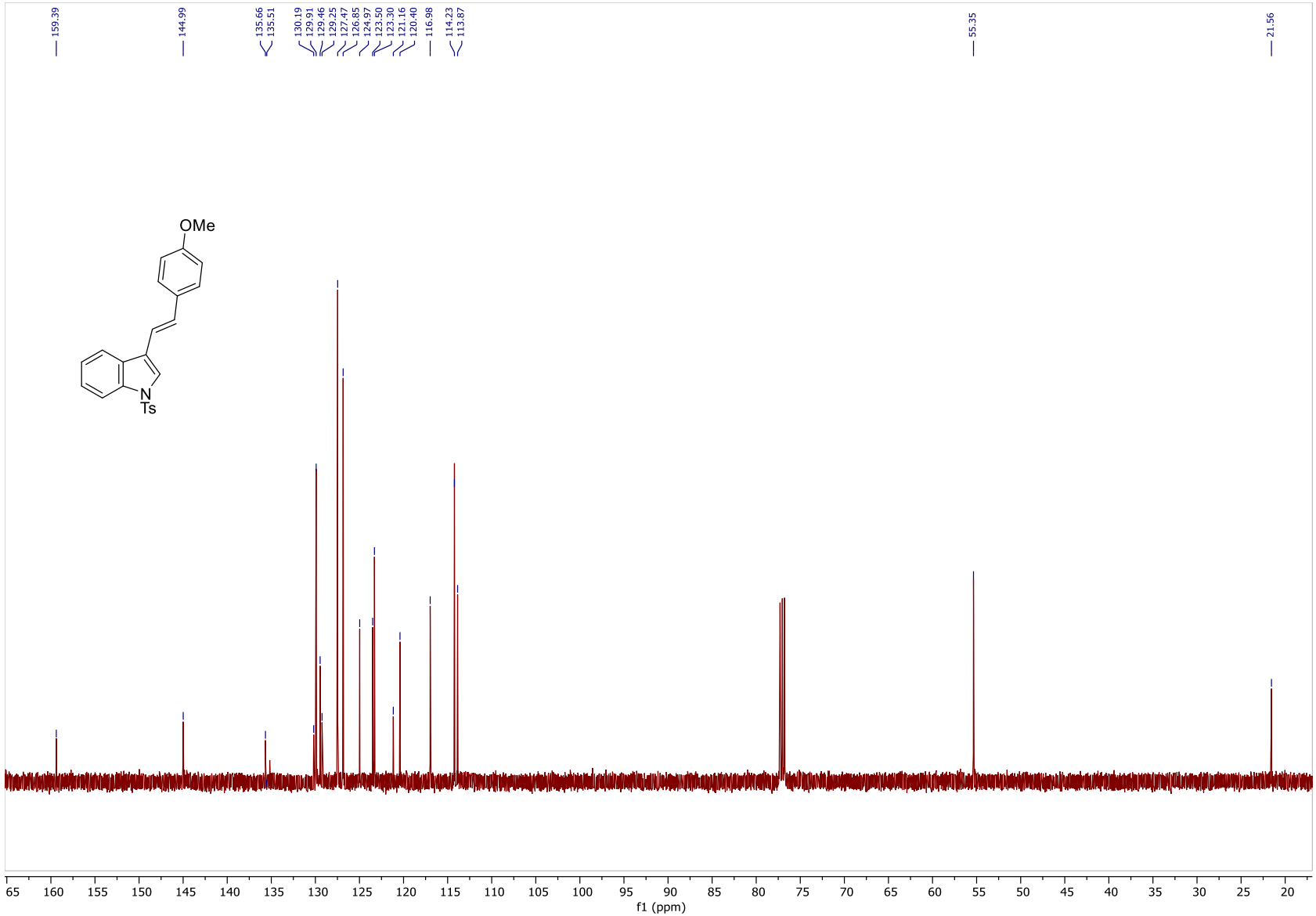

Figure 63: ^{13}C NMR Spectrum of **95o** (100MHz, $CDCl_3$)

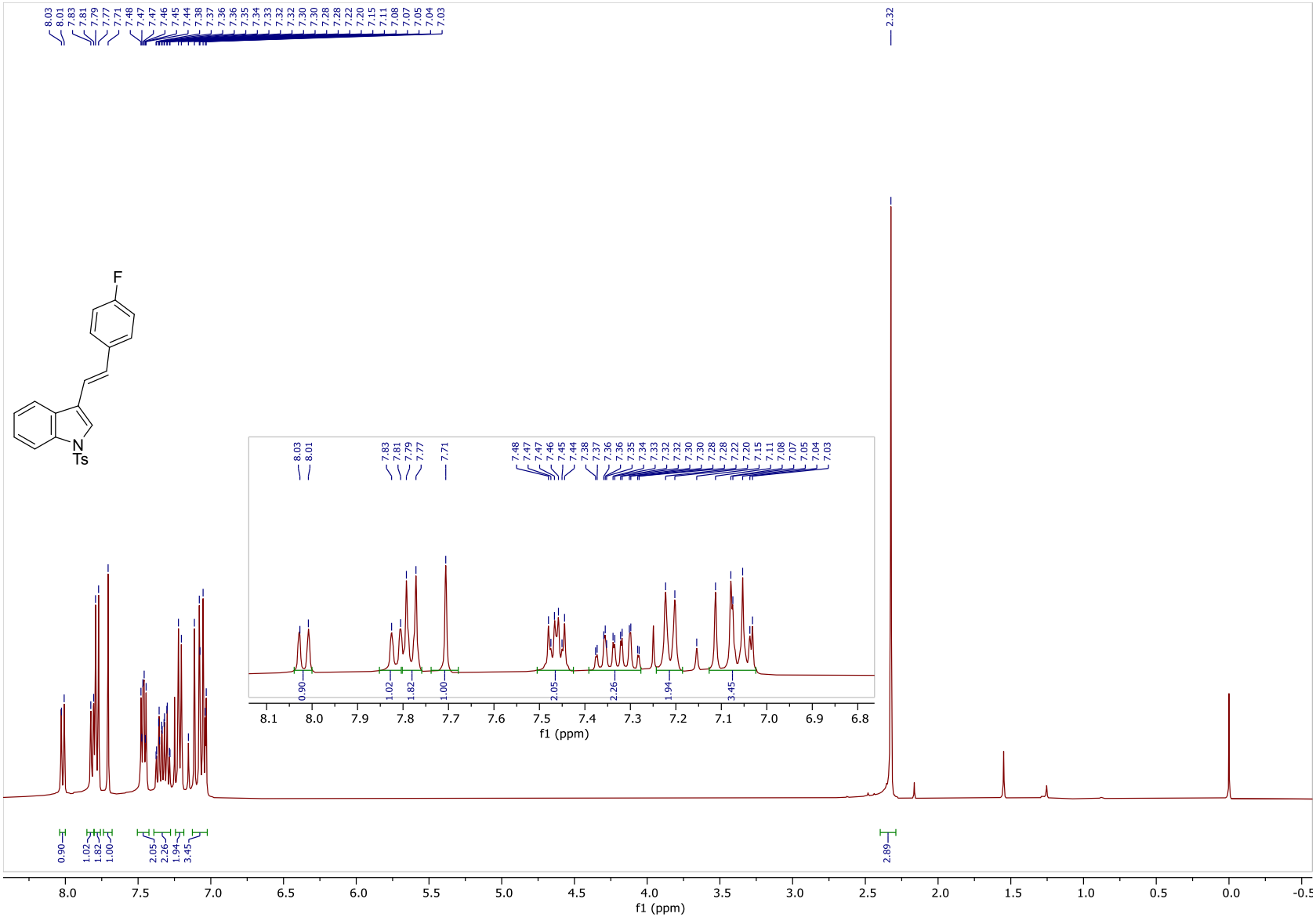

Figure 64: ^{1}H NMR Spectrum of **95p** (400MHz, $CDCl_3$)

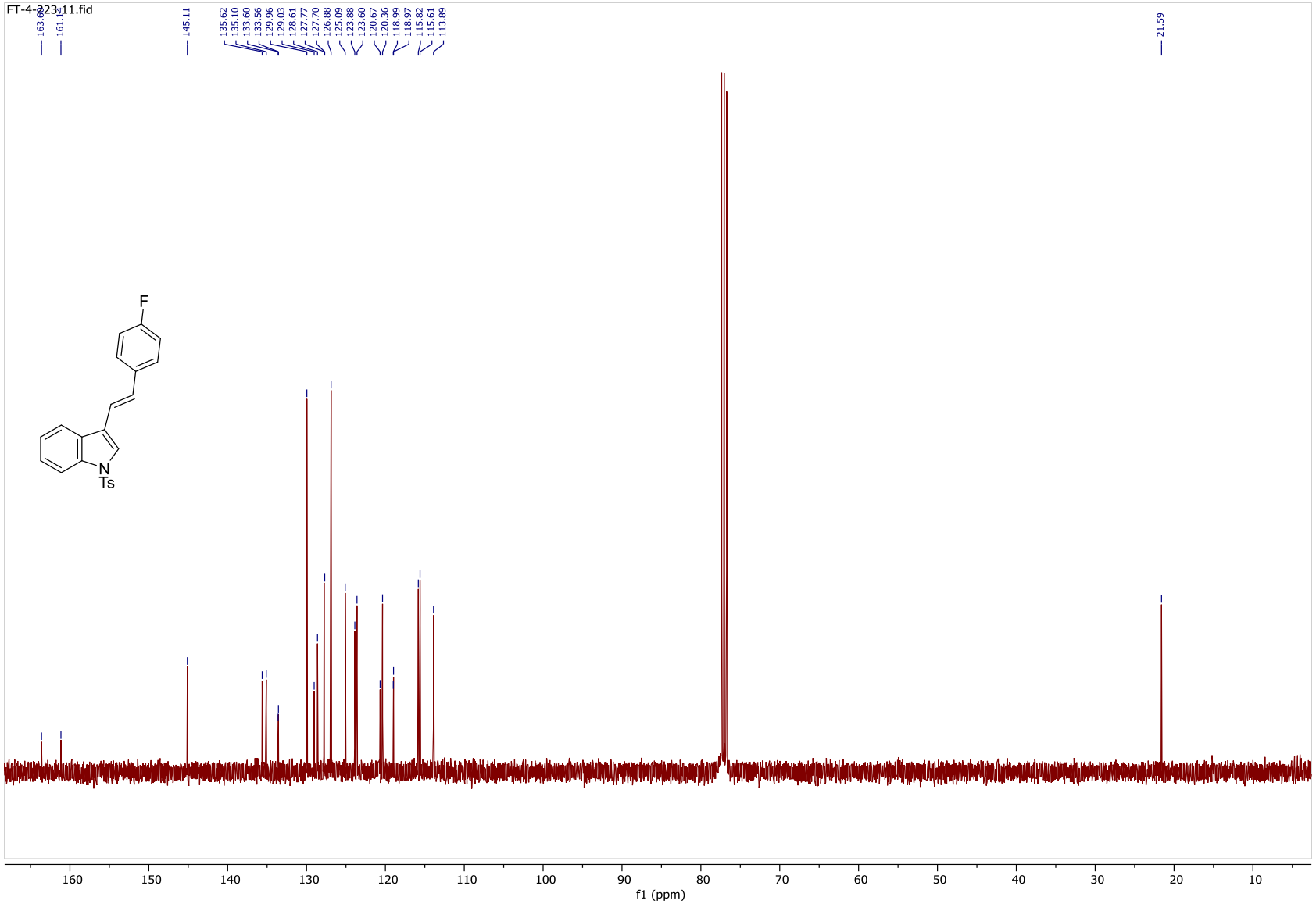

Figure 65: ^{13}C NMR Spectrum of **95p** (100MHz, $CDCl_3$)

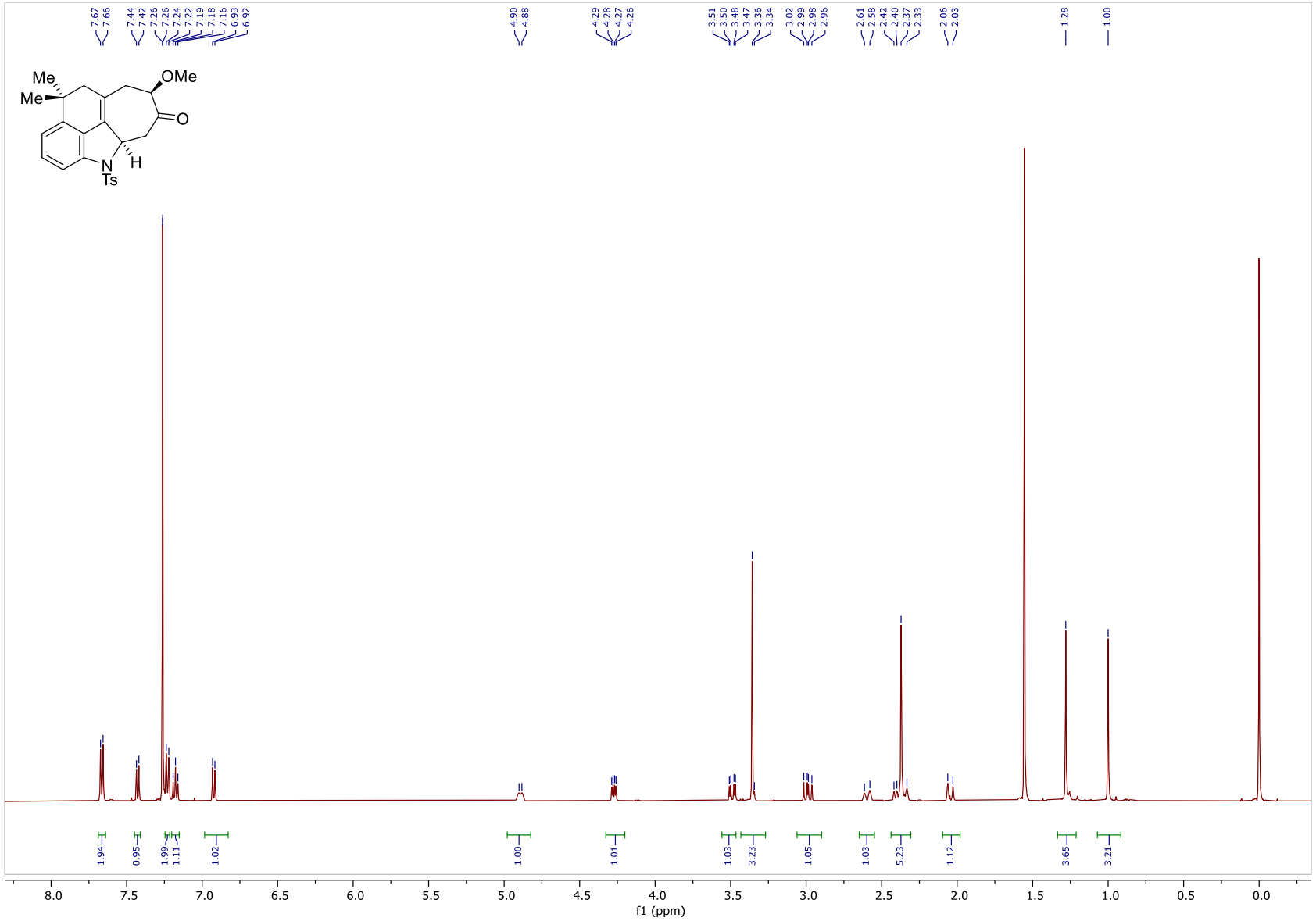

Figure 66: ^{1}H NMR Spectrum of **93** (500MHz, $CDCl_3$)

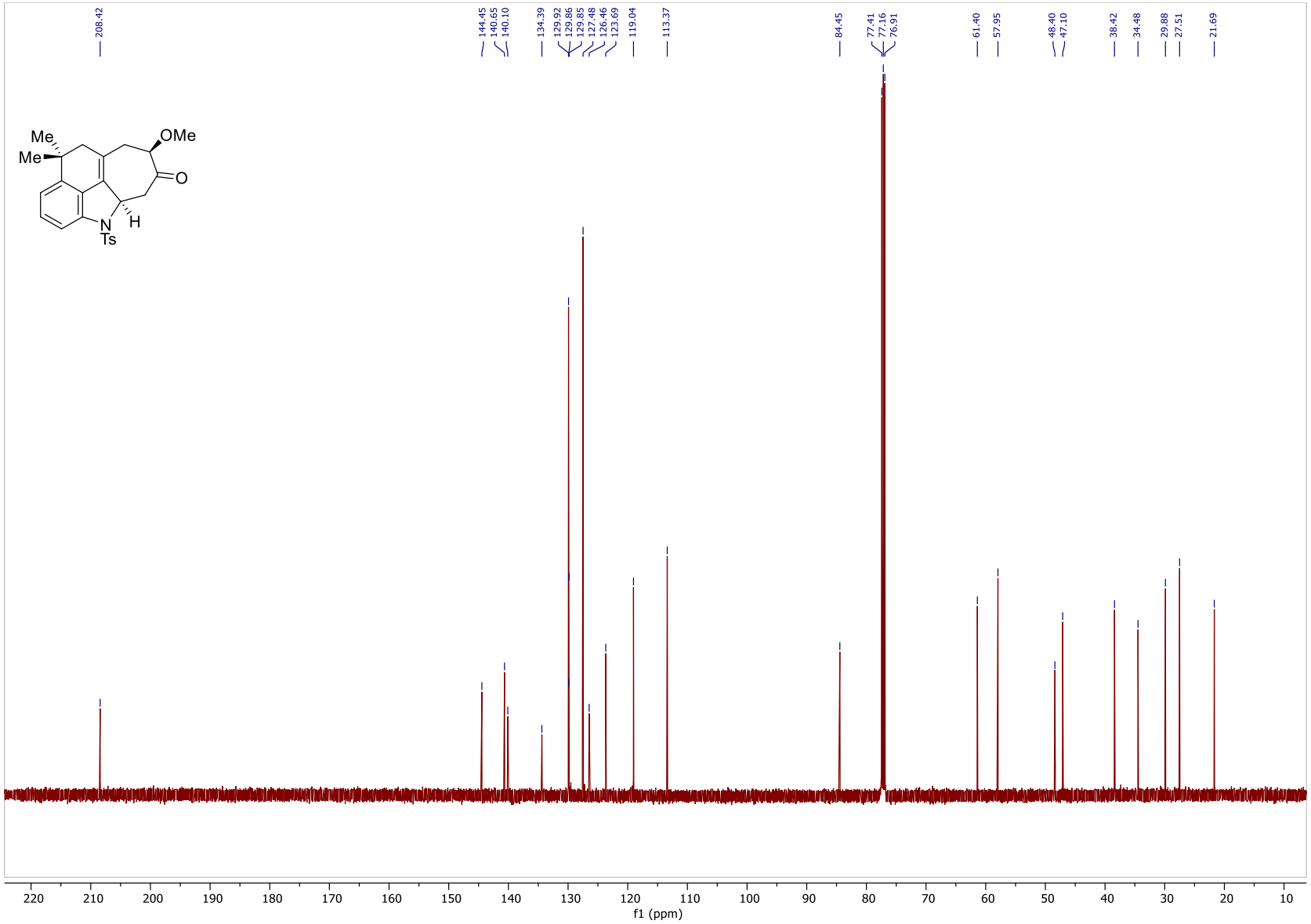

Figure 67: ^{13}C NMR Spectrum of **93** (100MHz, $CDCl_3$)

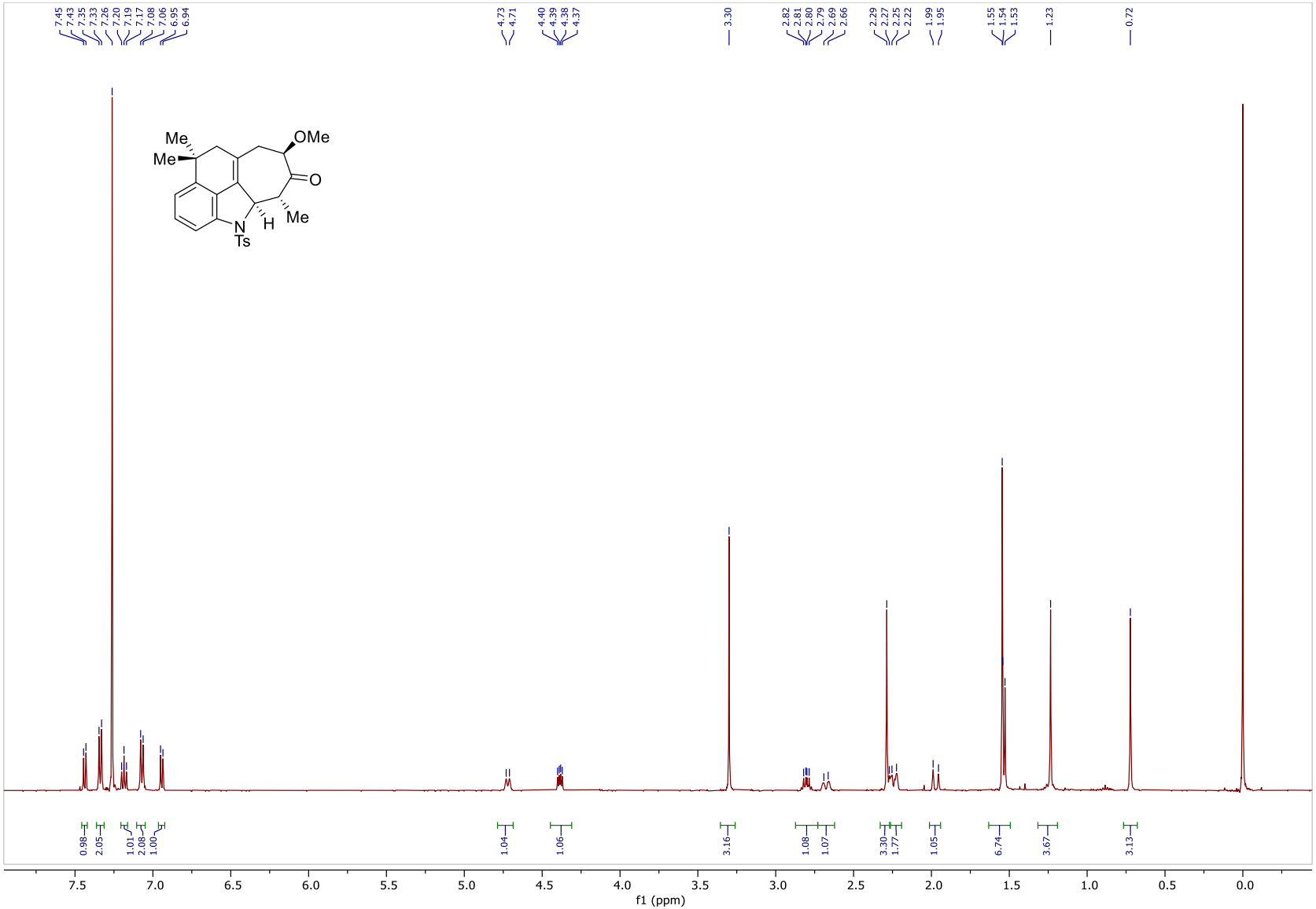

Figure 68: ^{1}H NMR Spectrum of **93b** (500MHz, $CDCl_3$)

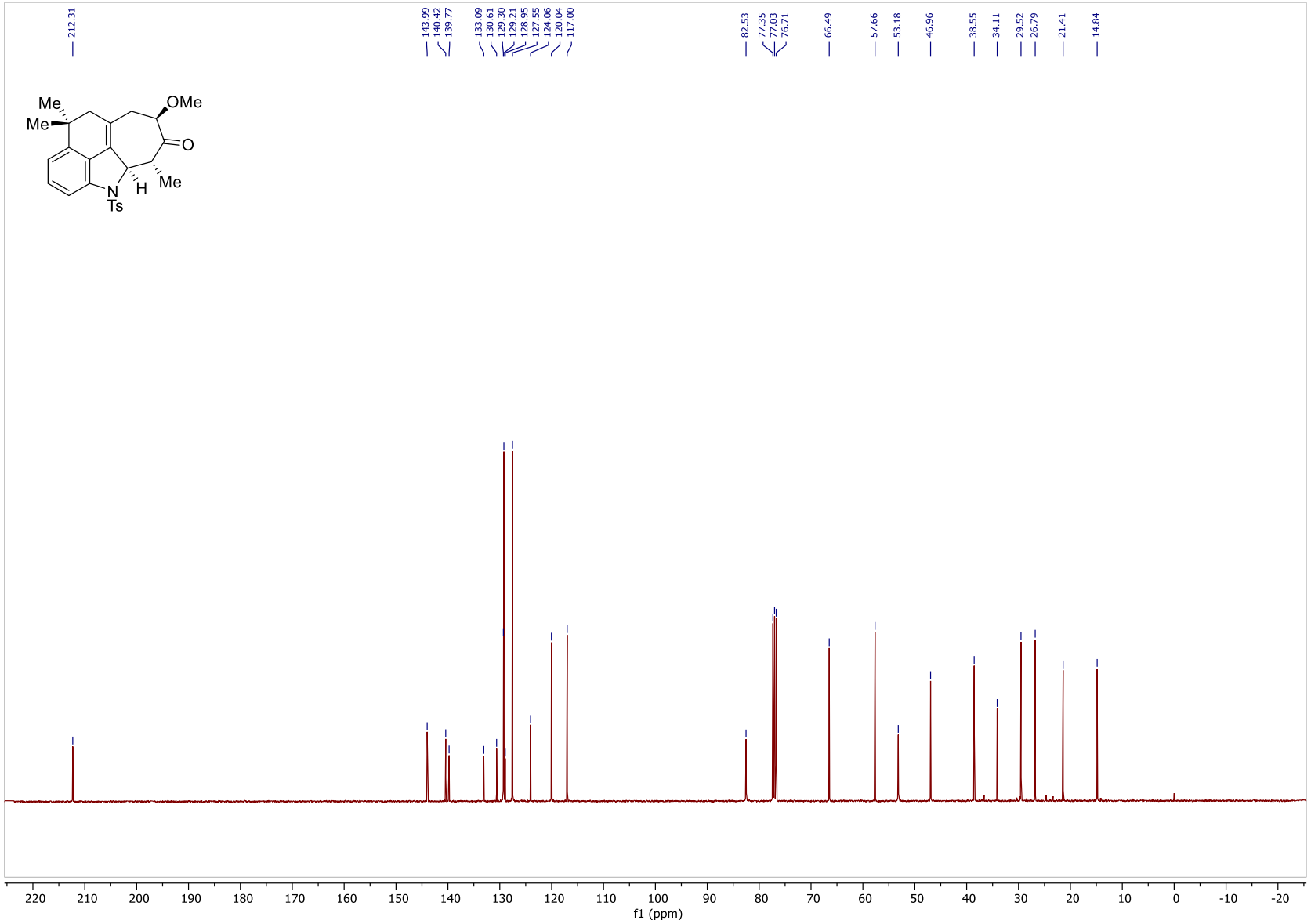

Figure 69: ^{13}C NMR Spectrum of **93b** (100MHz, $CDCl_3$)

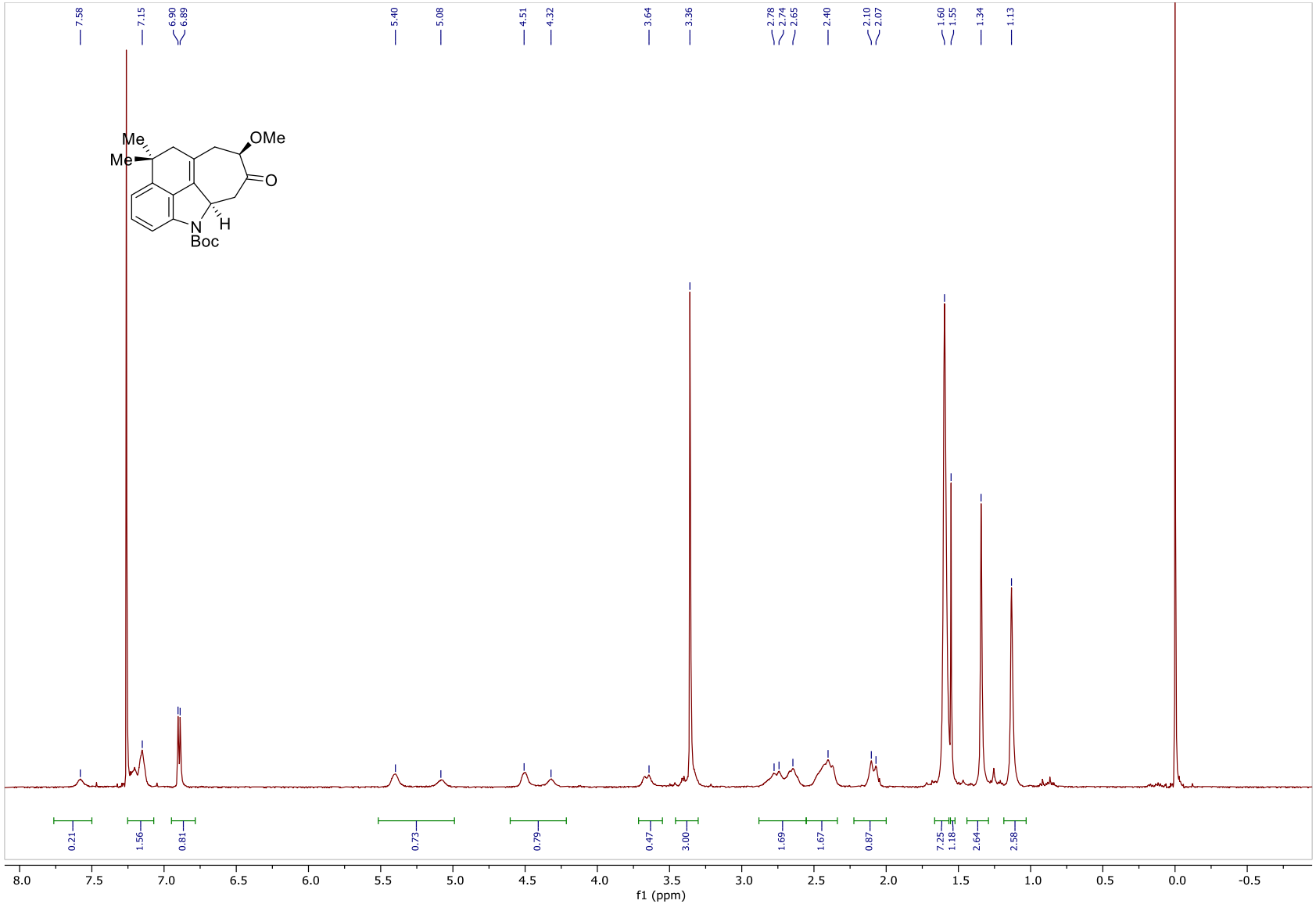

Figure 70: ^{1}H NMR Spectrum of **93c** (500MHz, $CDCl_3$)

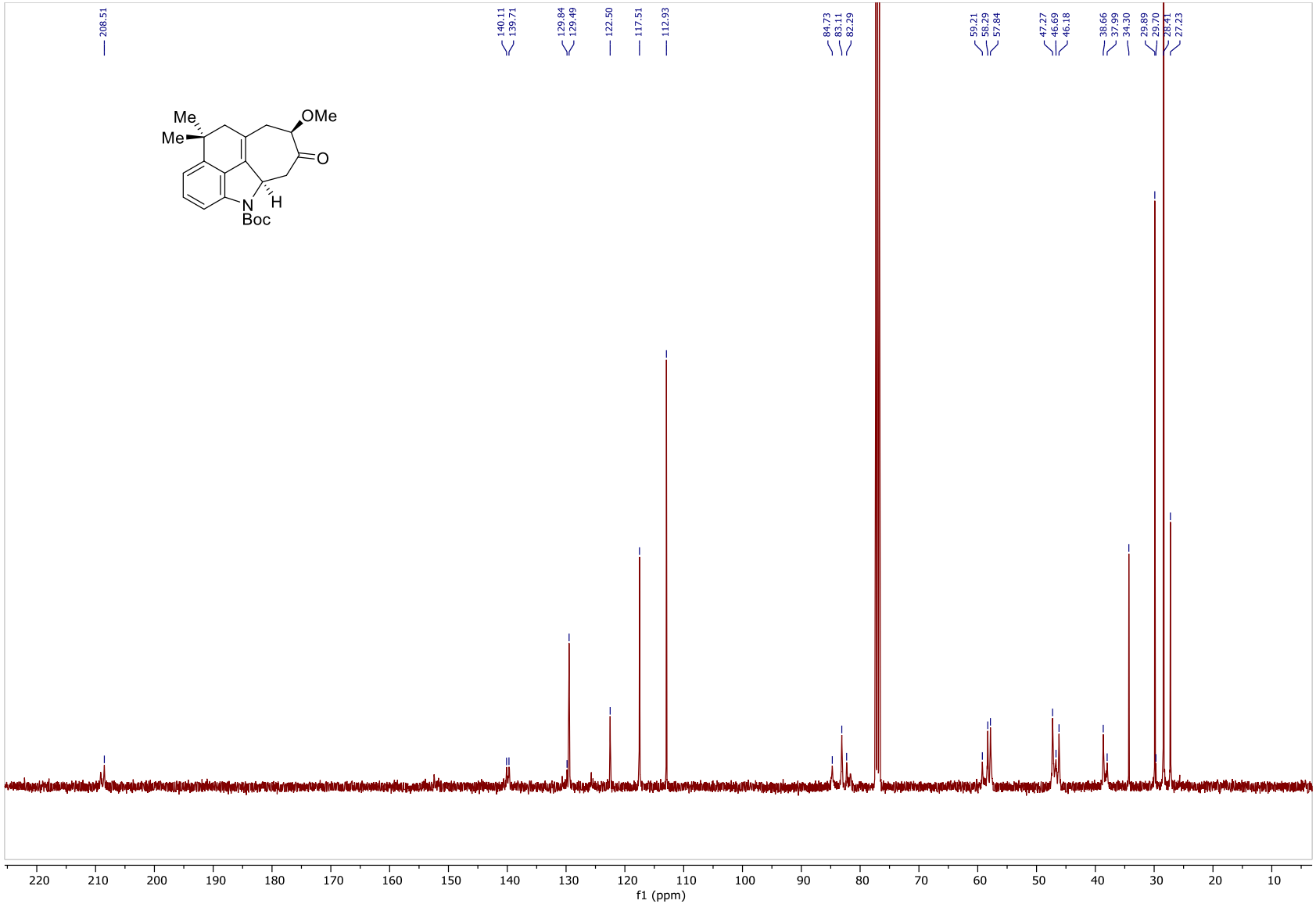

Figure 71: ^{13}C NMR Spectrum of **93c** (100MHz, $CDCl_3$)

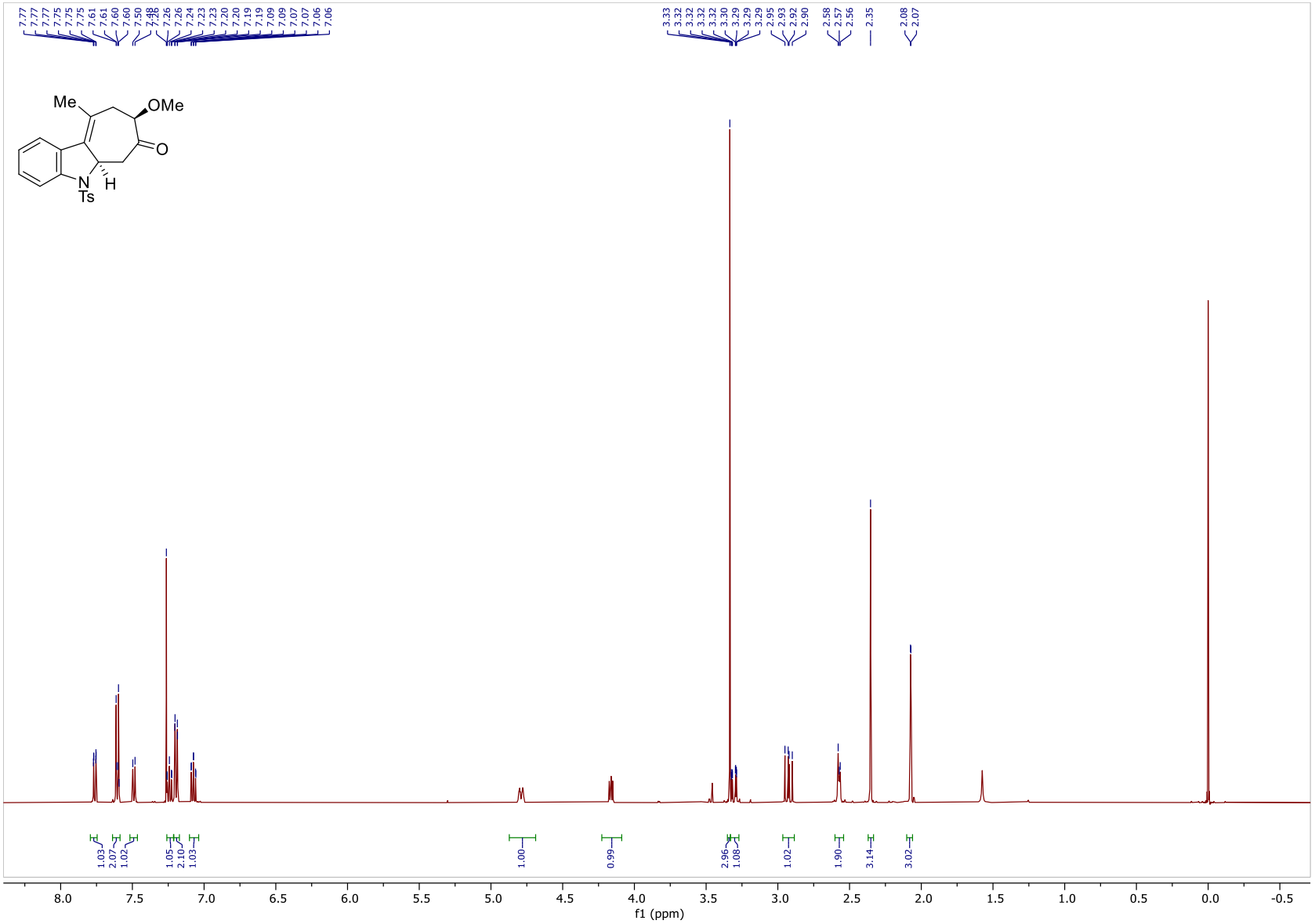

Figure 72: ^{1}H NMR Spectrum of **97a** (500MHz, $CDCl_3$)

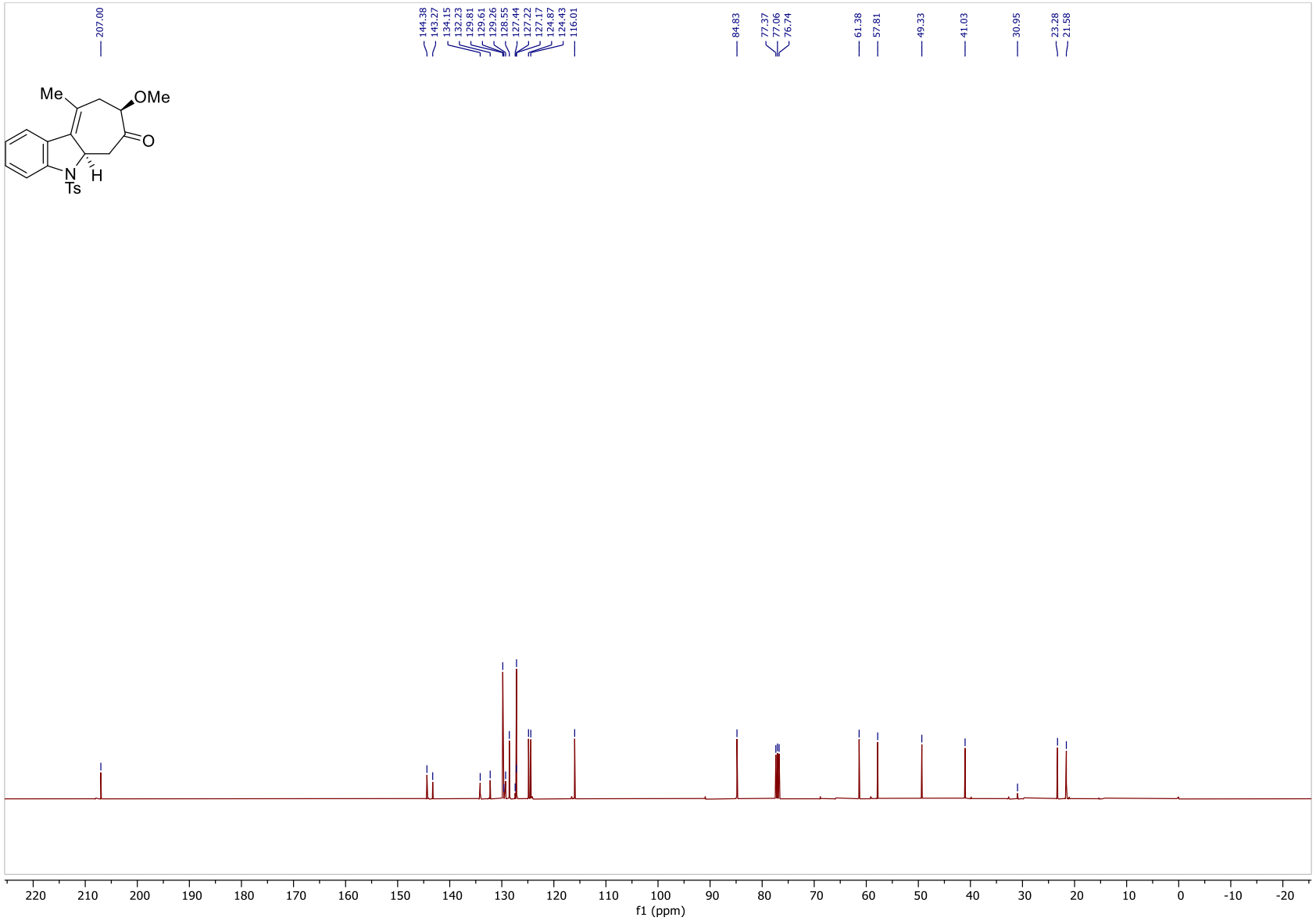

Figure 73: ^{13}C NMR Spectrum of **97a** (100MHz, $CDCl_3$)

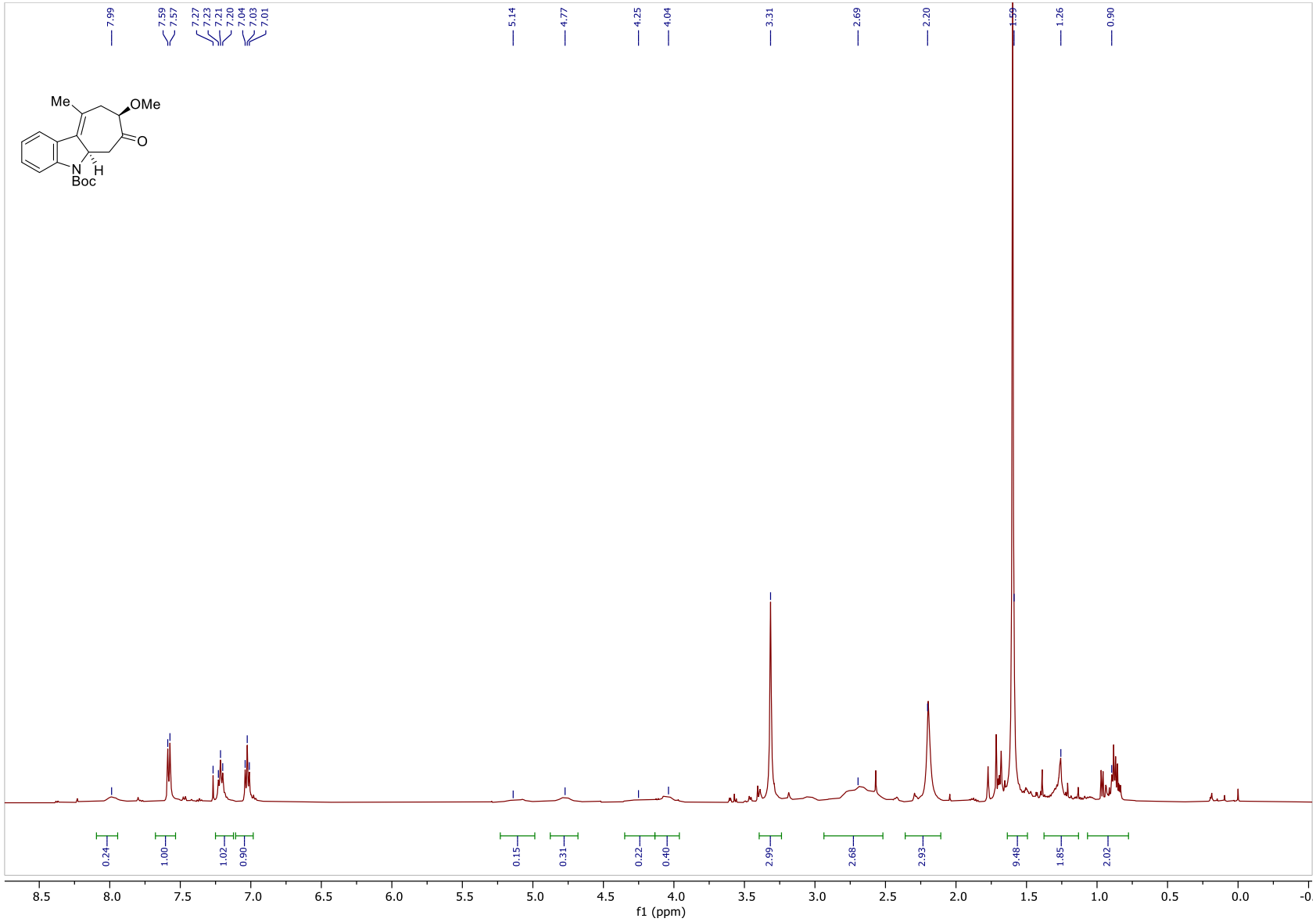

Figure 74: ^{1}H NMR Spectrum of **97b** (500MHz, $CDCl_3$)

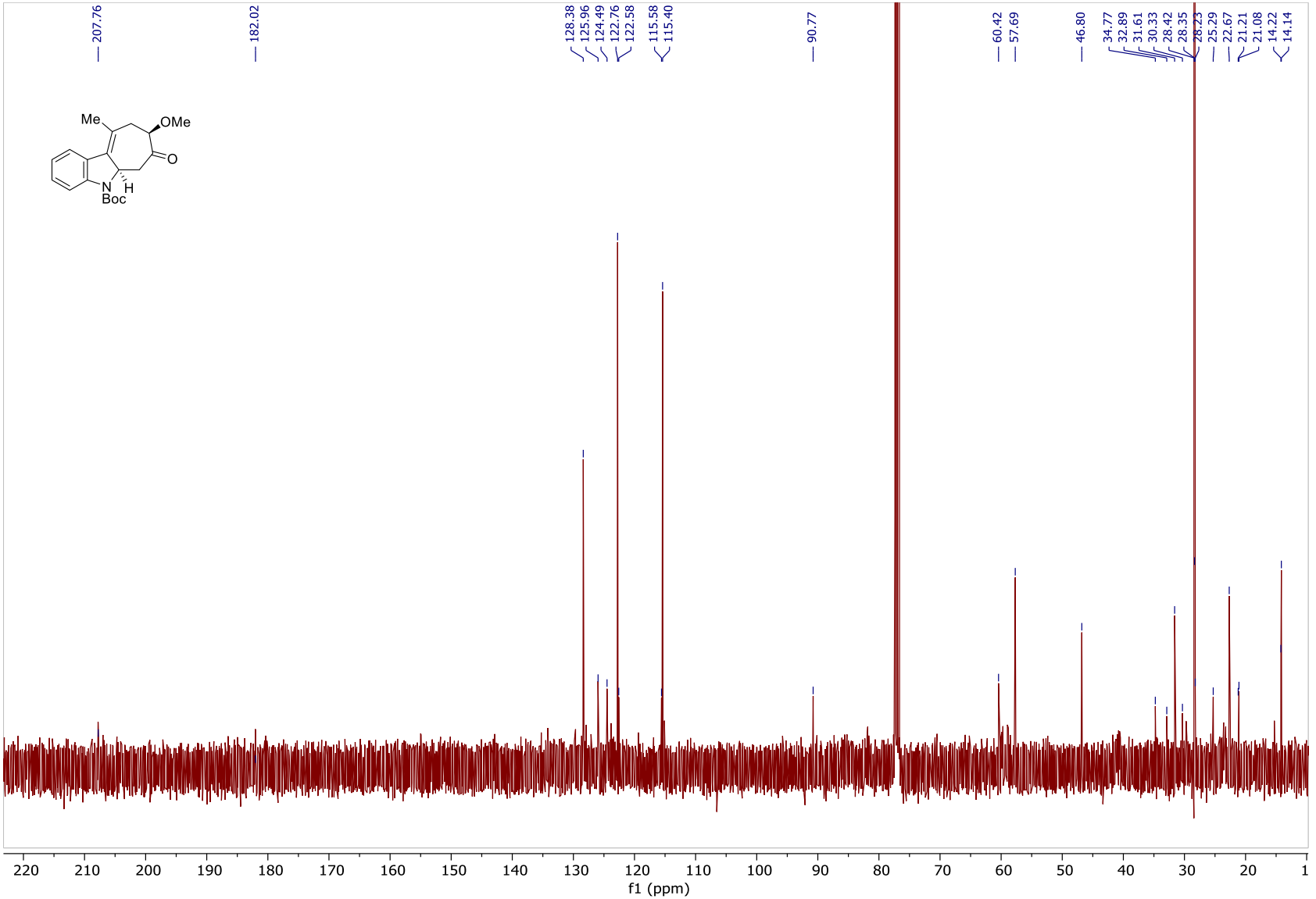

Figure 75: ^{13}C NMR Spectrum of **97b** (100MHz, $CDCl_3$)

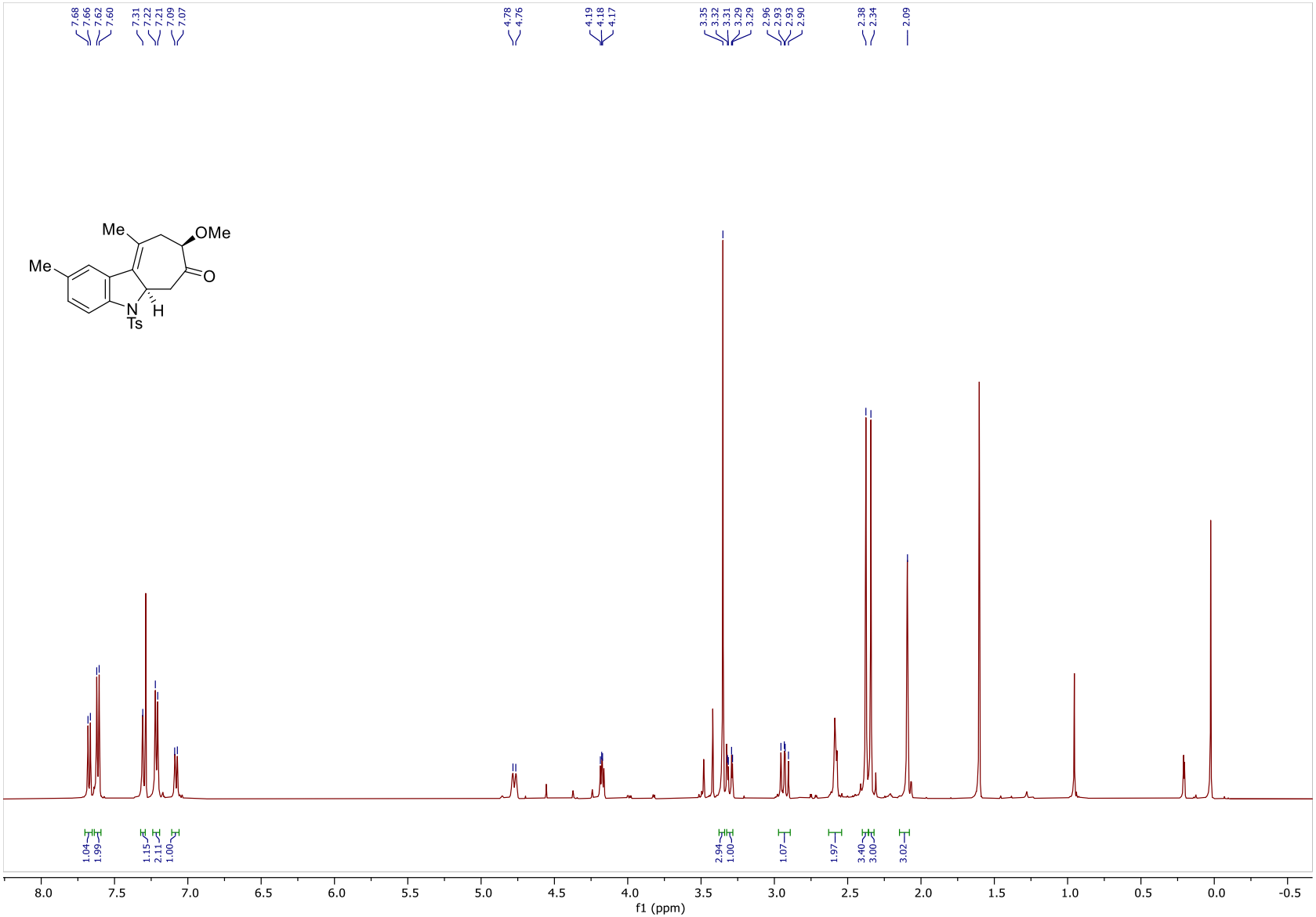

Figure 76: ^{1}H NMR Spectrum of **97c** (500MHz, $CDCl_3$)

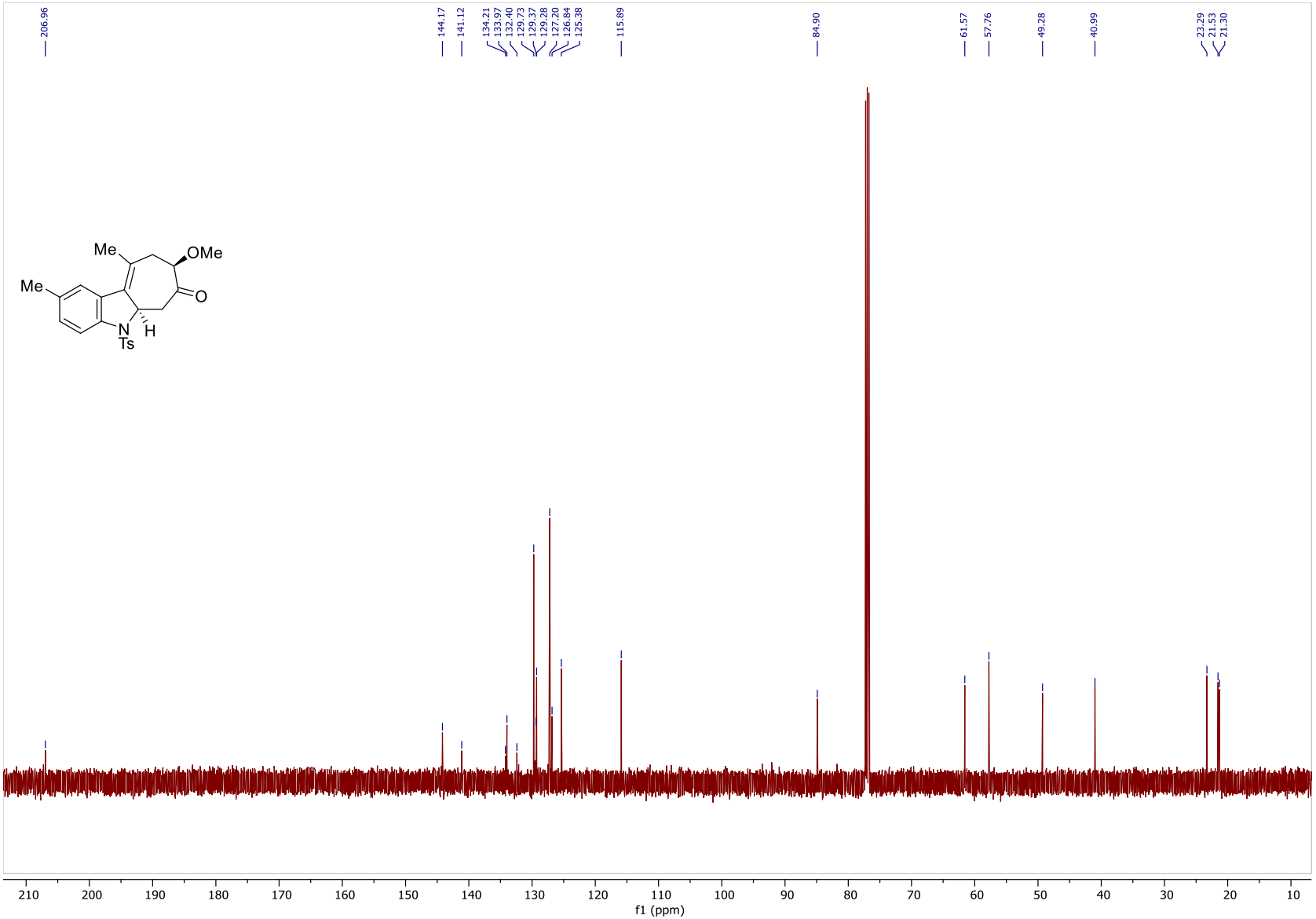

Figure 77: ^{13}C NMR Spectrum of **97c** (100MHz, $CDCl_3$)

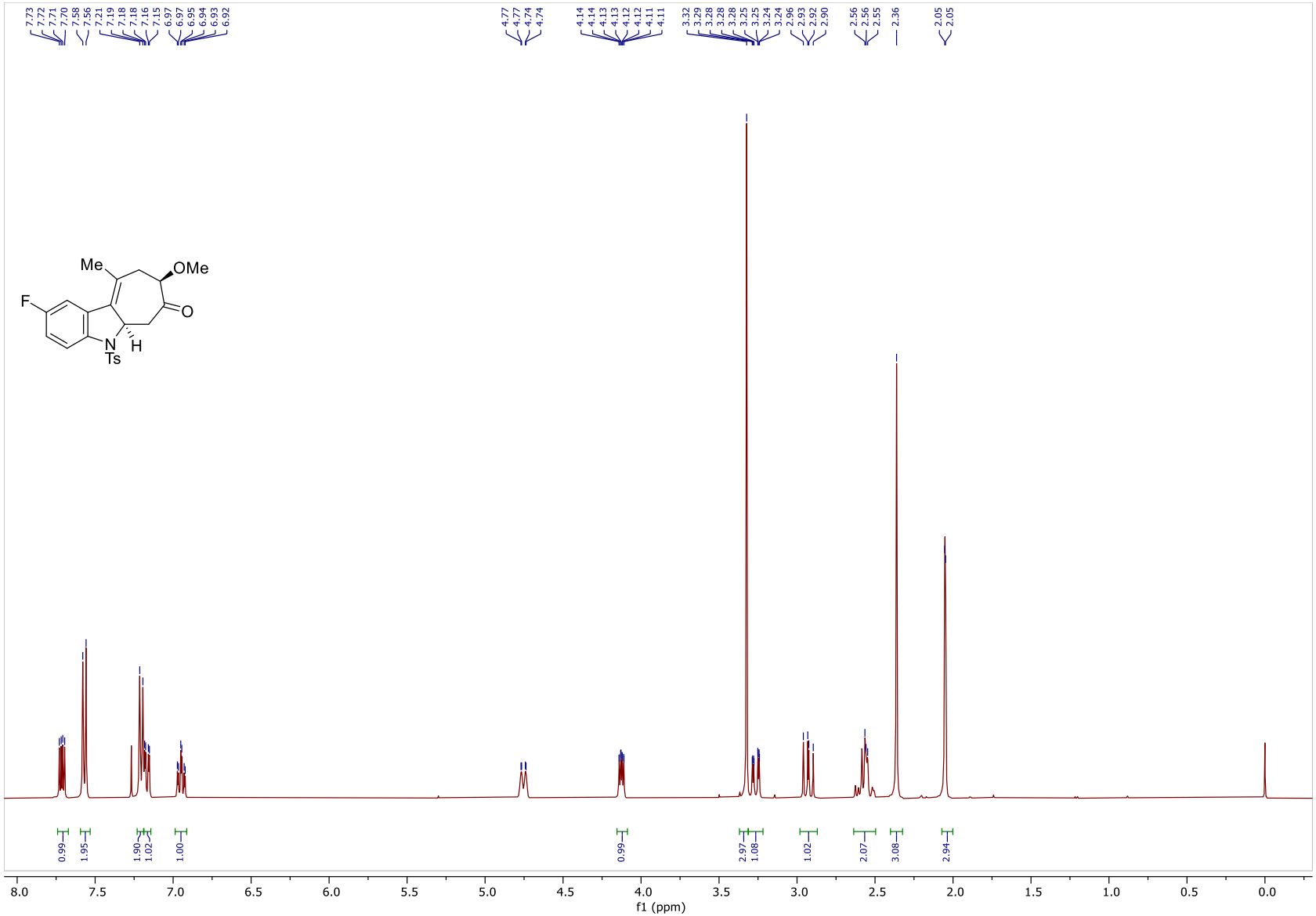

Figure 78: ^{1}H NMR Spectrum of **97d** (500MHz, $CDCl_3$)

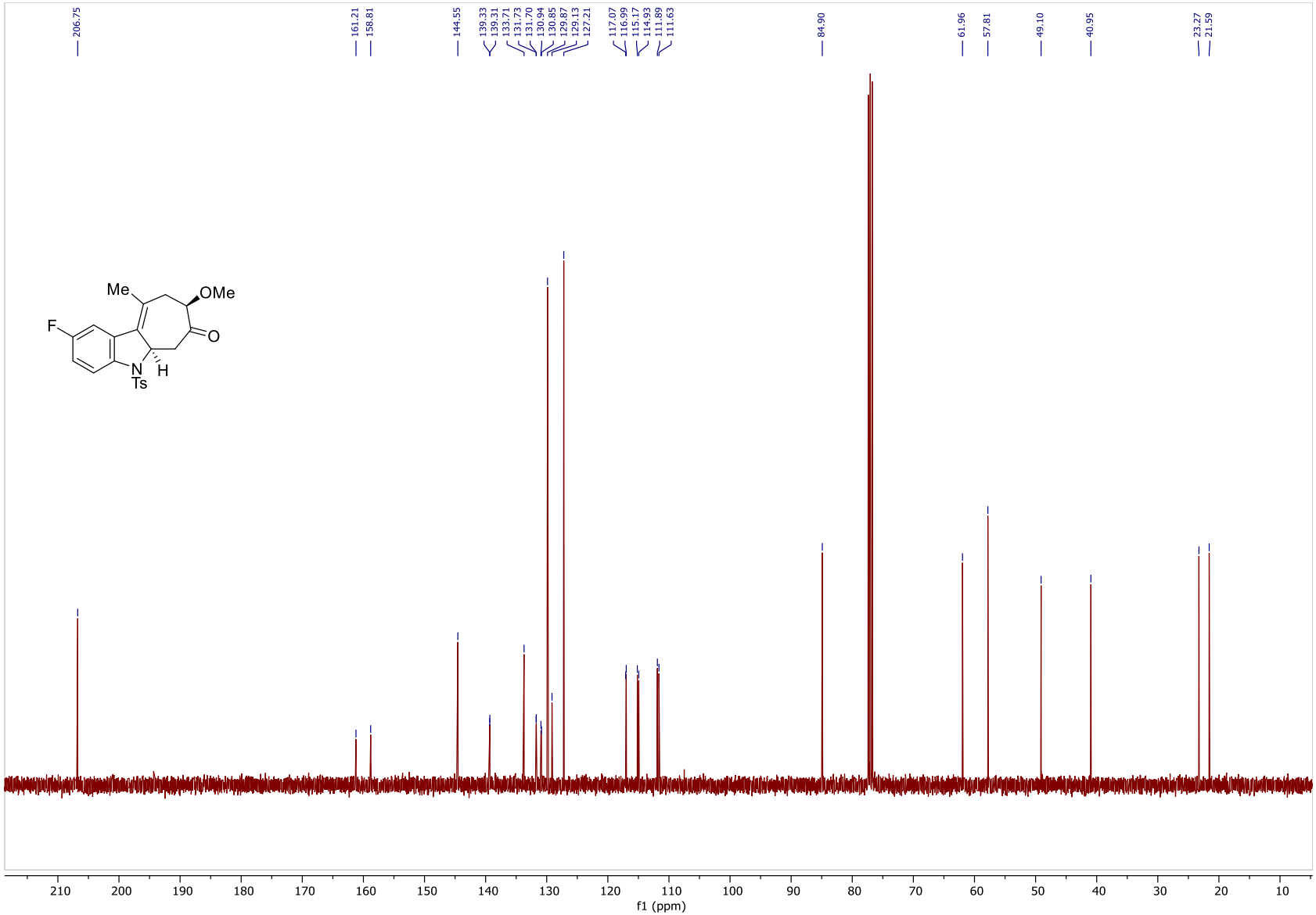

Figure 79: ^{13}C NMR Spectrum of **97d** (100MHz, $CDCl_3$)

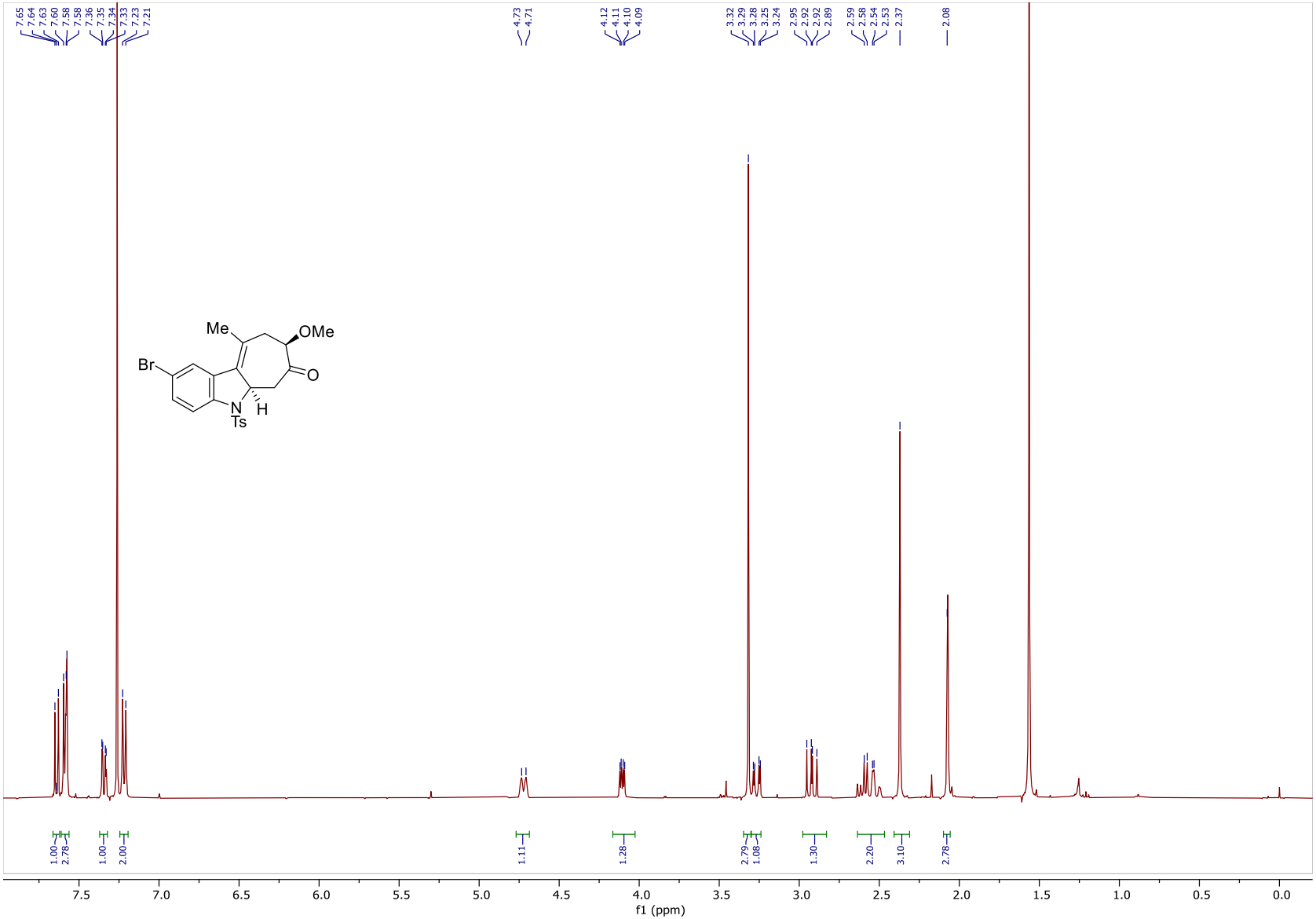

Figure 80: ^{1}H NMR Spectrum of **97e** (500MHz, $CDCl_3$)

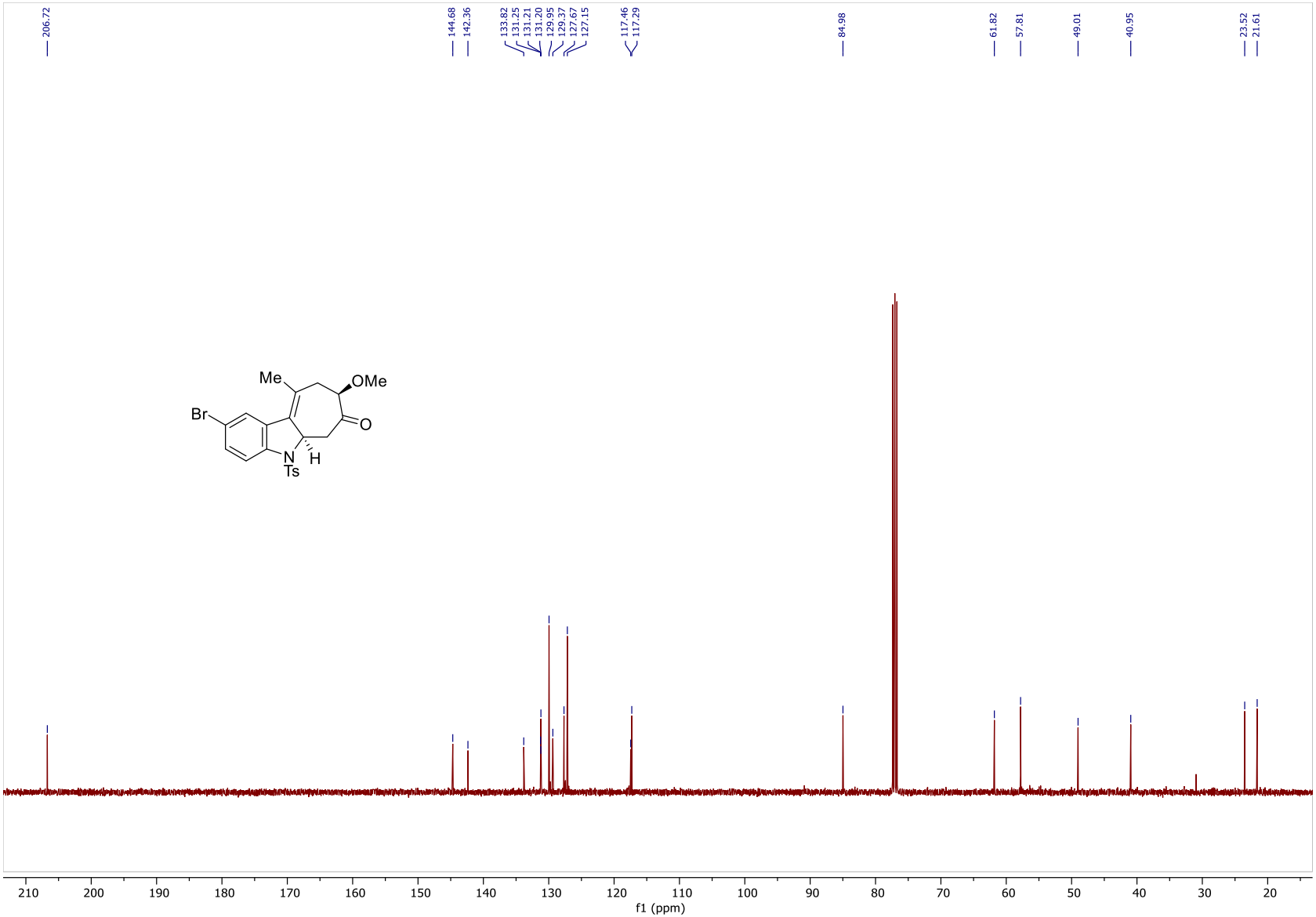

Figure 81: ^{13}C NMR Spectrum of **97e** (100MHz, $CDCl_3$)

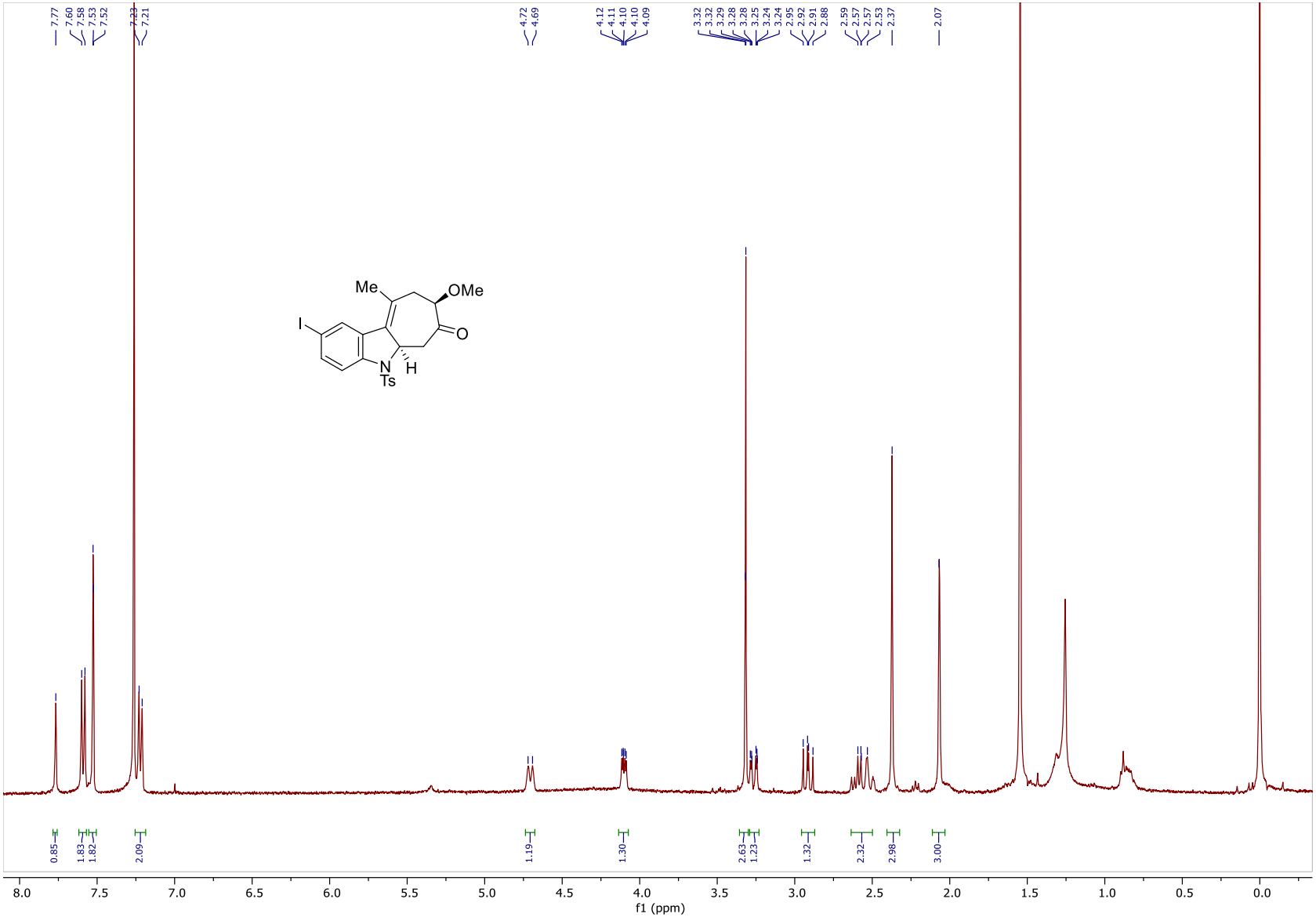

Figure 82: ^{1}H NMR Spectrum of **97f** (500MHz, $CDCl_3$)

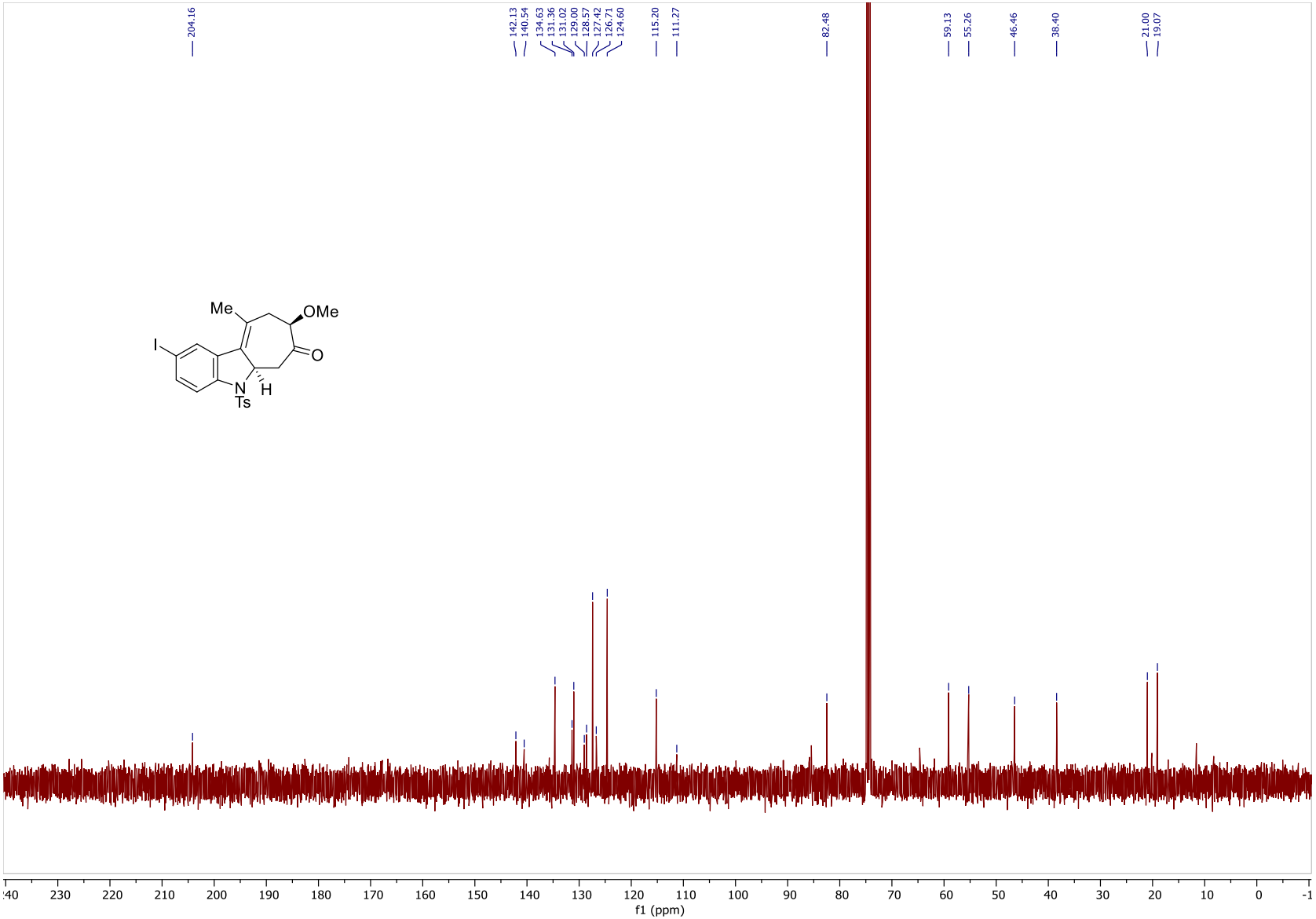

Figure 83: ^{13}C NMR Spectrum of **97f** (100MHz, $CDCl_3$)

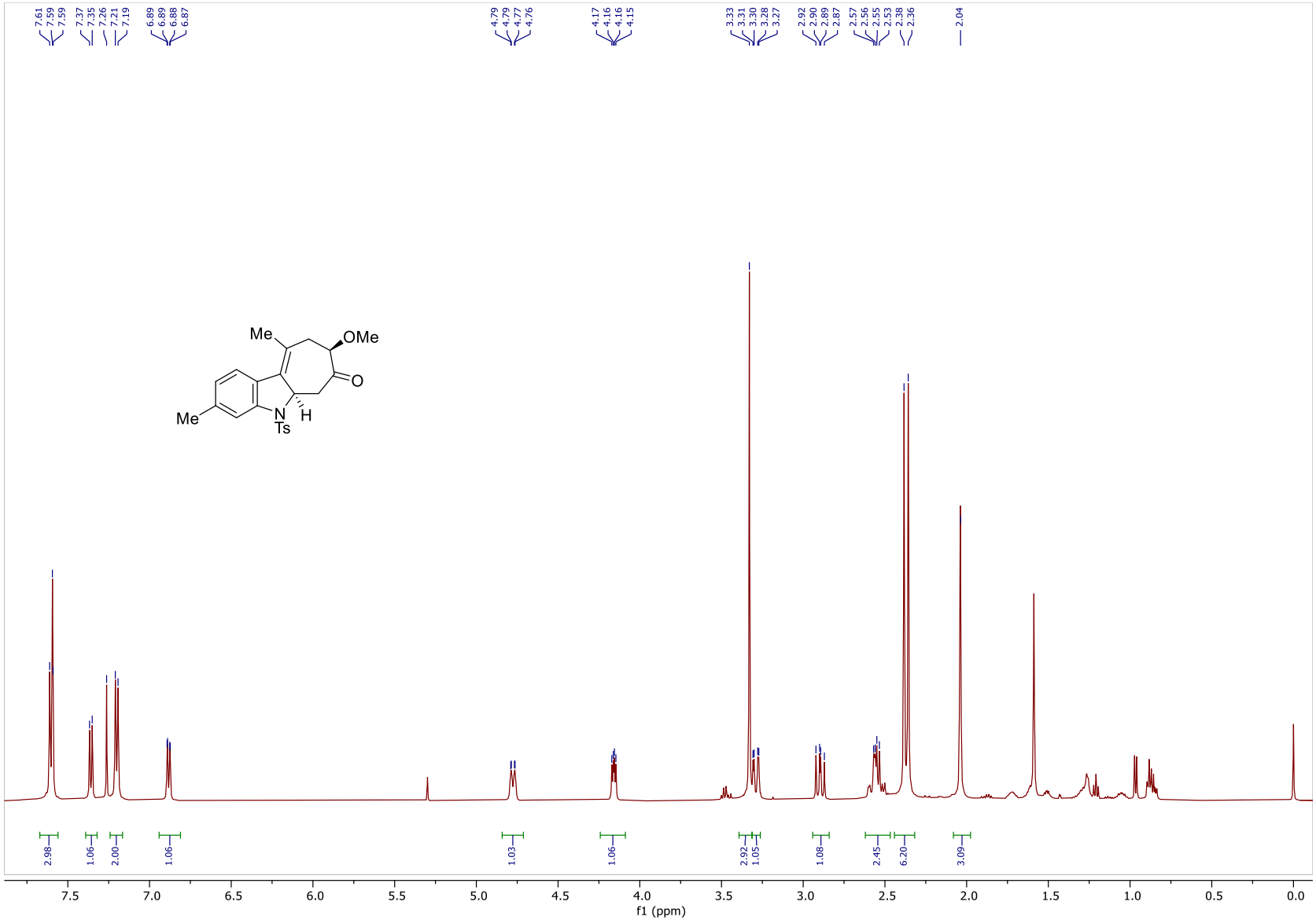

Figure 84: ^{1}H NMR Spectrum of **97g** (500MHz, $CDCl_3$)

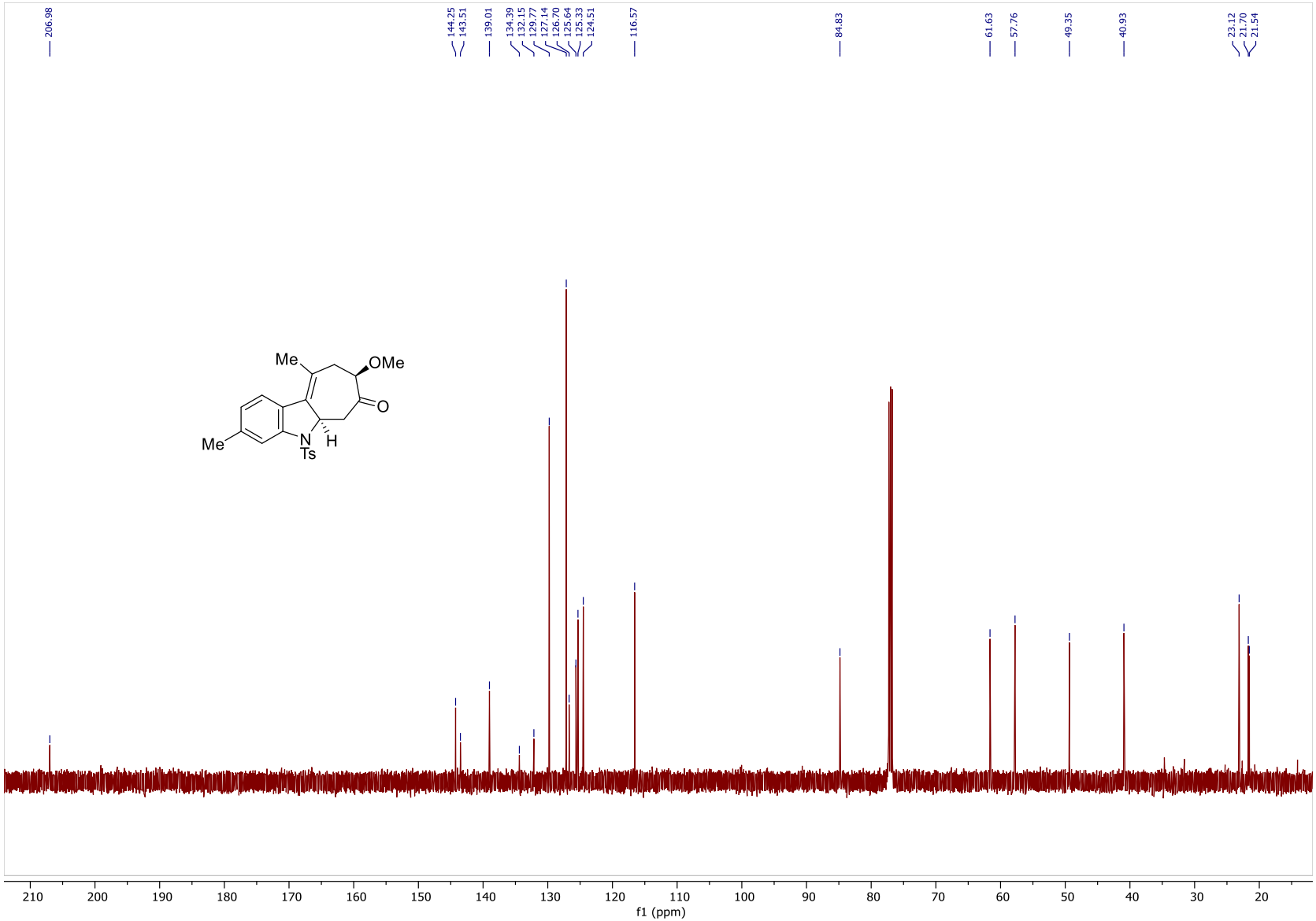

Figure 85: ^{13}C NMR Spectrum of **97g** (100MHz, $CDCl_3$)

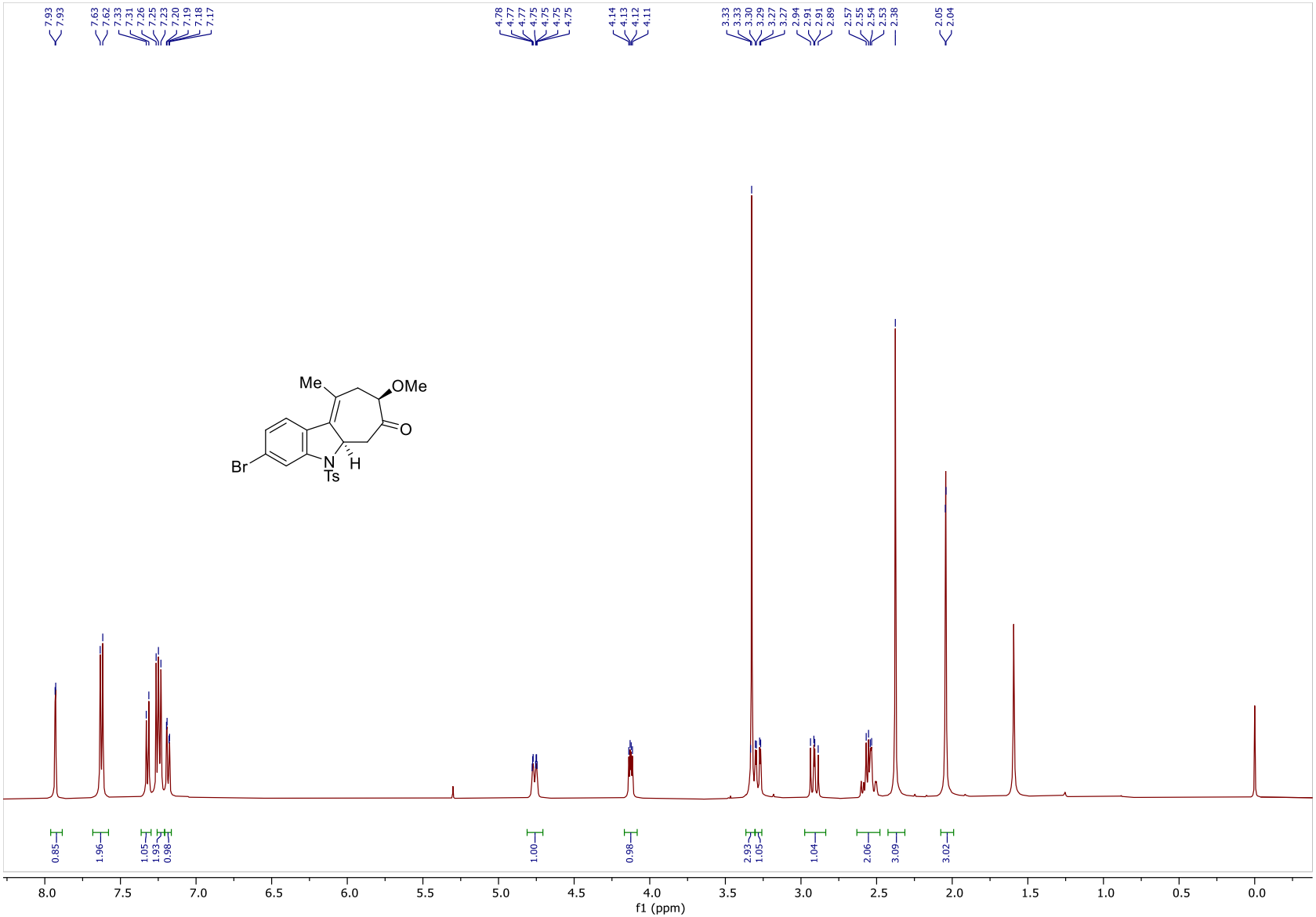

Figure 86: ^{1}H NMR Spectrum of **97h** (500MHz, $CDCl_3$)

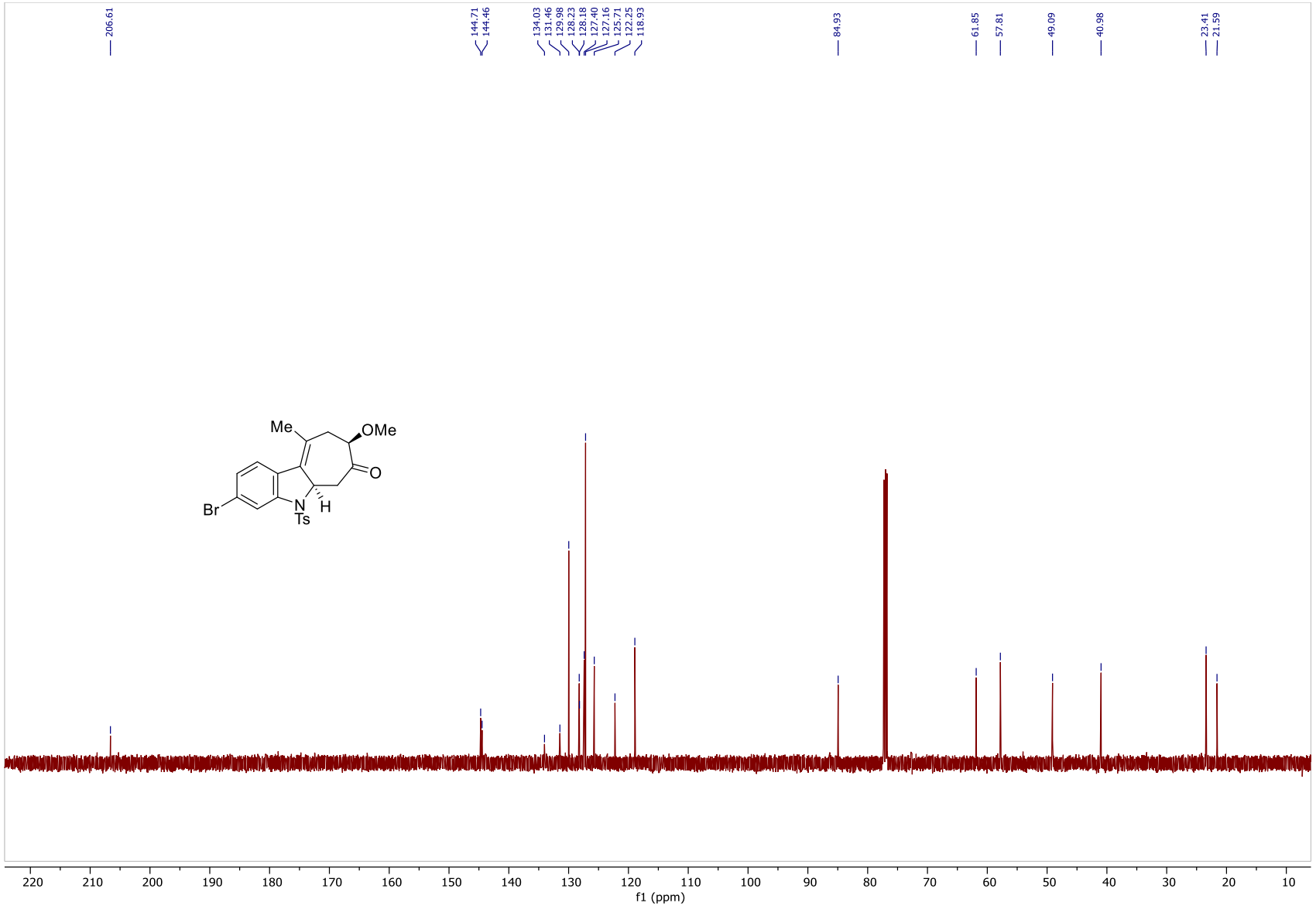

Figure 87: ^{13}C NMR Spectrum of **97h** (100MHz, $CDCl_3$)

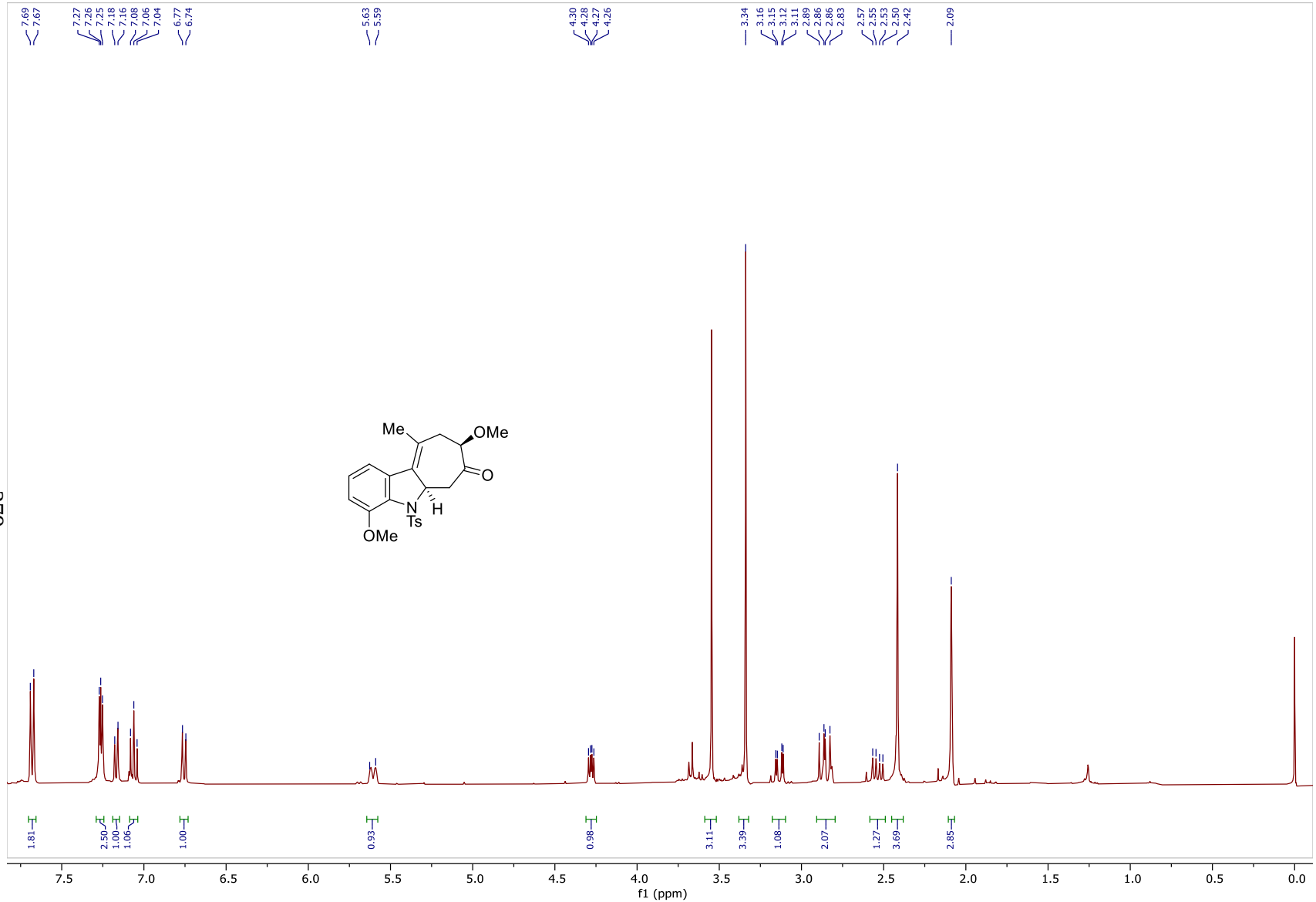

279

Figure 88: ^{1}H NMR Spectrum of **97i** (400MHz, $CDCl_3$)

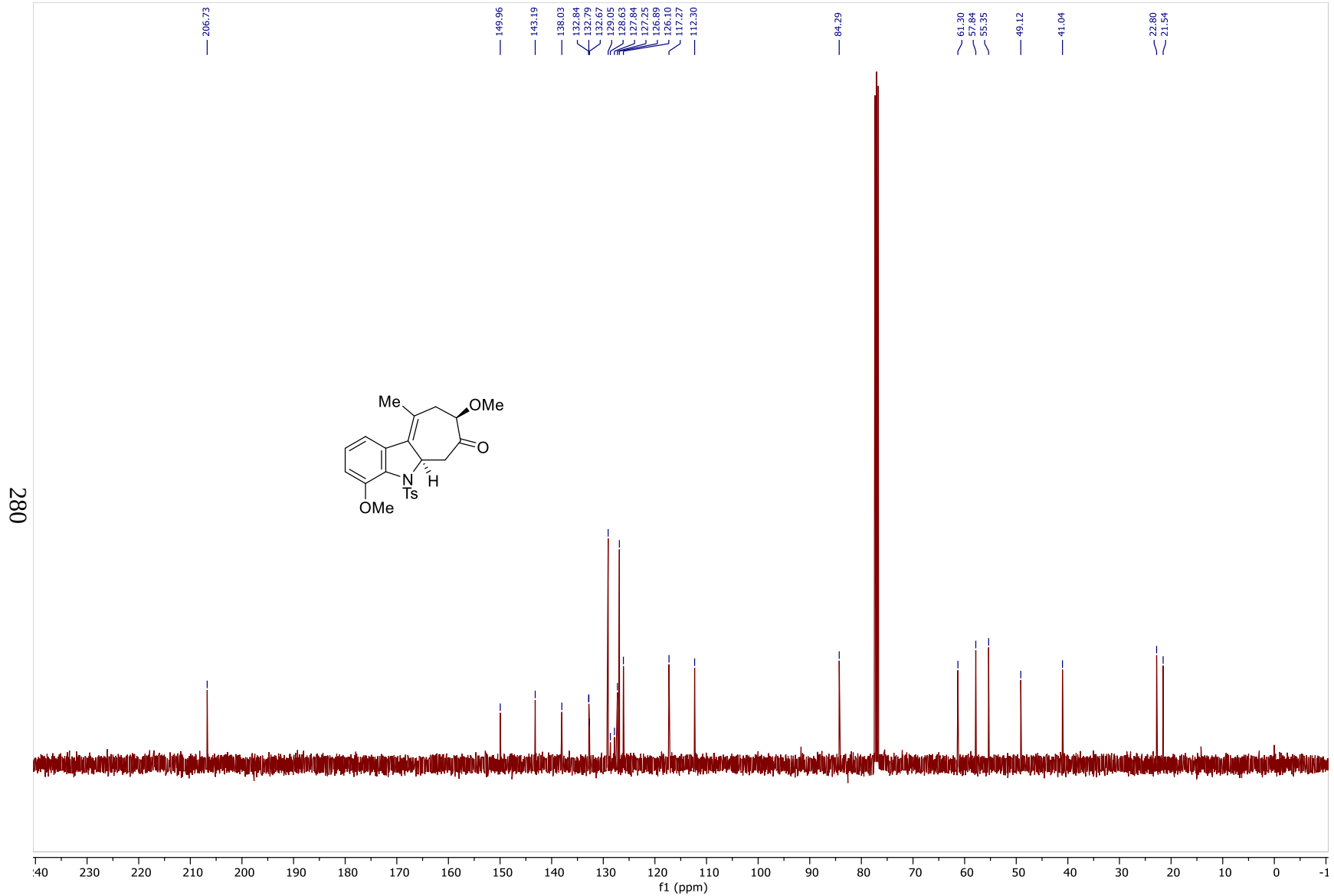

Figure 89: ^{13}C NMR Spectrum of **97i** (100MHz, $CDCl_3$)

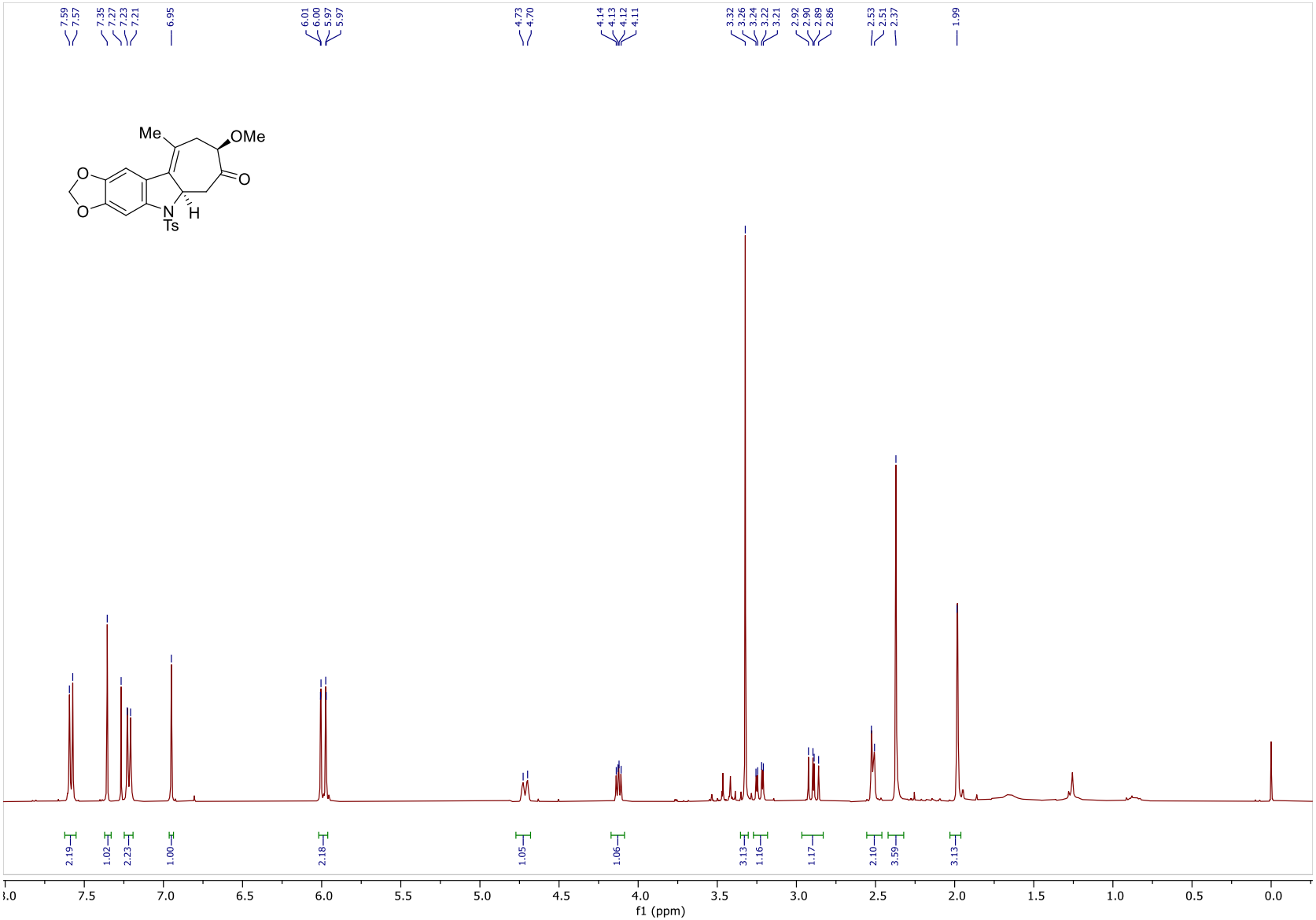

Figure 90: ^{1}H NMR Spectrum of **97j** (500MHz, $CDCl_3$)

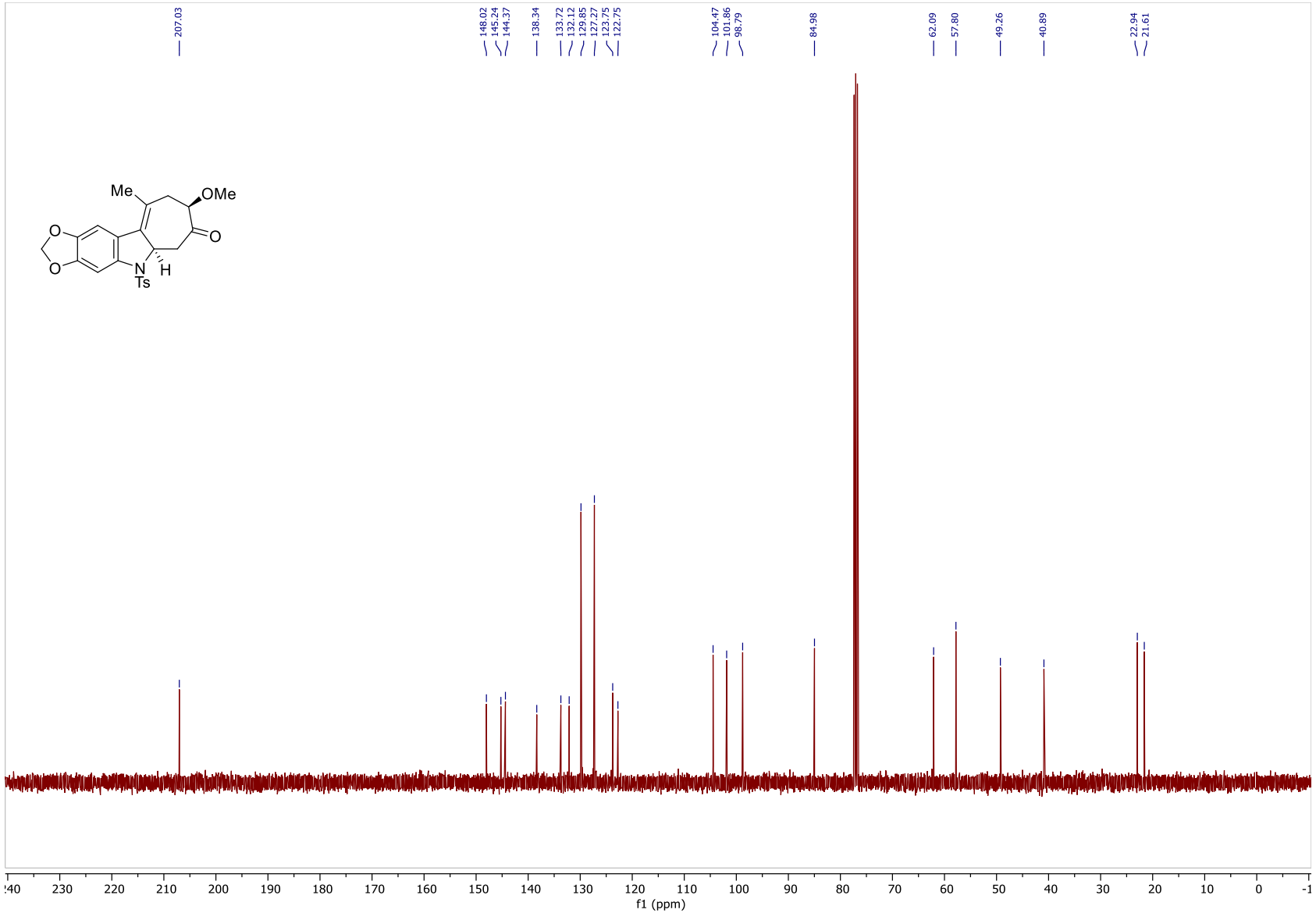

Figure 91: ^{13}C NMR Spectrum of **97j** (100MHz, $CDCl_3$)

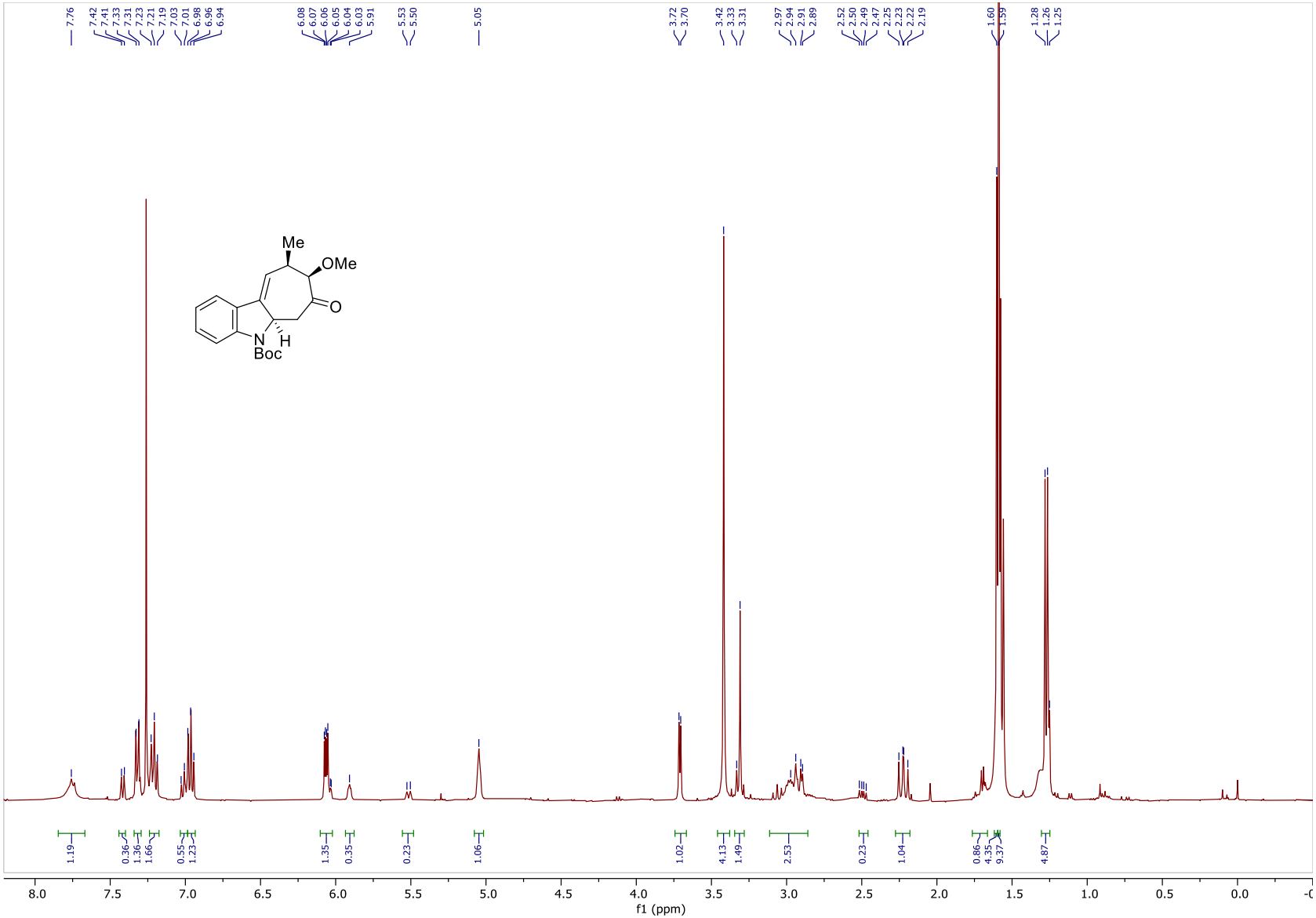

Figure 92: ^{1}H NMR Spectrum of **97k** (400MHz, $CDCl_3$)

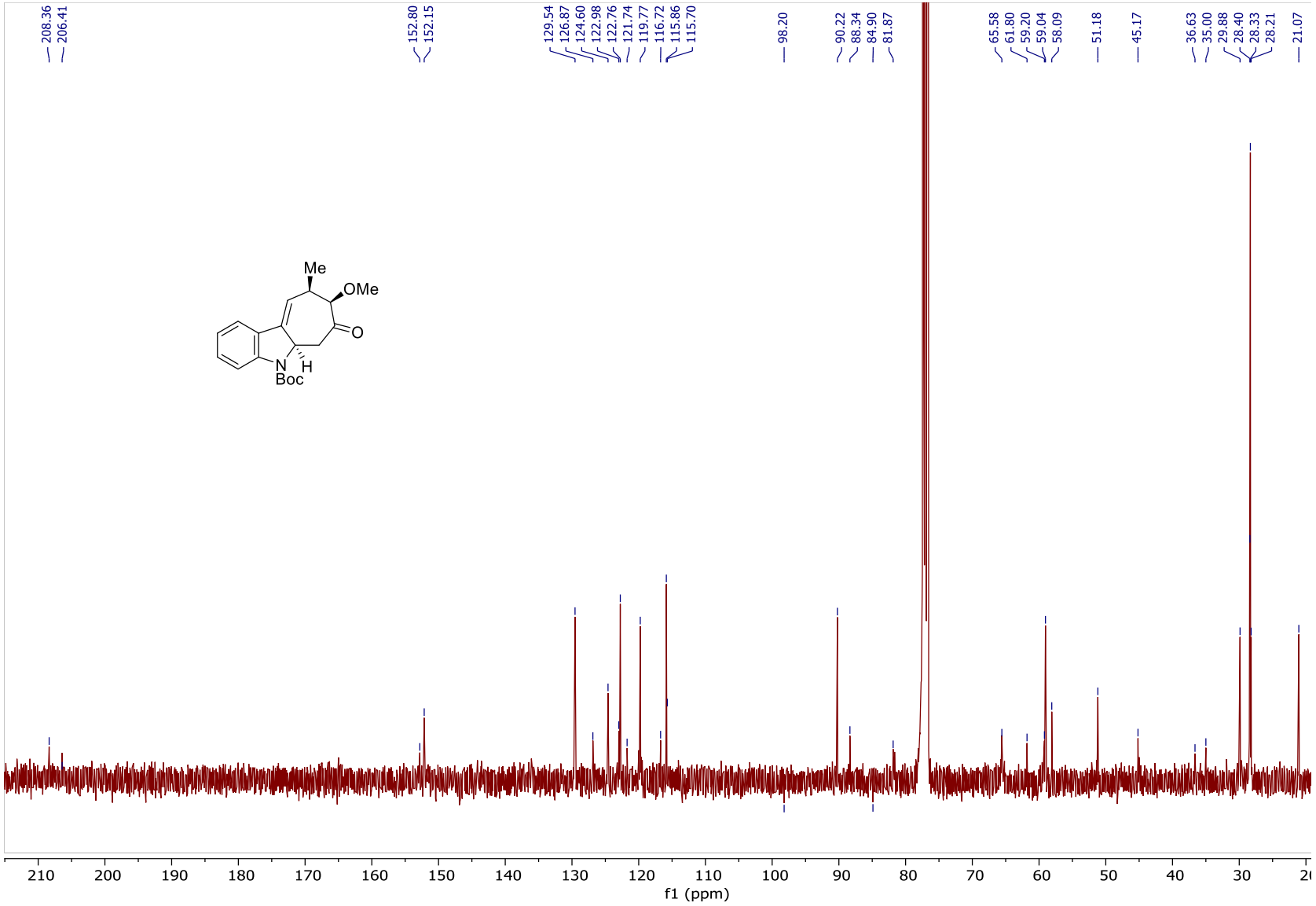

Figure 93: ^{13}C NMR Spectrum of **97k** (100MHz, $CDCl_3$)

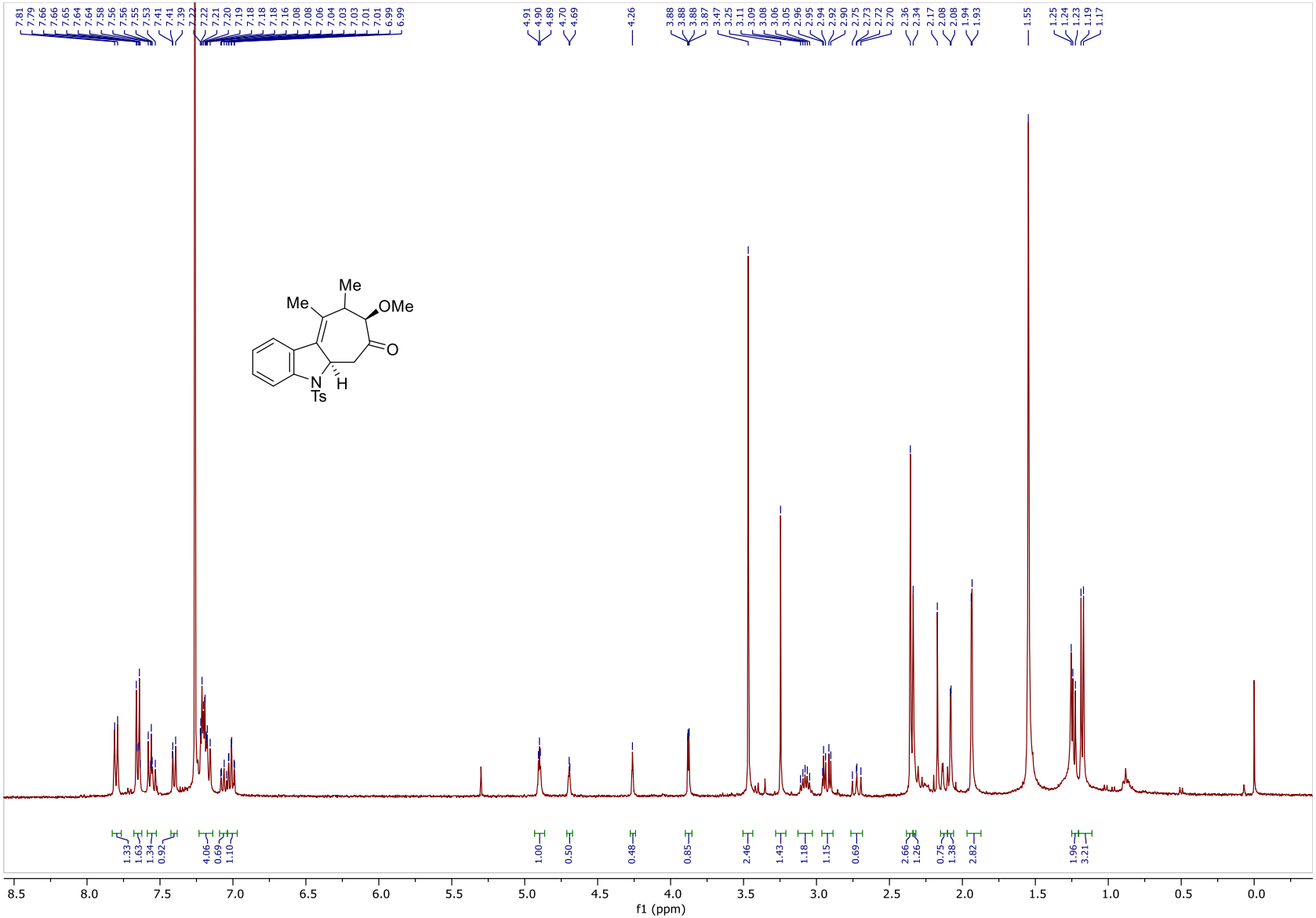

Figure 94: ^{1}H NMR Spectrum of **97l** (400MHz, $CDCl_3$)

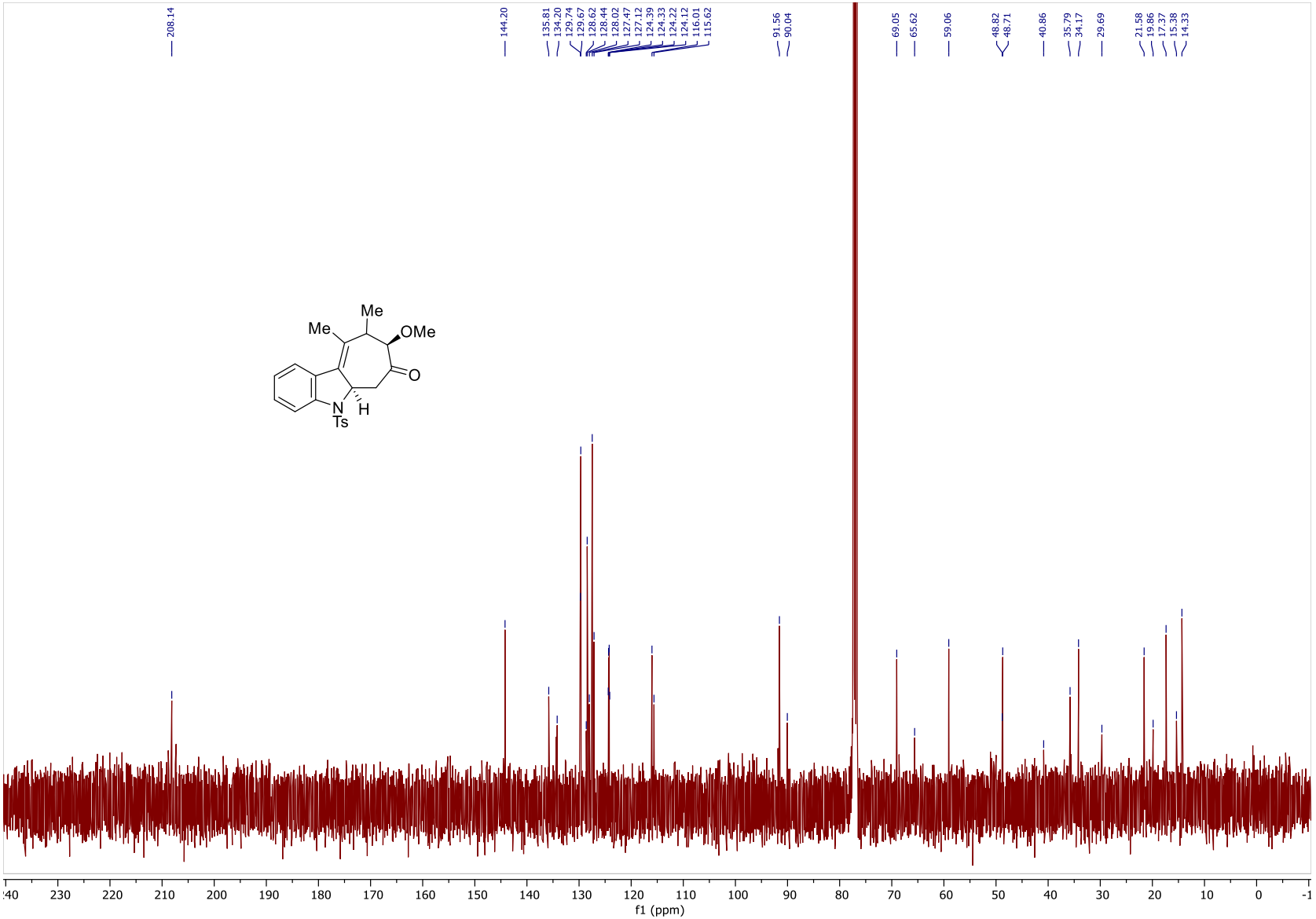

Figure 95: ^{13}C NMR Spectrum of **97l** (100MHz, $CDCl_3$)

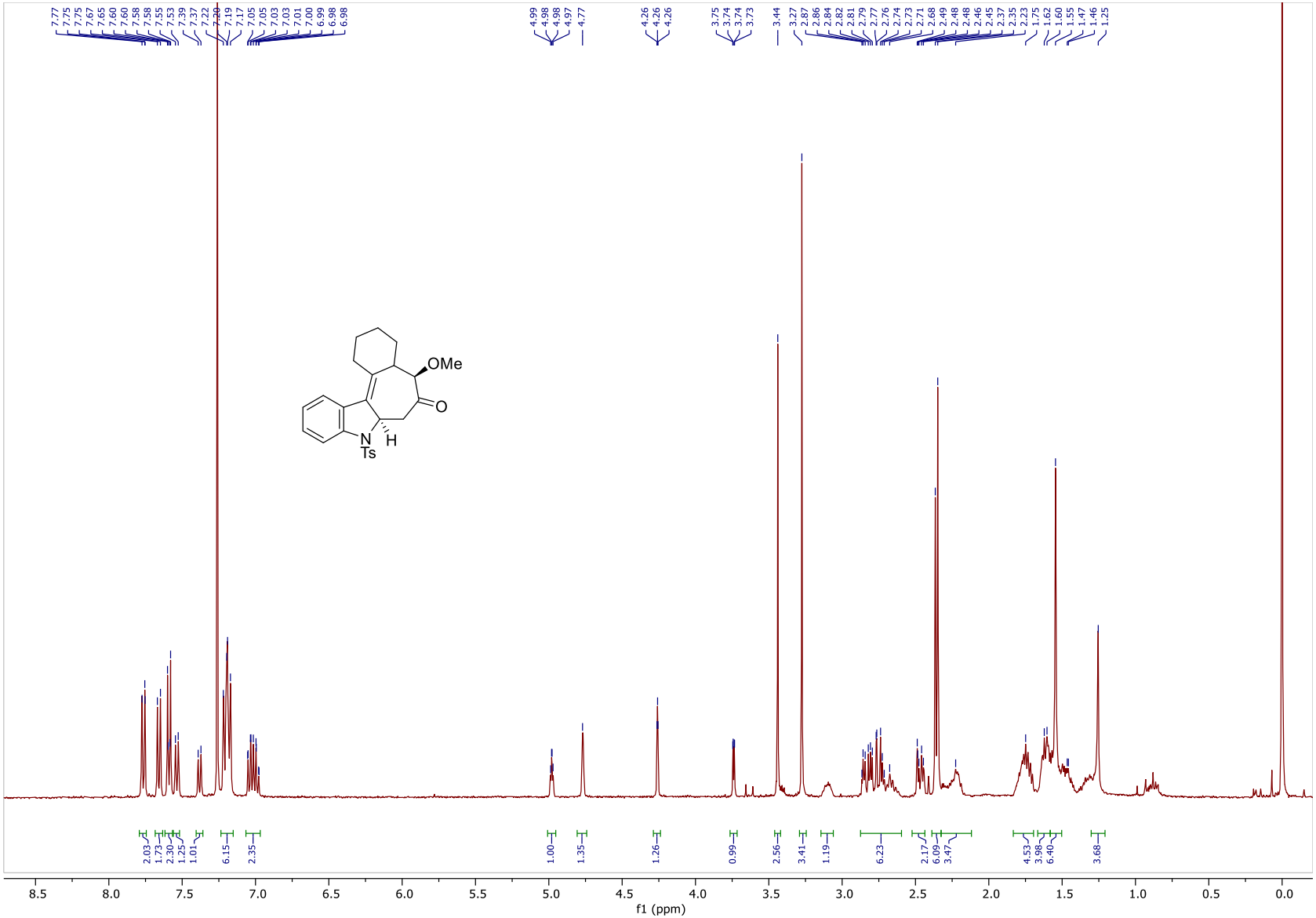

Figure 96: ^{1}H NMR Spectrum of **97m** (400MHz, $CDCl_3$)

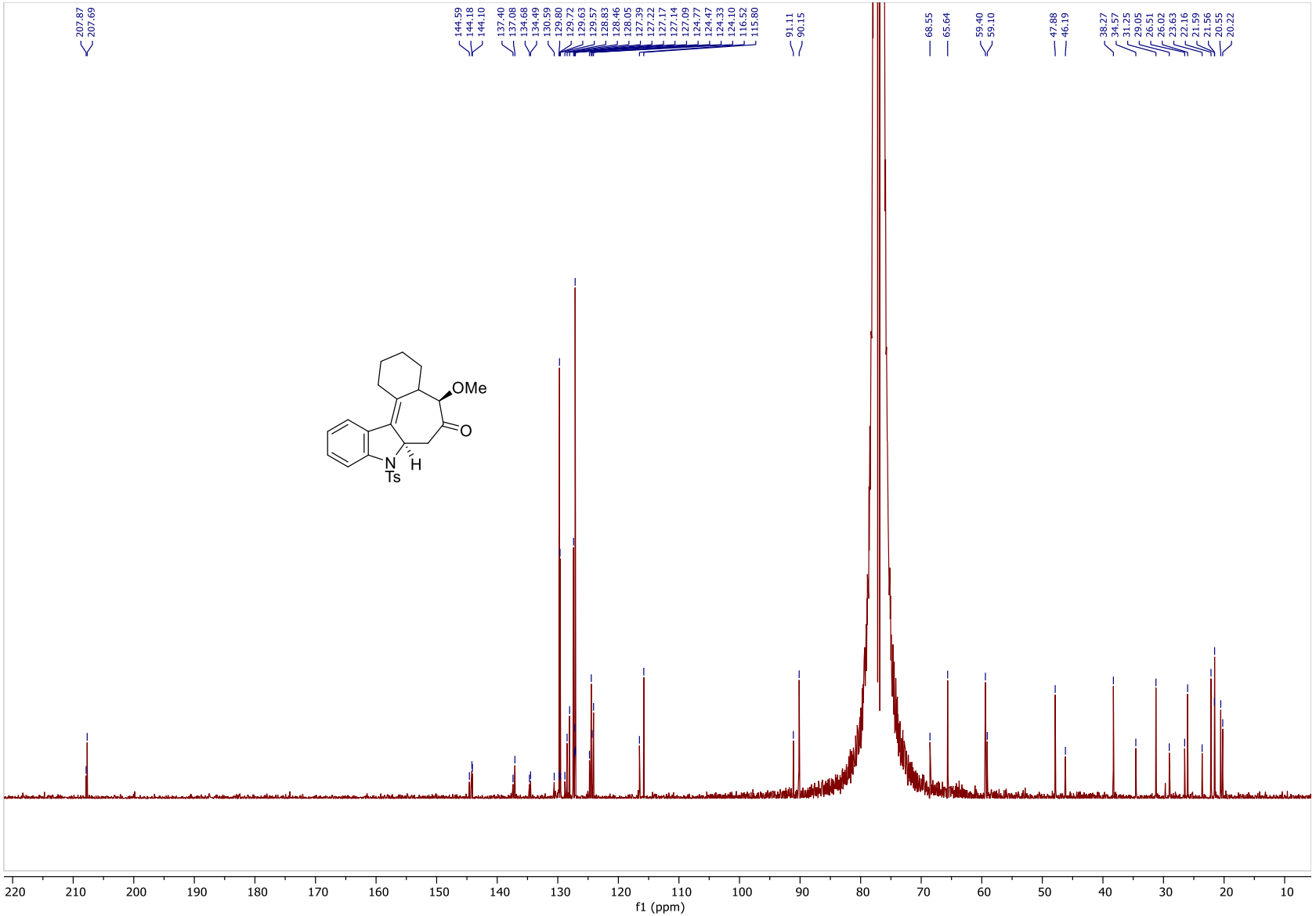

Figure 97: ^{13}C NMR Spectrum of **97m** (100MHz, $CDCl_3$)

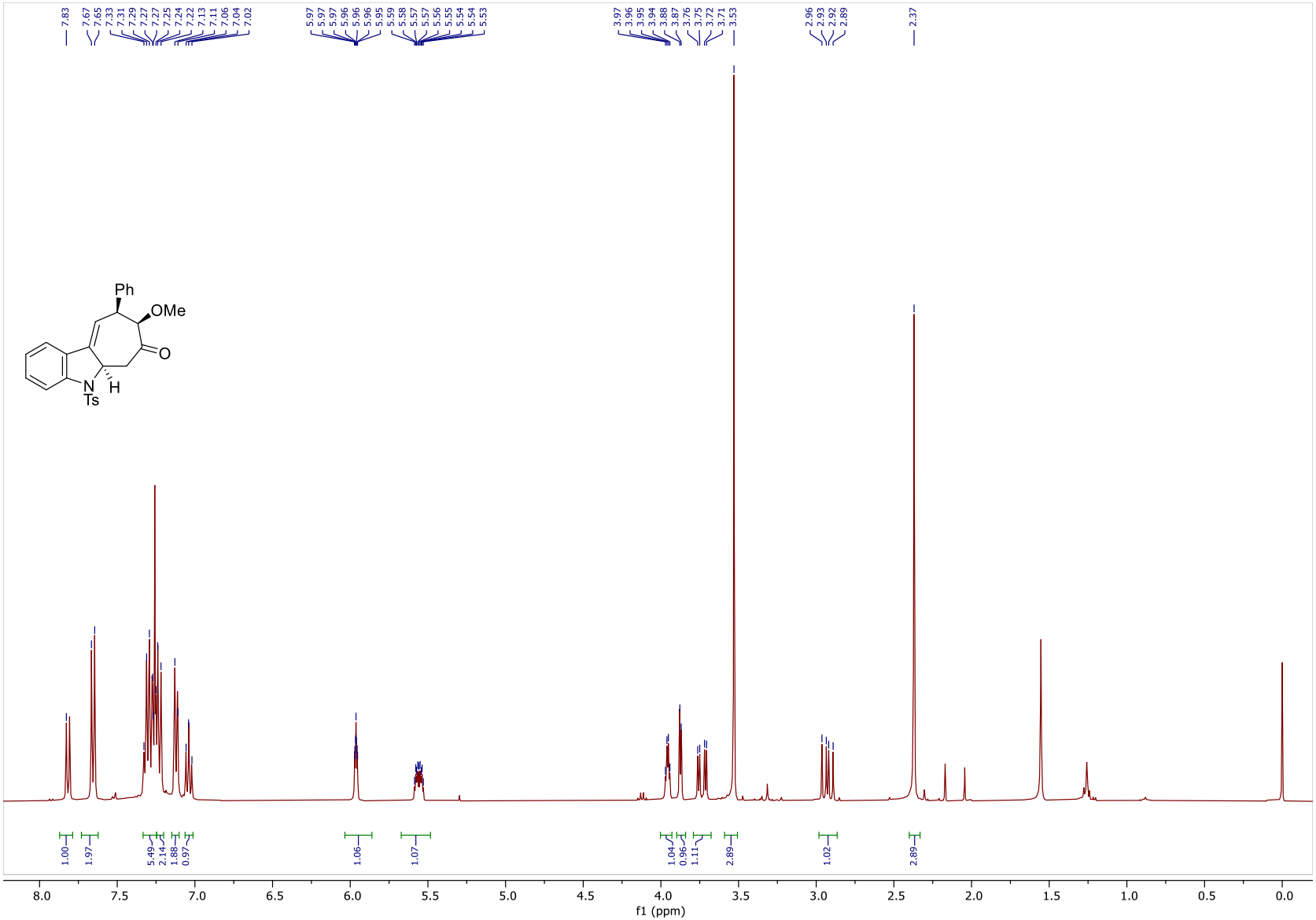

Figure 98: ^{1}H NMR Spectrum of **97n** (400MHz, $CDCl_3$)

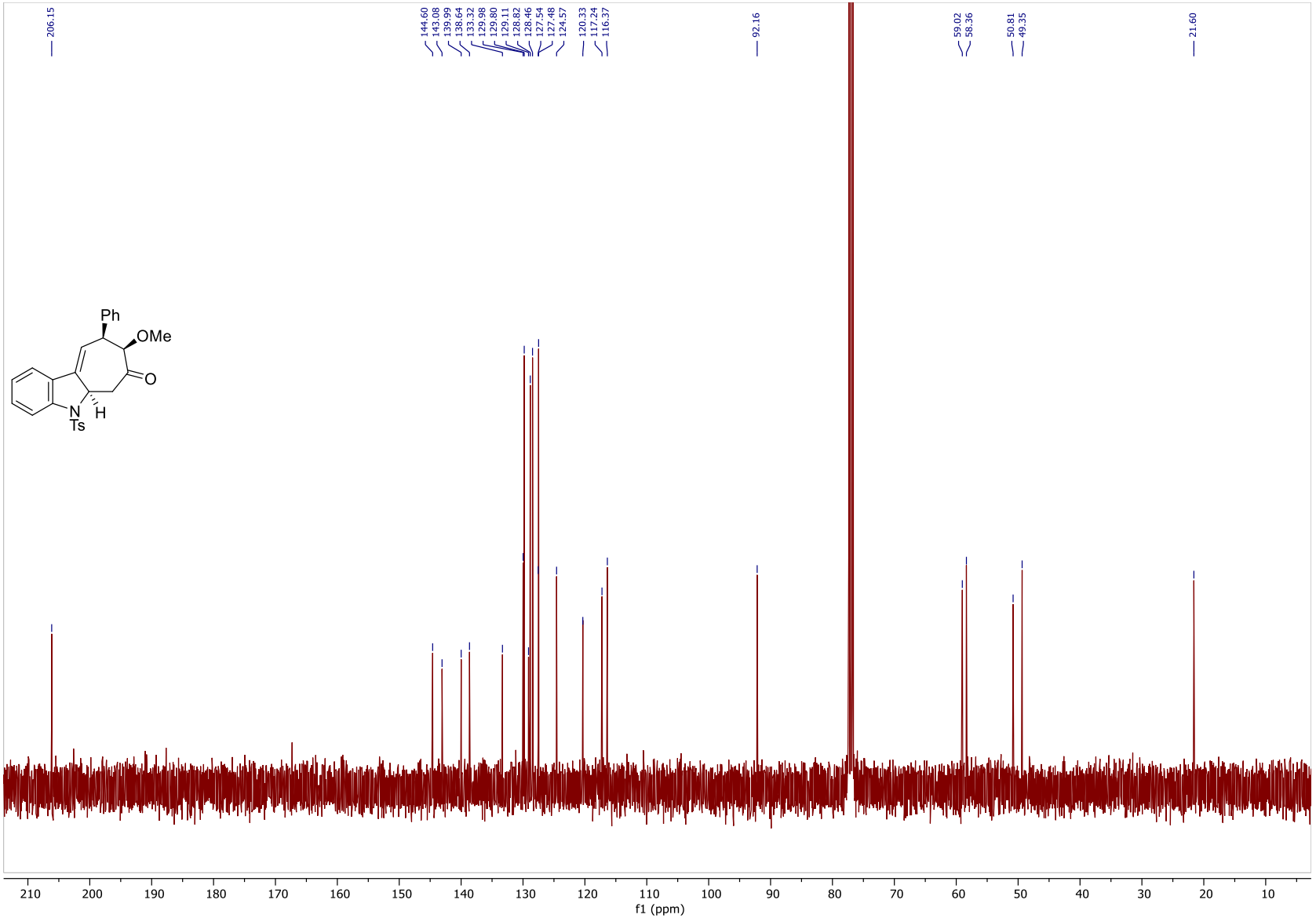

Figure 99: ^{13}C NMR Spectrum of **97n** (100MHz, $CDCl_3$)

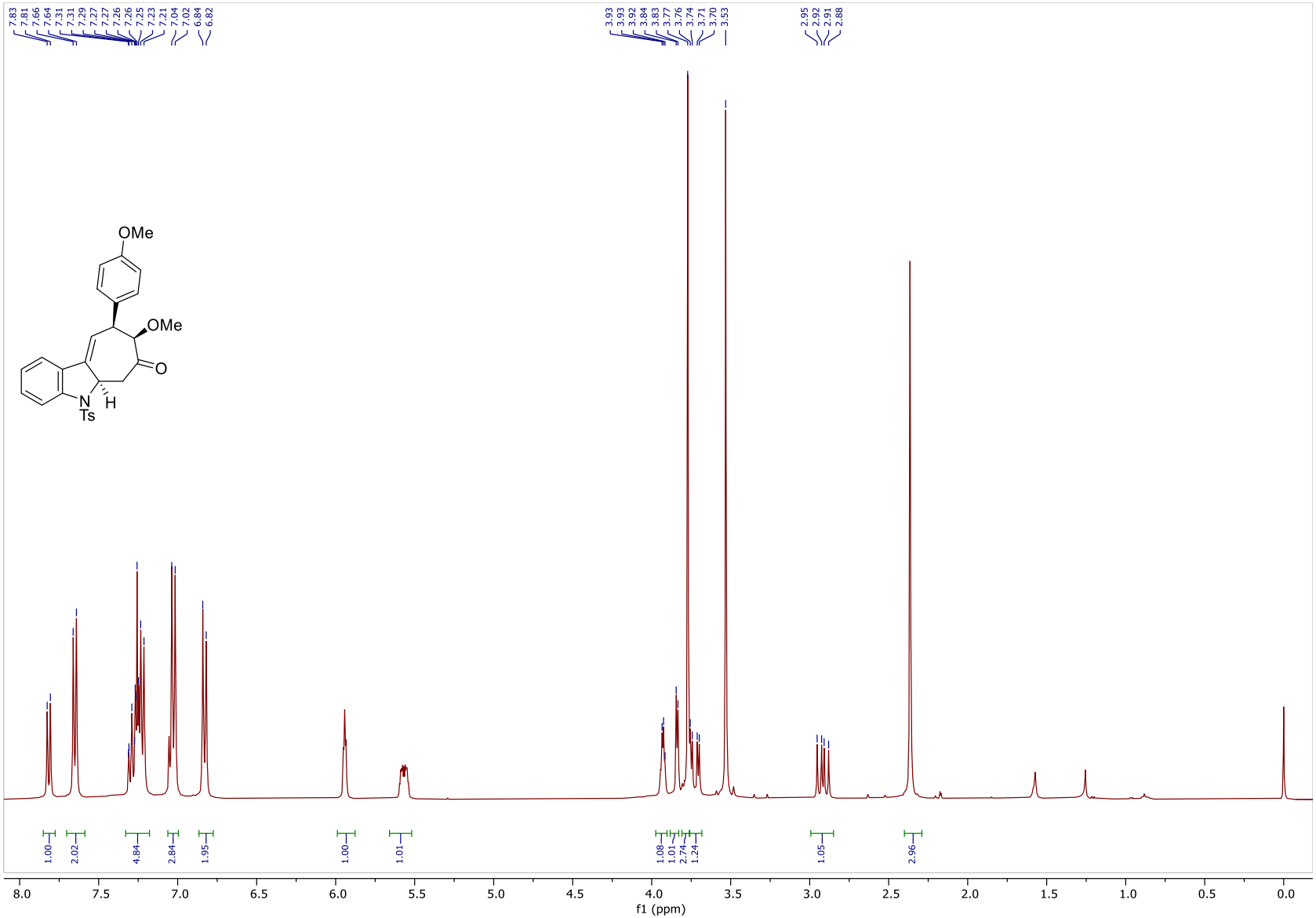

Figure 100: ^{1}H NMR Spectrum of **97o** (400MHz, $CDCl_3$)

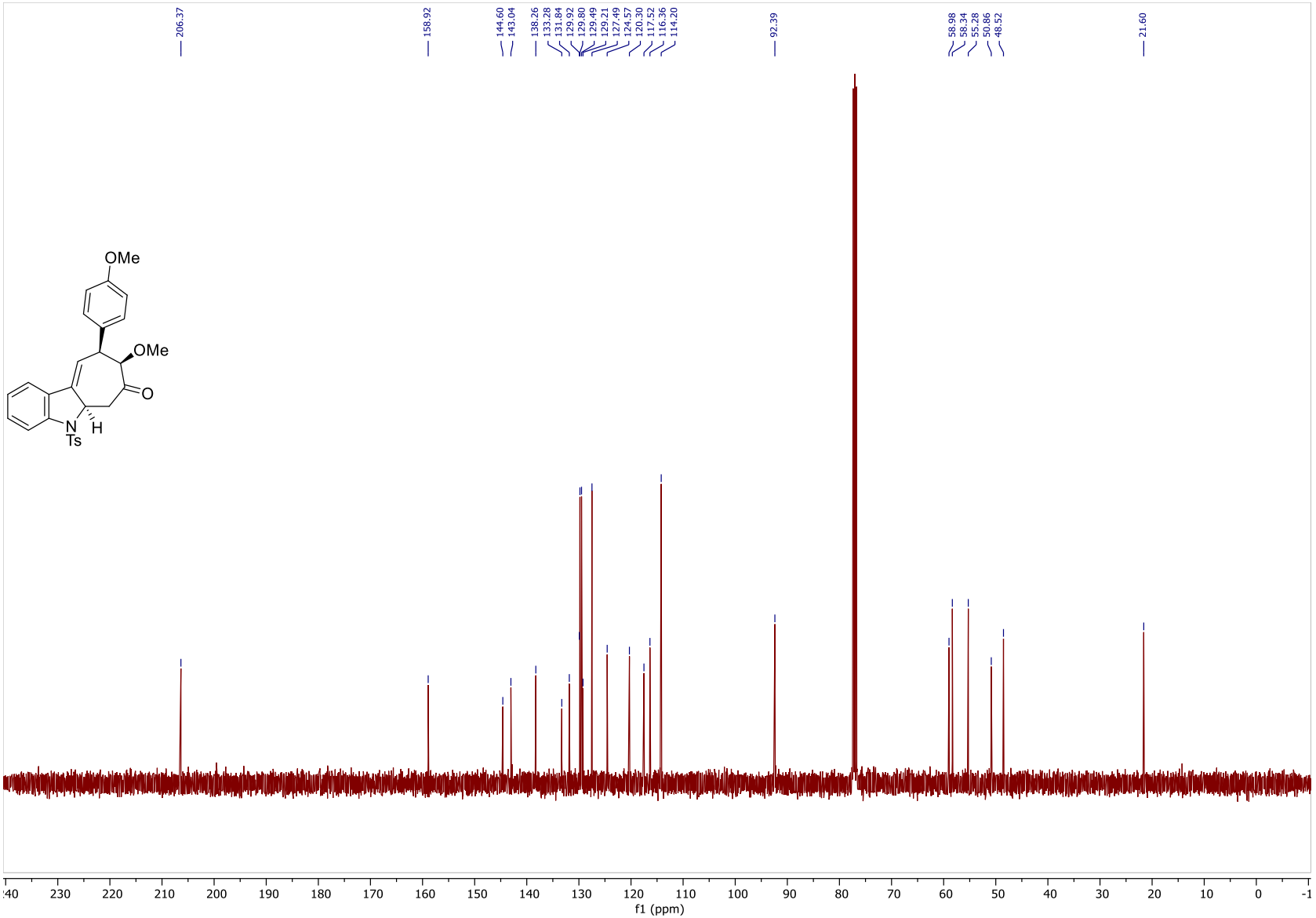

Figure 101: ^{13}C NMR Spectrum of **97o** (100MHz, $CDCl_3$)

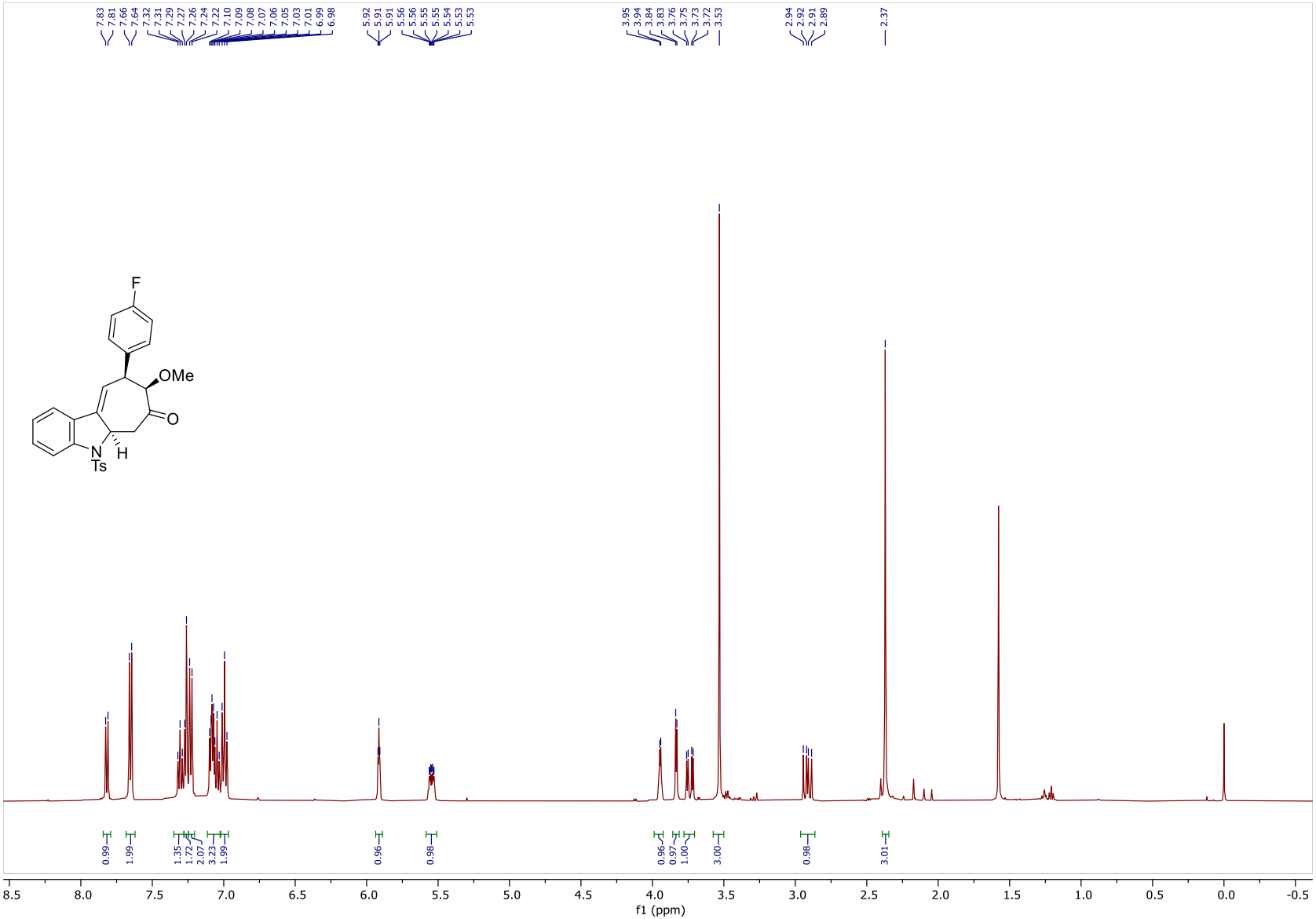

Figure 102: ^{1}H NMR Spectrum of **97p** (400MHz, $CDCl_3$)

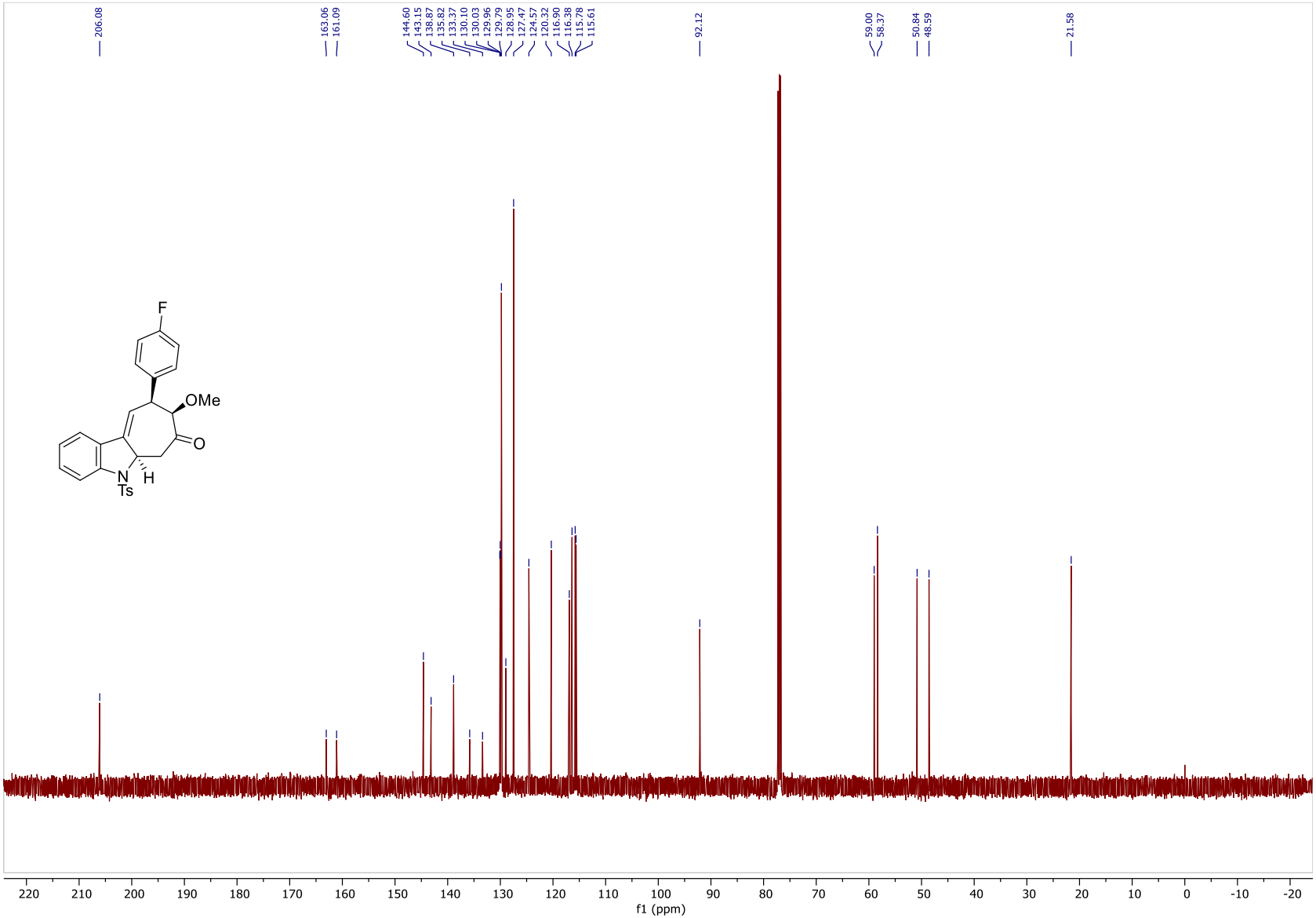

Figure 103: ^{13}C NMR Spectrum of **97p** (100MHz, $CDCl_3$)

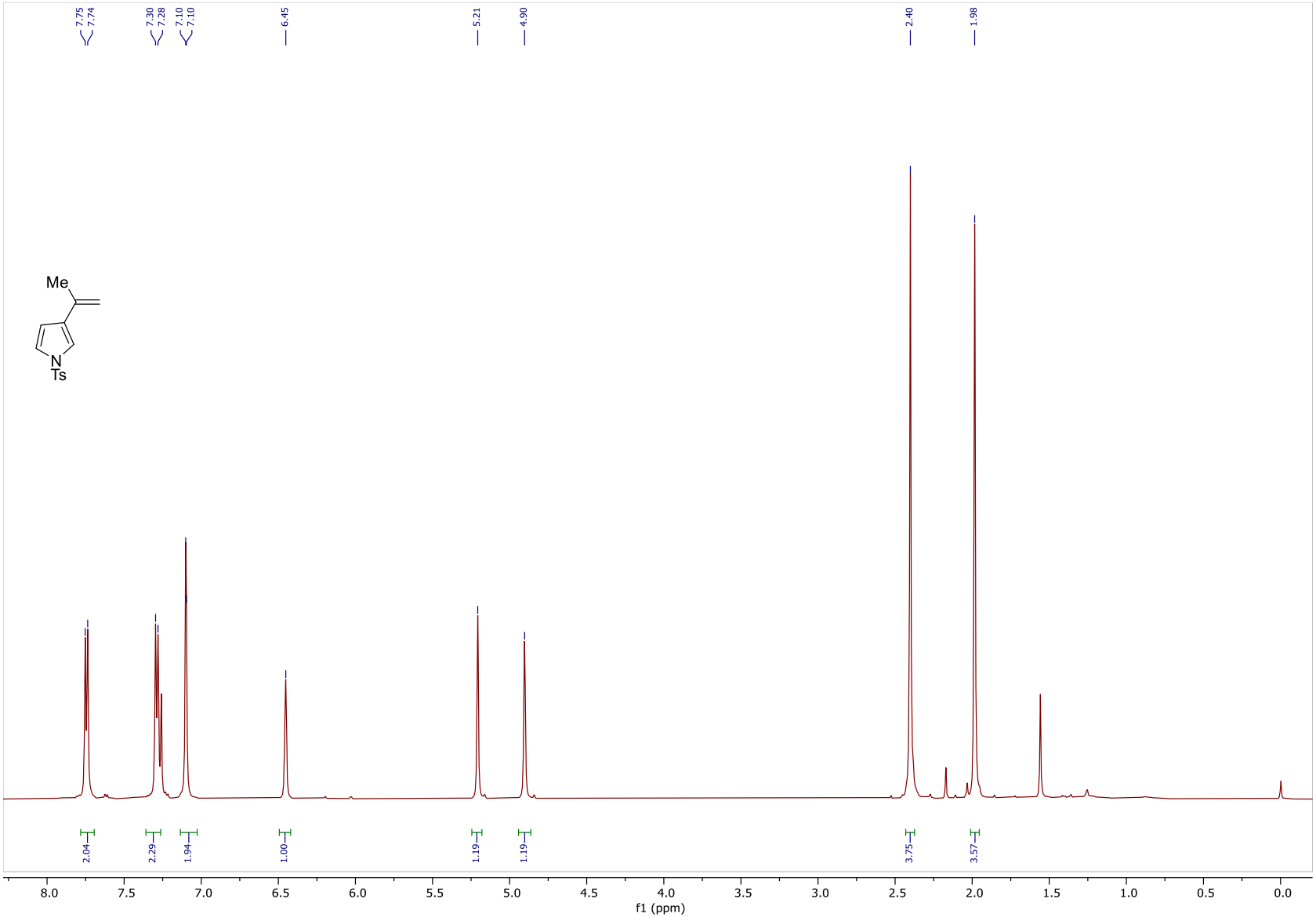

Figure 104: ^{1}H NMR Spectrum of **103** (500MHz, $CDCl_3$)

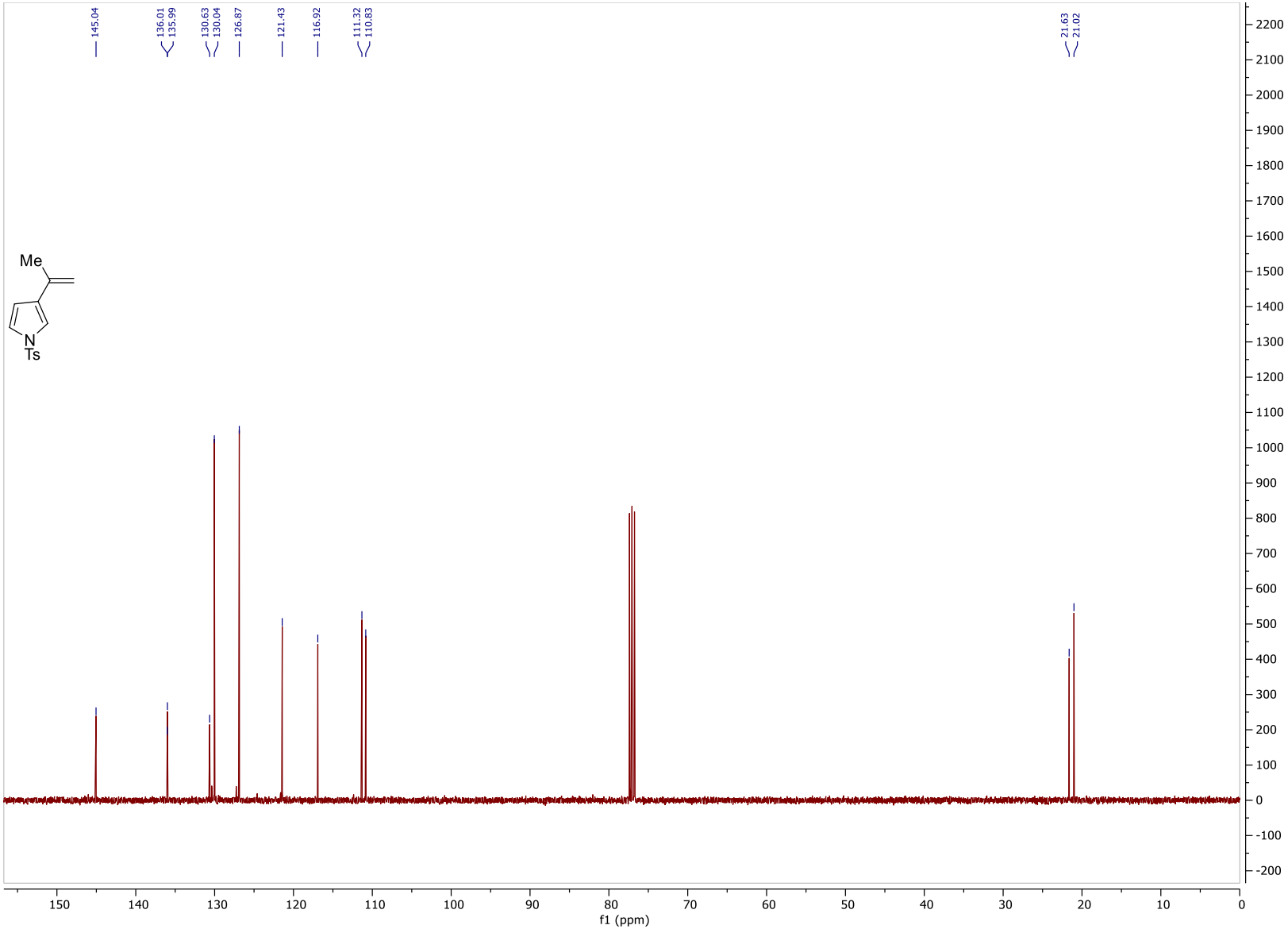

Figure 105: ^{13}C NMR Spectrum of **103** (100MHz, $CDCl_3$)

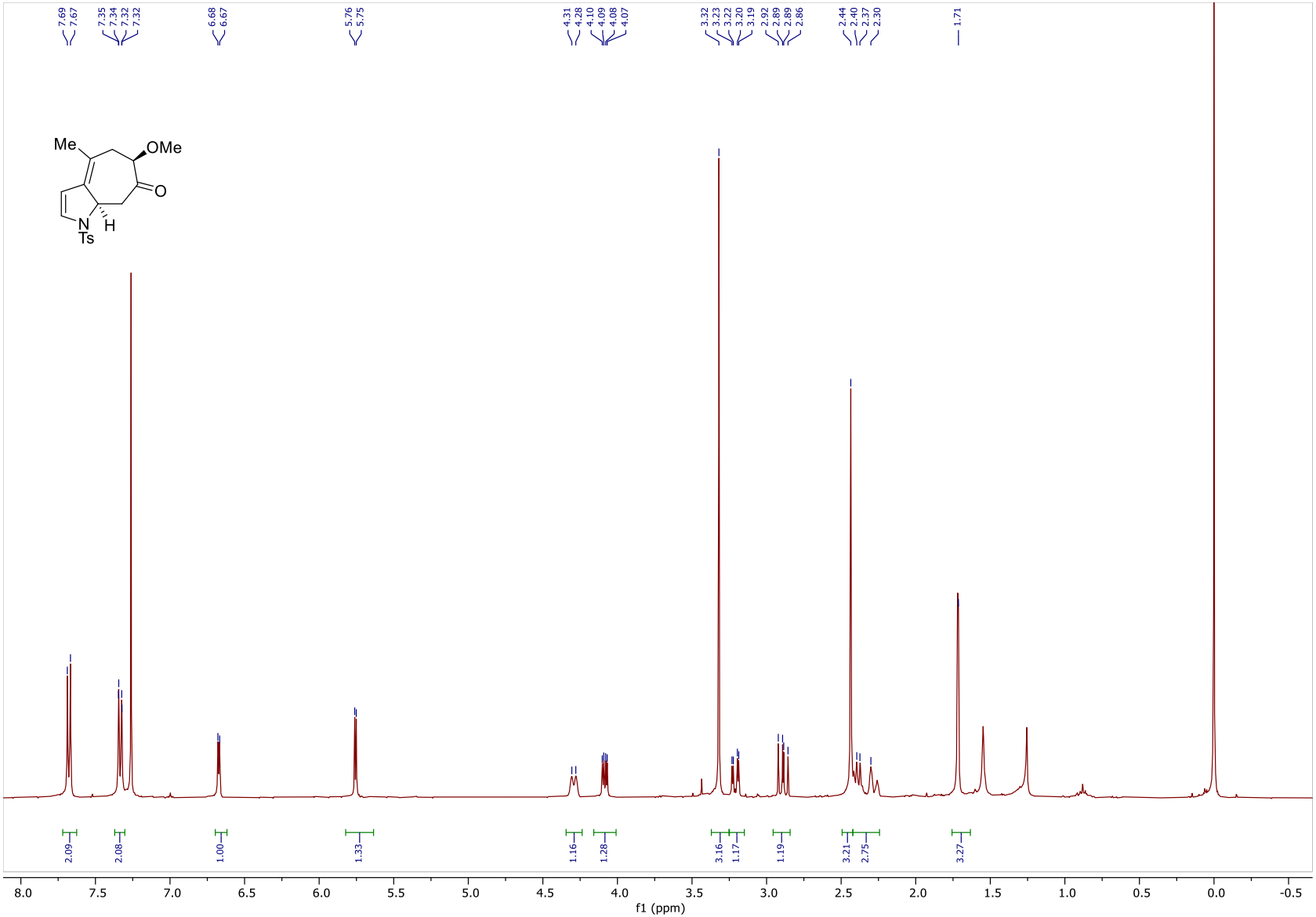

Figure 106: ^{1}H NMR Spectrum of **104** (400MHz, $CDCl_3$)

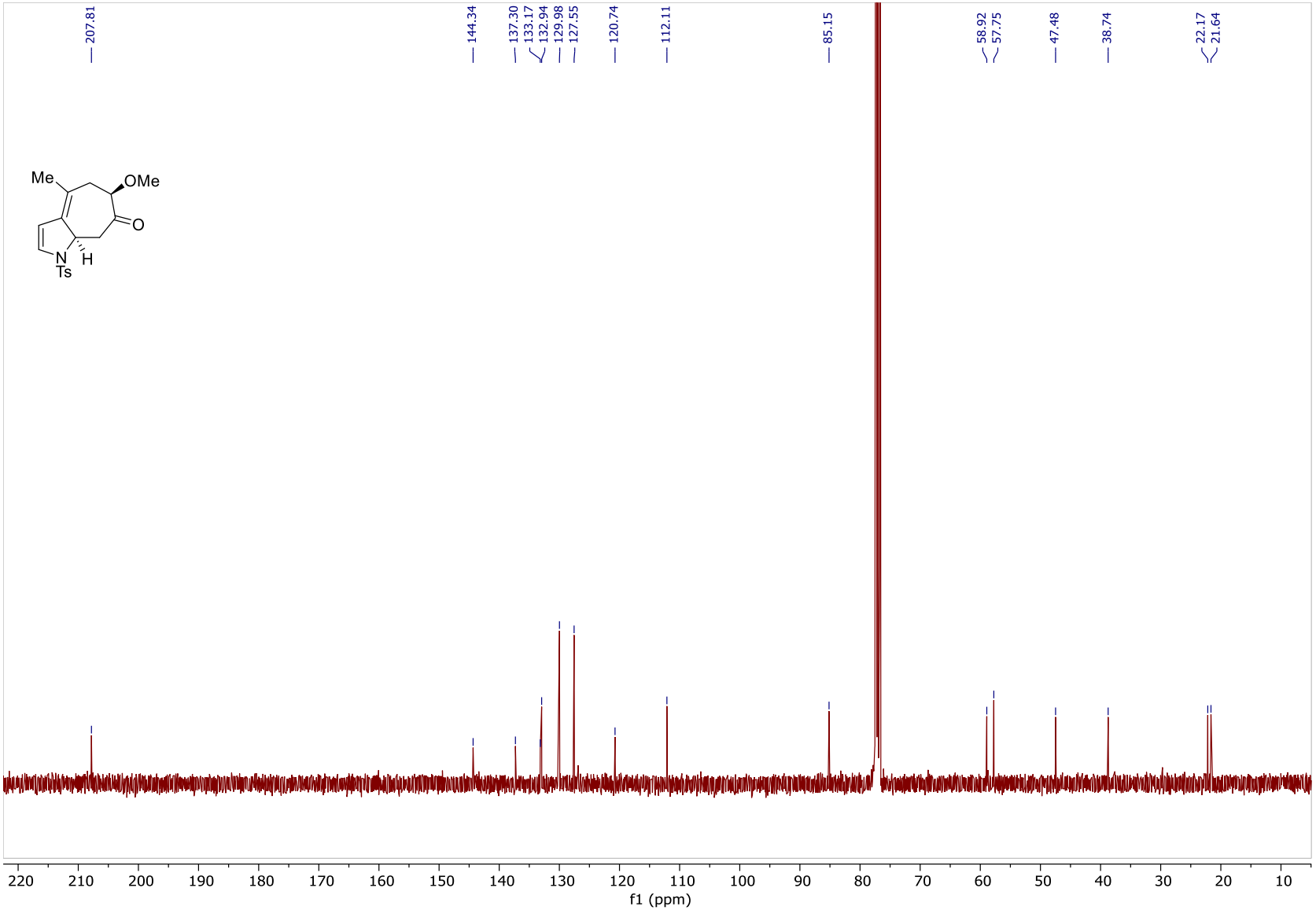

Figure 107: ^{13}C NMR Spectrum of **104** (100MHz, $CDCl_3$)

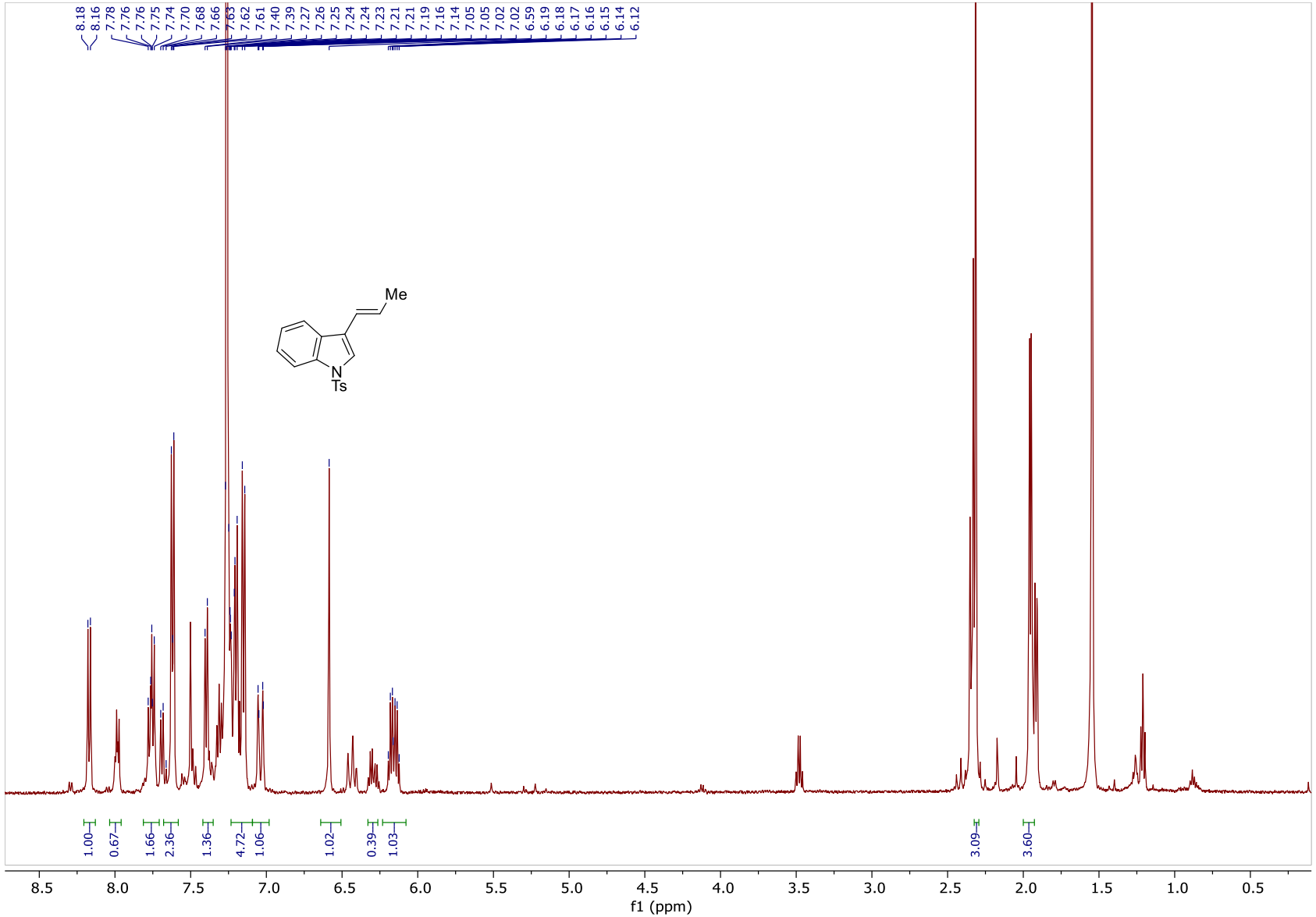

Figure 108: ^{1}H NMR Spectrum of **101a** (500MHz, $CDCl_3$)

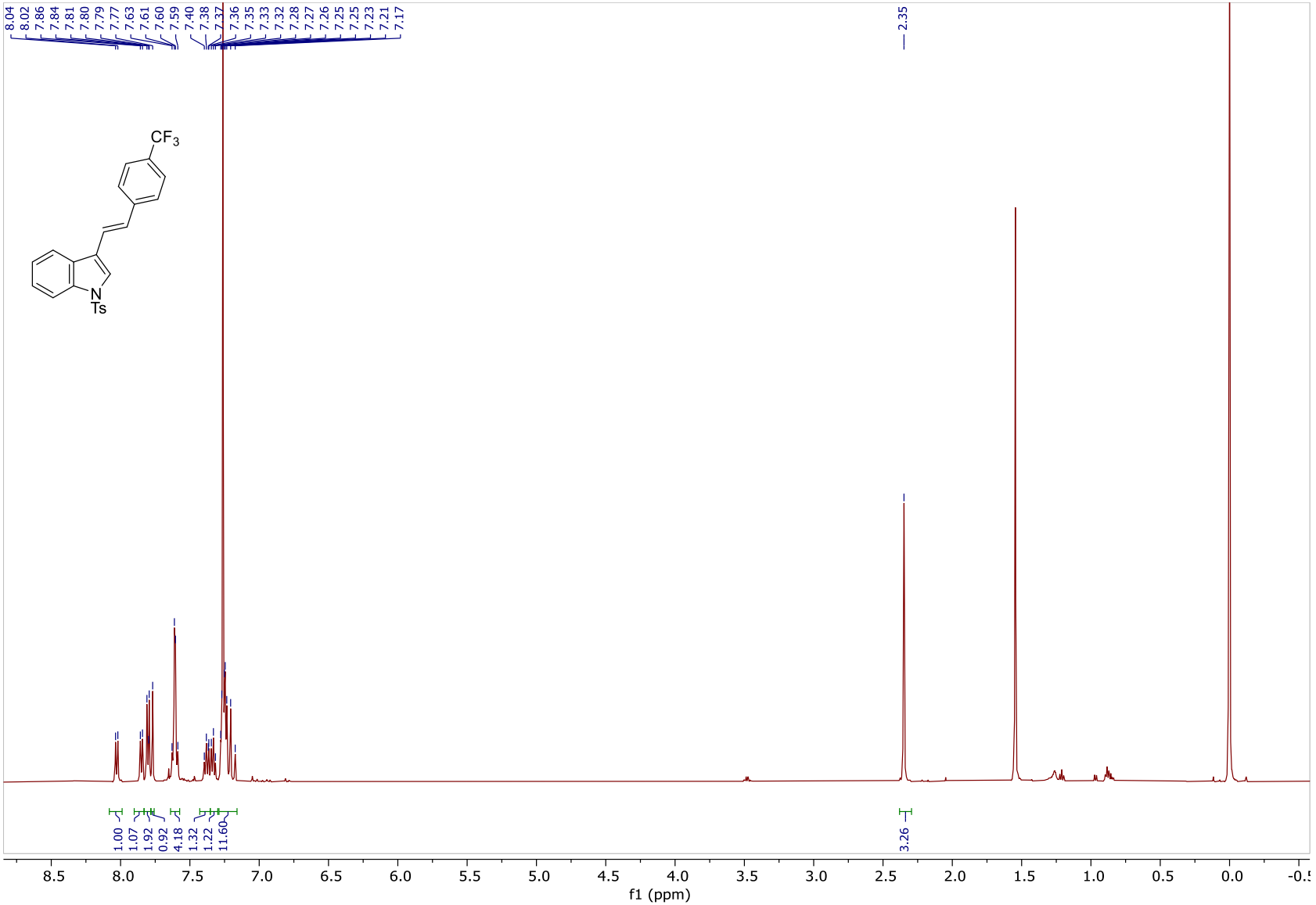

Figure 109: ^{1}H NMR Spectrum of **101b** (500MHz, $CDCl_3$)

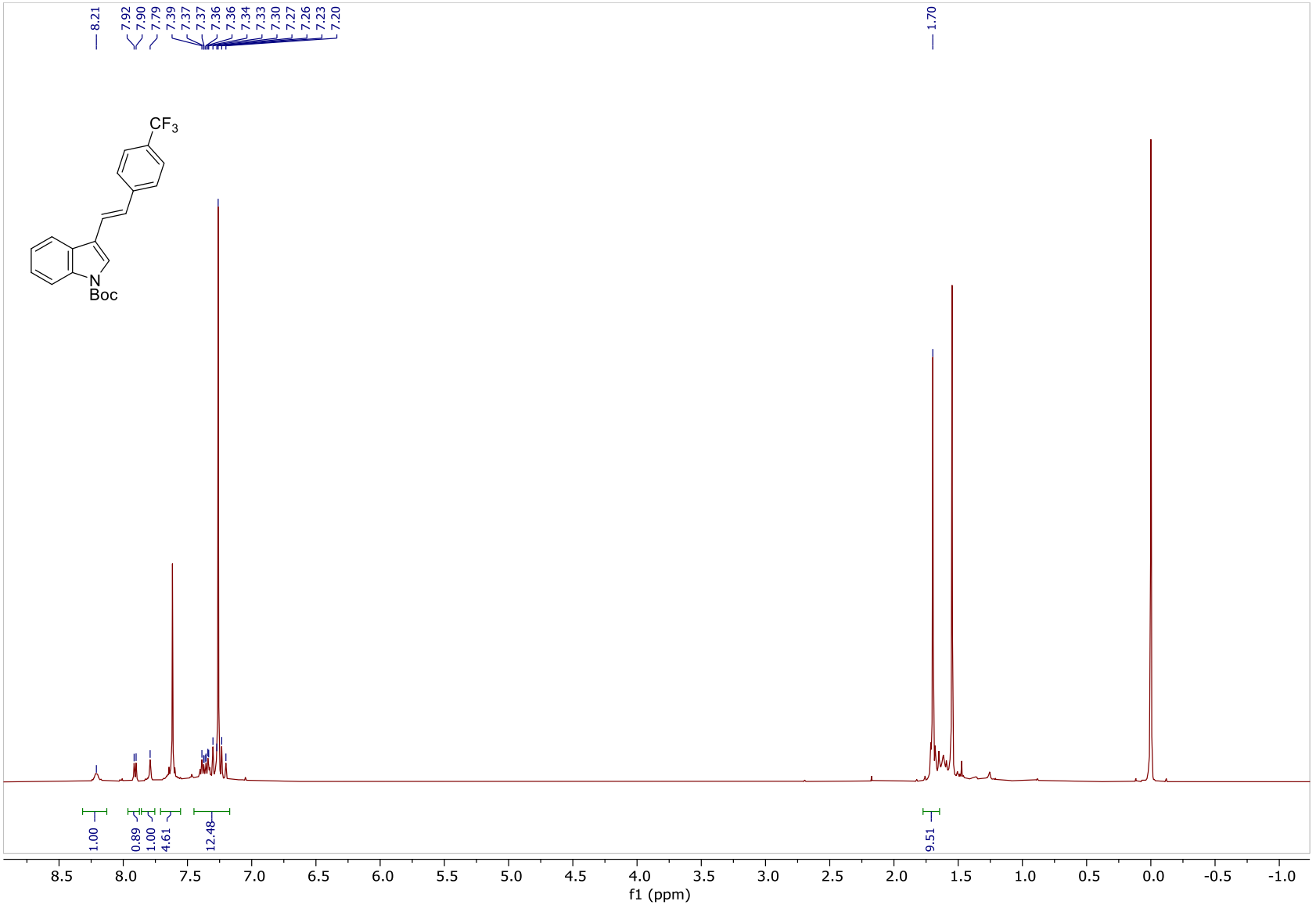

Figure 110: ^{1}H NMR Spectrum of **101c** (500MHz, $CDCl_3$)

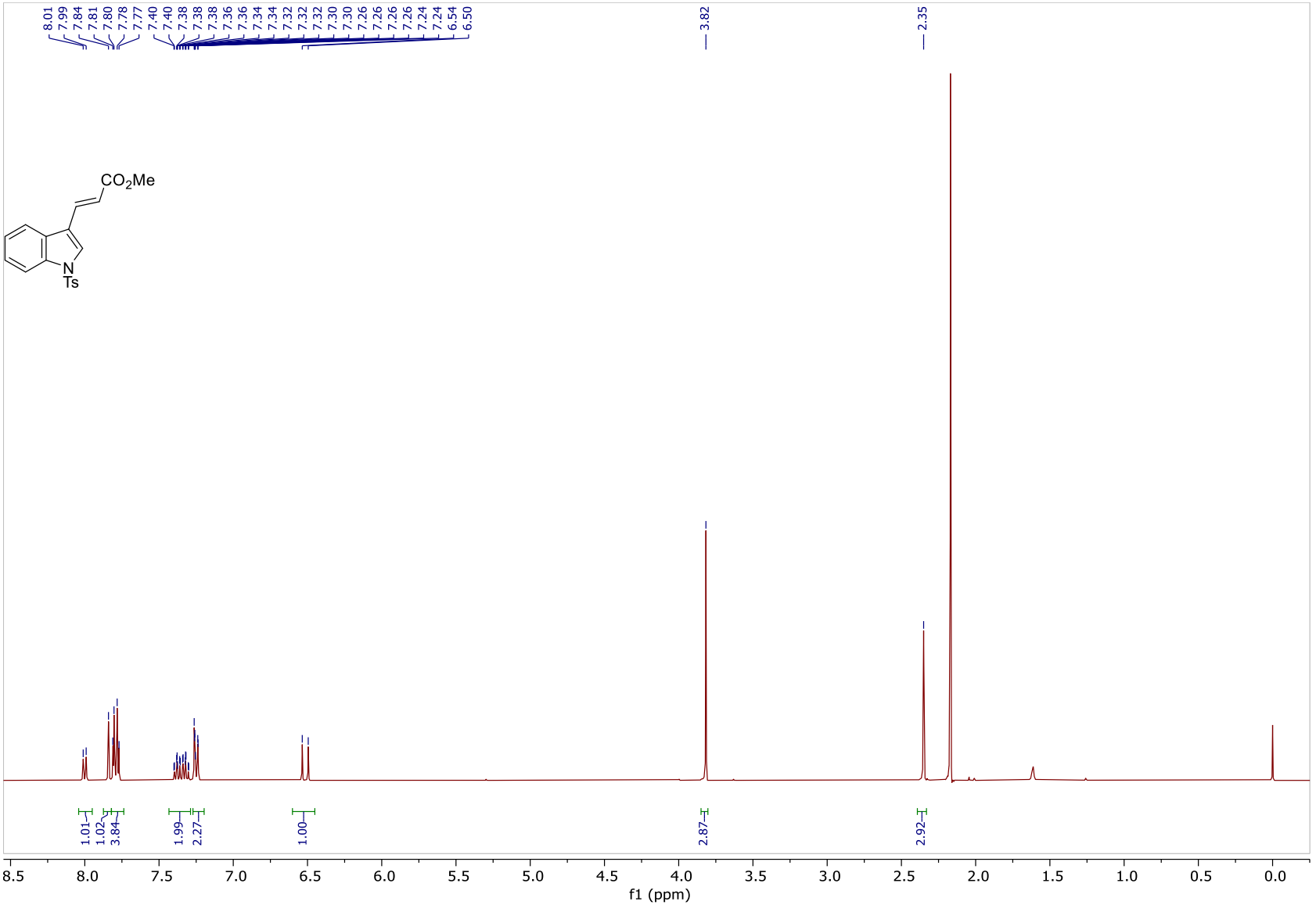

Figure 111: ^{1}H NMR Spectrum of **101d** (400MHz, $CDCl_3$)

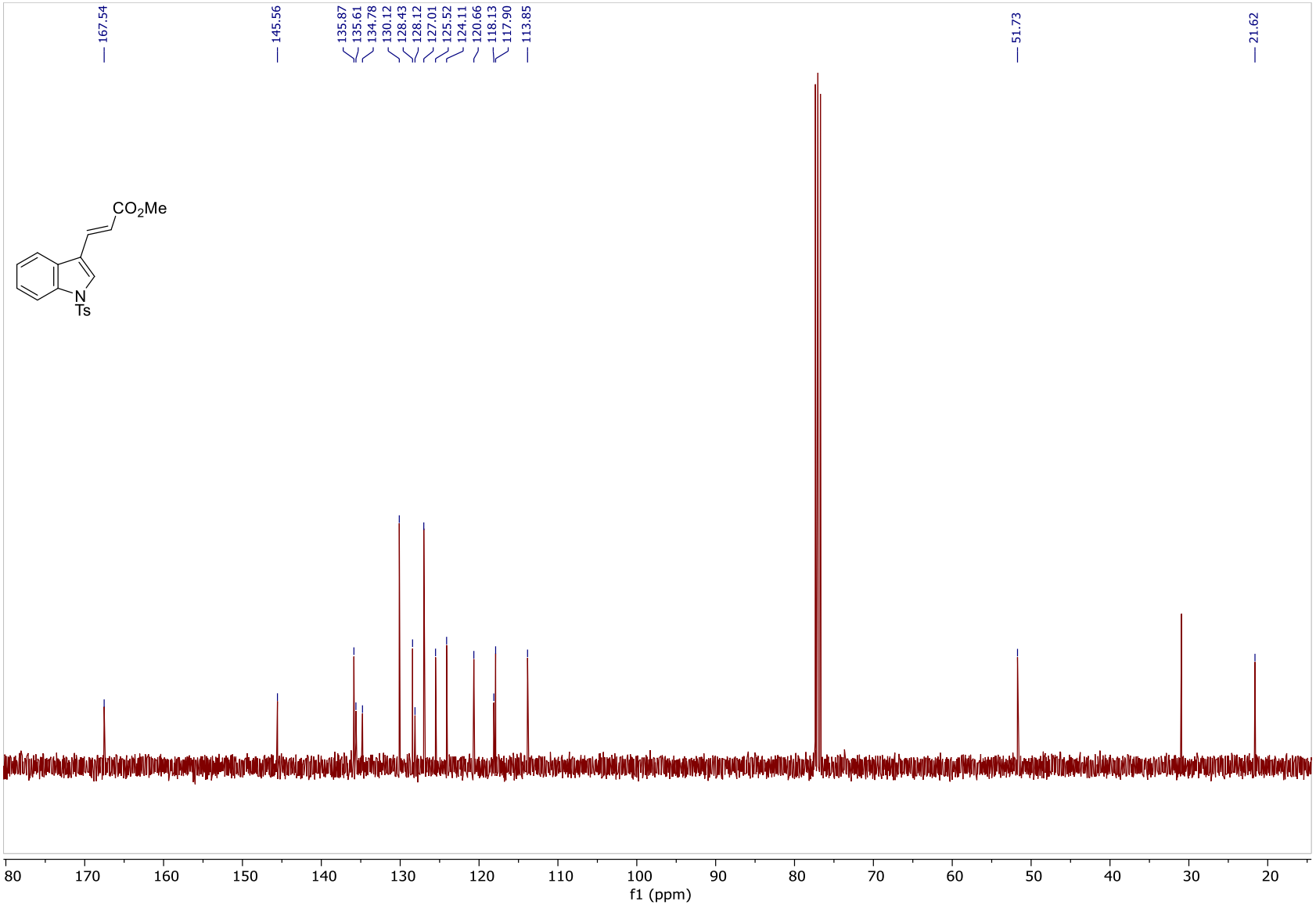

Figure 112: ^{13}C NMR Spectrum of **101d** (100MHz, $CDCl_3$)

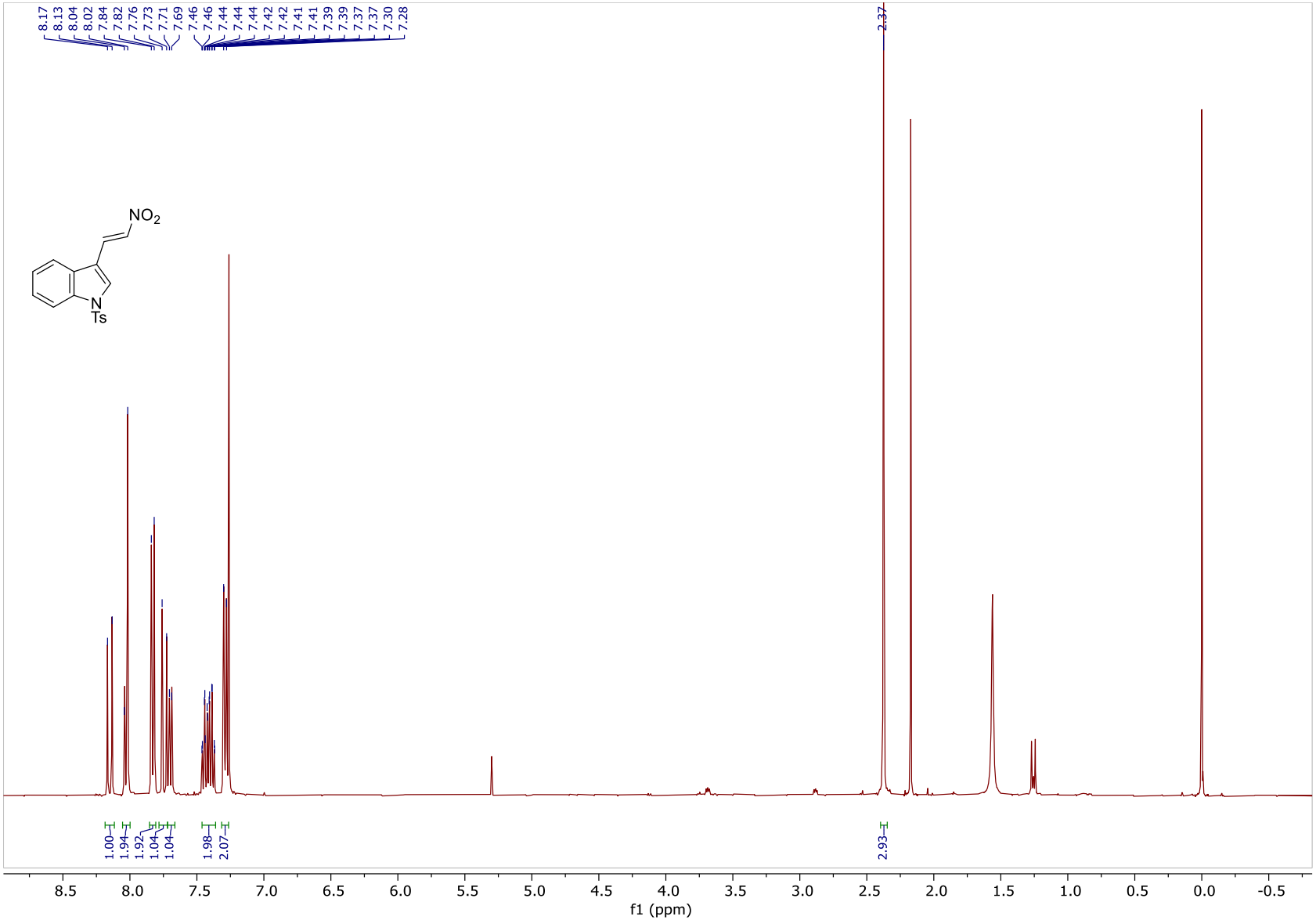

Figure 113: ^{1}H NMR Spectrum of **101e** (400MHz, $CDCl_3$)

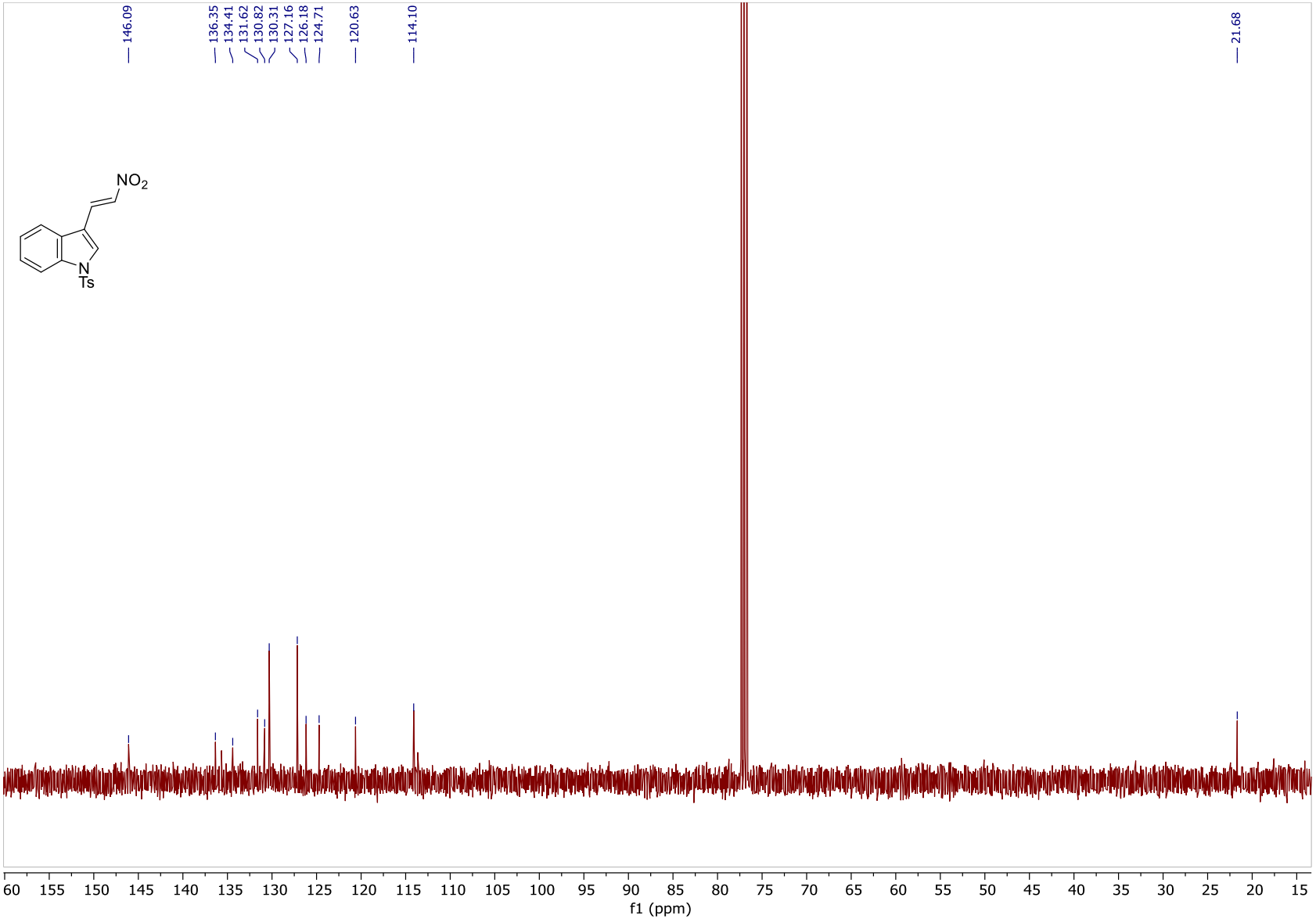

Figure 114: ^{13}C NMR Spectrum of **101e** (100MHz, $CDCl_3$)

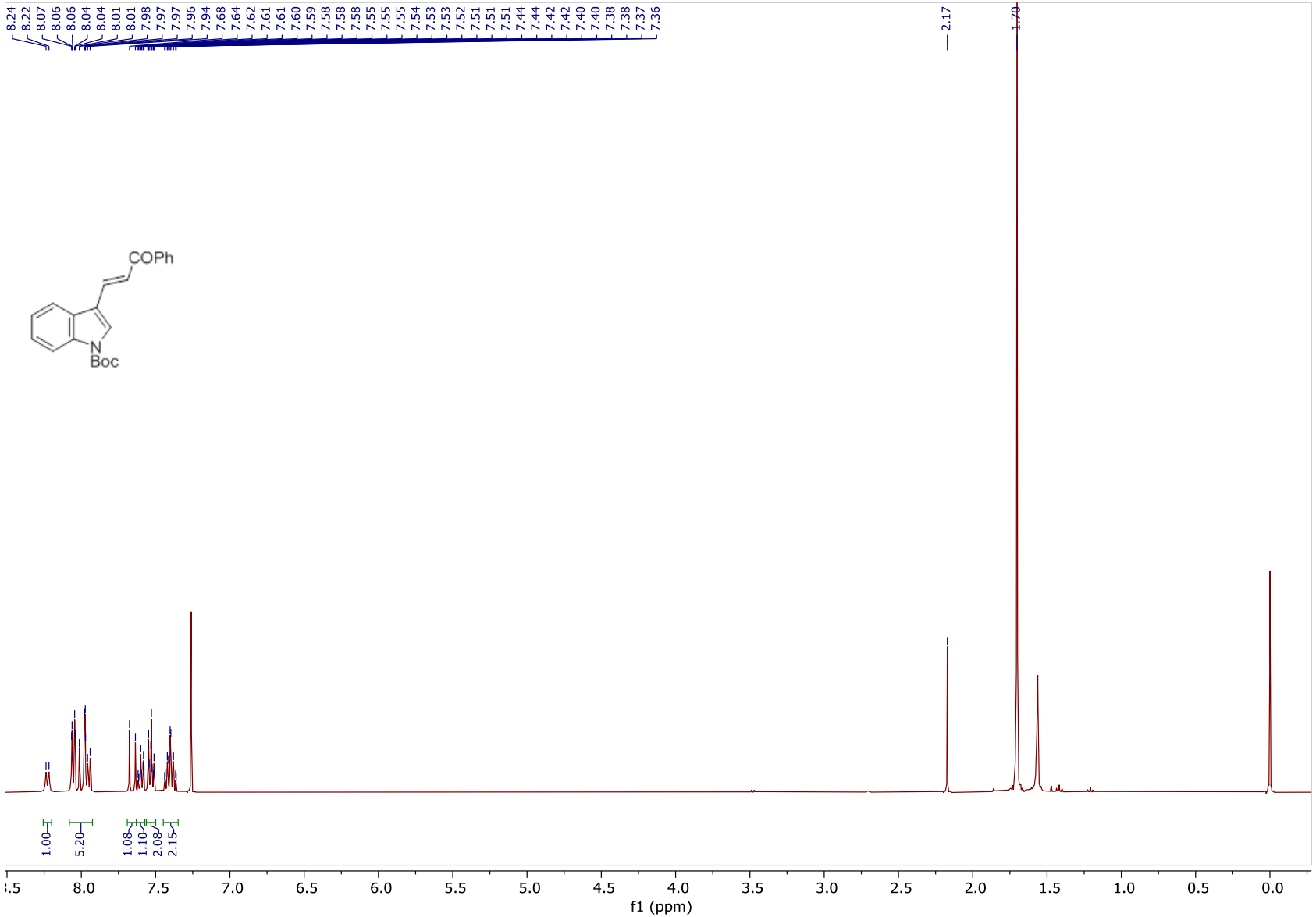

Figure 115: ^{1}H NMR Spectrum of **101f** (400MHz, $CDCl_3$)

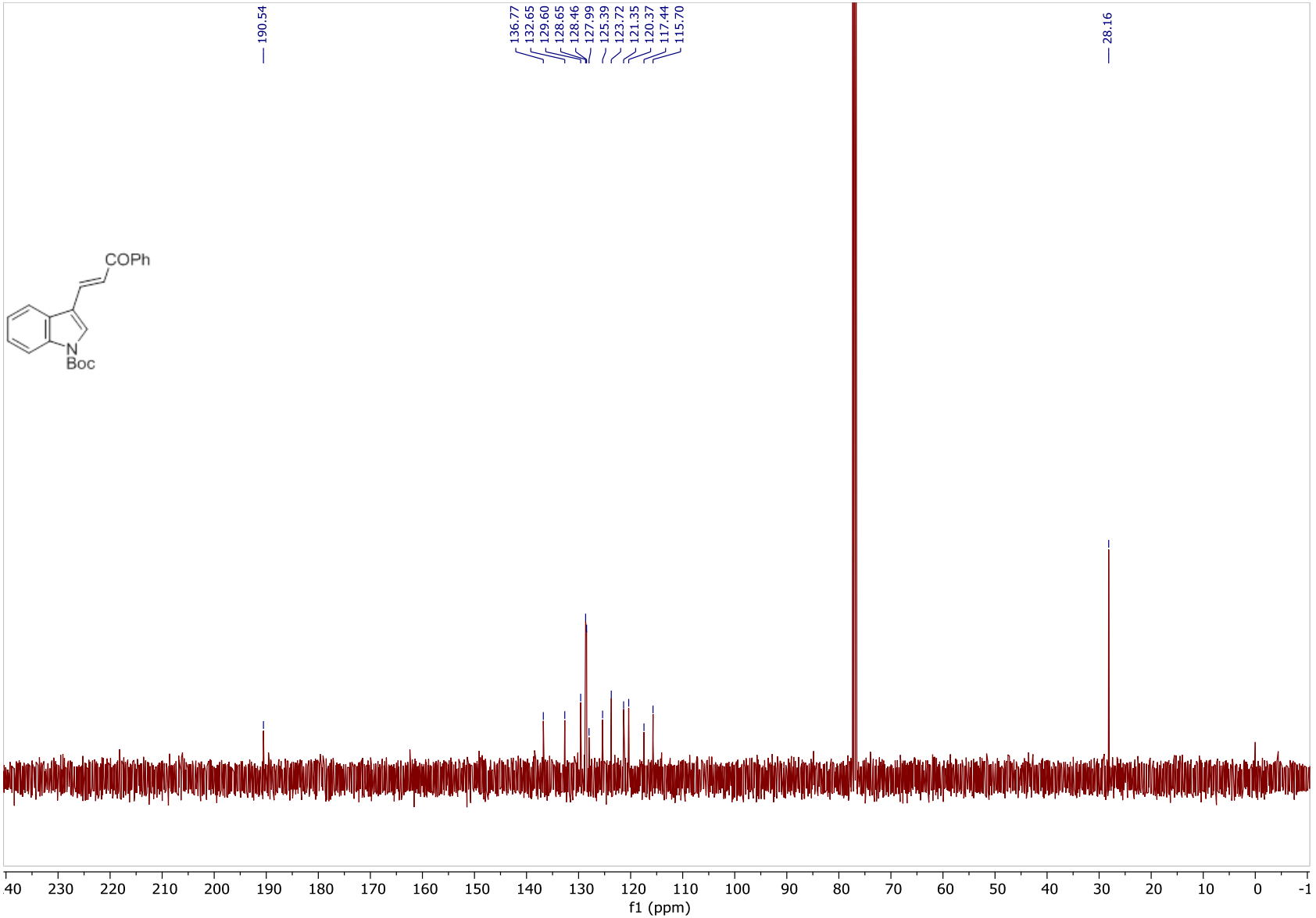

Figure 116: ^{13}C NMR Spectrum of **101f** (100MHz, $CDCl_3$)

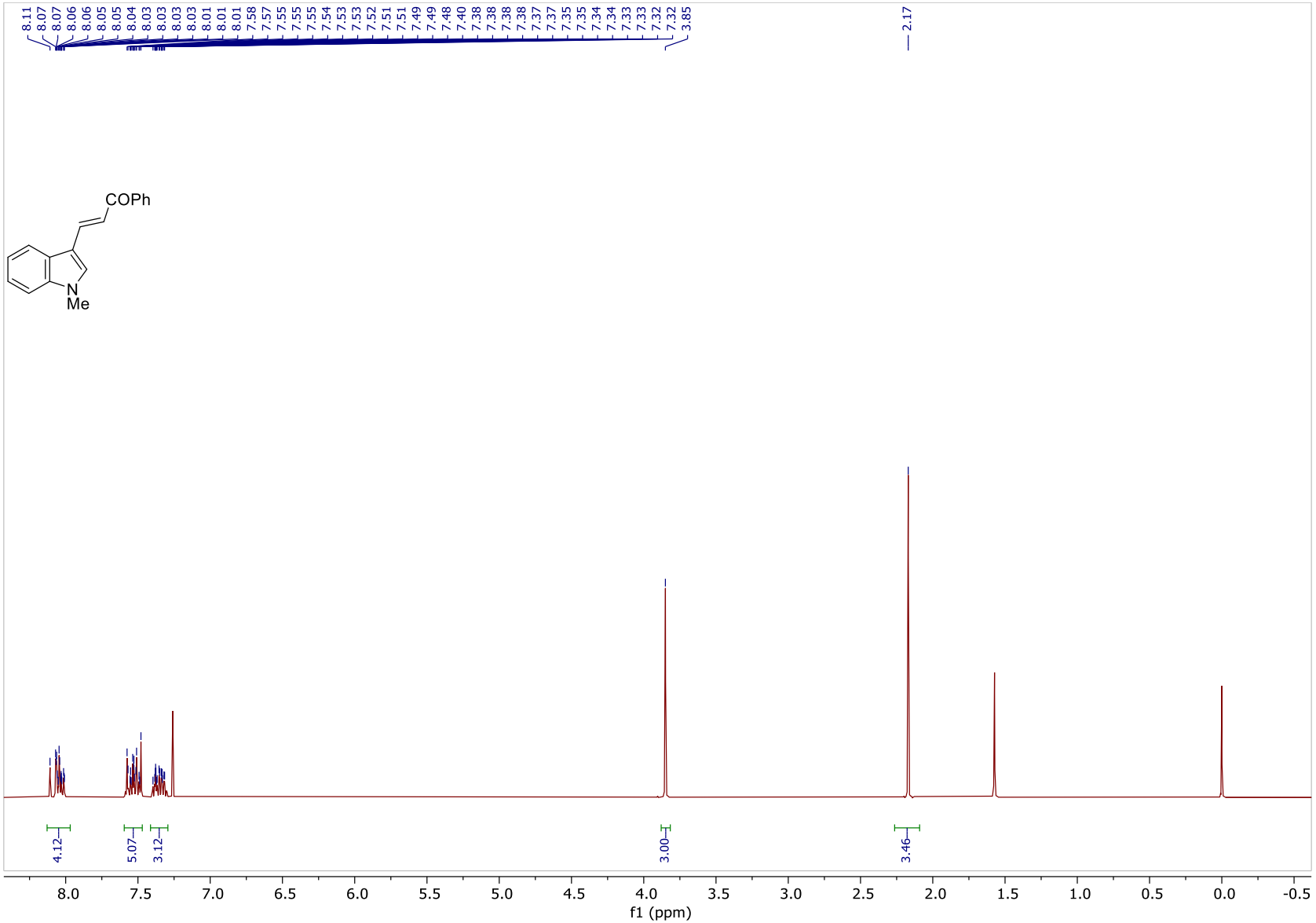

Figure 117: ^{1}H NMR Spectrum of **101g** (400MHz, $CDCl_3$)

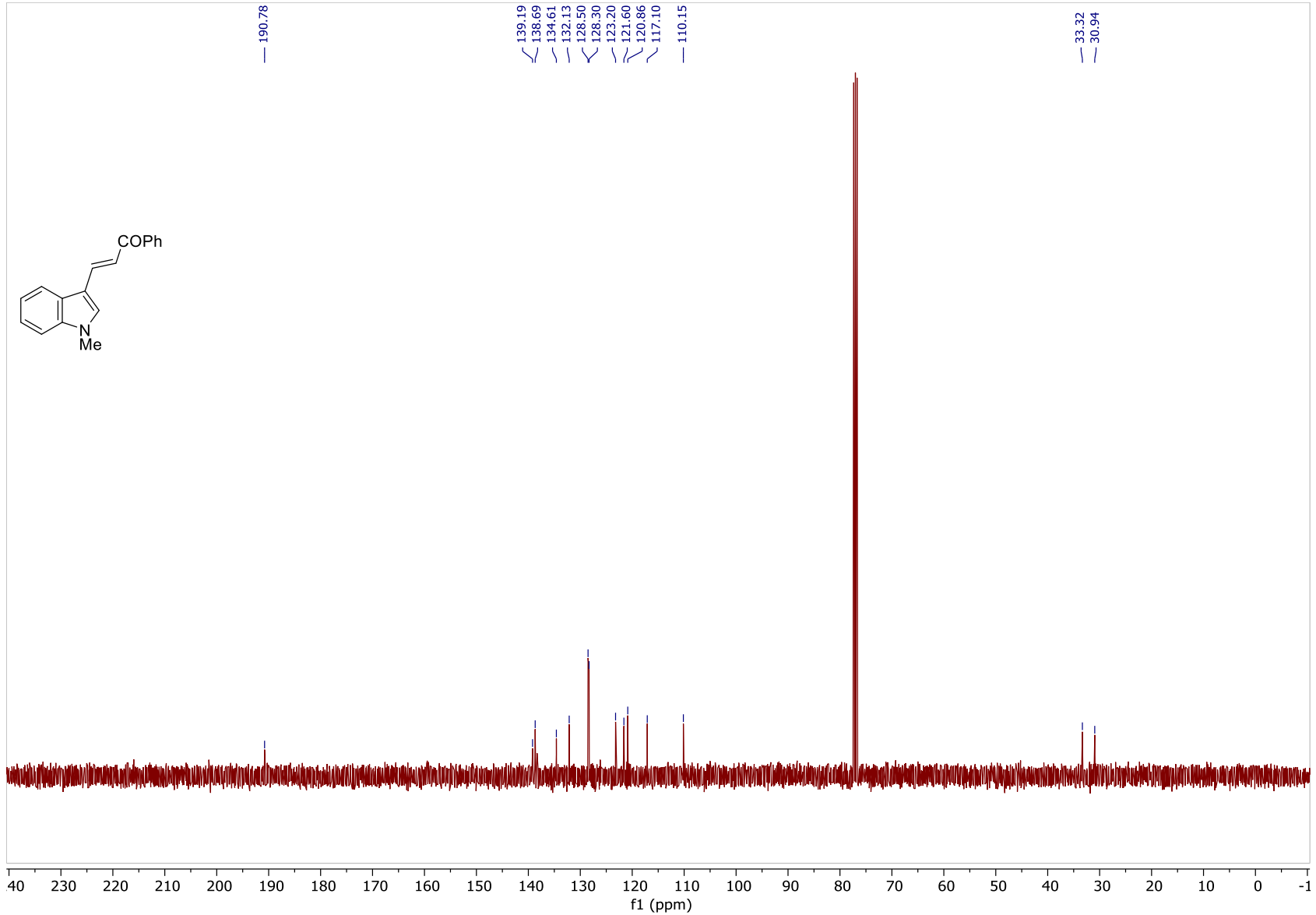

Figure 118: ^{13}C NMR Spectrum of **101g** (100MHz, $CDCl_3$)

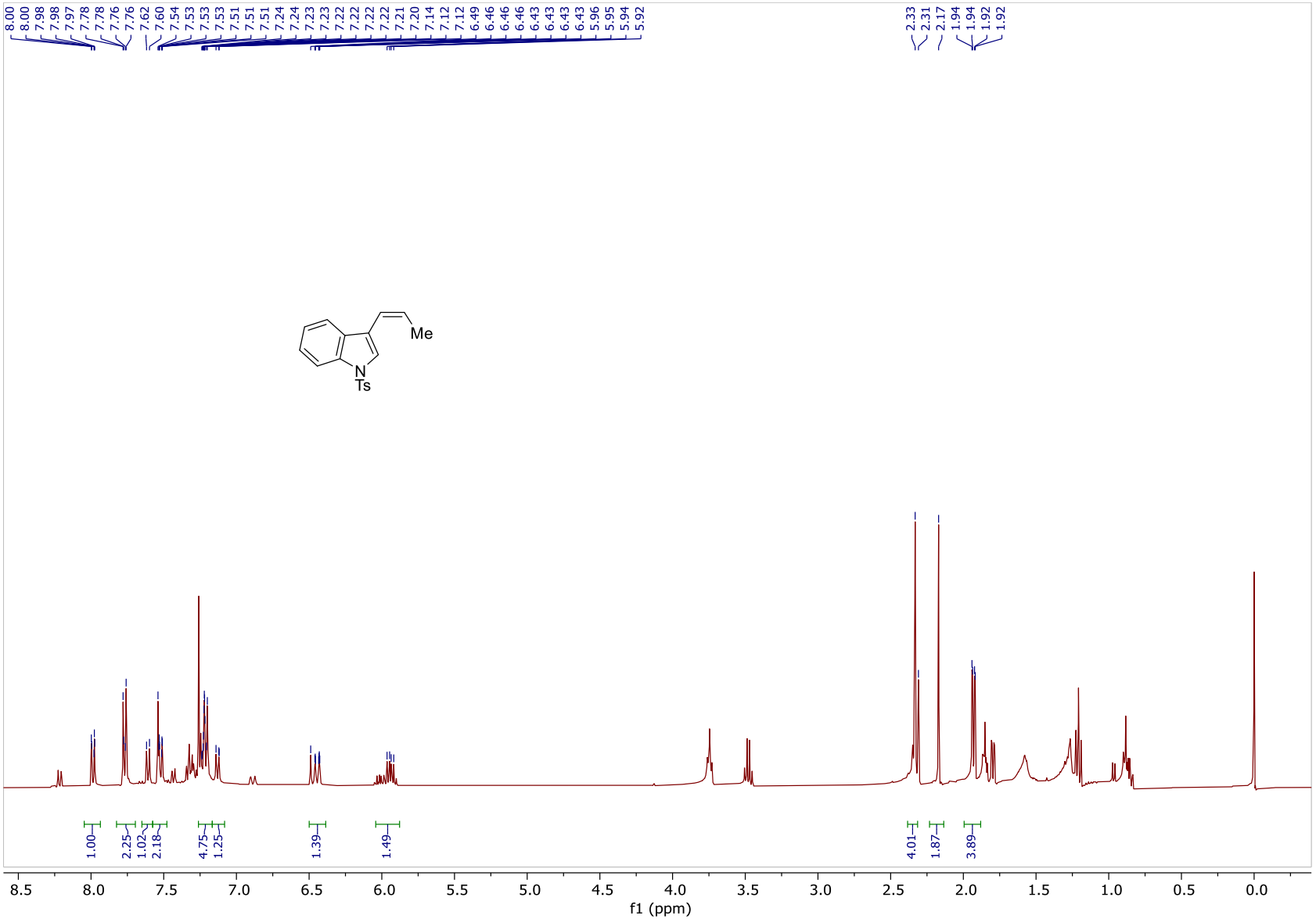

Figure 119: ^{1}H NMR Spectrum of **101h** (400MHz, $CDCl_3$)

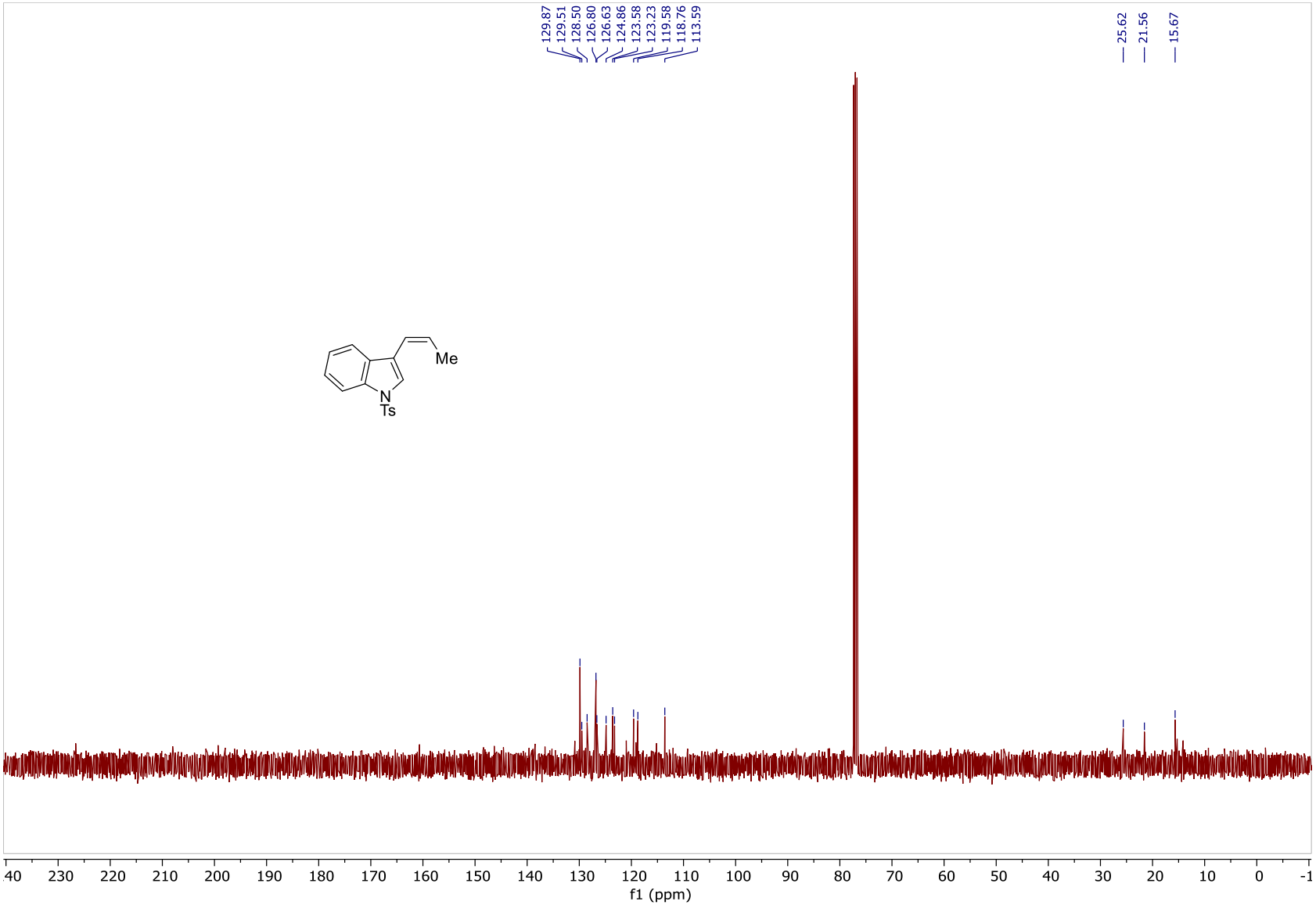

Figure 120: ^{13}C NMR Spectrum of **101h** (100MHz, $CDCl_3$)

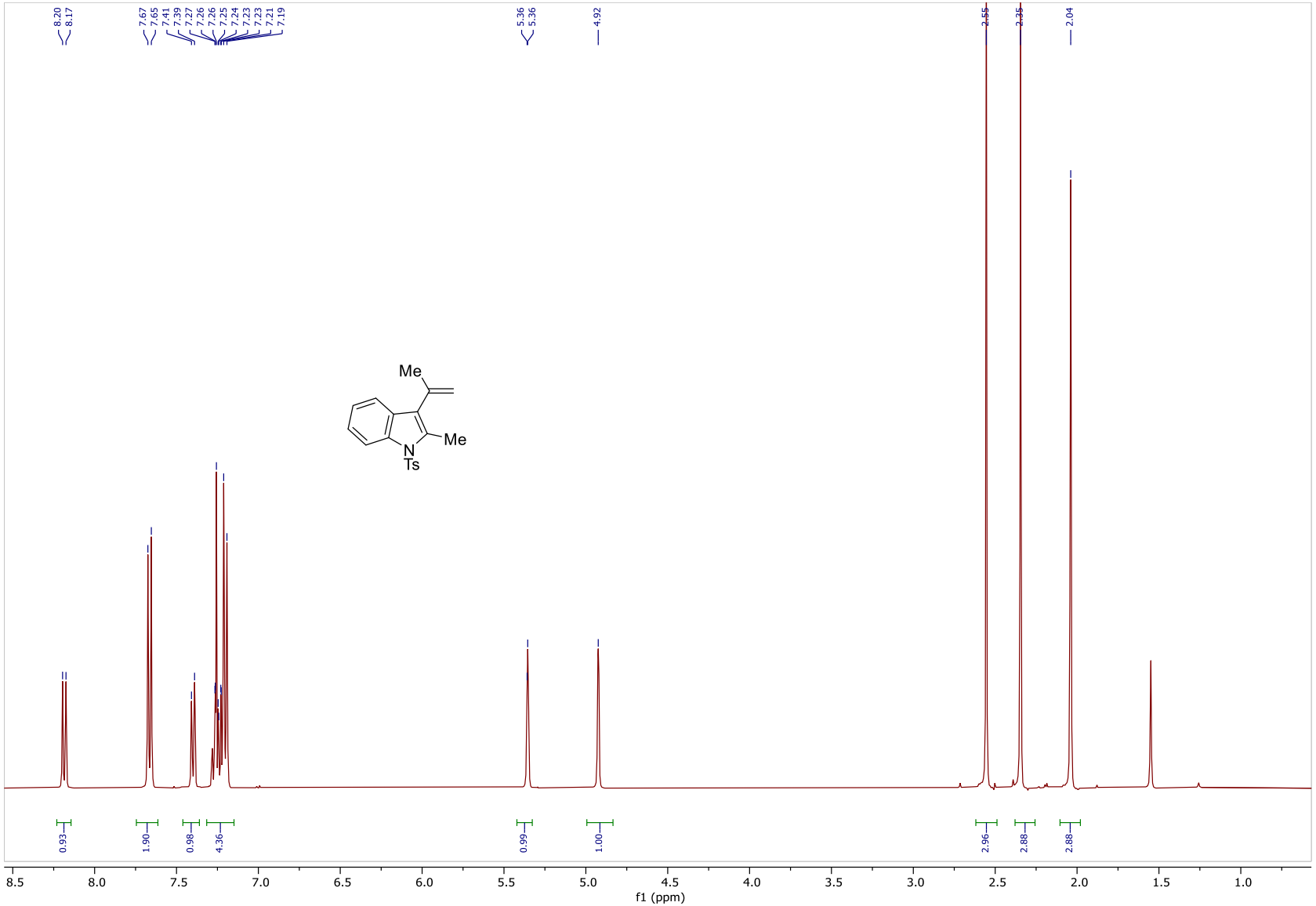

Figure 121: ^{1}H NMR Spectrum of **101j** (400MHz, $CDCl_3$)

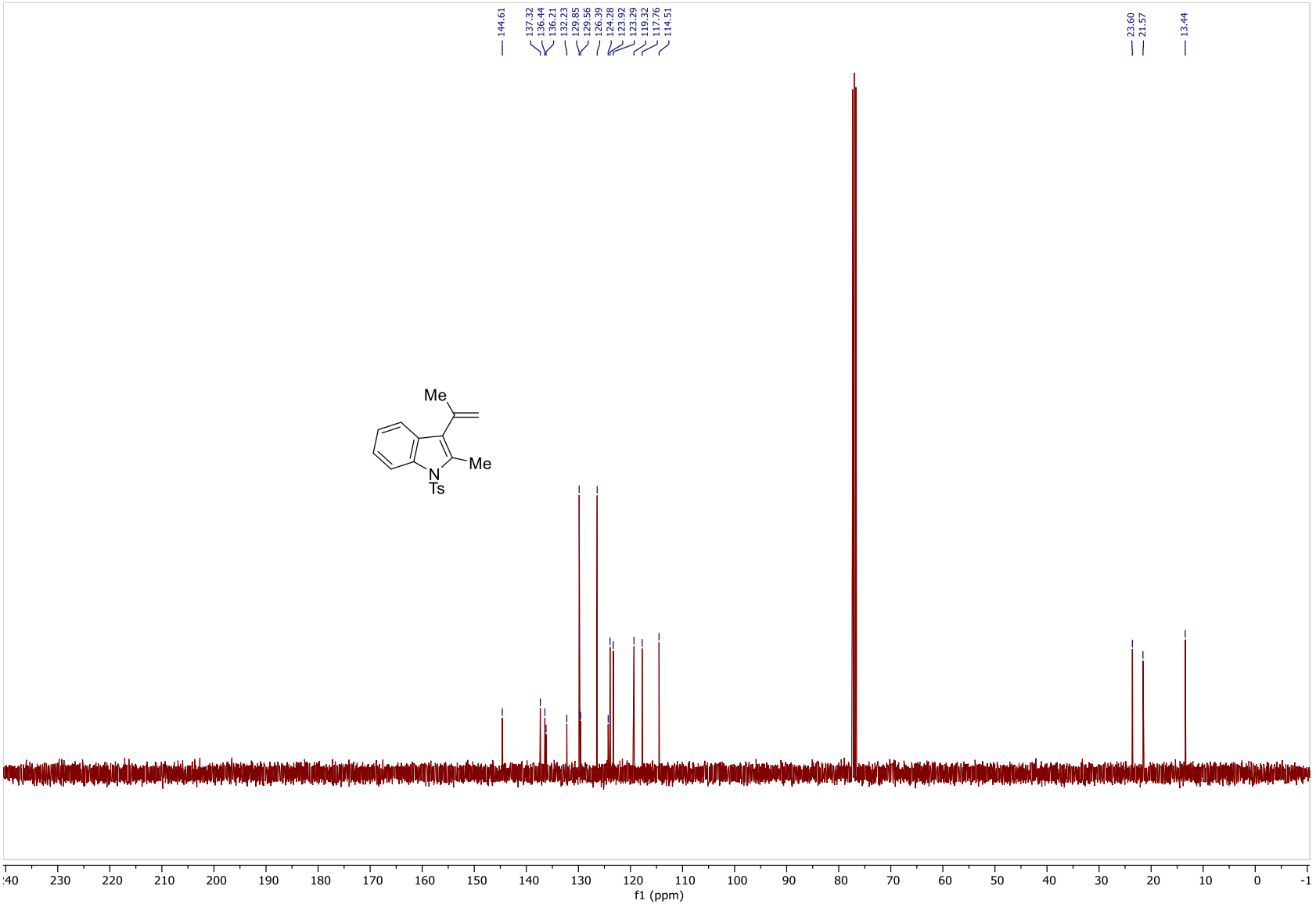

Figure 122: ^{13}C NMR Spectrum of **101j** (100MHz, $CDCl_3$)

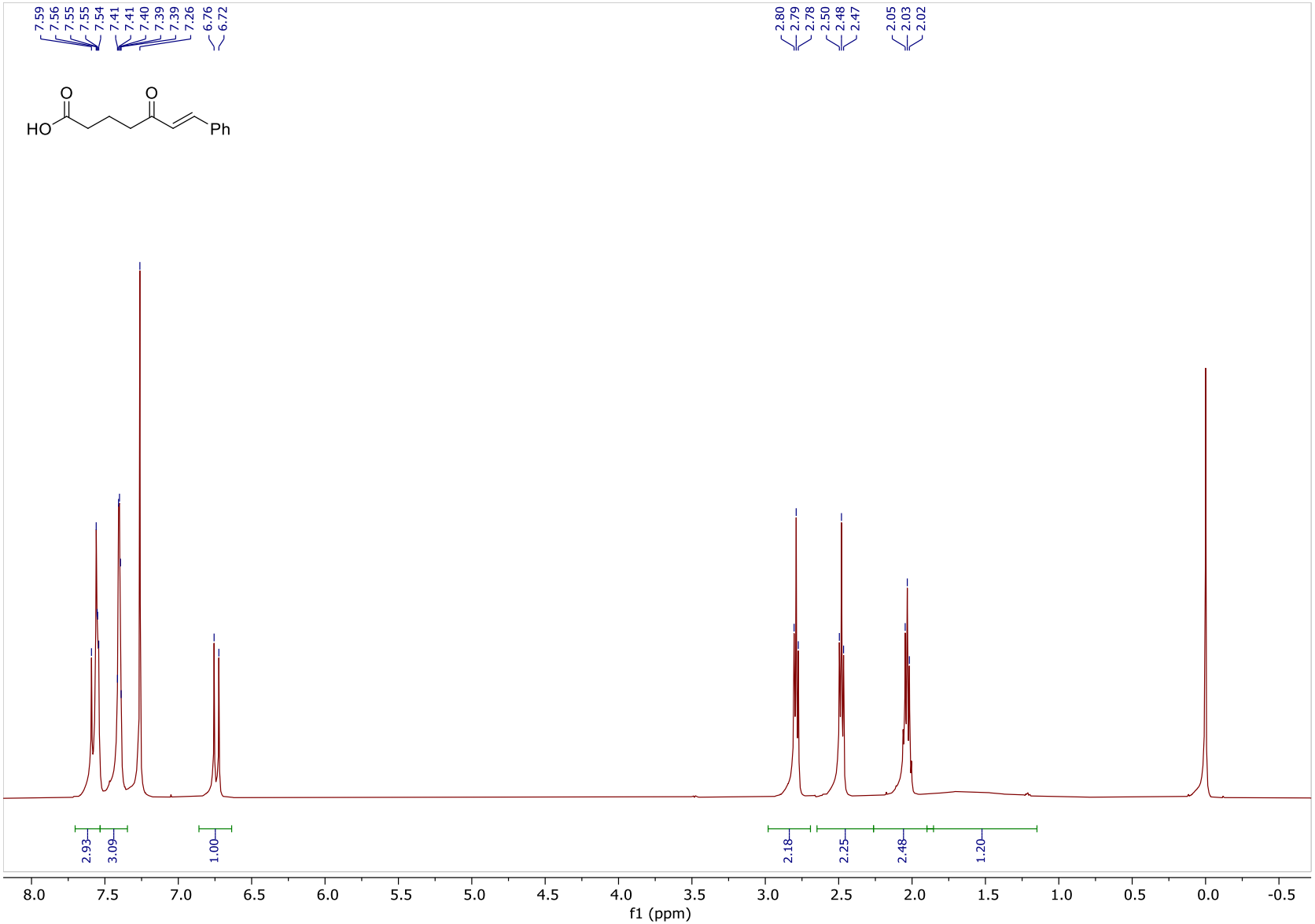

Figure 123: ^{1}H NMR Spectrum of **110** (500MHz, $CDCl_3$)

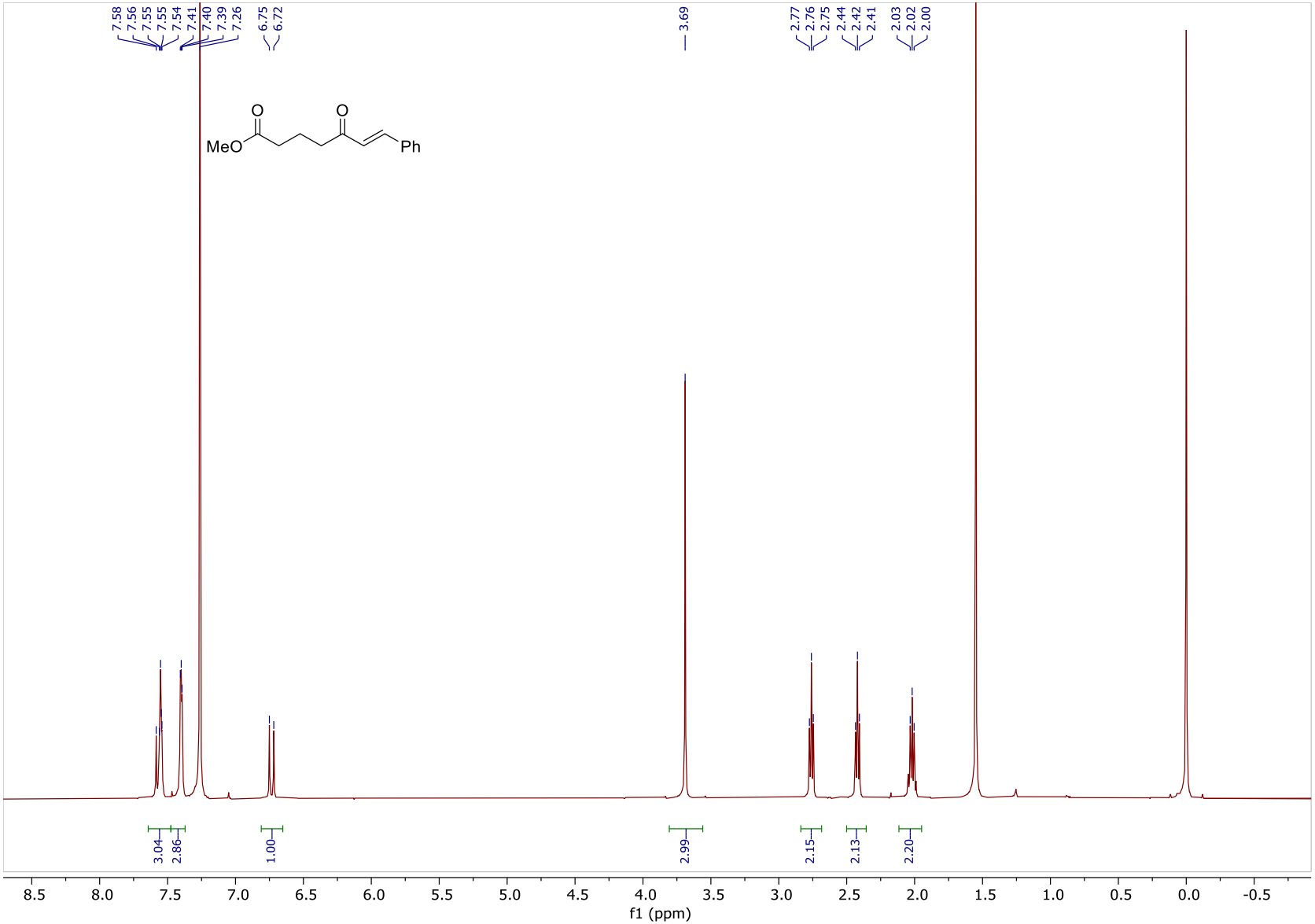

Figure 124: ^{1}H NMR Spectrum of **111** (500MHz, $CDCl_3$)

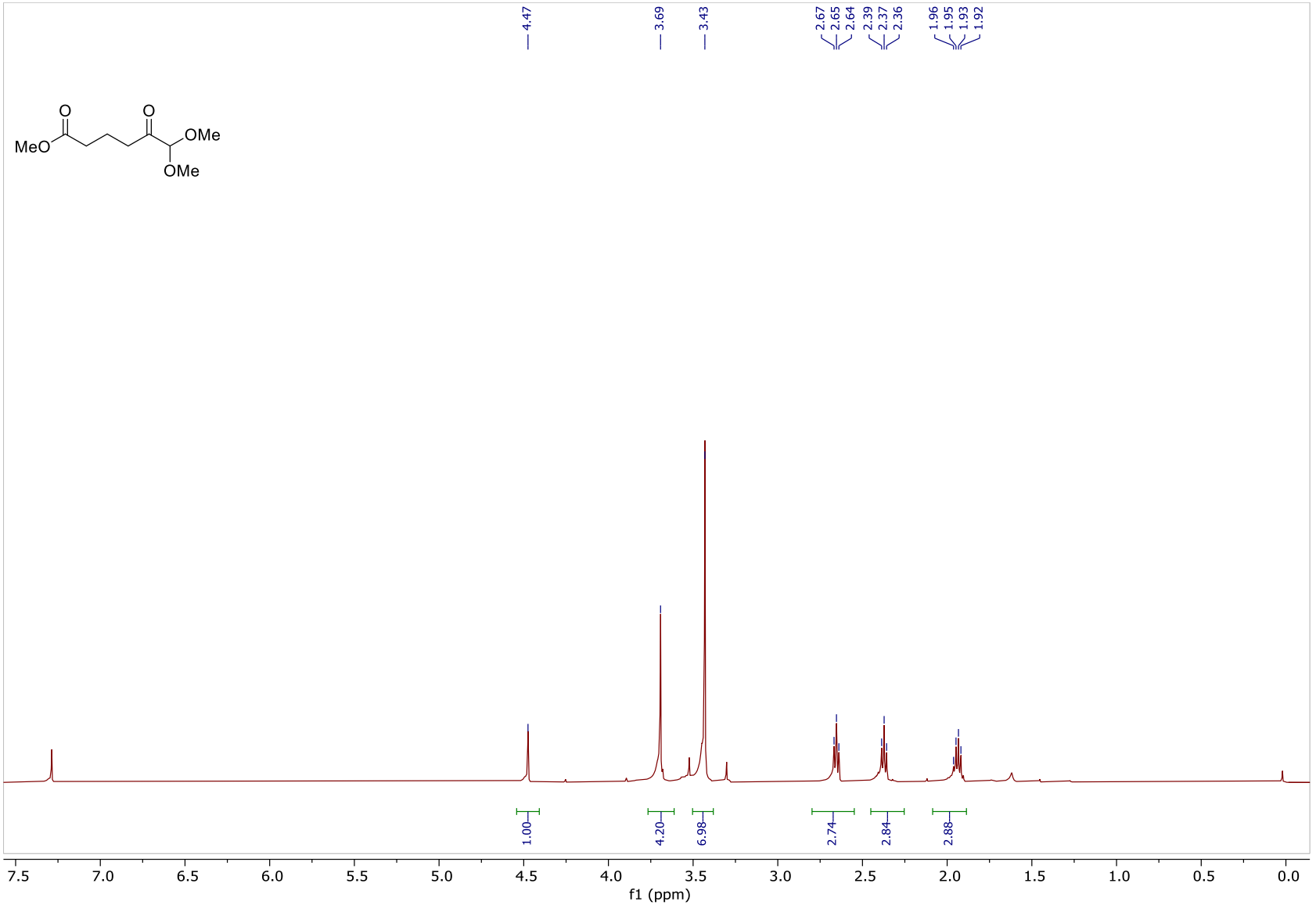

Figure 125: ^{1}H NMR Spectrum of **112** (500MHz, $CDCl_3$)

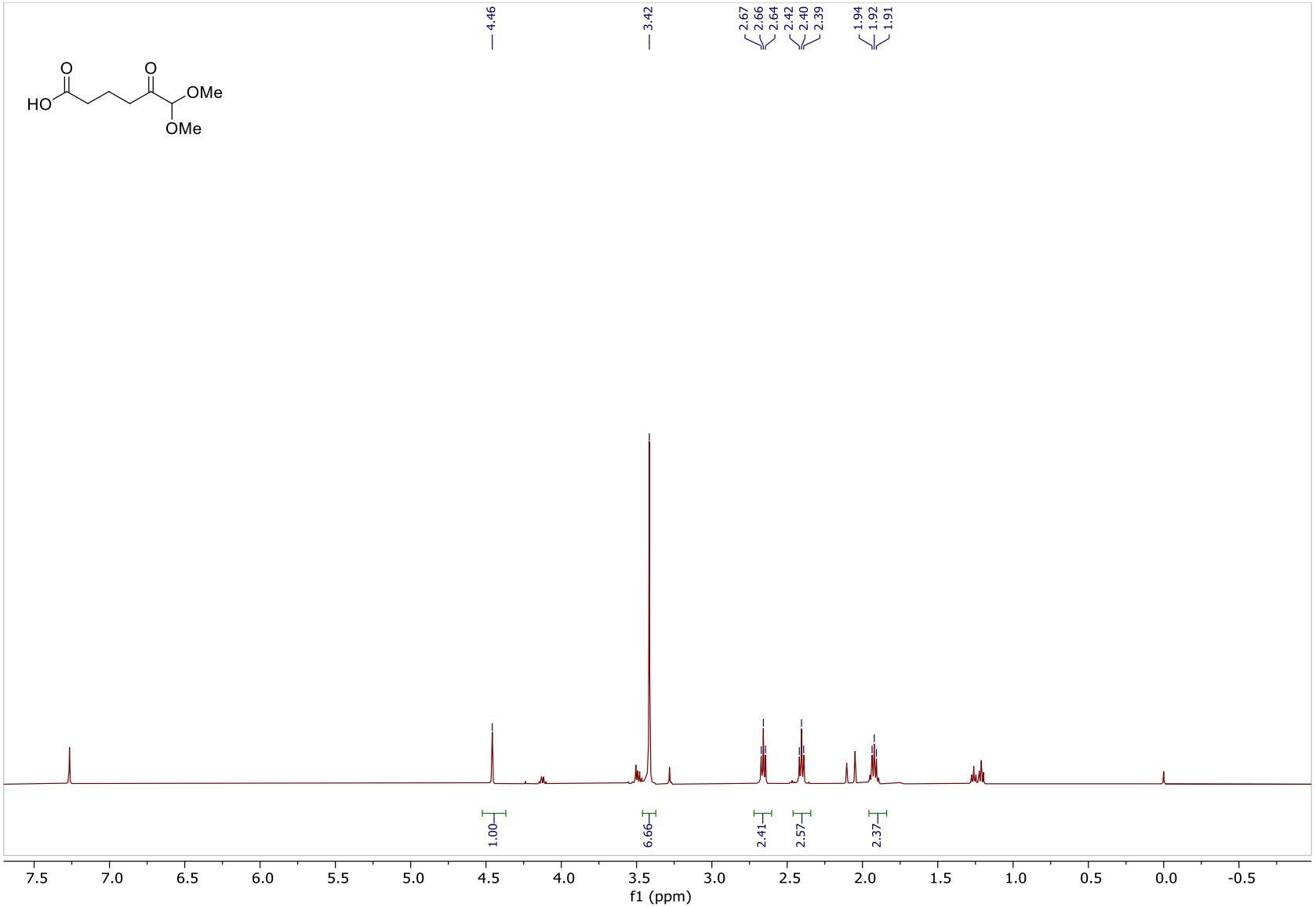

Figure 126: ^{1}H NMR Spectrum of **108** (400MHz, $CDCl_3$)

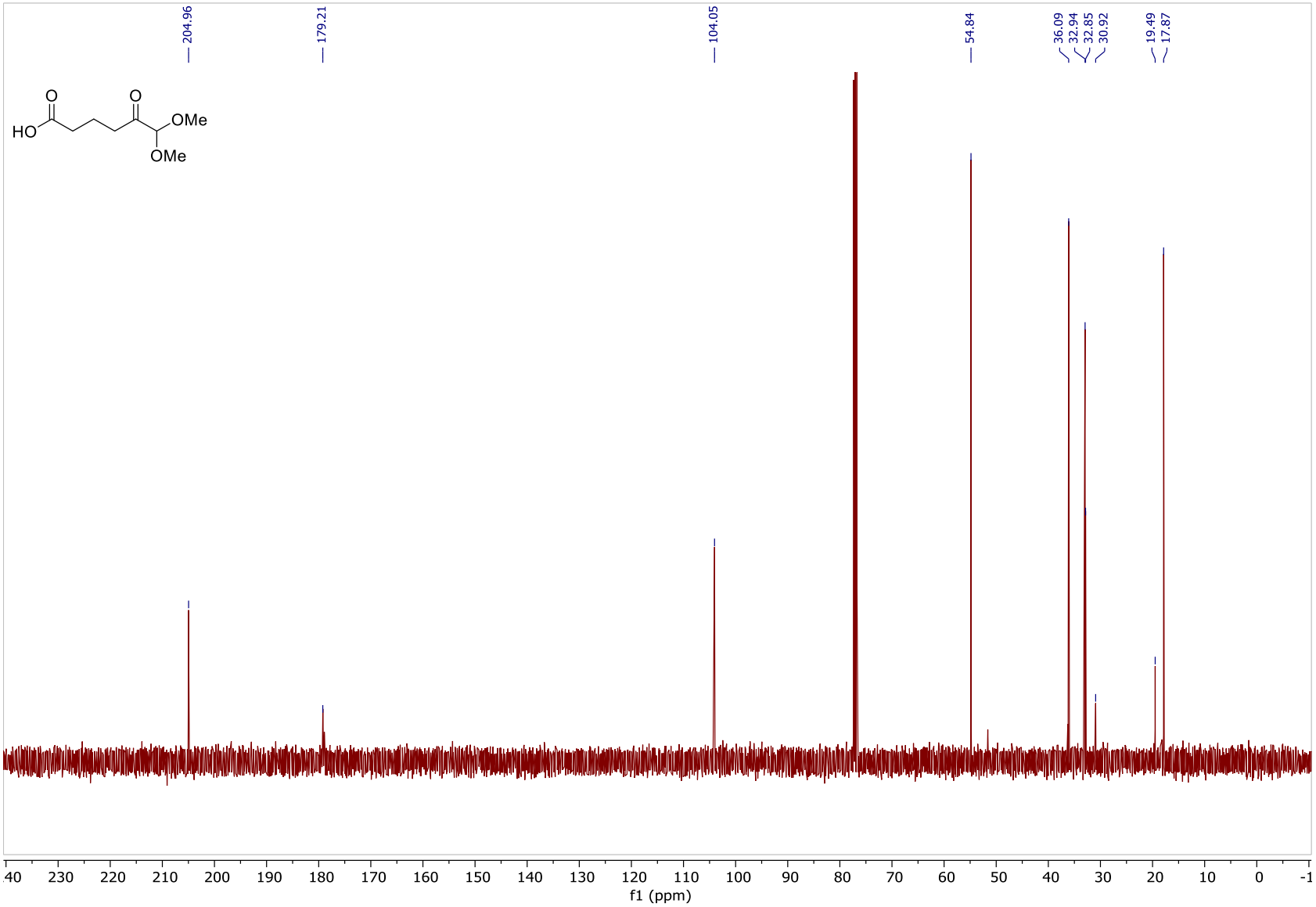

Figure 127: ^{13}C NMR Spectrum of **108** (100MHz, $CDCl_3$)

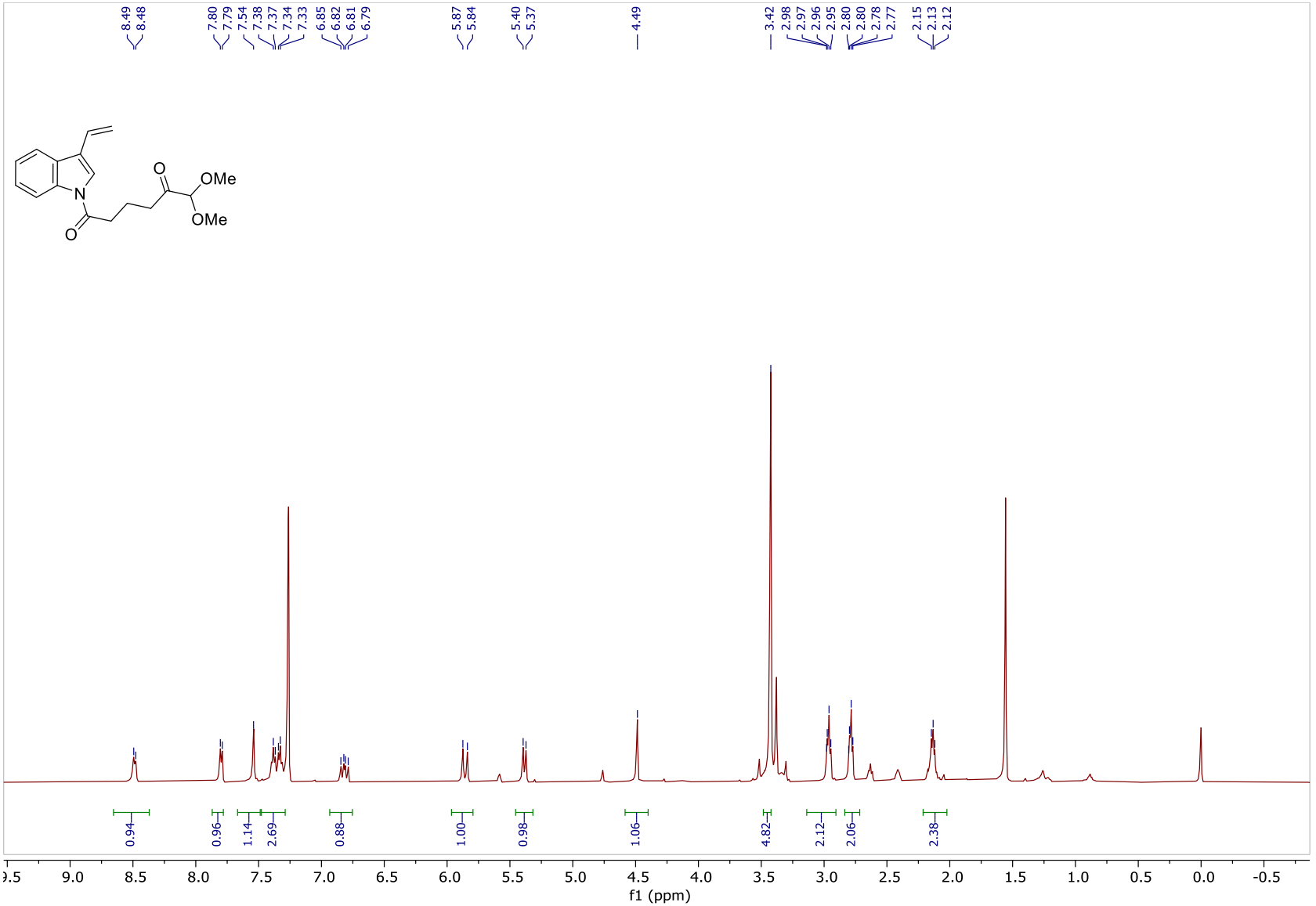

Figure 128: ^{1}H NMR Spectrum of **106** (500MHz, $CDCl_3$)

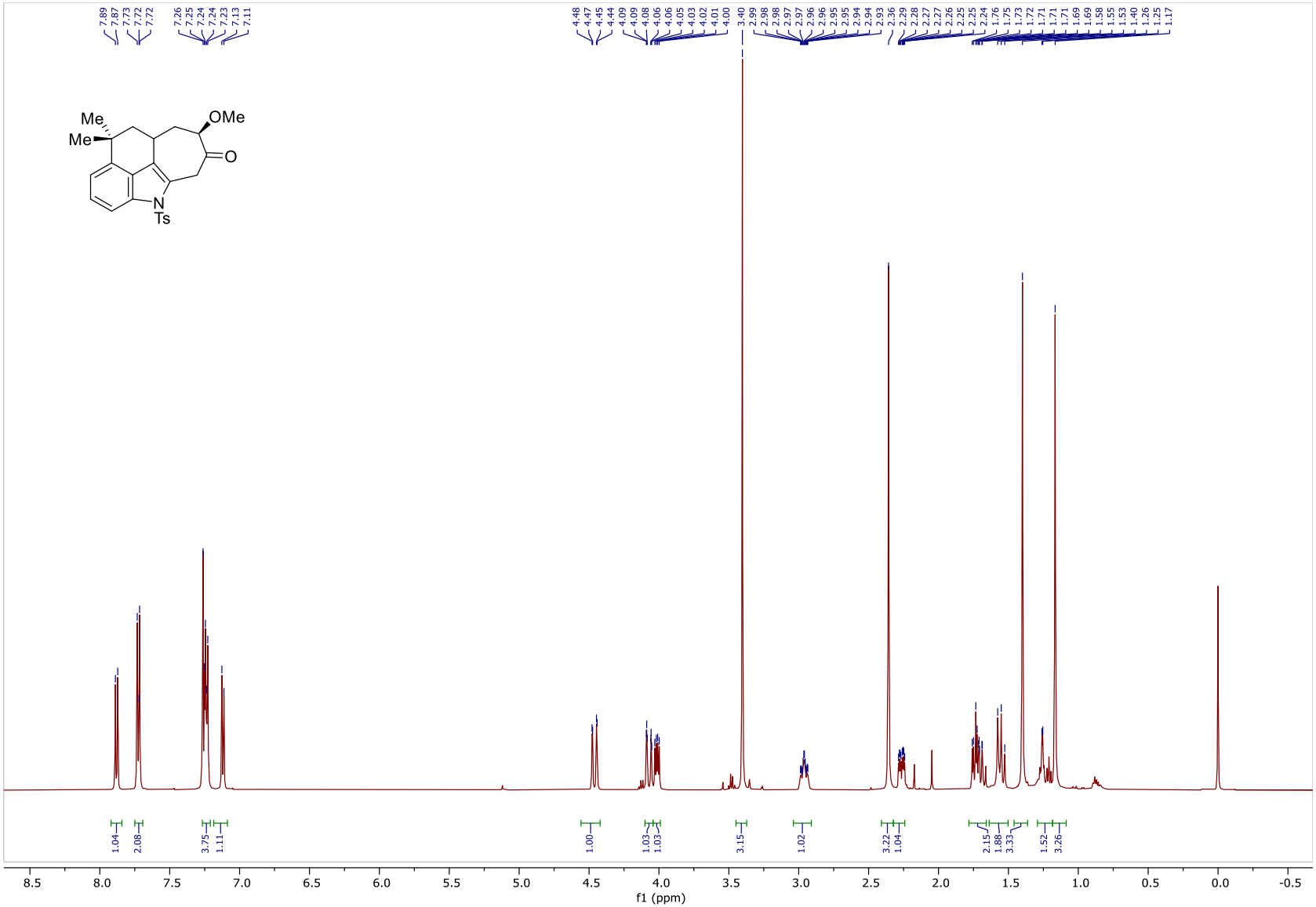

Figure 129: ^{1}H NMR Spectrum of **117** (500MHz, $CDCl_3$)

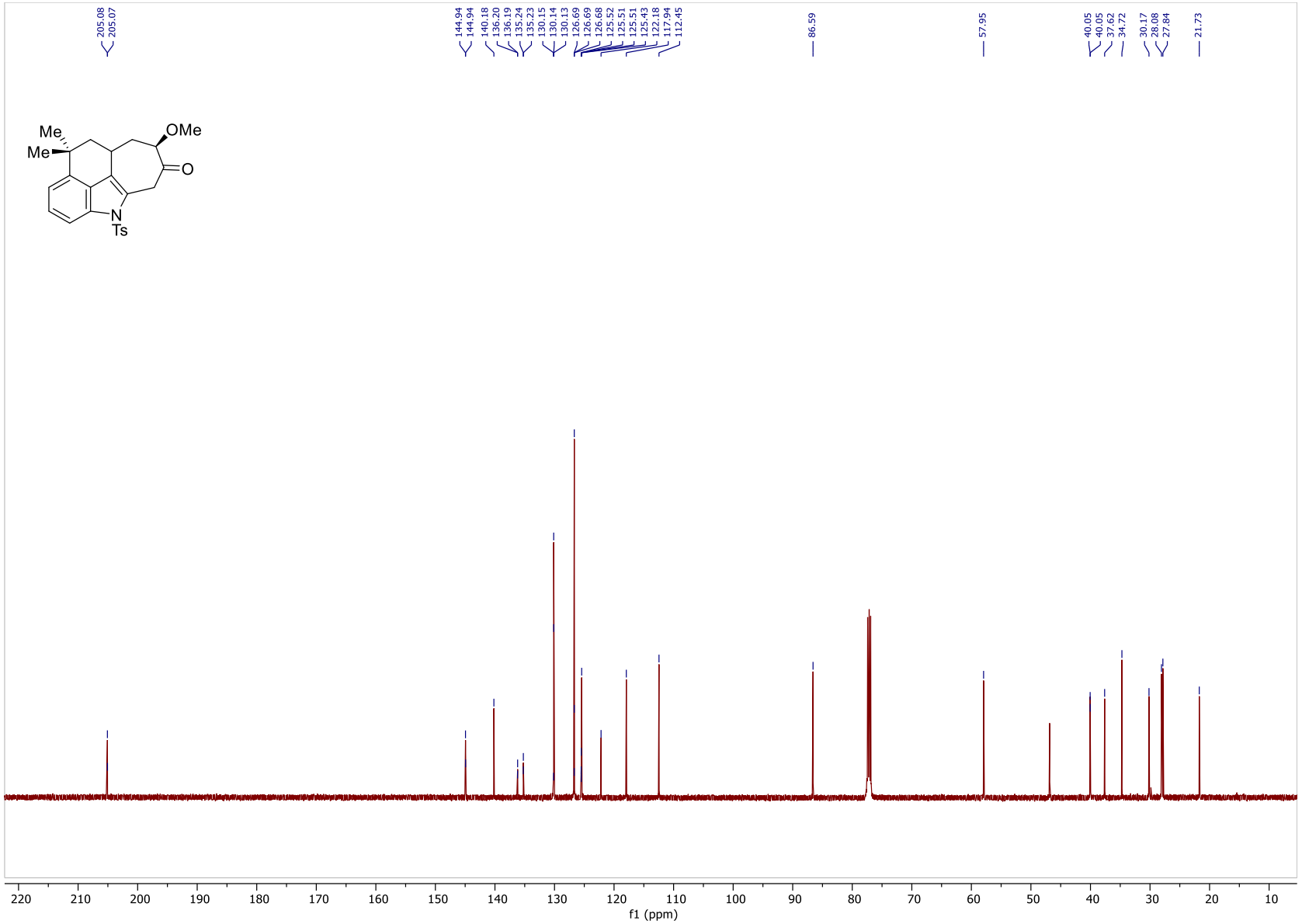

Figure 130: ^{13}C NMR Spectrum of **117** (100MHz, $CDCl_3$)

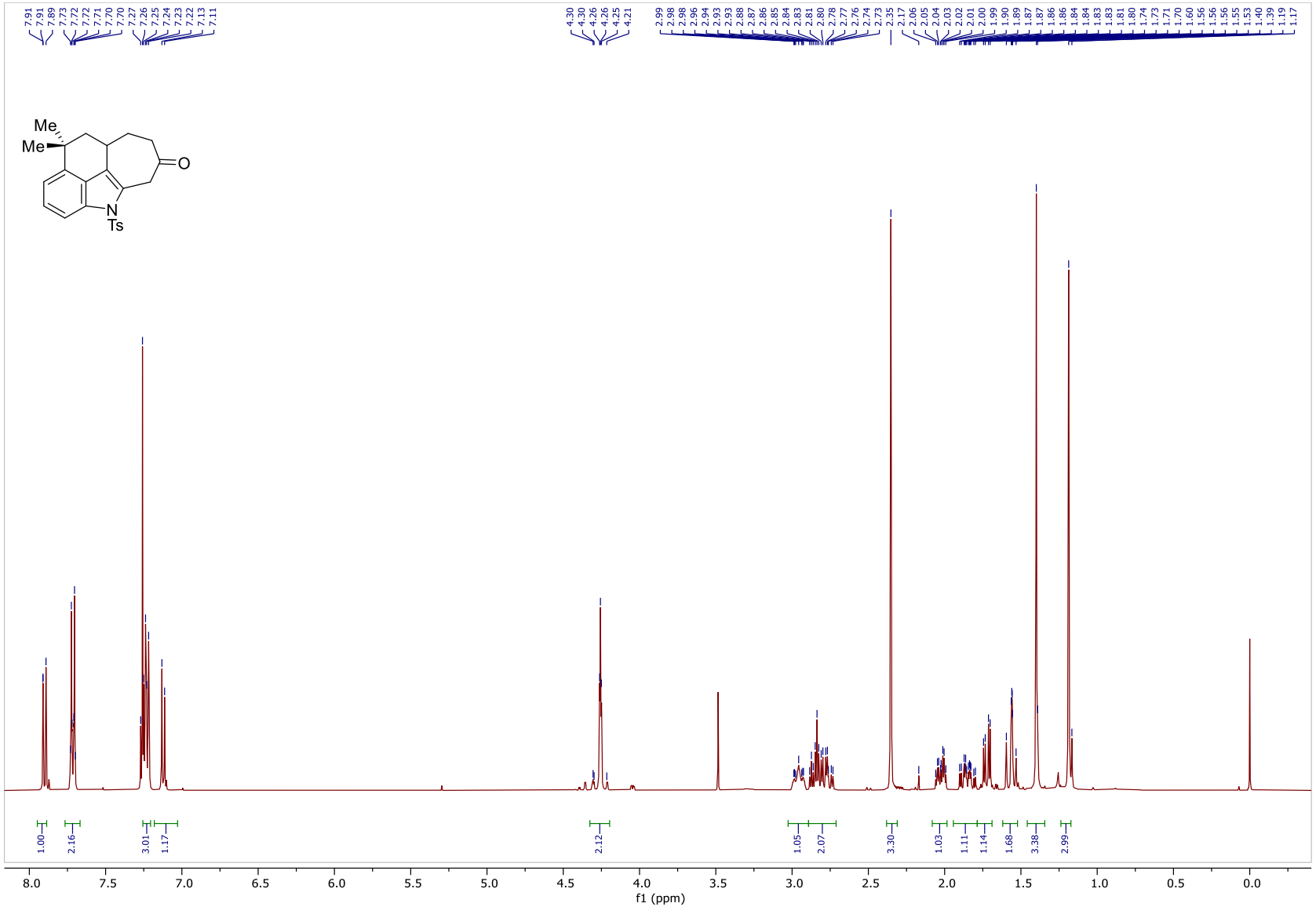

Figure 131: ^{1}H NMR Spectrum of **118a** (400MHz, $CDCl_3$)

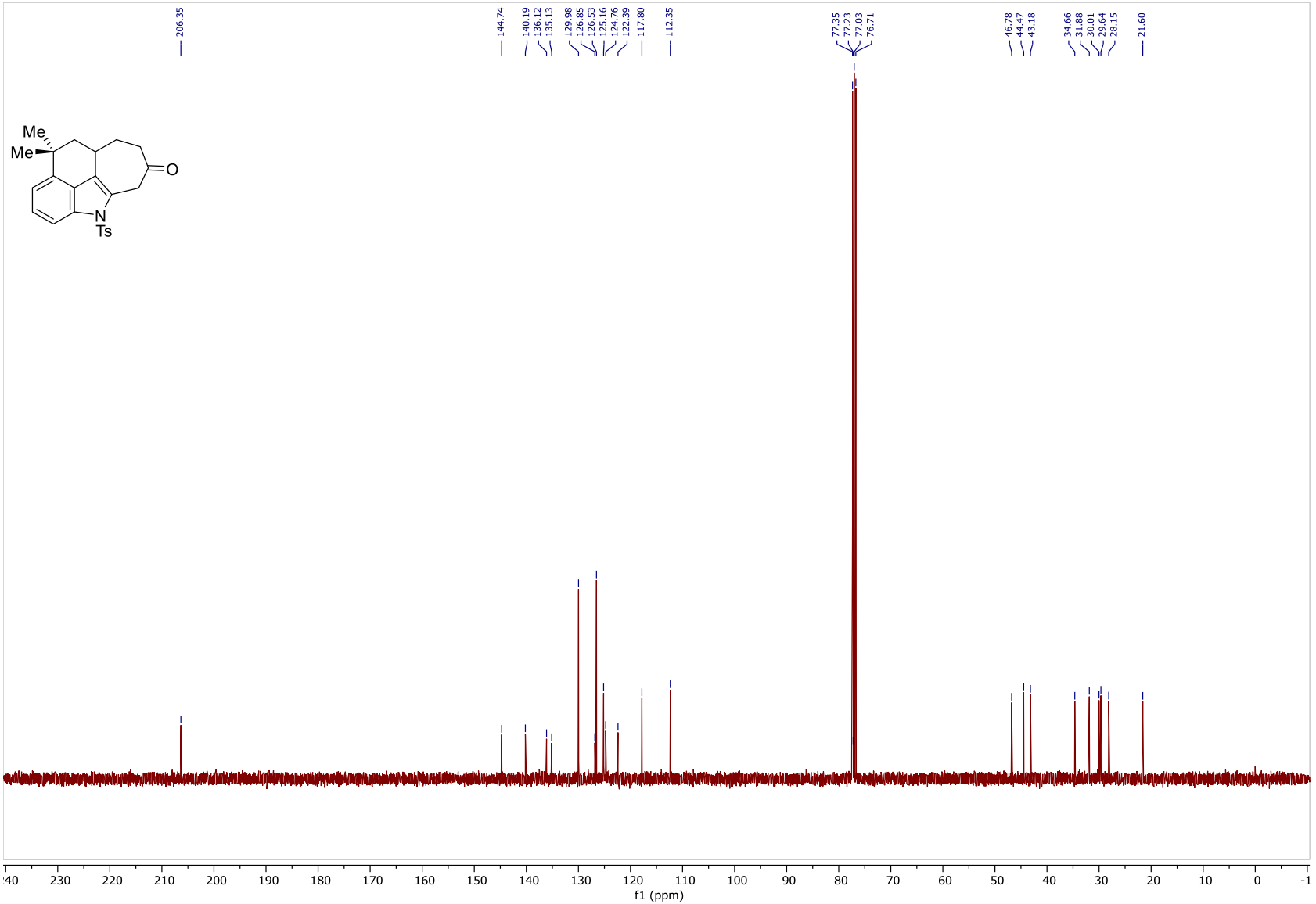

Figure 132: ^{13}C NMR Spectrum of **118a** (100MHz, $CDCl_3$)

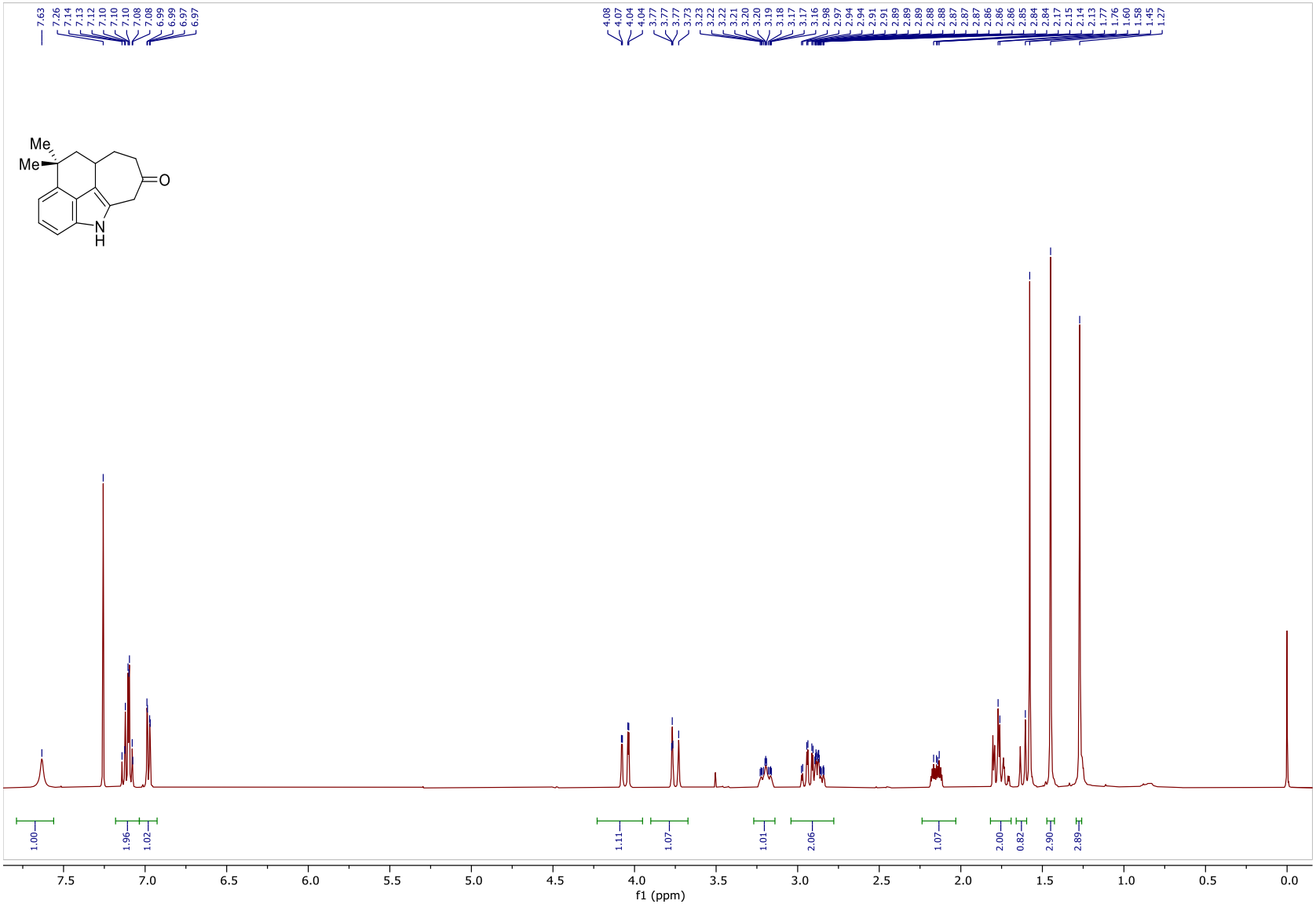

Figure 133: 1H NMR Spectrum of **118b** (400MHz, CDCl3)

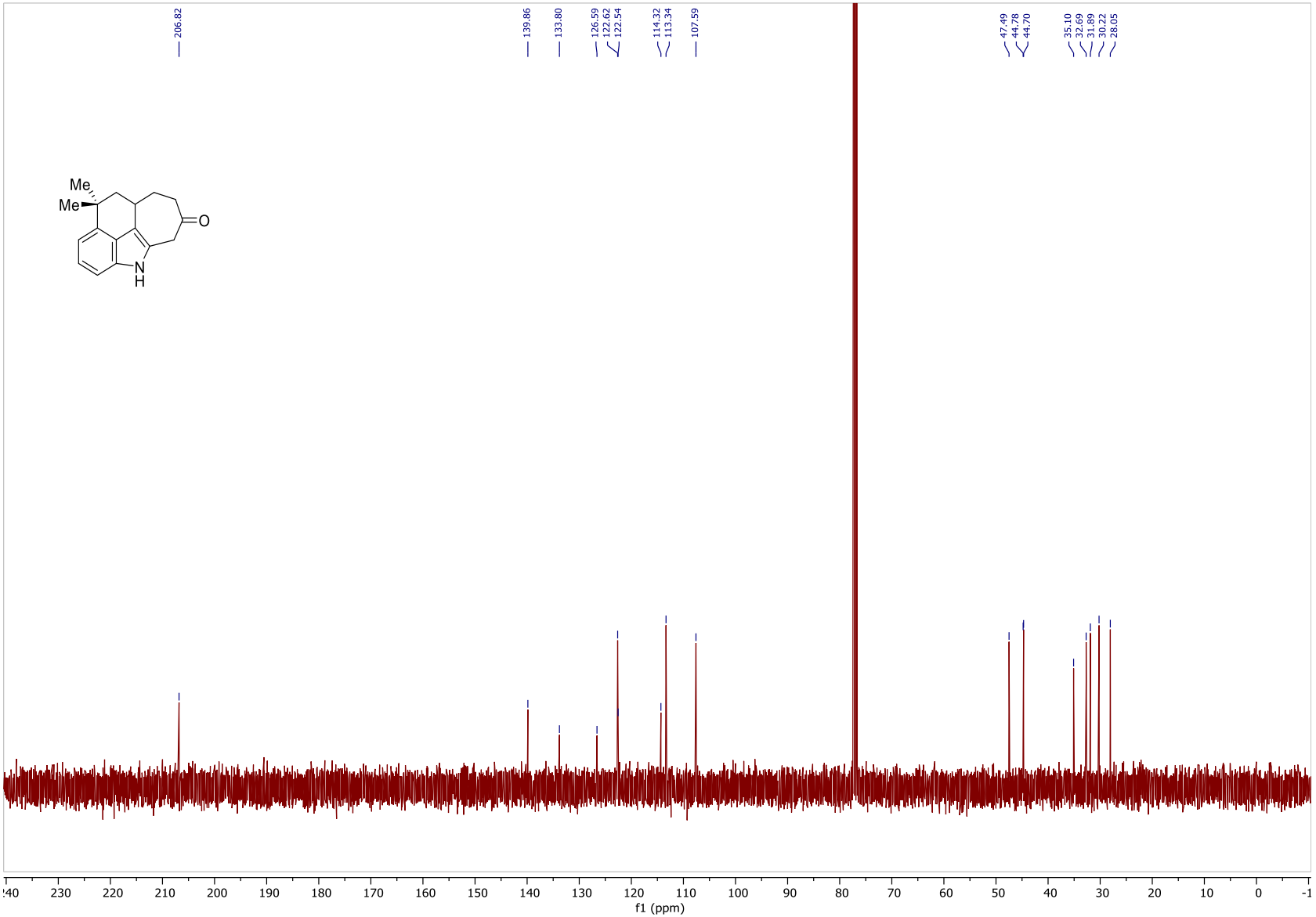

Figure 134: ^{13}C NMR Spectrum of **118b** (100MHz, $CDCl_3$)

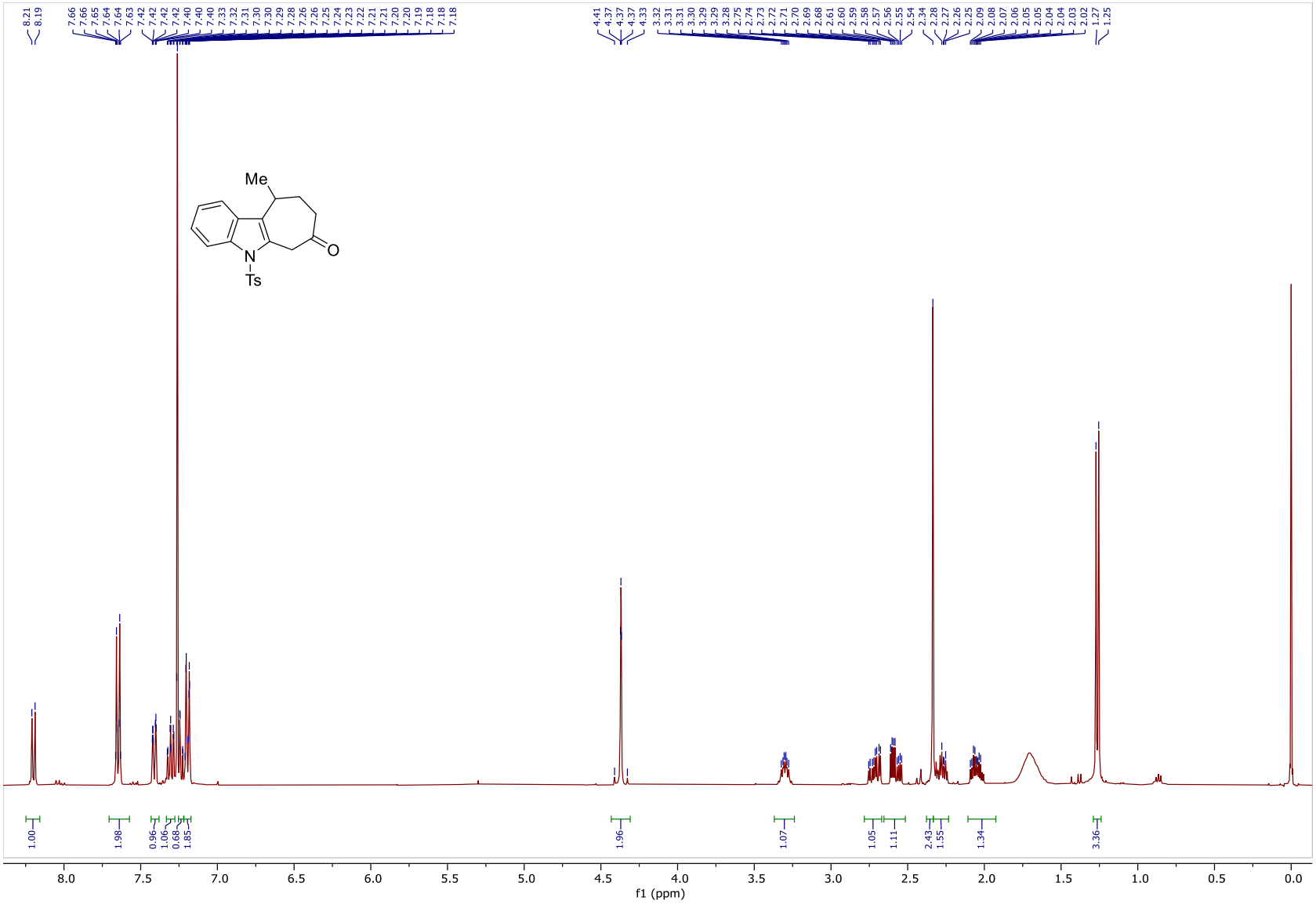

Figure 135: ^{1}H NMR Spectrum of **122** (400MHz, $CDCl_3$)

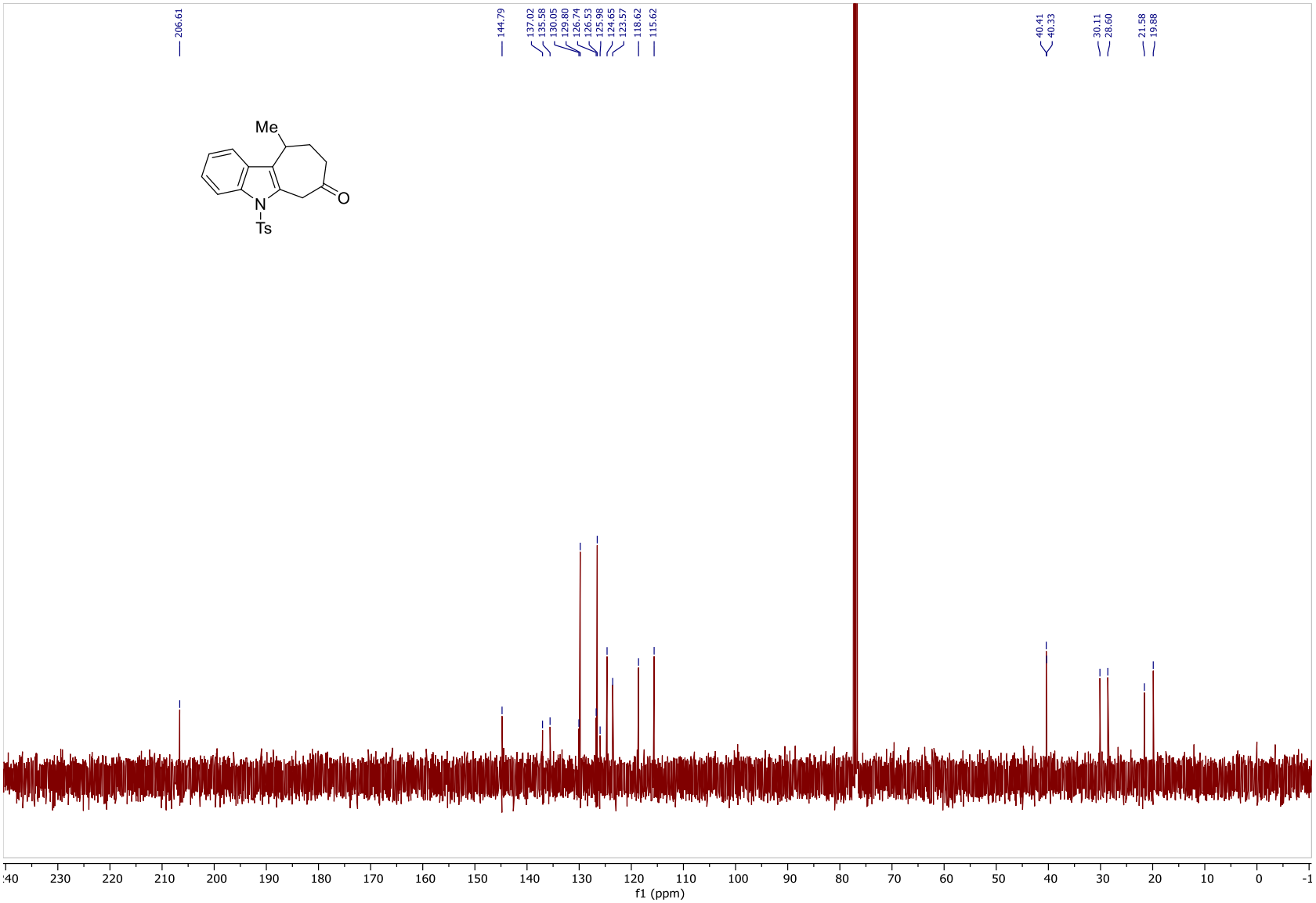

Figure 136: ^{13}C NMR Spectrum of **122** (100MHz, CDCl3)

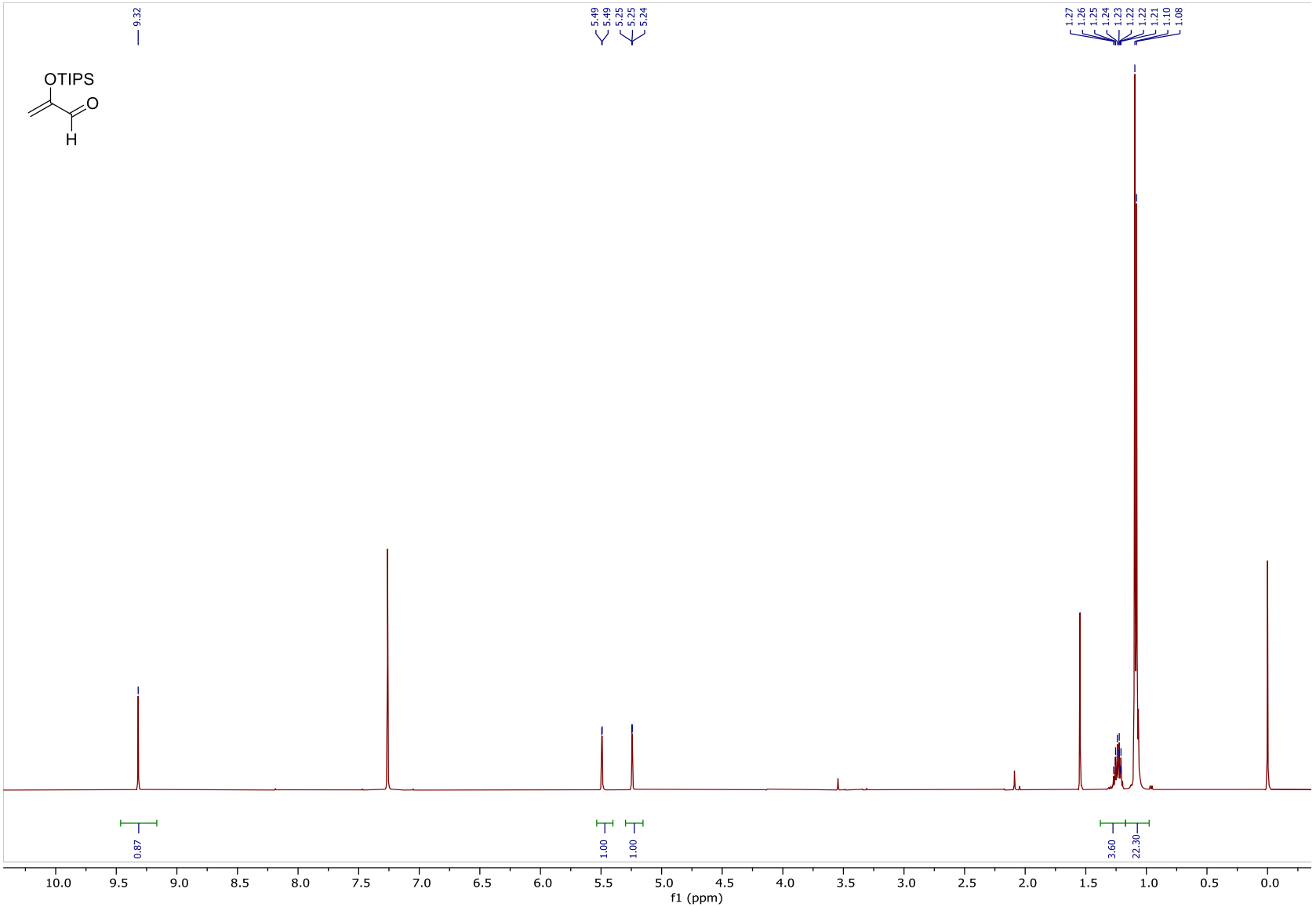

Figure 137: ^{1}H NMR Spectrum of **115b** (500MHz, $CDCl_3$)

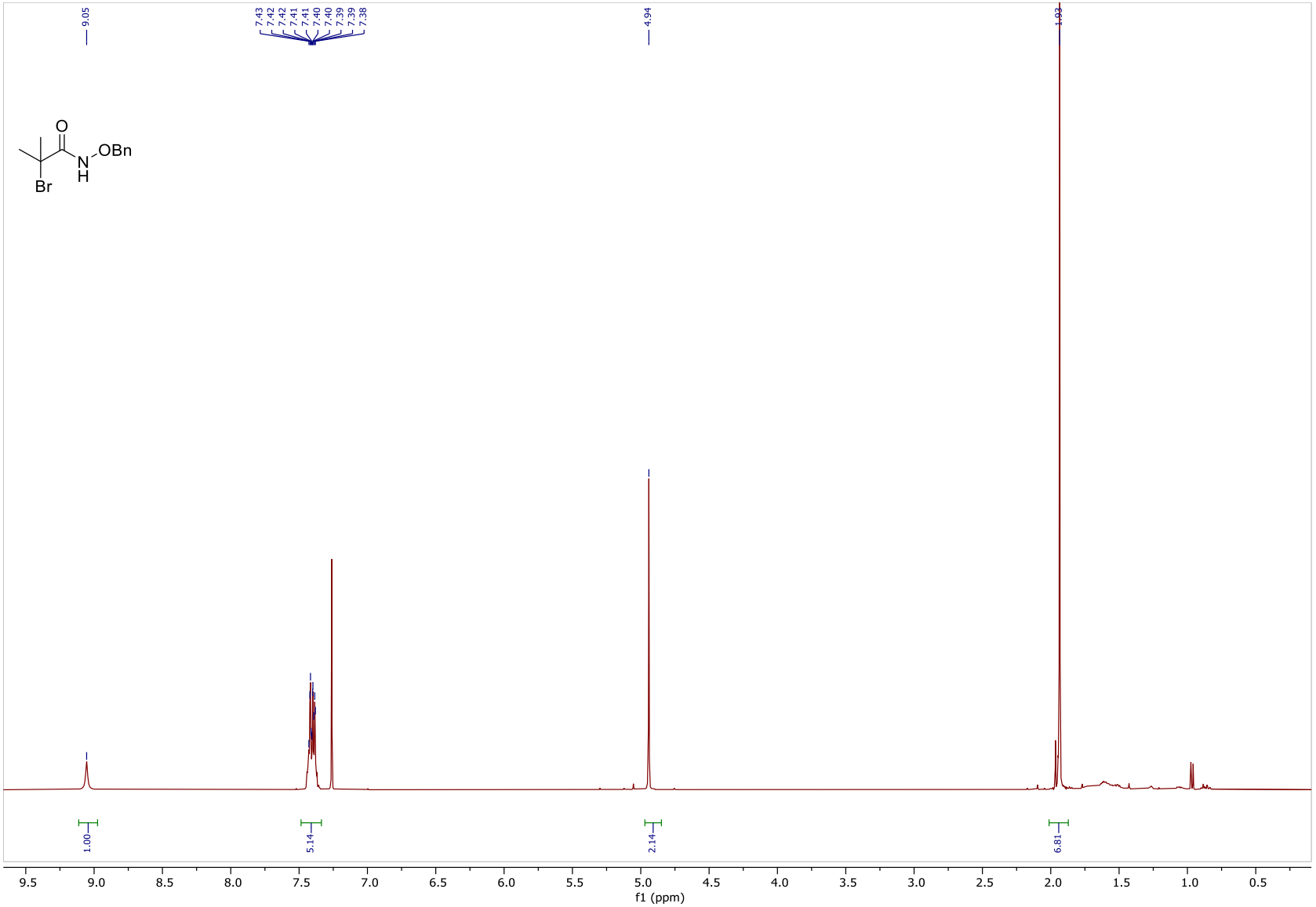

Figure 138: ^{1}H NMR Spectrum of **115c** (400MHz, $CDCl_3$)

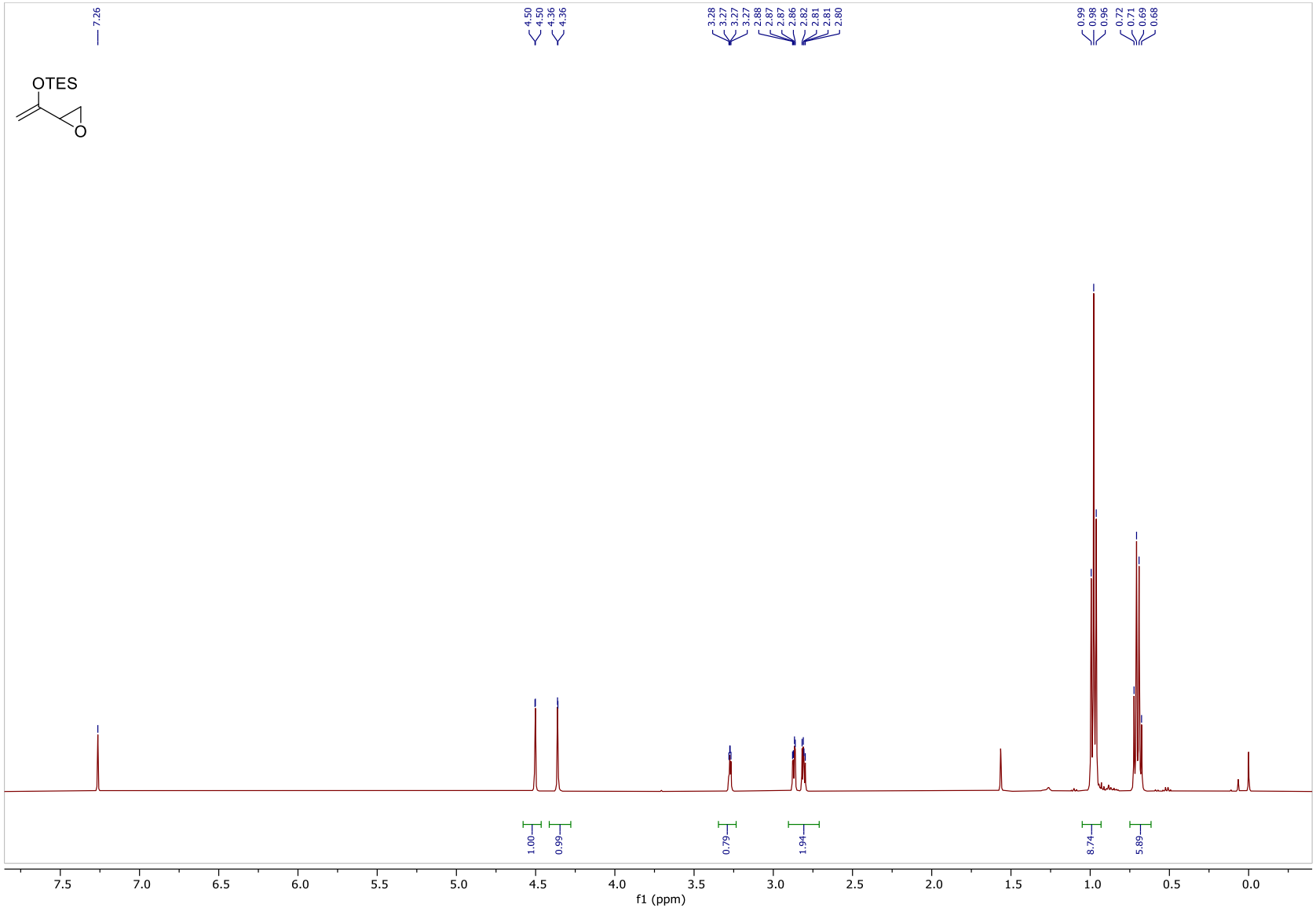

Figure 139: ^{1}H NMR Spectrum of **115d** (500MHz, $CDCl_3$)

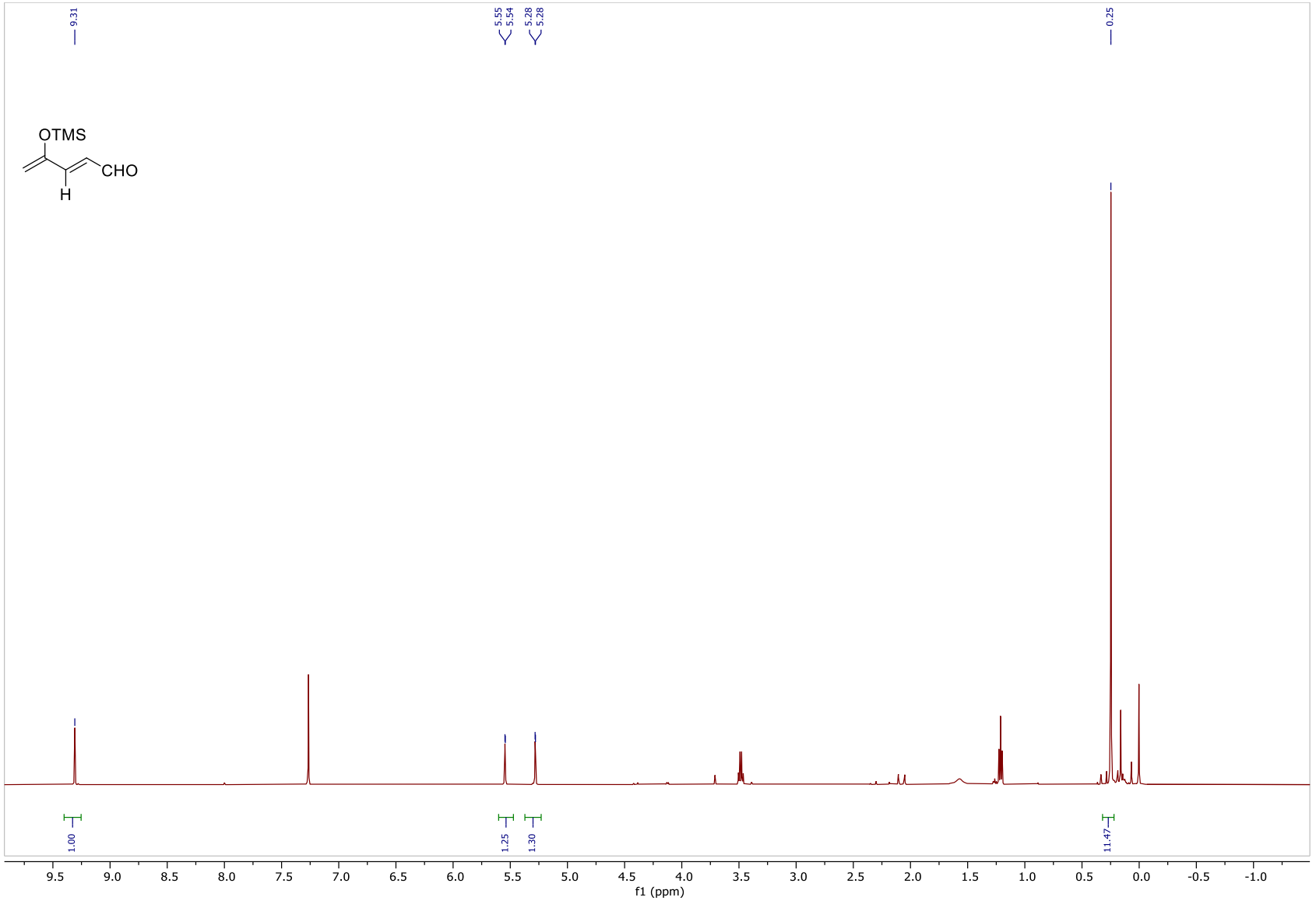

Figure 140: ^{1}H NMR Spectrum of **115e** (500MHz, $CDCl_3$)

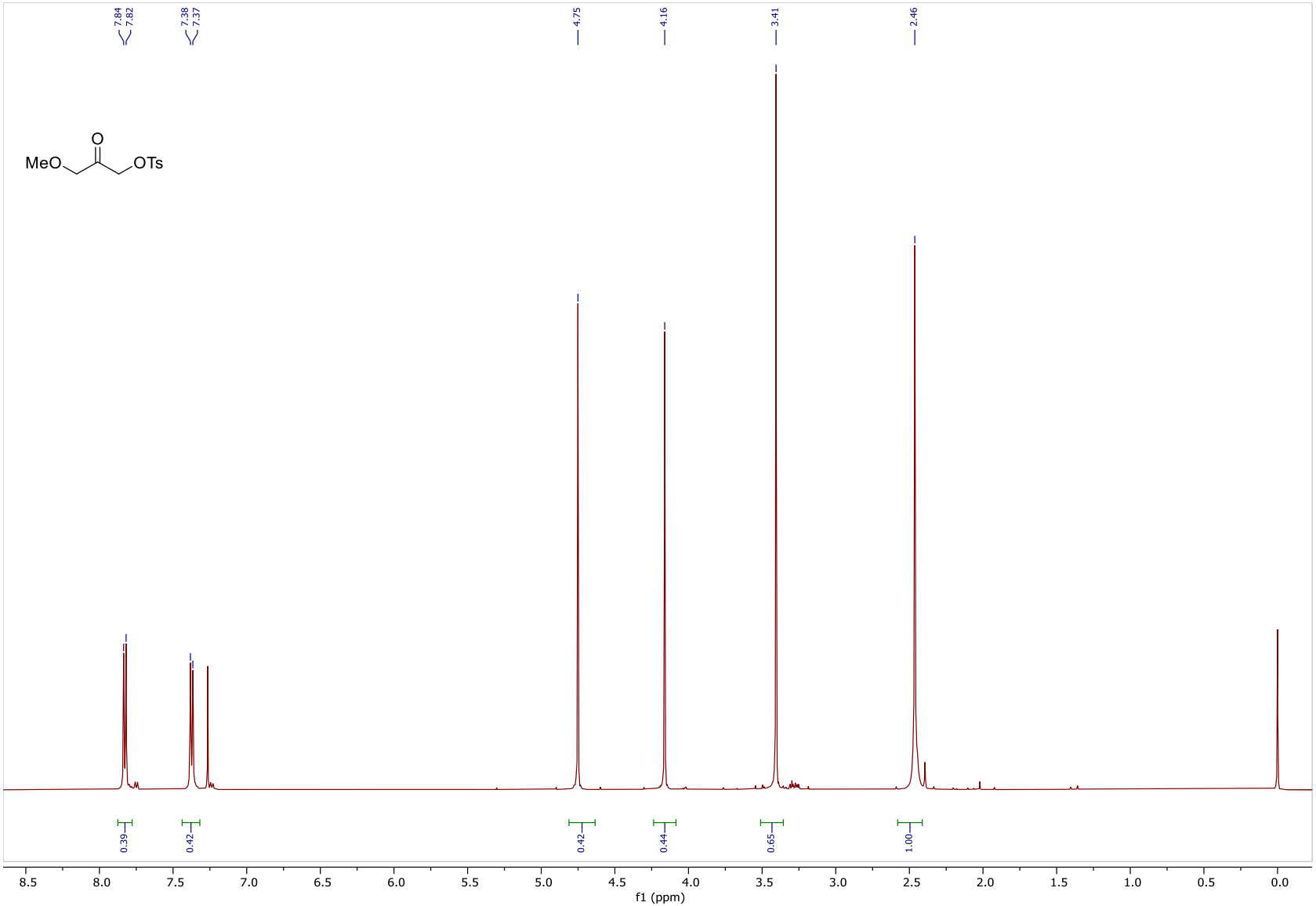

Figure 141: ^{1}H NMR Spectrum of **115f** (500MHz, $CDCl_3$)

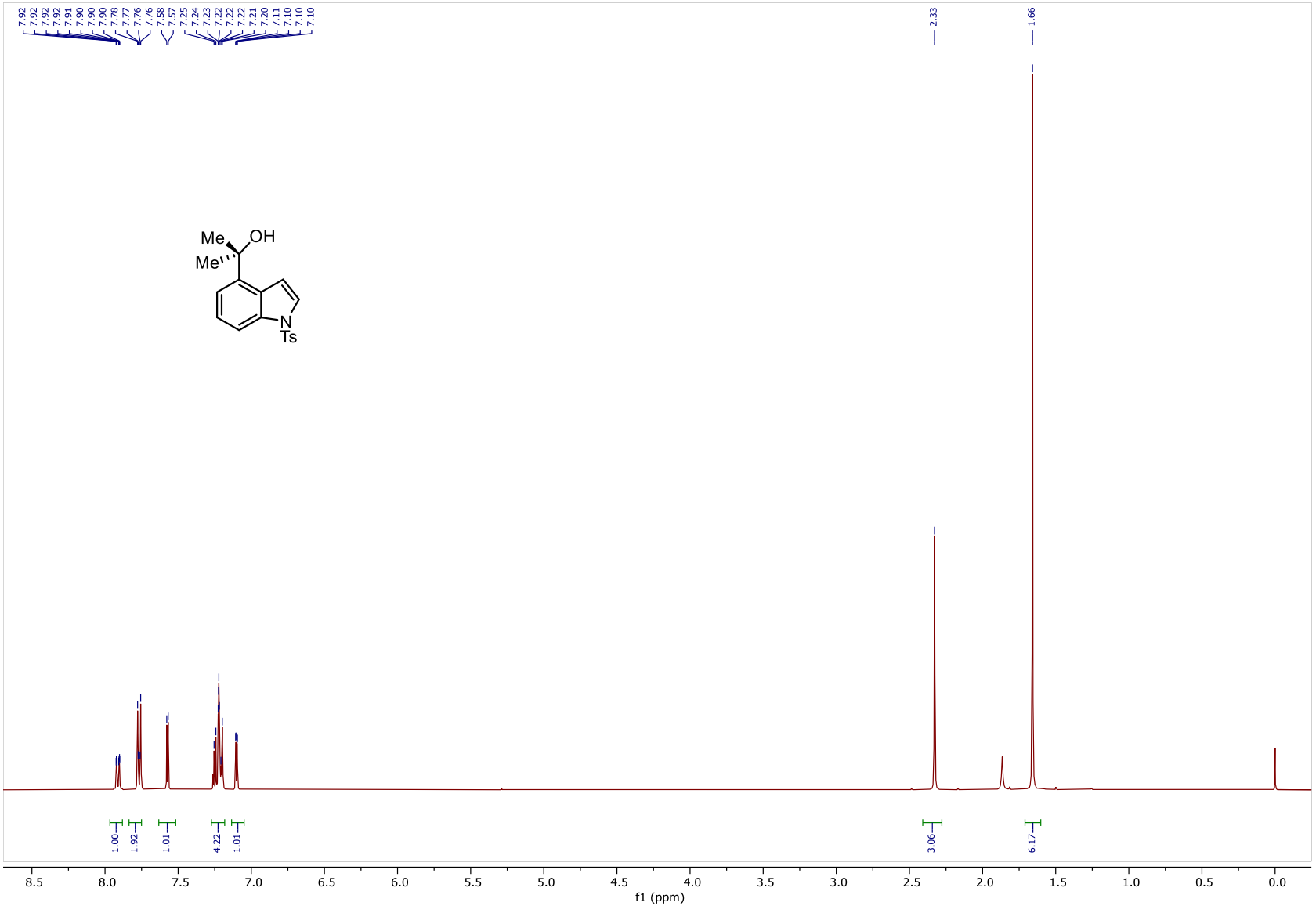

Figure 142: ^{1}H NMR Spectrum of **176** (400MHz, $CDCl_3$)

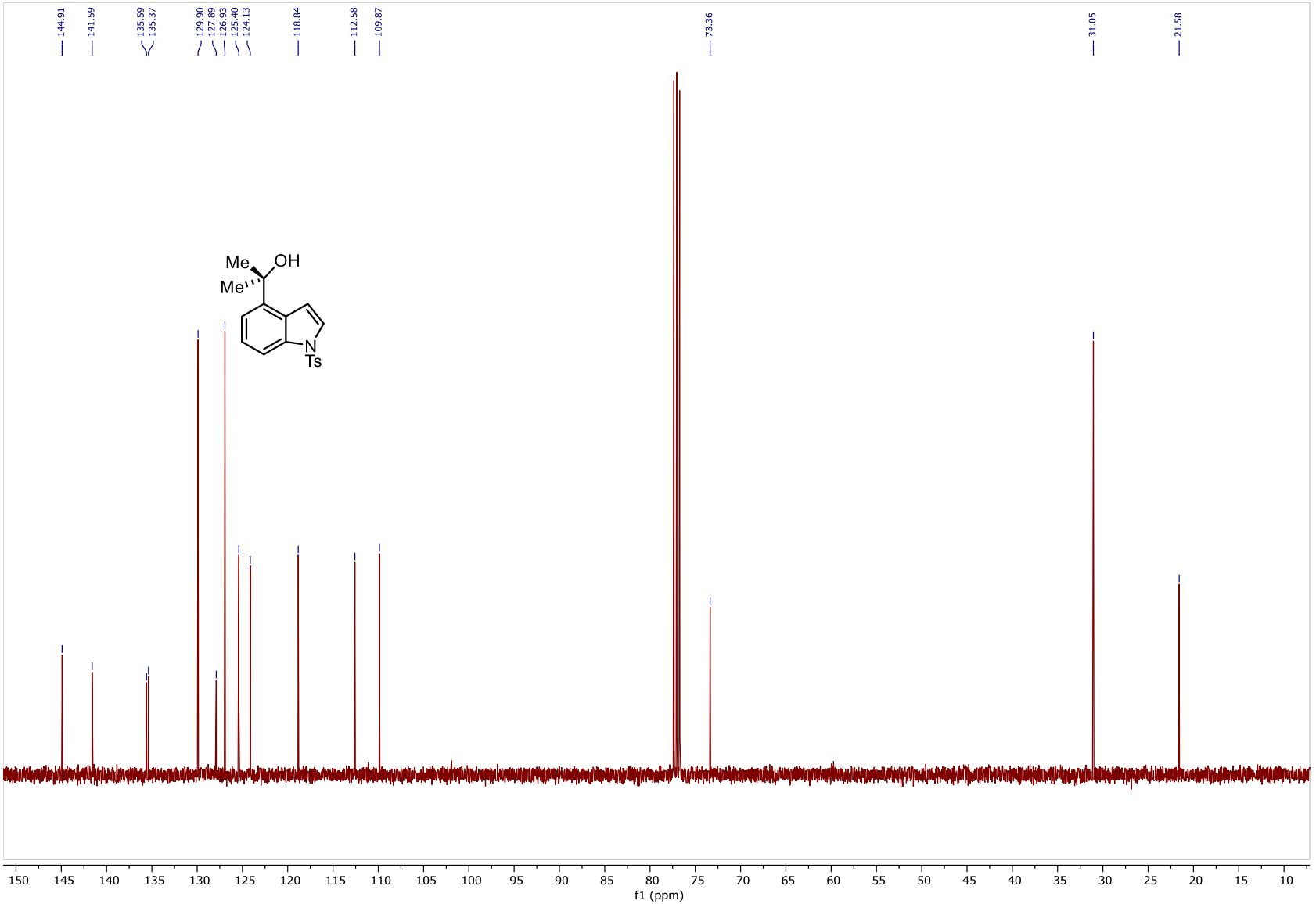

Figure 143: ^{13}C NMR Spectrum of **176** (100MHz, $CDCl_3$)

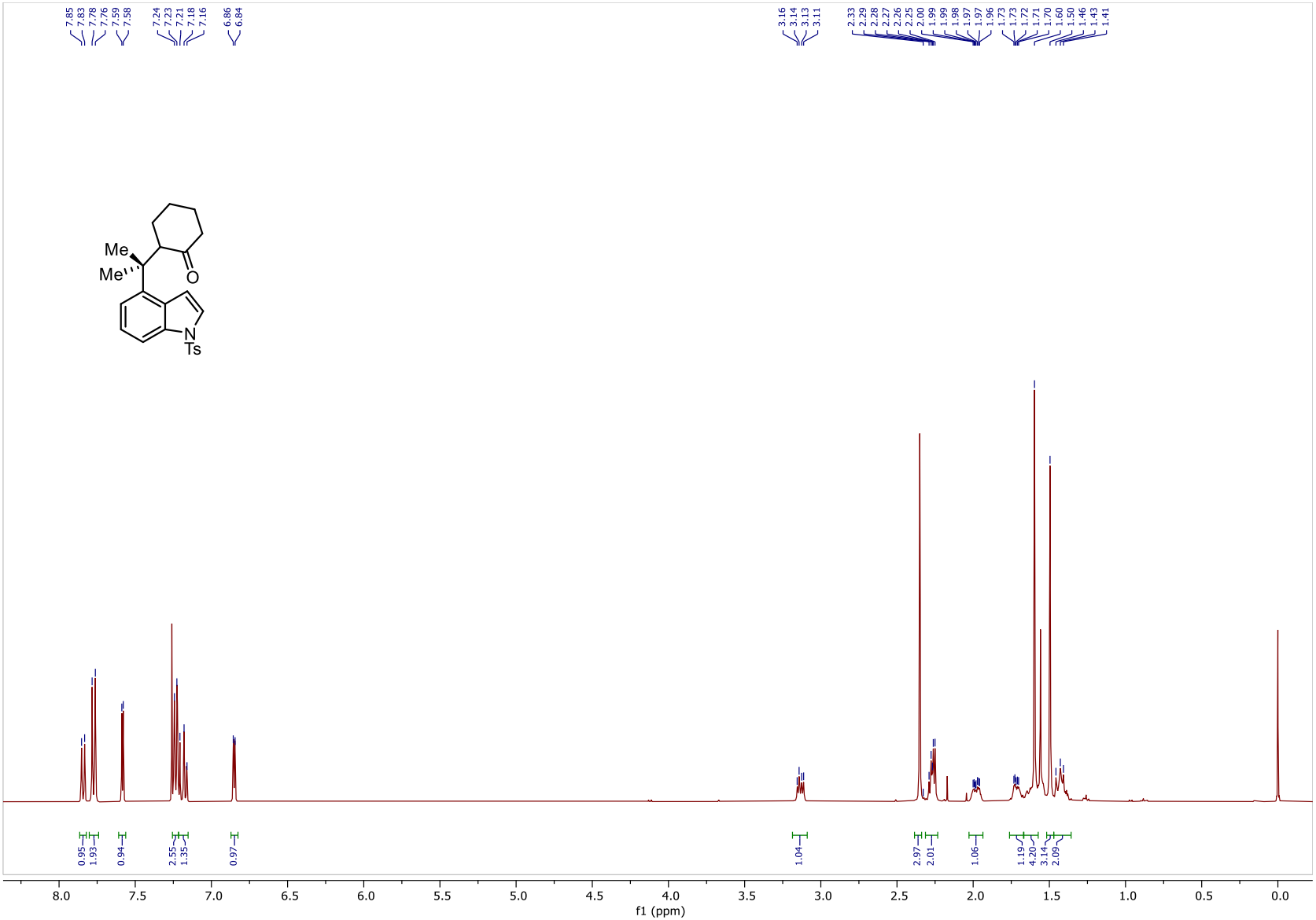

Figure 144: ^{1}H NMR Spectrum of **180** (400MHz, $CDCl_3$)

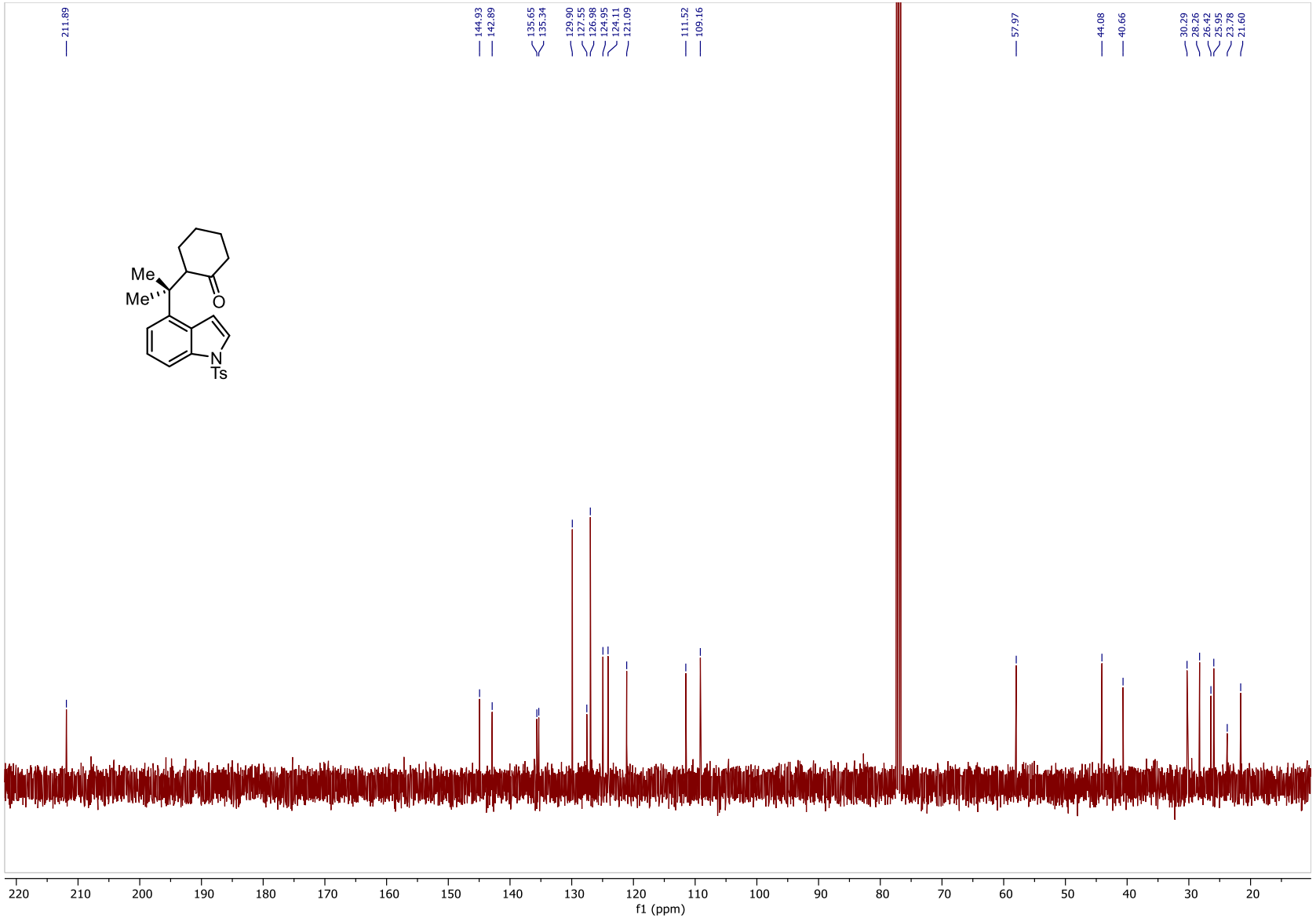

Figure 145: ^{13}C NMR Spectrum of **180** (100MHz, $CDCl_3$)

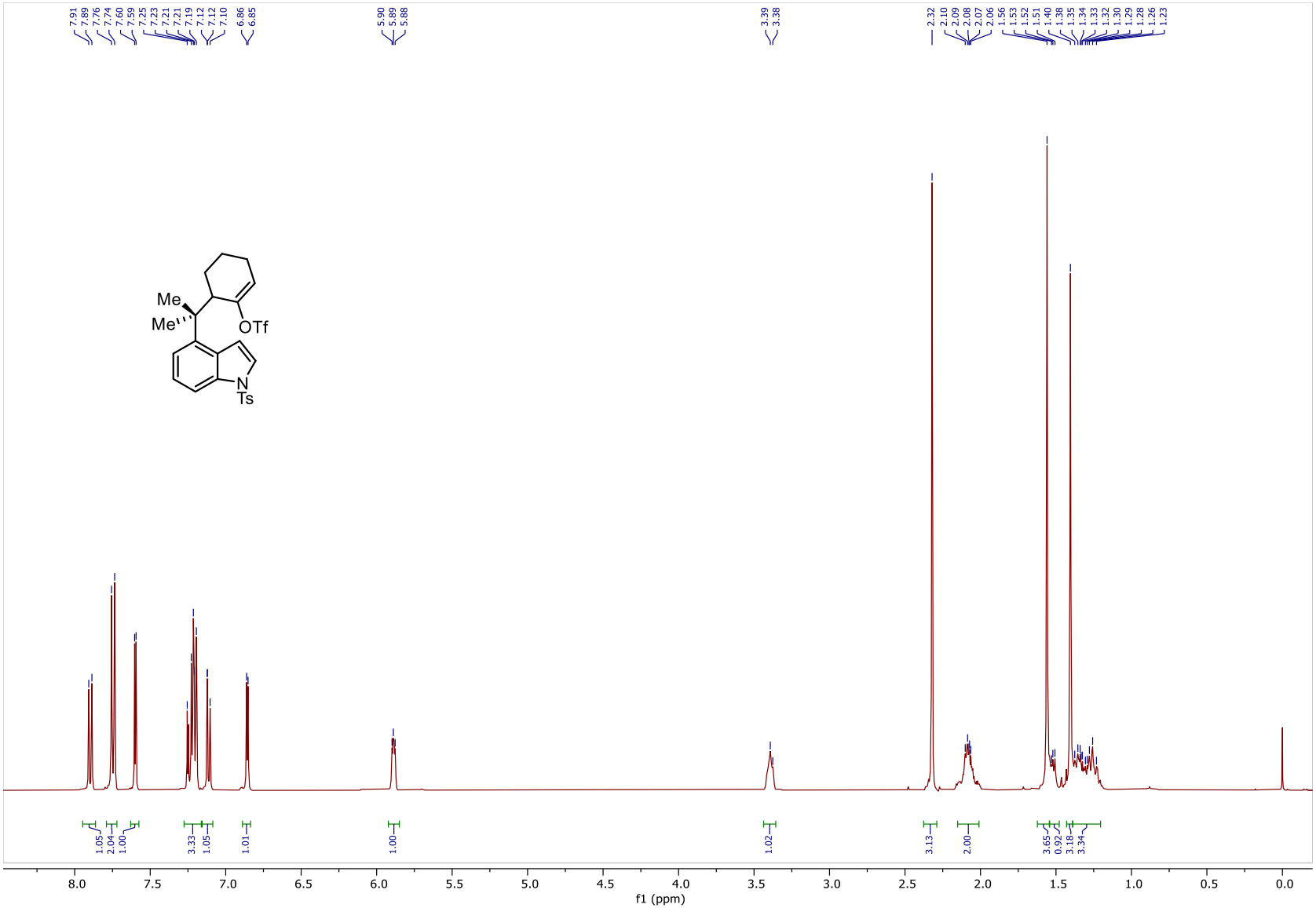

Figure 146: ^{1}H NMR Spectrum of **181** (400MHz, $CDCl_3$)

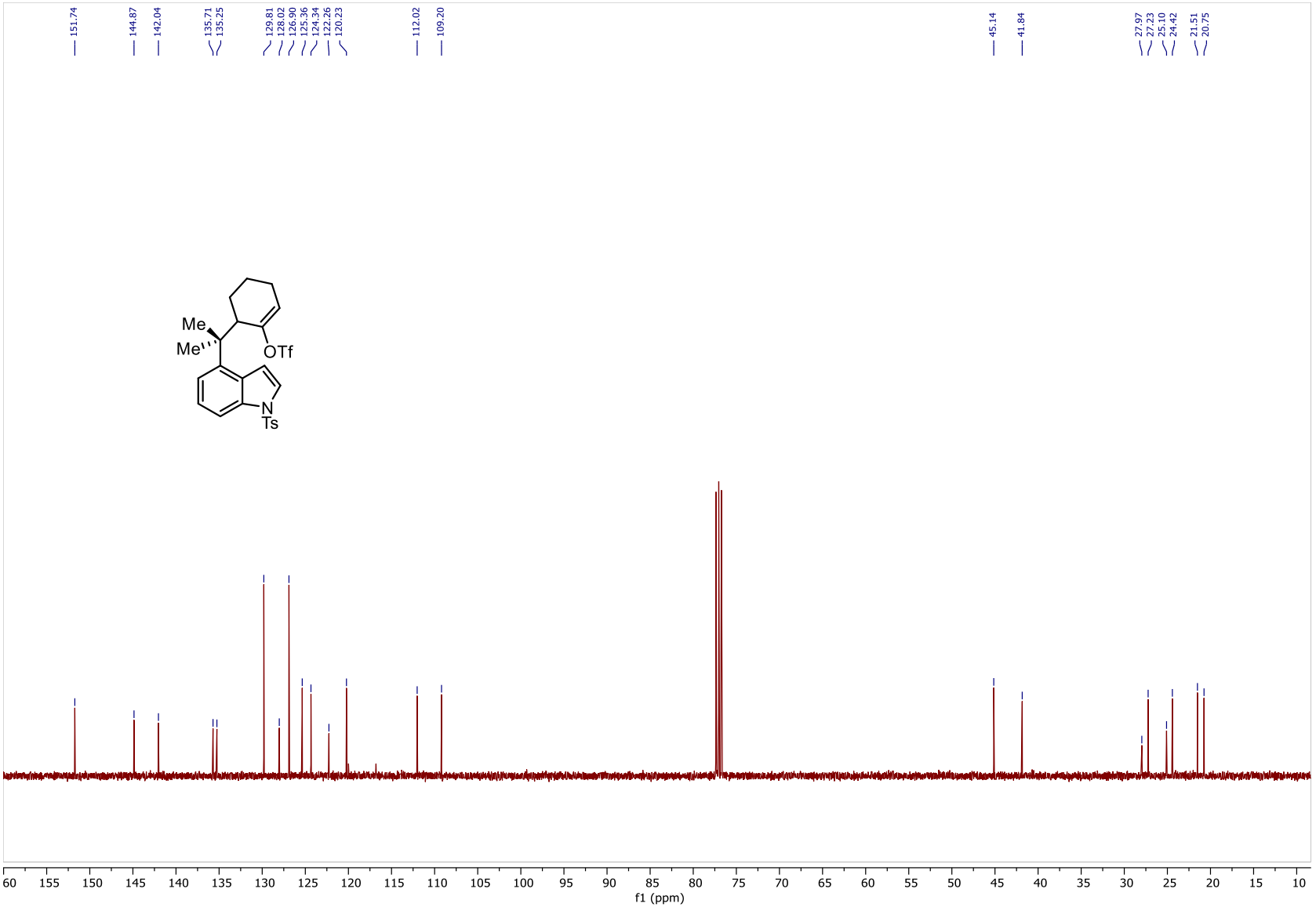

Figure 147: ^{13}C NMR Spectrum of **181** (100MHz, $CDCl_3$)

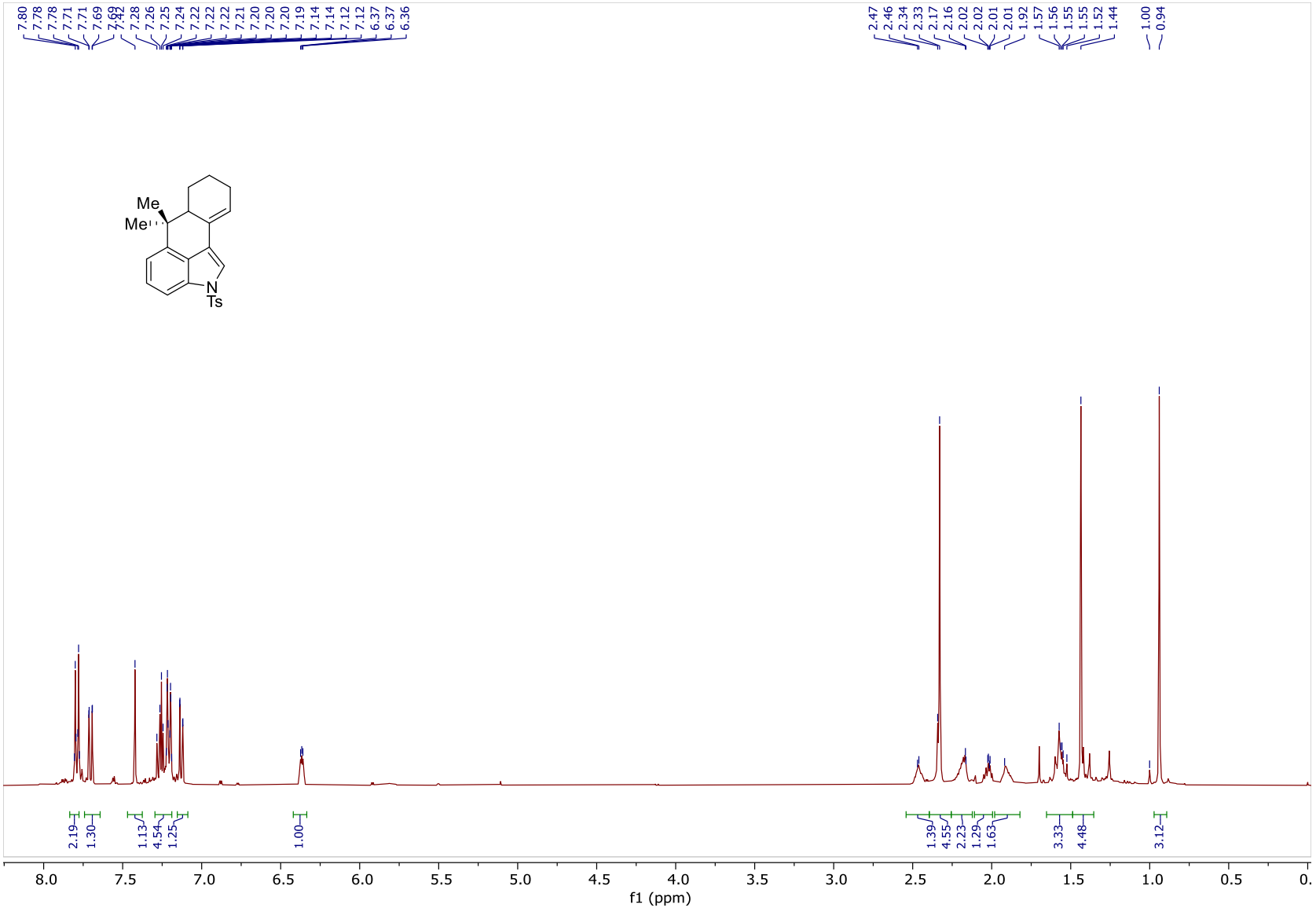

Figure 148: ^{1}H NMR Spectrum of **182** (400MHz, $CDCl_3$)

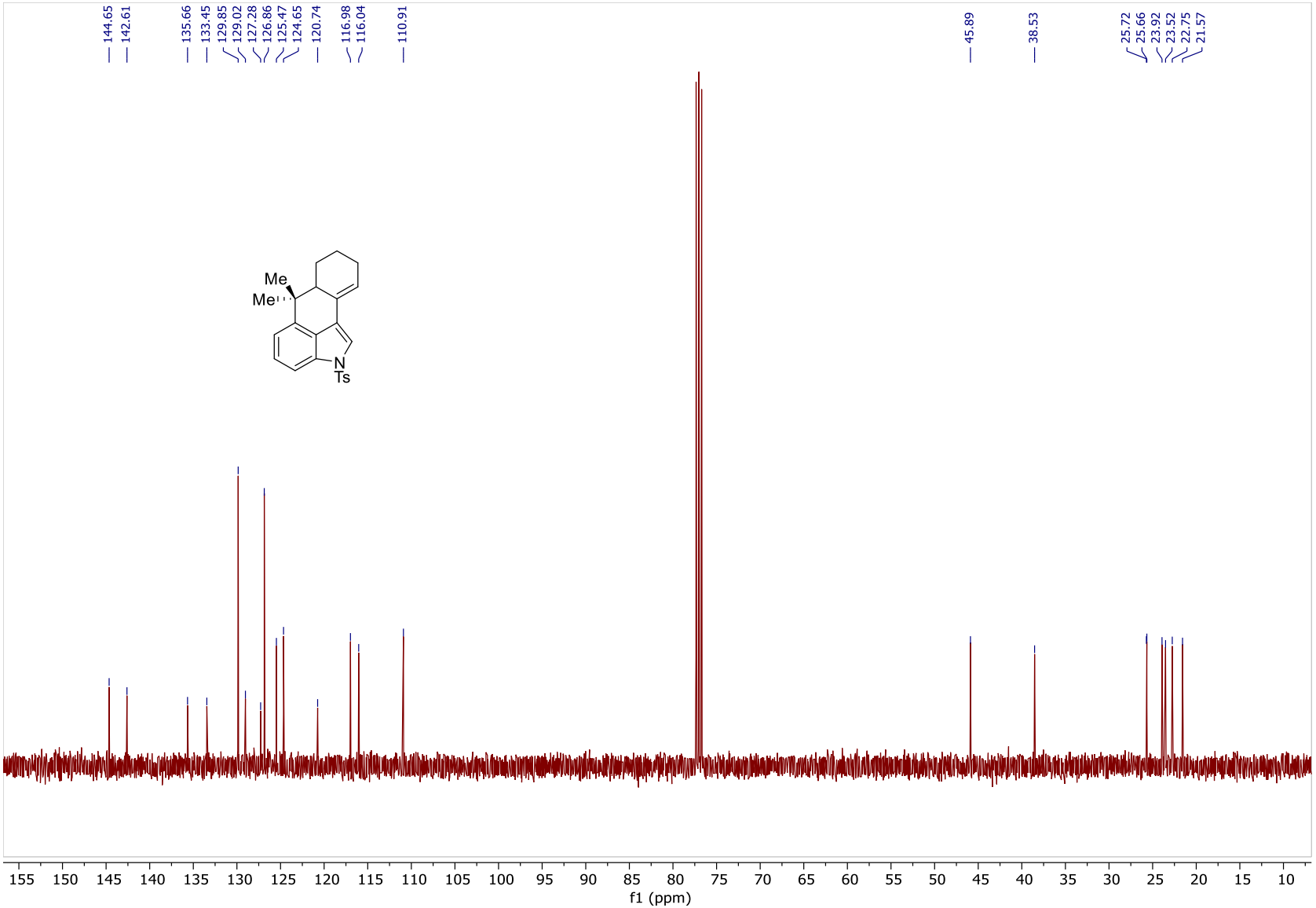

Figure 149: ^{13}C NMR Spectrum of **182** (100MHz, $CDCl_3$)

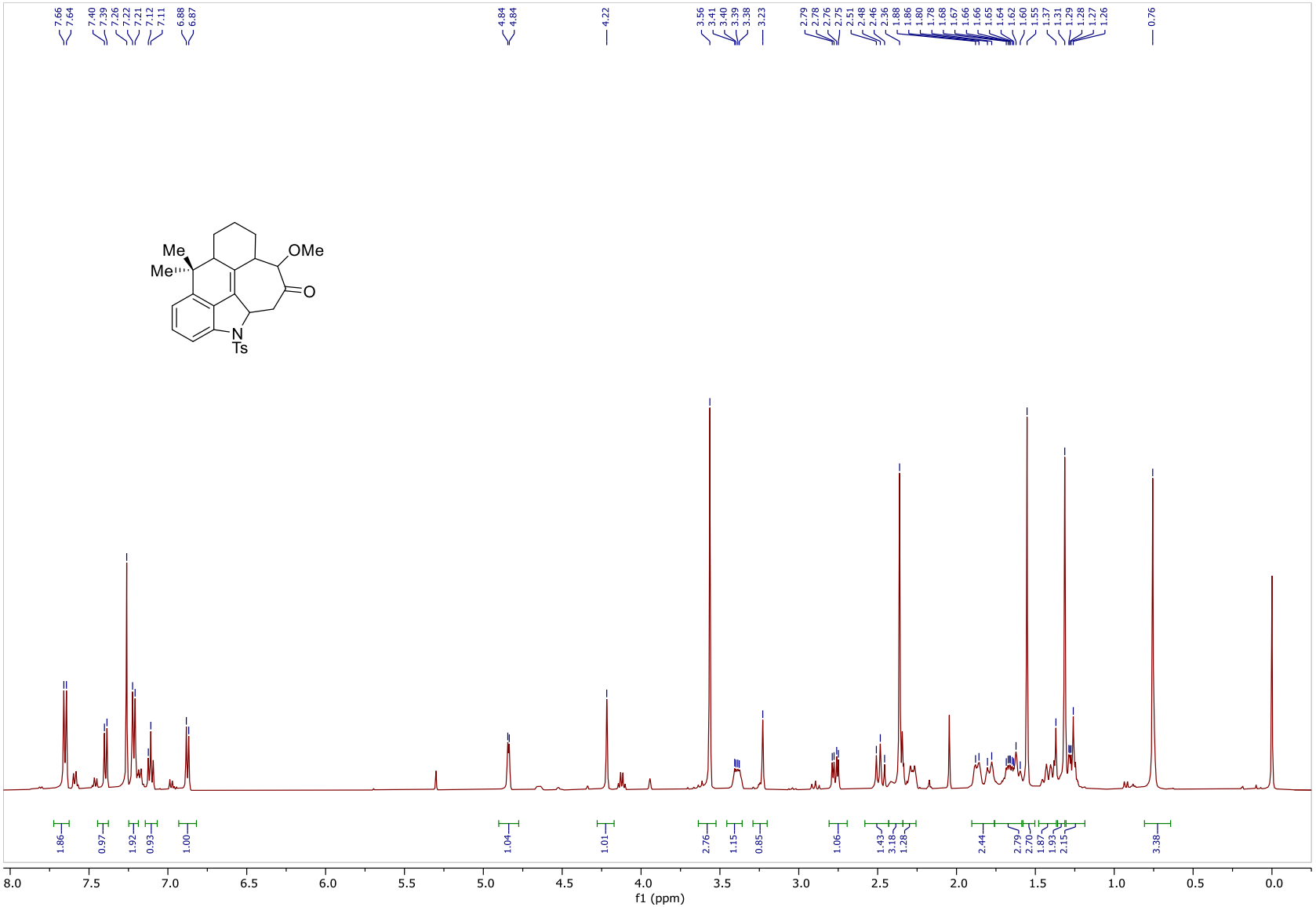

Figure 150: ^{1}H NMR Spectrum of **183** (400MHz, $CDCl_3$)

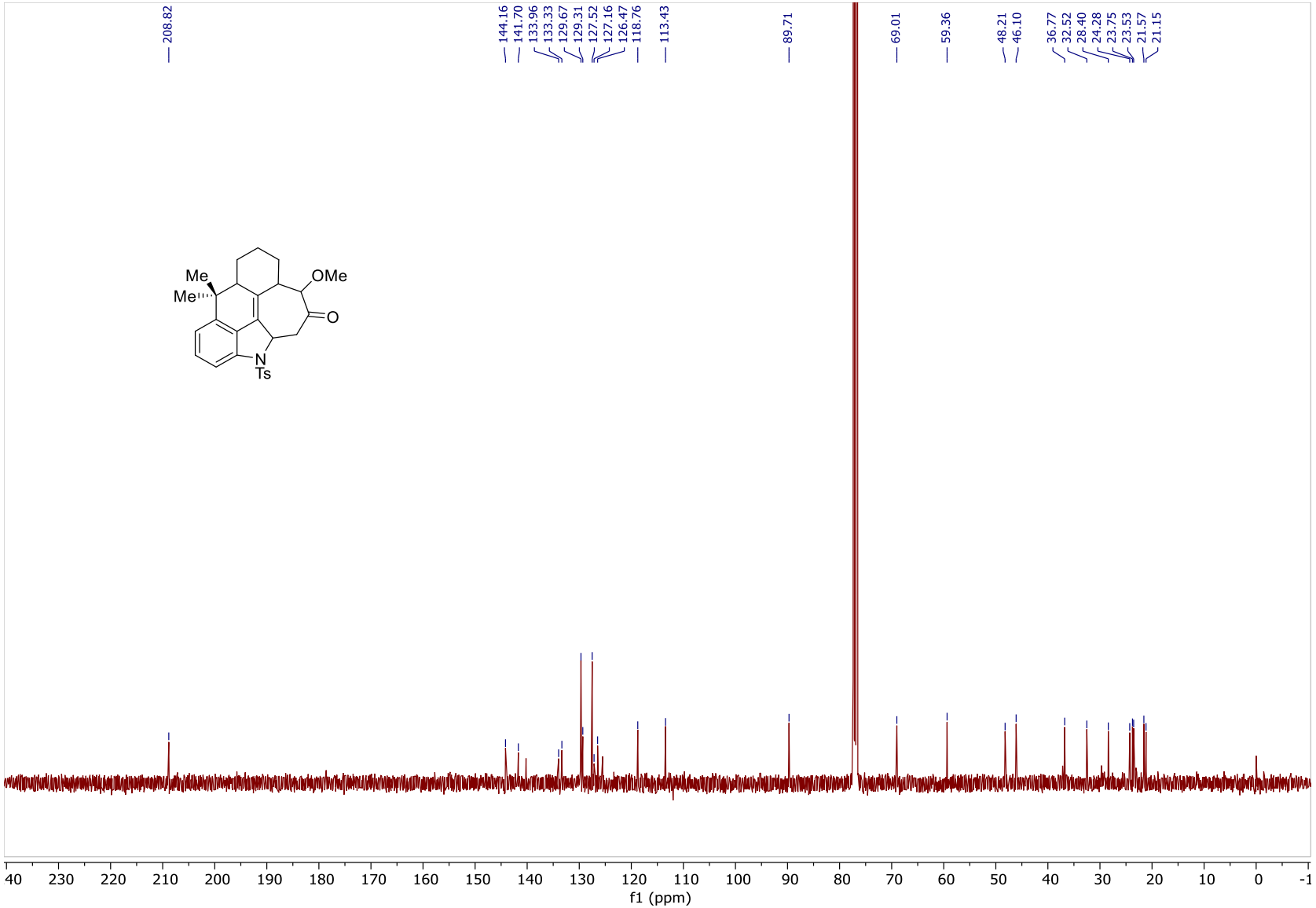

Figure 151: ^{13}C NMR Spectrum of **183** (100MHz, $CDCl_3$)

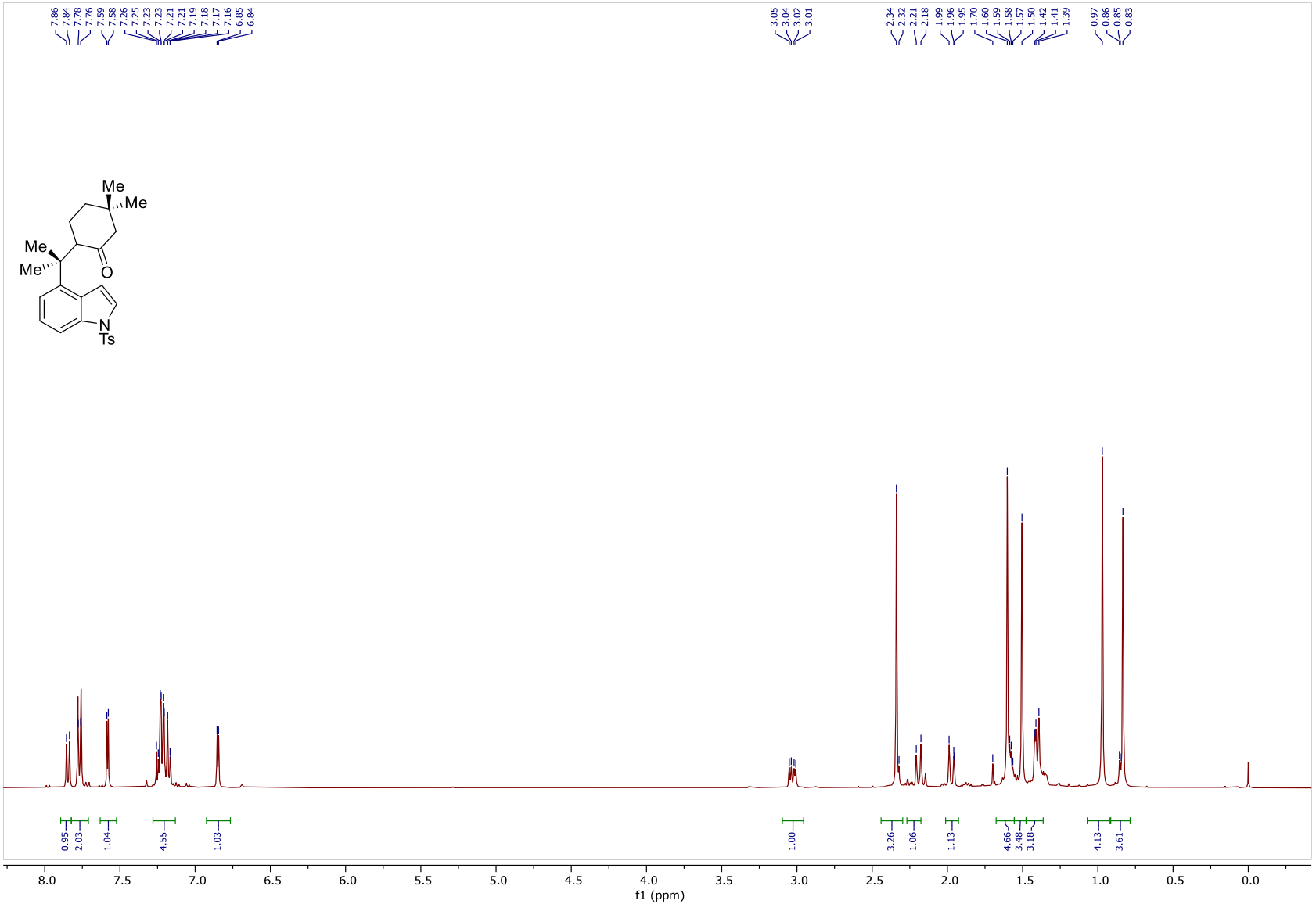

Figure 152: ^{1}H NMR Spectrum of **185** (400MHz, $CDCl_3$)

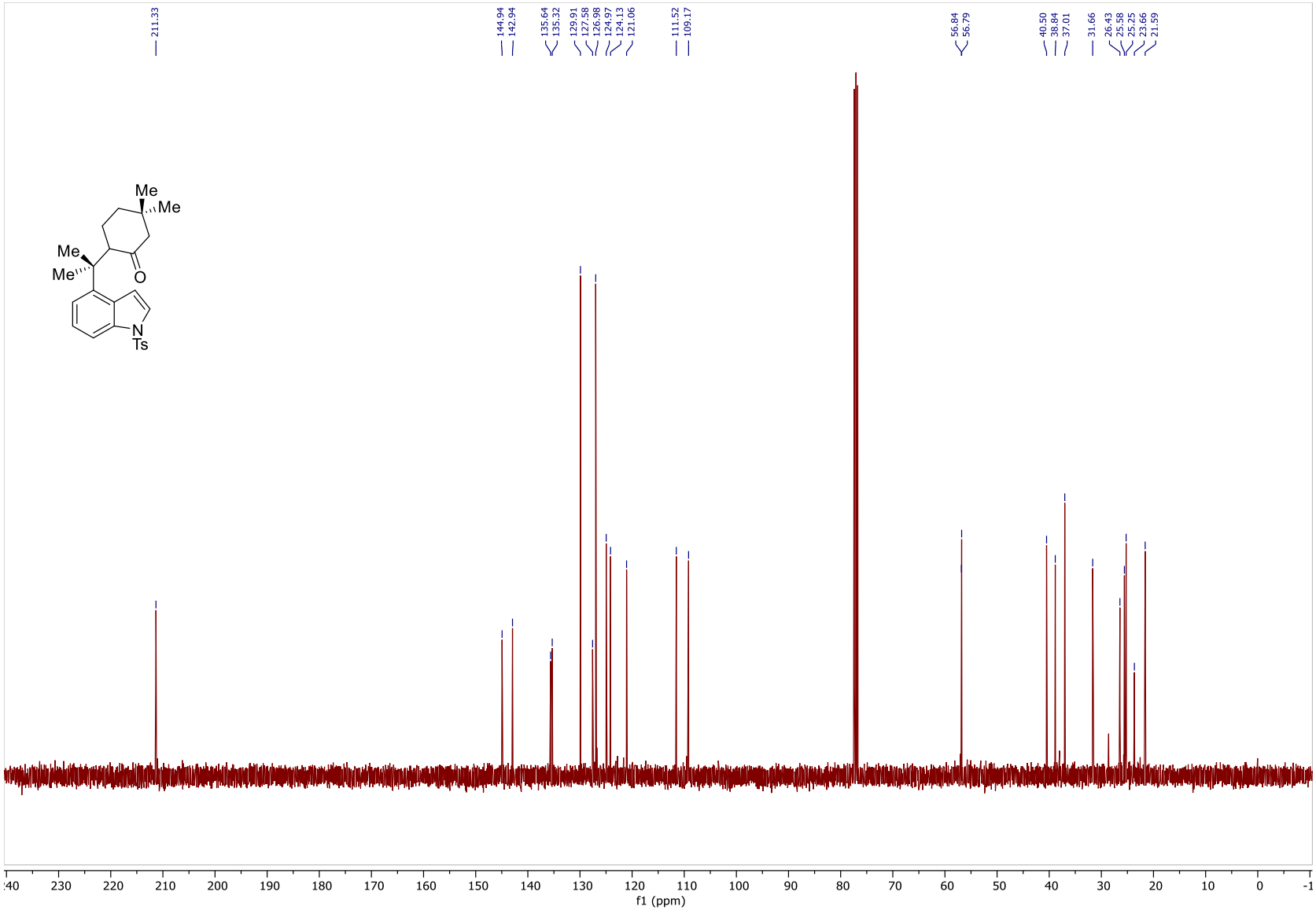

Figure 153: ^{13}C NMR Spectrum of **185** (100MHz, $CDCl_3$)

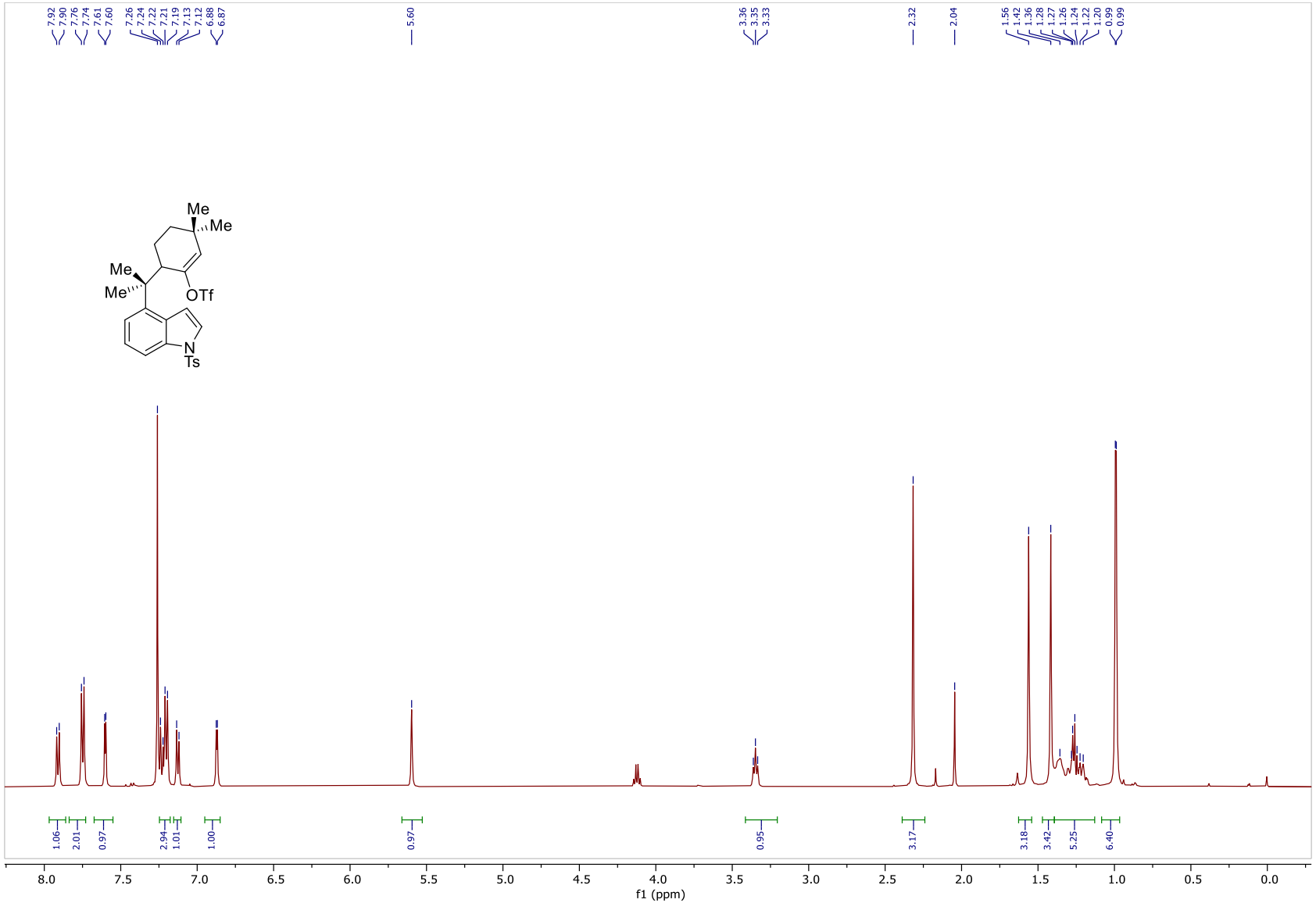

Figure 154: ^{1}H NMR Spectrum of **185b** (400MHz, $CDCl_3$)

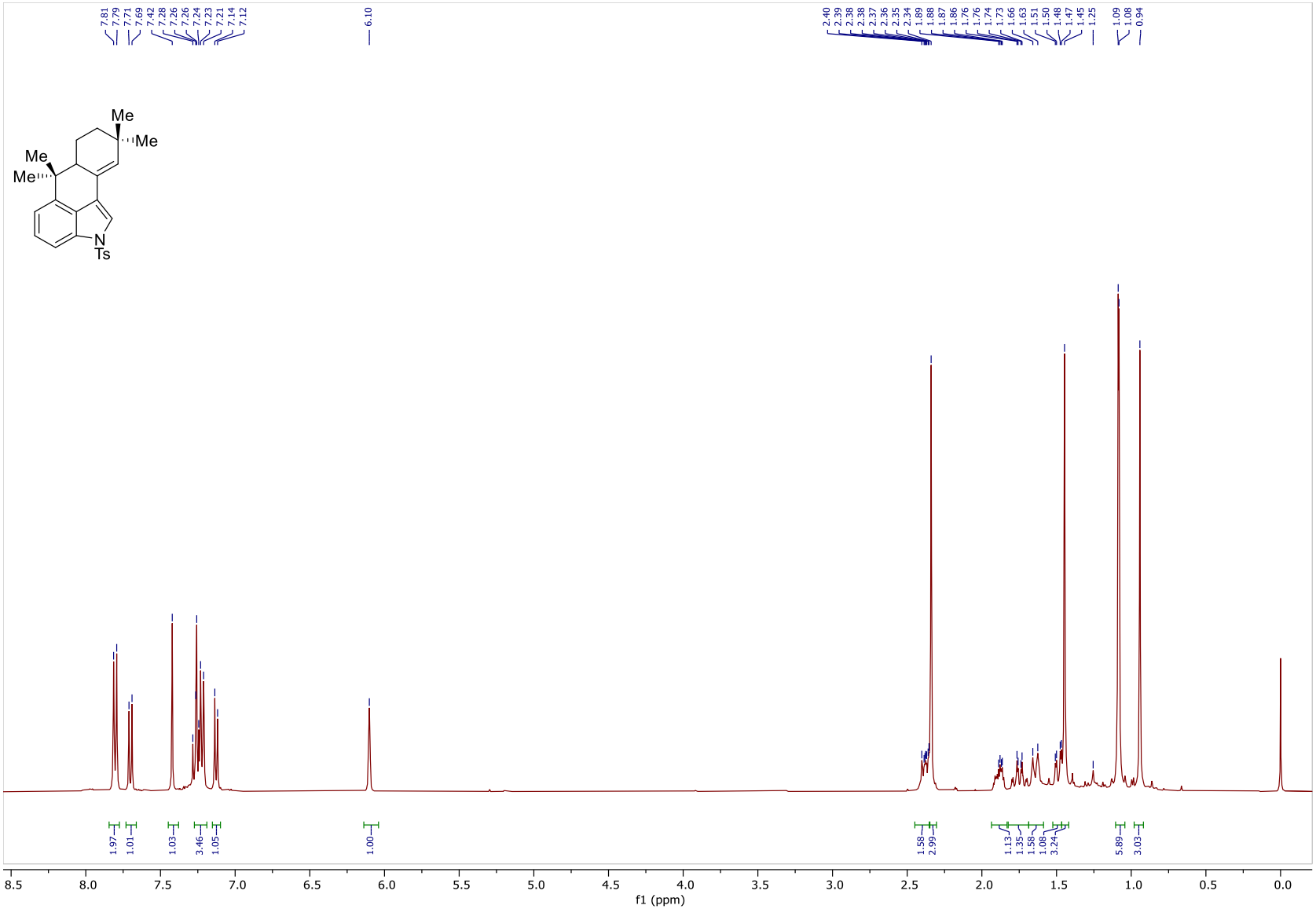

Figure 155: ^{1}H NMR Spectrum of **186** (500MHz, $CDCl_3$)

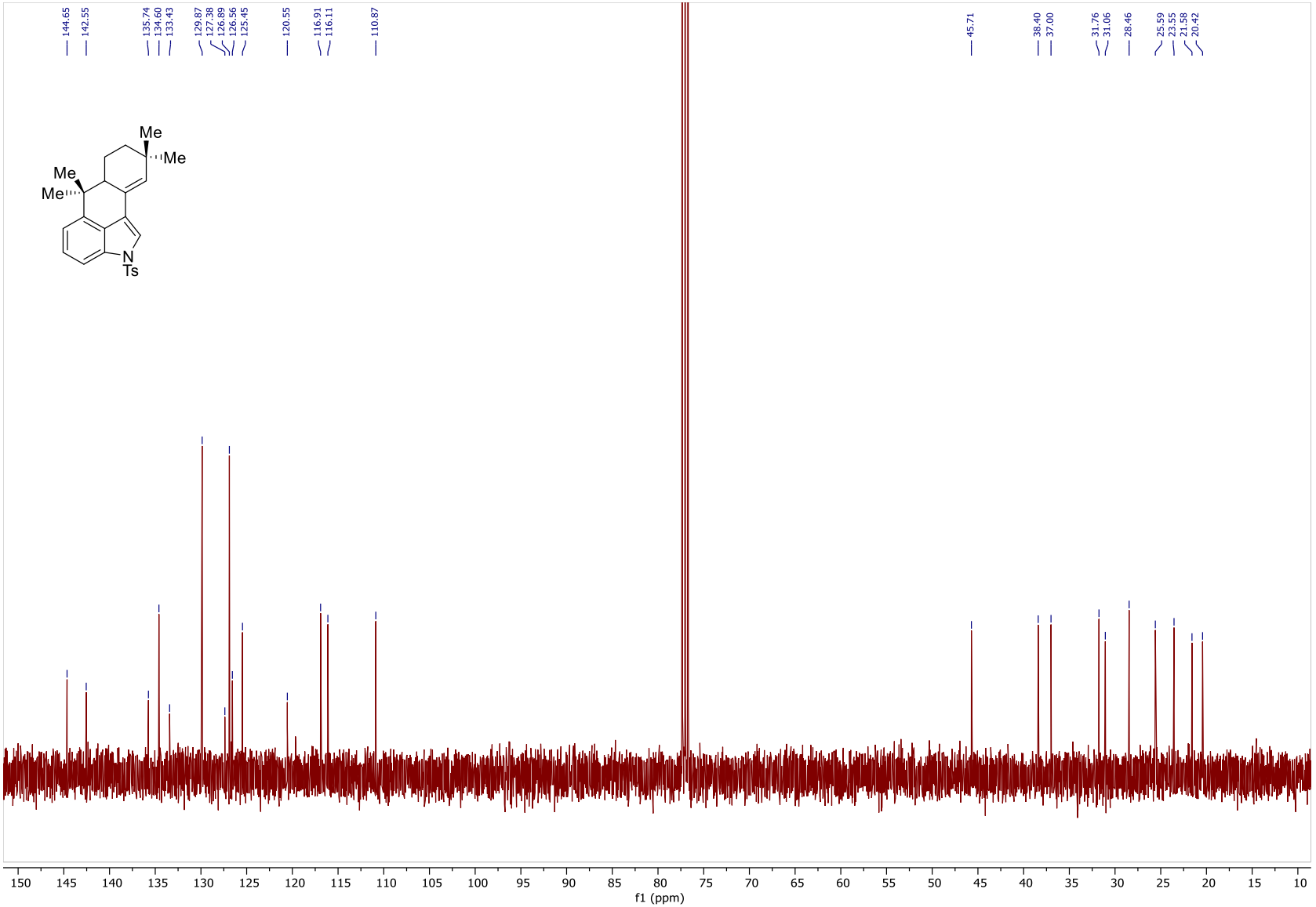

Figure 156: ^{13}C NMR Spectrum of **186** (100MHz, $CDCl_3$)

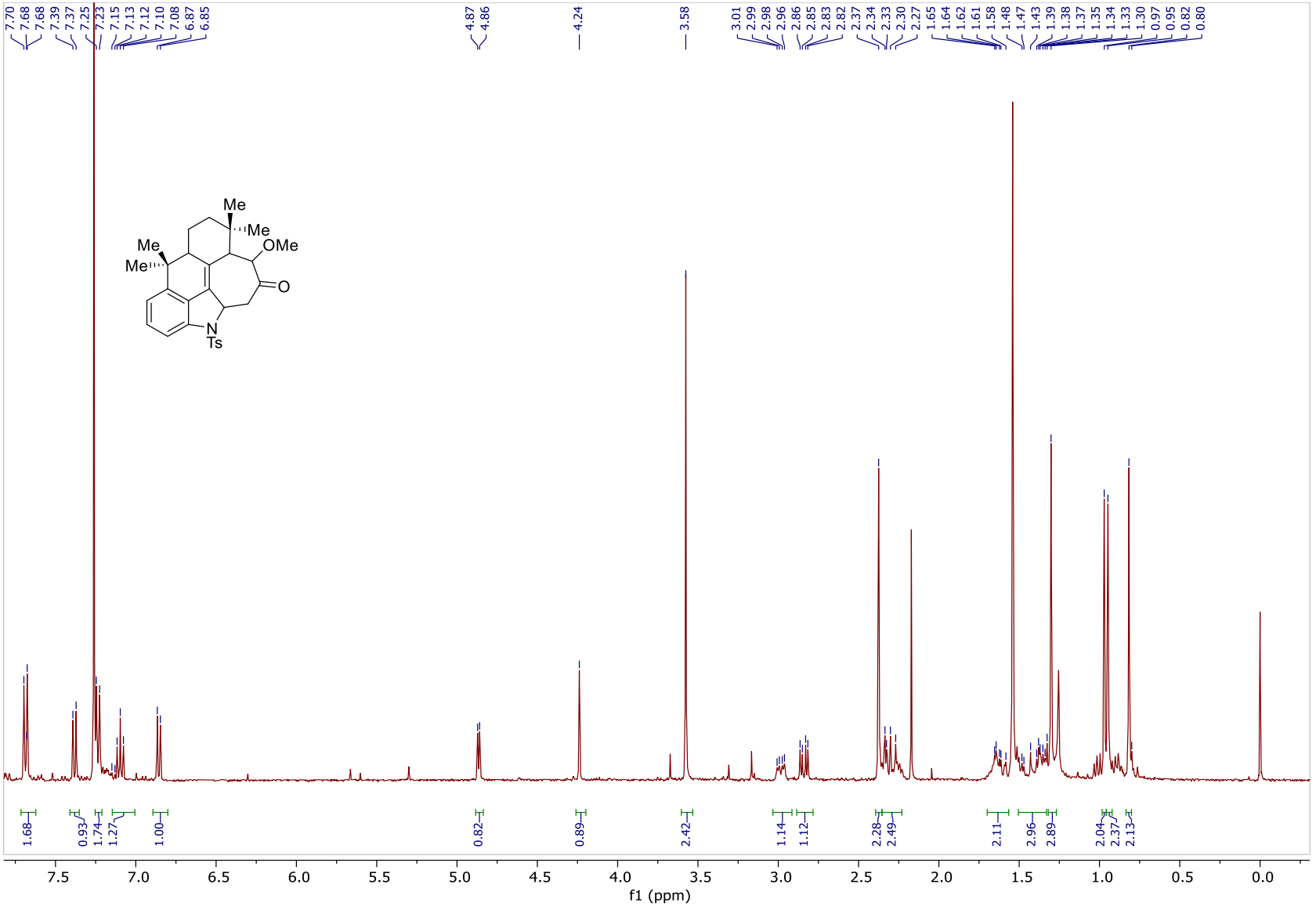

Figure 157: ^{1}H NMR Spectrum of **187** (500MHz, $CDCl_3$)

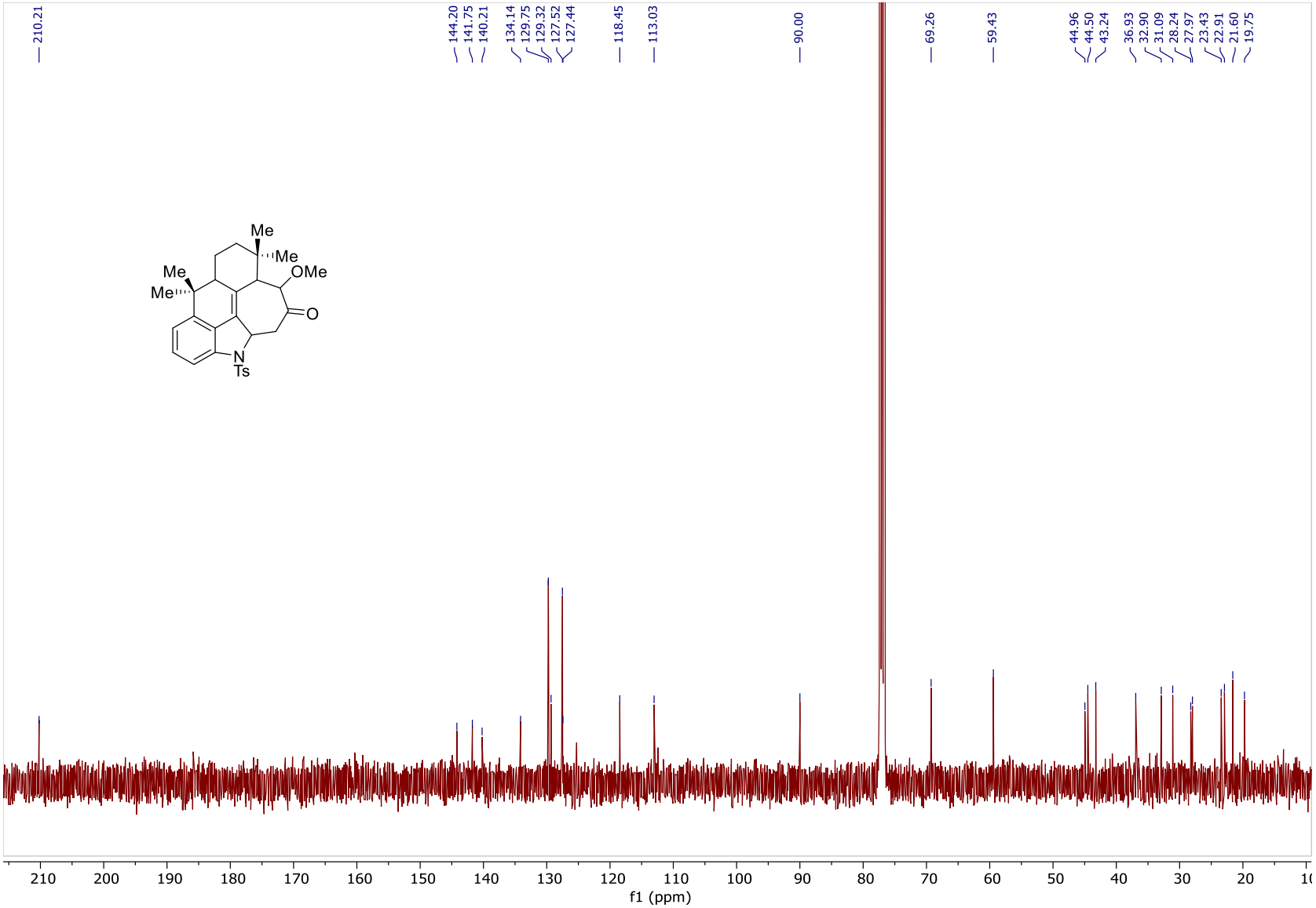

Figure 158: ^{13}C NMR Spectrum of **187** (100MHz, $CDCl_3$)

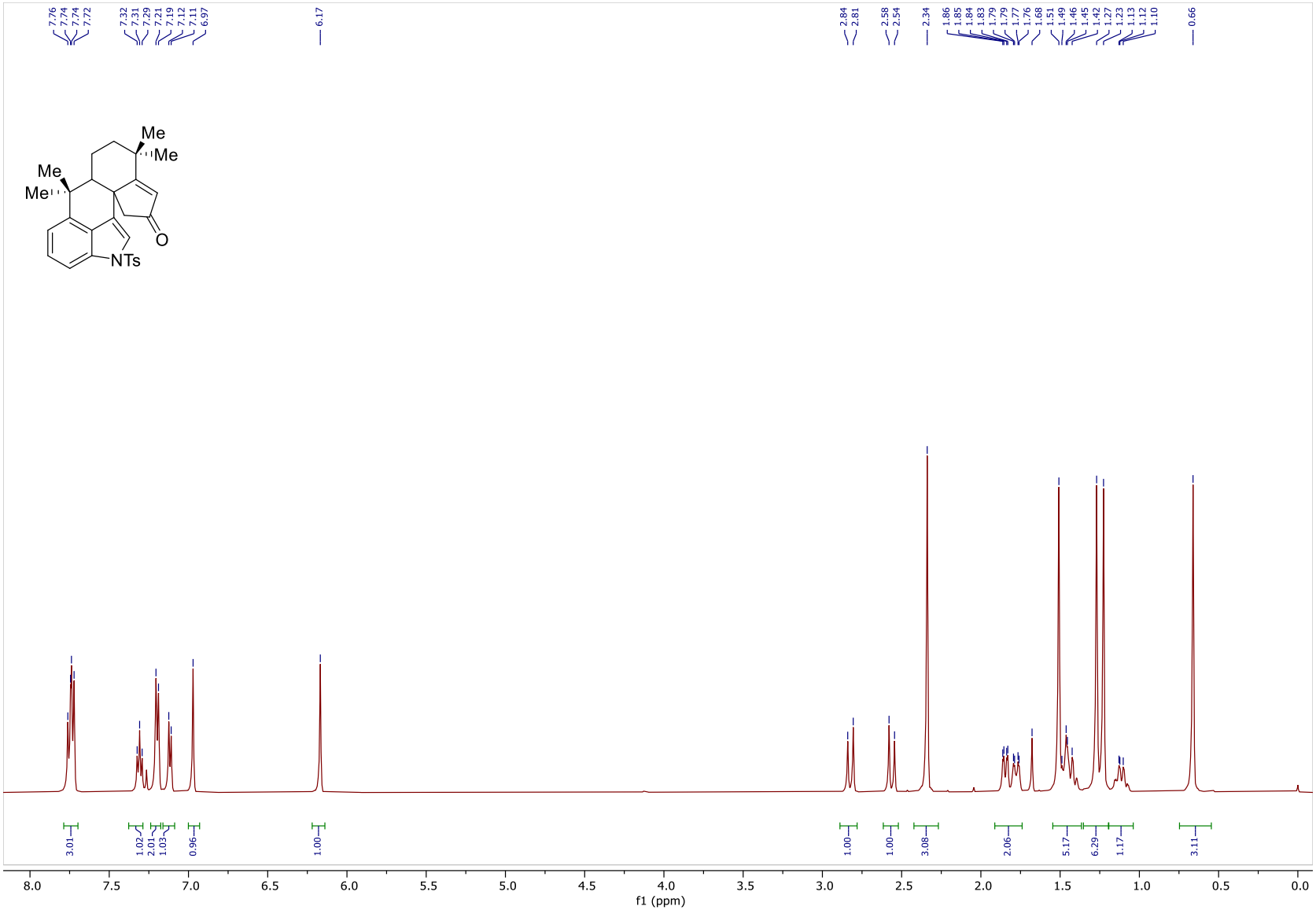

Figure 159: 1H NMR Spectrum of **188** (500MHz, $CDCl_3$)

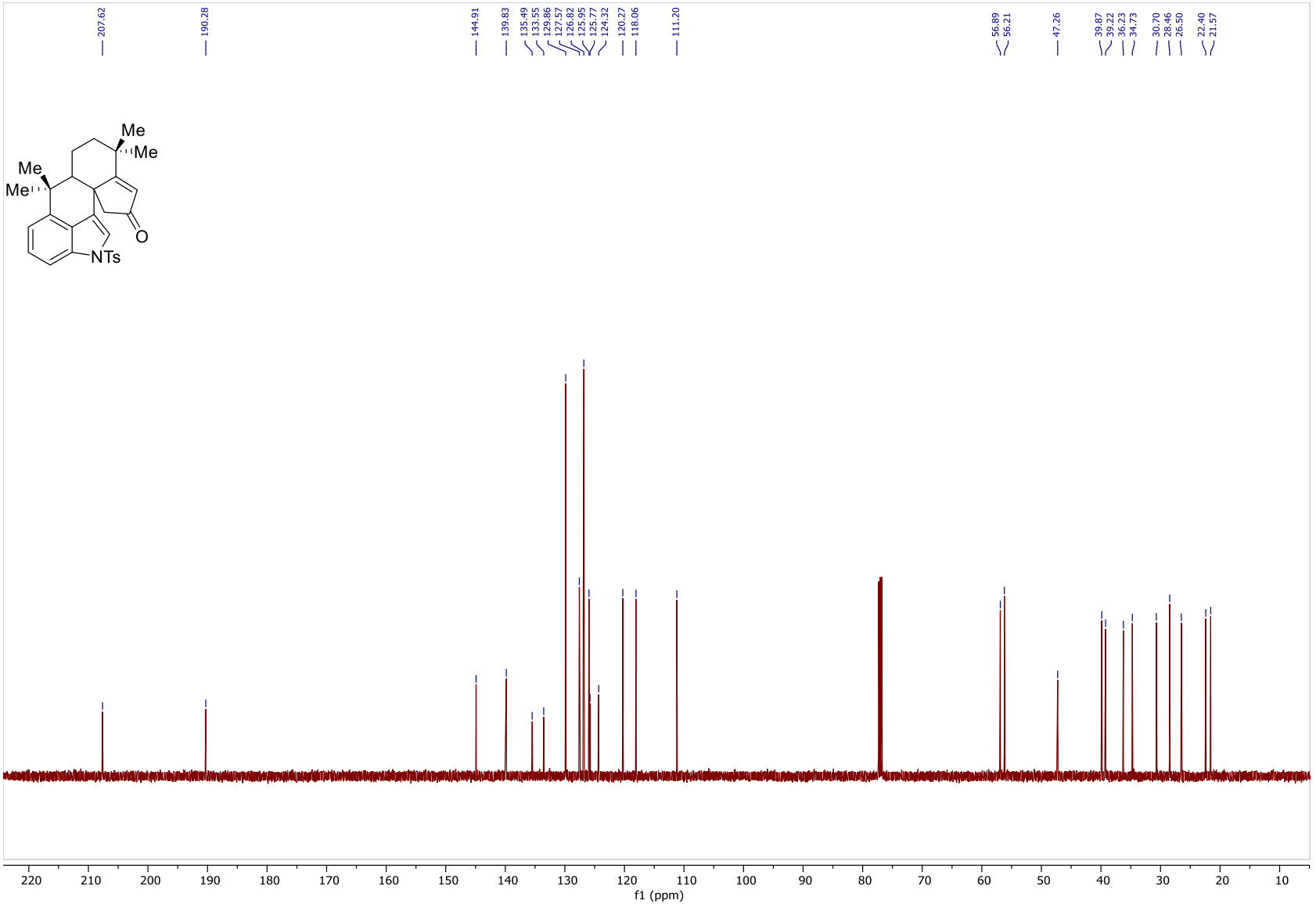

Figure 160: ^{13}C NMR Spectrum of **188** (100MHz, $CDCl_3$)

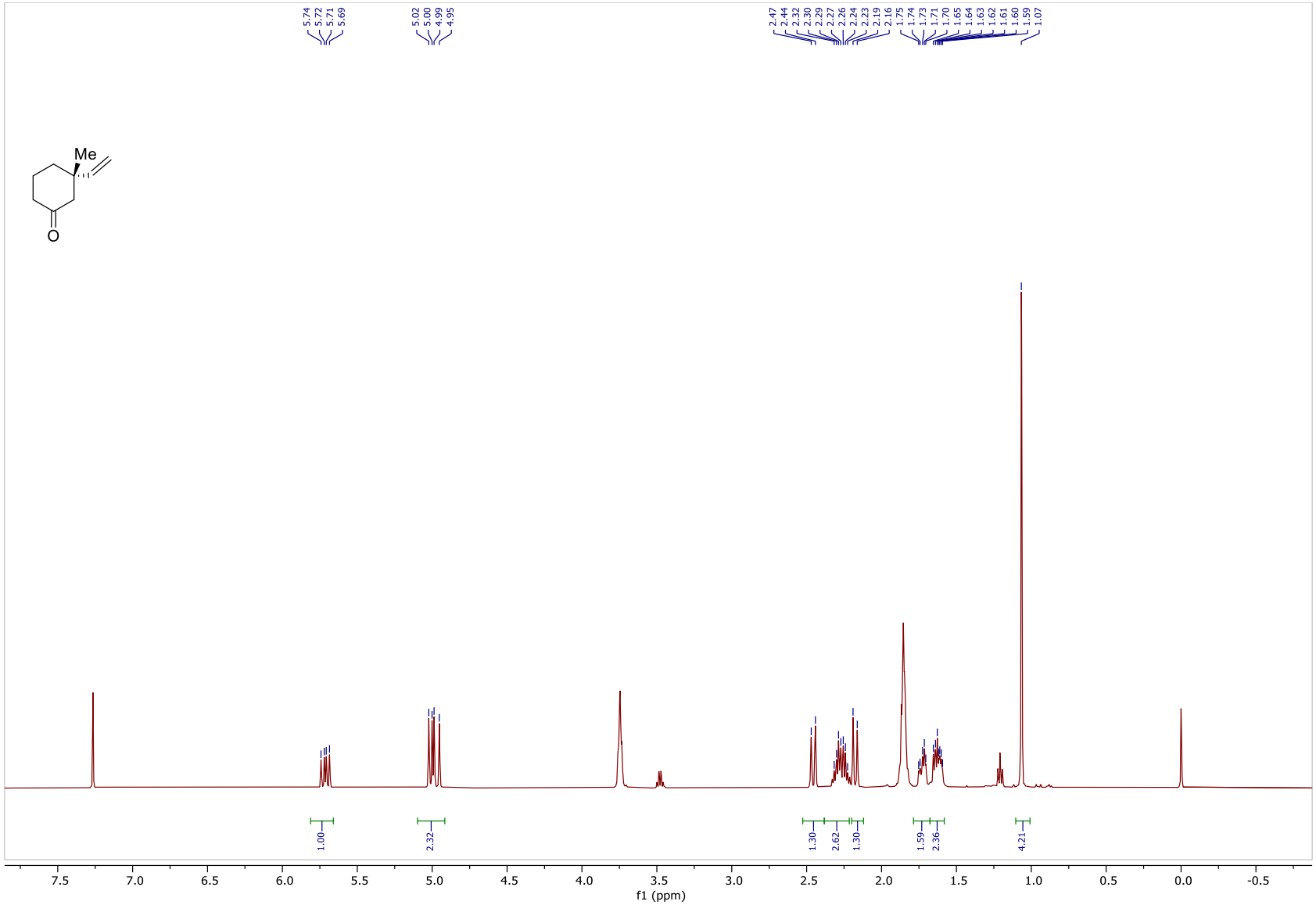

Figure 161: ^{1}H NMR Spectrum of **190** (500MHz, $CDCl_3$)

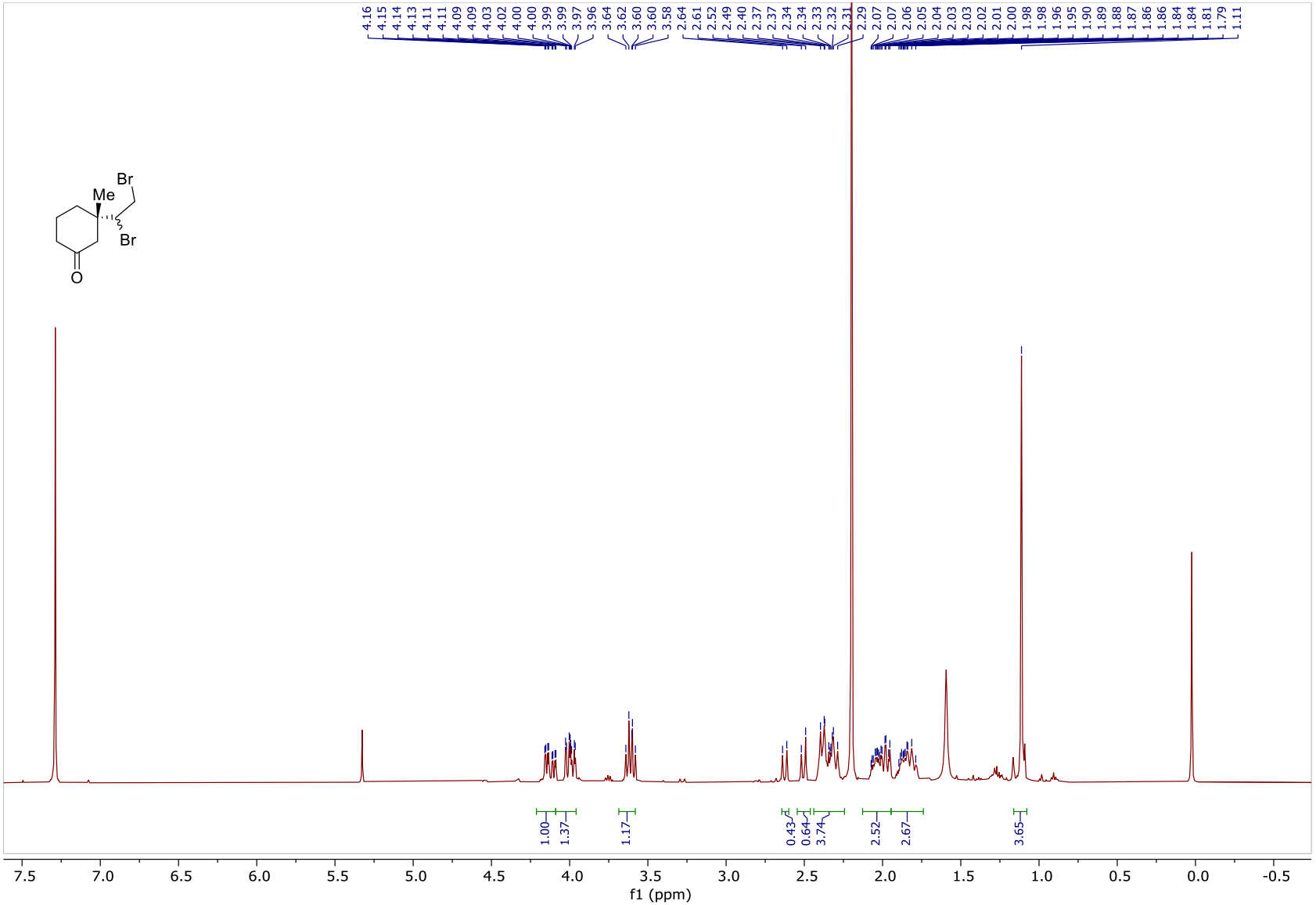

Figure 162: ^{1}H NMR Spectrum of **191** (500MHz, $CDCl_3$)

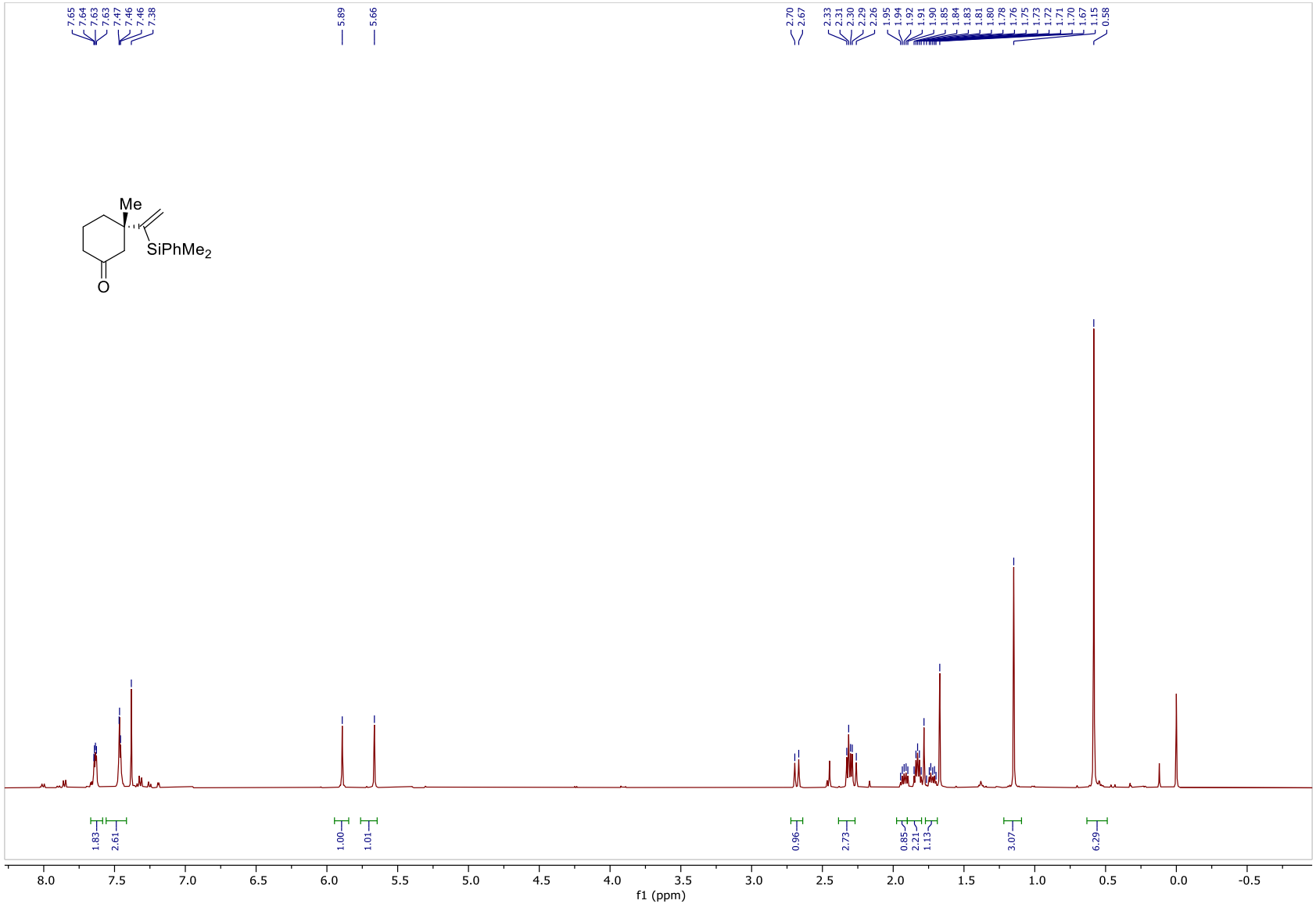

Figure 163: ^{1}H NMR Spectrum of **199** (500MHz, $CDCl_3$)

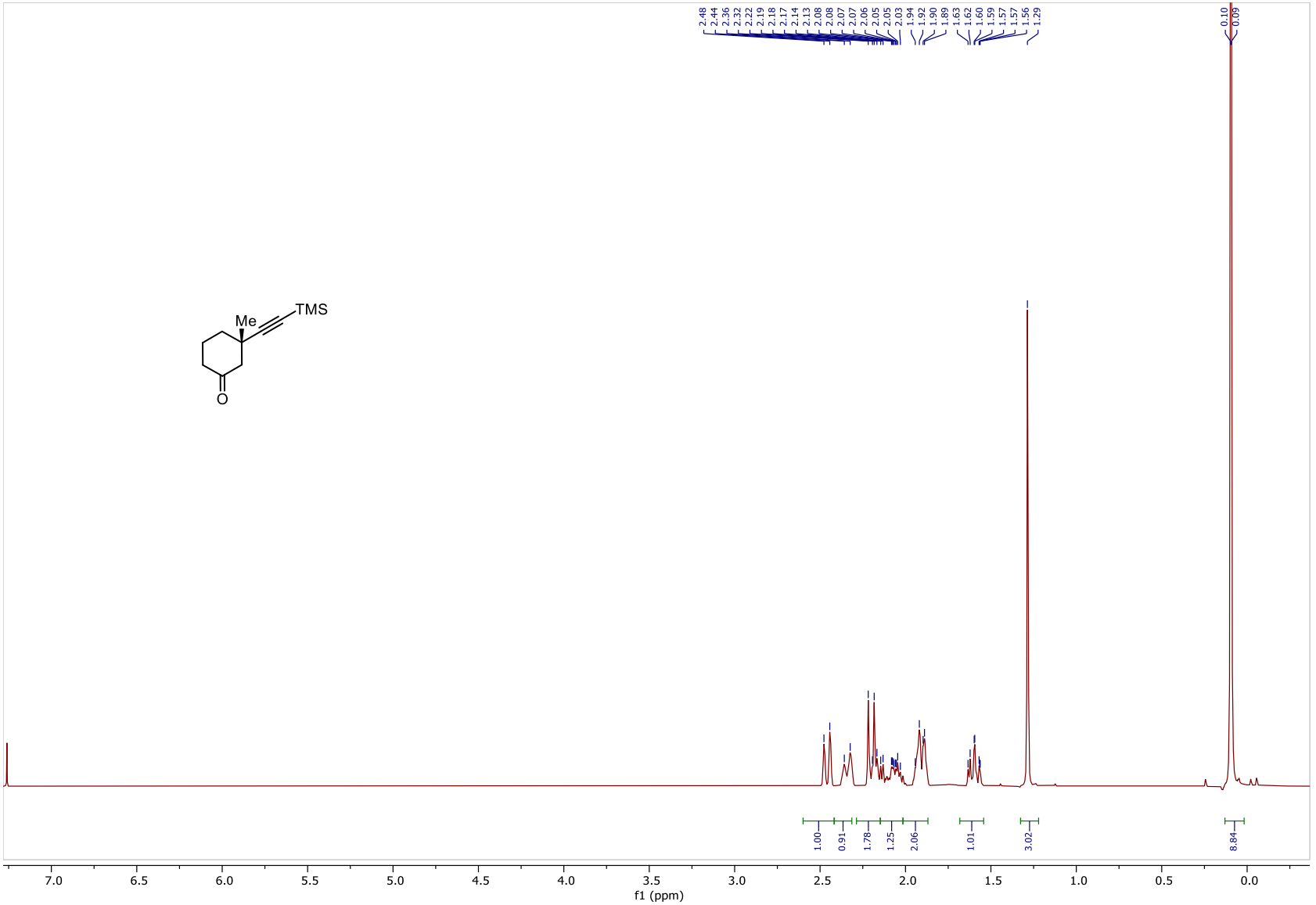

Figure 164: ^{1}H NMR Spectrum of **193** (400MHz, $CDCl_3$)

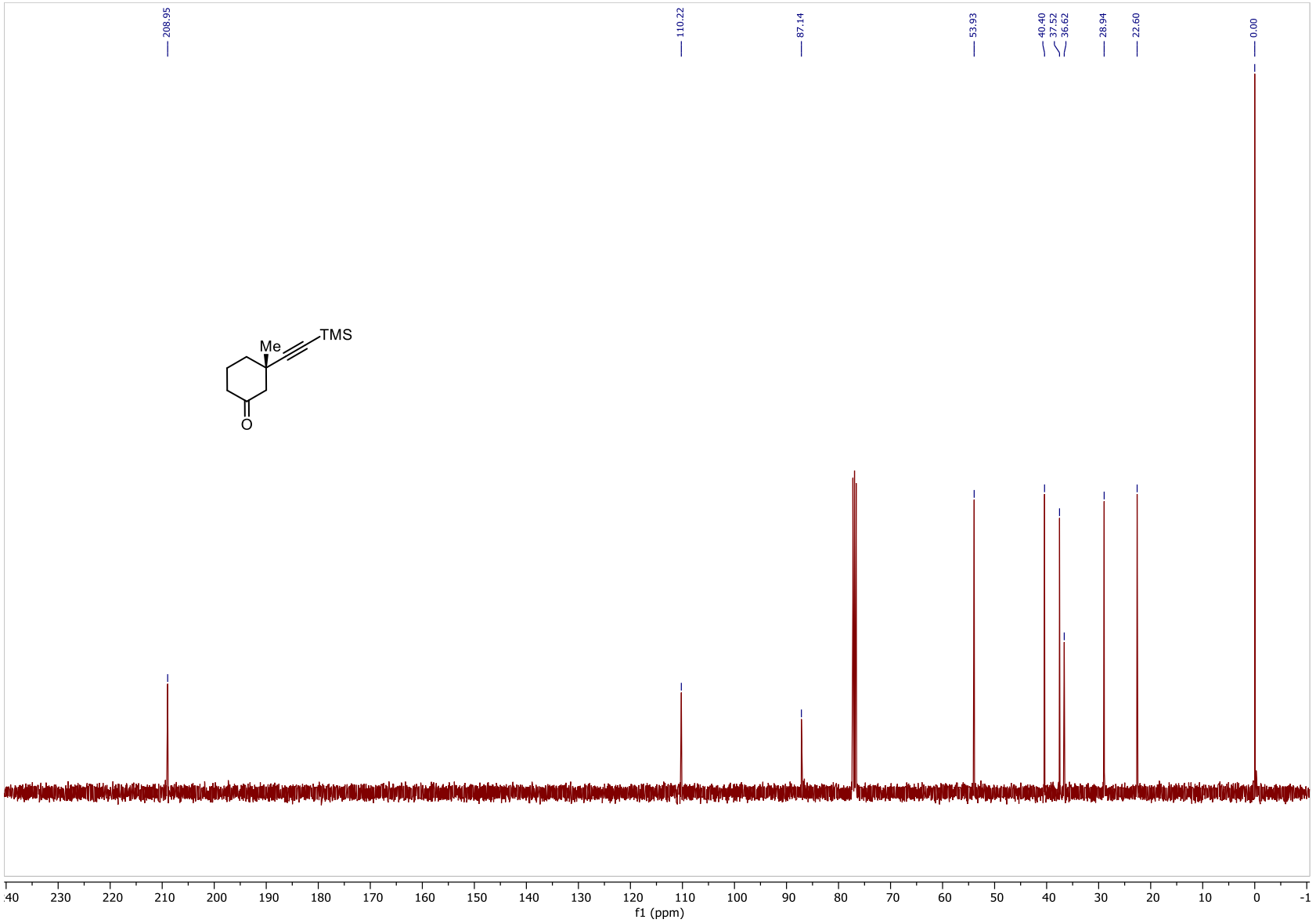

Figure 165: ^{13}C NMR Spectrum of **193** (100MHz, $CDCl_3$)

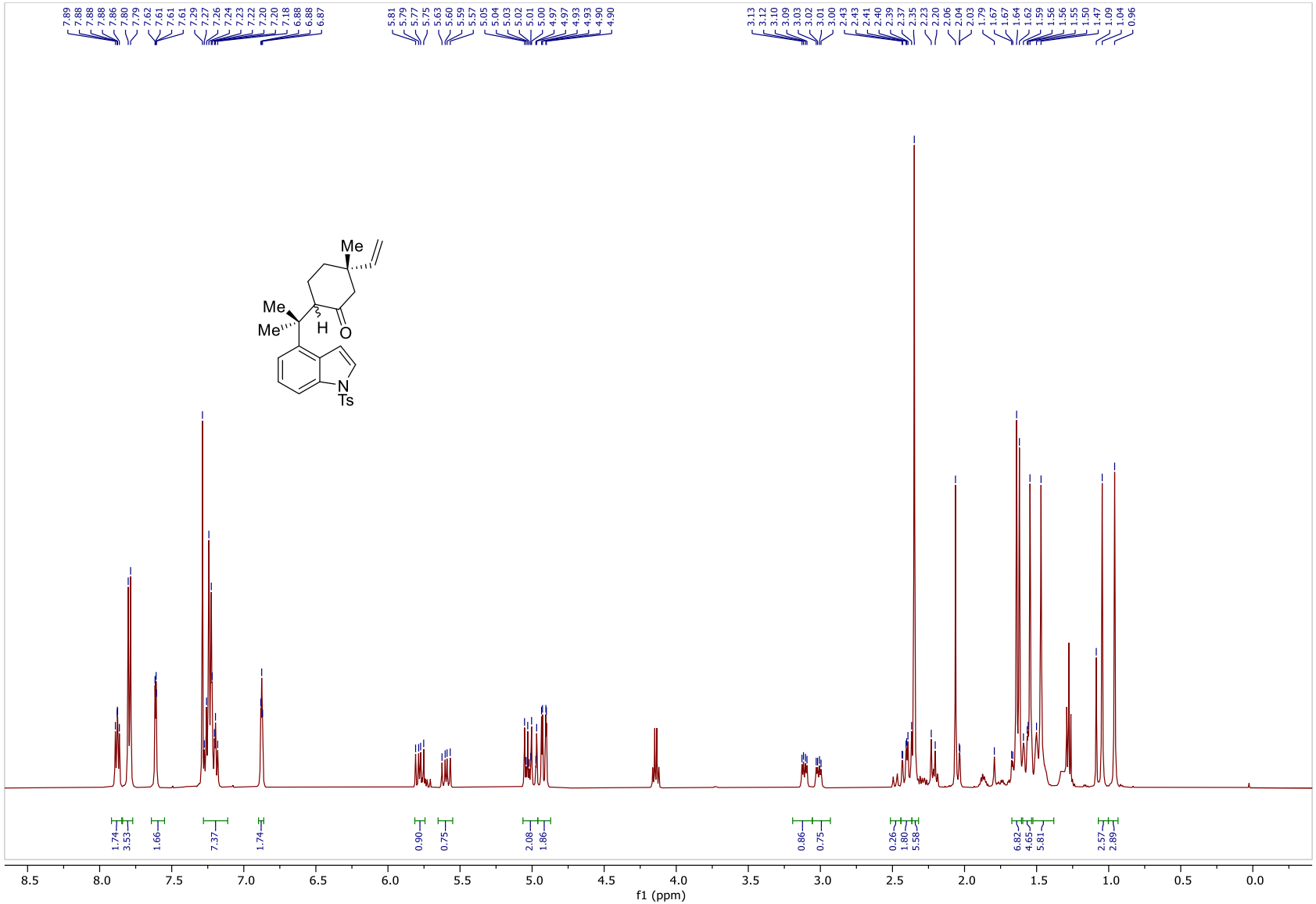

Figure 166: ^{1}H NMR Spectrum of **189a** (500MHz, $CDCl_3$)

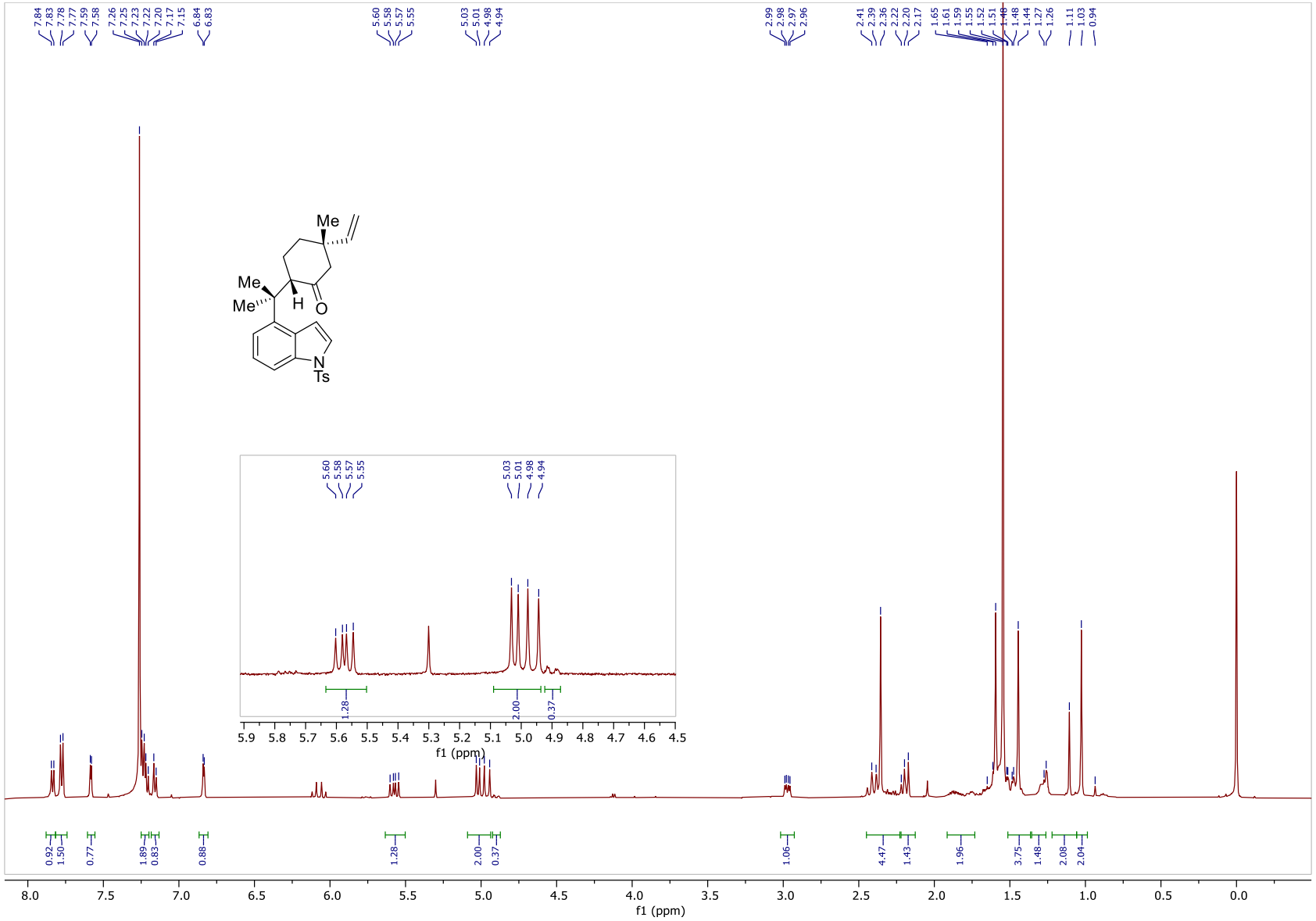

Figure 167: ^{1}H NMR Spectrum of **189b** (500MHz, $CDCl_3$)

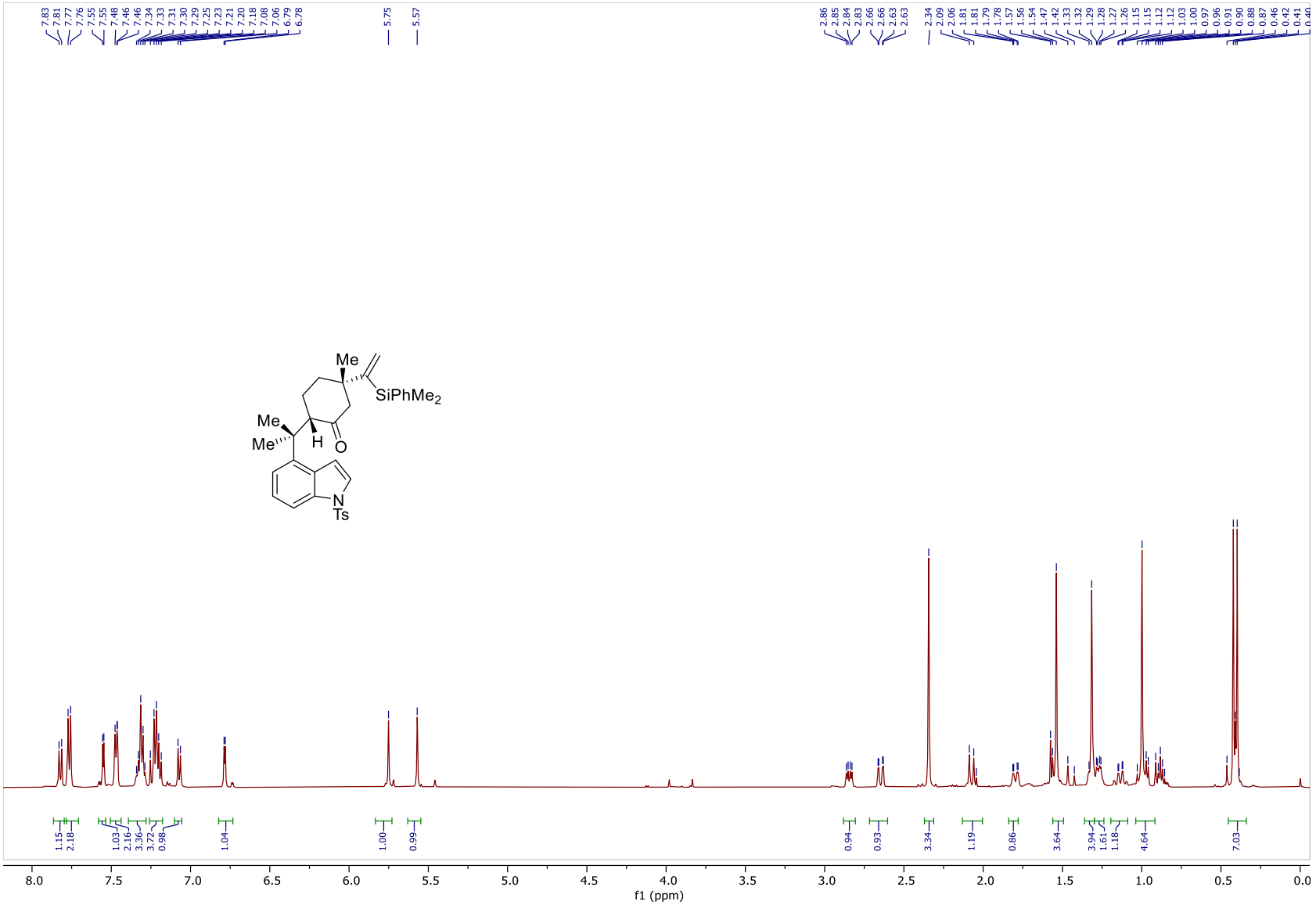

Figure 168: ^{1}H NMR Spectrum of **189c** (500MHz, $CDCl_3$)

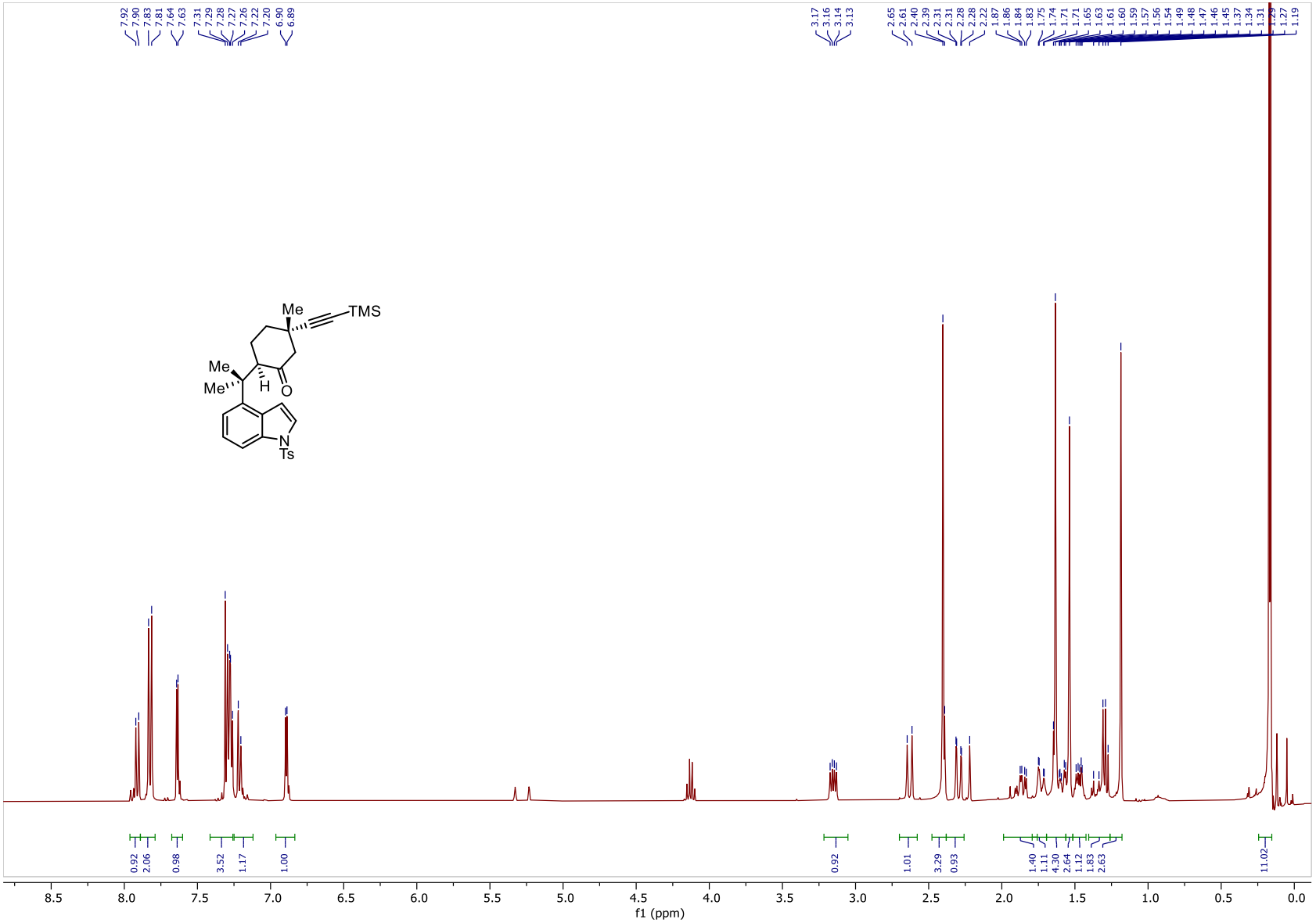

Figure 169: ^{1}H NMR Spectrum of **189d** (400MHz, $CDCl_3$)

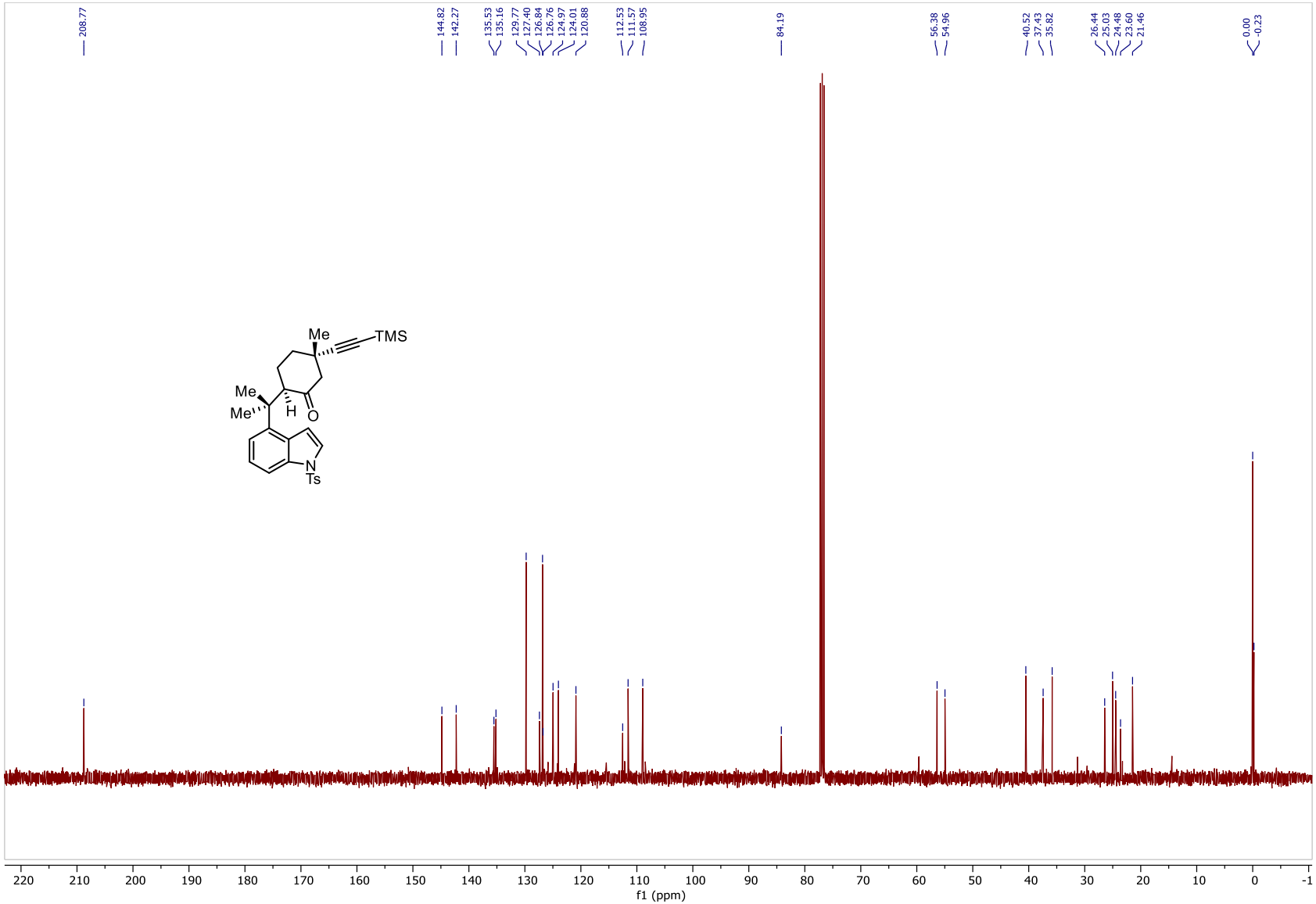

Figure 170: ^{13}C NMR Spectrum of **189d** (100MHz, $CDCl_3$)

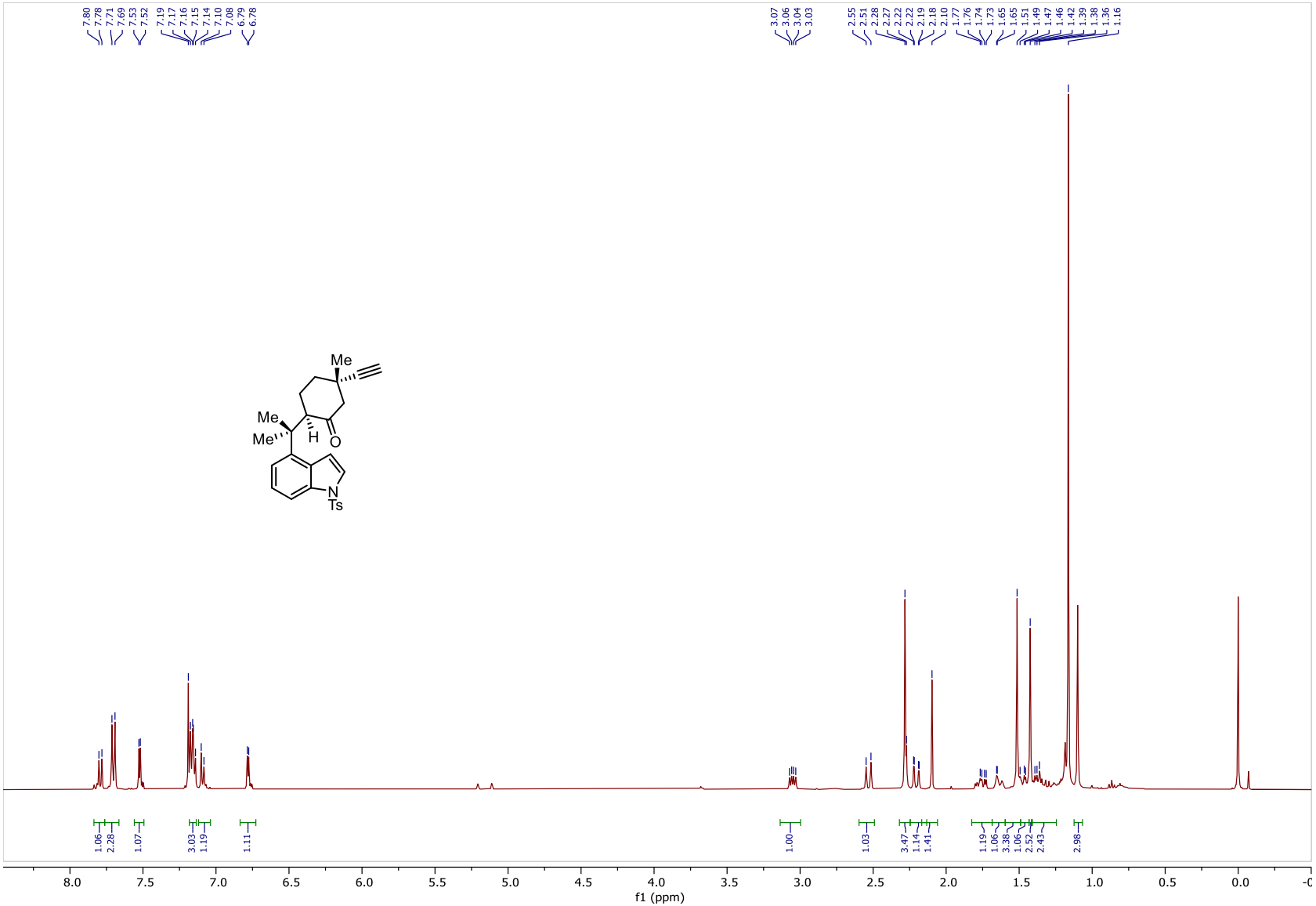

Figure 171: ^{1}H NMR Spectrum of **194** (400MHz, $CDCl_3$)

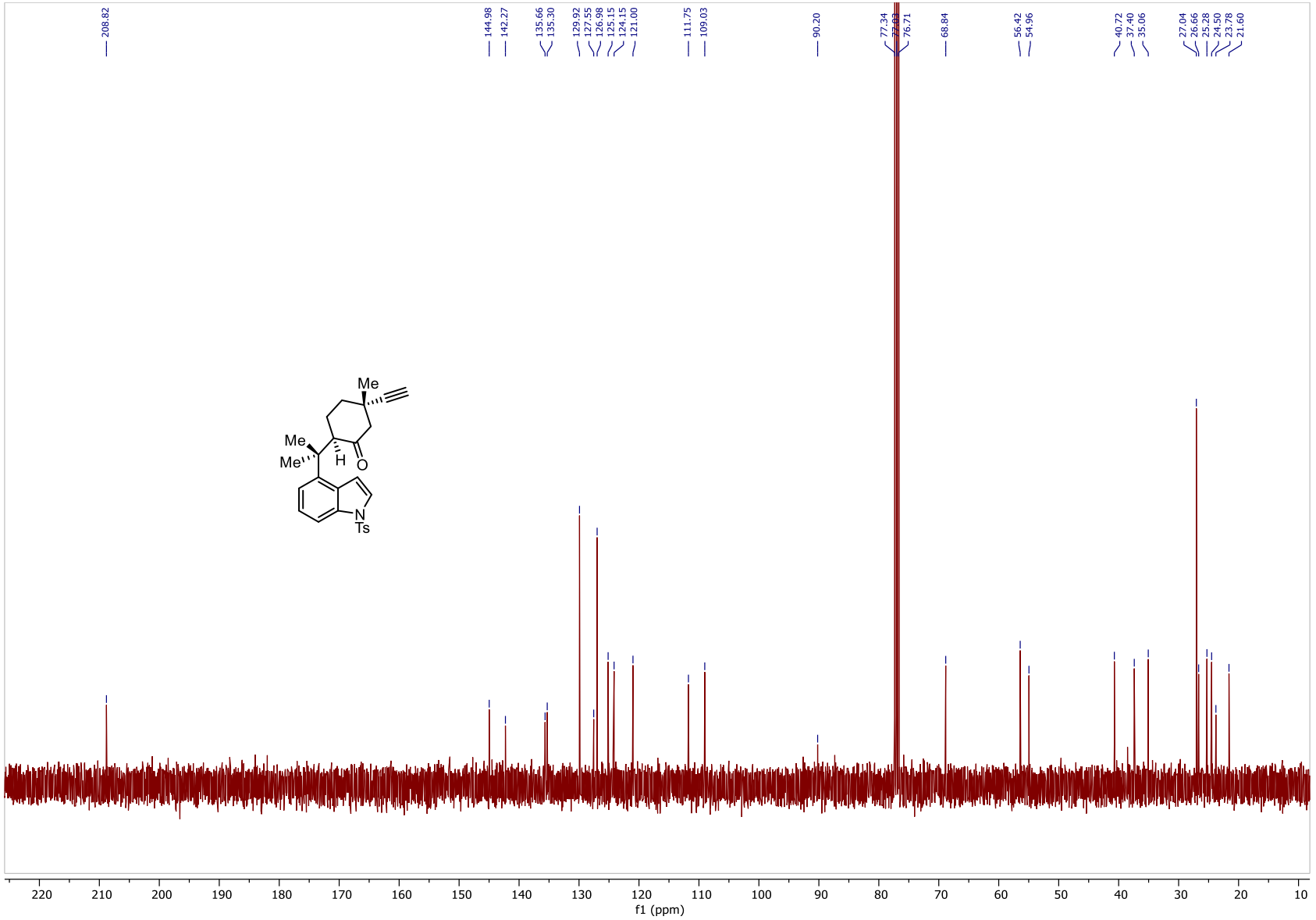

Figure 172: ^{13}C NMR Spectrum of **194** (100MHz, $CDCl_3$)

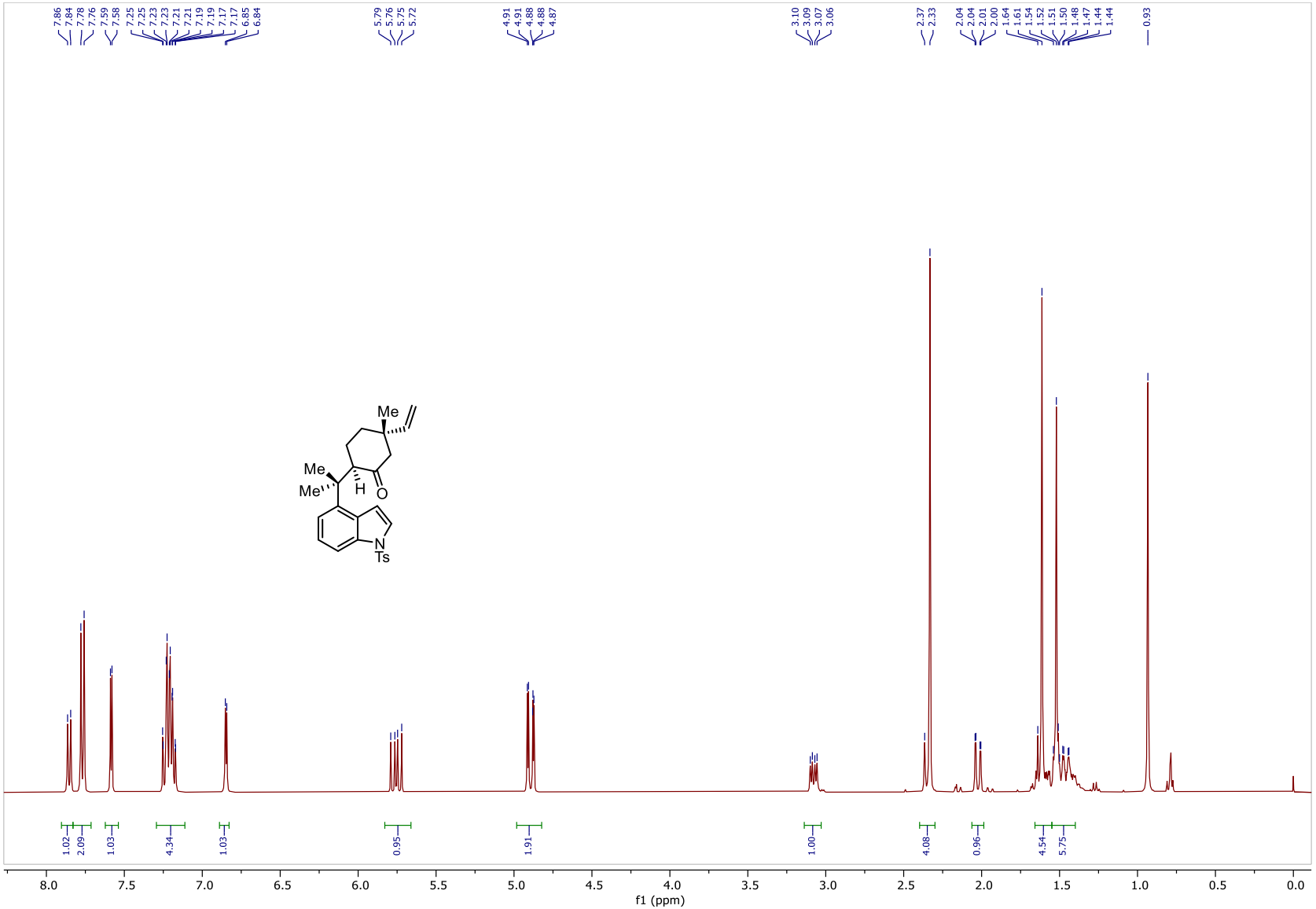

Figure 173: ^{1}H NMR Spectrum of **195** (400MHz, $CDCl_3$)

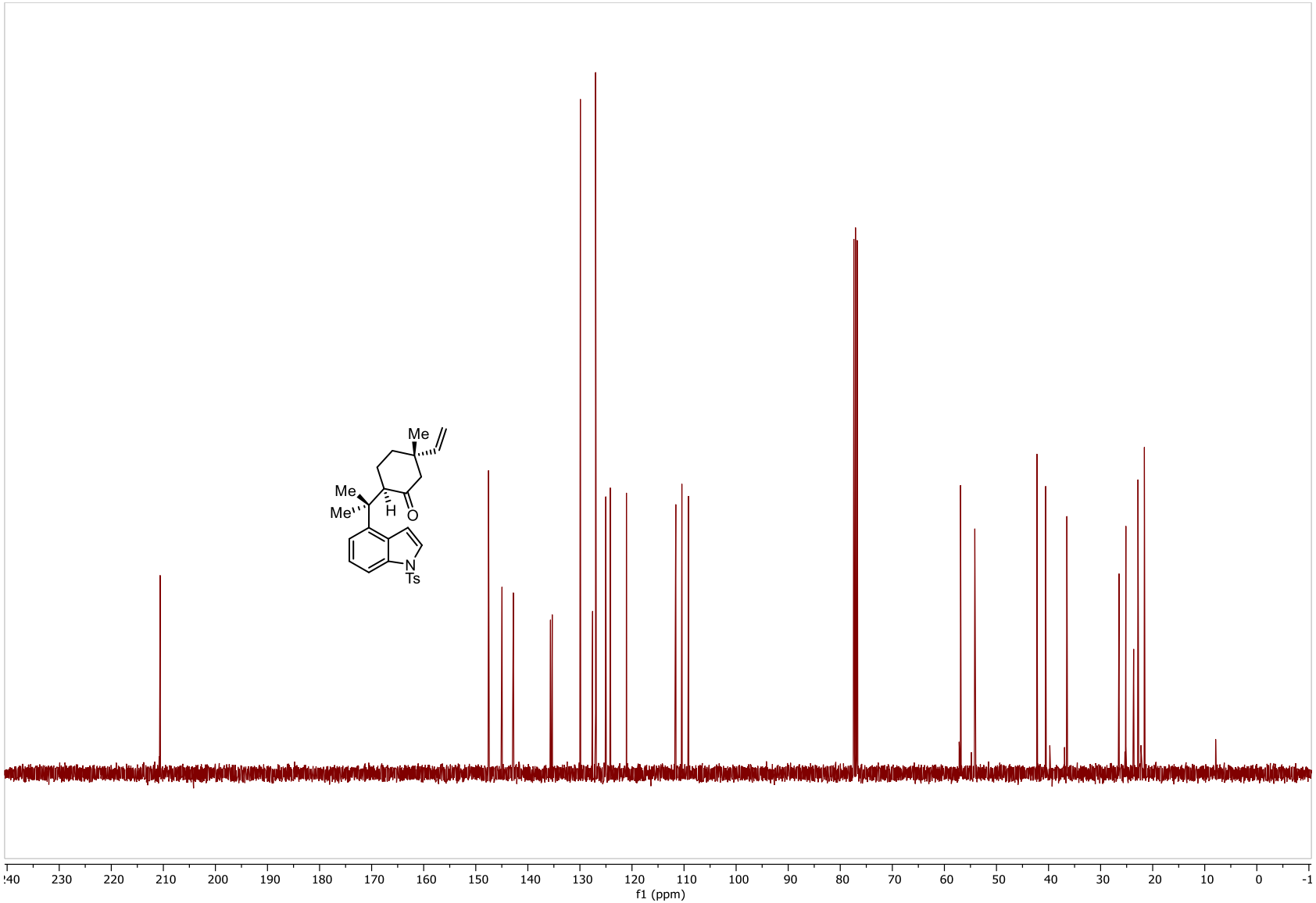

Figure 174: ^{13}C NMR Spectrum of **195** (100MHz, $CDCl_3$)

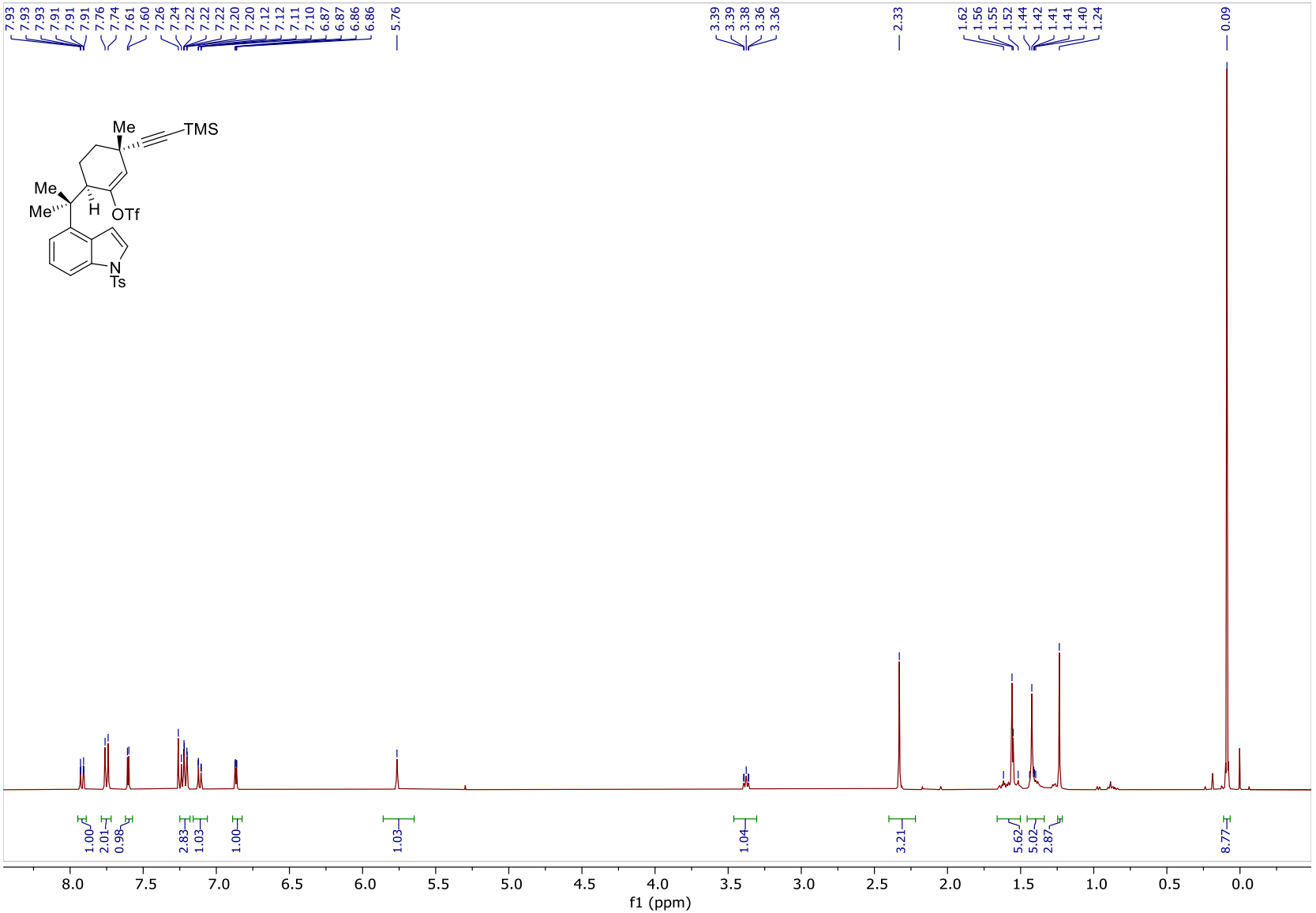

Figure 175: ^{1}H NMR Spectrum of **175b** (400MHz, $CDCl_3$)

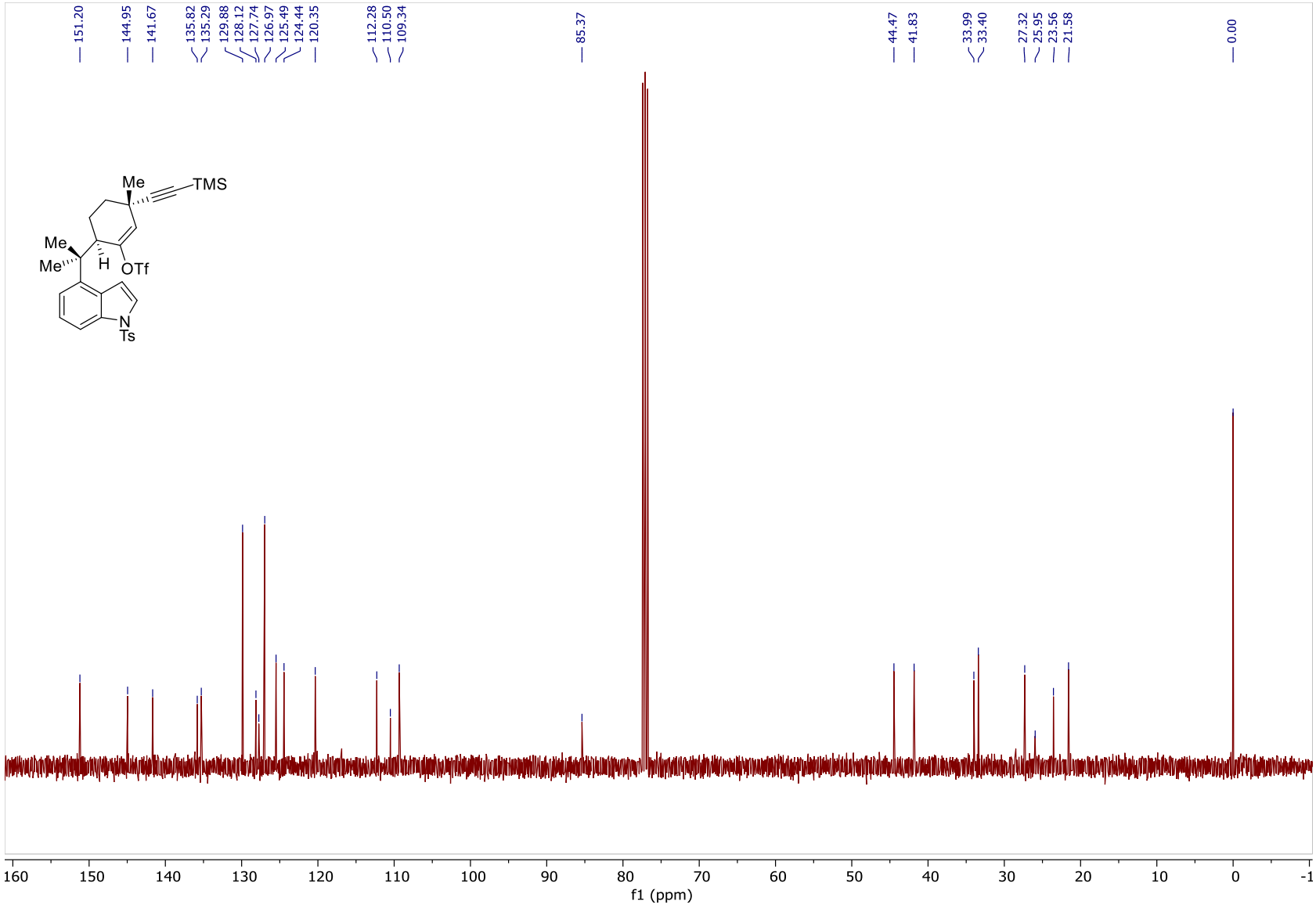

Figure 176: ^{13}C NMR Spectrum of **175b** (100MHz, $CDCl_3$)

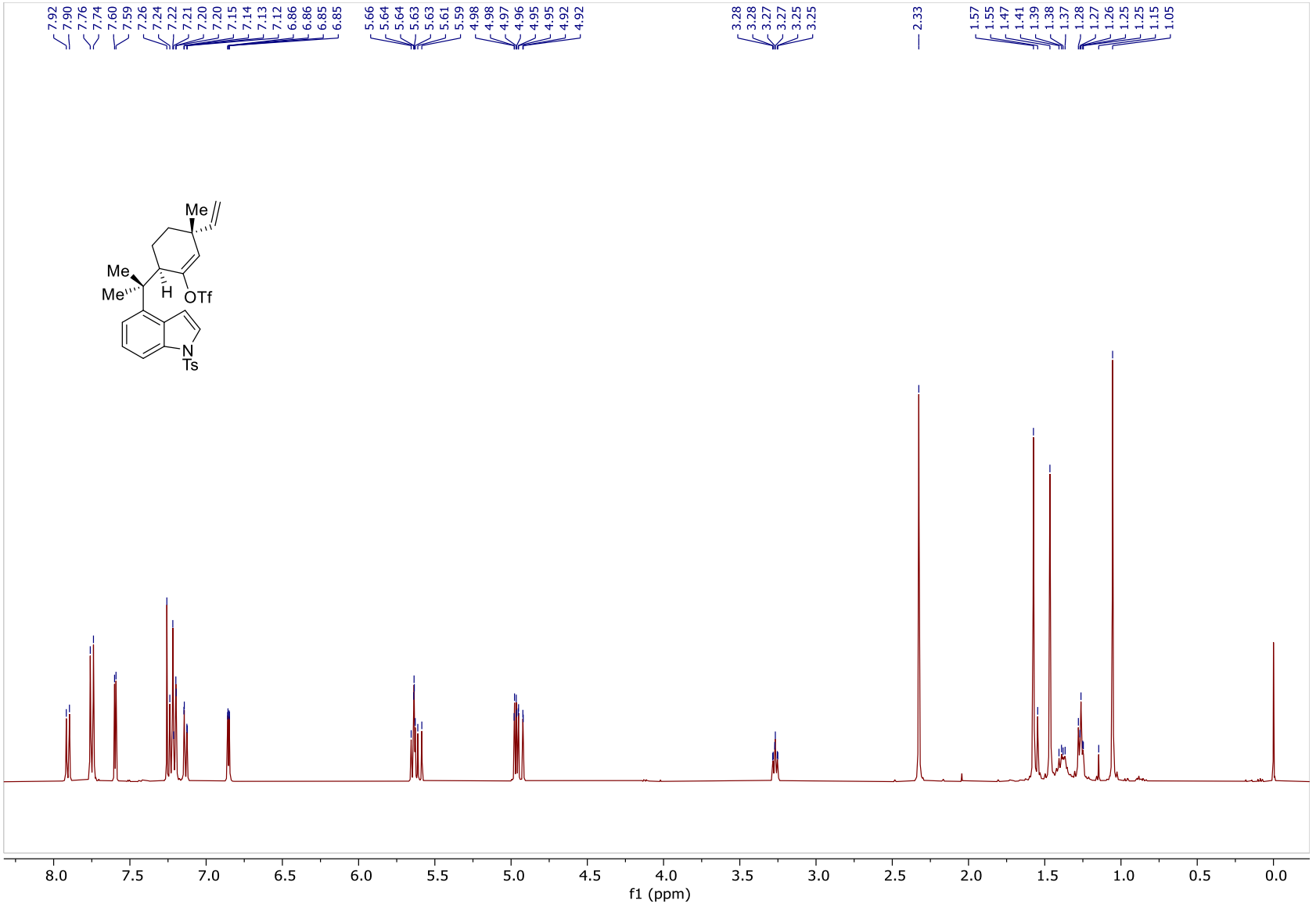

Figure 177: ^{1}H NMR Spectrum of **175** (400MHz, $CDCl_3$)

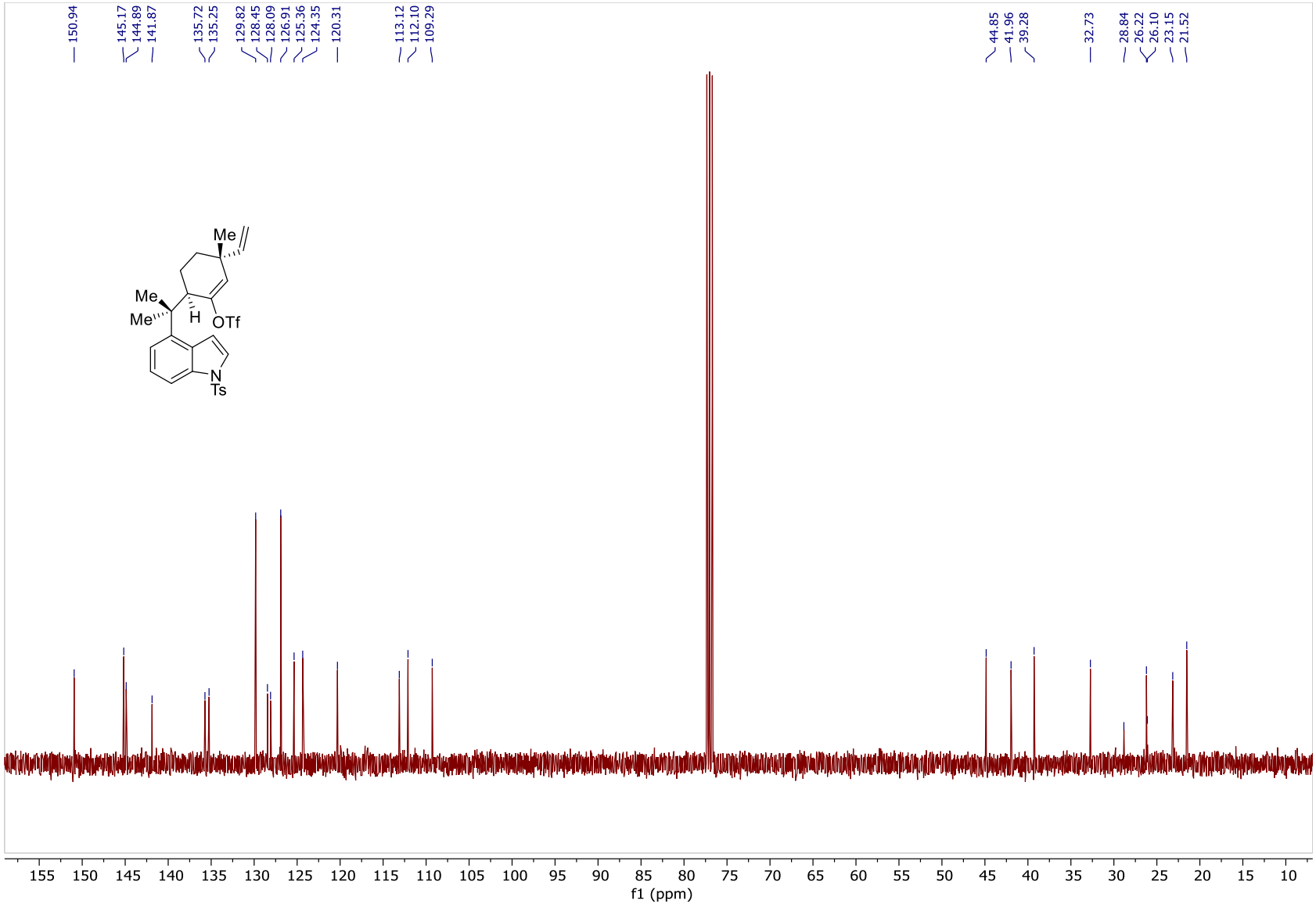

Figure 178: ^{13}C NMR Spectrum of **175** (100MHz, $CDCl_3$)

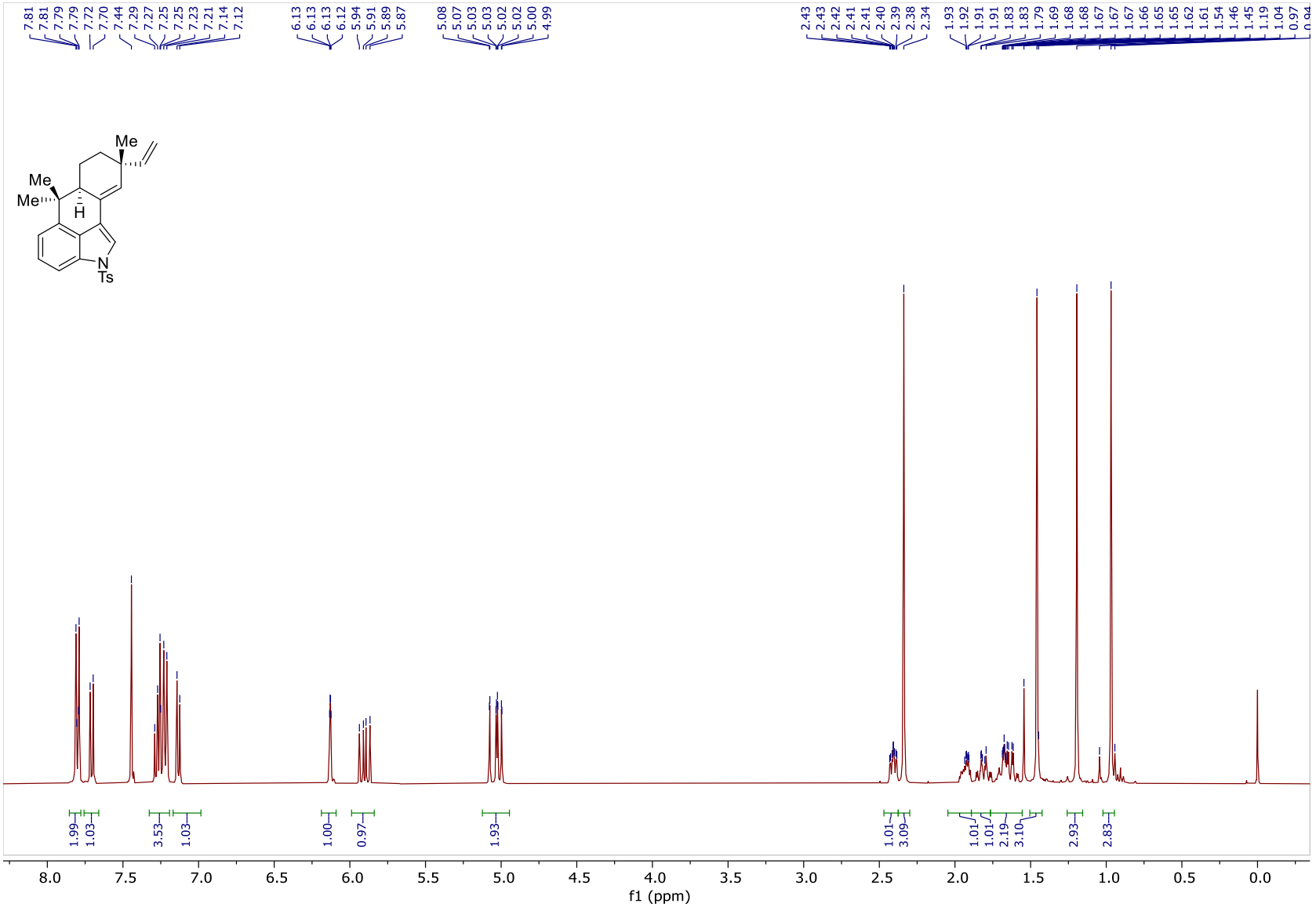

Figure 179: ^{1}H NMR Spectrum of **171** (400MHz, $CDCl_3$)

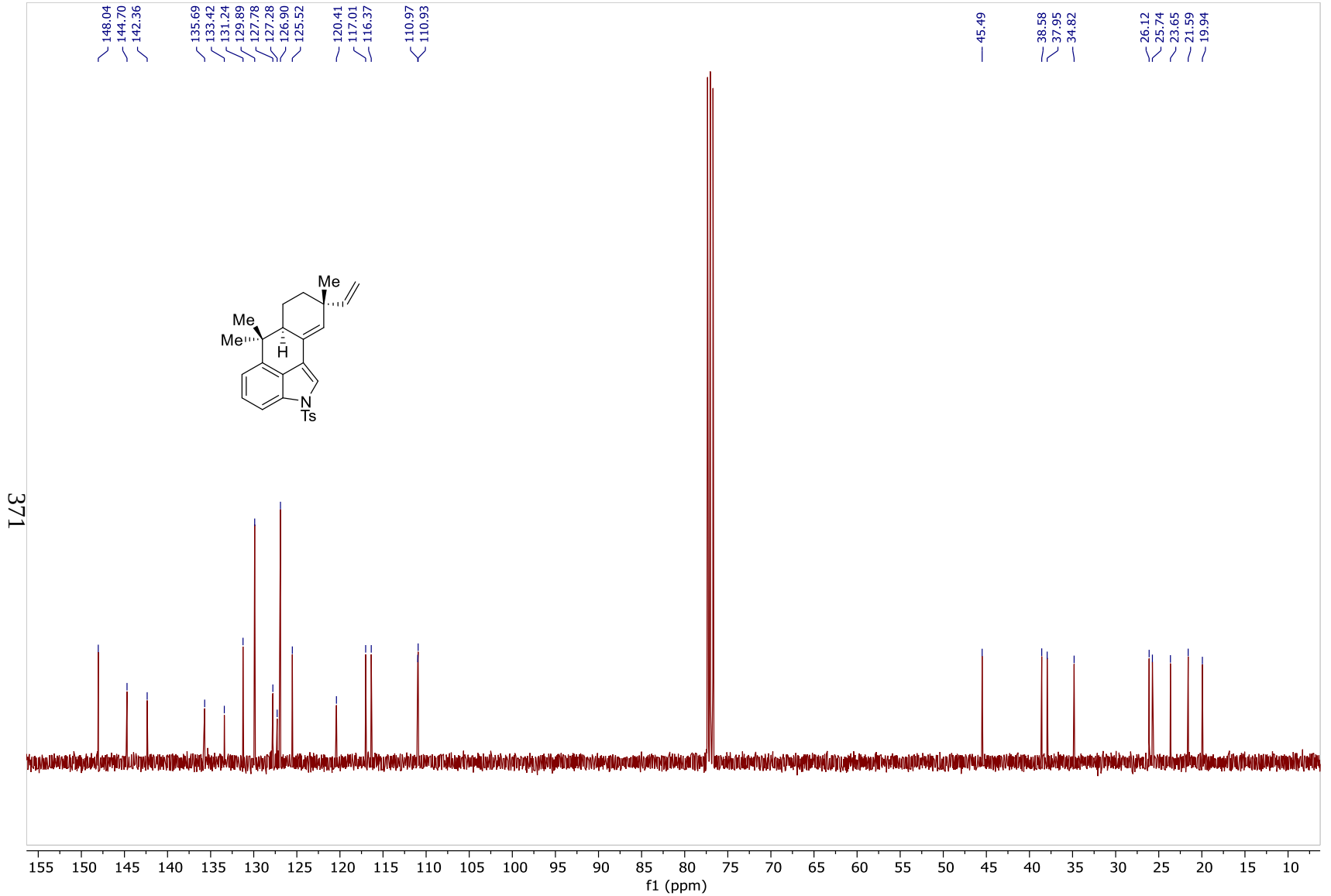

Figure 180: ^{13}C NMR Spectrum of **171** (100MHz, $CDCl_3$)

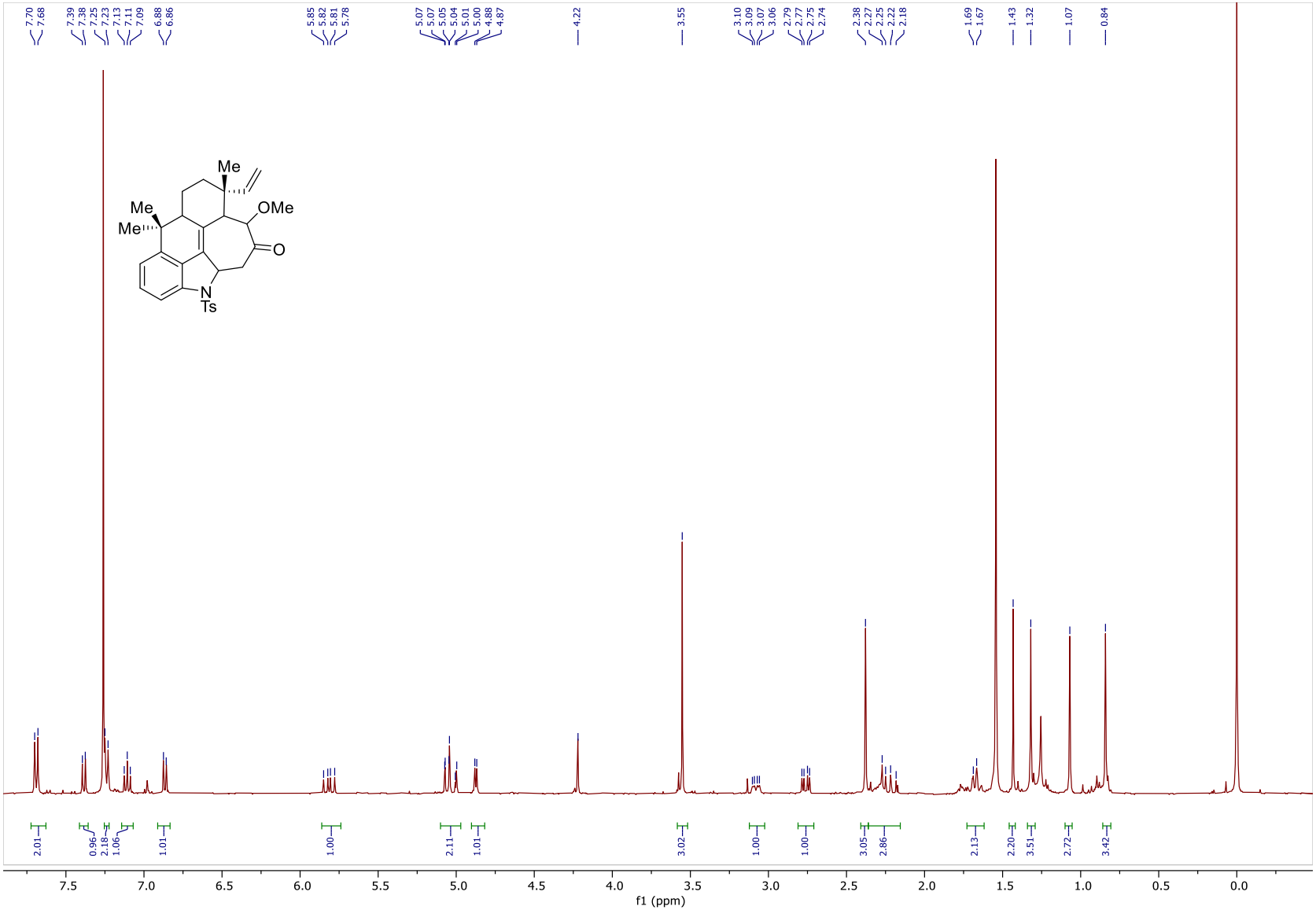

Figure 181: ^{1}H NMR Spectrum of **170** (400MHz, $CDCl_3$)

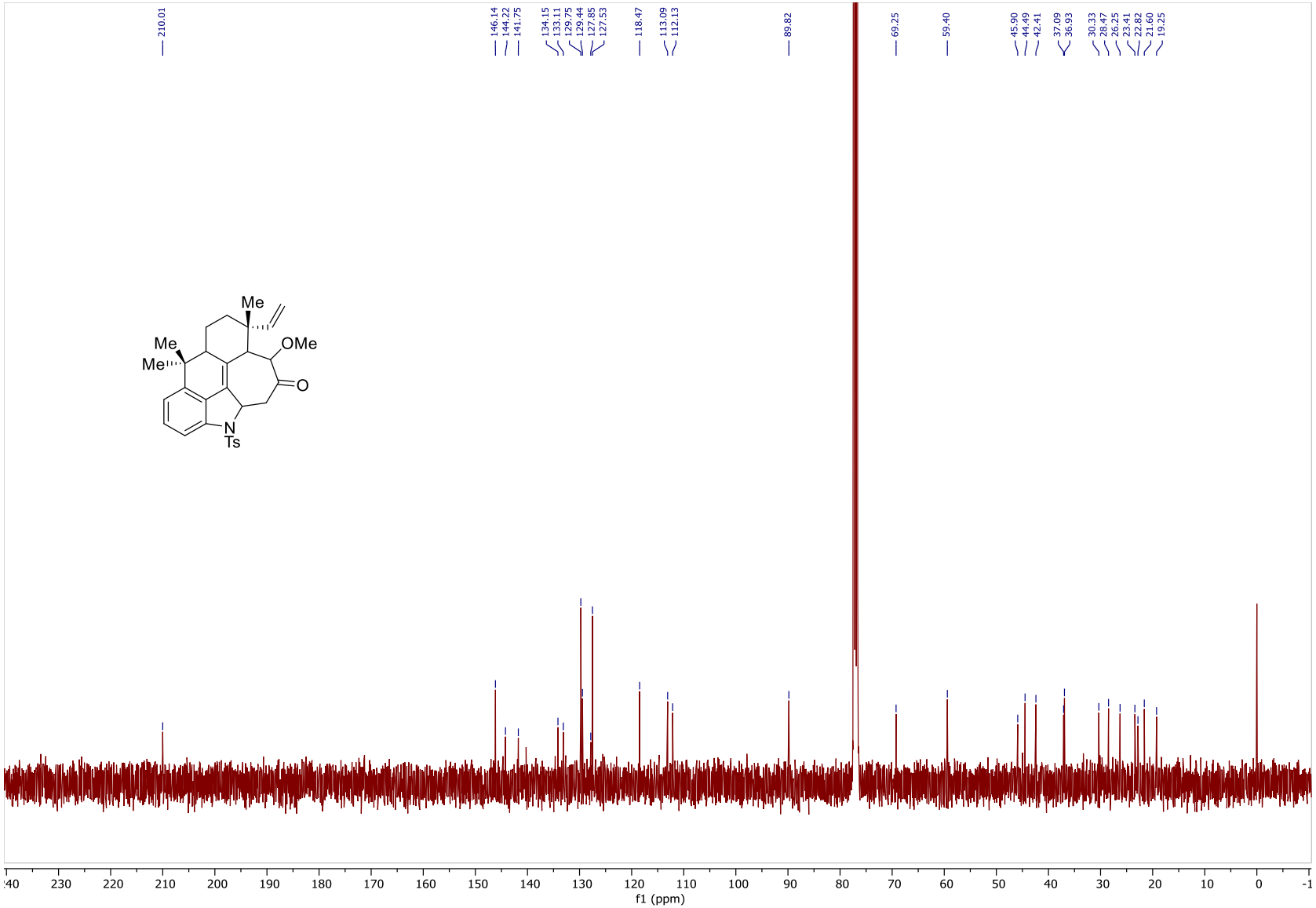

Figure 182: ^{13}C NMR Spectrum of **171** (100MHz, $CDCl_3$)

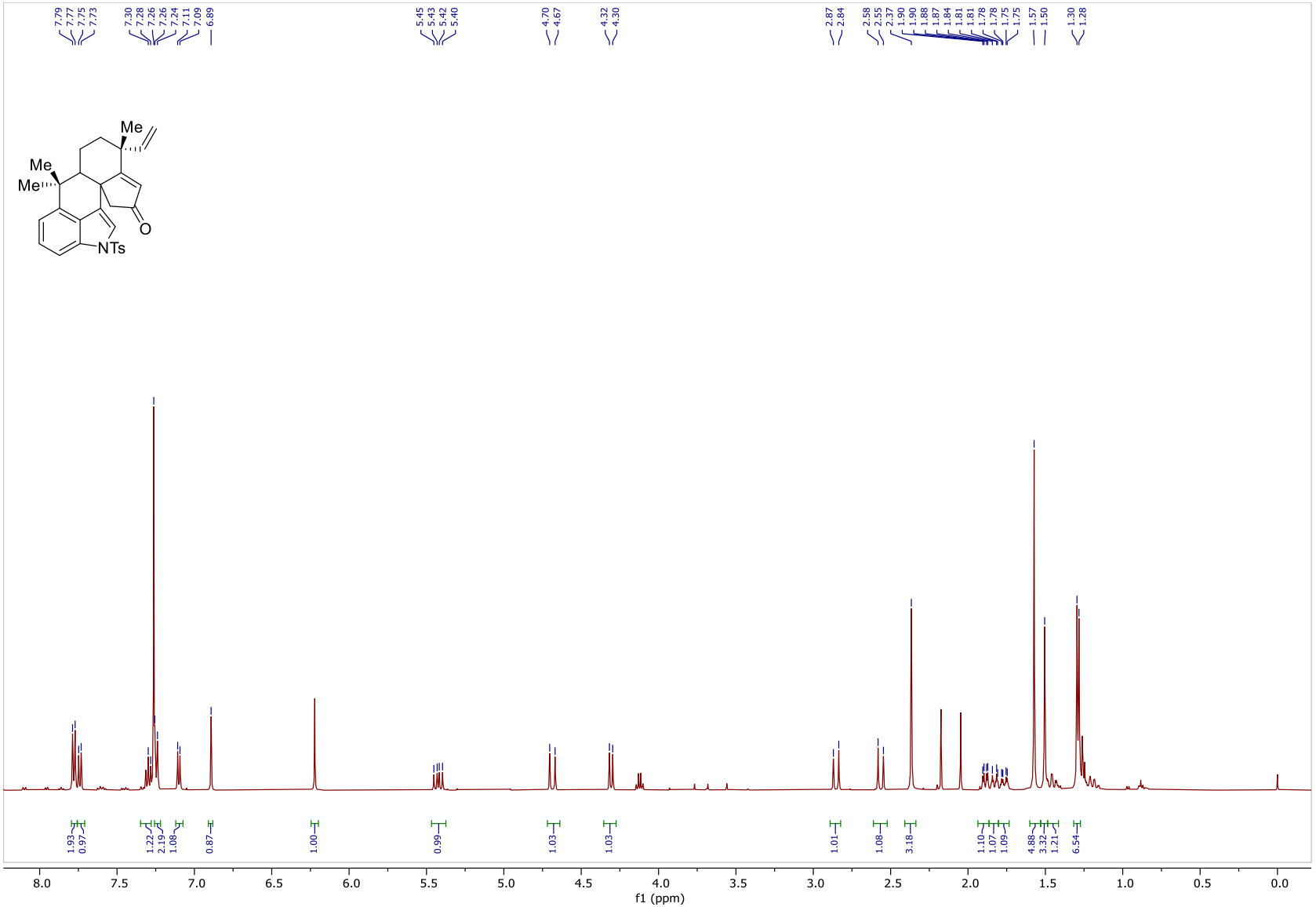

Figure 183: ^{1}H NMR Spectrum of **197** (400MHz, $CDCl_3$)

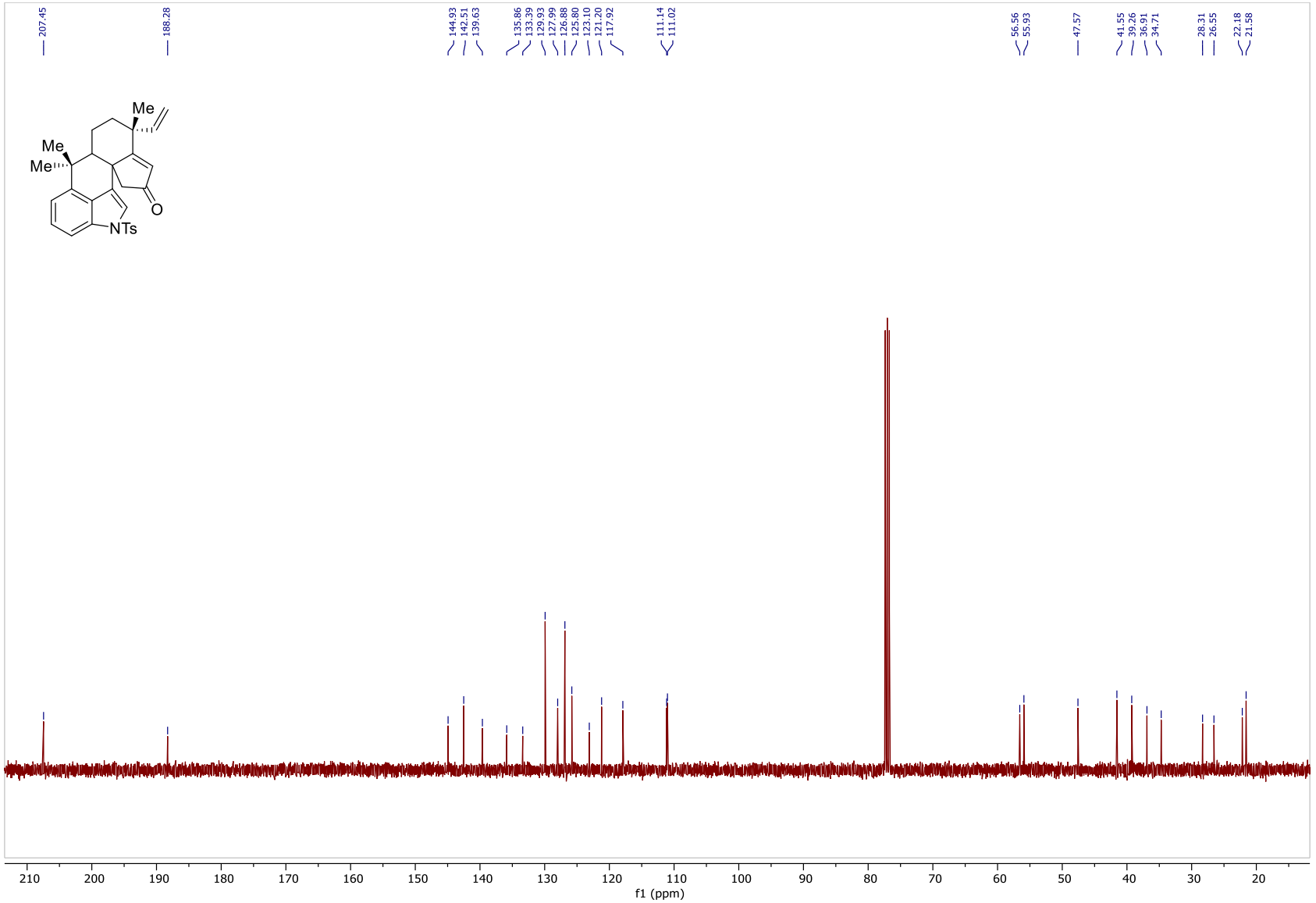

Figure 184: ^{13}C NMR Spectrum of **197** (100MHz, $CDCl_3$)

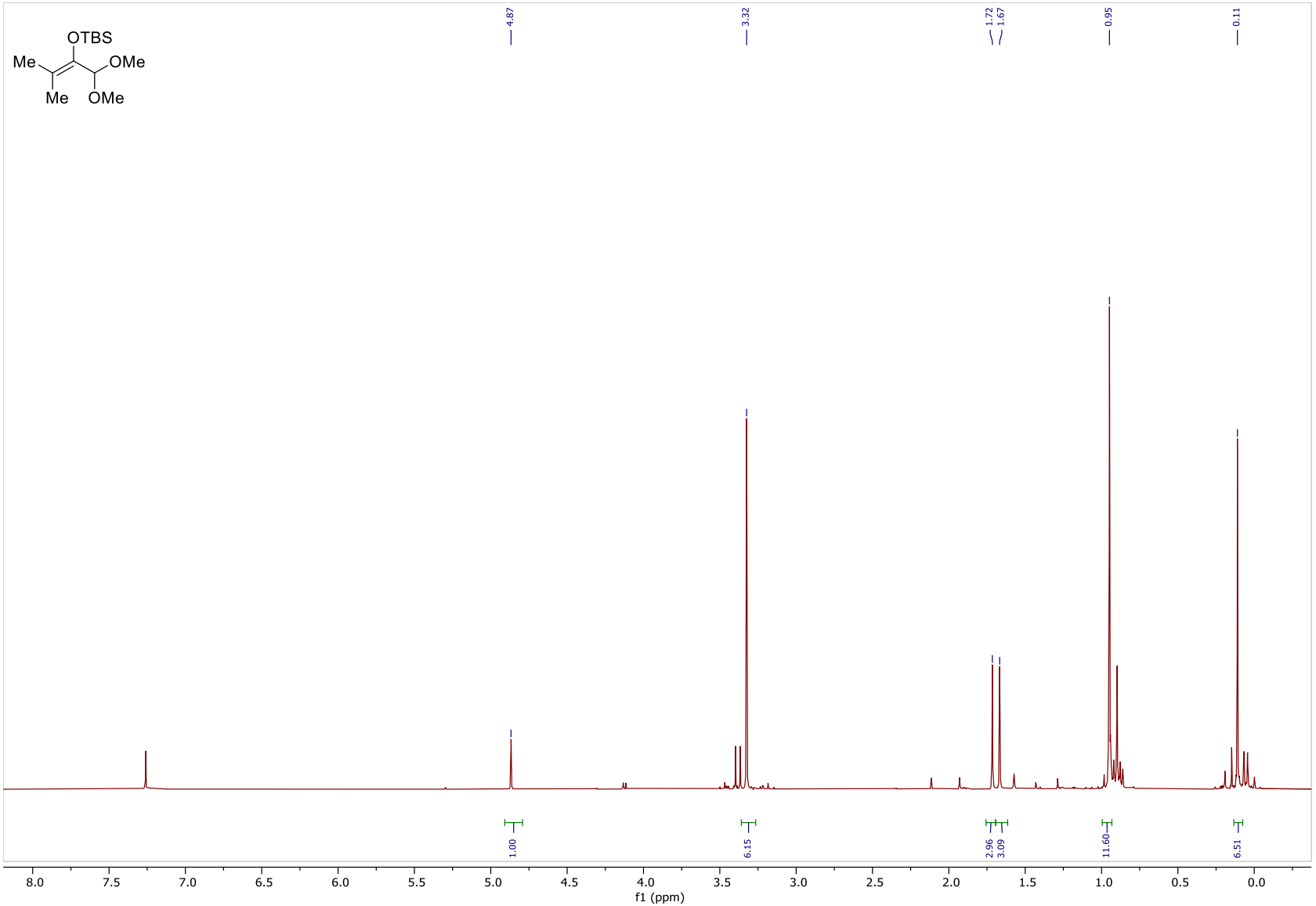

Figure 185: ^{1}H NMR Spectrum of **92c** (400MHz, $CDCl_3$)

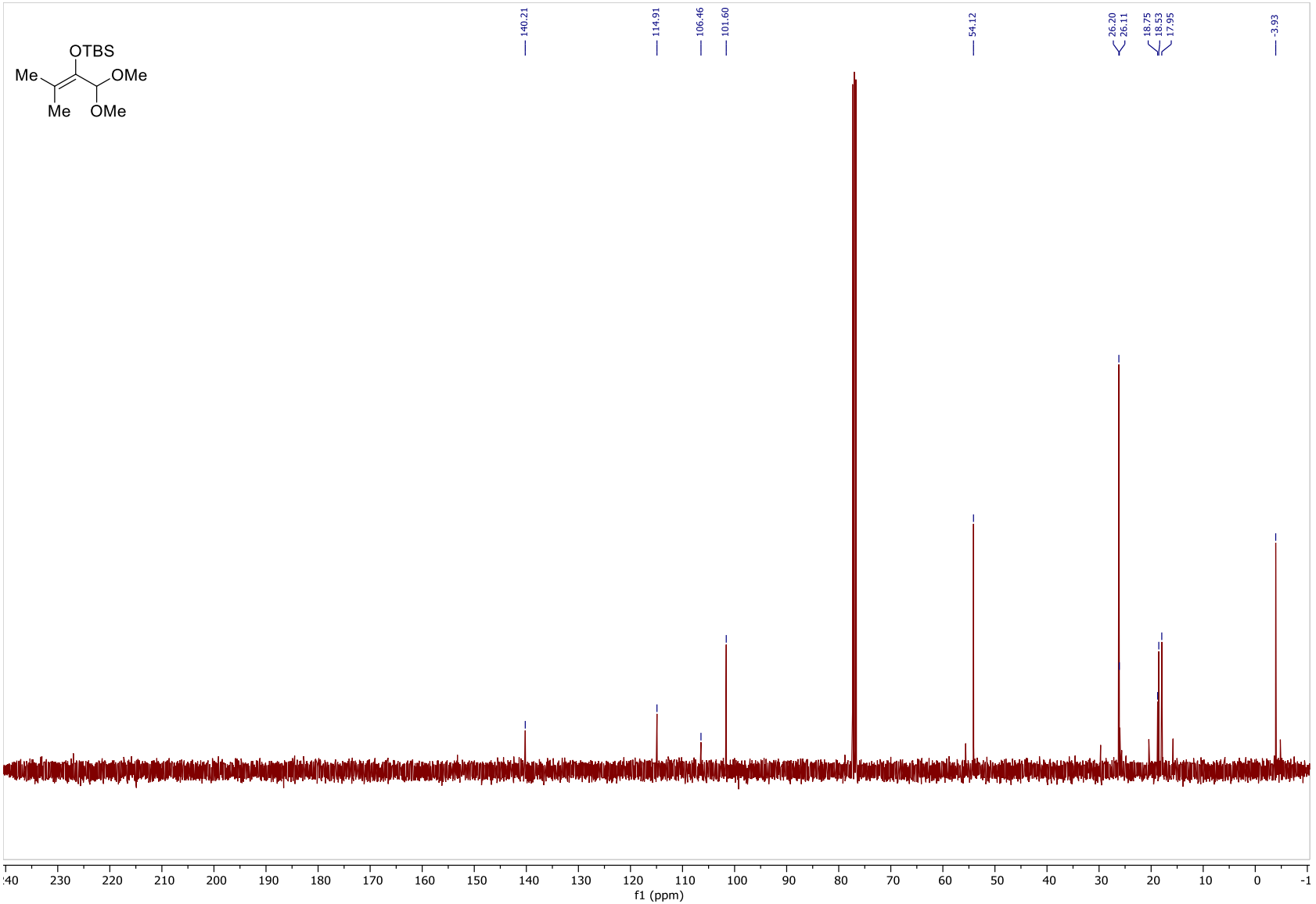

Figure 186: ^{13}C NMR Spectrum of **92c** (100MHz, $CDCl_3$)

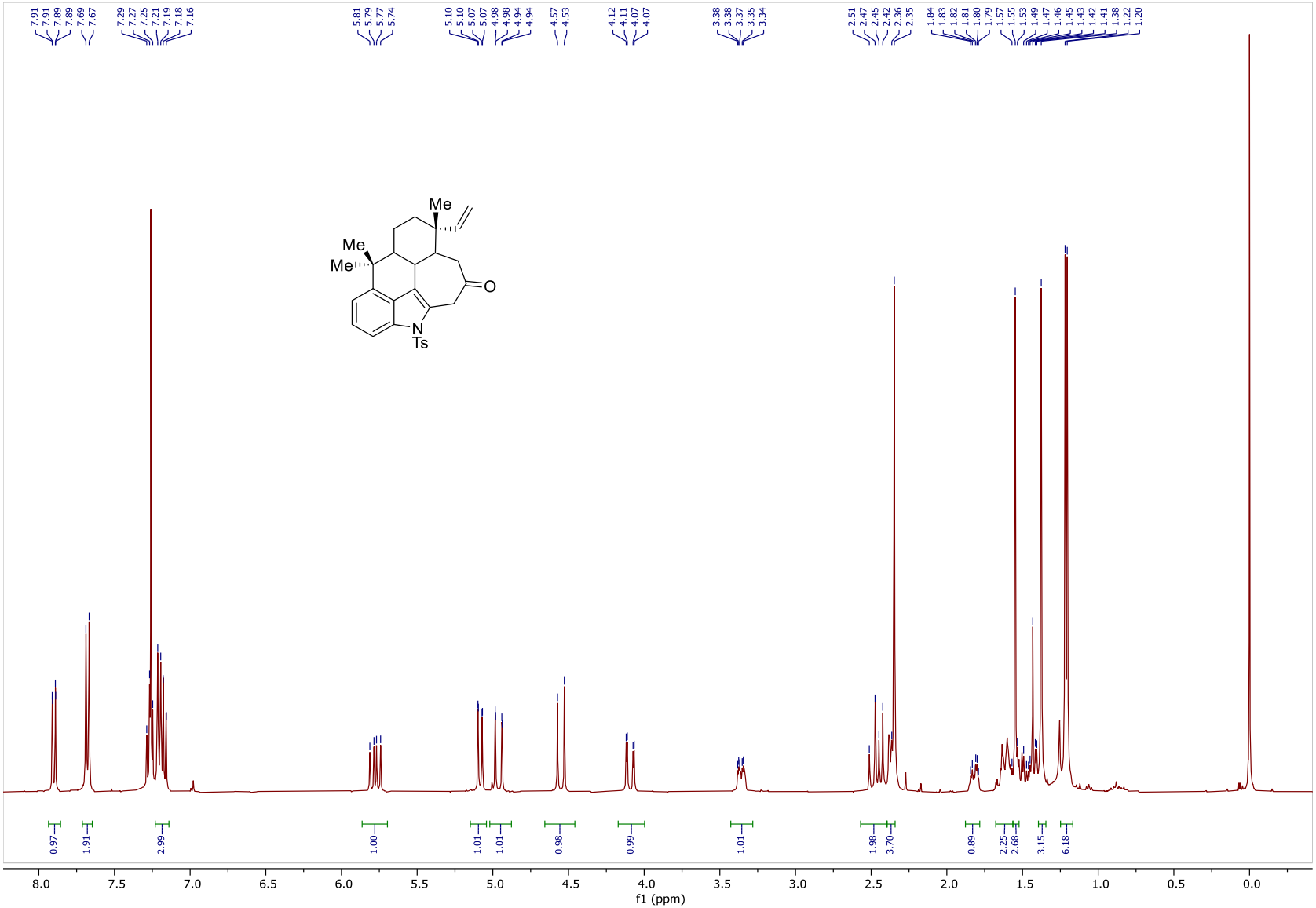

Figure 187: ^{1}H NMR Spectrum of **204** (400MHz, $CDCl_3$)

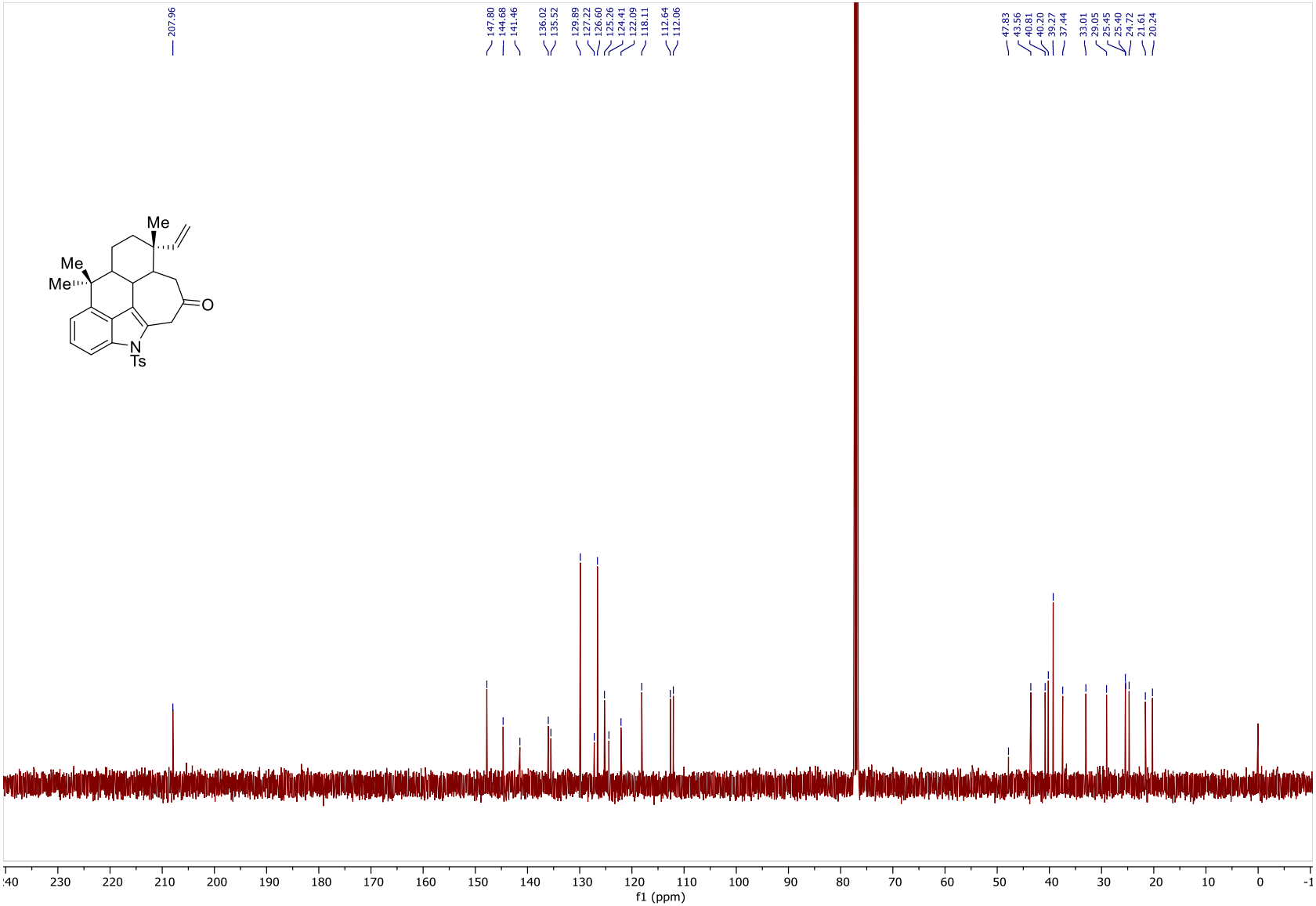

Figure 188: ^{13}C NMR Spectrum of **204** (100MHz, $CDCl_3$)

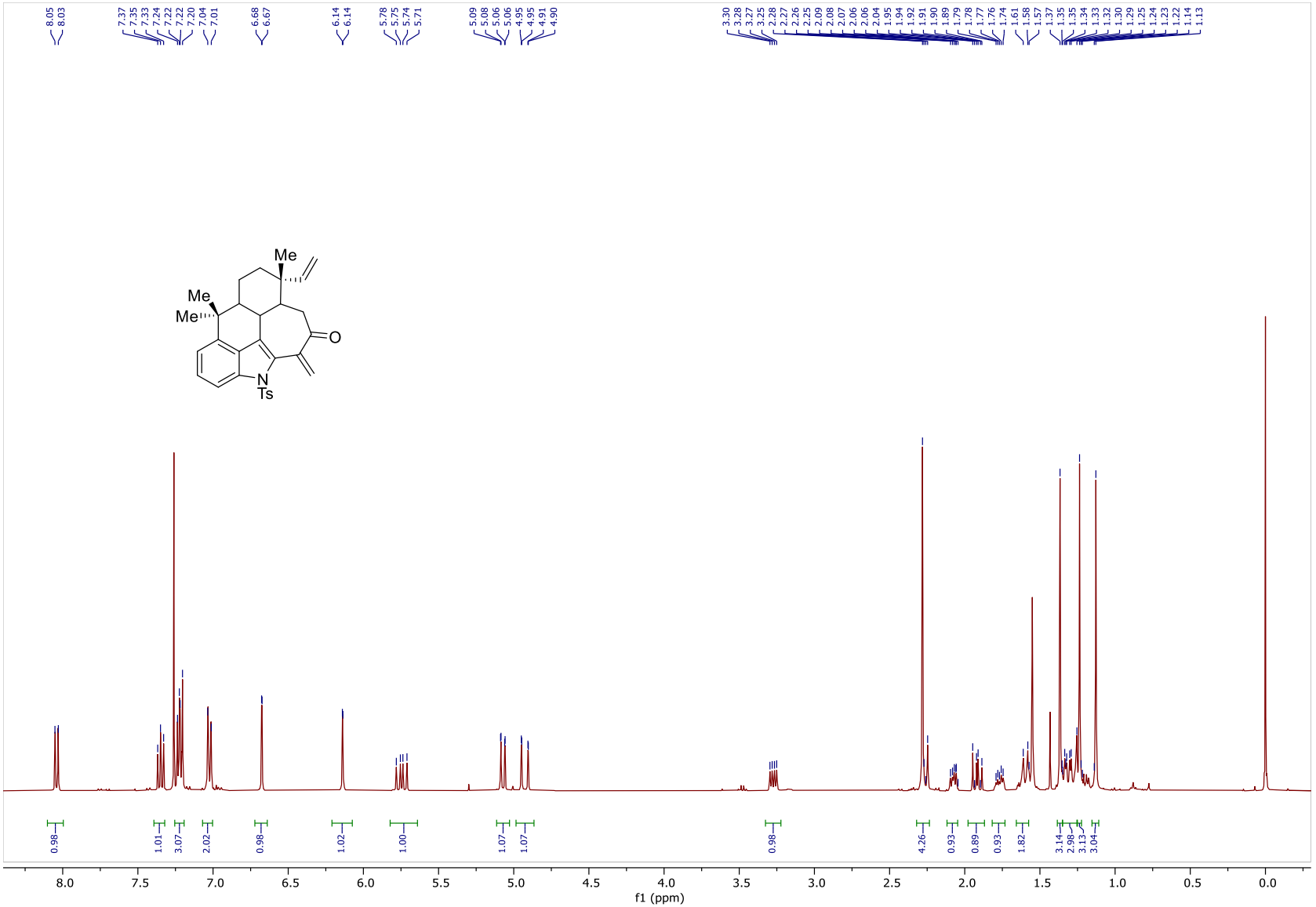

Figure 189: ^{1}H NMR Spectrum of **208** (400MHz, $CDCl_3$)

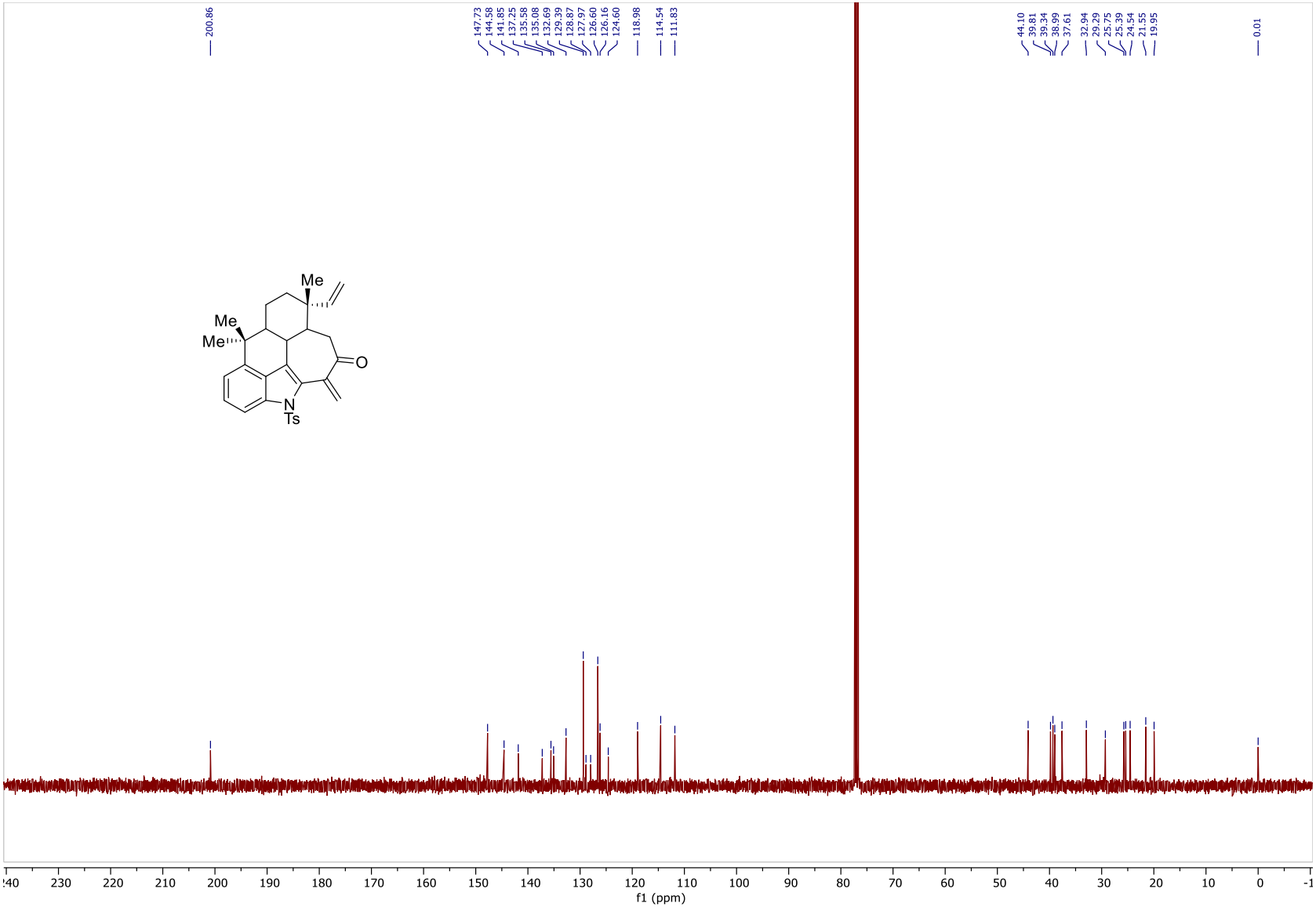

Figure 190: ^{13}C NMR Spectrum of **208** (100MHz, $CDCl_3$)

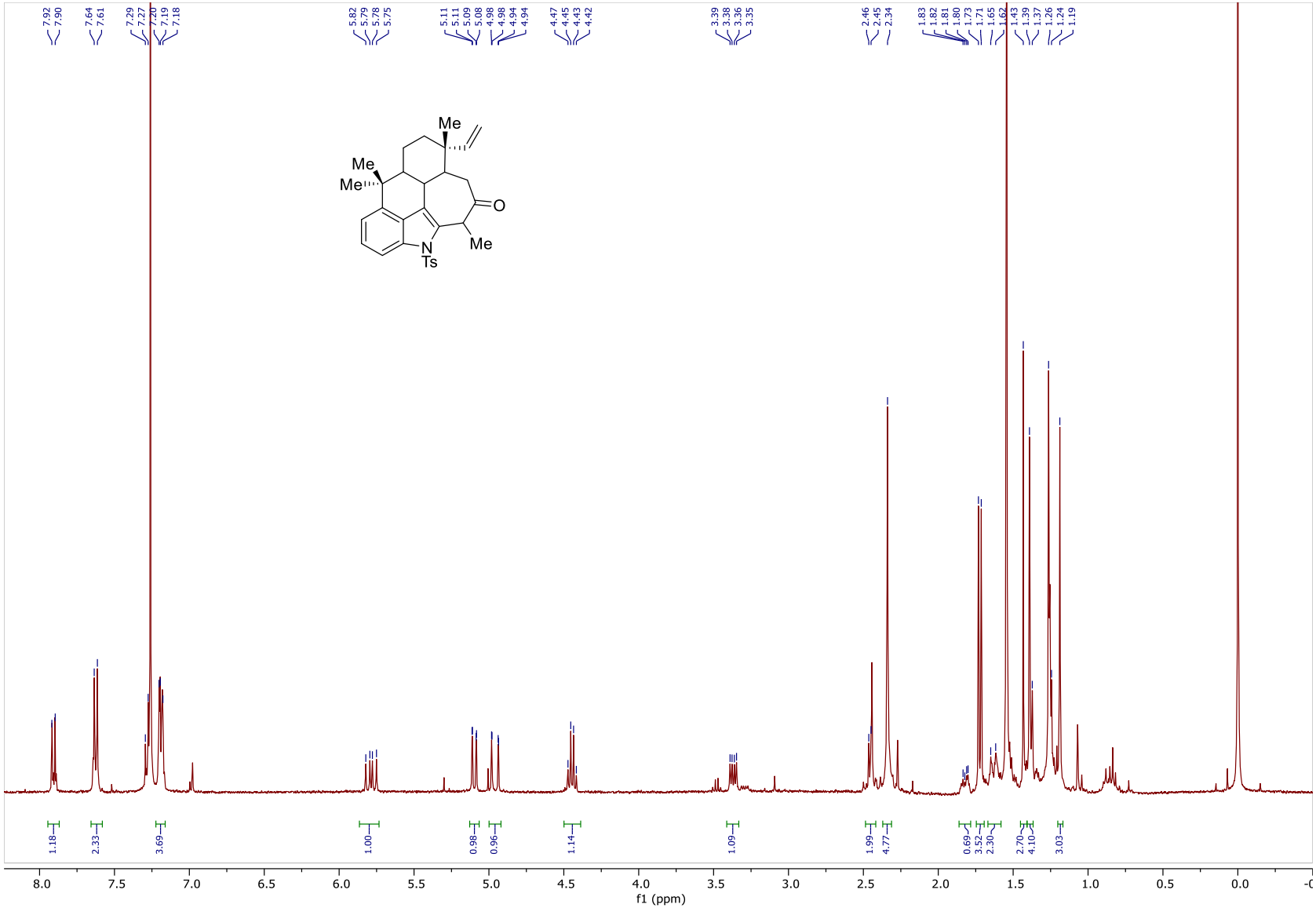

Figure 191: ^{1}H NMR Spectrum of **205** (400MHz, $CDCl_3$)

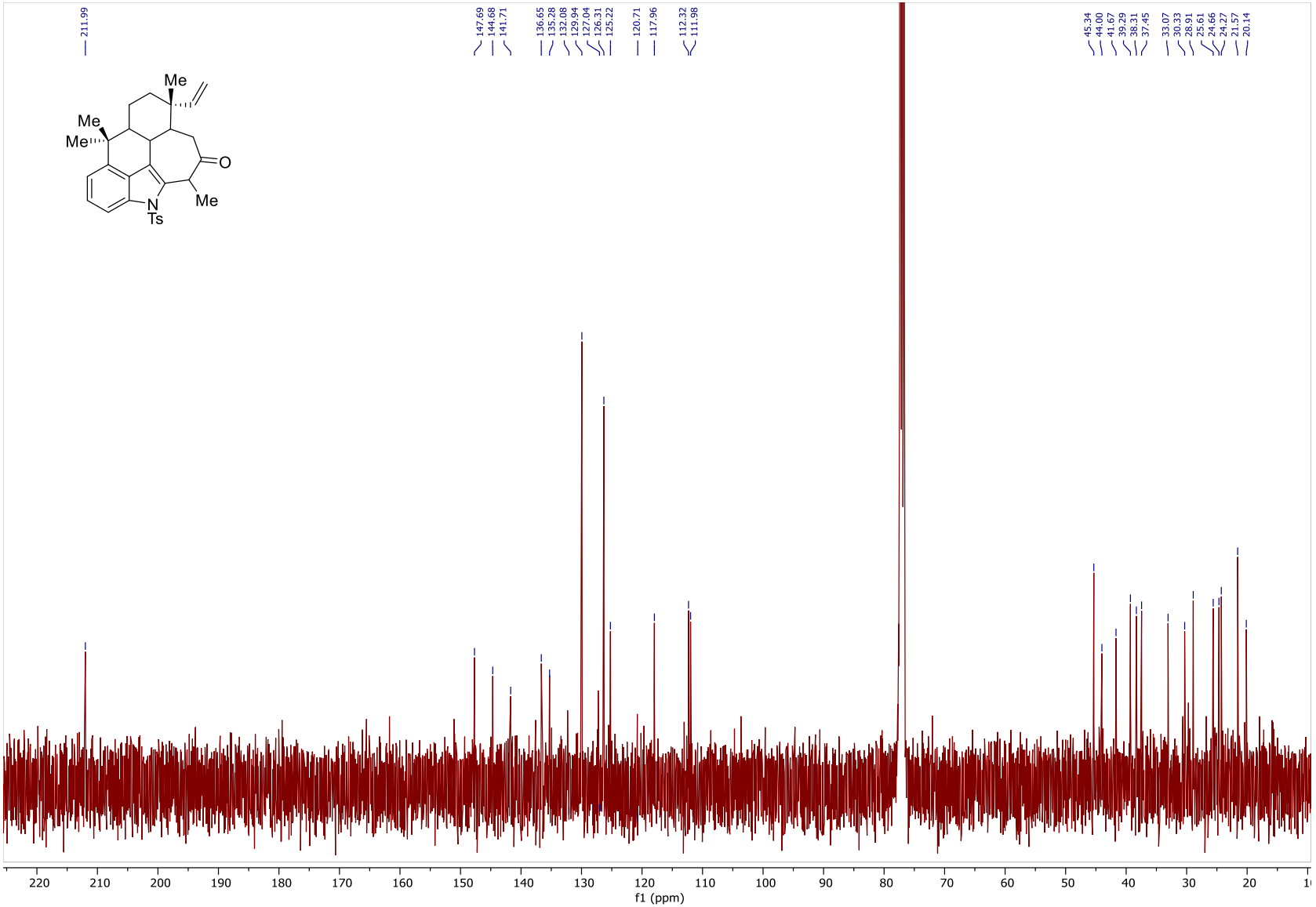

Figure 192: ^{13}C NMR Spectrum of **205** (100MHz, $CDCl_3$)

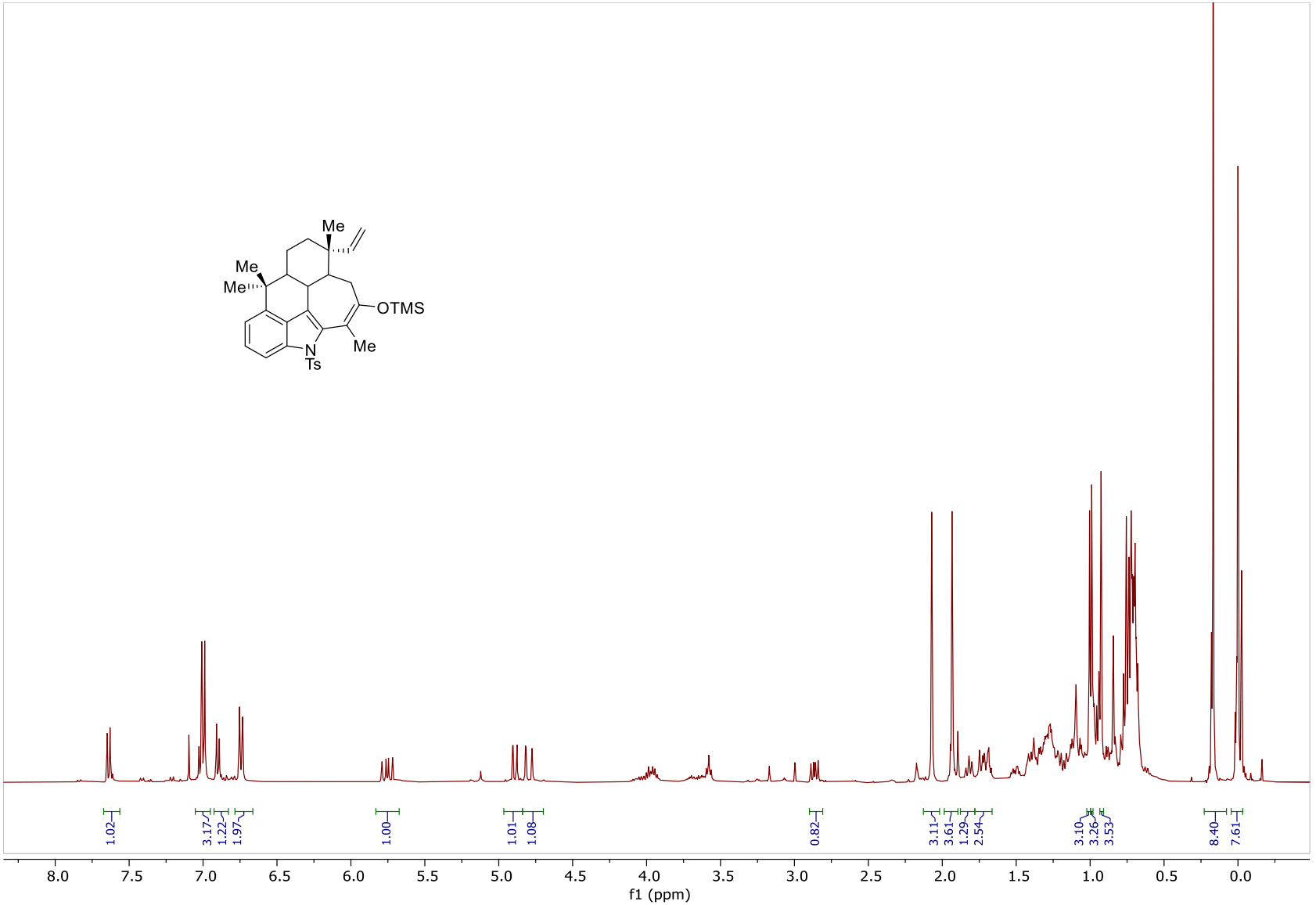

Figure 193: ^{1}H NMR Spectrum of **211** (400MHz, $CDCl_3$)

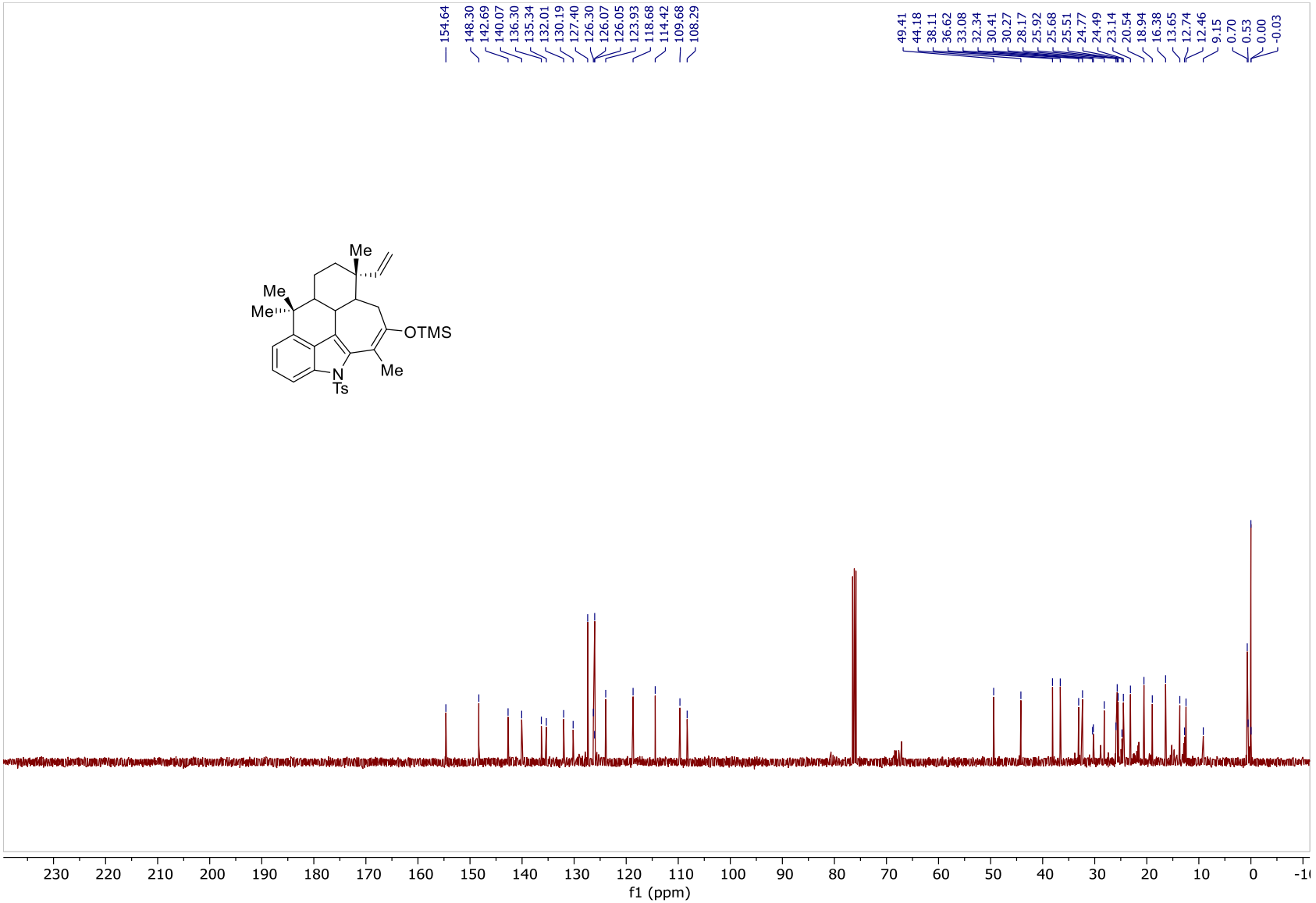

Figure 194: ^{13}C NMR Spectrum of **211** (100MHz, $CDCl_3$)

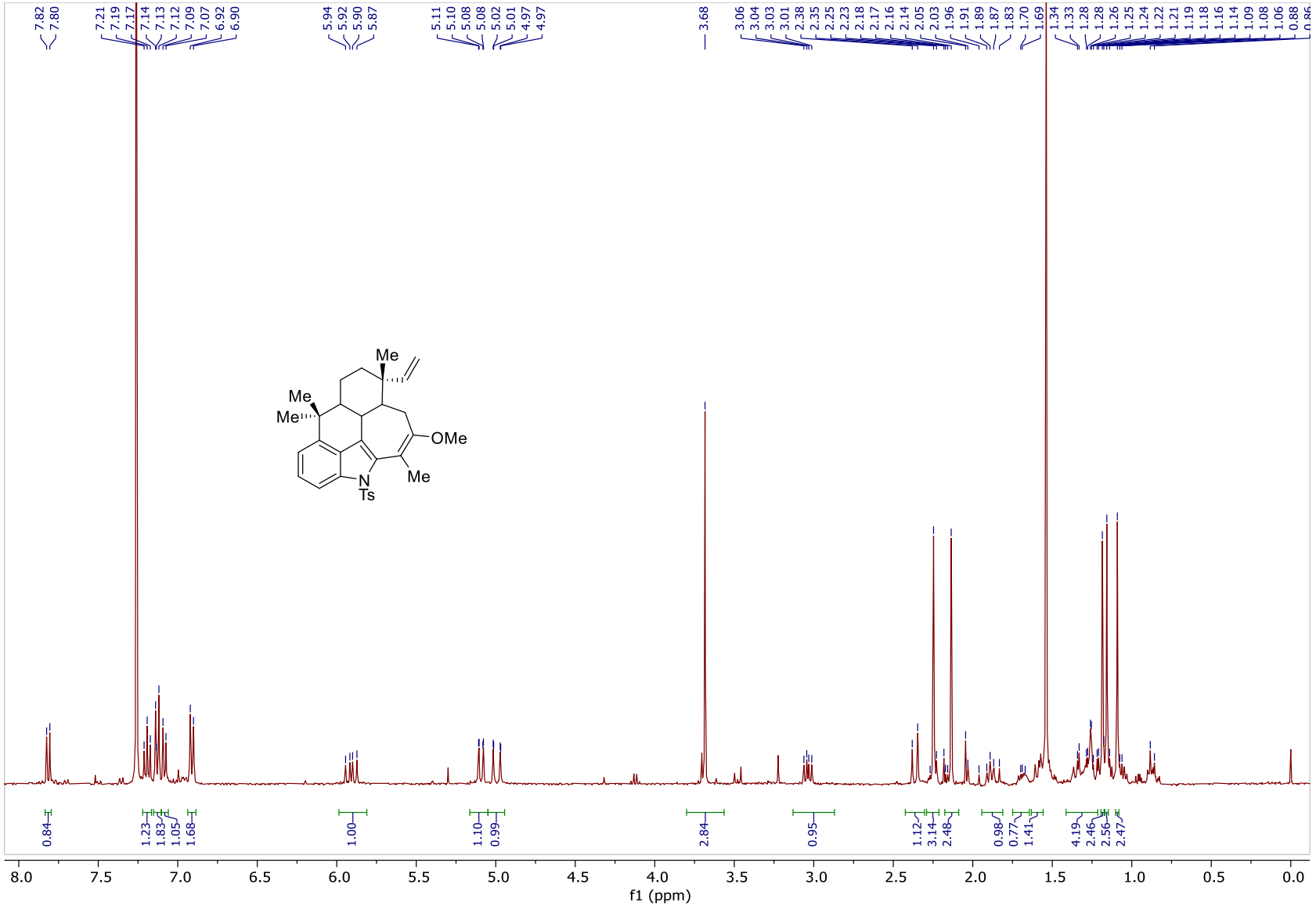

Figure 195: ^{1}H NMR Spectrum of **207** (400MHz, $CDCl_3$)

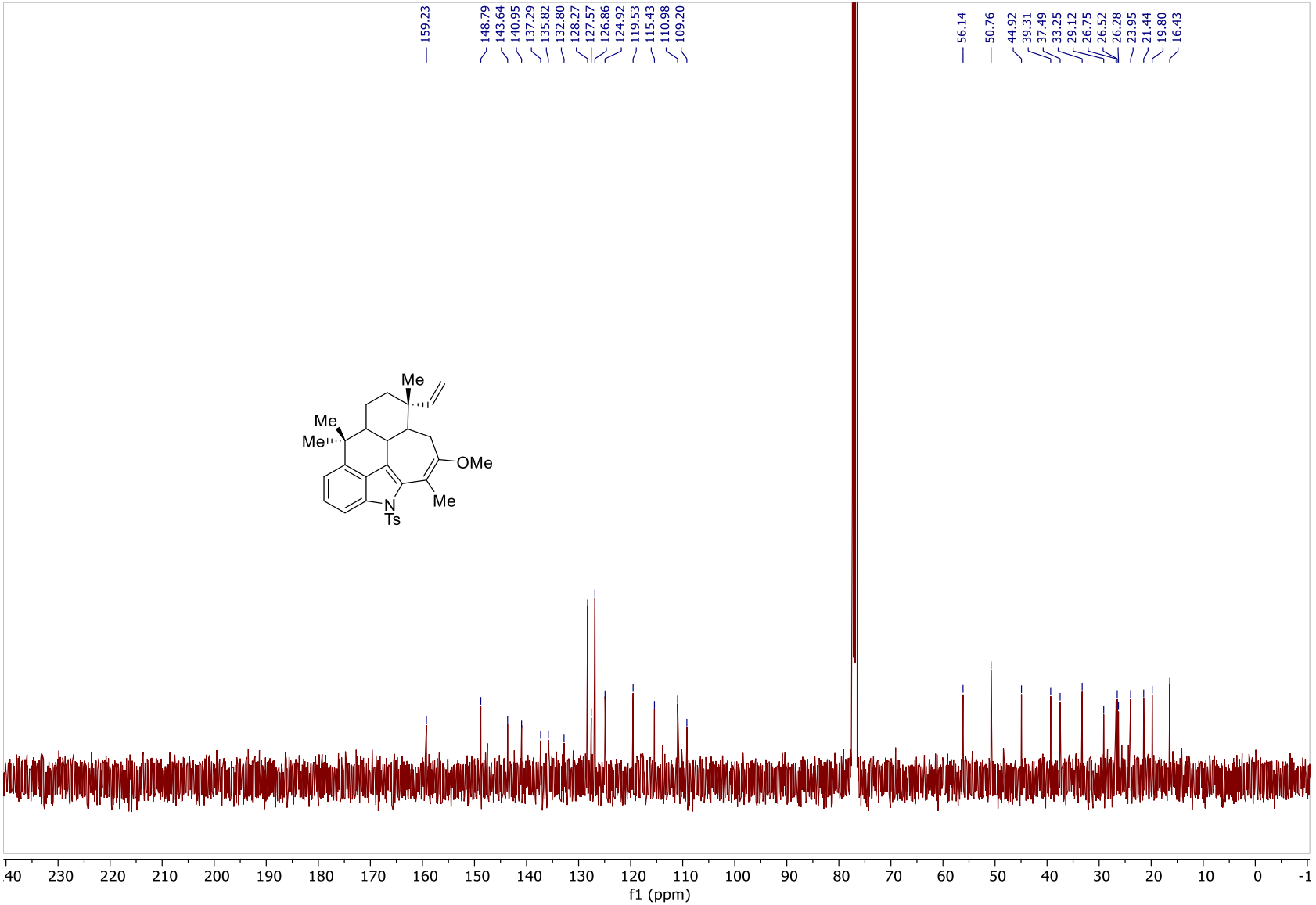

Figure 196: ^{13}C NMR Spectrum of **207** (100MHz, $CDCl_3$)

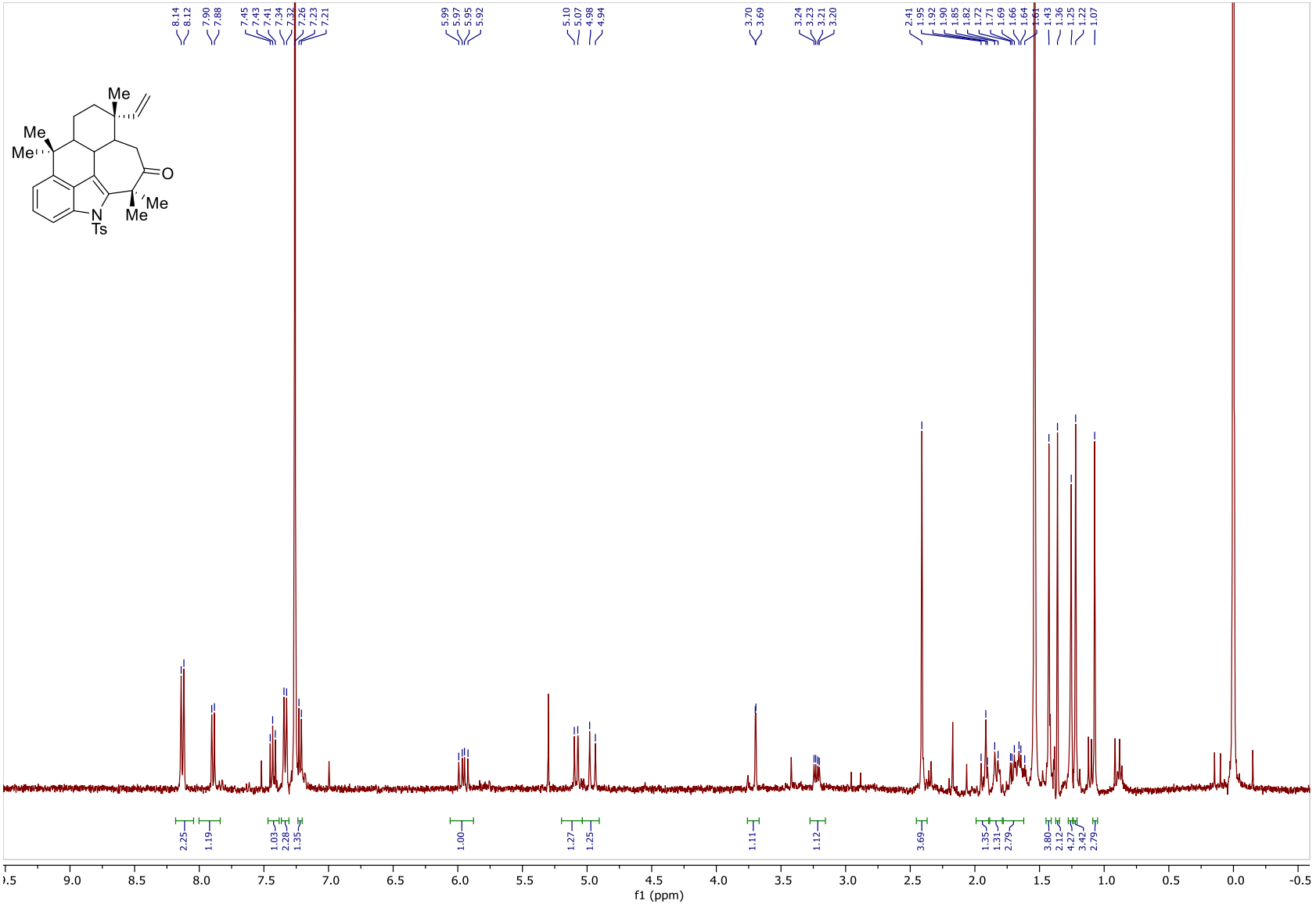

Figure 197: ^{1}H NMR Spectrum of **206** (400MHz, $CDCl_3$)

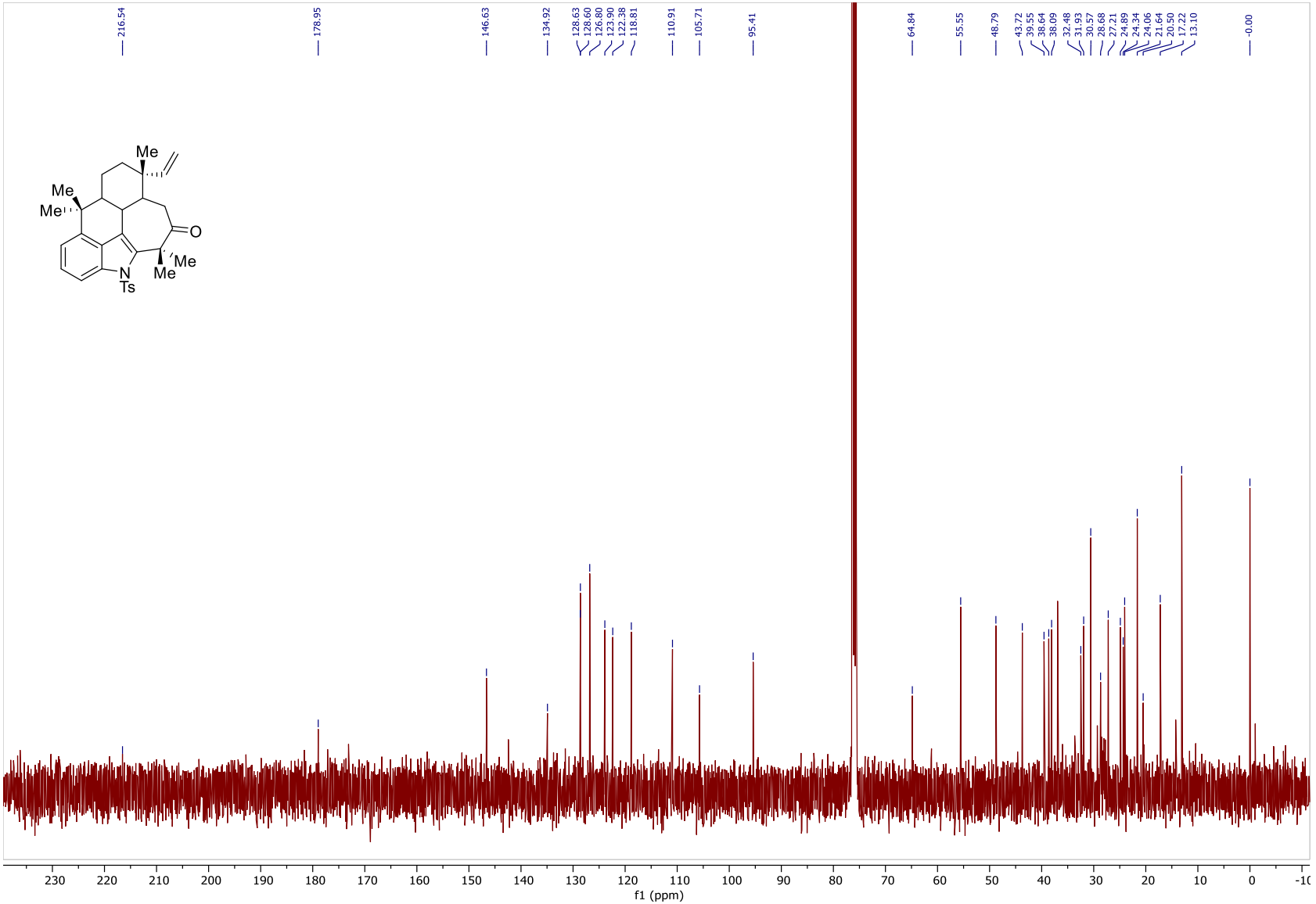

Figure 198: ^{13}C NMR Spectrum of **206** (100MHz, $CDCl_3$)

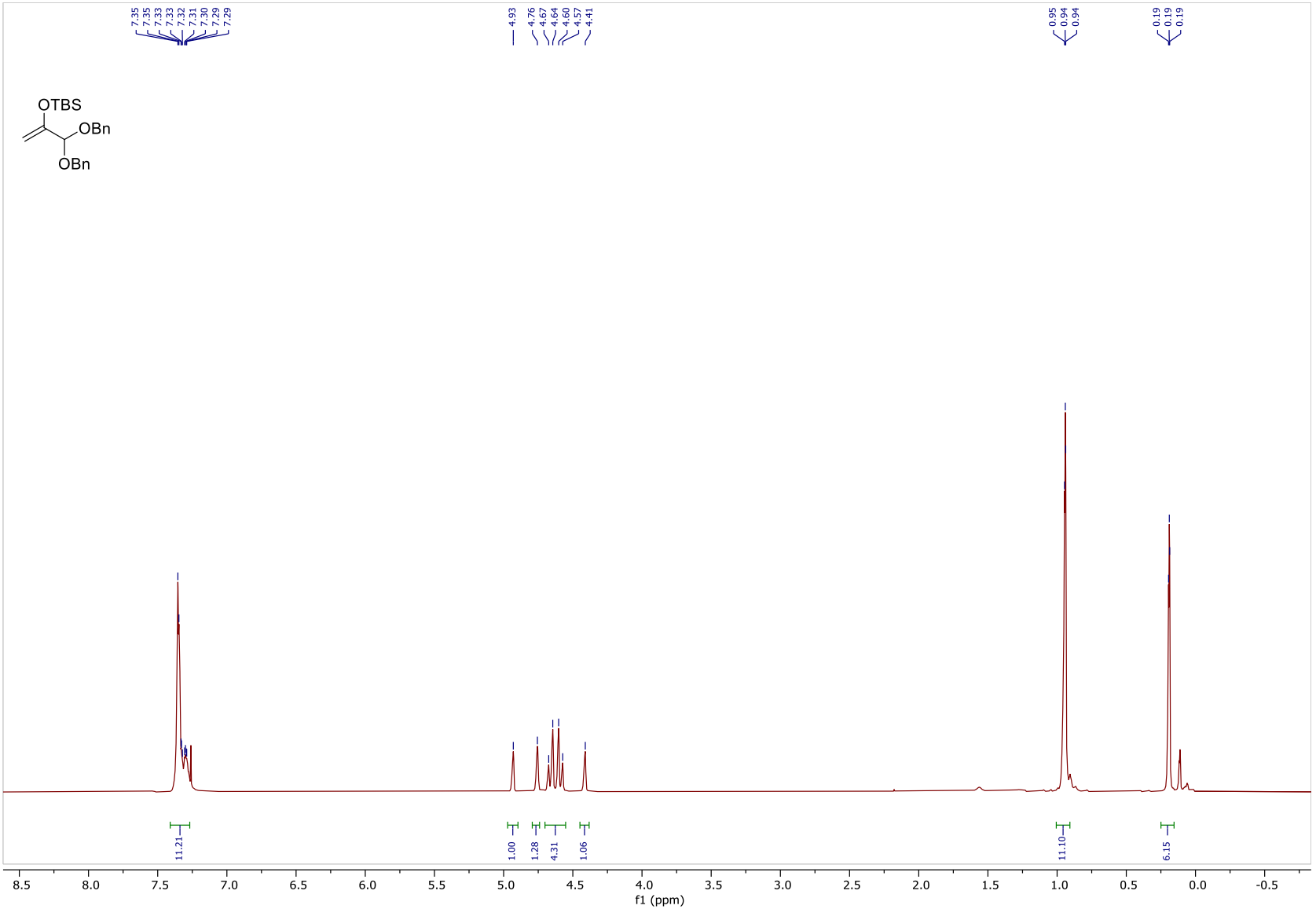

Figure 199: ^{1}H NMR Spectrum of **92d** (400MHz, $CDCl_3$)

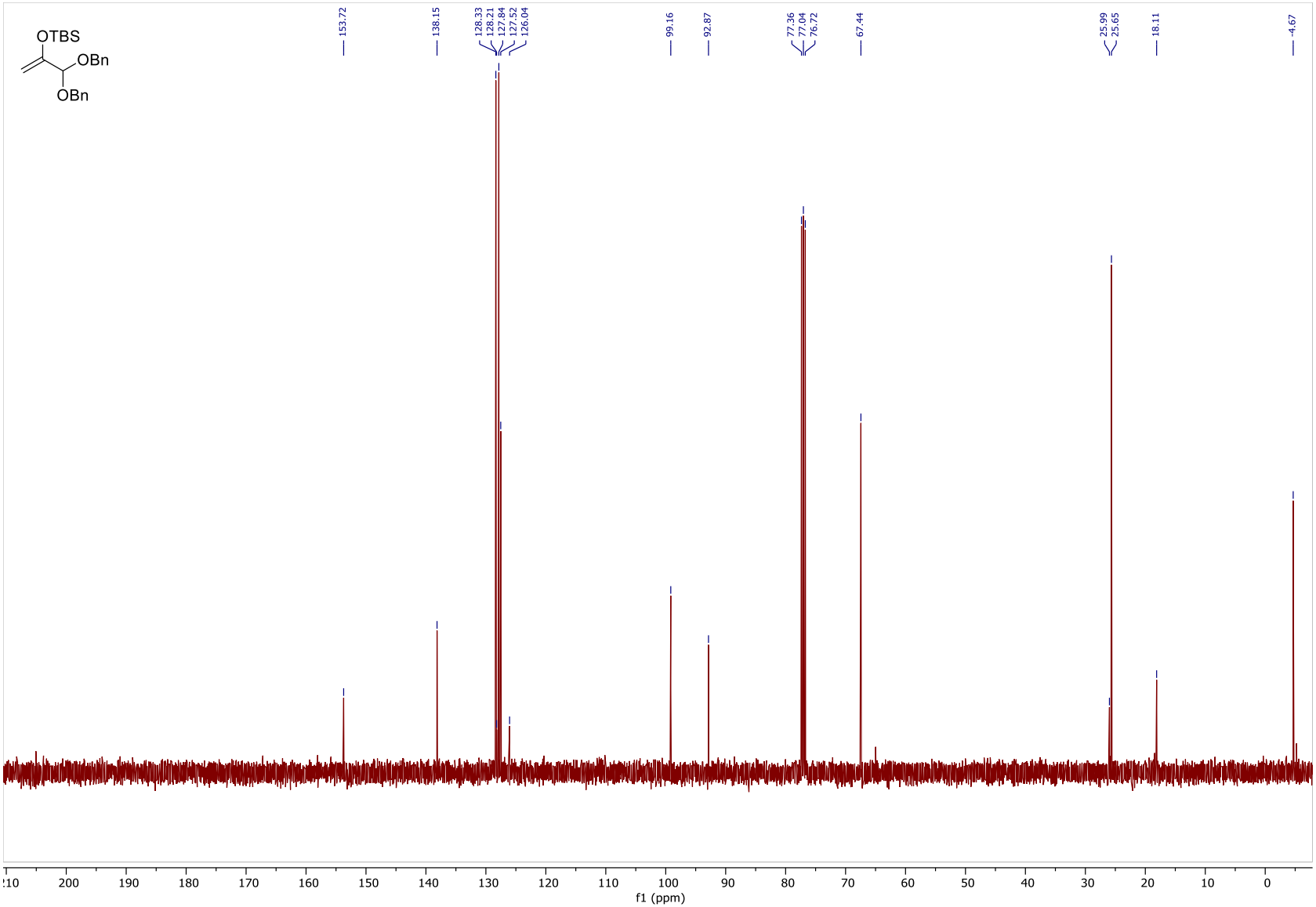

Figure 200: ^{13}C NMR Spectrum of **92d** (100MHz, $CDCl_3$)

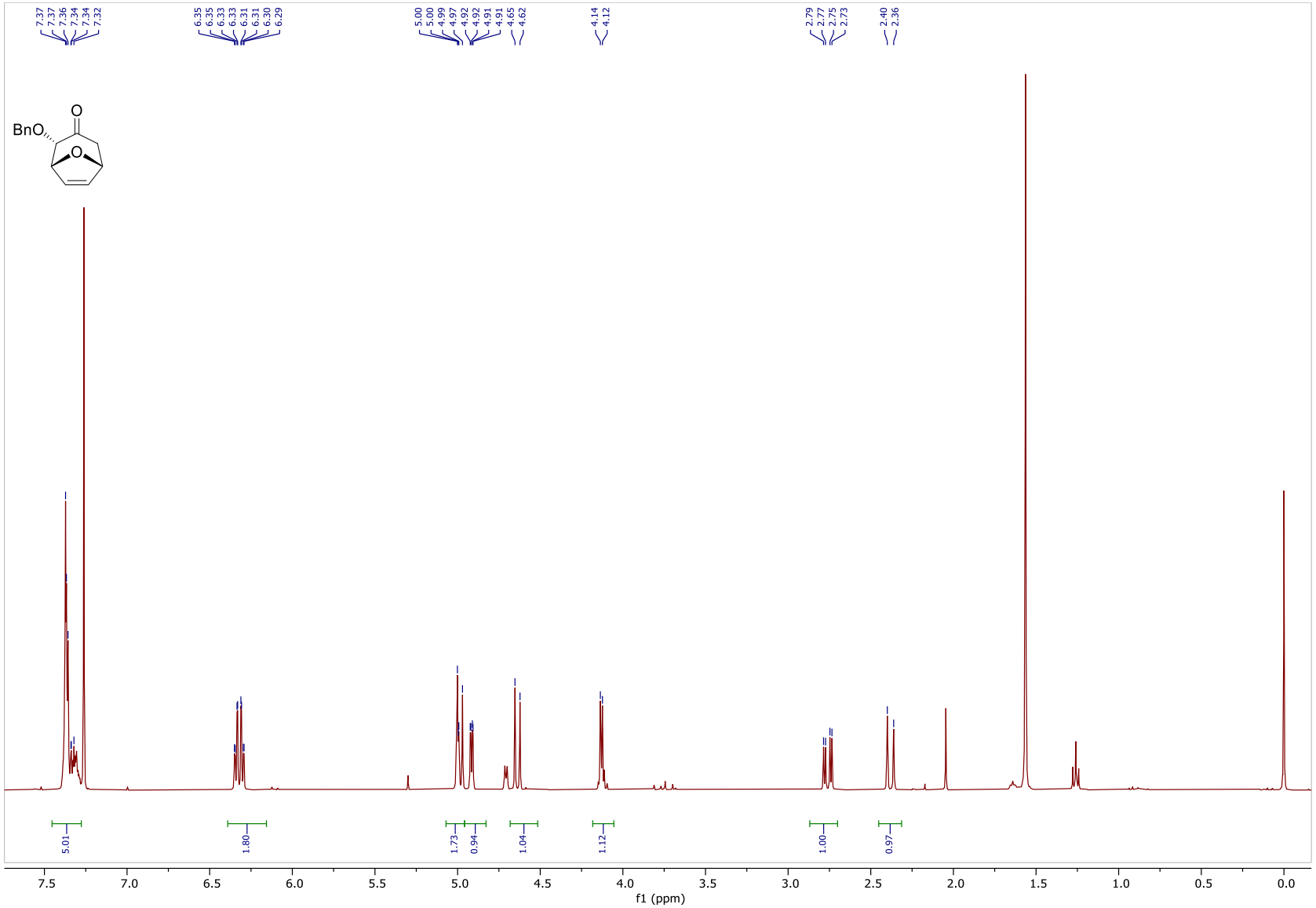

Figure 201: ^{1}H NMR Spectrum of **228** (400MHz, $CDCl_3$)

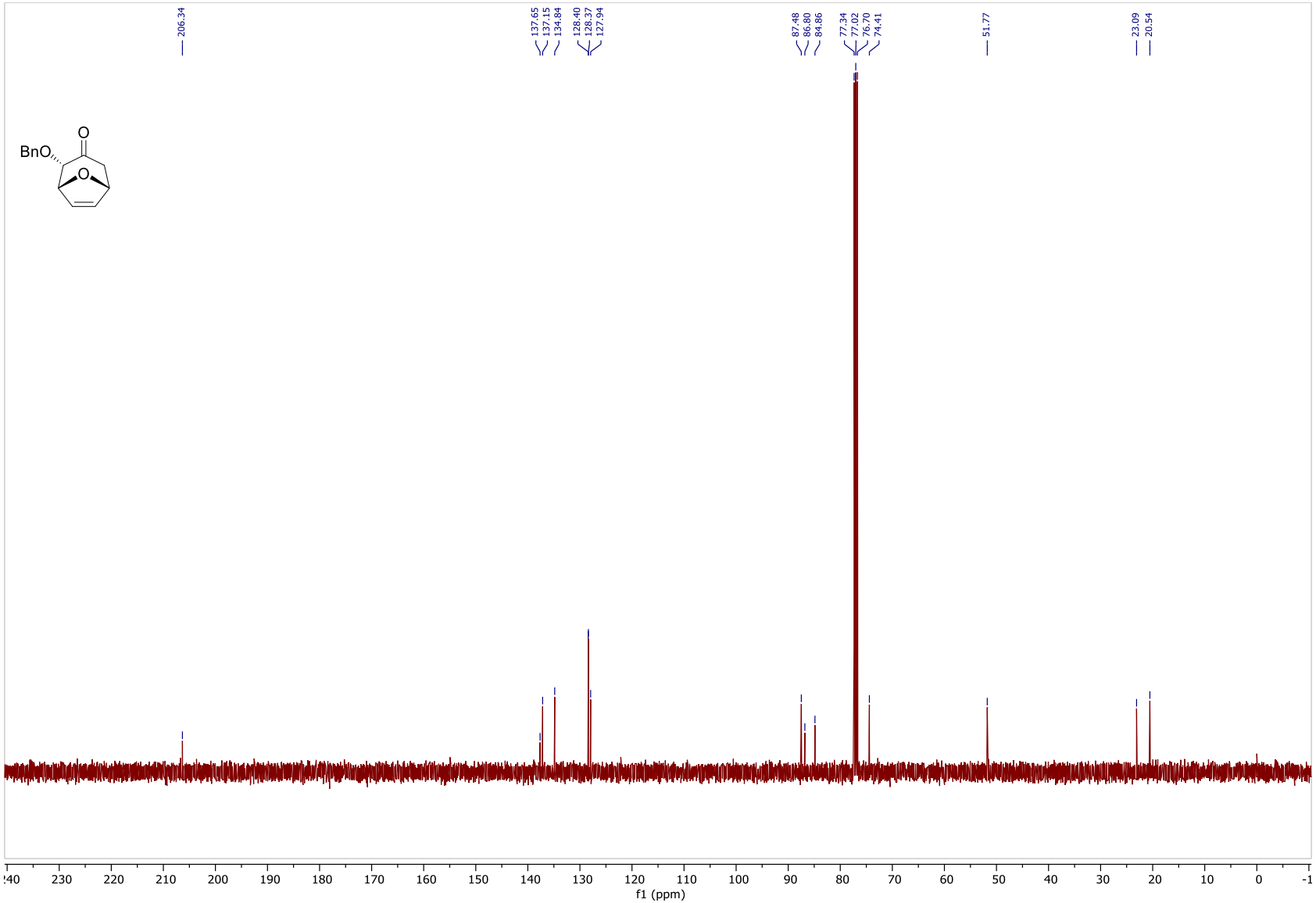

Figure 202: ^{13}C NMR Spectrum of **228** (100MHz, $CDCl_3$)

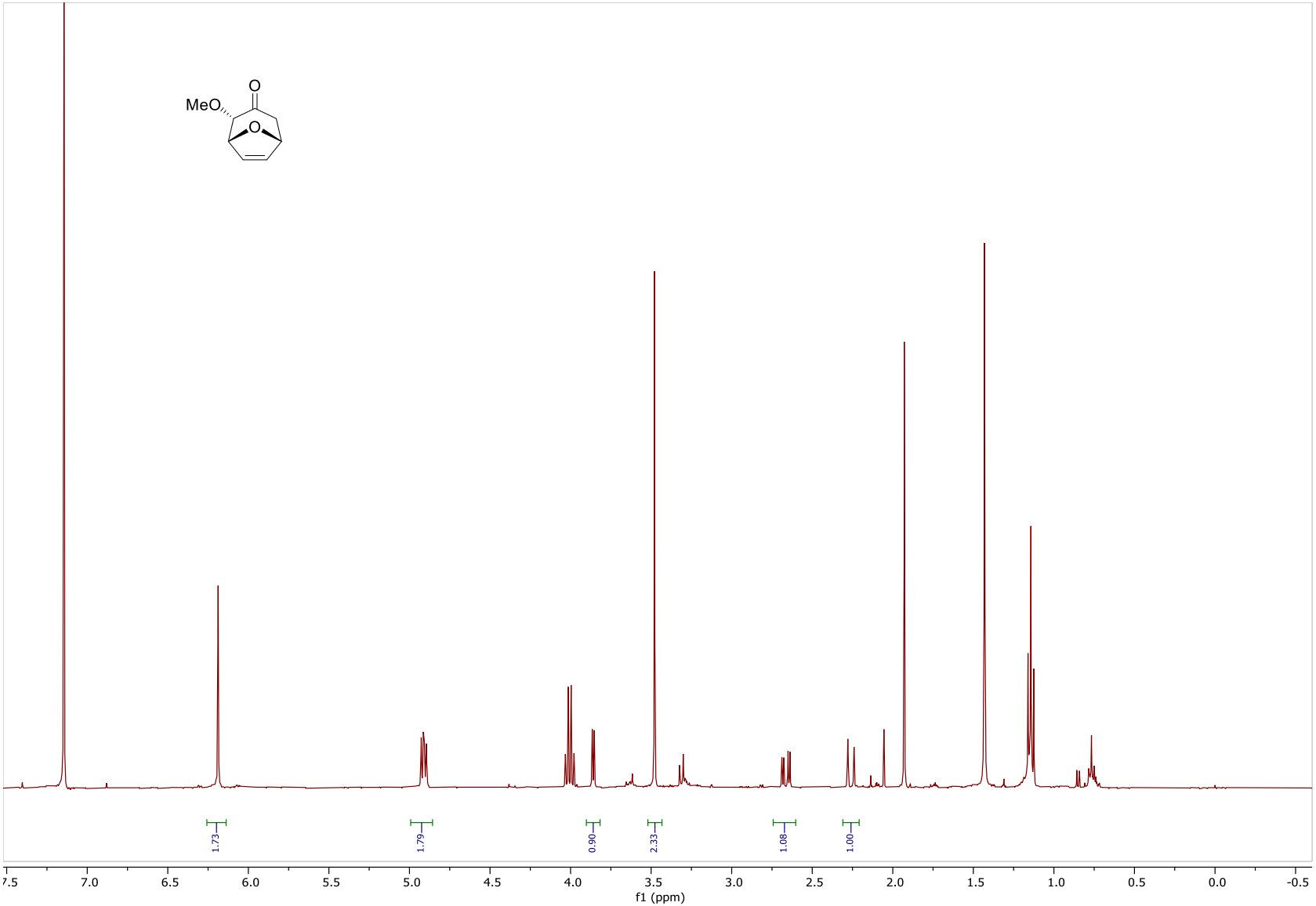

Figure 203: ^{1}H NMR Spectrum of **234a** (400MHz, $CDCl_3$)

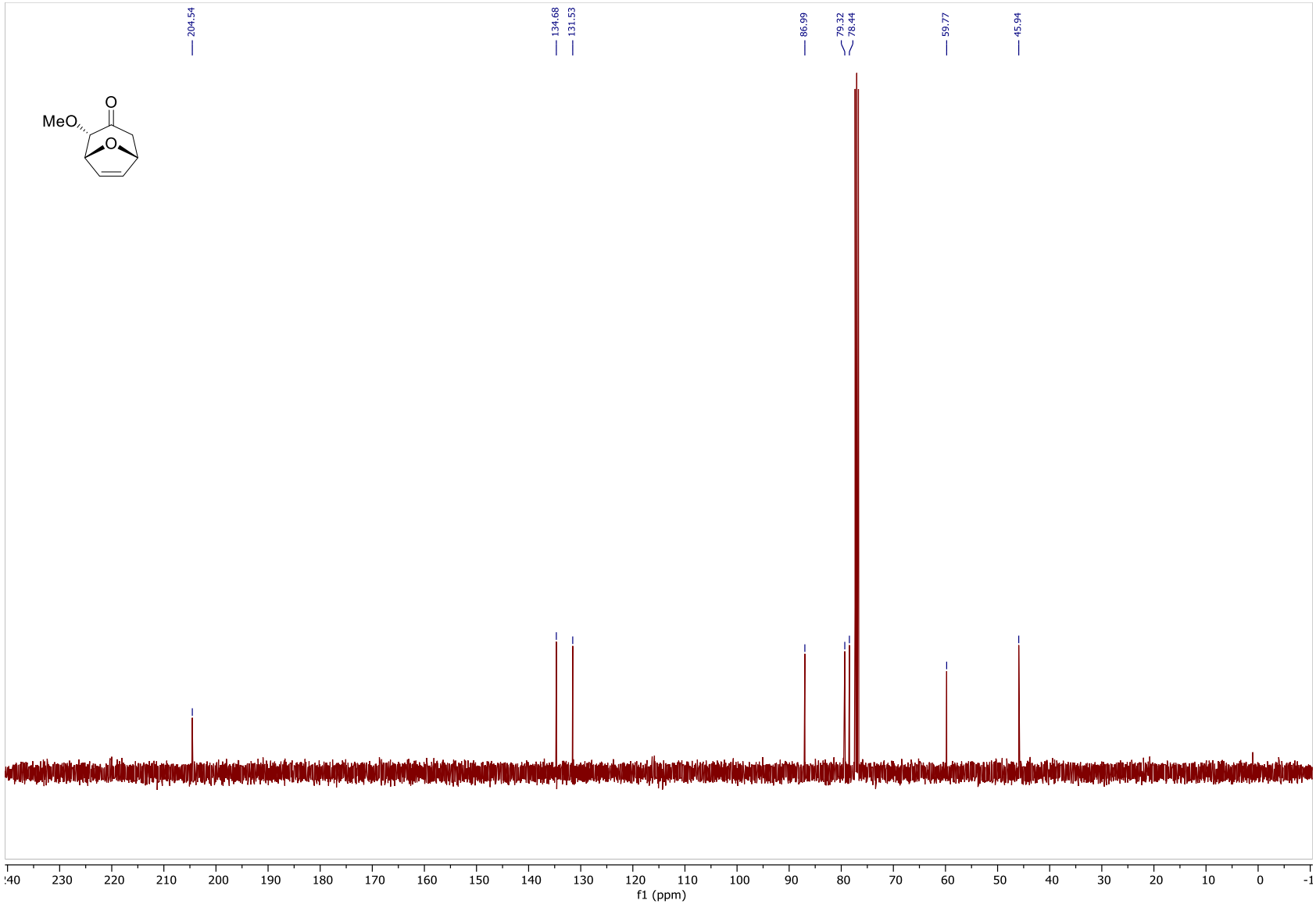

Figure 204: ^{13}C NMR Spectrum of **234a** (100MHz, $CDCl_3$)

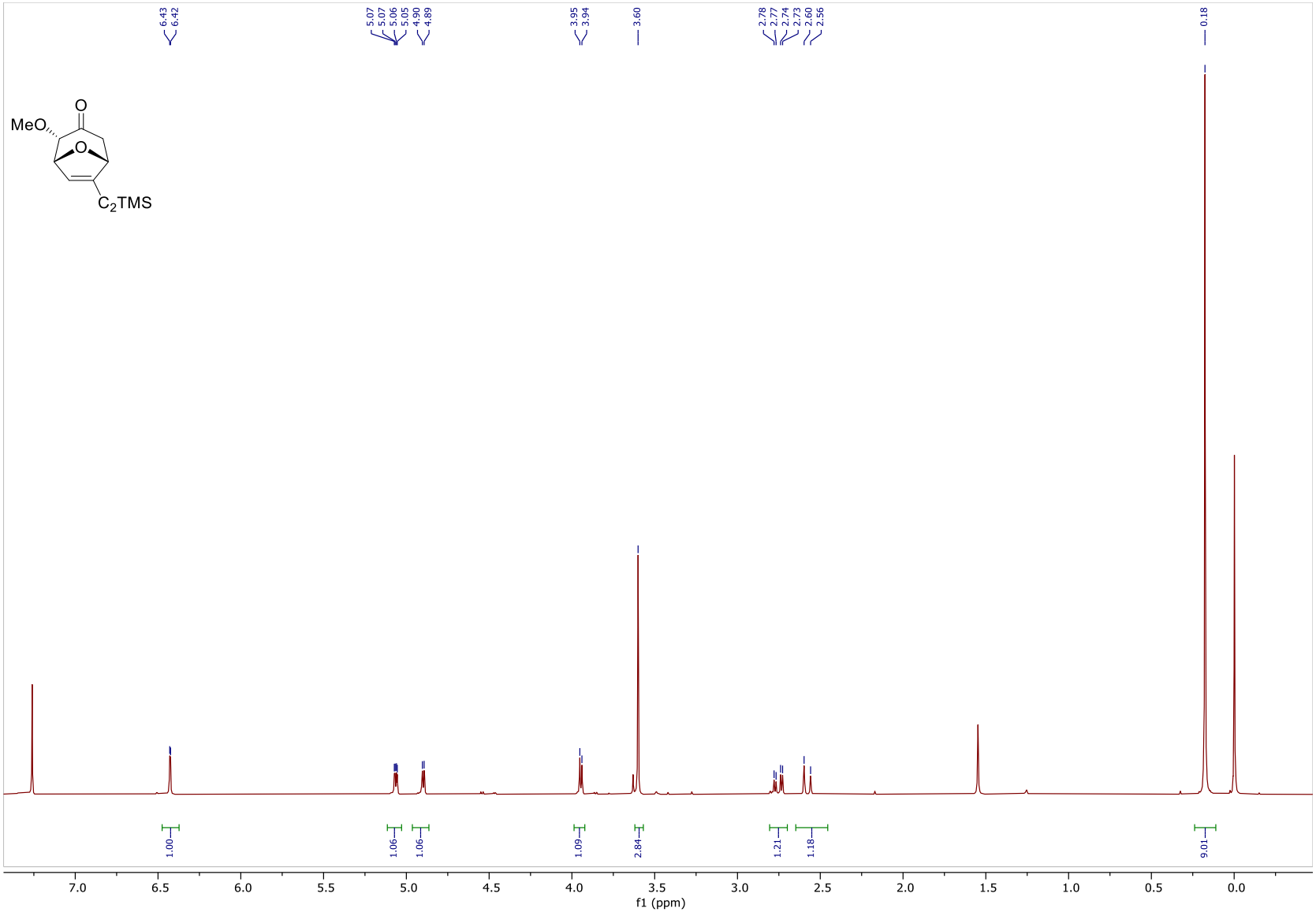

Figure 205: ^{1}H NMR Spectrum of **234b** (400MHz, $CDCl_3$)

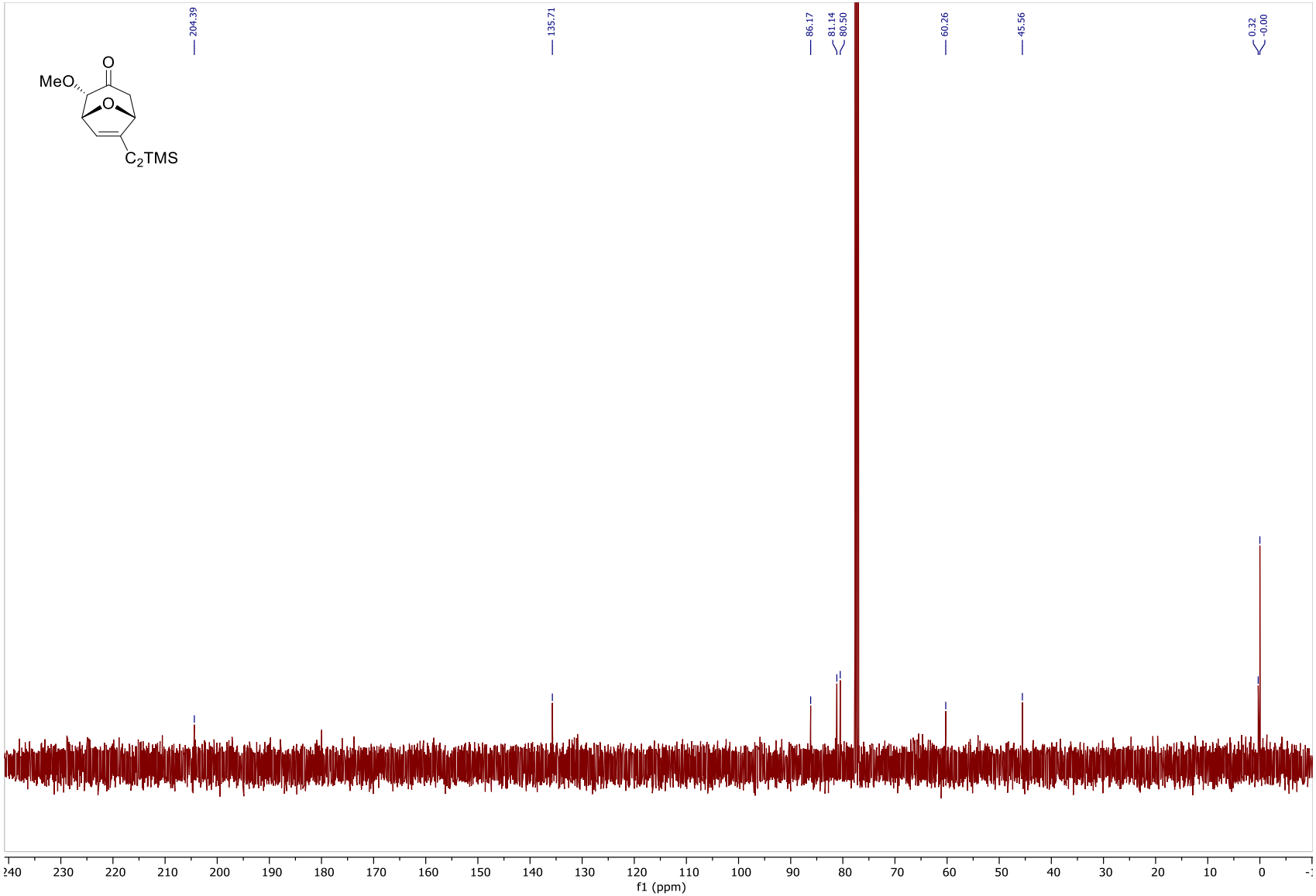

Figure 206: ^{13}C NMR Spectrum of **234b** (100MHz, $CDCl_3$)

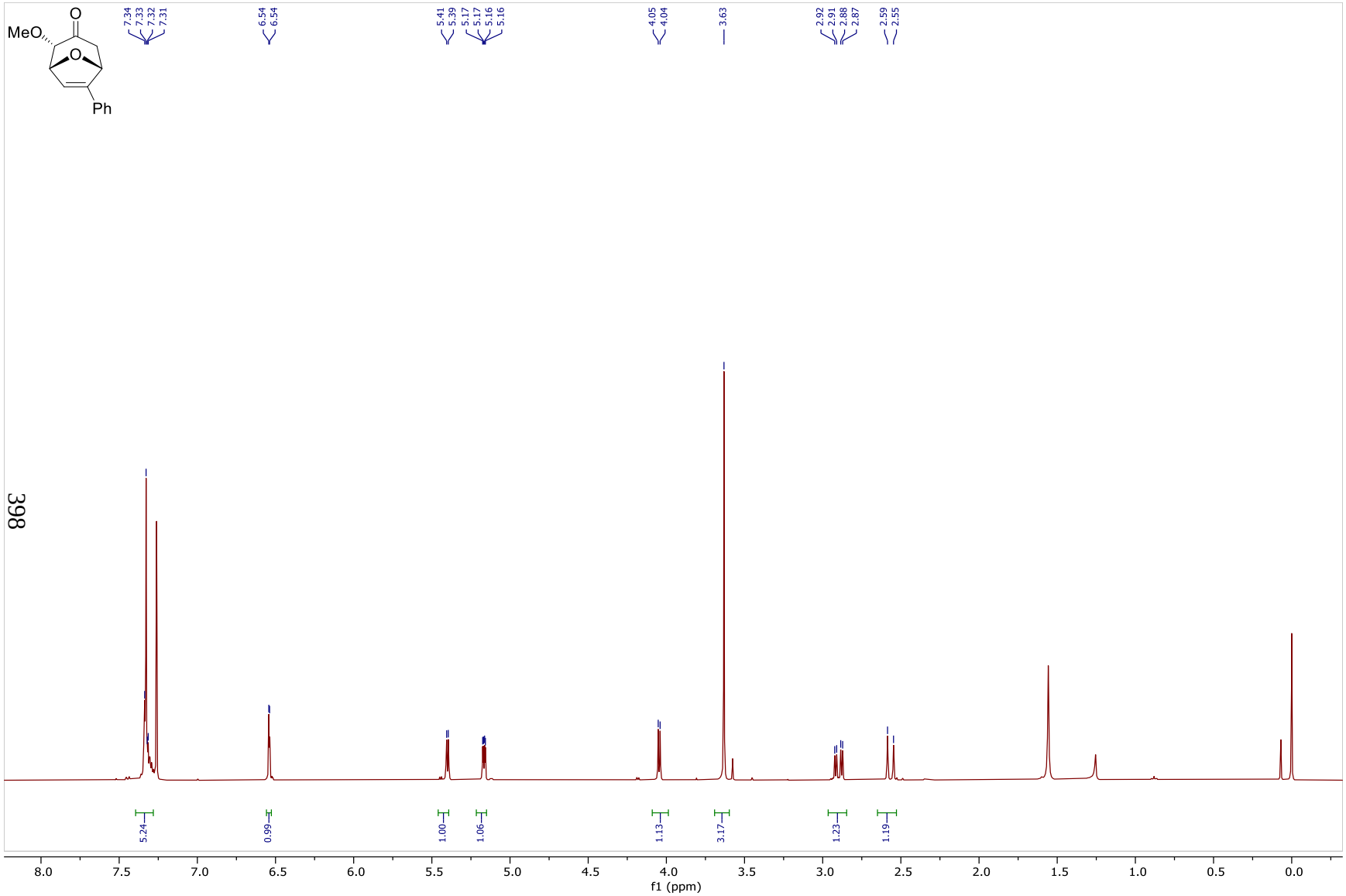

Figure 207: ^{1}H NMR Spectrum of **234c** (400MHz, $CDCl_3$)

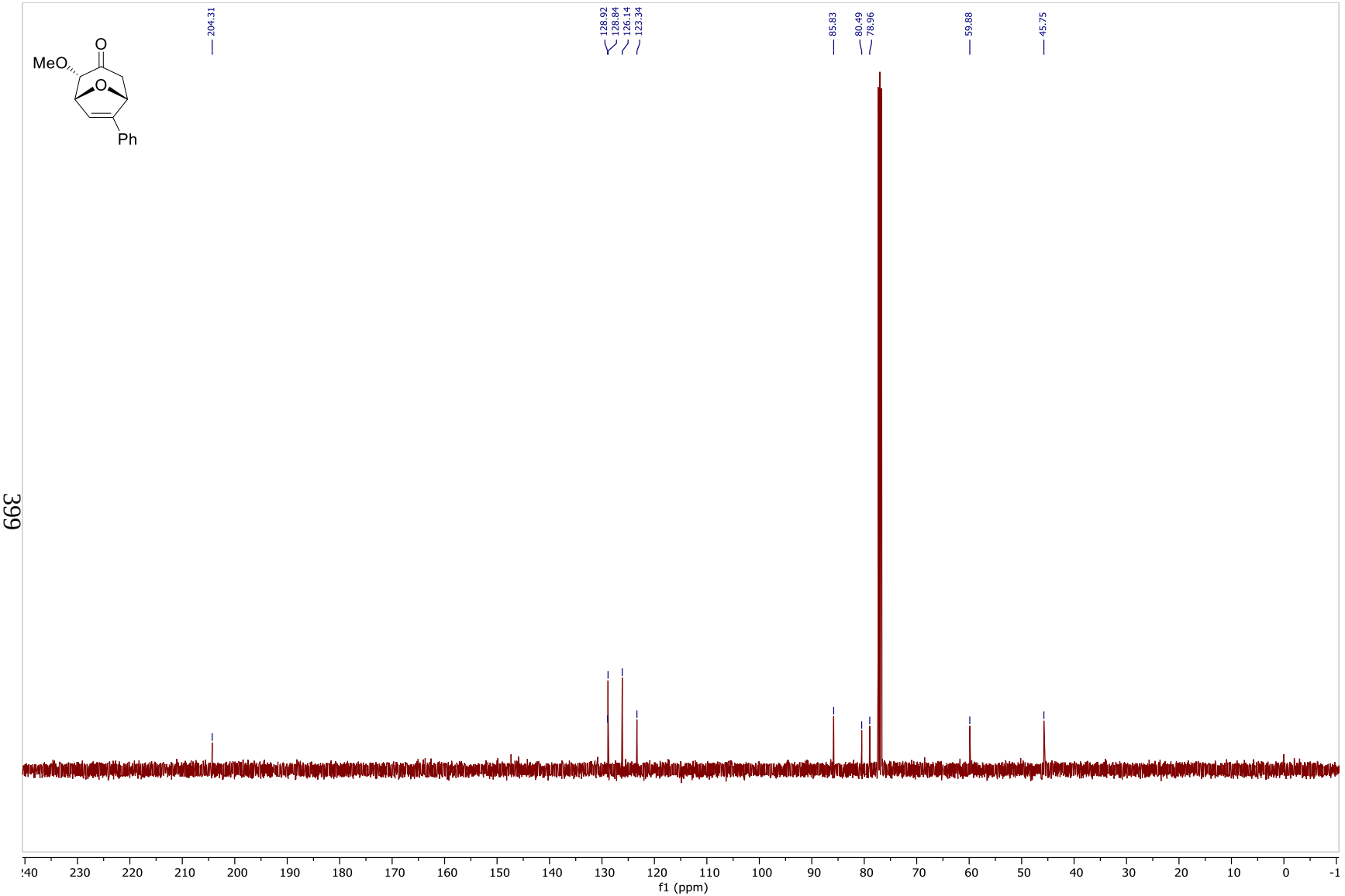

Figure 208: ^{13}C NMR Spectrum of **234c** (100MHz, $CDCl_3$)

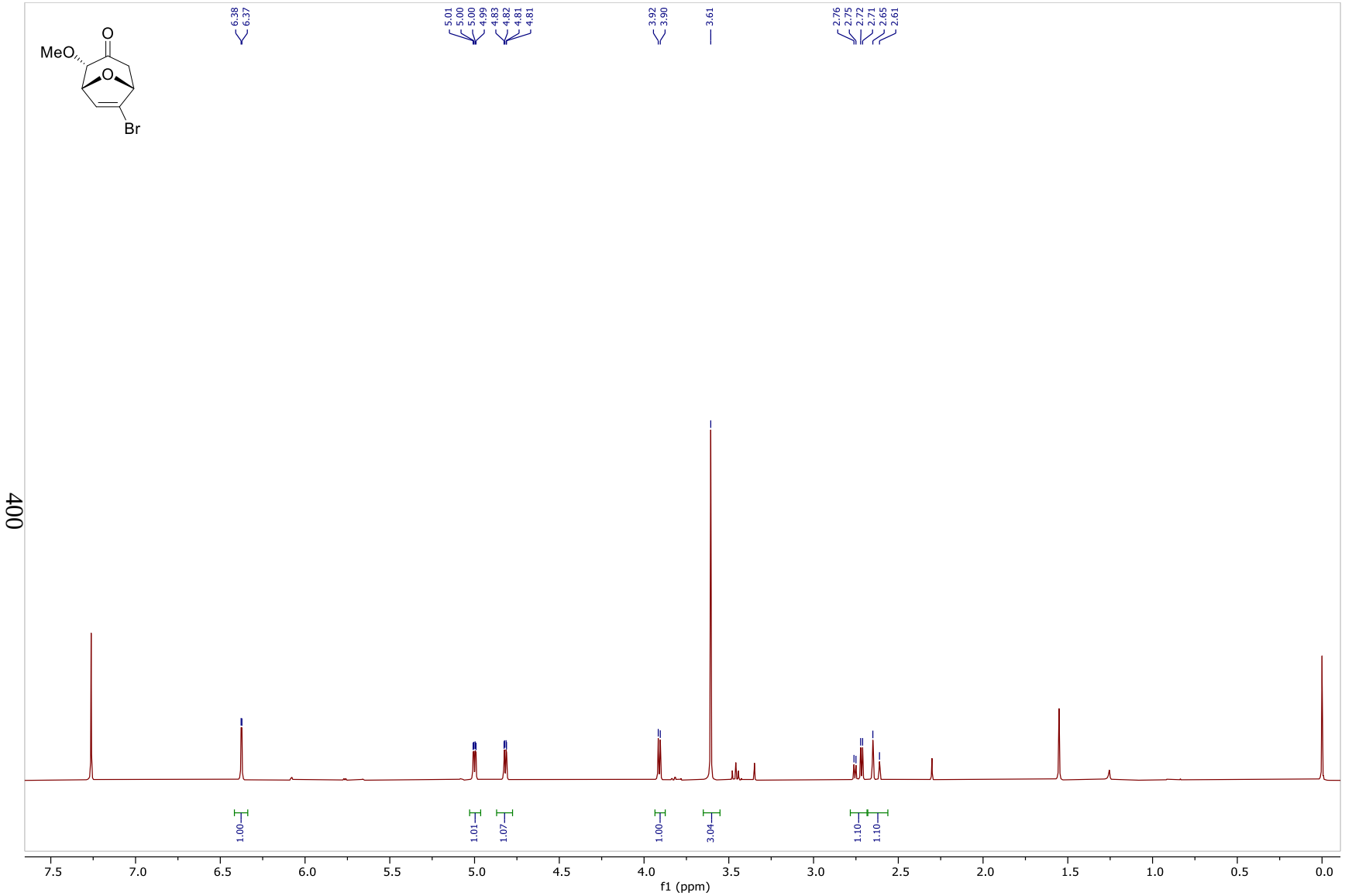

Figure 209: ^{1}H NMR Spectrum of **234d** (400MHz, $CDCl_3$)

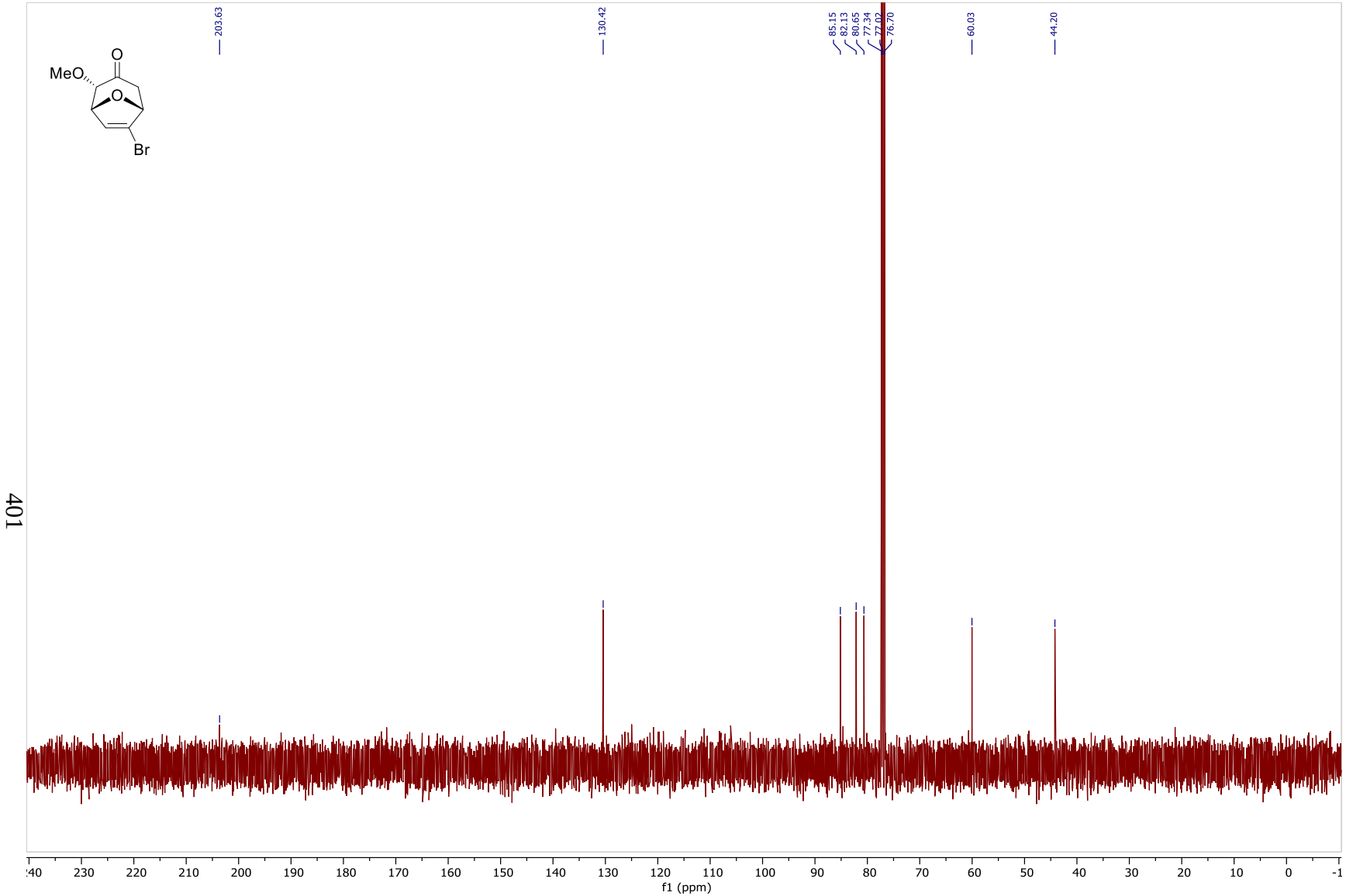

Figure 210: ^{13}C NMR Spectrum of **234d** (100MHz, $CDCl_3$)

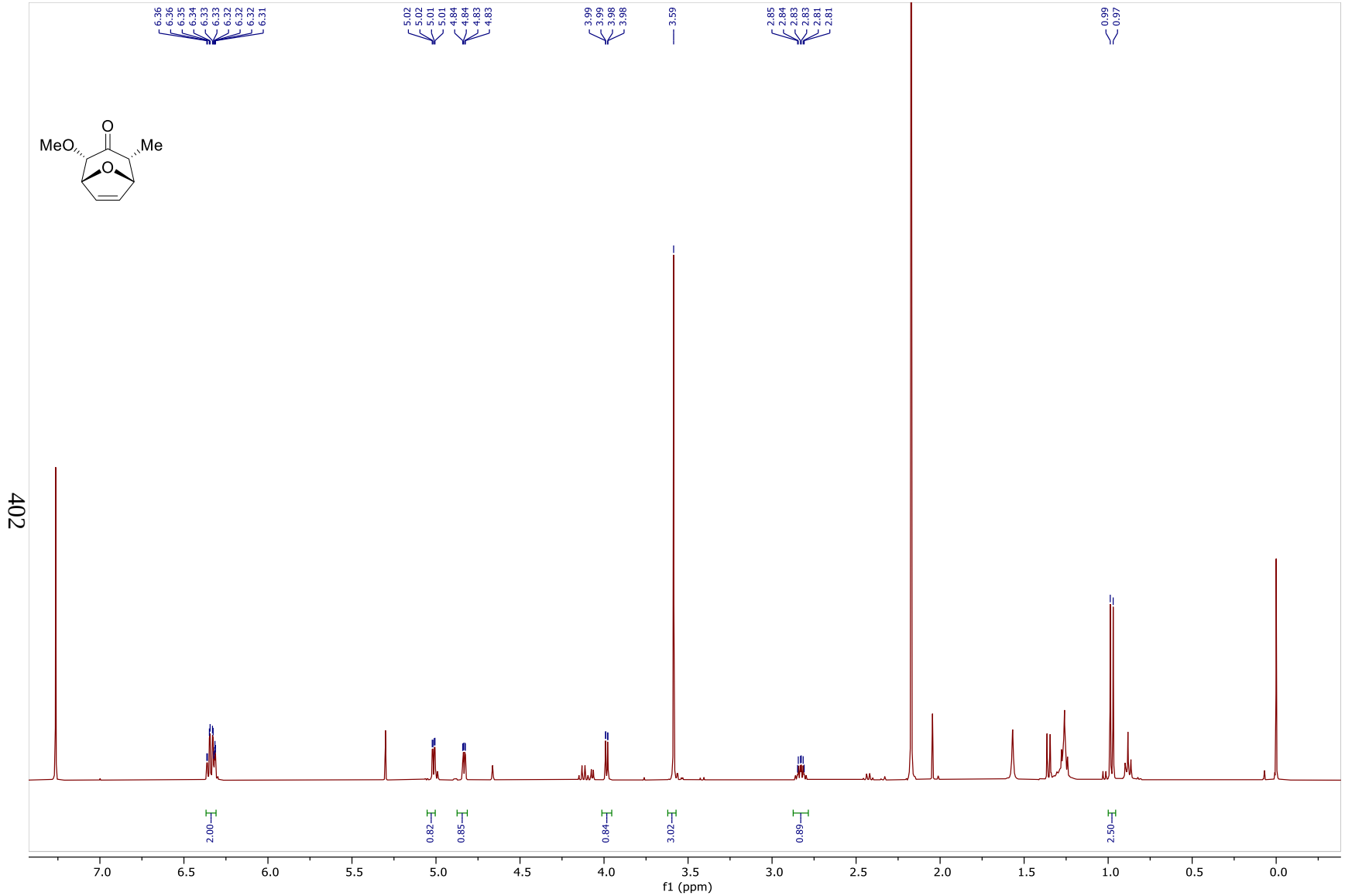

Figure 211: ^{1}H NMR Spectrum of **234e** (400MHz, $CDCl_3$)

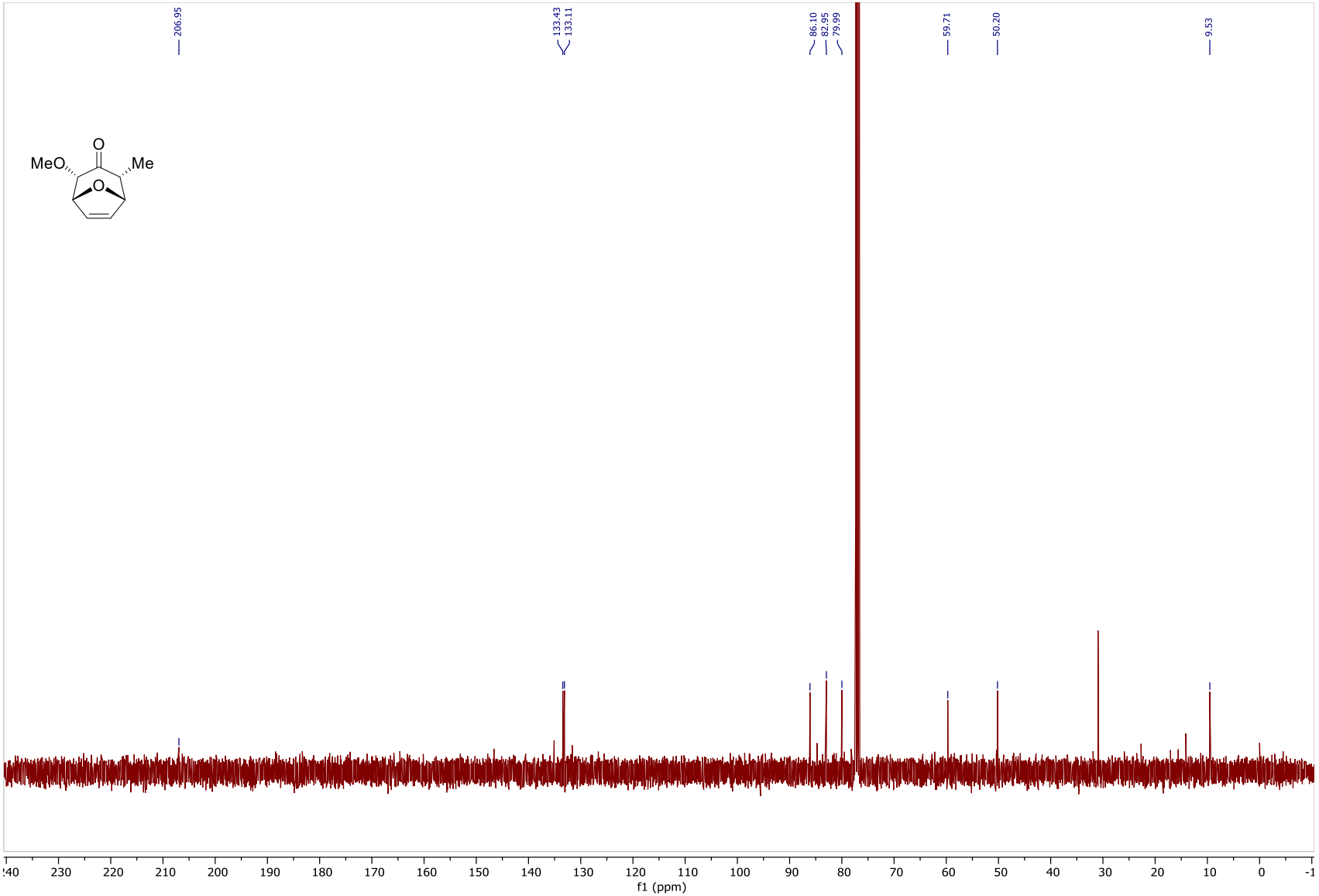

Figure 212: ^{13}C NMR Spectrum of **234e** (100MHz, $CDCl_3$)

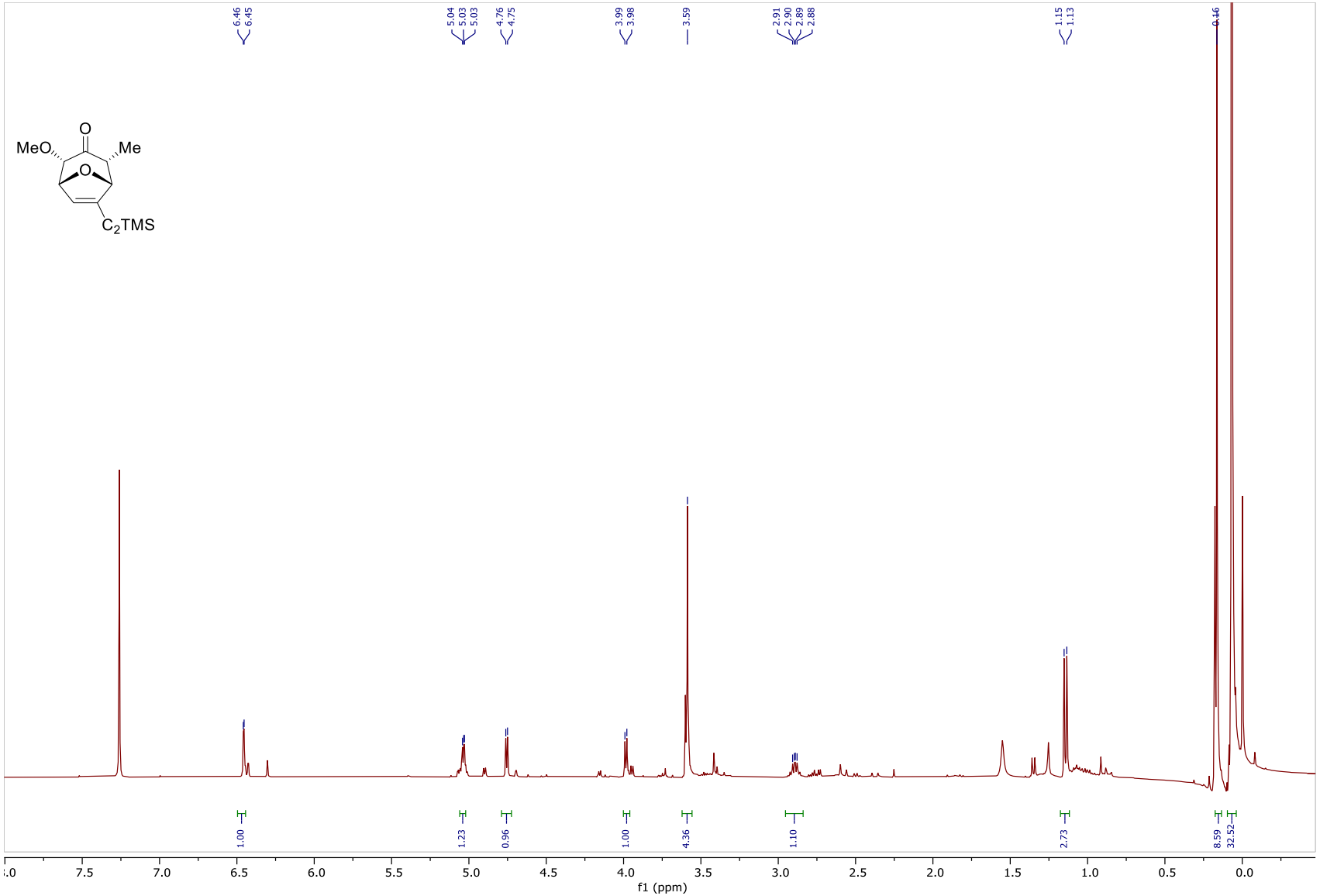

Figure 213: ^{1}H NMR Spectrum of **234f** (400MHz, $CDCl_3$)

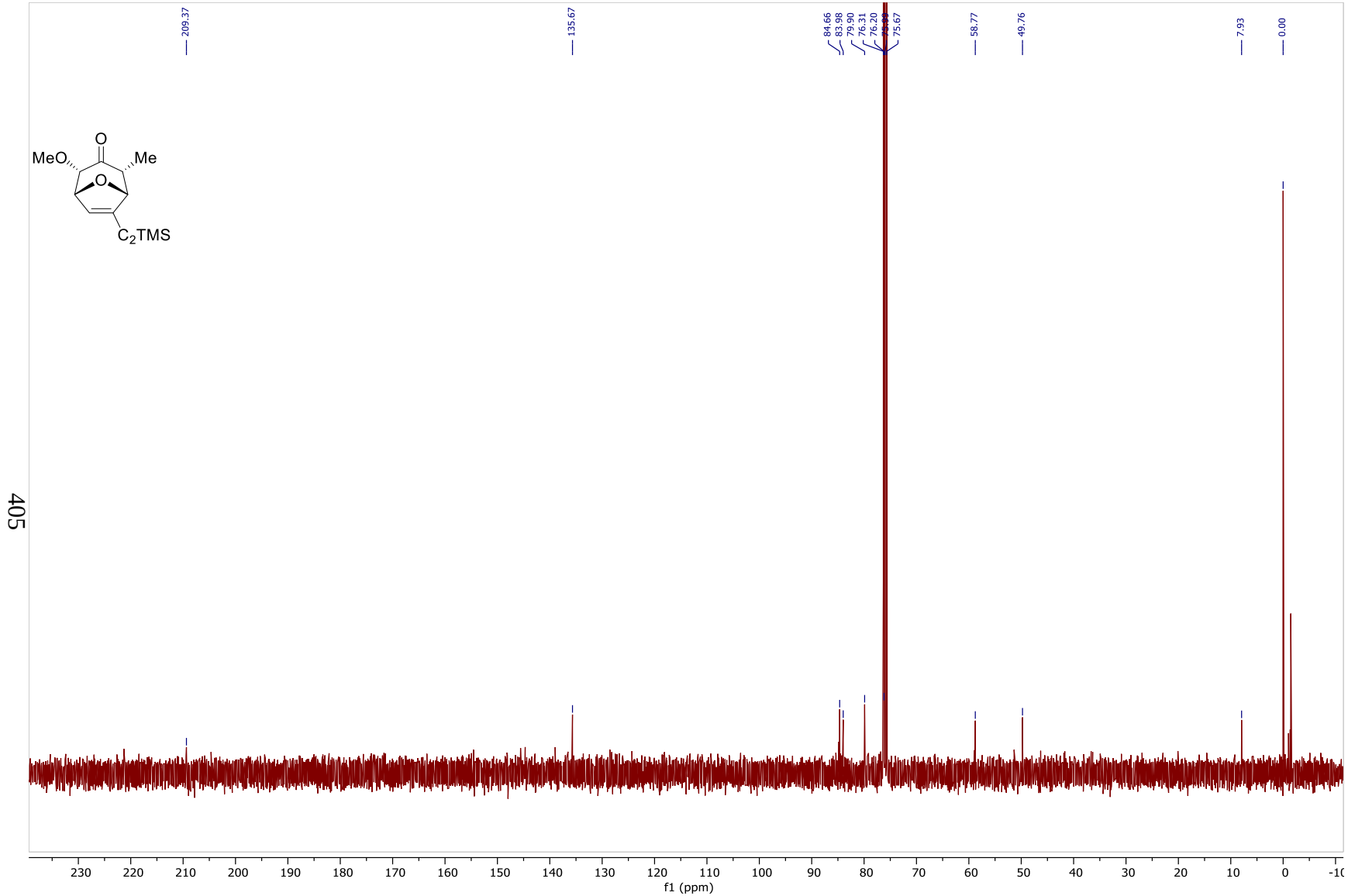

Figure 214: ^{13}C NMR Spectrum of **234f** (100MHz, $CDCl_3$)

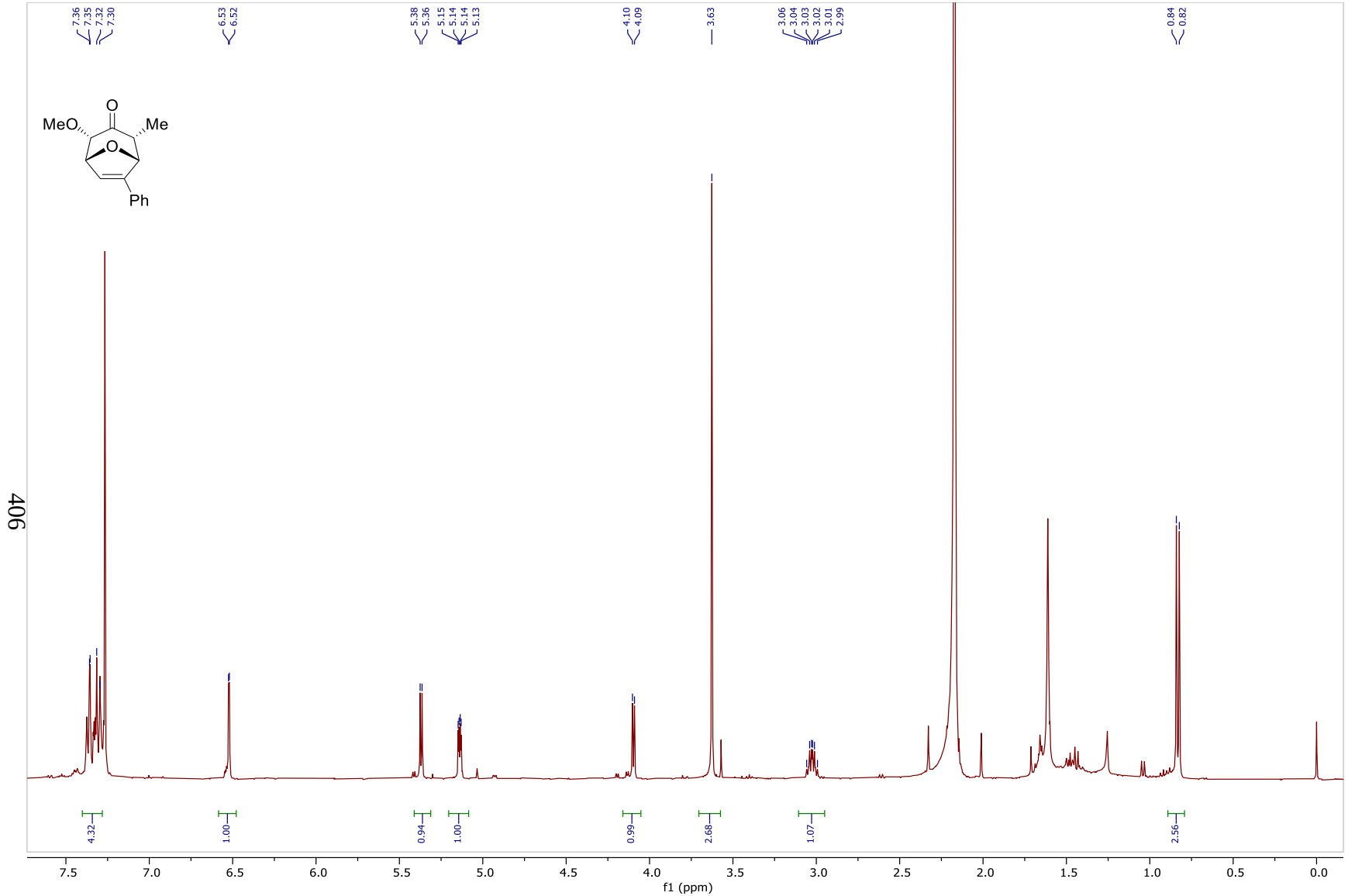

Figure 215: ^{1}H NMR Spectrum of **234g**(400MHz, $CDCl_3$)

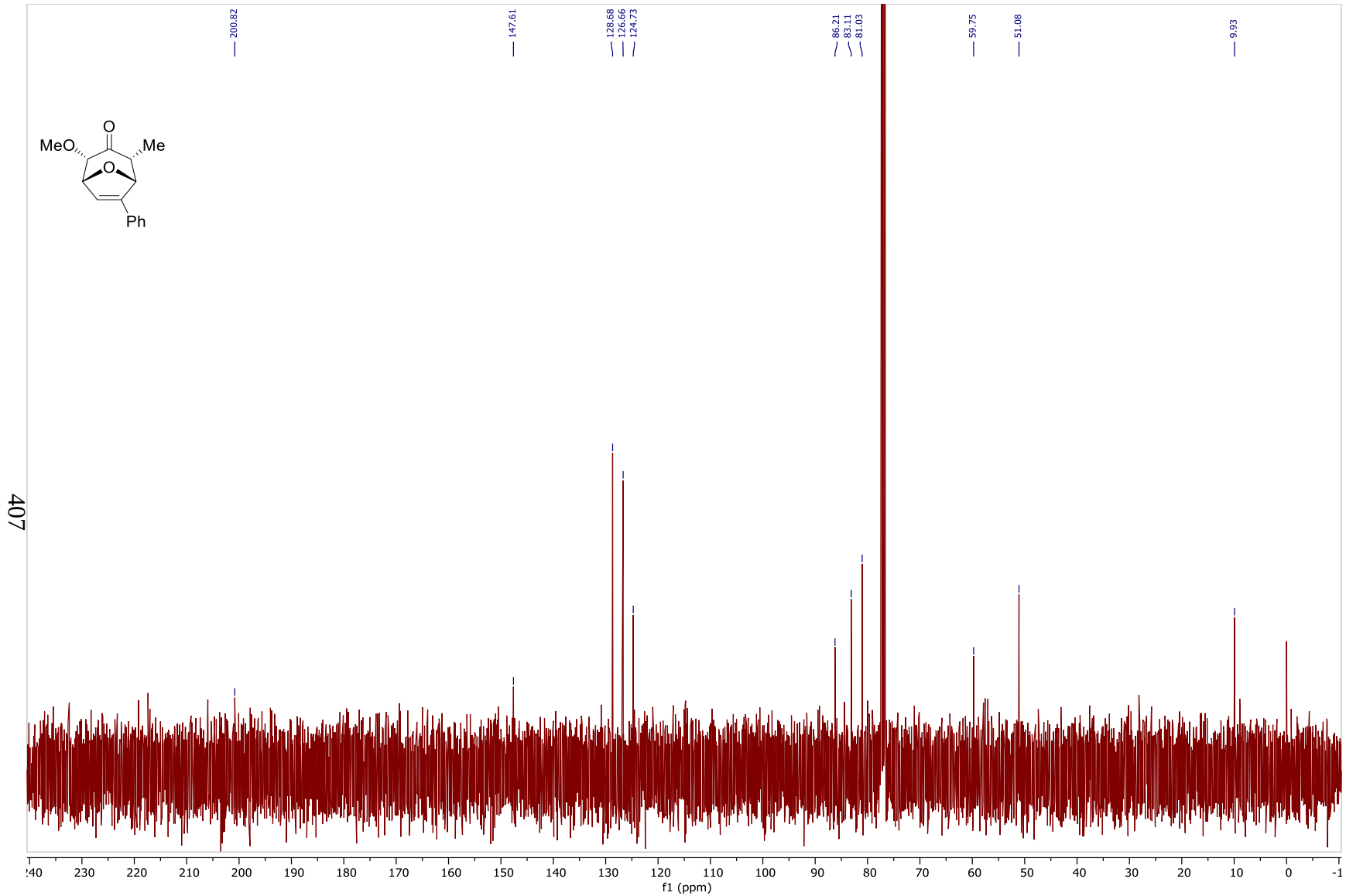

Figure 216: ^{13}C NMR Spectrum of **234g** (100MHz, $CDCl_3$)

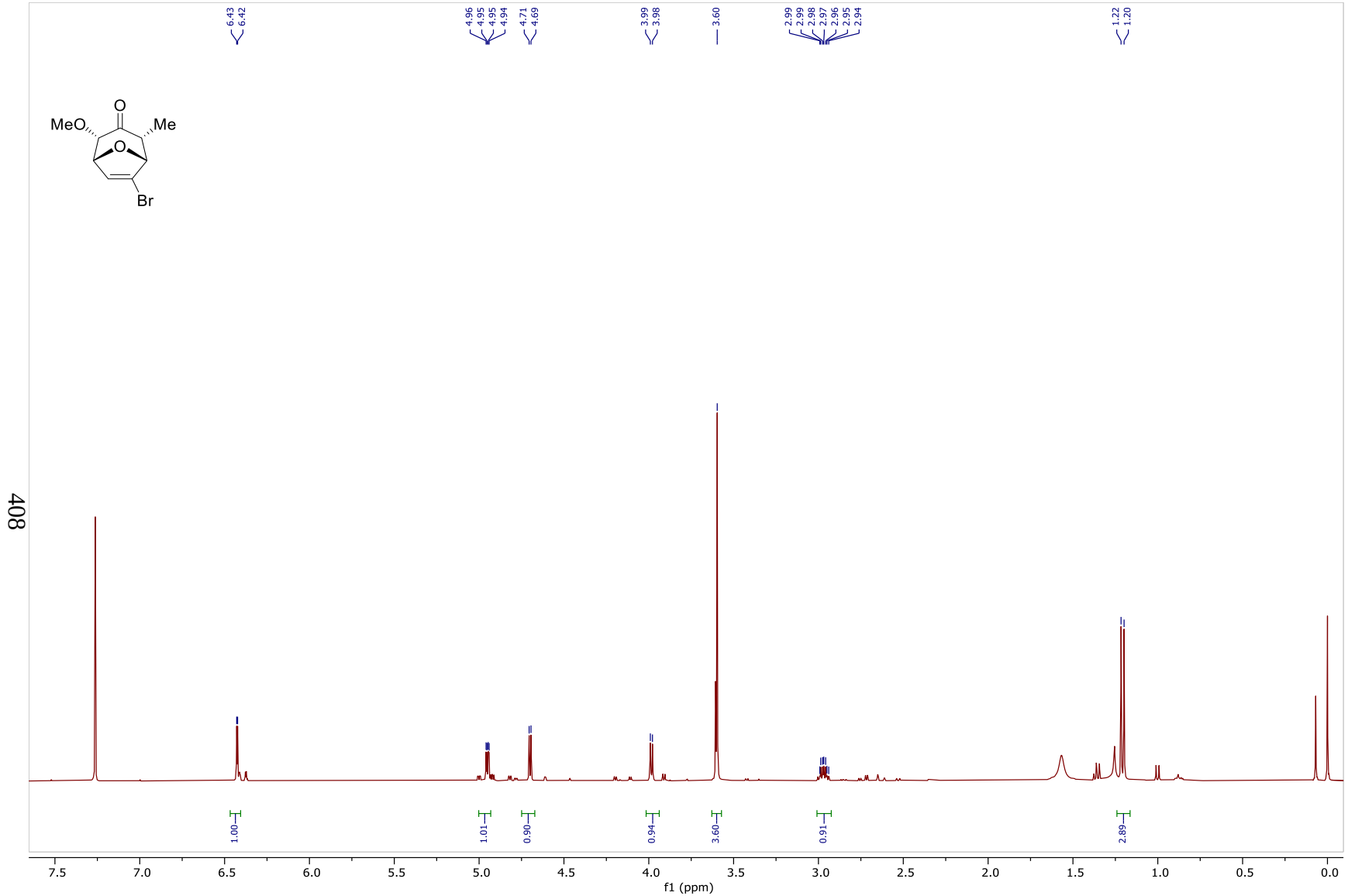

Figure 217: ^{1}H NMR Spectrum of **234h**(400MHz, $CDCl_3$)

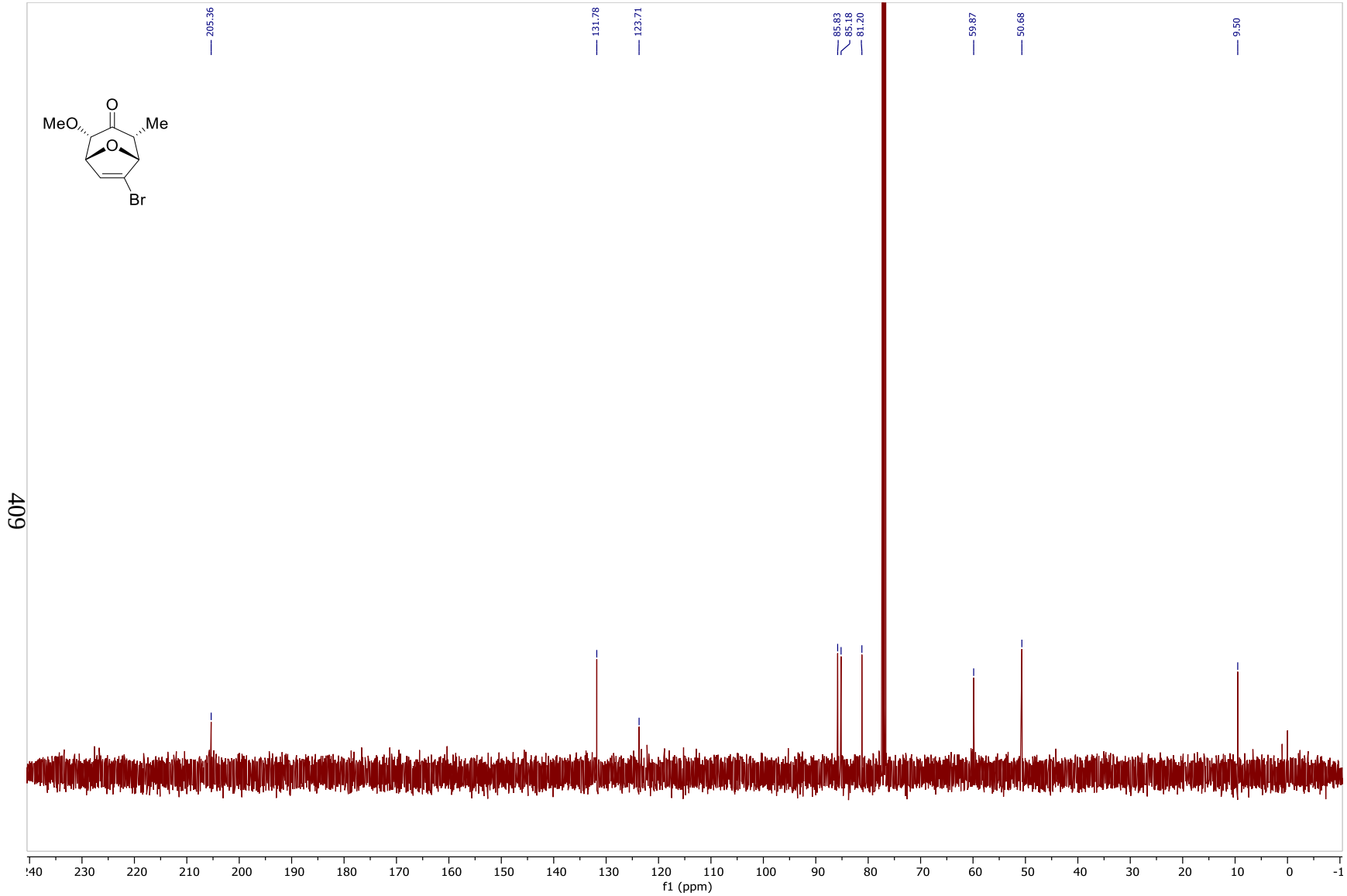

Figure 218: ^{13}C NMR Spectrum of **234h** (100MHz, $CDCl_3$)

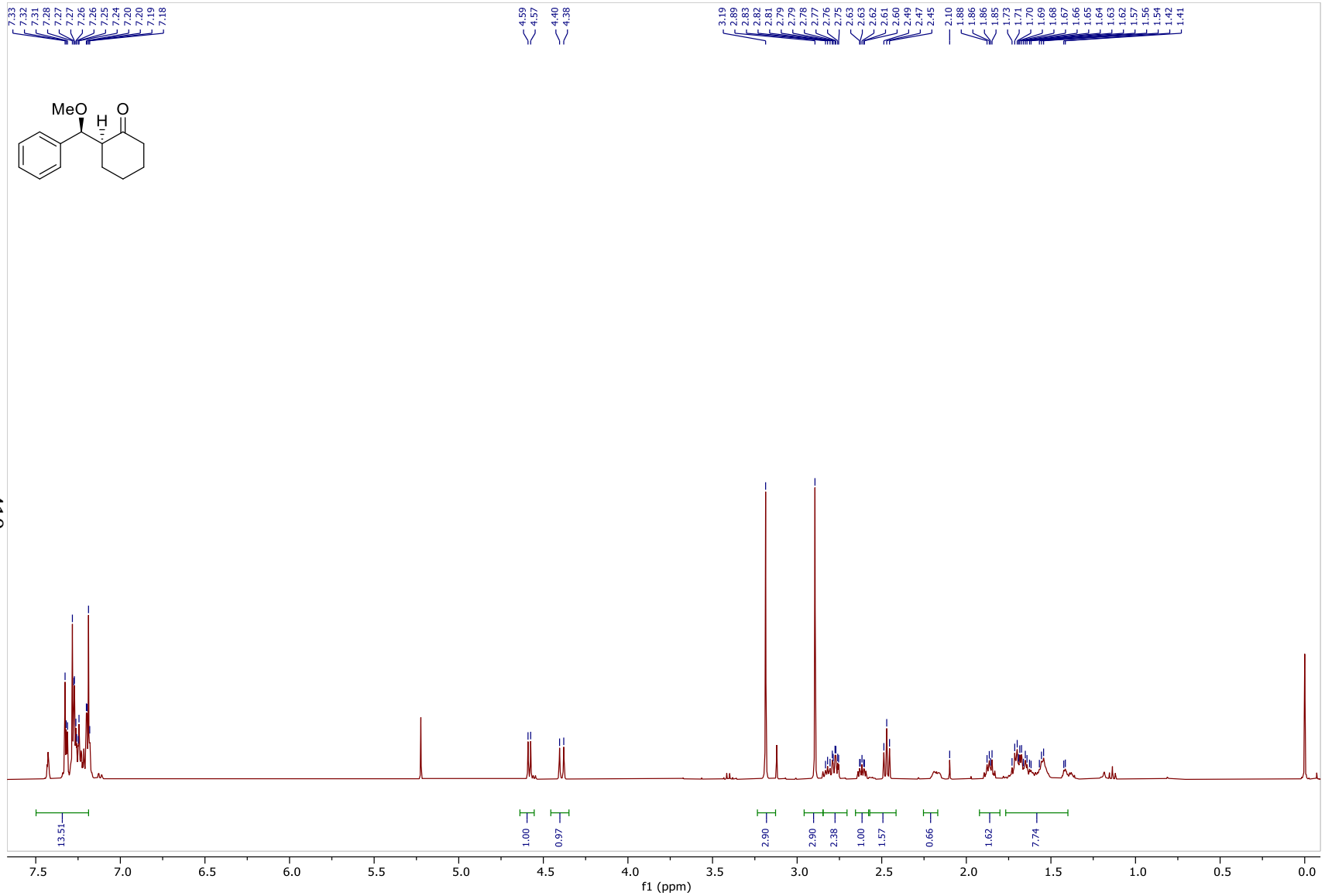

Figure 219: ^{1}H NMR Spectrum of **241**(400MHz, $CDCl_3$)

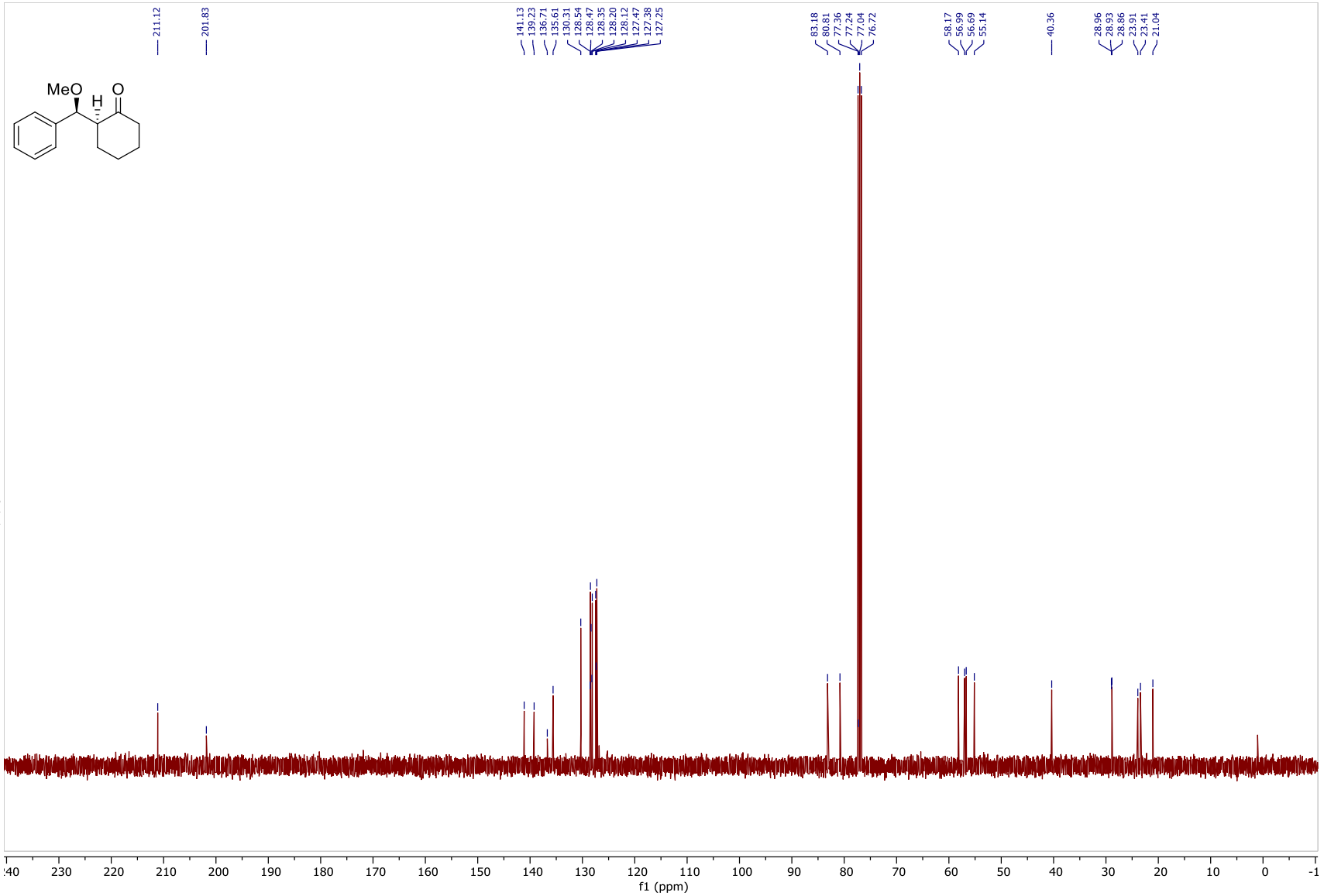

Figure 220: ^{13}C NMR Spectrum of **241** (100MHz, $CDCl_3$)

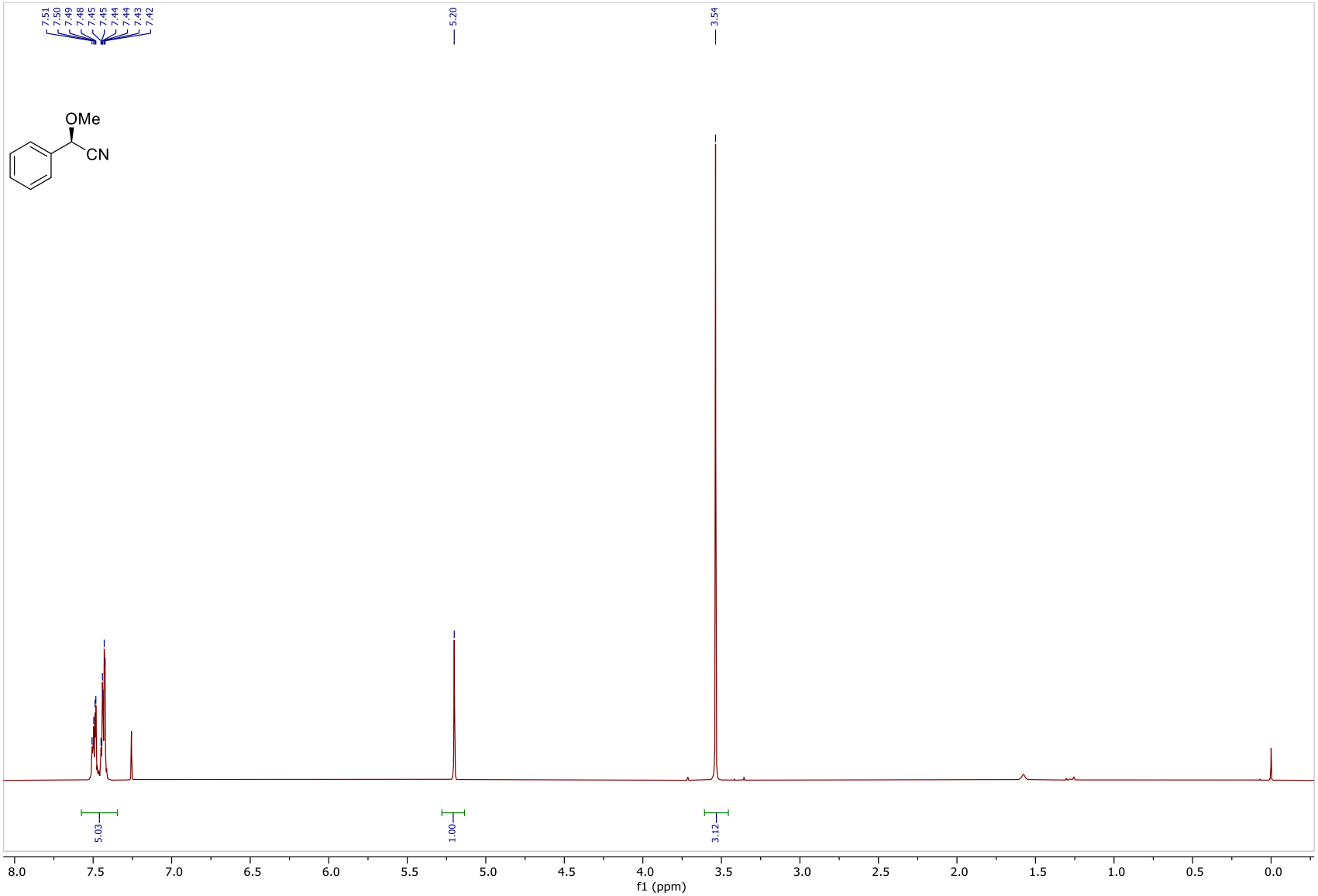

Figure 221: ^{1}H NMR Spectrum of **243 (**400MHz, $CDCl_3$)

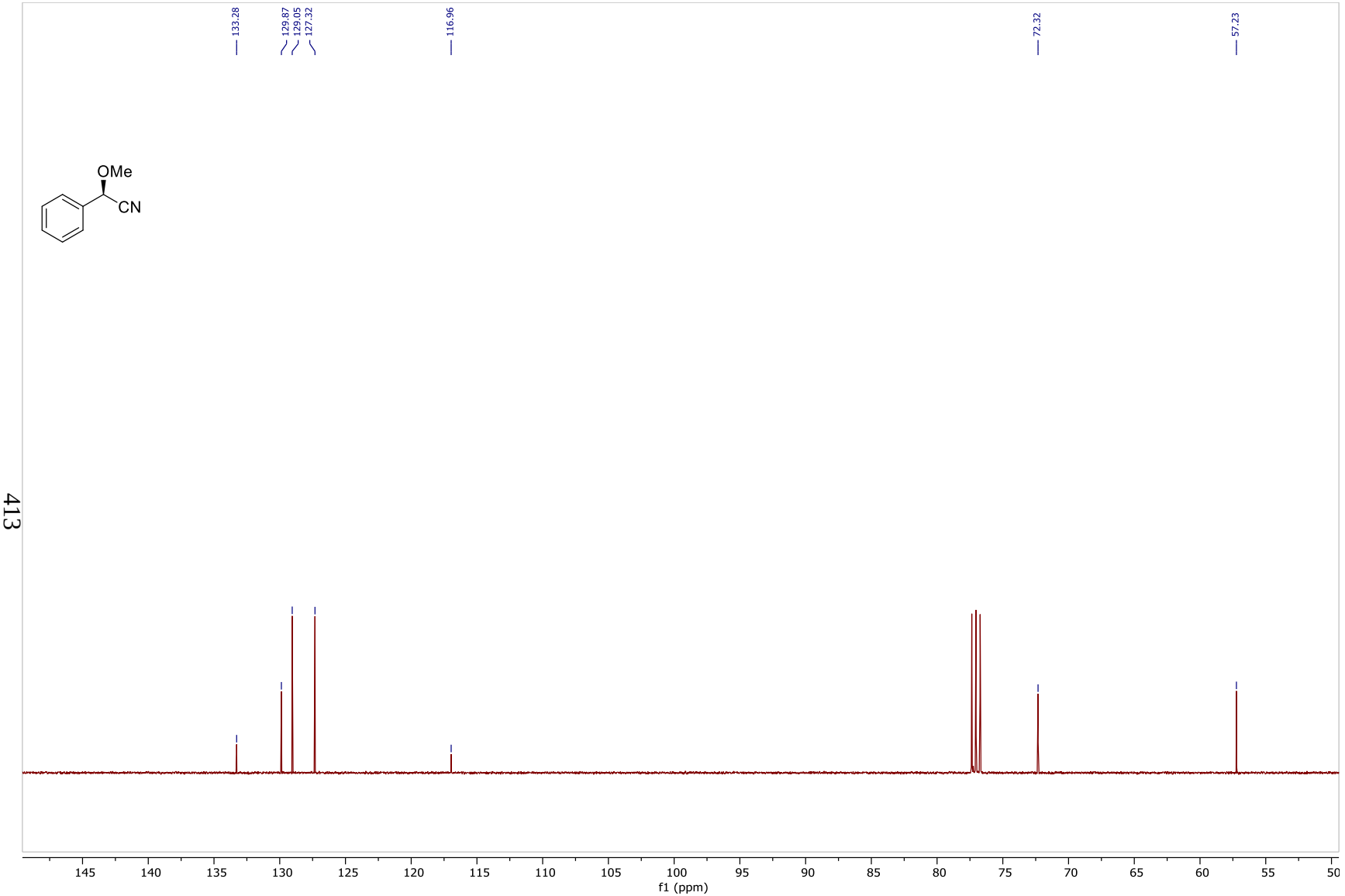

Figure 222: ^{13}C NMR Spectrum of **243** (100MHz, $CDCl_3$)

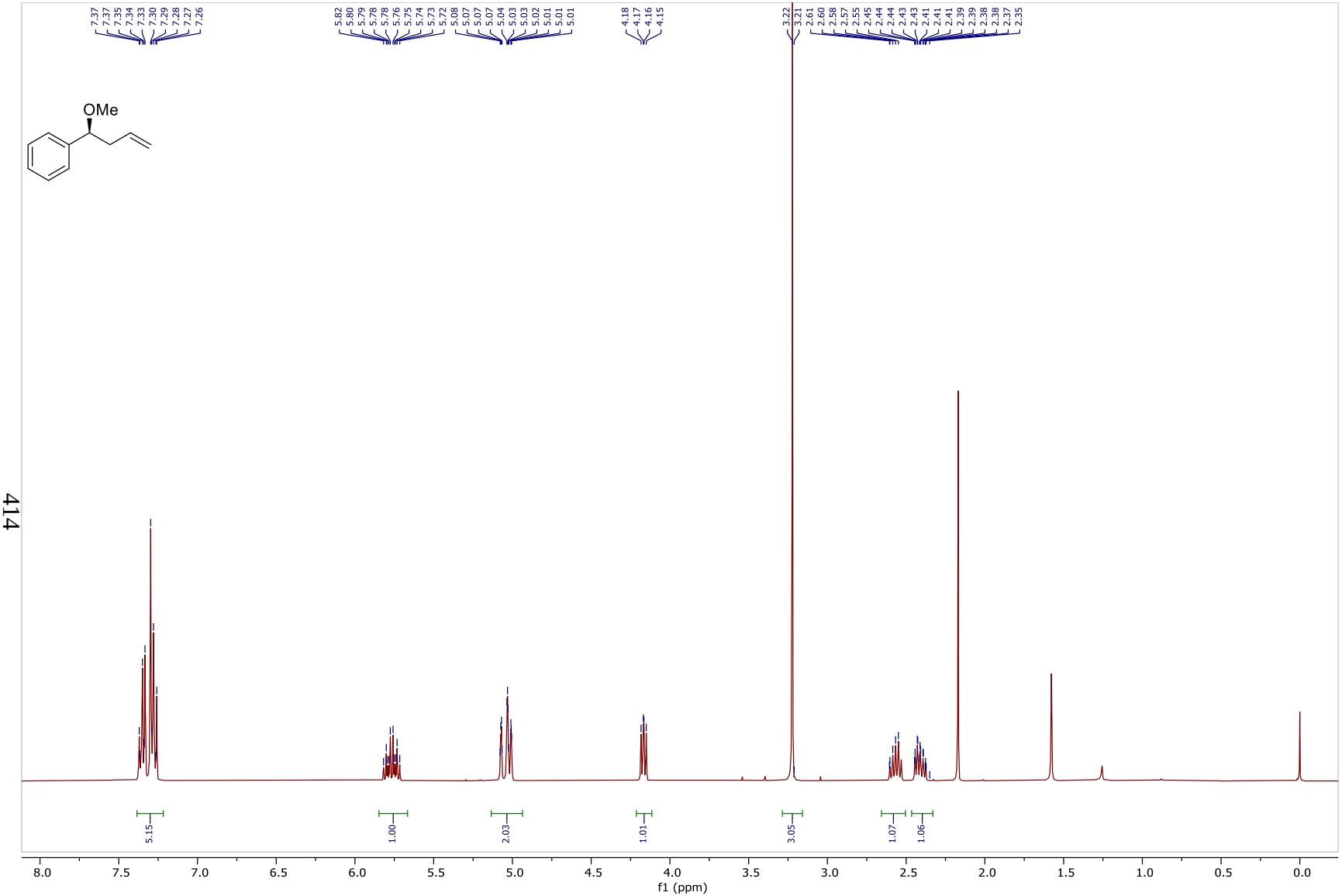

Figure 223: ^{1}H NMR Spectrum of **244 (**400MHz, $CDCl_3$)

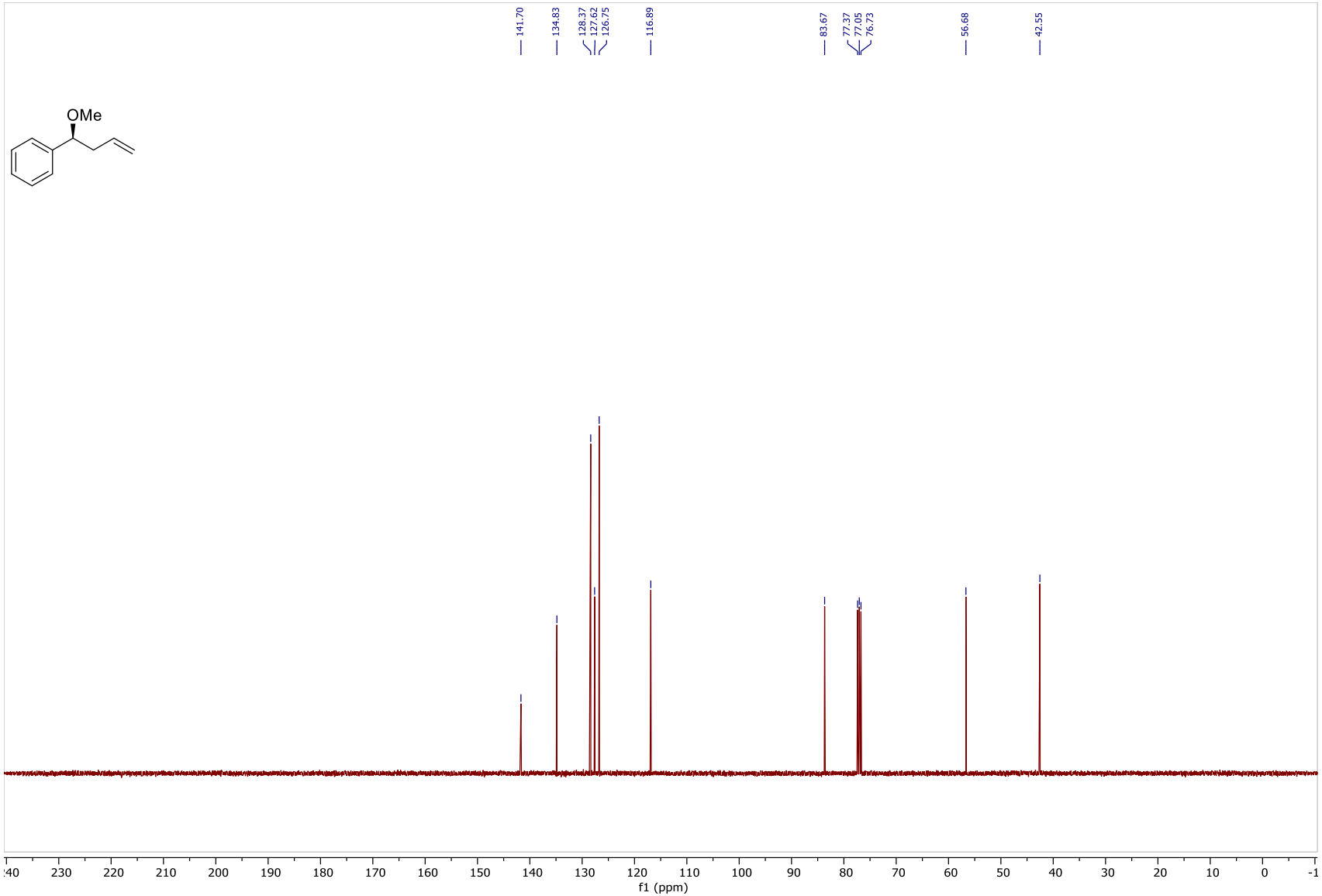

Figure 224: ^{13}C NMR Spectrum of **244** (100MHz, $CDCl_3$)

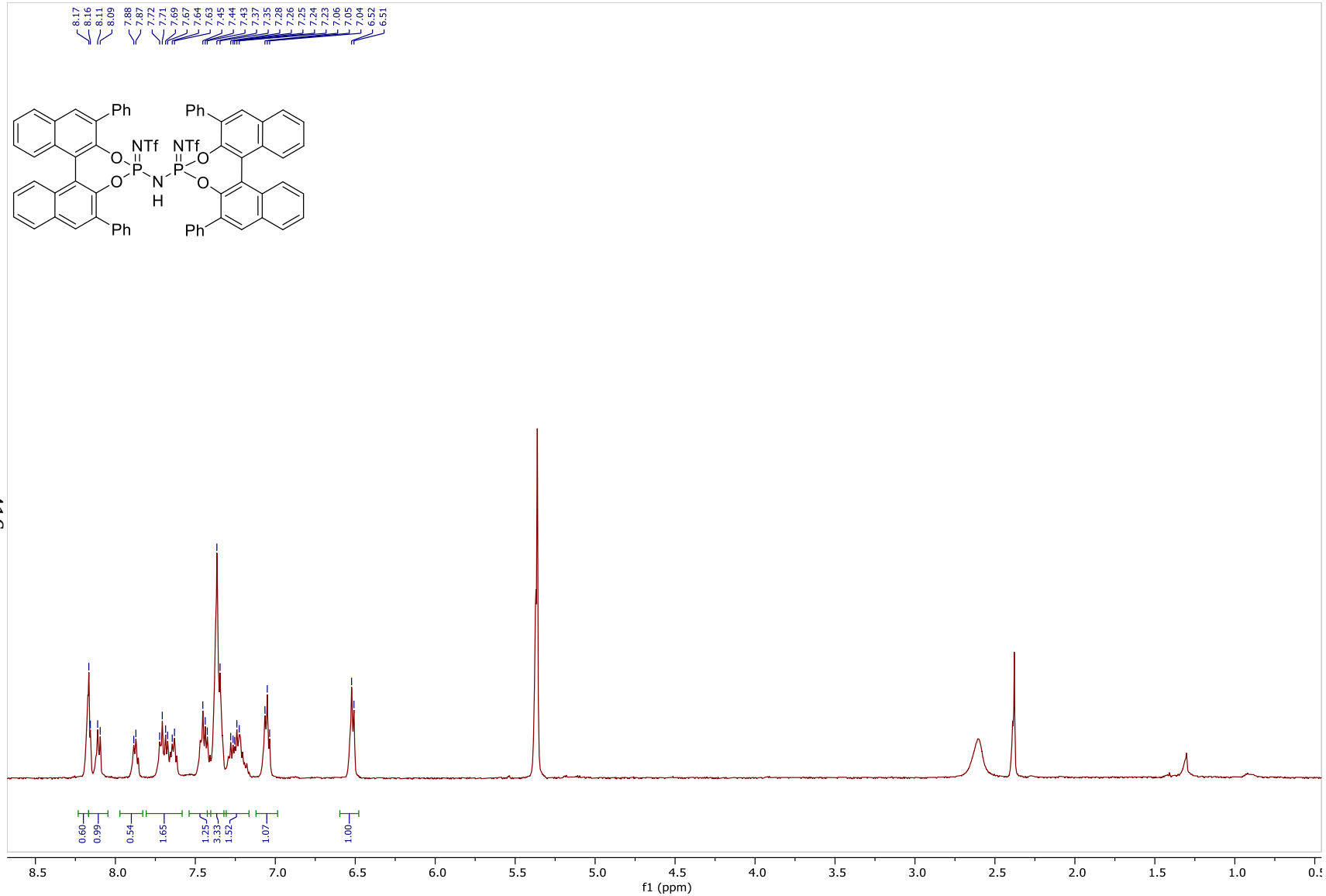

Figure 225: ^{1}H NMR Spectrum of **IDPi-a** (500MHz, $CDCl_3$)

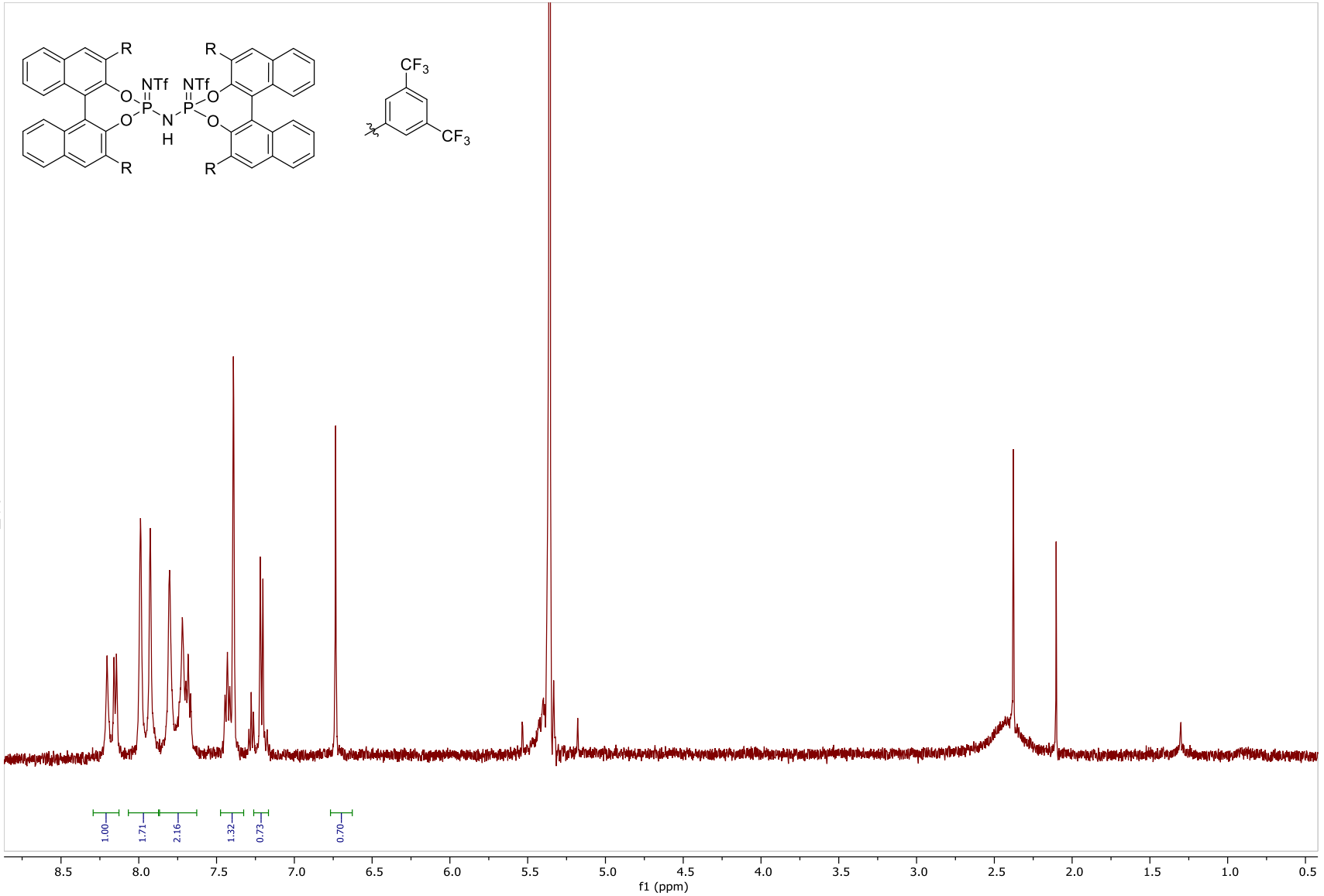

Figure 226: ^{1}H NMR Spectrum of **IDPi-b** (500MHz, CD_2Cl_2)

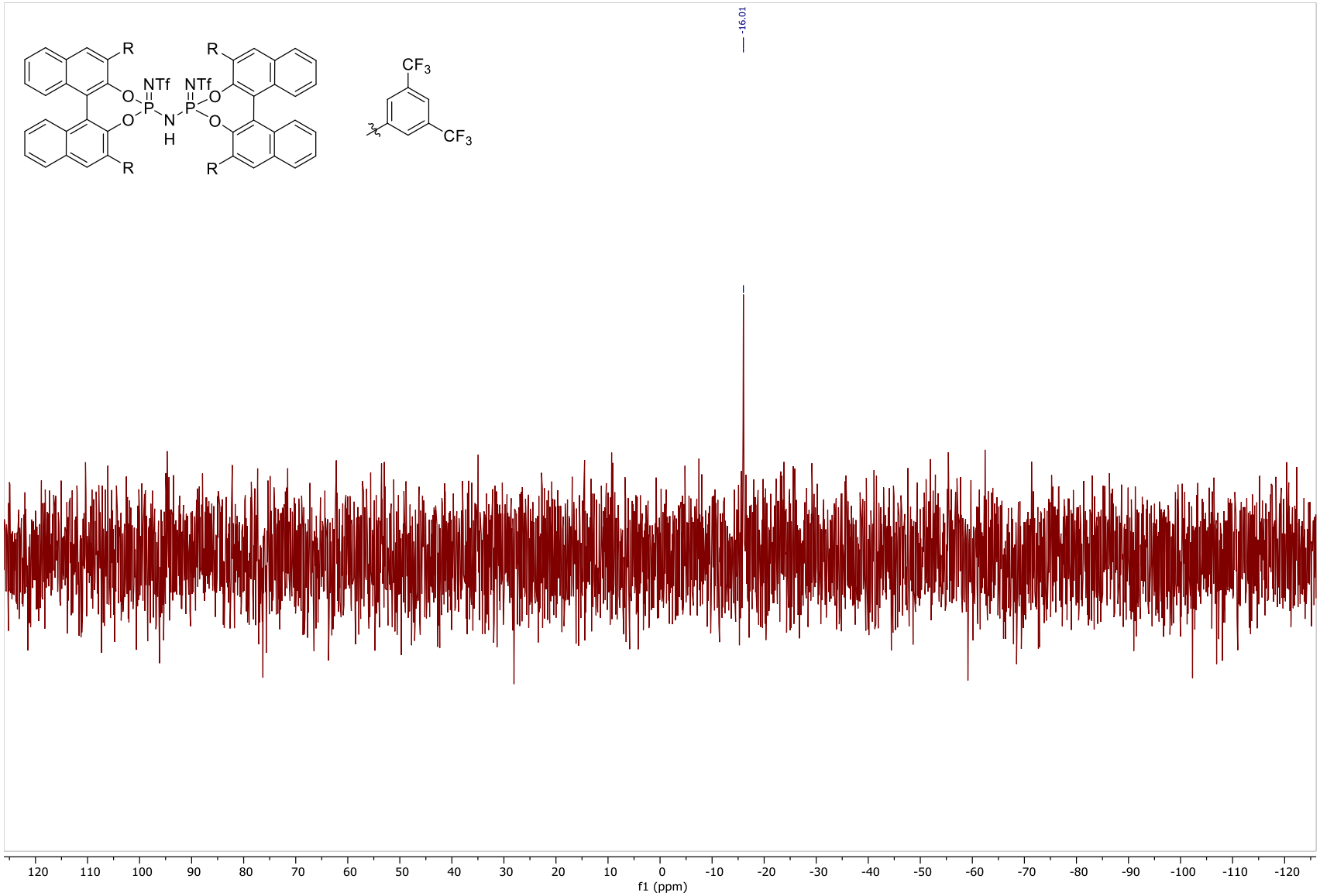

Figure 227: ^{1}H NMR Spectrum of **DPi-b** (202 MHz, CD_2Cl_2)

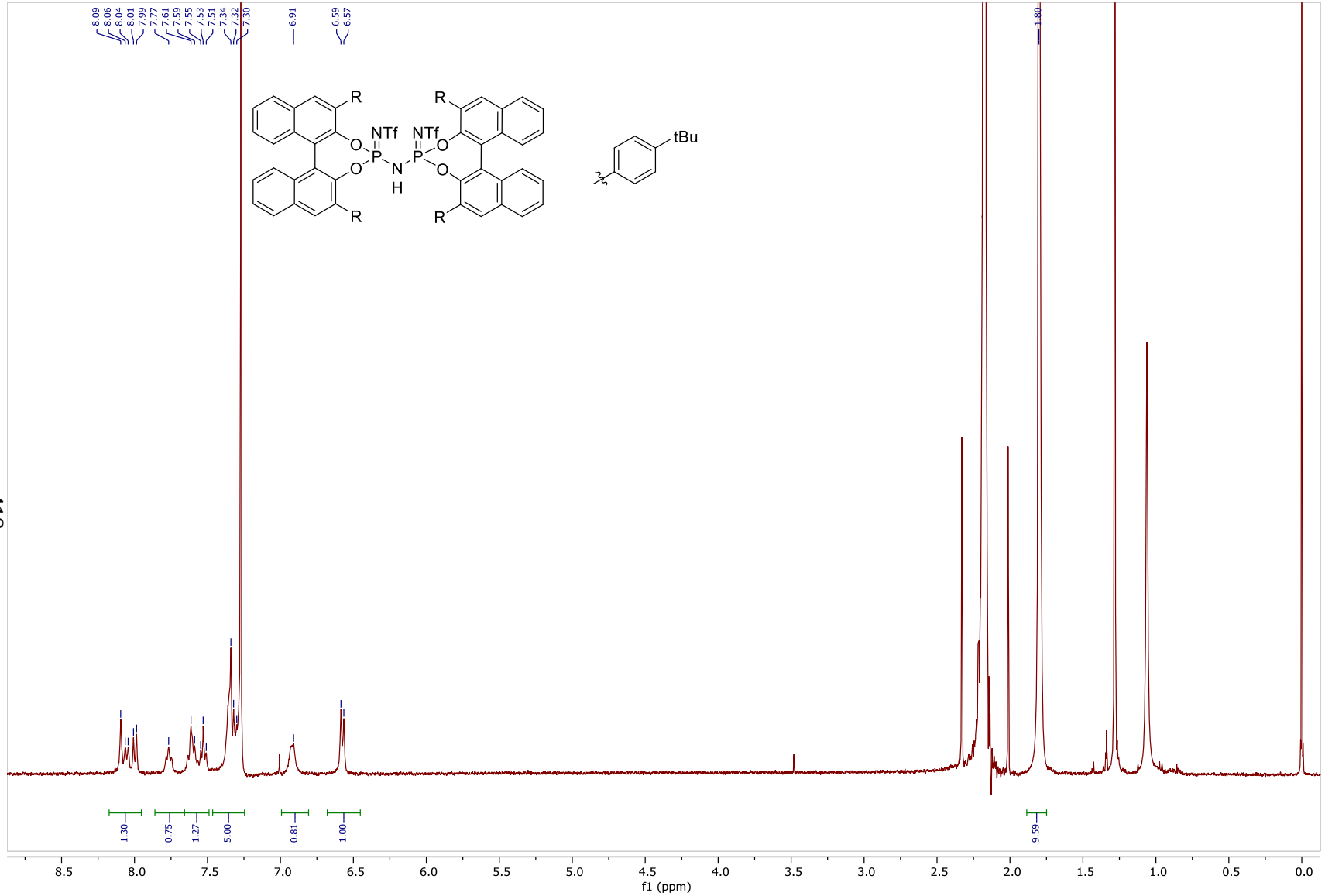

Figure 228: ^{1}H NMR Spectrum of **IDPi-c** (500MHz, $CDCl_3$)

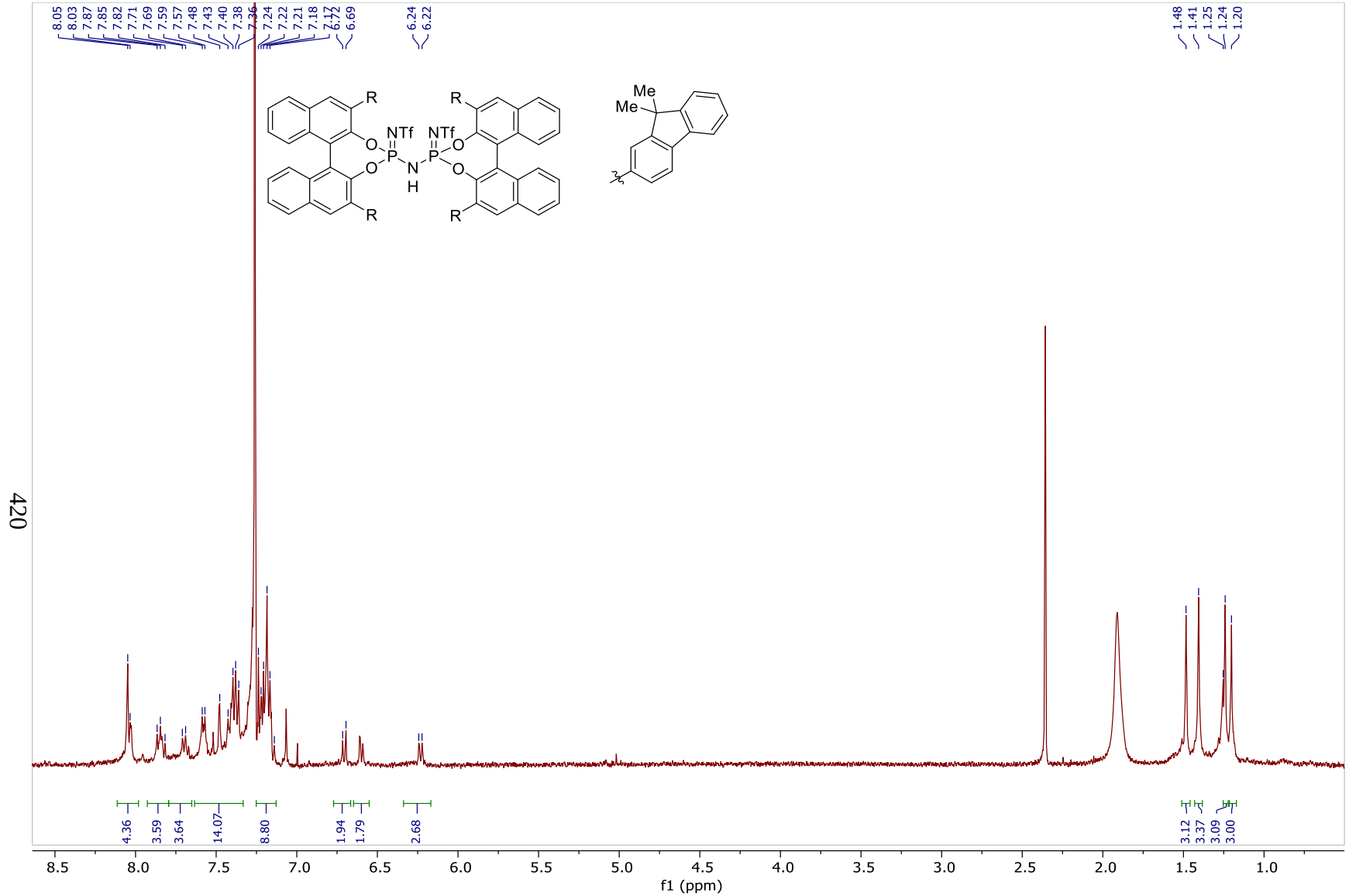

Figure 229: ^{1}H NMR Spectrum of **IDPi-d** (400MHz, $CDCl_3$)

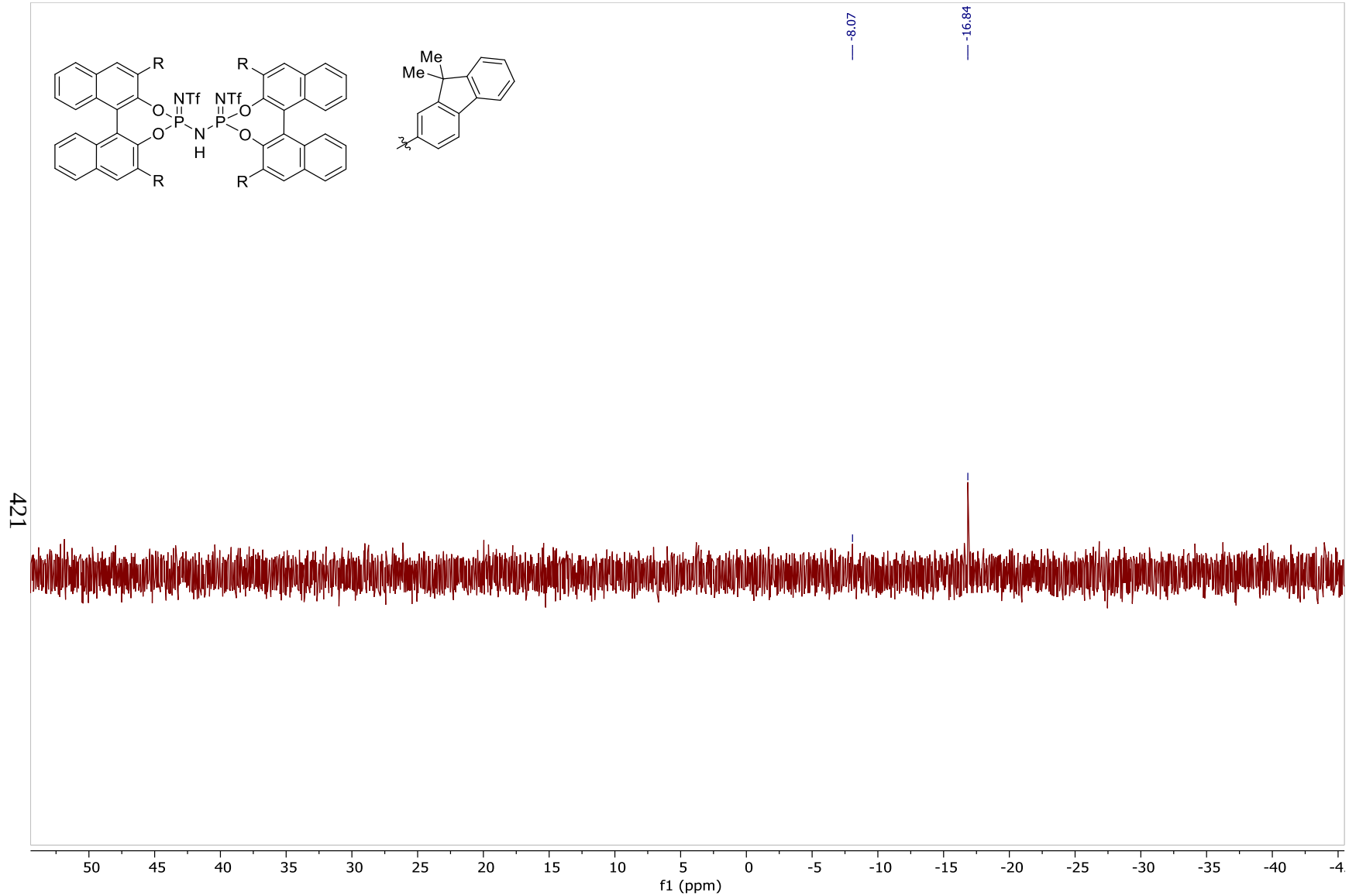

Figure 230: ^{31}P NMR Spectrum of **IDPi-d** (202MHz, $CDCl_3$)